Microprocessor Applications to the Phenomena Associated with High-Voltage Transmission Line Transients

A thesis presented by

Mark Munro

(Sponsoring establishment

Dundee College of Technology)

to the CNAA

in partial fulfilment of the

requirements for the degree of

Doctor of Philosophy

October 1986

Declaration

I declare that while registered as a candidate for the degree for which this thesis is presented I have not been a candidate for any other award. I further declare that except where stated the work contained in this thesis is original and was performed by the author. The author is grateful to Mr I Longair for the Low-Pass Digital Filter computer program employed in Chapter 6.

Signed

Mark Munro.

Advanced Studies

In addition to the original research reported in this thesis the author followed a programme of postgraduate study attending lectures on the Digital Techniques used in Transmission Line Energisation Transient Studies. Also the author attended and presented papers at the 1984 and 1985 Universities Power Engineering Conferences (UPEC) while contributing to the papers presented at UPEC in 1986 and the Liquid and Amorphous Semiconductors Meeting (Chelsea) in 1984.

Acknowledgements

The author is indebted to and wishes to thank the following without whose help this work would not have been possible.

Mr L Crowe for his supervision and encouragement throughout this investigation.

Dr J P Bickford for his advice and constructive criticism.

Mr W C R Legg, Mr J A B Hutton and Mr C J White for the discussions concerning the microprocessor aspects of this project.

Dr P L Bainbridge for extending to the author the use of the facilities of the Electrical and Electronic Engineering Department at Dundee College of Technology.

Mr W Harper, Mr W Butter and Mr S Sturrock for their advice and assistance concerning the technical aspects of the investigation.

The staff of the Computer Centre for their patience and considerable help in the preparation of this thesis.

The Scottish Education Department and Dundee College of Technology for providing the financial assistance which made this work possible.

Abstract

Microprocessor Applications to the Phenomena Associated

with High-Voltage Transmission Line Transients

Mark Munro

The methods for determining transmission line energisation overvoltages incorporate the traditional analogue Transient Network Analyser approach and the more recent mathematical techniques developed for the digital computer. The combination of the two technologies suggest a hybrid TNA system where switching and monitoring of the analogue transmission line model and its response are controlled by a decision-making microprocessor.

This study describes a new approach where the microprocessor is used to reduce the Gibbs phenomena present in uncompensated model line energisation responses. This has previously been achieved by incorporating resistor compensation in the model but the subsequent increase in attenuation reduces waveform rates of rise and affects global response.

Experimental Sigma Factors, analogous to those developed in Fourier Transform analysis, have been devised to locally average the digitised uncompensated line response. They have been applied to uncompensated line receiving-end waveforms resulting from ideal and inductive source energisation of single and 3-phase (simultaneous closure) open-circuited model lines.

These factors significantly reduce the magnitude of the oscillations and achieve the overvoltage accuracy obtained from the compensated line. The resulting processor responses however give steeper rates of rise at response discontinuities as line length increases and also improved global response.

Significant differences in peak overvoltage, between processor and compensated waveforms resulting from inductive source energisation, have been determined for source values of 0 - 0.2H the improvement in accuracy being apparent over an increasing range of source inductance as line length is increased.

Spectral analysis of the model line waveforms was also undertaken and has improved the understanding of the model. Attempts at reducing the Gibbs content by Digital Filtering were not successful.

The Experimental Sigma Factors do not completely reduce the Gibbs content but the results obtained indicate that a modified approach for their implementation may further improve the processor responses already obtained.

Table of Contents

CHAPTER 1

Transmission Line Energisation Transients

1.1 Introduction

In recent years the voltage at which electrical power is transmitted over long distance overhead lines has been continually increasing with systems of up to 750 kV now in operation. As system operating levels were increased above 300 kV it was found that the transient overvoltages arising from switching of the network became more significant than those associated with lightning discharges[1]. The two switching conditions which cause significant transient overvoltages to occur in Extra High-Voltage (EHV) transmission systems are:-

1. Circuit Energisation
2. Circuit Breaking

Both conditions results in the stressing of the system insulation while the latter also stresses circuit-breaker residual arc paths.

In EHV systems, therefore, insulation becomes a major factor in the cost and practicability of the network. In order to optimise the safety and economic factors associated with such systems that are in the design and planning stage of development it is necessary to be able to accurately predict the overvoltages which the system itself will generate.

Since the 1960s much work has been done in investigating the phenomena due to system switching with particular attention being paid to the transient overvoltages produced by overhead transmission line energisation[2, 3]. Line energisation from an ideal source can cause high overvoltages due to the voltage doubling phenomena which occurs at the open-circuited line receiving end. For this condition overvoltages of the order of twice the normal phase to earth voltage will be apparent at the receiving end but in an actual network a number of other effects such as source impedance, trapped charge and non-simultaneous circuit-breaker pole closure

will contribute to an increase in this value to 3 pu and above[4].

The traditional method of investigating and determining the magnitude of such transient phenomena has been to study the response of a lumped-parameter model of the actual overhead transmission line to energisation from a repetitive controlled point-on-wave switching device known as the Transient Network Analyser or TNA[5]. This analogue technique has been complemented since the 1960s, with the advent of powerful digital computers and microprocessors, by a variety of mathematical techniques applied to system switching[6]. The mathematical techniques are commonly described as Digital Methods (see section 1.8) since they require calculations to be carried out at discrete intervals of time and are programmed in computer software. Although these techniques are more accurate the TNA is an important investigative tool in this field which is still in frequent use[7].

1.2 The TNA Approach

The modern TNA (section 2.6) is a sophisticated device which allows energisation of model networks on a single and 3-phase basis from a 1-phase AC/DC or 3-phase model ideal source. With the ability to repeat this switching many times per second the transient waveform from a model system can be viewed on a CRO and/or its maximum overvoltage value recorded by a peak-reading digital voltmeter. In energising a 3-phase model transmission line the closing sequence of the switches on the TNA 3-pole switch card (section 2.6.4) can be varied so that the effects of non-simultaneous closure can be investigated quickly and the maximum overvoltages determined. However in simulating an overhead transmission line in the laboratory error is introduced due to the nature of the model representation used.

1.2.1 Overhead Transmission Line Models

For TNA studies an actual distributed-parameter overhead line is physically modelled by a number of lumped-parameter π-sections. Figure

1.1(a) shows a 1-phase π-section model of the series impedance and shunt capacitance of a 1-phase overhead line. This representation is accurate for steady-state analysis but for transient waveforms which have a far greater frequency spectrum accuracy is improved by cascading a number of these π-sections. However this representation acts as a low-pass filter and the high frequencies present in a step disturbance which are greater than the model cut-off frequency f_c are attenuated giving rise to Gibbs Oscillations[8] which are superimposed on the transient fundamental response. Figure 1.1(b) displays this phenomena in the response of an open-circuited 50 mile 1-phase line represented by 10 π-sections i.e. 1 π-section per 5 miles and energised from an ideal DC source. Increasing the number of π-sections used in the line representation will increase the accuracy of the response (see section 7.2) since the distributed-parameter case, where an infinite number is assumed[9], is being approached.

Figure 1.2 shows a 3-phase model line π-section with a frequency-dependent earth path based on Carsons equations[10]. Mutual coupling is also included in the earth-return since line transposition is assumed which greatly simplifies the model representation[11].

Transient analysis using the 3-phase model of Figure 1.2 was carried out until 1967 when Mullineux and Reed[12] suggested that resistor-compensation be introduced to damp out the Gibbs phenomena. The predominant frequency of the Gibbs Oscillations is dependent on the π-section L and C values i.e. the natural π-section frequency f_0 which is given by

$$f_0 = \frac{1}{2\pi\sqrt{L_p \frac{C_p}{2}}} \tag{1.1}$$

Subsequent investigation[13] determined the best values for the compensating resistors which gave the closest overvoltage magnitude (2 pu) and rate of rise to that expected for the case of energisation of an open-circuited line. A single-phase compensated π-section is shown in Figure 1.3(a) which

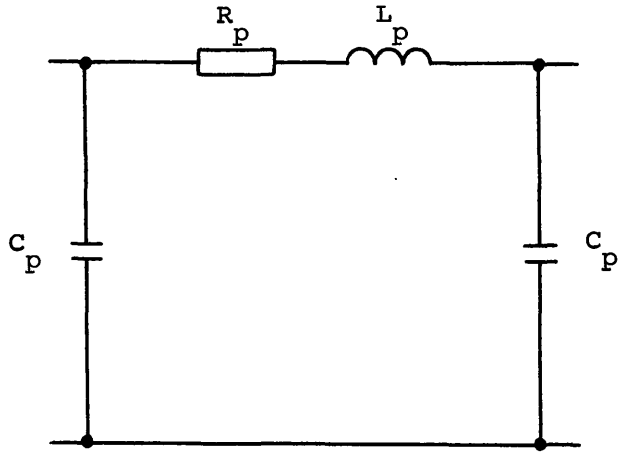

Figure 1.1(a) Single-phase uncompensated model line pi-section

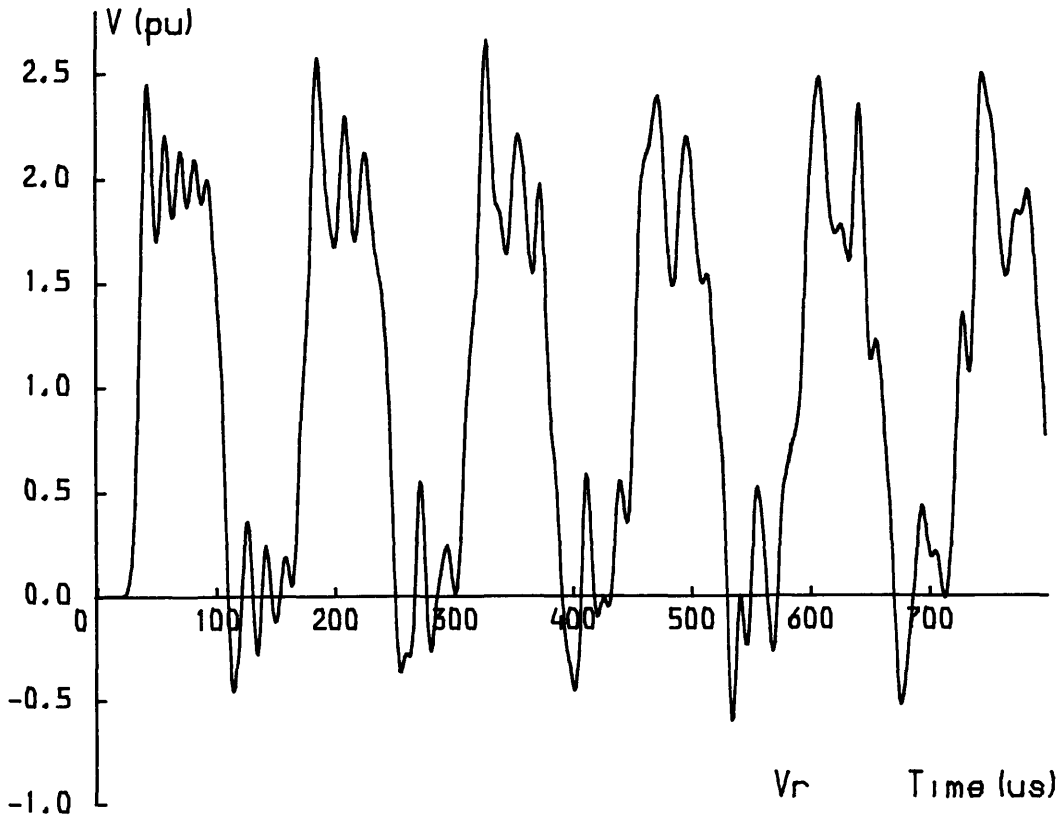

Figure 1.1(b) Receiving-end response of a 50 mile uncompensated line, represented by 10 pi-sections, to 1 pu step excitation.

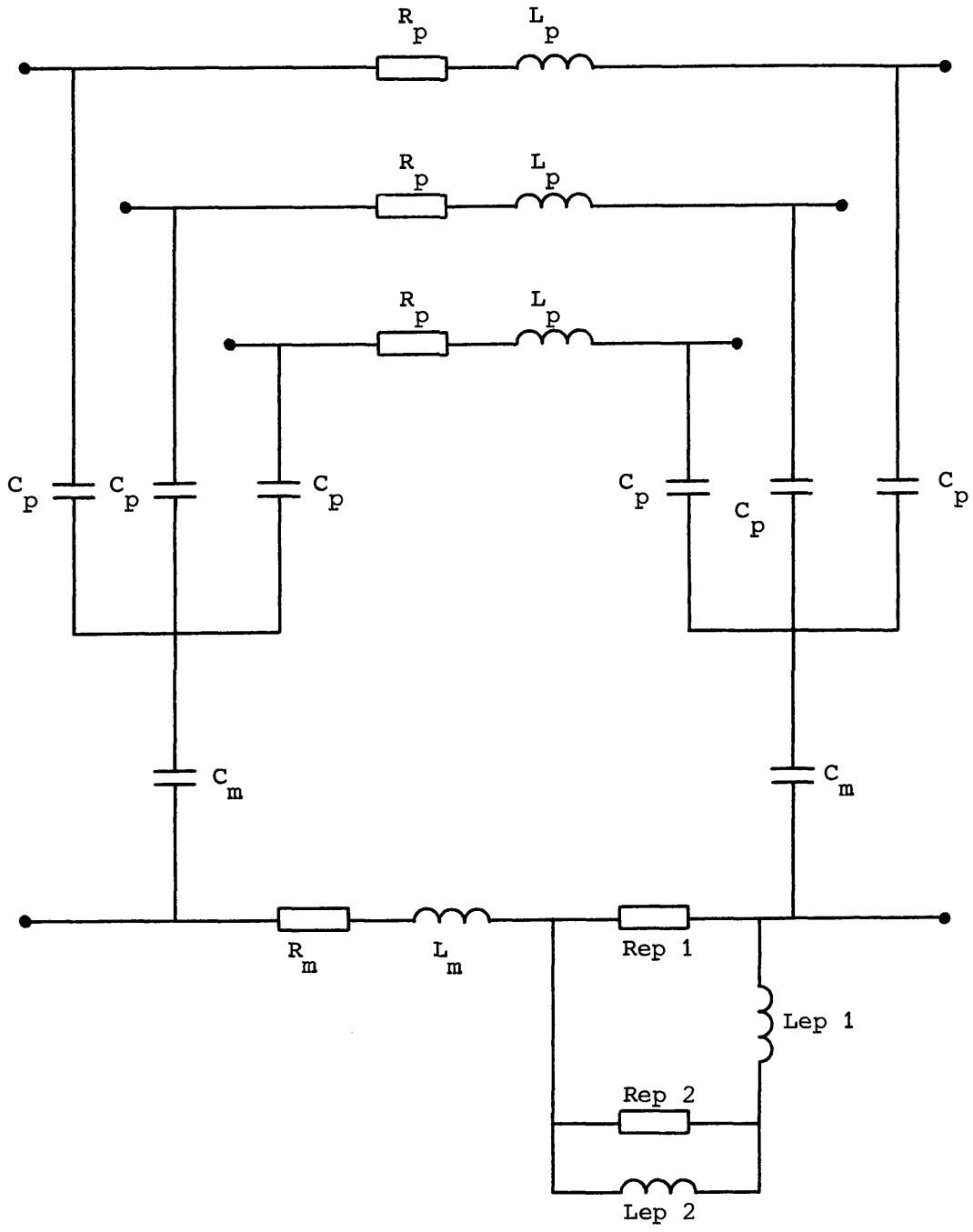

Figure 1.2 Single-pi-section of an uncompensated 3-phase model line.

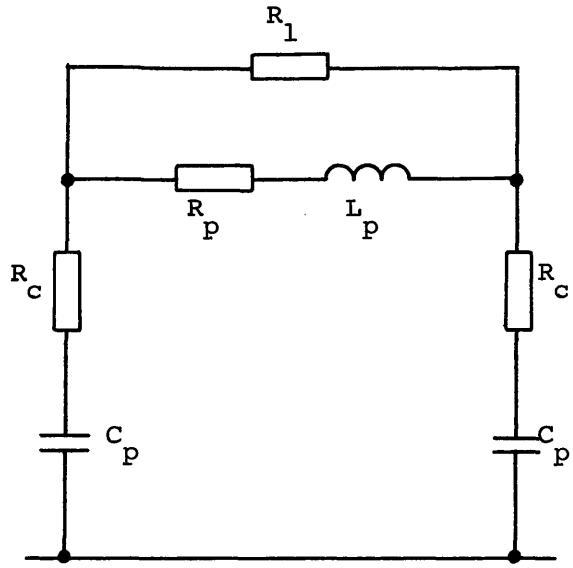

Figure 1.3(a) Single-phase compensated model line pi-section.

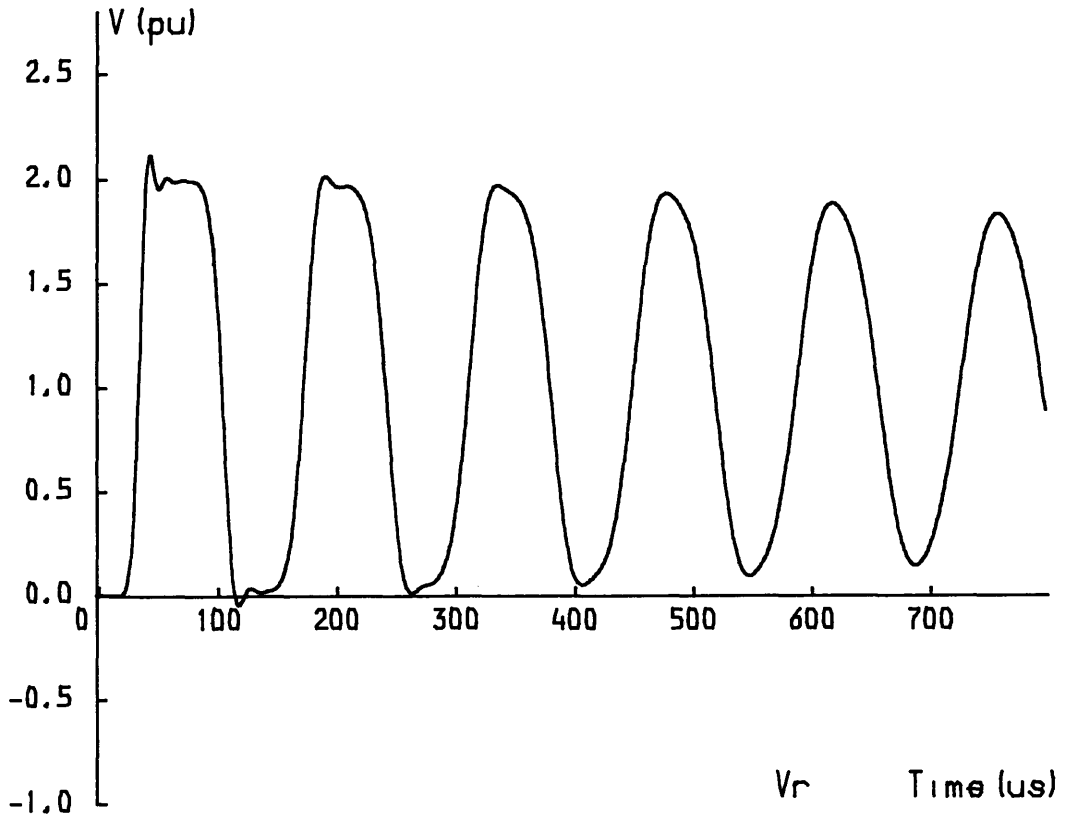

Figure 1.3(b) Receiving-end response of a 1-ph 50 mile compensated line to 1 pu step excitation.

incorporates a resistor in parallel with the line series impedance and a resistor in series in each shunt capacitance branch. Similar connections are made in each phase of the 3-phase model. The response for a 50 mile compensated line, shown in Figure 1.3(b), demonstrates that the oscillations are successfully reduced by the inclusion of the damping resistors in each π-section and gives greater accuracy when the TNA is used for transient overvoltage studies. Indeed this representation is still in use at the present time[14].

Using this model line with a TNA for transient overvoltage studies has a number of advantages and disadvantages. The advantages of the TNA approach are:-

1. The TNA is now a relatively low cost instrument due to the advances made in solid-state electronic technology.

2. It is an ideal teaching device for electrical engineers who are coming into the transient field for the first time. Since there is a direct physical relationship between the model network and the system it represents the corresponding elements of the two networks can be clearly identified.

3. The TNA, being an analogue device, allows system parameters to be varied easily which leads to a better understanding of the system under investigation. Unforeseen problematic conditions can therefore be studied effectively in this manner and the effects of parameter variation monitored. Non-simultaneous closure of the three poles of a circuit breaker and the overvoltages produced by certain closure sequences can also be quickly determined using the double frequency source method. The analyser can therefore produce results much more economically than the digital computer.

4. The analyser is suitable for carrying out a large number of

studies on one particular system. Once a system has been set up on the TNA a lot of information on its transient response can be quickly and easily obtained.

The main disadvantages of this approach are:-

1. Lines are modelled on a symmetrical component basis which assumes that the lines are transposed which is not the case, in this country, for the 275 and 400 kV EHV systems.

2. It is not suitable for carrying out a few studies on a large number of different systems unless the TNA equipment is flexible and the models are available to allow accurate network representation.

3. The work involved in representing a large system on a three-phase basis, especially when earth path effects are taken into account, is prohibitive due to the physical size of such a model.

1.3 The TNA-Microprocessor Hybrid Approach

With the advent of modern digital technology the initial consideration in the TNA field was to merge both the analogue and digital equipment to give a hybrid TNA arrangement. The control of TNA switching e.g. pole closure spread and variation of circuit parameters such as source impedance would be carried out, using interfacing equipment, by decision-making microprocessor software and with peak voltage metering and waveform sampling, overvoltages and rates of rise with their time of occurrence could then be determined[15, 16].

However Crowe[17] suggested that the microprocessor could also be used to improve the accuracy of the transient responses obtained from the uncompensated model line. When resistor-damping is included in the model to reduce the Gibbs Oscillations the resistors attenuate all transient waveform frequencies and not only those associated with the Gibbs phenomena. The

inherent disadvantage of this method is therefore an increase in line attenuation which reduces rates of rise and affects the global response of a compensated model line transient. This can be observed from the actual and model transmission line characteristics.

1.3.1 Actual and Model Transmission Line Parameters

In simulating an overhead transmission line the model line parameters should agree with those of the actual line over a wide frequency range. The parameters of interest are the line surge impedance (symbol Z_0), line attenuation (α) and phase change (β). These were calculated for the three lines, actual, uncompensated and resistor-damped to investigate their variation with frequency.

The design of the model line used in the investigation i.e. Figure 1.2 is based on the twin 0.4 sq. in. 275 kV system of the South of Scotland Electricity Board and was developed at Strathclyde University in 1971 for the investigation of Transient Recovery Voltages. Toland[11] discusses in depth how the analogue model line parameters are derived from those of the actual system. This model line is constructed on the basis of a single π-section representing 5 miles of actual line and has been built in sections representing 25 miles. The phase self surge impedances are 372Ω and the mutual surge impedances are 75Ω i.e. line transposition is assumed. The 1-phase line with zero earth impedance has a surge impedance of 297Ω.

For the actual line the following base values are assumed:-

Base Power = 1000 MVA

Base Voltage = 275 kV

Base Frequency = 50 Hz

The base impedance is given by

$$1 \text{ pu} = \frac{\text{X.MVA}}{\text{kV}^2} = 75.625\ \Omega$$

The model line has the following base values:-

Base Power = 1000 MVA

Base Impedance = 200 Ω

Base Frequency = 398 Hz

This gives the conversion factors between the actual system and the model representation:-

Frequency Scale	$= \frac{f_s}{f_m}$	=>	1/8 : 1
Time Scale	$= \frac{1/f_s}{1/f_m}$	=>	8 : 1
Impedance Scale	$= \frac{Z_s}{Z_m}$	=>	0.38 : 1
Inductance Scale	$= \frac{Z_s/f_s}{Z_m/f_m}$	=>	3 : 1
Capacitance Scale	$= \frac{Z_m f_m}{Z_s f_s}$	=>	21 : 1
Velocity Scale	$= \sqrt{\frac{L_m C_m}{L_s C_s}}$	=>	1/8 : 1

The distance scale is therefore 1 : 1 i.e. 5 miles on the model represents 5 miles of the actual line.

1.3.1.1. Actual Line

The equations relating Z_0, α and β to the positive-sequence resistance R, inductance L and capacitance C of an actual single-phase overhead line, derived in Appendix I.1, are given by

$$Z_0 = \sqrt{\frac{L}{C} - j\frac{R}{\omega C}} \quad \Omega$$

$$\alpha = \frac{R}{2}\sqrt{\frac{C}{L}}\left[1 - \frac{R^2}{8\omega^2 L^2}\right] \quad \text{nepers/mile}$$

$$\beta = \omega\sqrt{LC}\left[1 + \frac{R^2}{8\omega^2 L^2}\right] \quad \text{radians/mile}$$

The variation of these parameters with frequency were calculated for a 5 mile length of line using the resistance values, taking into account conductor skin

effect, given by Toland[11] and are tabulated in Appendix I.2.

1.3.1.2. Uncompensated Model Π-Section

The surge impedance Z_0 of the uncompensated π-section (see Appendix I.3) is given by

$$Z_0 = \sqrt{\frac{\frac{L}{C} - j\frac{R}{\omega C}}{1 - \frac{\omega^2 LC}{4} + j\frac{\omega CR}{4}}} \quad \Omega$$

where R, L and C are the values per π-section i.e per 5 miles where the variation of R with frequency i.e. skin effect, is taken from the values determined experimentally by Toland.

For frequencies where the terms $\frac{\omega^2 LC}{4}$ and $\frac{\omega CR}{4}$ are small Z_0 of the uncompensated model is the same as that of the actual line.

The attenuation and phase change per π-section are given by

$$\alpha = \frac{\omega CR}{2Q}$$

and

$$\beta = \sin^{-1} Q$$

where Q is the imaginary part of

$$(R + j\omega L)/Z_0$$

The results are shown in Appendix I.4.

1.3.1.3. Compensated Model Π-Section

The variation of parameters with frequency for the compensated π-section model were taken from analysis previously carried out by Ovenstone[18] and are listed in Appendix I.5.

1.3.1.4. Analysis of Line Parameter Characteristics

Using the values of Z_0, α and β from the tables in Appendices I.2, I.4 and I.5 the characteristics were plotted to a base of pu frequency

using the base frequency values previously defined. The characteristics of Z_0, α and β are shown in Figures 1.4 - 1.6 respectively.

The surge impedance characteristics of Figure 1.4 show that good agreement between both model line configurations and the actual line is obtained up to 90 pu i.e. 4.5 kHz based on the actual line operating frequency of 50 Hz. Above this frequency the compensated π-section characteristic is closer to the actual line characteristic. The phase characteristics in Figure 1.6 show that both model representations closely follow the linear phase characteristic of the actual line for the greater part of the frequency range with the compensated line phase response again closer to that of the actual case for the highest frequencies calculated.

However the attenuation characteristics of Figure 1.5 clearly display the effect of including the damping resistors in the model line. The compensated π-section displays a far higher attenuation than the actual and uncompensated lines for frequencies above 40 pu while the uncompensated π-section attenuation remains similar to the actual line case for frequencies of up to 120 pu i.e. 6 kHz at the actual operating frequency. This demonstrates the increased attenuation of the compensated model line and explains why the compensated waveform discontinuities and global response are adversely affected. These effects are noticeable in Figure 1.7 when comparing the receiving-end responses obtained from energisation of a 25 mile 5 π-section model line, with and without resistor-damping, from an ideal DC source.

1.4 Microprocessor Reduction of Gibbs Phenomena

To improve these transient waveform features Crowe suggested that the uncompensated line could be used since its attenuation characteristic is closer to that of the actual line. This however implied that the resulting Gibbs phenomena would have to be significantly reduced by other means in order to obtain the overvoltage accuracy given by the compensated line.

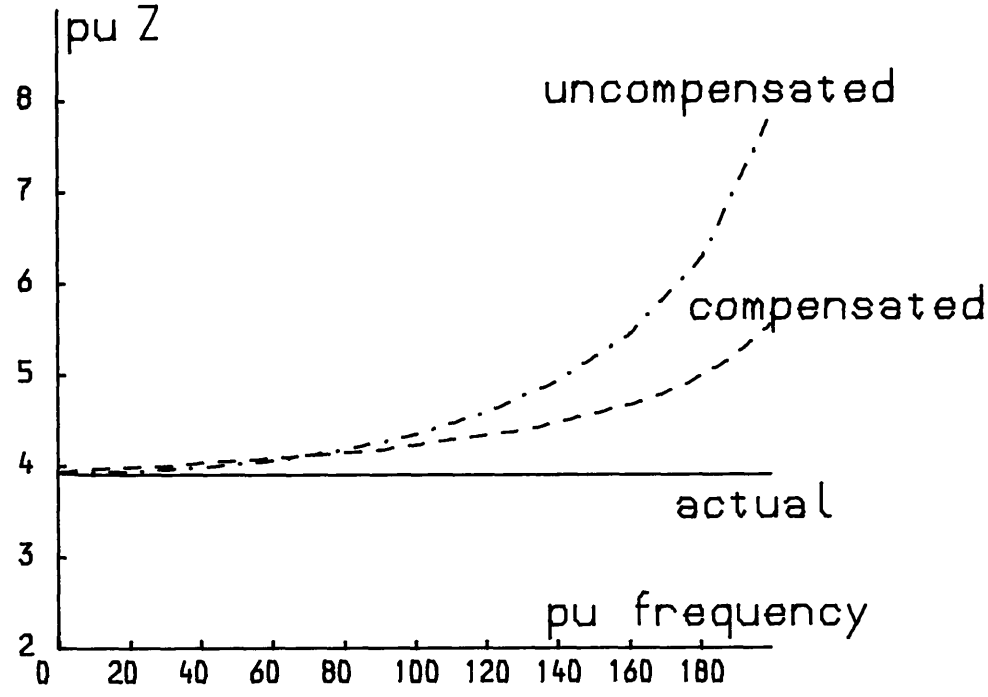

Figure 1.4 Variation of model and actual line surge impedance with frequency.

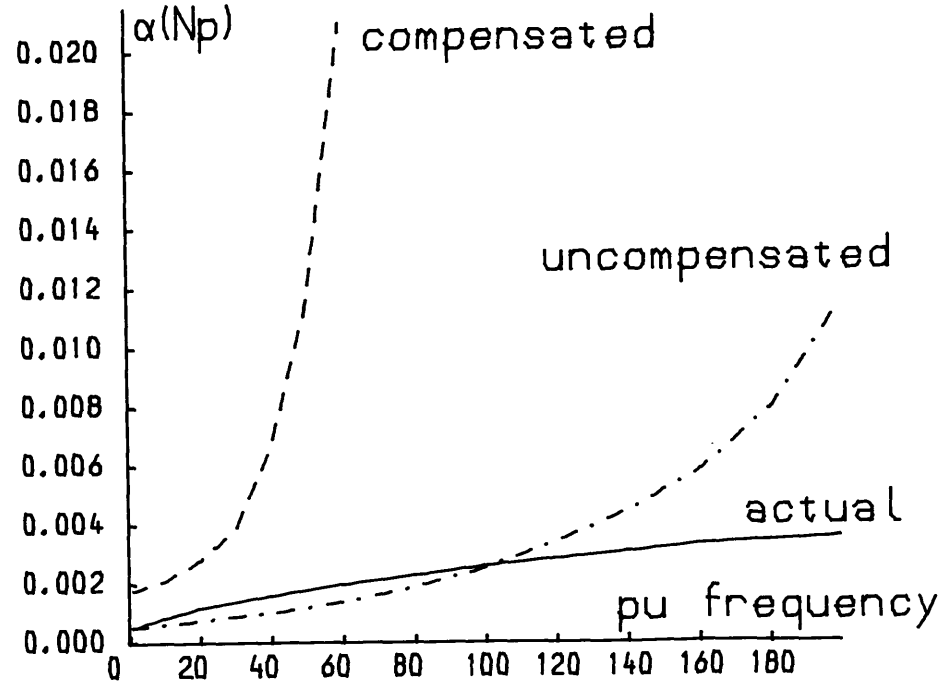

Figure 1.5 Variation of model and actual line attenuation with frequency.

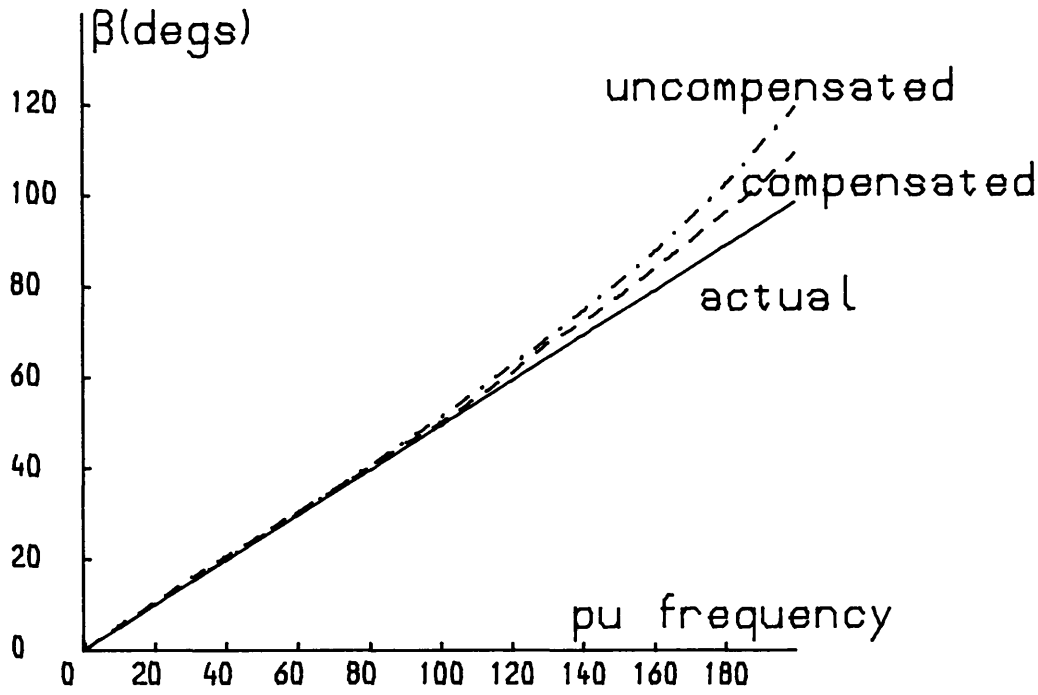

Figure 1.6 Variation of model and actual line phase change with frequency.

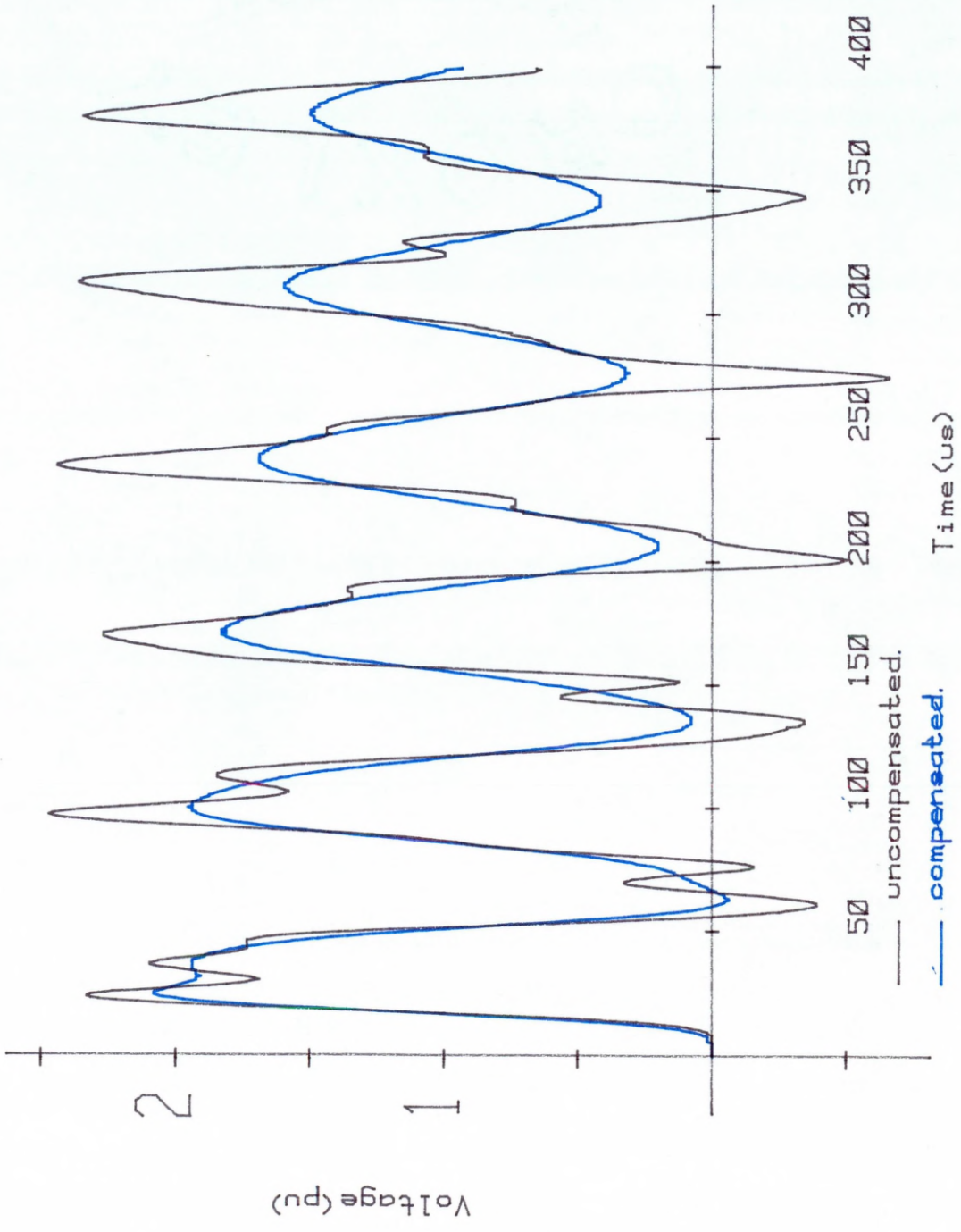

Figure 1.7 Receiving-end responses of a 25 mile, 5 pi-section line, compensated and uncompensated.

1.4.1 Waveform Modification by Local Averaging

In Fourier Analysis Gibbs phenomena also occur when an infinite Fourier series is truncated or the limits of an inverse Fourier Integral are made finite for digital computation. In the latter case this is necessary when no analytical solution of the function can be obtained and integration must be carried out numerically. In this instance Lanczos[8] devised the mathematical Standard Sigma Factor σ_s which employs the idea of locally averaging the function to successfully reduce the oscillatory phenomena (section 1.8.4).

Crowe suggested that this technique could also be applied to digitally sampled uncompensated line waveforms since the Gibbs Oscillations in such a line response are analogous to those in the Fourier case. If the oscillations could be significantly reduced, thereby improving overvoltage accuracy, then the lower attenuation of this model could give improved waveform rates of rise and global response. Since the Gibbs phenomena are basically sinusoidal, and the average of a sine wave over one period is zero, the oscillations could be reduced by locally averaging over a period determined by their frequency. The predominant frequency of the model line Gibbs phenomena can be determined by equation (1.1). Using the model line values of L_p and C_p (section 2.4) f_0 was calculated as 65.18 kHz. However a method of determining the local averaging range from the waveform itself was derived and is discussed in Chapter 4. In the experimental technique the microprocessor software performs local averaging and has the same effect as the use of the Sigma Factor in the Fourier Integral. The term Experimental Sigma Factor is therefore used to describe in an analogous manner the effect of microprocessor local averaging.

The locally averaged waveform is defined as the 'processed' or 'processor' response since it is calculated by microprocessor software from the sampled uncompensated line transient.

1.5 Objective of Research

The objective of the research work was therefore to record sampled uncompensated model line transient waveforms with the intention of significantly reducing their Gibbs content by the method of local averaging. The technique would have to give accurate system overvoltages and to determine if improvements in processor waveform rates of rise and global response could be achieved each processor response would have to be compared directly with the equivalent compensated line waveform. Model lines with and without resistor-damping would be required for immediate waveform comparison.

The receiving-end response of an actual open-circuited line from an ideal DC source is well documented which would allow comparison of the processor and resistor-compensated waveforms with the distributed-parameter case. Therefore the simplest equivalent model line configuration was chosen as the starting point for the investigation of the local averaging technique. 1-phase model lines with zero earth impedance were therefore required.

The equipment necessary for such a study is now discussed.

1.6 Equipment Requirements and Availability

The investigation for microprocessor modification of uncompensated line transient waveforms would require:-

1. The recording of model line receiving-end waveforms. For microprocessor modification using local averaging these would have to be sampled by a device capable of recording fast transient waveforms such as a Transient Recorder.

2. A microprocessor so that the uncompensated waveforms could be modified by the appropriate software.

3. A visual display with colour would be required for comparison of uncompensated, processed and resistor-damped waveforms so that

the effectiveness of the averaging technique could be immediately determined. The display should be an integral part of the processor system.

4. A means of obtaining hard copies of waveforms for discussion and analysis i.e. a plotter under processor control.

The electrical department already had a 3-phase compensated model line with frequency-dependent earth path based on the Strathclyde design and a TNA and Transient Recorder were also available having been used in overvoltage studies previously[18, 19]. Hard copies of model line waveforms could also be obtained by linking one of the digital plotters available to the microprocessor system. This left the choice of a microprocessor system to be decided upon in order to fulfil the basic equipment requirements.

The required system block diagram is shown in Figure 1.8.

1.7 Developments from the Initial Research Objective

Although the local averaging technique forms the basis of Chapter 4, the knowledge gained from this initial study led to the development of other averaging techniques (also Chapter 4), the investigation of the effects of inductive source energisation (Chapter 5) and the analysis of the frequency content of the model line waveforms using spectral analysis techniques (Chapter 6).

1.7.1 The Experimental Modified Sigma Factor S_{me}

Day et al[3] devised the Modified Sigma Factor σ_m (section 1.8.4) which, using an arbitrary period of averaging, improved the rates of rise of the waveform discontinuities with respect to those calculated by the Standard Sigma Factor in the Fourier Analysis. The arbitrary range which achieved this operated over a shorter time period than that implemented by σ_s and the analogy with the local averaging of waveform samples was also

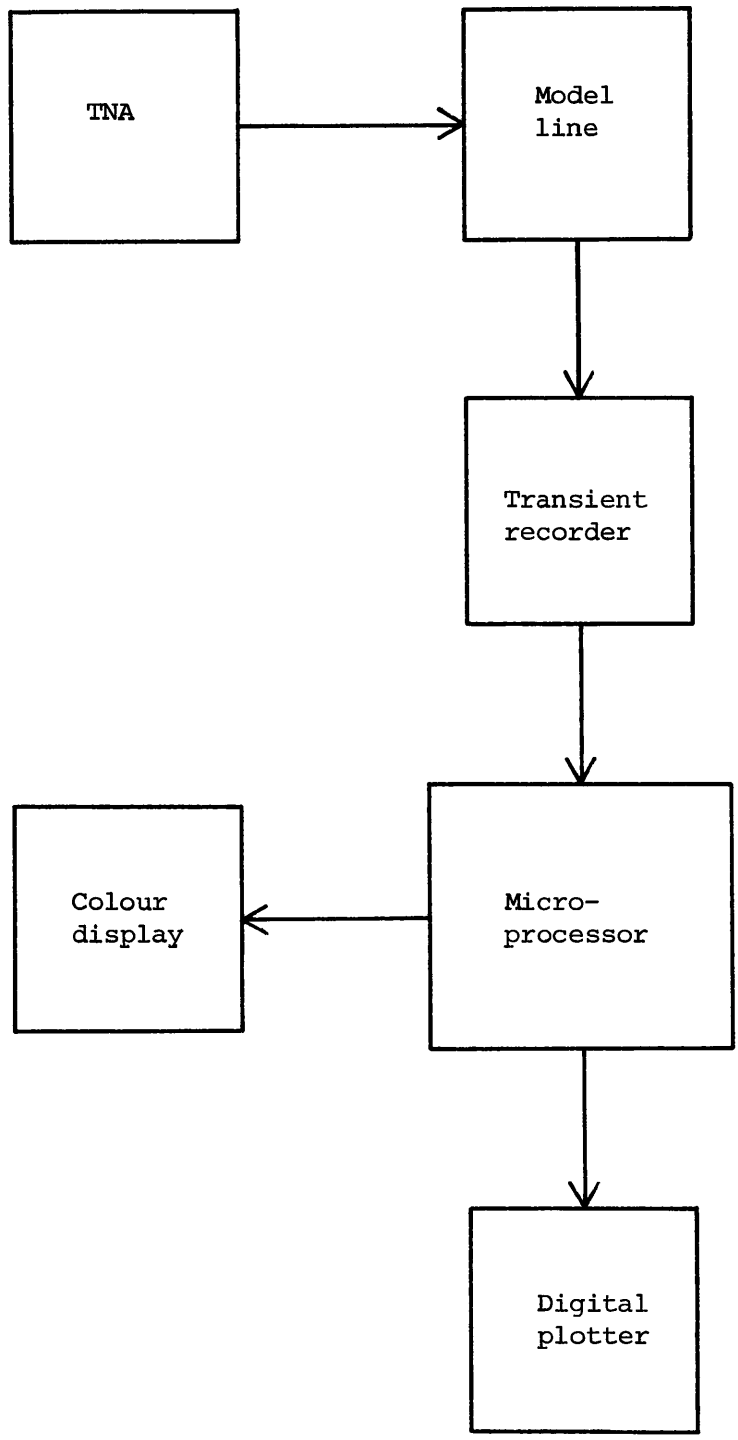

Figure 1.8 Required system block diagram.

investigated. The Experimental Modified Sigma Factor S_{me} was therefore derived. Day also stated that the two averaging techniques could be applied at the relevant parts of a transient response i.e. σ_s being implemented for regions of Gibbs Oscillations and σ_m at waveform discontinuities. Due to the decision-making capability of the microprocessor software this more complex process could be implemented (section 4.7).

1.7.1.1. Energisation from an Inductive Source

The Gibbs phenomena arise due to attenuation of the high-frequency content of the step input which results from ideal DC or AC source energisation. An actual generator can be simply approximated however by introducing inductance in the model source representation. The effects of this parameter on transient waveshape and overvoltage has been the subject of detailed investigation by Bickford[4, 20, 21] but in uncompensated model line energisation the effect of this parameter in modifying the sending-end voltage becomes significant.

The sending-end voltage now rises exponentially with a time constant dependent on the source inductance and line surge impedance such that the high-frequency content of the line input disturbance is reduced. A value of source inductance will be encountered such that the frequency content of the input will lie below that of the cut-off frequency of the model line. Therefore no Gibbs phenomena should be apparent in the receiving-end response which implies that no averaging would be required (see Chapter 5). Simultaneous closure of the 3-phase model line was also included as it represented a step towards the more realistic situation of non-simultaneous circuit breaker pole closure when energising a 3-phase line.

1.7.1.2. Spectral Analysis of Uncompensated Line Transients

From the results of ideal source energisation, with specific reference to the waveforms obtained from the longer uncompensated 1-phase lines investigated (section 4.4.1.1), spectral analysis of the uncompensated line

transient waveforms was undertaken. It was envisaged that, with a clearer understanding of the Gibbs phenomena generated in the line, improved local averaging techniques could be devised or that Digital Filtering could be employed to reduce the Gibbs phenomena. Spectral analysis was achieved by applying the Discrete Fourier Transform or DFT to the transient waveforms and is discussed in Chapter 6.

1.8 Digital Techniques in Overvoltage Studies

Before proceeding with a description of the equipment required for the research (Chapter 2) a discussion of the Digital Techniques available to engineers for the analysis of EHV system transients must be given. As the investigation developed some of the Digital Methods available were implemented as a means of comparison with the results obtained from the model line responses.

The existing techniques available for the calculation of voltage and current in a power system using Digital Software Techniques can be listed as follows:-

1. Lumped Parameter Method
2. Lattice-Diagram Method
3. Schnyder-Bergeron Method
4. Fourier Transform Method
5. Laplace Transform Method

1.8.1 Lumped Parameter Method

In this method the differential equations of the system are solved using a numerical integration technique such as the fourth-order Runge-Kutta algorithm. System representation is the same as that used on a TNA i.e. a distributed parameter line is represented by a number of cascaded π-sections. Using this representation solutions to single and 3-phase problems can be obtained. Line energisation studies are carried out by applying a voltage

across the breaker contacts while transient recovery voltages can be calculated by injecting a current at the circuit breaker terminals[22].

The use of the Runge-Kutta technique in solving compensated and uncompensated model line transients forms the basis of Chapter 7 where a full discussion of the method is given. The programs developed were used to verify the responses obtained from the two model line representations.

1.8.2 Lattice Method

For a distortionless line i.e. one in which the voltages and currents are subjected to the same attenuation, the voltage and current at any point in the line can be expressed, from equations (8.7) and (8.8), as

$$V = e^{-\alpha t} [f_1(x - ut) + f_2(x + ut)] \tag{1.2}$$

$$I = e^{-\alpha t} [f_1(x - ut) - f_2(x + ut)]/Z_0 \tag{1.3}$$

where Z_0 is the surge impedance of the line.

Thus the general solutions consist of combinations of forward and backward travelling waves each with a propagation velocity of u m/s.

If the line is lossless then the waves are propagated without attenuation and this assumption forms the basis of the Lattice Method. With $\alpha = 0$

$$V = f_1(x - ut) + f_2(x + ut) \tag{1.4}$$

$$I = [f_1(x - ut) - f_2(x + ut)]/Z_0 \tag{1.5}$$

The function $f_1(x - ut)$ represents the wave which is travelling in the forward or positive x-direction while the function $f_2(x + ut)$ represents the wave travelling in the backward or negative x-direction. The relationship between voltage and current in the forward direction is $V/I = Z_0$ and that between voltage and current in the reverse direction is $V/I = -Z_0$.

Consider two lines of surge impedance Z_0 and R_e which meet at a

junction. If an incident voltage and current, V_i and I_i, are travelling towards the junction on the line of surge impedance Z_0, the equations relating these quantities with the reflected voltage and current (V_r and I_r) and transmitted voltage and current (V_t and I_t) are given by:-

$$\frac{V_i}{I_i} = Z_0 \qquad \frac{V_r}{I_r} = -Z_0 \qquad \frac{V_t}{I_t} = R_e$$

and

$$V_t = V_r + V_i \qquad I_t = I_r + I_i$$

from which

$$V_t = \frac{2R_e}{R_e + Z_o} * V_i = K_t V_i$$

where K_t is termed the transmission coefficient and

$$V_r = \frac{R_e - Z_o}{R_e + Z_o} * V_i = K_r V_i$$

where K_r is termed the reflection coefficient. These coefficients are related by the equation

$$K_r = (K_t - 1) \tag{1.6}$$

If K_t and K_r are known the transmitted and reflected voltages can then be determined from the incident voltage. The voltage at a point on the line can be determined graphically using the lattice diagram developed by Bewley[23]. While adequate for simple 1-phase problems, extended 1-phase and 3-phase systems have been investigated using the 'branch timetable' technique devised by Bickford and Doepel[4] which is non-graphical and therefore suitable for digital computation.

This technique represents lines and cables by their surge impedances and propagation times. The coefficient K_t at each busbar is calculated for each line connected to that busbar and using equation (1.6) K_r for each case can be calculated. Thus all reflected and transmitted voltage surges can be determined. The technique requires the choice of a 'basic time

interval' θ such that it is a fraction e.g. a half of the propagation time of the shortest line in the system. All line propagation times are then re-defined as multiples of θ. For convenience the propagation velocity used is the speed of light which necessitates that lines and cables with lower propagation velocities are increased in length to compensate. The voltage at any point in the system at a time 't' can be obtained by summing all the voltage waves that have arrived at the point up to that time. The calculation is performed in the time domain and in terms of voltage alone.

Lumped reactive elements can also be represented by approximating them as short transmission line stubs[24]. The stub has a surge impedance Z_0 and a travel time τ given by

$$Z_0 = \sqrt{L/C} \tag{1.7}$$

$$\tau = \sqrt{LC} \tag{1.8}$$

where L and C represent the stub line inductance and capacitance.

An inductor is represented by the inductance of the stub line which is short-circuited at the remote end. Substituting equation (1.8) into equation (1.7) gives the surge impedance of the stub

$$Z_0 = L/\tau$$

and the capacitance of the line

$$C = \tau/Z_0$$

For accurate representation C and hence τ must be small.

In a similar manner the capacitance of the stub line can represent a capacitor where

$$Z_0 = \tau/C$$

and the inductance is given by

$$L = \tau Z_0$$

As before L and hence τ must be small for accurate representation of the reactive component. Therefore in both cases the value of τ must be small and it becomes the basic time interval. The surge impedances of inductive and capacitive stubs should be, respectively, greater than ten times and less than one tenth the combined equivalent surge impedance of all other circuits connected to the same busbar[4].

Non-linear elements can be represented and attenuation and distortion included in the single-phase line transient calculation. In the latter case the Lattice and Fourier Transform Methods are combined to take account of line losses. The step response of the line is calculated once using the Fourier Transform and each voltage step applied in the Lattice calculation is modified according to this response. Subsequent reflections however are treated as travelling on a lossless line.

For 3-phase calculations the individual surge impedances are replaced by surge impedance matrices which include the mutual effects between phases. Due to mutual coupling, voltage changes in one phase are functions of the voltages in the other phases and losses cannot be represented by attenuating and distorting the voltages in each phase. However Wedepohl[25] shows that all voltages in the phase domain can be transformed into a modal domain in which modal voltages are free from mutual effects and where each modal component has its own velocity of propagation and attenuation. Losses may therefore be applied to each mode as in the 1-phase conductor case. The step response for each modal line is calculated using the Fourier Transform Method and each modal voltage step is modified accordingly and then transmitted to the remote end of the line where they are transformed back into the phase domain. The phase surge impedance matrix calculated at the predominant frequency of the transient is used to determine the values of K_t and K_r at each termination and junction and all

reflected and transmitted voltage surges are therefore calculated in the phase domain.

1.8.3 The Schnyder-Bergeron Method

This technique also applies to lossless lines with equations (1.4) and (1.5) being rearranged as

$$V + Z_0 I = 2f_1(x - ut)$$
$$V - Z_0 I = 2f_2(x + ut)$$

The interpretation of these equations is that if an imaginary observer were to travel along a line in the direction of x increasing with the same velocity u as the wave such that (x - ut) is constant then $(V + Z_0 I)$ is constant for every point visited. Similarly an observer travelling in the opposite direction with the same velocity will see $(V - Z_0 I)$ constant at every point. Furthermore the two observers at the same point at the same moment in time must see the same voltage and current.

Consider the transmission line AC with B as its midpoint in Figure 1.9(a). At time t_1 assume that known forward waves start from A and known backward waves start from C. At A, at $t=t_1$ the current and voltage lie on the line

$$V + Z_0 I = 2f_1(-ut_1) = \text{constant}$$

At B, at $t=t_2$ where $t_2=t_1 + l/u$, the current and voltage will lie on the same line i.e.

$$V + Z_0 I = 2f_1(l - ut_1 - l)$$
$$= 2f_1(-ut_1)$$

Similarly at C, at $t=t_1$, current and voltage lie on the line

$$V - Z_0 I = 2f_2(l + ut_1) = \text{constant} \qquad (1.9)$$

At B, at $t=t_3$ where $t_3=t_2$ then

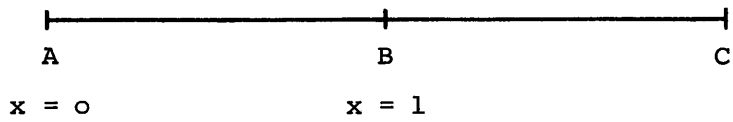

(a)

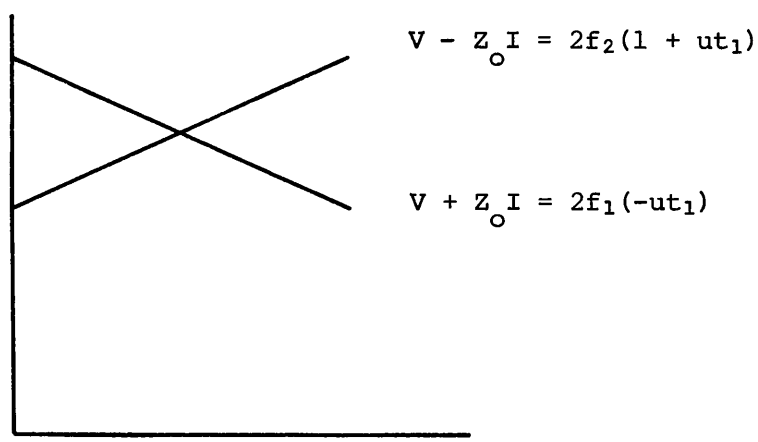

(b)

Figure 1.9 (a) 2 equal sections of single-phase line

(b) voltage-current characteristics.

$$V - Z_0 I = 2f_2(0 + ut_1 + l)$$
$$= 2f_2(l + ut_1)$$

and the current and voltage again lie on the line given in equation (1.9). Consequently the intersection of these two lines on the voltage-current characteristic give the voltage and current at B at time t_2 (see Figure 1.9(b)).

This is the basis on which the graphical method for solving transient problems involving transmission lines was developed by Bergeron.

In applying this technique all transmission lines must be divided into sections with the same travel time. Lumped inductive and capacitive elements are considered as transmission line stubs as in the Lattice Method and for a multiconductor system the phase components are transformed into independent modes of propagation where each component is dealt with on a 1-phase basis. The solution does not take account of the frequency dependent nature of line parameters and as an approximation the line parameters are calculated at the dominant frequency of the transient as in the Lattice Technique[6].

1.8.4 The Fourier Transform Method

A function with period T can be expressed in the complex exponential Fourier Series form

$$f(t) = \sum_{k=-\infty}^{\infty} C_n \, e^{jk\omega t} \tag{1.10}$$

where

$$C_n = \frac{1}{T} \int_{-T/2}^{T/2} f(t) \, e^{-jn\omega t} \, dt \tag{1.11}$$

and

$$\omega = \frac{2\pi}{T}$$

However by allowing T to become infinite the expression

$$f(t) = \frac{1}{2\pi} \int_{-\infty}^{\infty} F(\omega)\ e^{j\omega t}\ d\omega \qquad (1.12)$$

is obtained[26] where

$$F(\omega) = \int_{-\infty}^{\infty} f(t)\ e^{-j\omega t}\ dt \qquad (1.13)$$

Equations (1.12) and (1.13) form the Fourier Transform pair. Therefore the transient response f(t) of a system can be determined from a knowledge of its frequency response $F(\omega)$.

The frequency response of a transmission line is given by

$$F(\omega) = e^{-\gamma(\omega)x}$$

where $\gamma(\omega) = \sqrt{Z(\omega).Y(\omega)}$. $Z(\omega)$ and $Y(\omega)$ are the series impedance and shunt admittance respectively of the line. The propagation constant $\gamma(\omega)$ can be evaluated at various frequencies[27, 28].

The response of the line to a unit step voltage is given by

$$F(\omega) = e^{-\gamma(\omega)x}/j\omega$$

The transient response of the line is found by applying the inverse Fourier Transform of equation (1.12). To evaluate an inverse transform of the form of equation (1.12) which has no analytic solution requires the use of a digital computer to perform the numerical integration and therefore the range of integration must be made finite i.e.

$$f_{\Omega}(t) = \frac{1}{2\pi} \int_{-\Omega}^{\Omega} F(\omega)\ e^{j\omega t}\ d\omega \qquad (1.14)$$

and as in the case of a finite Fourier series the truncation of the frequency range gives rise to Gibbs phenomena. However by averaging the function locally over the range $\pm\frac{\pi}{\Omega}$ from t

$$f_\sigma(t) = \frac{\Omega}{2\pi} \int_{t-\frac{\pi}{\Omega}}^{t+\frac{\pi}{\Omega}} f_\Omega(\tau)\, d\tau$$

$$f_\sigma(t) = \frac{1}{2\pi} \int_{-\Omega}^{\Omega} \sigma_s\, F(\omega)\, e^{j\omega t}\, d\omega \qquad (1.15)$$

the oscillations are significantly reduced. σ_s is the Standard Sigma Factor for integrals and is given by

$$\sigma_s = \frac{\sin \pi\omega/\Omega}{\pi\omega/\Omega} \qquad (1.16)$$

The Modified Sigma Factor σ_m can be used to improve the rates of rise of the response by averaging arbitrarily around t by $\pm m^3$. Substituting $\pm m$ for $\pm\frac{\pi}{\Omega}$ in $f_\sigma(t)$ gives

$$\sigma_m = \frac{\sin \omega m}{\omega m} \qquad (1.17)$$

In evaluating the response of a system by equation (1.12), the poles of the frequency response of the system, $F(\omega)$, may and in some cases do lie close to the line of integration i.e. the real axis. This causes the integrand to peak over a series of small intervals lying in the neighbourhood of the poles and hence for accurate integration it is necessary to take very short step lengths.

This can be overcome by using the Modified Fourier Transform. For a function $f(t) = 0$ for $t < 0$, $f(t)$ is multiplied by e^{-at} where $a > 0$ giving

$$F(a+j\omega) = \int_0^{\infty} f(t)\ e^{-(a+j\omega)t}\ dt \qquad (1.18)$$

and the inverse transform is defined

$$f(t) = \frac{1}{2\pi} \int_{-\infty}^{\infty} F(a+j\omega)\ e^{(a+j\omega)t}\ d\omega \quad \text{for } t > 0$$

$$0 = \frac{1}{2\pi} \int_{-\infty}^{\infty} F(a+j\omega)\ e^{(a+j\omega)t}\ d\omega \quad \text{for } t < 0$$

This process has the effect of moving the poles away from the real axis by a distance 'a' which can be arbitrarily chosen but it has been shown[29] that the best results are obtained for the particular case of the open-circuited transmission line with $a = 10^4$.

The inverse transform for numerical computation is given by

$$f(t) = \frac{e^{at}}{2\pi} \int_{-\Omega}^{\Omega} F(a+j\omega)\ e^{j\omega t}\ d\omega \qquad (1.19)$$

The receiving-end response of an open-circuited 1-phase line to step energisation, using (1.19) and incorporating σ_s, is shown in Figure 4.1(b).

The Fourier Transform technique is applied to the solution of transient problems in both 1-phase and 3-phase systems[30, 28, 31]. By making the substitution $s = (a + j\omega)$ the Modified Fourier Transform converts to the Laplace Transform.

1.8.5 The Laplace Transform Method

The Laplace Transform is an integral transformation of a function of a real variable t to a function of a complex variable s. Application of the

transformation reduces a partial differential to an ordinary differential equation and reduces an ordinary differential equation in the variable t to linear algebraic equation in the variable s. If f(t) is a function which is defined for all $t \geq 0$ the Laplace Transform of f(t), denoted by F(s), is given by

$$F(s) = \int_0^\infty f(t)\ e^{-st}\ dt$$

The Laplace Transform of the differential operator $\frac{df(t)}{dt}$ is

$$\mathcal{L}\{\frac{d}{dt}\} = s\ F(s) - f(0)$$

In line energisation studies f(0) is very often zero.

The partial differential equations of a single-phase transmission line, given by equations (8.3) and (8.4), are

$$\frac{\delta^2 V}{\delta x^2} = \gamma^2 V$$

and

$$\frac{\delta^2 I}{\delta x^2} = \gamma^2 I$$

On applying the Laplace Transform

$$\frac{dV(x,s)}{dx} + (sL + R)\ I(x,s) = 0 \qquad (1.20)$$

and

$$\frac{dI(x,s)}{dx} + sC\ V(x,s) = 0 \qquad (1.21)$$

The general solutions of (1.20) and (1.21) are

$$V(x,s) = A(s)\ e^{-\gamma(s)x} + B(s)\ e^{\gamma(s)x} \qquad (1.22)$$

and

$$I(x,s) = \frac{1}{Z_0(s)}\ [A(s)\ e^{-\gamma(s)x} - B(s)\ e^{\gamma(s)x}] \qquad (1.23)$$

where

$$\gamma^2 = sC(sL + R) \tag{1.24}$$

and

$$Z_0(s) = \sqrt{\frac{sL + R}{sC}} \tag{1.25}$$

A(s) and B(s) can be determined from the boundary conditions.

By using the Heaviside Shifting Theorem and taking the inverse Laplace Transform of (1.22) and (1.23), equations (1.2) and (1.3) are obtained i.e.

$$V = e^{-\alpha t} [f_1(x - ut) + f_2(x + ut)]$$

$$I = e^{-\alpha t} [f_1(x - ut) - f_2(x + ut)]/Z_0$$

When dealing with a 3-phase system the transmission line is assumed to be transposed and the line parameters are calculated at the transient frequency. Due to the mutual coupling between phases the application of the Laplace Transform to the phase voltages gives three interdependent second order differential equations. These equations are separated, using matrix algebra, by transforming the voltages into independent modes which have no mutual coupling and therefore the modal voltages travel on the line without interaction. Two of the modes (positive and negative sequence) travel close to the speed of light with low attenuation while the third mode (zero sequence) travels at about 75% of the speed of light with high attenuation. For each mode, the applied waveform is attenuated and delayed when it appears at the far end of the line. The phase voltage waves, however, are distorted due to the different modal attenuation and speed of propagation. The phase voltages are found by the addition of the forward and reverse modal waves and then applying the inverse modal transformation[32, 33].

1.9 Comparison of Analogue and Digital Methods

Results from line energisation studies calculated using the aforementioned Digital Techniques and from TNA studies are given in references[16, 2]. These are compared with actual system test results and good agreement between responses are obtained. In most cases differences which occur are in the high-frequency content of the transient response. It can therefore be stated that the analogue and digital methods are capable of giving adequate results.

The Lattice, Schnyder-Bergeron and Laplace Transform Methods are all solutions of the transmission line wave equations and should give equivalent results. The Schnyder-Bergeron method is preferred when the voltages and currents at many points in a system are required while the Lattice method is more suitable for the calculation of voltage at a few points in the system. The Lattice Method is more accurate since the frequency dependence of line losses is taken into account using Fourier methods. In each method the frequency dependence of line parameters is ignored and as an approximation the values of line parameters used are calculated at the transient frequency or if this is not known at a frequency based on the transit time of the line being switched. Methods have been recently developed, however, that incorporate continuous line parameter frequency-dependence[6]. These methods are not used in the instance where all system parameters are highly frequency dependent i.e. transient induction in a pilot cable close to a power cable in which there is dielectric failure. In this case the Fourier Transform must be used.

The Fourier Transform can take into account the frequency dependence of system parameters and is capable of giving the highest accuracy of all the methods of calculation. However this accuracy is only achieved at the high cost of computation and since the frequency response of all system parameters over the transient spectrum may not be readily

available the use of this method cannot always be justified. One use of this method is the investigation of validity in the assumptions made in the other techniques.

In conclusion, there is no one particular method which can be considered as the best one to use in all circumstances. Each method has its own advantages and disadvantages and the choice of technique depends on the particular problem to be solved and the degree of accuracy required.

CHAPTER 2

Transient Analysis System Hardware

2.1 Choice of a Microprocessor System

As discussed in section 1.6 the availability of equipment left the task of choosing a suitable microprocessor system for the experimental work to be undertaken. In order to compare model line and processor waveforms, good graphics and input/output facilities would be of the highest priority in the system chosen with the need for fast computing and data storage in a lower category. The input/output facilities would have to transfer data from the Transient Recorder (TR) to the processor and from there to the plotter. With these criteria in mind various 8-bit microprocessor systems were investigated, the three most readily available now being discussed.

1. After studying the HP-85 system it became apparent that it would be unsatisfactory due to the lack of input/output facilities and the small (6") monochromatic monitor used for display. Differentiation between waveforms was extremely difficult when a test program was executed and this indicated that a larger monitor with colour facilities would be needed. The storage of waveform data to cassette tape, the only storage medium available, was very slow and the required use of the BASIC language would further slow down program execution.

2. The APPLE 2 mini-computer is a 6502 CPU-based system. BASIC is also the main programming language but PASCAL could also be used and this had the added advantage of being linkable to a relocatable assembler package which would be used for managing input/output routines for data transfer to and from the microprocessor system. However, the colour graphics did not have satisfactory resolution (280x192 pixels) as test programs showed and the disc storage was limited to 143K.

3. Investigation of a Cromemco Z-2D system with colour graphics used in another department of the College indicated that this system would

satisfy the criteria defined for transient waveform analysis for the following reasons:-

- It is constructed around the Z-80 CPU which is one of the most powerful 8-bit processor available.
- It has a relocatable assembler package which can be linked to FORTRAN or BASIC. FORTRAN was selected because of its faster execution times than BASIC.
- A working area of ~46K RAM, expandable up to 512K, is available.
- Disc storage of 386K from each of the 2 disc drives used is provided.
- Good colour graphics with resolution of 754x482 pixels.
- The 21-card mother board allowed S-100 bus system cards to be inserted into the system for specific user-system design i.e input/output cards and system expansion.
- Experience had been gained by other users within the College which would prove helpful in the initial stages of system-user contact.
- The software packages that would be needed were already available within the College.

Therefore for an operational system the Z-2D standard system would be needed with additional graphics and I/O cards included. When funds became available from the Scottish Education Department the Z-2D system was purchased (March 1982).

2.2 The Development System

The hardware used for the initial development system is as follows:-

1. Cromemco Z-2D standard system plus 8PIO, TUART, SDI and

48KTP memory cards.

2. 5 π-section 1-phase model line with zero earth path impedance.
3. A College-built 20 π-section, 3-phase model line with frequency dependent earth-return path based on the original design by Strathclyde University.
4. Reyrolle Transient Network Analyser.
5. Datalab DL920 Transient Recorder plus DL019 Line Disturbance Monitor.
6. Hewlett-Packard 7225A Digital Plotter.
7. Microvitec RGB Colour Monitor.
8. Dacoll Monitor.

2.3 Cromemco Z-2D Standard System

The Z-2D microcomputer provides the processing power for waveform display and modification and for input/output to and from the aforementioned devices. With the addition of other Cromemco cards to the standard system the requirements of the project would be satisfied. The Z-2D required only a terminal (Dacoll VDU) to become operational. It is a self-contained unit housed in a cage with 21 slots to allow for expansion or specific system design through the S-100 bus.

The Z-2D comes as a complete package which consists of four main modules:-

1. Z-80 Central Processing Unit (CPU).
2. 64K Dynamic Random Access Memory (RAM).
3. Floppy Disc Controller with Twin Floppy Disc Drives.
4. 21-Slot S-100 Card Cage and Power Supply.

The software packages that were used consisted primarily of a FORTRAN-77 compiler and a Z-80 Macro Assembler. Other software facilities

included a Text Editor, an SDI graphics package and a Debug routine which proved invaluable in eliminating errors in the input/output and graphics routines written.

The following boards were required to enhance the standard system in order to meet the experimental requirements of the development system.

2.3.1 The 8PIO Board

The 8PIO is used to transfer waveform data from the Transient Recorder memory to the microprocessor memory by means of a software-controlled parallel data transfer.

This board has eight independent parallel input/output ports, each consisting of a separate input port and a separate output port with the same address. Three ports were used (section 3.4) by the software with the remaining five reserved for system expansion.

2.3.2 TUART Board

The TUART board was required for the serial data transfer between the Z-2D and the Hewlett-Packard digital plotter.

The Cromemco TUART (Twin Asynchronous Receiver and Transmitter) provides two channels of duplex serial data and two channels of parallel data exchange. Two TMS 5501 chips, known as Device 'A' and Device 'B', each drive one serial and one parallel port. The TUART has twenty-eight registers each of which is viewed by the system CPU as an I/O port. However for transfer of data with handshaking to the Hewlett-Packard plotter, only four registers are necessary for communication over the RS-232 interface, with only three pin connections (Transmit, Receive and Ground) required for operation. The four registers are:-

- The IN status register which is read into the accumulator to check the transmit and receive buffers.

- The OUT Baud register which is loaded from the CPU to set the baud rate and required stop bits, which for the plotter is 2400 Baud and 1 stop bit.
- The IN receiver data register which is read by the CPU to obtain the assembled byte of data from the serial receiver and used for software handshaking with the plotter.
- The OUT transmitter data register which is loaded from the CPU with a data byte for serial transmission to the plotter.

2.3.3 SDI Graphics Board

The SDI consists of two boards which plug directly into the S-100 bus. These boards act as an interface between the computer and the RGB Colour Monitor. Board 1, the Direct Memory Access board takes picture information from the computer memory and Board 2 converts this information to analogue outputs for an RGB video signal.

Normal resolution (378x241 pixels) is used as this allows a choice of 16 colours for the display of waveforms whereas high resolution (756x482 pixels) allows only two colours. However normal resolution is still superior to that of the APPLE 2. Displays are drawn using FORTRAN and assembler language graphics subroutine calls from the graphics software package.

In the basic system, using the 64KZ memory board, the SDI and the main CPU must share the data bus. This results in an increase in execution time of the user program, decreasing CPU efficiency from 100% to 65% at best, the actual reduction in efficiency being determined by the amount of memory used to store the picture image. This restriction is overcome by using the Cromemco's 48K Twin-Port memory boards. These boards now store the picture information leaving the CPU to continue operation of program execution.

2.3.4 48K Twin-Port Memory Board

The 48KTP card stores picture information as either a low resolution nybble(4-bit)-mapped or a high resolution bit-mapped image. It supplies the SDI with picture information while the system CPU can independently and simultaneously execute a user program, since the 48KTP card responds to an SDI refresh signal via its own address and data lines. This card is connected directly to the SDI therefore bypassing the S-100 bus, but it can also be accessed by the CPU through another port via the S-100 bus as if the SDI were not present (Figure 2.1).

2.3.5 Disc Drives and FDC Card

Program and waveform data storage in the Z-2D is provided by floppy disc in the form of two 5" double-sided, double-density discs each capable of 386K of storage. Total storage is therefore ~770K. Storage and retrieval of information and programs are controlled by the Floppy Disc Controller (FDC) card which is serviced by the Cromemco Disc Operating System (CDOS) software. The FDC also provides an RS-232 link for operation of the Z-2D via the Dacoll VDU.

2.4 Five Π-Section Model Line

This 1-phase 5 π-section line with zero earth impedance was constructed to allow easy connection/disconnection of compensating resistors when necessary for acquisition of compensated and uncompensated waveforms. The compensated π-section is as shown in Figure 1.3(a). The values for the individual components are as follows:-

$$L_p = 2.71 \text{ mH}$$

$$R_p = 0.83 \ \Omega$$

$$C_p = 2200 \ \rho\text{F}$$

Compensating Resistors

$$R_c = 33 \ \Omega$$

$$R_l = 6800 \ \Omega$$

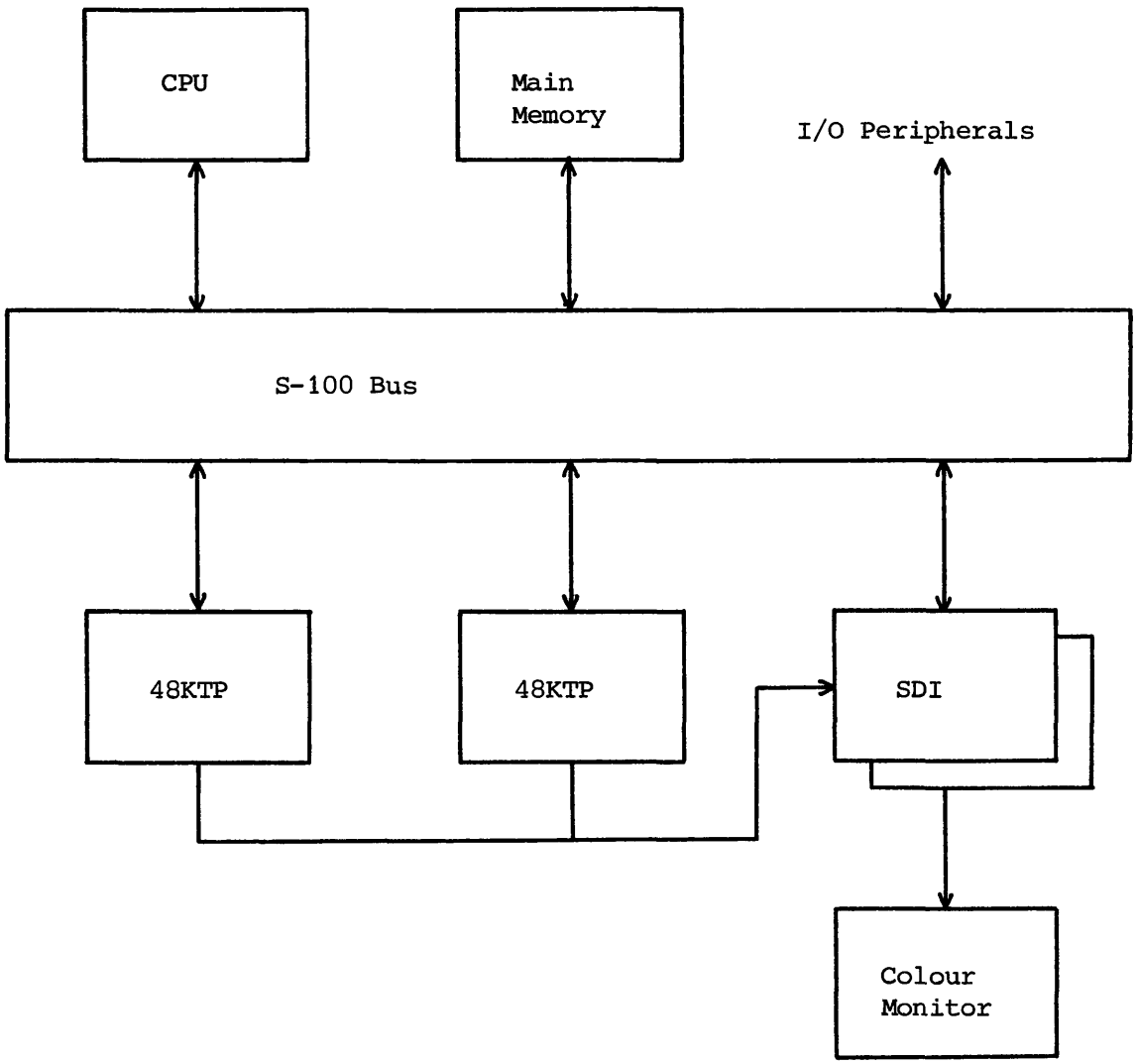

Figure 2.1
SDI Graphics System

This relatively simple line configuration was used in order to aid software development for the Z-2D and allowed initial development of the Runge-Kutta technique since the simple line design gave differential equations of low complexity.

2.5 20 Π-Section, 3-Phase Model Line

This model of a 100 mile, 275 kV twin 0.4 sq.in. double-circuit line was designed at Strathclyde University. Using this design a line was constructed in the College previously for transient overvoltage studies[18, 19]. A 3-phase π-section is shown in Figure 1.2. The values for individual components are as follows:-

$$L_p = 2.71 \text{ mH}$$

$$R_p = 0.83 \ \Omega$$

$$C_p = 2200 \ \rho\text{F}$$

$$C_m = 8600 \ \rho\text{F}$$

$$R_m = 0.79 \ \Omega$$

$$L_m = 0.68 \text{ mH}$$

$$R_{ep1} = 69.0 \ \Omega$$

$$R_{ep2} = 9.25 \ \Omega$$

$$L_{ep1} = 0.376 \text{ mH}$$

$$L_{ep2} = 0.324 \text{ mH}$$

Compensating Resistors

$$R_c = 33 \ \Omega$$

$$R_l = 6800 \ \Omega$$

This line was modified for 1-phase tests on 10 and 20 π-section lengths of line with and without earth impedance in Chapter 4. The line in its original form was used for 3-phase overvoltage analysis with source inductance in Chapter 5.

2.5.1 Line Modification

In order to obtain both uncompensated and resistor-damped line responses quickly from the longer lengths of model line some method of switching the damping resistors in and out of each π-section would be required. From Figure 2.2 it can be seen that six switching operations are needed per 5 π-section length of line to meet this requirement.

An initial idea was to use 4-pole relays to carry out the switching which would be processor controlled through an interface circuit (shown in Figure 2.3). However, the wiring from the appropriate parts of each π-section to the relays became lengthy and cluttered and added to the fact that each relay would have to be screened because of possible coupling effects made this method impractical. Connection of the processor to each relay via the interfacing circuitry would have added further to the problem.

Alternatively the use of single-pole, double-throw switches meant that they could be distributed such that line-switch connection lengths could be kept to a minimum. A 20 π-section line with earth return path was tested with this design but the results obtained showed that the waveforms, the uncompensated response in particular, were attenuated by an unacceptable amount. This was thought to be caused by the switches containing some magnetic material thereby increasing attenuation due to frequency-dependent magnetic losses.

Therefore the method of physically removing and reinserting the damping resistors was used to obtain the uncompensated and resistor-damped responses. Since line lengths up to a maximum of only 20 π-sections were tested 1-phase responses were obtained without any problems from the modified 3-phase line. However in the 3-phase tests of Chapter 5 waveforms had to be taken separately for the 20 π-section lines which inhibited immediate waveform comparison. Responses were obtained immediately however for uncompensated and compensated 5 and 10 π-section lengths.

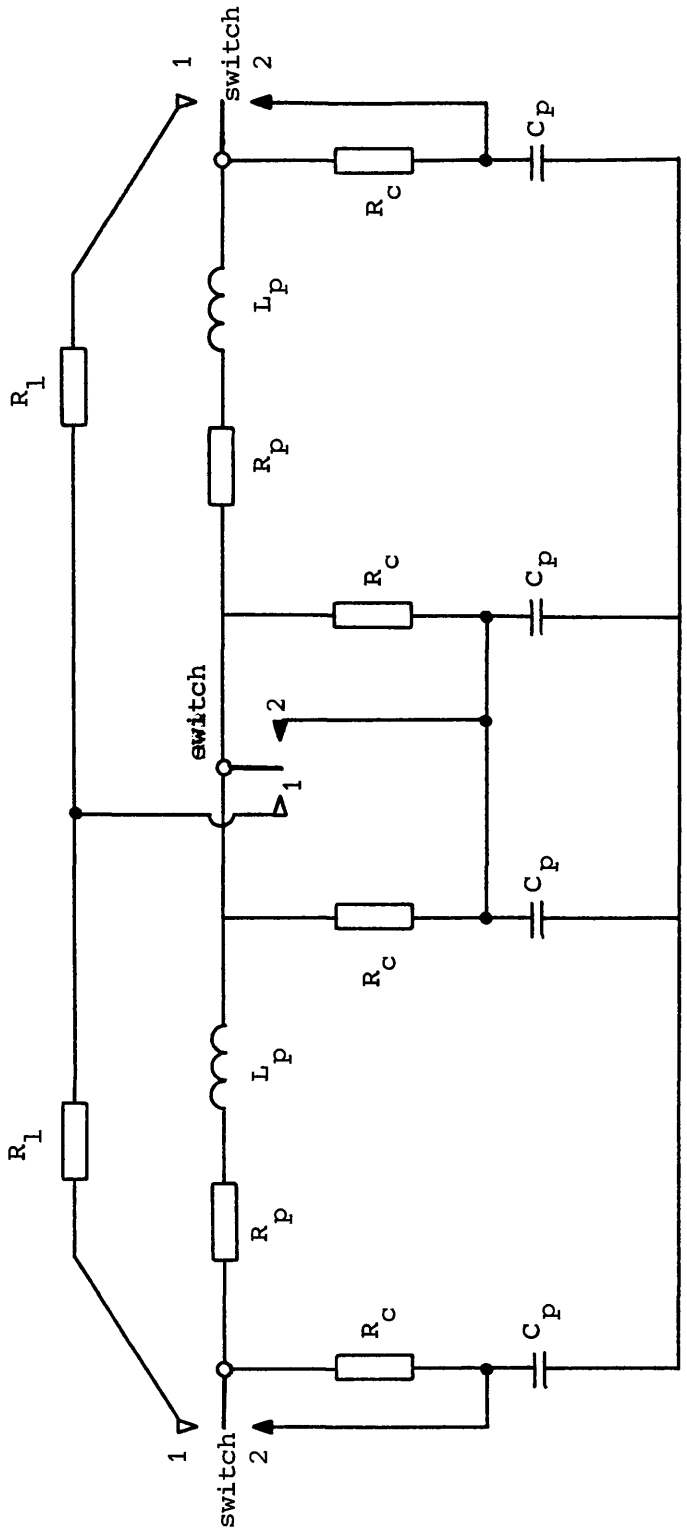

Figure 2.2
Switching the damping resistors in and out of the model line. Switches in position 1, damping resistors in.

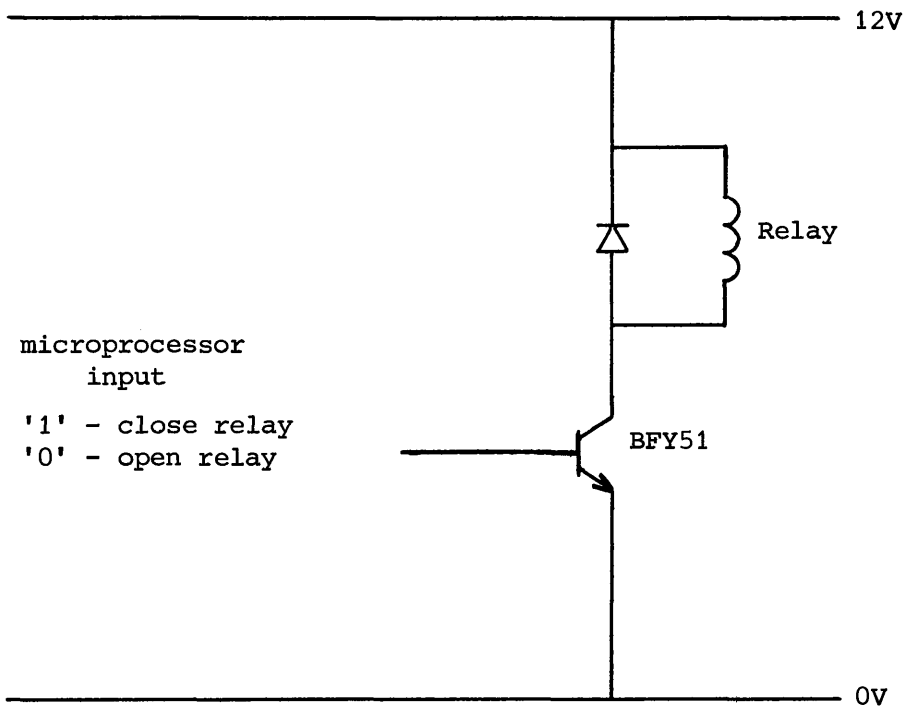

Figure 2.3
Interfacing circuit between microprocessor and relay

2.6 Reyrolle Transient Network Analyser

The Transient Network Analyser (TNA) is an accurate point-on-wave switch, which controls all the switching to be investigated. Using this device it is possible to determine the effects of switching on model power systems. It can be used to investigate model line responses to single or 3-phase sinusoidal energisation or with an external DC source, 1-phase step excitation. It can also determine transient overvoltages due to non-simultaneous closure using the double frequency source method[16]. The TNA has four main modules.

2.6.1 Three-Phase Oscillator Unit

This unit comprises a variable frequency, variable phase, 3-phase oscillator. It produces two sets of 3-phase signals , one for the generator unit and one for the master control unit. The frequency range of the oscillator is 40-3870 Hz, this being divided into 4 overlapping ranges of frequency set by the coarse frequency control:-

Range 1) 40 - 127 Hz

2) 120 - 386 Hz

3) 380 - 1224 Hz

4) 1197 - 3870 Hz

The fine frequency control enables the operator to achieve the frequency desired in the chosen range. The variable phase-angle control has a dial calibrated in degrees to enable direct reading of the phase angle between the master control and generator unit 3-phase supplies.

2.6.2 Generator Card

The ideal generator would be a sinusoidal voltage source with zero internal impedance but since this is difficult to achieve in practice, power operational amplifiers are used which give an extremely low output impedance. The unit has overall amplitude control and individual phase

amplitude adjustment to enable a balanced 3-phase supply to be set up. Although the amplifiers can source a maximum current of 1A, the transistor switches in the 3-pole switch card can only sink 400mA so limiting resistors were introduced. This card was used for 1-phase sinusoidal and 3-phase simultaneous closure line energisation tests.

2.6.3 Master Control Card

This unit is the heart of the TNA as it produces the timing pulses from which all the switches operate. The information which the card generates is in two forms:-

1) Cycle pulses
2) A six-phase supply for fine control purposes

This information is picked up by the 3-pole switch cards from the information buses. The master control card can be reset at any number of cycles between 1-99 by the thumbwheel switch on the card front panel thus determining the repetition rate.

The six-phase supply is generated from the 3-phase oscillator supply by means of inverting and non-inverting unity gain amplifiers while the cycle pulses are derived from comparators fed from the reference signal of the oscillator 3-phase supply producing a train of pulses synchronised to the reference signal.

2.6.4 Three-Pole Switch Card

These cards simulate circuit-breaker switching for the model lines under investigation. The TNA has four of these cards, each one having 3 pole switches with the following timing options:-

(i) Simultaneous Open and Close
(ii) Simultaneous Open and Sequential Close
(iii) Simultaneous Close and Sequential Open

Either of these options can be selected by a switch located on the card. The reference pole (pole 3) can be closed and opened relative to the repetition rate on the master control card by two thumbwheel switches (set between 1-99). The other two poles can be closed or opened simultaneously with the reference pole or delays can be introduced to simulate pole-scatter by means of two potentiometers on the card.

The ideal switch should have infinite impedance when open, zero impedance when closed and operate at the same point in the cycle with respect to the fundamental frequency. The transition from the on to the off state should be absolute and take zero time. The solid state switching used best fits these criteria having an open impedance of approximately 4MΩ and a closed impedance of 0.5Ω. As mentioned previously the transistor current rating is 400mA and this should not be exceeded.

The transistor switches must be electrically isolated as they can be inserted at any point in a model system and this is done by the use of isolating transformers in the circuitry. With the need for isolation, the switches must also have their own power supply and this is achieved by using rechargeable batteries, one for each switch, which are charged up via separate charging circuits brought into operation by a switch on the card panel.

2.6.5 New TNA Equipment

In November 1983 new TNA equipment was ordered from NEI Reyrolle to enhance the capabilities of the existing system. The active unit which controls the switching is virtually identical to that of the existing TNA but additional passive units were incorporated for the modelling of lumped parameter series and shunt resistor/inductor elements e.g. loading, source impedance.

This equipment eventually became available during the latter stages of the experimental work and was used to extend the investigation

into the effects of source inductance on the uncompensated line transient waveforms.

Initial results using this source impedance had been taken on a 1-phase basis only, the range having an upper limit of 0.1H. The new equipment had the capability of extending this range on a 1-phase basis and allowed 3-phase analysis to be carried out. Since the units supplied consisted basically of resistor and inductor elements in parallel, slight modification to the units internal wiring had to be made for the use of the inductive section alone.

2.7 Datalab DL920 Transient Recorder

The decision to use a device of this nature as temporary storage for model line waveform data as opposed to using computer Direct Memory Access (DMA) to capture the waveform(s) was made for a number of reasons.

Transients in the model system will contain frequencies of up to approximately 100 kHz i.e. line cut-off f_c = 92.2 kHz and for good visual representation of a transient waveform it was deemed necessary to have at least 10 samples per cycle. Therefore for one such waveform, one sample every microsecond (10x100 kHz = 1 MHz) would be needed. The project however would require three waveforms to be recorded at a later stage which defined a DMA device with a data transfer rate of ˜3Mbytes per second. Since no devices were available at the time with the necessary criteria the idea was discarded.

The Transient Recorder (TR) is a digital instrument designed to capture single-shot or low repetition events and present them for continuous display on a CRO and readout to an analogue plotter. The model available in the department was the Datalab DL920 which has a 4096 byte memory with an amplitude resolution of 1 in 256 i.e. 8 bits (block diagram Figure 2.4). Since it incorporates a 20 MHz A/D converter it easily satisfies the

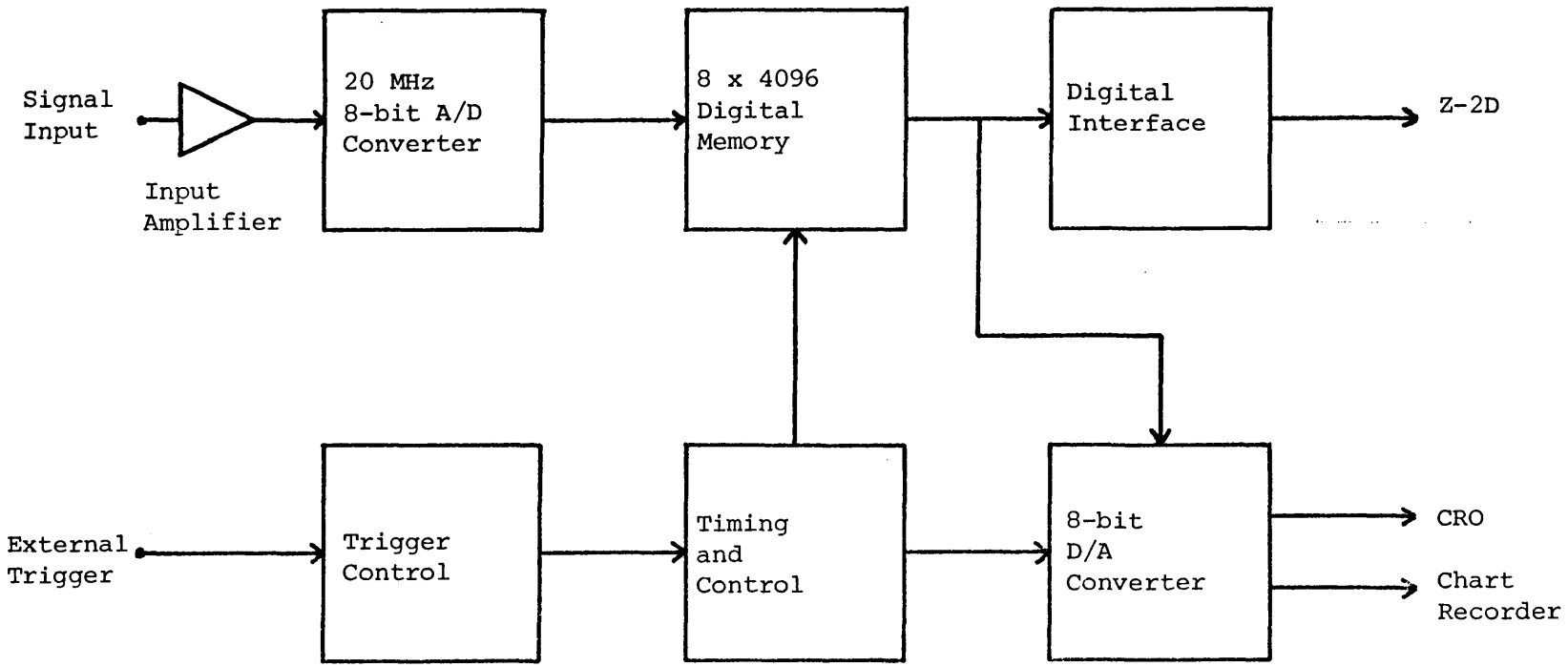

Figure 2.4
Transient Recorder Block Diagram

1 sample/μs criteria. It also has an interface board which allows digital transfer of data to a computer or other peripheral, the data being read out in sequence under peripheral control.

As with any sampling device it is necessary to consider the sample interval and the relationship with the frequency content of the signal to be recorded. The number of samples is fixed at 4000 (4096 if digital output is used) therefore a change in the TR sweep time is accompanied by a change in sample time. Sweep A on the TR selects the time over which 4000 equally-spaced samples are recorded therefore the sample time is given by:-

$$\text{sample time} = \text{sweep time}/4000$$

For a range of sweep time values up to 4 ms good waveform representation is achieved, this being the maximum sweep time allowable. As the memory consists of 4096 bytes the recording sweep continues for 96 more sample intervals than sweep A indicates, this additional data being available only through the digital interface card.

The sweep mode used was the delayed-sweep mode and the TR was externally triggered by the TNA so that it records the line response from the instant at which the line is energised. From the waveform plotted on the RGB monitor the line travel time can be easily observed.

The TR Volts Full Scale dial was set to 20V as a 5V (1 pu) step applied to the line generated voltages in the range +13 to -3V. For step energisation this gave a voltage range of 4 pu. For sinusoidal energisation, the peak voltage used was 3.125V which gave a voltage range of 6.4 pu. The amplitude resolution is therefore 20/256 V and this figure was used for voltage scaling when displaying waveforms on the RGB monitor (see section 3.5).

2.8 Datalab DL019 Line Disturbance Monitor

The DL019 is intended for use with the TR to enable transients and other disturbances that occur on AC power lines to be isolated and recorded for visual presentation or digital analysis. This instrument was initially included for the analysis of the 1-phase lines with earth-return path of section 4.4.2. It was discovered that signal input of the TR provided an additional earth path in parallel with that of the earth impedance line (with the zero impedance line this had been shorted out) and the DL019 was used to isolate the required line receiving-end waveform.

This problem was realised when the model response did not match the theoretical Runge-Kutta waveforms for this line. The DL019 was therefore also used for the 3-phase tests carried out.

2.9 Hewlett-Packard 7225A Digital Plotter

The HP 7225A is a microprocessor-based, RS-232 compatible plotter that produces high quality graphic plots on A4 size paper. It can address moves as small as 0.032mm and contains 39 different 'built-in' instructions which give the plotter capabilities such as point-digitising, labelling, character-sizing, scaling and window-plotting. With the 17603A personality module the plotter can be connected via an RS-232 interface to a host computer[34], in this case the Z-2D. A plot of a waveform from the 7225A can be seen in Figure 1.7.

The plotter exchanges data over the serial interface at a maximum rate of 2400 Baud. It is connected to the Z-2D by means of an RS-232 interface cable which plugs directly into the plotter, the computer connection being made from the TUART board in the Z-2D. The 7225A has other facilities such as 'paper load', setting of graphics limits, pen up, pen down, reset and error detection indicators, 'ERROR' and 'OUT OF LIMIT' on the facia.

Since the 7225A will take various lengths of time to perform

plotting and lettering commands, a buffer has been included to accept 630 bytes of data. Obviously the buffer must never be allowed to overflow as this would cause loss of plot data and so the plotter incorporates various handshake modes to cater for this. It would be inefficient for the Z-2D to send one character at a time and so data in sent in blocks of 100 bytes. After a block is sent the processor 'asks' the plotter if there is room in the buffer for another block, the plotter monitors the buffer and replies accordingly. Two methods are employed for this handshaking procedure, a Hardwire mode which requires modification of the interface cable and a Software mode which uses control instructions for handshaking. The latter method is employed as it eliminates hardware modification and can be programmed in Z-80 assembly language. The fault indicators when lit, signify a program or communication error and the 7225A when given a control instruction is programmed to output 1 of 7 possible error messages to the Z-2D therefore aiding in debugging of computer/plotter communication software.

2.10 Microvitec 1409/BS RGB Colour Monitor

This is a Z-2D compatible 14" RGB colour monitor used for graphical display of waveforms. It has a resolution of 452x585 pixels which gives good low and high-resolution graphics. It was decided to purchase this monitor in place of the Cromemco model, as it gave the graphic quality desired and was considerably cheaper (£265 as opposed to £2000).

2.11 Dacoll VDU

This monitor is used to communicate with the Z-2D, for creating, editing, executing and debugging of software and is connected to the Z-2D via the FDC Board RS-232 interface. Most terminals can operate with the Z-2D but the Dacoll was used as it was readily available.

The equipment for the development system has been described and is shown in block diagram form in Figure 2.5.

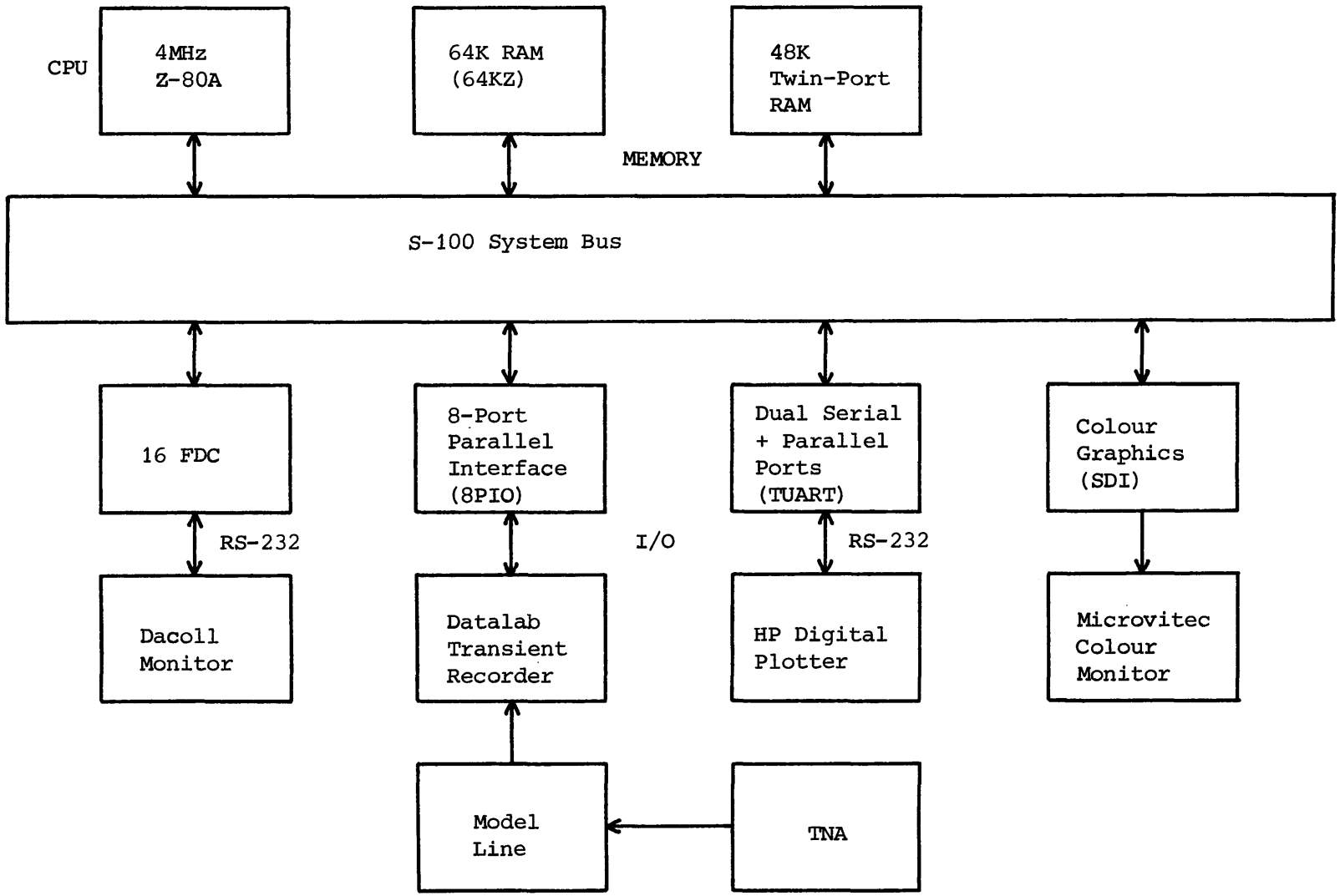

Figure 2.5
Development System Block Diagram

2.12 CAMAC Computer System

As the investigation proceeded to the analysis of the 3-phase line energised from an inductive source (section 5.4.3) the use of a CAMAC 24-bit computer system was investigated as a possible data acquisition device for the simultaneous storage of 3-phase transient waveforms. Since the TR could only record one phase at a time the use of this system would be beneficial in terms of the automation and speed of waveform capture.

The CAMAC system[35] is essentially modular. Separate plug-in units may be accommodated in any one of 24 positions or stations in a crate. The station situated at the right when viewed from the front is the control station (Figure 2.6). This station does not connect to all data bus-lines, but instead has additional control lines to and from the remaining normal stations. The 7025 controller used in the system occupies 3 stations since it requires access to the data bus and the control lines. This module is responsible for supervising operations on the data bus. The controller takes instructions from the program store module which consists of a 64 instruction diode plugboard and executes these to perform the various operations associated with each module in the system.

The 9082 16K store would be used to store the 3 waveforms from the line with the 9090 module interfacing the model line and store. The data would be passed to the Z-2D via the 9013 module to the RS-232 line of the 5072 module which would be controlled by software handshaking between the two computer systems.

However various factors meant that this method of data acquisition had to be abandoned, after considerable work was done in understanding and designing a system configuration, due to the unreliability of the CAMAC equipment. The system was old (purchased in 1972 for medical data acquisition and analysis) and it was eventually discovered that some of the modules did not work properly. Other factors which added to

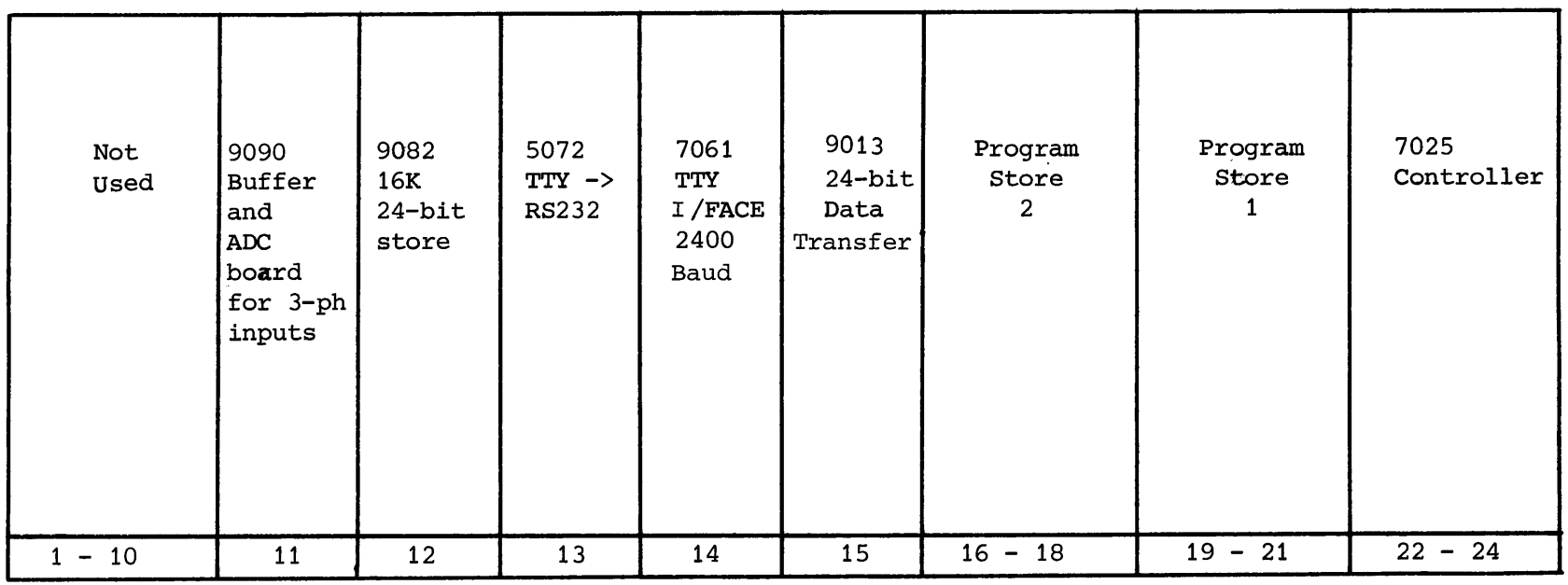

Figure 2.6
Module locations in CAMAC system

this decision were the difficulty in changing the CAMAC software (diode plugboard) and that no debug facilities were available. Indeed the documentation was relatively sparse in software detail which made the task of writing programs difficult.

With the prospect at some future time of the Department being able to purchase new multi-channel Datalab recording equipment and with the experience already gained in using Datalab equipment the CAMAC system was shelved.

Recording of 3-phase waveforms was accomplished using the method for 1-phase results although this entailed switching and recording the model line response three times in order to obtain a 3-phase response.

2.13 Development System Overview

The hardware system described coped easily with the analysis of 1-phase waveforms. 3-phase results were also obtained by means of energising the same circuit and recording different phases. This was more time consuming but proved to be adequate. Another problem, although not serious, arose due to the fact that the Z-2D memory working area was limited to 46K RAM. When dealing with 3-phase results, disc storage had to be used extensively and this slowed down program execution. Cromemco claim that memory is expandable using other memory cards but this memory can only be used as data storage space. Routines were obtained which allowed the use of another 64K memory board which worked to a certain extent. However the operating system software had to be modified and when the program used the system routines the program invariably crashed. Consequently this idea was abandoned. The use of floppy disc as a storage medium is discussed in section 3.8.

However, the processing, display and plotting of waveforms proved to be satisfactory. With hindsight and with the availability of more powerful microprocessors it is becoming increasingly apparent that the Cromemco,

although a fairly powerful system, should be replaced by one of the new generation of 16-bit processors. For example the SAGE IV system has all the facilities of the Z-2D but with a 0.5Mbyte working memory area and of course faster data processing or by the new 32-bit MG-1 workstation, both systems being financially comparable or cheaper in relation to Z-2D costs.

CHAPTER 3

Z-2D Software

3.1 Introduction

The task of linking devices such as the Transient Recorder, Plotter and Colour Monitor to the Z-2D system through the 8PIO and TUART boards was relatively straightforward if initially time consuming. To get the processor to use this equipment to fulfil the needs of the investigation is then a software problem which is more difficult. Given also that the model line transient waveforms were to be verified by computer using a Runge-Kutta technique and transient waveform analysis carried out by other Digital Methods, the project required two sets of software to be written:-

1. The microprocessor software to allow acquisition, display, modification and storage of the experimental waveforms obtained from the model line.

2. The software written on the College DEC-20 mainframe to:-
   - predict actual transmission line responses by the Modified Fourier Transform in Chapter 4 and the Lattice Method in Chapter 5.
   - 'process' the uncompensated line waveforms by Digital Filtering techniques in Chapter 6.
   - verify the experimental results by the Runge-Kutta numerical integration technique in Chapter 7.

Since the techniques in 2 require a very large number of calculations, the mainframe was used because of the greater arithmetic power available to the programmer i.e. a 36-bit CPU. The DEC-20 software, as well as uncompensated waveform modification by the Experimental Sigma Factors, will be discussed in following chapters. This chapter describes the software developed in order to achieve a single-user system for acquisition, display and plotting of model line results. The software referred to throughout the

chapter relates to that written for the analysis of 3-phase results as it incorporated the most recent ideas which were developed from the initial programming concepts (Appendices II.1 - II.6). The text cannot describe the software step-by-step but will aid in the understanding of what are regarded as the salient points.

3.2 Cromemco Z-2D Software Packages

The Z-2D system can be used with both high and low-level language packages such as BASIC, FORTRAN, COBOL and a Z-80 macro assembler. For the development system used it was decided that the FORTRAN and assembler languages would be used, which when compiled and assembled could be linked to form a final program. The Z-2D system software allows the user to create individual programs and routines at both levels and after machine-code generation of each program links their relocatable files together therefore forming a user program from several program modules. This was achieved by using a main FORTRAN program which 'called' five assembler modules all stored in separate files on floppy disc.

The reason for using languages of different levels is that should the need for complex mathematical routines arise, they can be easily written in a high-level language such as FORTRAN while simple routines and input/output are more efficiently handled by assembly language. Packages are also provided for the creation and development of programs and also for software debugging. Since processor waveforms are not calculated in real-time the debug software proved to be very helpful in correcting assembler program errors and to a lesser extent FORTRAN program errors.

The memory map of the Z-2D system is shown in Figure 3.1. The Disc Operating System (CDOS) occupies two areas as can be seen, the rest being available for user software (~46K).

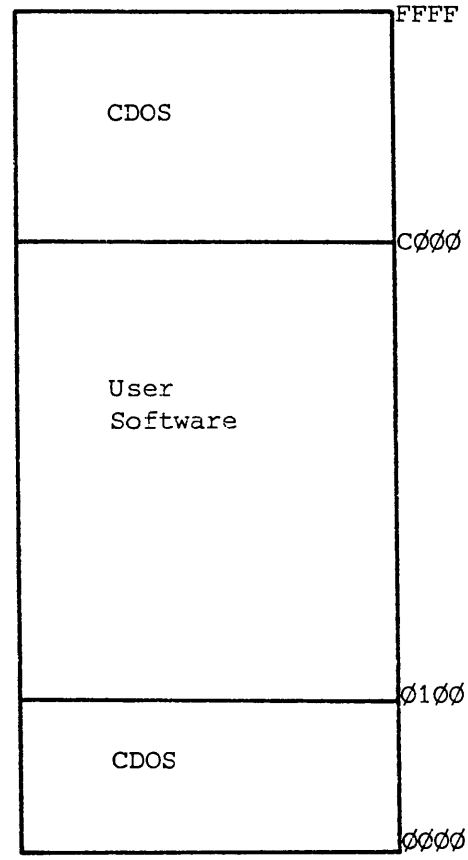

Figure 3.1
Cromemco System Memory Map

3.3 The Z-80 CPU

To understand the assembly language software written it is necessary to be familiar with the CPU configuration of the Z-80[36, 37]. The CPU contains 22 registers consisting of 208 bits of static RAM which are arranged into two banks of eight 8-bit registers, fourteen general purpose registers and two flag registers (see Figure 3.2). Only one bank of registers may be active at any given time, but the accumulator and flag registers of one bank may be used with the six general purpose registers of the other bank if required (the banks are usually exchanged when dealing with interrupts). The six general purpose registers may be used as six 8-bit registers or as three 16-bit register-pairs. The other registers are special purpose registers:-

- The stack pointer (SP) holds the current top of the stack address located in RAM.
- The index registers IX and IY are two 16-bit registers that permit indexed addressing.
- The interrupt register (I) is used for storing the higher-order 8-bit address of an interrupt-handling routine when an external device demands use of the CPU.
- The memory refresh register (R) provides a refresh signal when external dynamic RAM is used.

Since interrupts were not used the I and R registers and bank two of the general purpose registers were not required for the software developed.

3.4 Waveform Data Acquisition

After the model line transient waveforms have been captured by the TR they must be passed to the microprocessor for modification and/or display. This is achieved by the assembler program DI3.Z80 (Appendix II.2) which transfers the data by a handshaking routine from the TR memory through an on-board parallel digital interface card to the Z-2D 8PIO board.

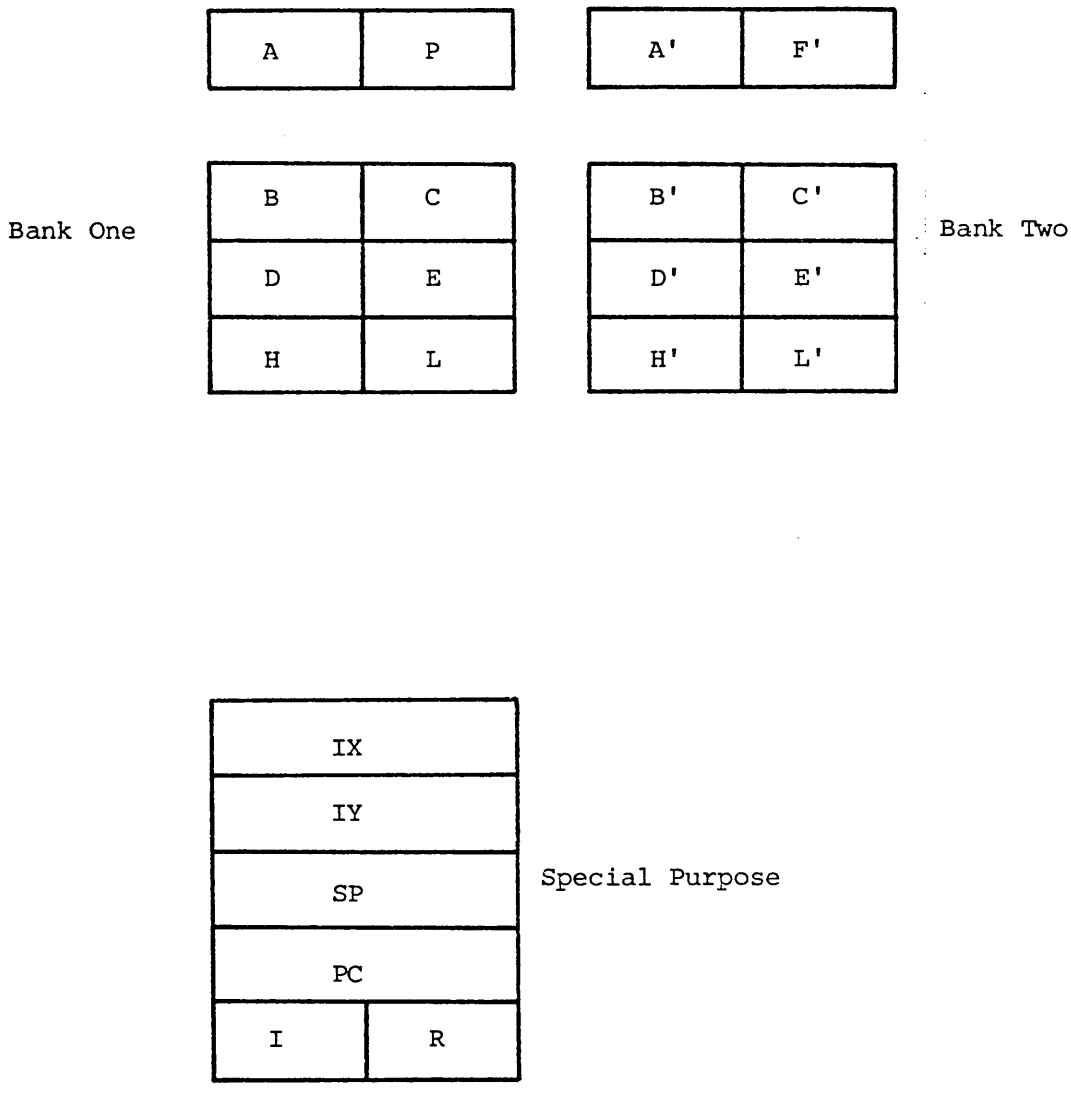

Figure 3.2
Z80 CPU Configuration

Software control places the data into the FORTRAN array IDATA(4096). An area of Z-2D memory common to both the FORTRAN and DI3 modules is therefore defined. Since the Z-2D graphics routines require the data to be in two-byte integer form, the single byte from the TR, which is loaded into the accumulator during data transfer, is then stored along with a zero value byte in the B-register into memory thereby satisfying the above criteria i.e.

From Z-2D	From TR
MS Byte	LS Byte
00000000	11001011
00000001	10010110 value x2 i.e. shift right

It was decided to use the most significant byte to some effect by doubling the discrete-point values of the TR waveforms so that the processor waveforms would have an amplitude resolution which was twice that of the model line responses. Bit 1 of the least significant byte is therefore always zero for the compensated and uncompensated waveforms but may be either 1 or 0 after local averaging has been implemented. Therefore processor waveform amplitude resolution is increased which will lead to more accurate overvoltage determination.

For handshaking between the TR and Z-2D systems the following control signals were necessary:-

TR --> Z-2D	Z-2D --> TR
Digital output flag (DOF)	Digital output enable (DOE)
Data ready (DR)	Digital output request (DOR)
	Word request (WR)

To enable the initiation of output from the TR the Digital Output Enable (DOE) is set high. This indicates to the TR that a device is present. Output is then initiated by setting DOR high. When output starts (within

4 ms) the DOF is set by the TR and then DR goes high to indicate to the Z-2D that valid data is available at the TR output. To read out further data bytes, the WR line is set by Z-2D software. This forces DR low, signalling the TR to fetch the next byte of data. WR is then reset low and when new data is available from the TR output DR goes high again. When all TR data has been transferred the DOF goes low and this terminates handshaking.

The flow chart for handshaking and the port connections used are shown in Figures 3.3 and 3.4.

3.5 Axes Display and Waveform Amplitude Scaling on Monitor

The time and pu voltage axes are displayed on the colour monitor and the pu voltage axis scaled using the program BL3.Z80 (Appendix II.3). The initial reason for writing this assembly language module was due to the zero volts level recorded by the TR varying thereby not giving a constant digitised value for 0V. This level is controlled by the DC offset dial on the TR but can easily be disturbed when using the device. It was therefore necessary to assume that the value for 0V was that given by the initial data byte taken from the TR. This value was then stored in the relevant common memory locations to be used by the Z-80 module to draw and scale the axes.

When waveforms from the 1-phase line with earth impedance were captured using the Line Disturbance Monitor (section 2.8), a slight oscillation superimposed on the 0V level was observed (see Figure 4.13(a)). Even though this irregularity (due to the use of the equipment) was attenuated in a few microseconds it could give a false reading for the 0V value using the previously discussed method. A software routine was then developed in the FORTRAN module to find the correct value for this parameter. The routine determined the most frequent occurrence of values at one digitised level for the initial part of the waveform and assumed this value to be 0V. Again this value was passed to the BL3.Z80 module for drawing and scaling of the axes.

The pu voltage axis scaling depends on the excitation voltage

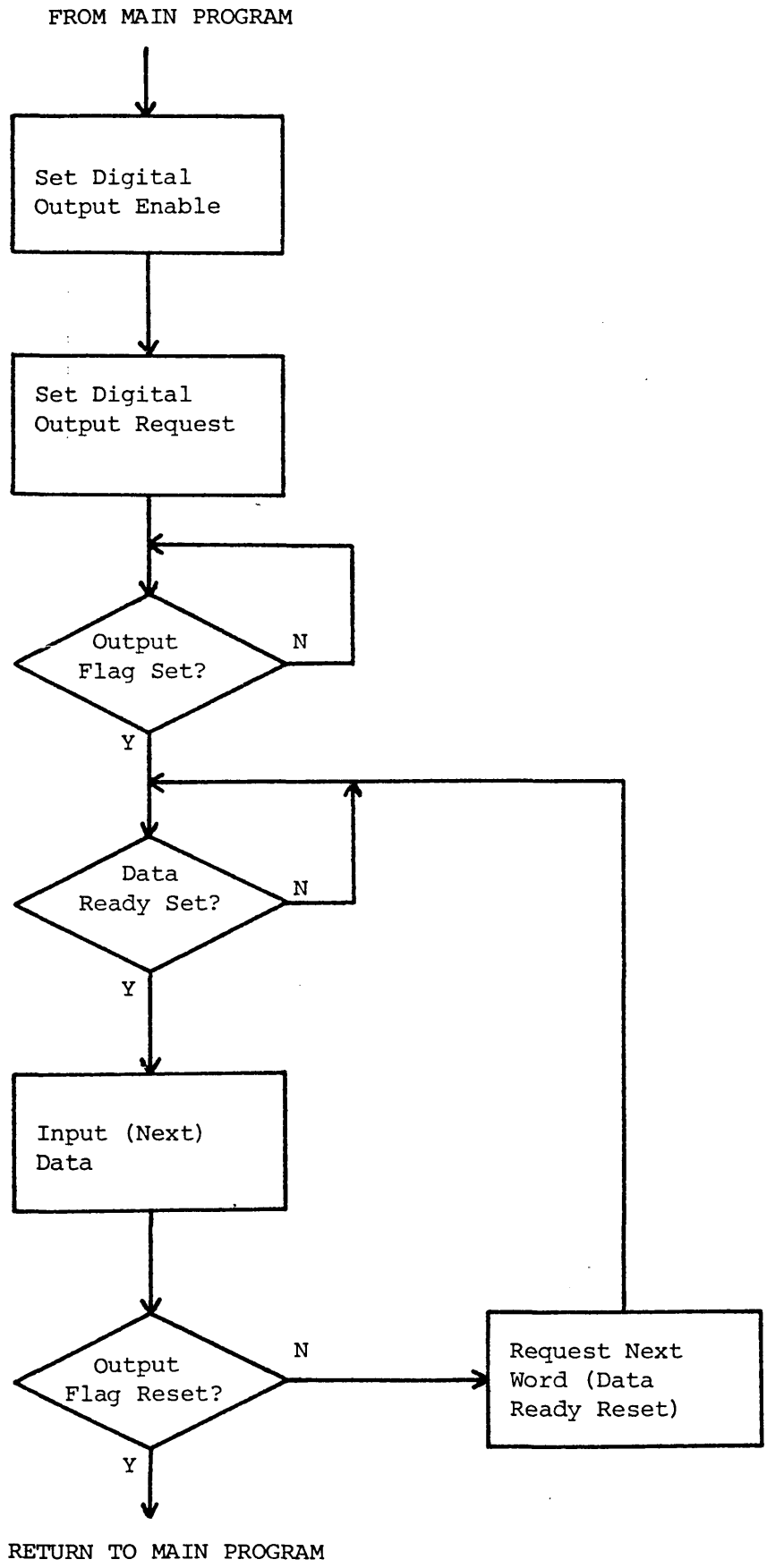

Figure 3.3
Handshaking Flowchart for Data Acquisition

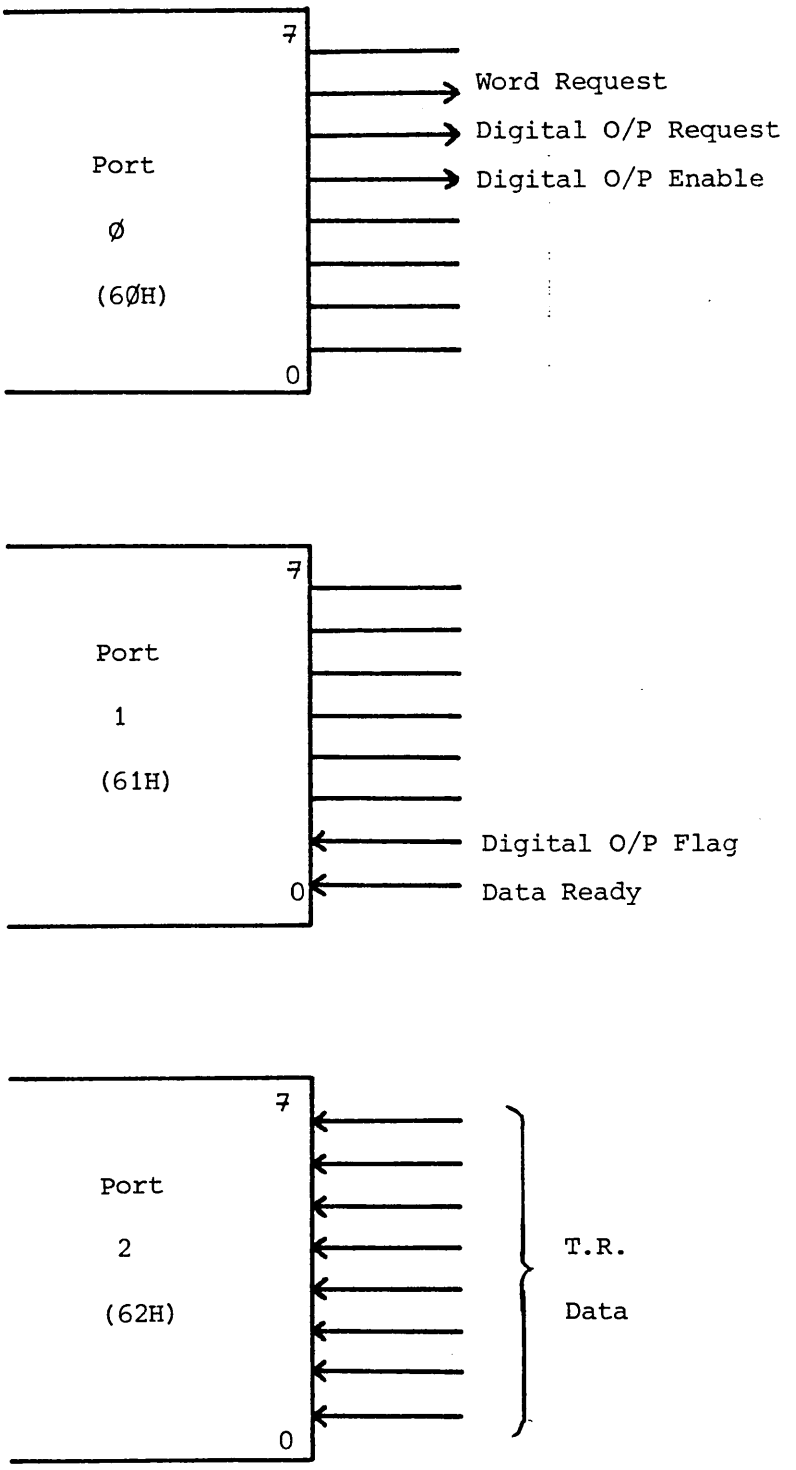

Figure 3.4
Z-2D Port Connection for TR Handshaking

defined as 1 pu and the Volts Full Scale setting on the TR. In 3-phase analysis the peak source voltage used was 3.125V and the TR set for a voltage range of 20V. This gives a range of 6.4 pu i.e. -3.2 pu -> +3.2 pu. Since the TR is an 8-bit device, this gives a resolution of

$$256/6.4 = 40 \text{ bits/pu}$$

and because all TR response values are doubled, the final figure is 80 bits/pu which was used in the scaling software. The pu axis is then marked at intervals of 1 pu and numbered. The monitor was scaled so that it only displayed a voltage range of -2.8 -> +2.8 pu as Runge-Kutta results indicated that peak overvoltages of no more than 2.7 pu were to be expected. For sinusoidal energisation the 0V level was given a value such that the y-coordinate of the time axis lay exactly midway in the vertical plane of the monitor, all TR waveforms being shifted in software so that their calculated 0V value lay on this axis (see Figure 4.20(a)).

To clear the monitor of plotted waveforms in preparation for a new display, the same responses are plotted again but in background colour which effectively removes them. When this is done however the axes can be visually corrupted and to correct this they are drawn again by calling the routine REAXE in the BL3 module.

All graphic routines can be used in both high and low-level languages, the latter using a system of indirect and double-indirect addressing (address pointers stored in BC, DE and HL) for pointing to the data for the relevant graphics subroutine[38].

3.6 Waveform Display and Time Axis Labelling

The compensated, processor and uncompensated waveforms are displayed on the Microvitec RGB monitor by calling the low-resolution graphics subroutines provided by Cromemco. The waveforms are displayed as discrete points instead of continuous lines because of the poorer waveform

representation which the low-resolution graphics gave when a line was drawn between adjacent samples. High-resolution graphics with the boards available allowed only two colours and for three waveforms on a background with axes required a minimum of five. High-resolution with 8 colours was possible but the cost of the extra boards required for this was restrictive when considering that the improvement would be qualitative and not of necessity.

The FORTRAN software was written to give the capability of displaying any section of a waveform. Since the monitor was scaled, using a graphics subroutine, to display a maximum of 800 points the time range of a waveform section (in μs) is determined by the time between waveform samples i.e. the TR sweep time. This range is calculated by multiplying the sample time by 800 i.e.

$$\begin{aligned} \text{TR Sweep time} &= 2 \text{ ms} \\ \text{sample time} &= \text{sweep time}/4000 \\ &= 0.5\ \mu\text{s} \\ \text{Time range of waveform section} &= 800 \text{ x } 0.5\ \mu\text{s} \\ &= 400\ \mu\text{s} \end{aligned}$$

To display a waveform sample the sample voltage value represents the Y-coordinate while the variable JXTIM gives the corresponding X(time)-coordinate for the XDOT subroutine. A degree of flexibility was introduced so that for the same sweep time, a half or twice-range display can be shown if desired. This allows closer inspection of the waveform at points of interest using the half-range, while the twice-range display allows inspection of the waveform in a global sense. Half-range display is achieved by incrementing the JXTIM variable by 2 for each voltage sample while the twice-range option increments by 2 through the voltage sample array IDATA (or IBUFF if from disc, section 3.8) for each JXTIM value. The program informs the user of the normal display time range and allows any waveform combination to be displayed.

The software also allowed the user to display any combination of three waveforms in the single and 3-phase software so that waveform comparison could be carried out visually on the monitor.

Initially a colour key was displayed so that the user could easily determine which waveforms were shown. In the 1-phase software this was carried out using the high-level graphics commands to permanently display the letters U (uncompensated), P (processor) and R (resistor-compensated) in the corresponding waveform colour but because of increased number of possible waveform combinations for display in the 3-phase program, small assembler routines were written to temporarily indicate the waveforms on display.

The assembly language module CV3.Z80 (Appendix II.4) is also implemented in this section of the software for the labelling of the time-axis. Since any waveform section can be displayed and then removed from the monitor the time axis values shown must be changed accordingly.

Time values are converted from their decimal value to an ASCII equivalent (carried out by the ASCON subroutine) as the graphics text subroutine XTEXT defines that data must be in ASCII code[38]. Storage of the ASCII equivalent number uses 6 bytes, 5 for the decimal digits, and a single byte text delimiter which ends execution of the graphic subroutine. The 5 digits therefore give an upper time limit of 99,999 μs. Since most time values will not use the full five bytes (e.g. 20 would be stored as 30,30,30,32,30) a routine was added to 'eliminate' these ASCII zeroes by incrementing the IX register to point to the first ASCII non-zero number required for display which in this case would be '32').

When displaying times of the order of 1000 μs and above i.e. of four digits, they appeared on the monitor as a continuous stream of digits with no discernable gap e.g.

so the subroutine includes a method of recognising a time value which consists of more than 3 digits and displays each time at alternative Y-coordinates i.e.

1000 1040 1080
1020 1060

When a new display is required by the user, the time values are removed by plotting them in background colour.

3.7 Waveform Plots

When desired, the display on the RGB monitor could be plotted thereby ensuring hard-copy records of results which were of particular interest. This was achieved using the final section of the main FORTRAN program and the two assembly language modules IP3.Z80 and PL3.Z80 (Appendices II.5 and II.6).

To obtain a plot of the display, communication between the plotter and the Z-2D must be initialised. IP3.Z80 carries this out by defining the baud rate between the two devices (2400 Baud). It also specifies the output mode and the handshake protocol of the plotter. Handshaking is carried out by the optional software mode and is realised by sending commands to the plotter to disable the hardwire handshake by using the following control instruction sequence

ESC . I 100 ; DC1 ; DC2 : (All ASCII code)

This informs the plotter that the processor will send data in blocks of 100 bytes. After each block is transmitted the Z-2D asks the plotter if there is space in the buffer for another 100 byte block by sending the hexadecimal equivalent of DC1. When there is sufficient space the plotter sends back the hexadecimal equivalent of DC2, thereby allowing the Z-2D to continue sending plot information. This routine of transmitting data and handshaking

is carried out by the TRANS subroutine in which the D-register counts the number of bytes transmitted. When the D-register reaches 100 bytes program control remains in a handshake communication loop until the plotter indicates it is ready for the next data block, after which the D-register is reset to zero.

The 7225A instruction set contains a useful instruction which allows the user to scale the plot output area. This means that the plotter can be scaled exactly to the RGB monitor scaling dimensions therefore eliminating any need for conversion of data from one scale to another. The IP3 module also draws and scales the axes by taking parameters from the main and assembler programs. Other functions carried out by the 7225A instruction set allow plotting of absolute points and scaling and labelling of the axes.

The plotting of waveforms is carried out by the PL3.Z80 module. Since the plotter only accepts information in ASCII code, the waveform data must be converted from two-byte integer form to its ASCII equivalent. Again this is achieved by calling the subroutine ASCON in CV3.Z80. The macro assembler allows calling of routines in other modules using the EXTERNAL and ENTRY pseudo-operators[39].

There is a plotter command and data block defined in this routine (Appendix II.6) which moves the pen to an absolute plotting position defined by the waveform sample coordinates. Two 3-byte areas in this block (for variables XCOORD and YCOORD) give the X and Y coordinates of the next pen position. These areas are filled with the converted waveform ASCII data before the block is sent to the plotter. Since the value XCOORD will always consist of three decimal digits i.e.

XCOORD => 110 - 910 i.e. 800 points

it will always give a 3-byte ASCII code when converted. However the

variable YCOORD may be less than 3 digits (range 0 -> 450) so that '25', which in ASCII is 30,32,35,would be plotted as '025'. The software therefore includes a CHECK0 routine to replace any preceding '30' bytes with a plotter 'no operation' byte which when undertaken by the plotter carries out no function until the next operative byte.

The processor effectively takes the relevant data from the main program, converts it to ASCII-code, loads the converted data into the 'plot' block of PL3 and transmits the block to the plotter. The flowchart for waveform plotting is shown in Figure 3.5 with the plotting procedure of a mainframe computer shown for comparison.

A complete normal-range plot, which draws and labels axes and copies three waveforms takes ~3 minutes.

The PL3 module also takes information from the main program to draw a waveform key diagram similar to that on the monitor. The waveforms are differentiated by changing the plotting pens of which there are various colours.

3.8 Storage and Retrieval of Data on Disc

The development of data storage on disc was necessary in the initial stages of the investigation as the software written eventually overran the available working area of ~46K. With the problems encountered in using extra memory boards (section 2.13) it proved to be invaluable when the research moved to 3-phase analysis. The first programs written for 1-phase transient analysis incorporated the graphics file SDIFOR which was 22K in size. In order to use the graphics facilities and subroutines all 22K of this package had to be included in the final program which significantly reduced the area available for user software. After consultation with Cromemco, their new graphics files FGRAF1 and GRAF2 were acquired which allowed the user to load FGRAF1 (the 8K graphics initiation package) and search through GRAF2 for only those graphic subroutines required by the user.

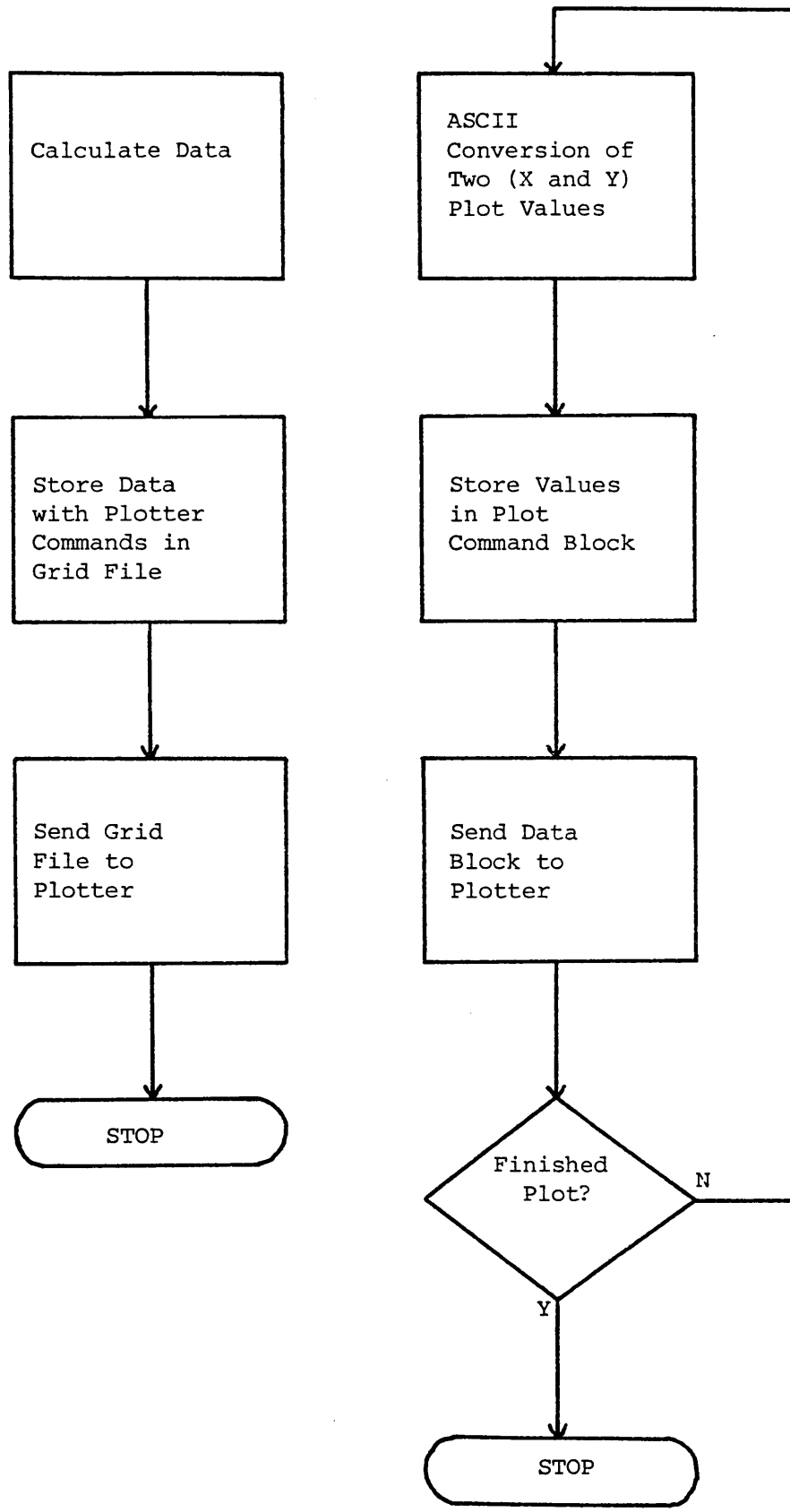

Figure 3.5
Comparison of Waveform Plot Flowcharts

Even with this saving in memory space, program development meant that the 46K limit was again approached. At that stage the uncompensated and processor waveforms were stored in 2 x 8K arrays and it proved impossible to allocate storage for the resistor-damped response. For this reason floppy disc had to be used as a storage medium for the processor and resistor-compensated responses. This left a 1 x 8K data working area in memory to which the uncompensated waveform was assigned since it was to be modified by the Experimental Sigma Factors.

The use of sequential formatted files[40] was inefficient since waveform segments, required for display and plotting, near the end of a file necessitated the reading of the file from the beginning. Retrieval of data in this instance took ~25 seconds. The use of formatted random access files caused the generation of extra data (control characters i.e. end of file, carriage return etc.) so that storing 8K of waveform data generated a 20K data file which also gave a long data access time. Therefore data had to be stored in an unformatted manner.

Non-sequential unformatted storage was finally used which generated an 8K data file on disc which could be loaded into the Z-2D memory in ~9 seconds. The disc I/O buffer holds 128 bytes which is the maximum record length specified by Cromemco for a 5" floppy disc. To utilise this space fully an integer array IBUFF(64) was created to store 64 two-byte integer values which would then be stored on disc in their unconverted binary forms. Therefore each time the IBUFF array was written to disc a record was stored. To write data onto disc the command WRITE(6,REC=NBLOCK)IBUFF was used where 6 represents the disc logical unit number and NBLOCK signifies the record number which is incremented in software everytime IBUFF is stored e.g.

NBLOCK=1 ==> Record 1 ==> 128 Bytes

NBLOCK=2 ==> Record 2 ==> 128 Bytes

When transferring the model line responses from the TR, the 8K working area in memory is used as a temporary store for these waveforms before they are saved on disc. This area is then overwritten with the uncompensated response ready for processor modification. FORTRAN subroutine STOBUF carries out data storage (see Appendix II.1). Retrieval of disc data is carried out by the FORTRAN subroutine GETBUF.

Waveform display or plotting is carried out by the FORTRAN subroutine WAVDOP which calls GETBUF for data. The first sample required is given by the time variable ITIM1 (user-defined). Dividing this value by 64 will give the appropriate data record number with which IBUFF is loaded and the subroutine software then points to the first sample in IBUFF which is required. The disc data is then read sequentially until time ITIM2 is reached which terminates the procedure.

3.9 Z-2D Software Overview

The basis of the software written to perform the various functions mentioned in the preceding text was mostly written in the first year of the investigation as understanding of the equipment was gained. Modifications were necessary when problems occurred (e.g. the introduction of the DL019 equipment) or when moving from 1-phase step energisation through 1-phase sinusoidal energisation to 3-phase analysis.

The main criticism that can now be made is that the separate modules written are too rigid in the sense that if, for example, the pu source excitation is changed, then certain parameters in most modules have to be changed. For the original programmer it is a fairly easy task to locate and change these variables but a new user wishing to modify the software would find this difficult. However to introduce a degree of flexibility into all of the modules would require more common data areas and the necessary software for handling the data.

The main modification would be in the FORTRAN module which

could be modified to ask for data such as the peak-to-peak pu excitation voltage, the full scale voltage range on the TR and the sweep time to be used. The program could then calculate the number of bits/pu necessary for scaling and the time ranges available for waveform display and plotting. This would improve the software written but due to the lack of a reasonable size working memory area in the Z-2D, would prove impossible. For these reasons the software includes comments and indicates where necessary the parameters which have to be changed if modifications are required.

CHAPTER 4

Waveform Modification by the Experimental Sigma Factors

4.1 Introduction

As described in section 1.8.4 the Modified Fourier Transform has been used previously to calculate the transient response of transmission lines to energisation[30]. In order that this could be carried out accurately the reduction of the Gibbs phenomena, which arise when numerically evaluating the truncated inversion integral, has been achieved by incorporating Lanczos Standard Sigma Factor σ_s[3]. This uses a local averaging range determined by the highest frequency Ω present in the integral calculation and incorporating σ_s gives a response with a significantly reduced Gibbs content. However it also reduces the rates of rise at the waveform discontinuities.

As a result the Modified Sigma Factor σ_m was developed where local averaging is implemented over an arbitrarily chosen shorter time range. This improves the rates of rise of the response[3] but is not as effective in reducing the Gibbs phenomena. These observations suggested however that both factors could be applied at the appropriate parts of a response[29] to give the most accurate representation attainable, σ_m at the response discontinuities and σ_s elsewhere.

The uncompensated model line waveforms also exhibit these high-frequency oscillations since the finite number of cascaded π-sections used for actual line representation is equivalent to limiting the transform integral frequency range. Previously the inclusion of damping resistors in the model line has significantly reduced the Gibbs content but the inherent increase in attenuation affects the transient waveform discontinuities and global response. It was suggested by Crowe[17] that analogous Sigma Factors could be derived from the ideas developed by Lanczos in an attempt to effectively reduce these oscillations by locally averaging sampled uncompensated line waveforms in the time domain. The reduced attenuation of the uncompensated model

line may therefore give improved waveform rates of rise and global response if the oscillatory content could be significantly reduced by these time-domain Sigma Factors.

The following text describes the Experimental Standard Sigma Factor S_{se} and how it is derived. The expertise gained and the processor responses obtained by applying S_{se} to the uncompensated model line transients allowed the more complex Experimental Adaptive Sigma Factor S_{ae} to be developed. Both of these techniques, equivalent to σ_s in the Fourier analysis, were used in the modification of uncompensated transient responses of 1-phase lines, with and without earth-return path, for ideal DC source energisation. Subsequently they were applied to the responses from AC source excitation for the same line configurations.

An Experimental Modified Sigma Factor S_{me} was also devised (section 4.7) to simulate σ_m although the range of local averaging in the case of S_{me} is variable throughout the modification process. As in the Fourier case, improvements in processor waveform rates of rise were expected using this technique.

The model lines tested varied in length from 5 to 20 π-sections i.e. equivalent to 25 - 100 miles of 1-phase transmission line and the investigation commenced with the simplest model line configuration available i.e. the 5 π-section zero earth impedance line.

4.2 Modified Fourier Transform Responses

The processor responses for the 5 π-section line were initially compared with the waveforms obtained from a distributed-parameter line which were calculated using the Modified Fourier Transform incorporating σ_s.

The receiving-end response of an open-circuited transmission line due to the application of a voltage step was calculated from the inversion integral

$$V_r = \frac{1}{2\pi} \int_{-\Omega}^{\Omega} \frac{e^{(a + j\omega)t}}{(a + j\omega) \cosh d \{[R + (a + j\omega)L][(a + j\omega)C]\}^{1/2}} d\omega \qquad (4.1)$$

where the line parameters of series inductance, series resistance and shunt capacitance per mile used are for a 5 π-section model line. This allowed a straightforward comparison with the damped model line and processor responses so that scaling (see section 1.3.1) would not be required. Equation (4.1) is derived in reference[29] and was numerically integrated by the program written in Appendix III.1.

The receiving-end response obtained by evaluating (4.1) with Ω=1 MHz and dω=2 kHz can be seen in Figure 4.1(a) and shows the Gibbs phenomena due to the truncated frequency range. By including the Standard Sigma Factor of equation (1.16) in the integral equation the oscillations are effectively reduced but the rates of rise of the discontinuities are also affected (Figure 4.1(b)). The Standard Sigma Factor σ_s is shown to be effective in reducing the Gibbs oscillations using the upper frequency limit of integration Ω as the basis for local averaging.

4.3 The Experimental Standard Sigma Factor S_{se}

The receiving-end response for 1 pu step energisation of a 5 π-section uncompensated model line is shown in Figure 4.2. This is the model line equivalent to the waveform calculated by equation (4.1) i.e. Figure 4.1(a). In this case the Gibbs phenomena occur because the frequency content of the step input which exceeds the model cut-off frequency f_c is attenuated from the response.

The Gibbs content can be viewed as a high-frequency sinusoidal waveform superimposed on an essentially square wave, the initial oscillations being dependent on the L and C values of the π-section (equation (1.1)) and the 'square wave' a product of the line travel time and sending and

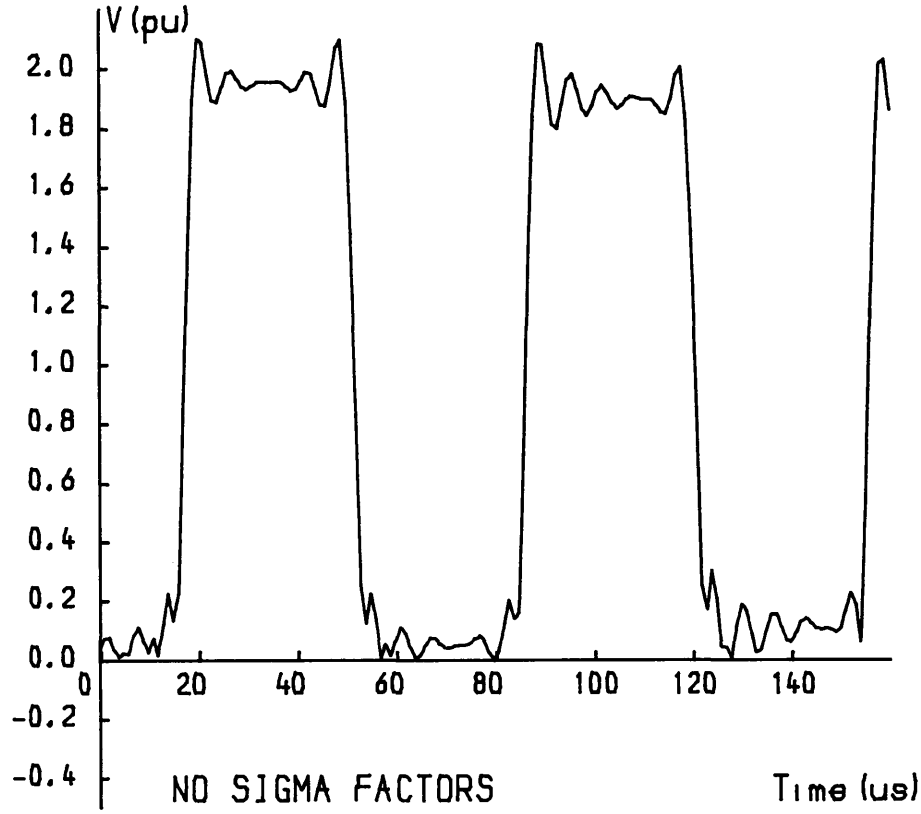

(a)

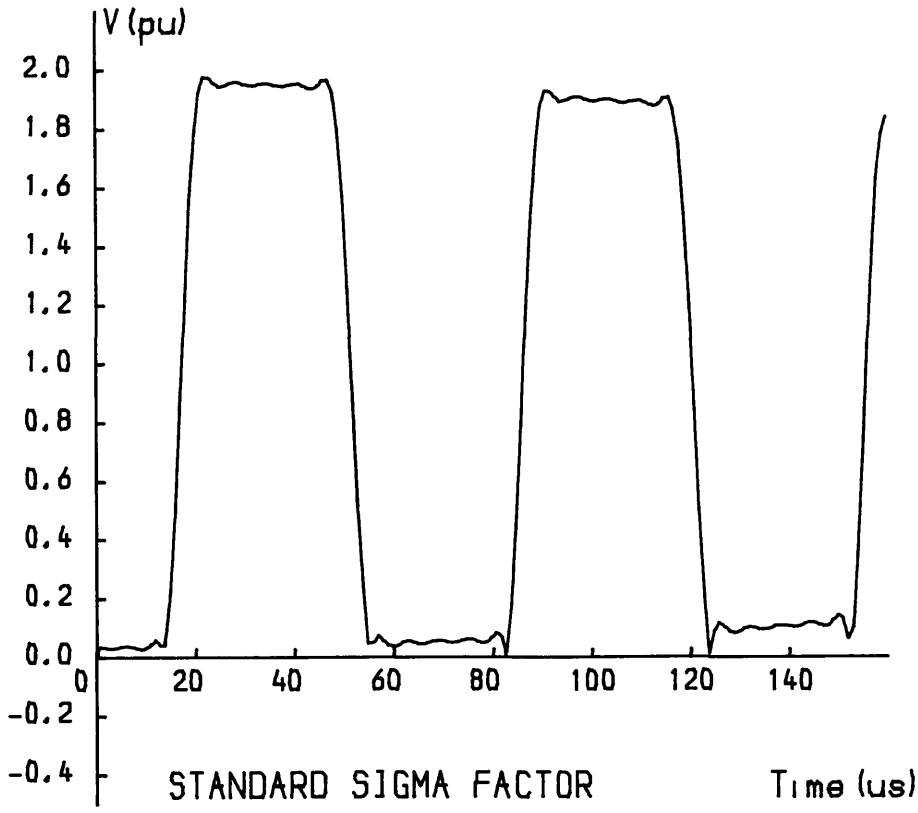

(b)

Figure 4.1(a) Receiving-end responses of an open-circuited 25 mile actual line calculated by the Modified Fourier Transform (b) σs significantly reduces the Gibbs phenomena.

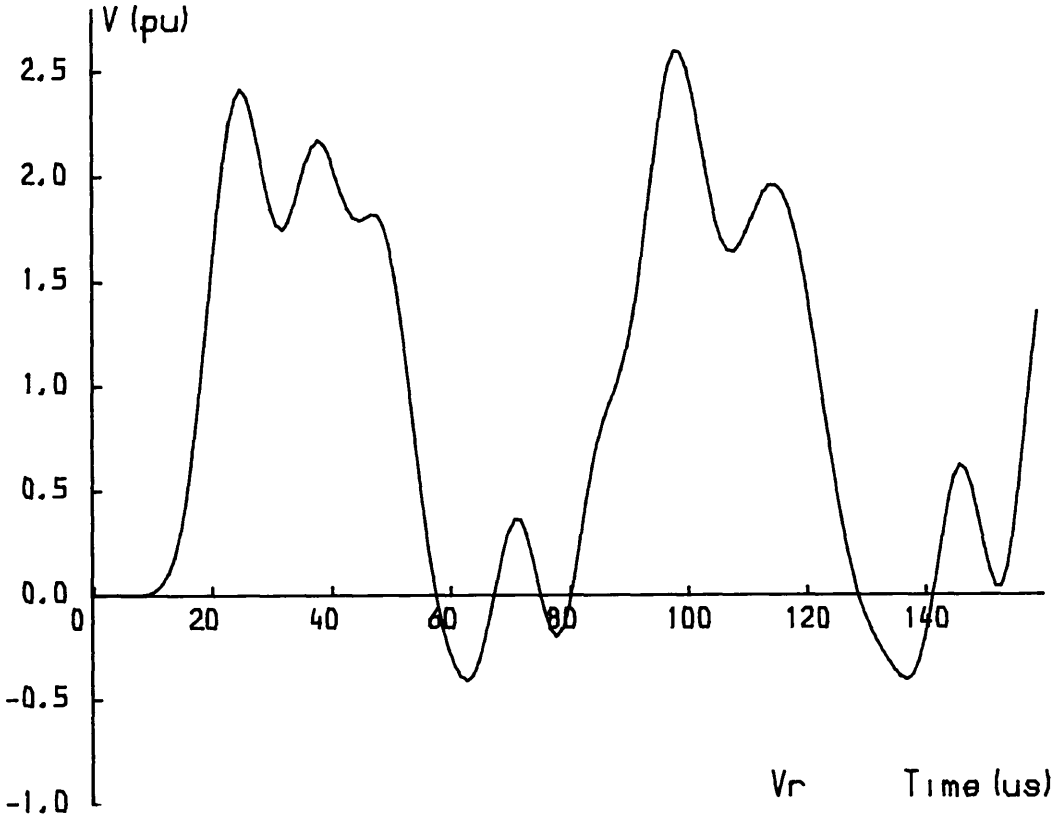

Figure 4.2 Receiving-end response of an open-circuited 25 mile uncompensated model line.

receiving-end conditions. The method of locally averaging a sine wave, represented by a number of discrete samples, forms the basis of the Experimental Standard Sigma Factor.

If a sine wave, as shown in Figure 4.3(a), is locally averaged over the period 'ae' in the time domain the result is zero. From the figure, the distance ac $\approx$ bd so that if the points B and D can be determined from the waveform then distance bd approximates to distance ac. If bd is now doubled this will give the period of the sine wave. Figure 4.3(b) is a representation of a sampled sine wave and indicates the first peak (sample 6) which must be detected. Its sample number n_{pk} is noted and the first trough is then determined by the software to give another sample value n_{tr} (in this case sample 16). So 'H' the 'half-range' value is calculated,

$$H = n_{tr} - n_{pk} \tag{4.2}$$

and N_s, defined as the Experimental Standard Averaging Range is determined,

$$N_s = 2H + 1 \tag{4.3}$$

where N_s is defined in microseconds. From Figure 4.3(b) H = 10 and therefore N_s = 21 μs assuming 1 sample/μs.

Implementing the Experimental Standard Sigma Factor S_{se} gives

$$v_{np} = \sum_{k = n - H}^{n + H} (v_k/N_s) \tag{4.4}$$

where v_{np} is the processed or processor voltage value of the n^{th} sample v_n of the uncompensated waveform. 'H' sample values before and after v_n are summed to v_n and the total is divided by N_s. This process is repeated for each uncompensated waveform sample giving the 'processor' response.

Using the technique described S_{se} can therefore be automatically determined from the initial Gibbs oscillation i.e. the region of the highest

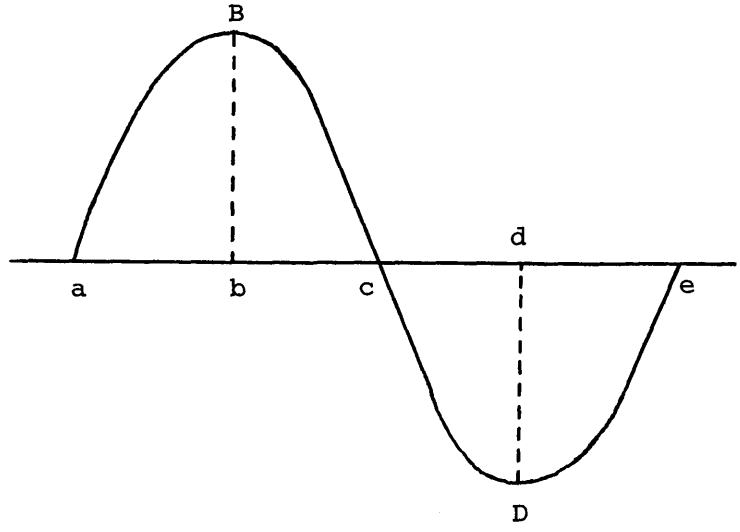

(a)

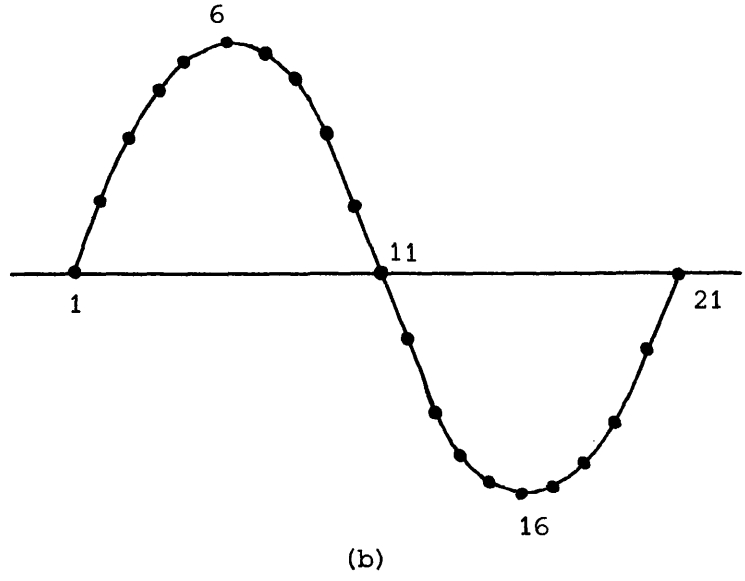

(b)

Figure 4.3 Determination of the sine wave period.

frequencies present in the response of Figure 4.2. Programming (4.4) in Z-2D software and implementing the software described in Chapter 3 allowed the Experimental Standard Sigma Factor S_{se} to be applied to the uncompensated waveforms.

4.4 Response of 1-phase Lines to Step Energisation

To investigate the ability of S_{se} to reduce model line Gibbs phenomena the simplest model line available from which responses could be obtained was chosen. This was the 5 π-section line with zero earth impedance of section 2.4 which was energised from an ideal DC source. This also allowed development of the Runge-Kutta method (Chapter 7), used to verify the model transients recorded, because of the relatively uncomplicated circuit model.

Earth-path impedance was also introduced to investigate frequency-dependent earth effects and allowed gradual development towards the more complex 3-phase model line.

4.4.1 Lines with Zero Earth Impedance

4.4.1.1. 25 Mile, 5 Π-Section Line

Figure 4.4 shows the receiving-end response from this uncompensated line due to DC excitation and the corresponding processor response using S_{se}. The processor waveform shows that the unwanted oscillations are effectively reduced by S_{se} but the initial rate of rise is also greatly reduced due to S_{se} being implemented from the beginning of the uncompensated waveform. As an initial improvement it was decided that the point at which S_{se} should become effective was where the two waveforms intersected, the processor response up to that point being copied directly by software from the uncompensated waveform itself. Averaging from this point improved the continuity of the processor waveform as averaging beginning earlier or later did not achieve this (see Figures 4.5(a) and (b)). The software was modified accordingly and the response of this line with and without

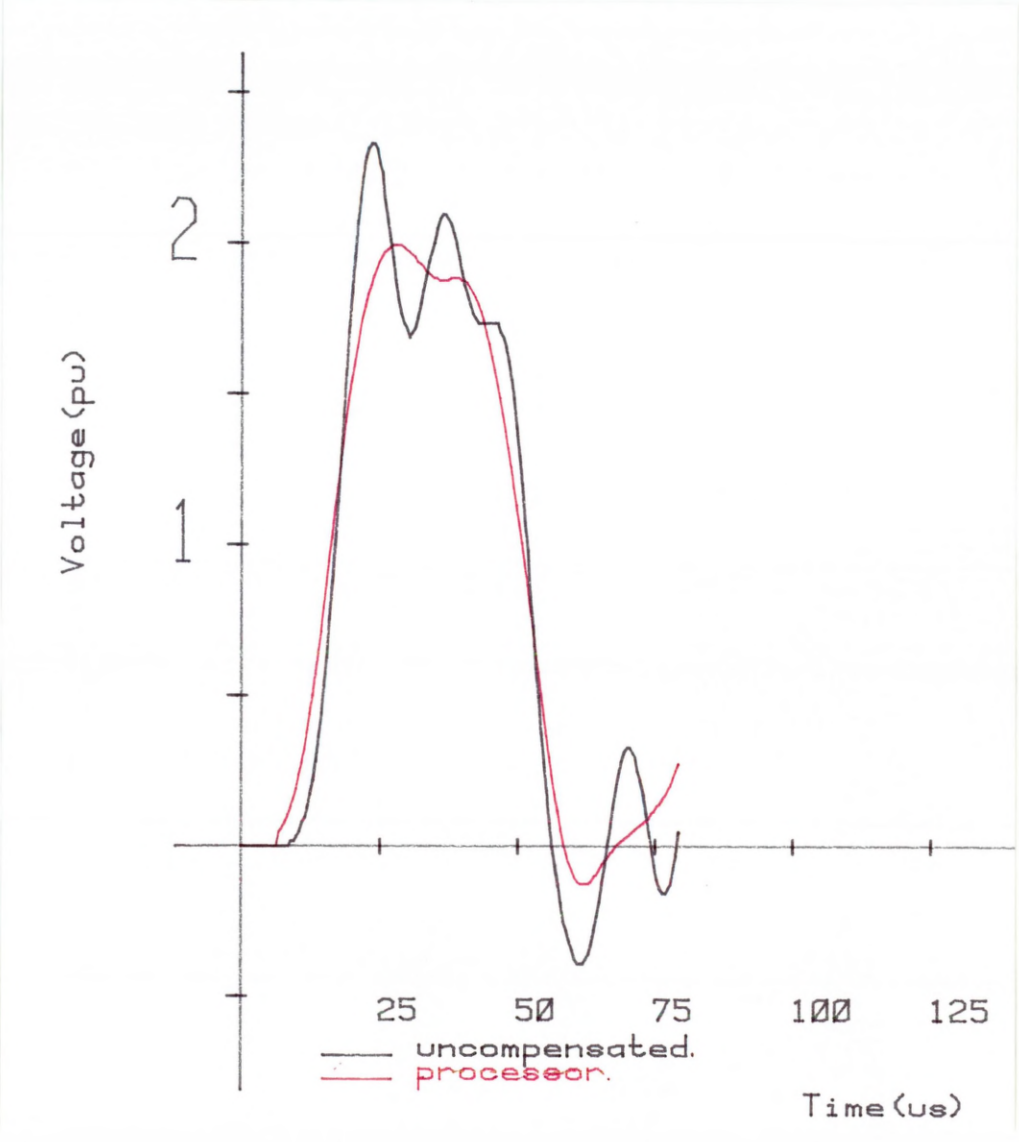

Figure 4.4 S_{se} implemented from t = 0 reduces the initial rate of rise.

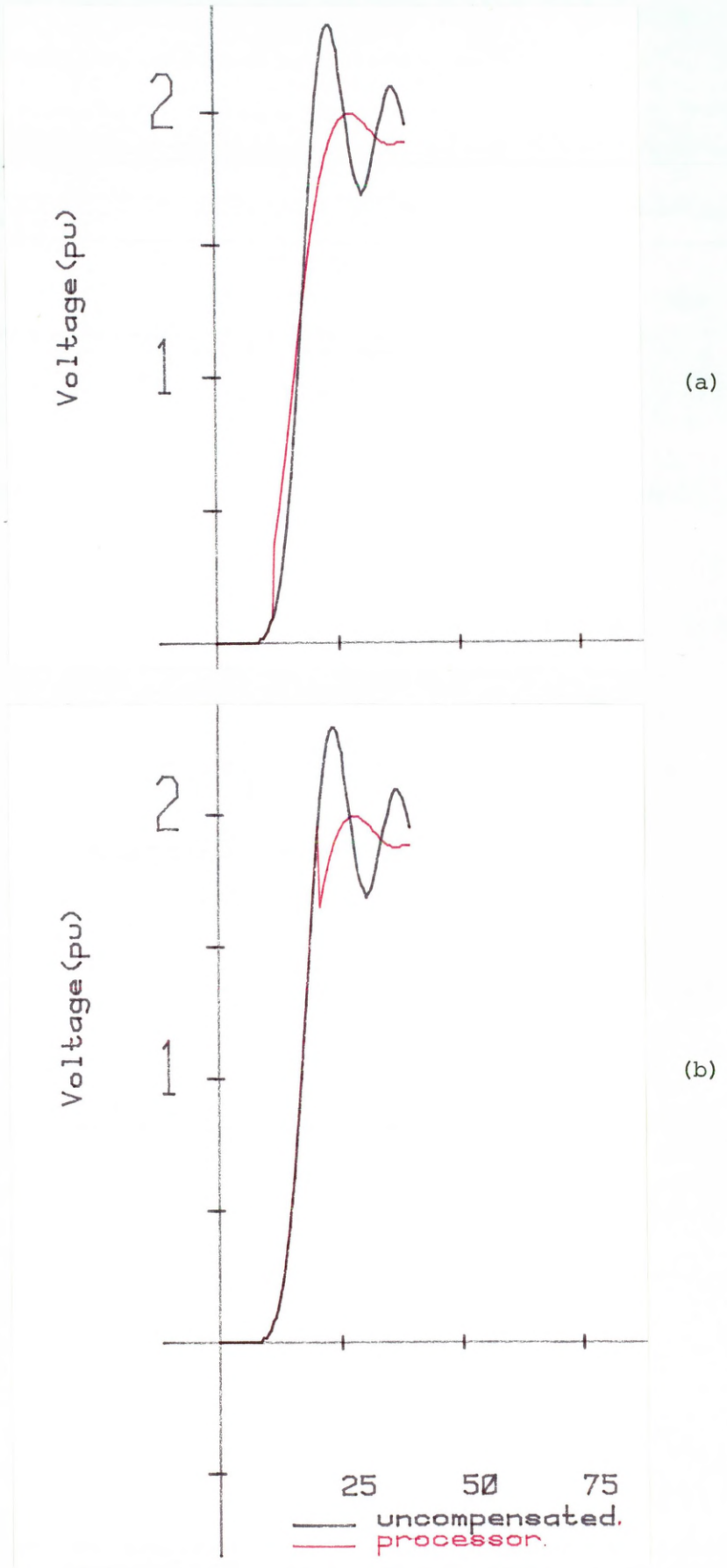

Figure 4.5 Loss of processor response continuity due to averaging being implemented (a) too early; (b) too late.

resistor damping was then recorded (Figures 4.6(a) - (d)).

The Standard Averaging Range N_s was automatically determined from the uncompensated response as 15 μs and the processor response calculated shows that the oscillations are reduced quite effectively for the whole waveform using this value of N_s. A 15 μs period corresponds to a Gibbs frequency of 66.7 kHz which is approximately equivalent to the natural π-section frequency of 65.18 kHz. From the initial surges of the uncompensated response (Figure 4.6(a)) it appears that although the Gibbs Oscillations are not constant in frequency S_{se} significantly reduces their voltage magnitudes. The processor response also displays improved rates of rise at the discontinuities (apart from the initial rate of rise) and improved global response when compared to the resistor-damped waveform which after the first transient cycle displays the effects of the increased line attenuation. In commenting on the initial rate of rise of the processor waveforms this characteristic is considered from the point where S_{se} is implemented as the processor waveform up to that point is copied directly from the uncompensated response.

However the processor response lies outwith the expected 0 - 2 pu range in the region 90 - 500 μs even though Gibbs phenomena are not apparent. This implies that the averaging range N_s calculated is not effective in this region. Therefore N_s was varied to 13 and 17 μs by changing H by ±1 and the processor waveforms for these averaging ranges are shown in Figures 4.7 and 4.8 respectively.

With N_s equal to 13 μs the initial surge and rate of rise are improved and more closely resemble the resistor-damped response but subsequent surges show however that the Gibbs phenomena are not so successfully reduced. By increasing N_s to 17 μs the initial rate of rise is poorer than in the processor responses previously obtained although subsequent reflections show a slight improvement with respect to voltage

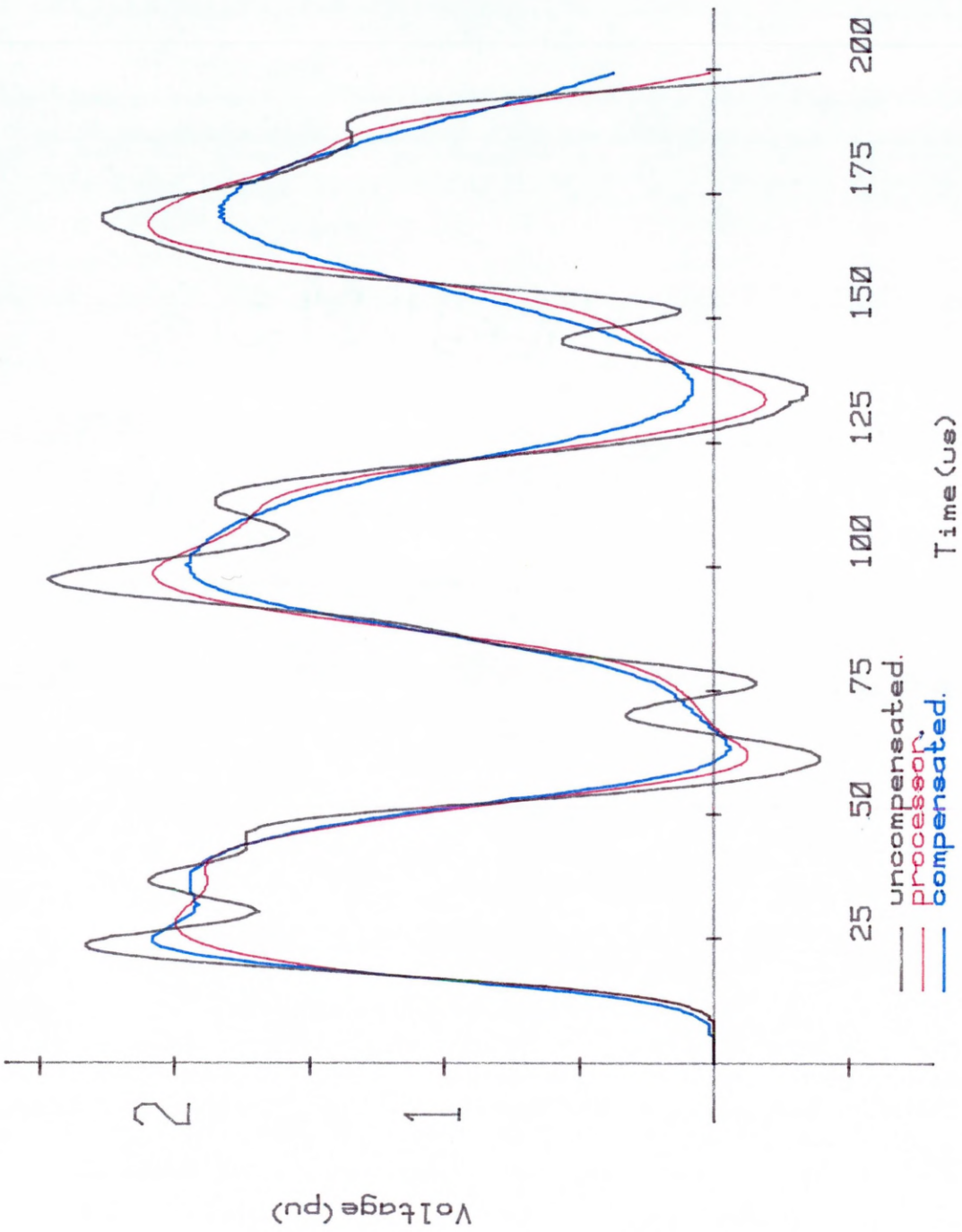

Figure 4.6(a) Responses of 5 pi-section lines with zero earth impedance (0 - 200 μs). Processor response calculated by S_{se} with N_s = 15 μs.

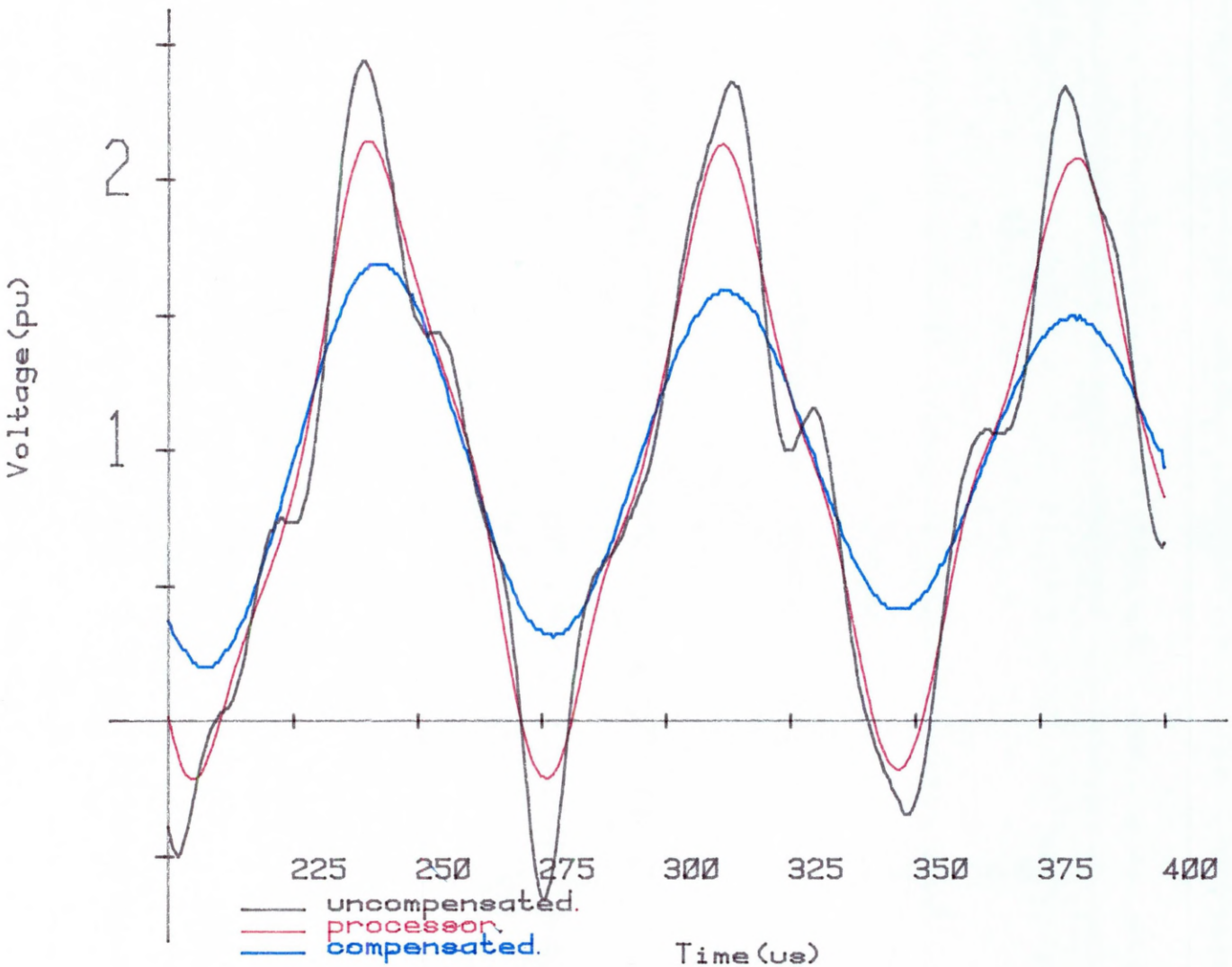

Figure 4.6 (cont'd) (b) 200 - 400 us.

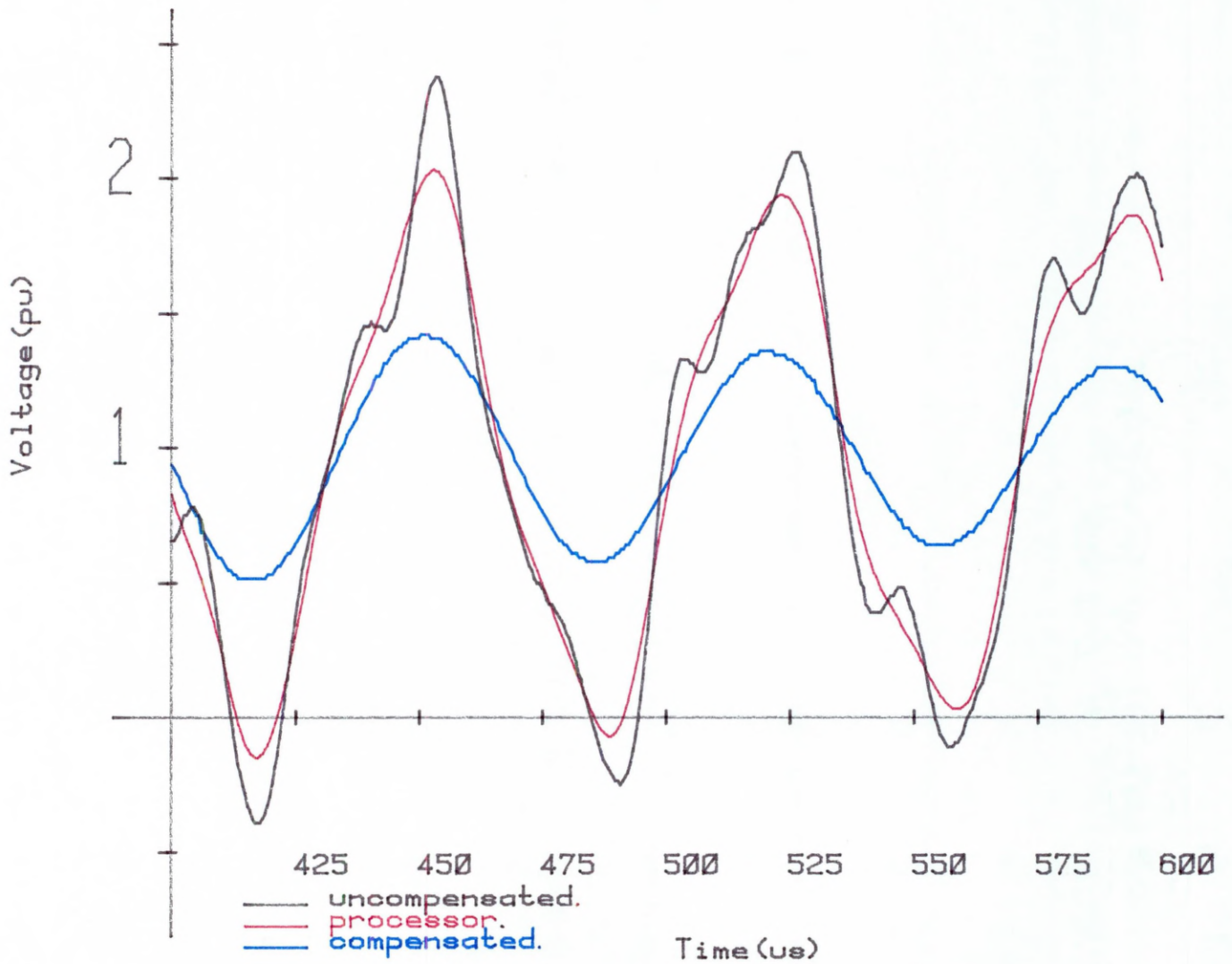

Figure 4.6 (cont'd) (c) 400 - 600 us.

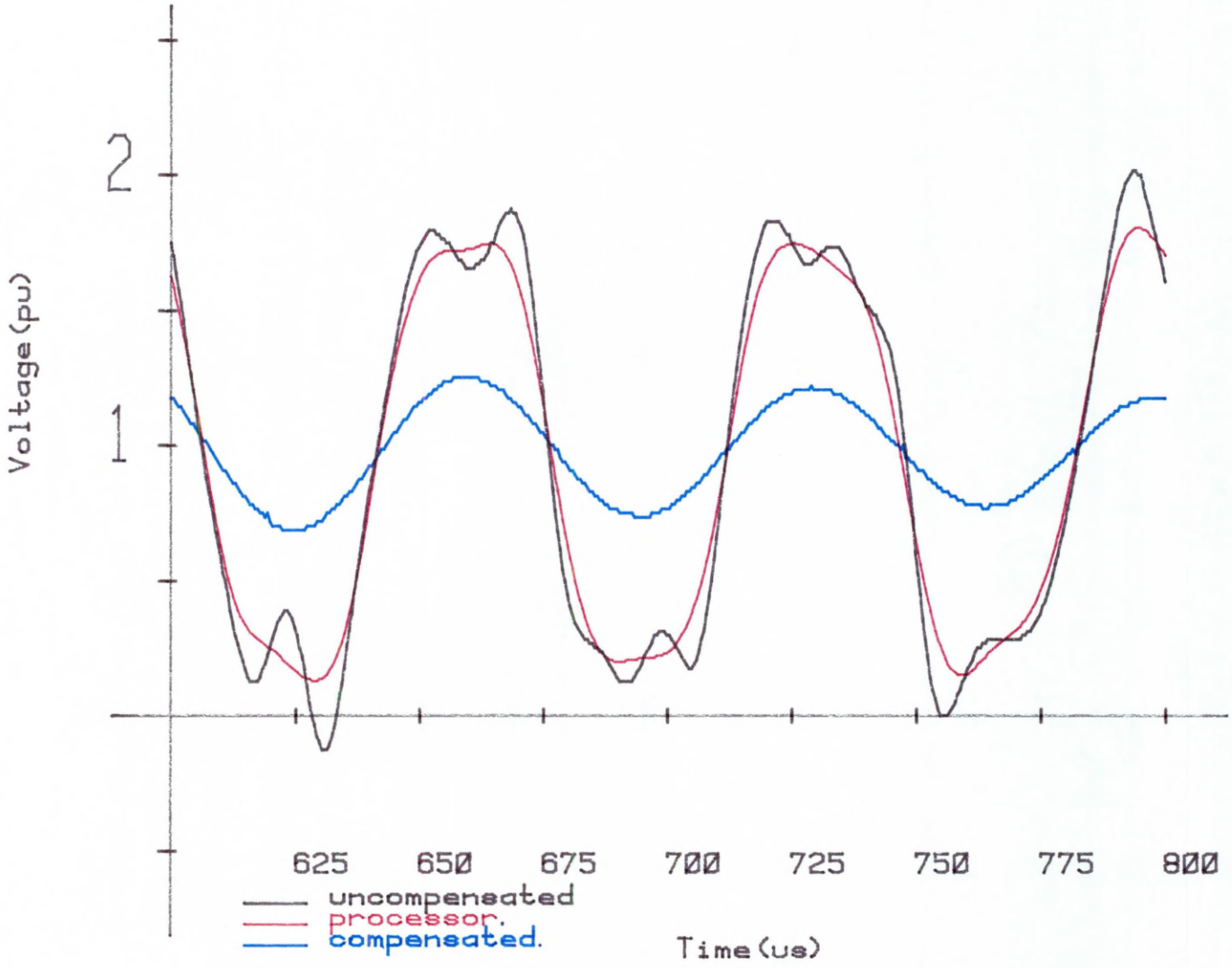

Figure 4.6 (cont'd) (d) 600 - 800 us.

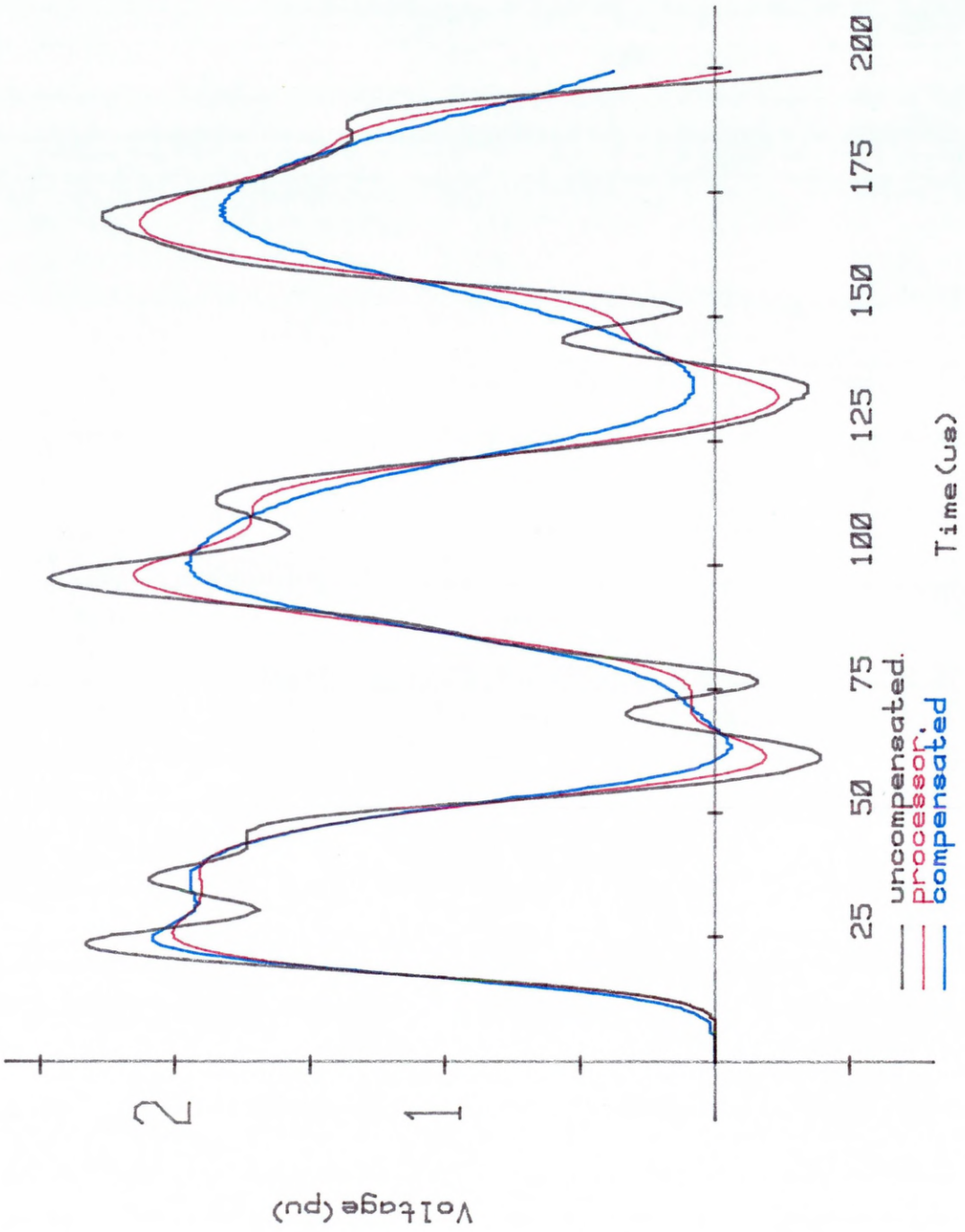

Figure 4.7 5 pi-section zero earth impedance line responses.
Processor response calculated by S_{se} with N_s = 13 μs.

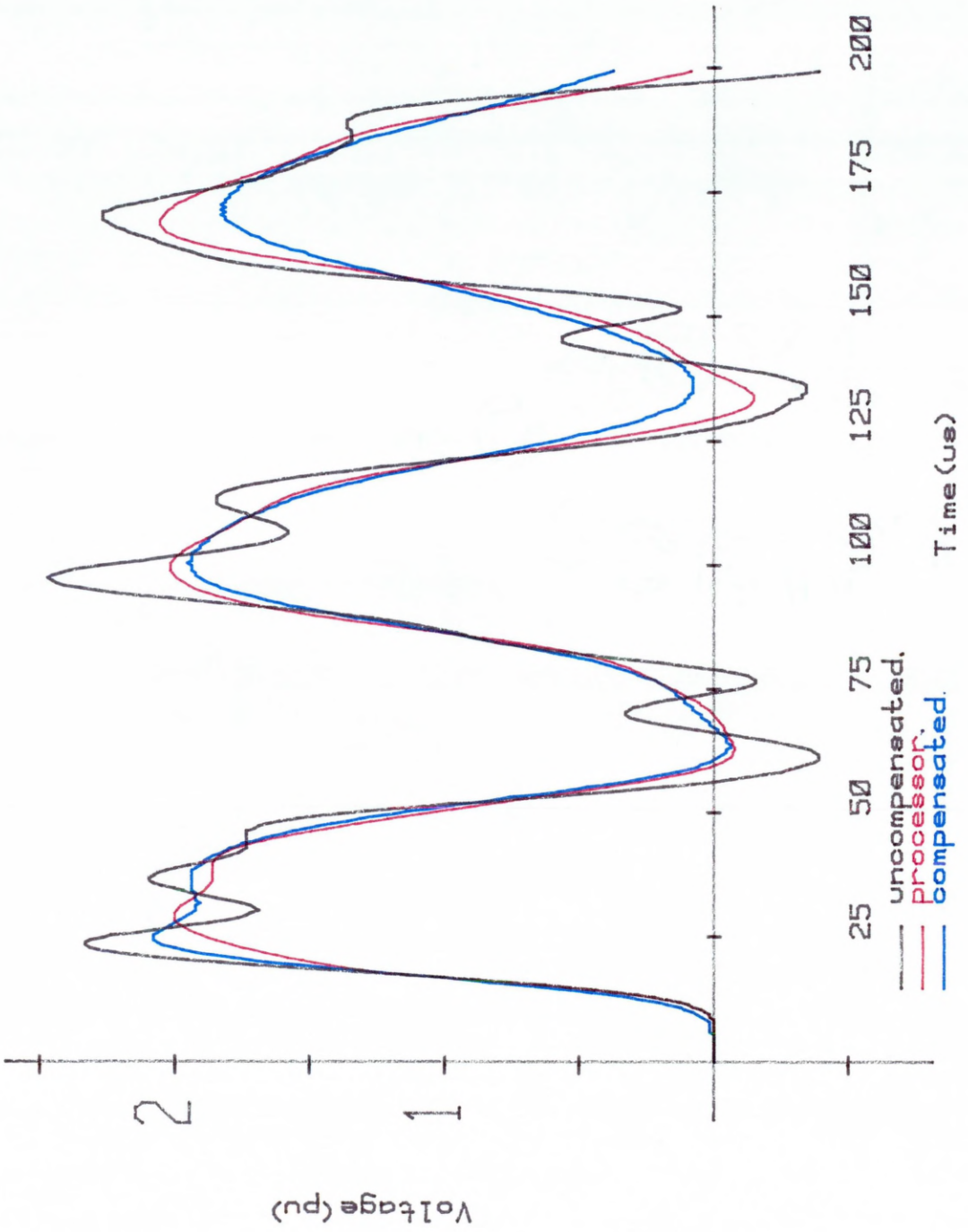

Figure 4.8 5 pi-section zero earth impedance line responses.
Processor response calculated by S_{se} with N_s = 17 μs.

magnitude i.e. those parts of the processor responses outside the 0 - 2 pu range. The greater averaging range however reduces all processor waveform rates of rise.

These observations indicate that the high-frequency Gibbs content of the uncompensated waveform changes with time.

The transient fundamental frequency for this line was determined from the responses as 14.3 kHz.

4.4.1.2. 50 Mile, 10 Π-Section Line

The 10 π-section responses in Figures 4.9(a) - (c) show the processor waveform calculated by the automatically determined N_s of 17 μs. Although the Gibbs phenomena of the initial surge are significantly reduced in magnitude, the processor response still displays a small high-frequency content in this region. S_{se} then becomes ineffective for subsequent surges until approximately 1600 μs. After this time the uncompensated waveform no longer displays a square-wave characteristic and N_s again becomes relatively successful in reducing the remaining high-frequency uncompensated waveform components. A higher value of N_s may then satisfactorily reduce all the Gibbs phenomena apparent in the uncompensated response after this time.

By using an operator-defined value of N_s of 13 μs an improved initial rate of rise, steeper than in the damped case, is obtained (Figure 4.10). The initial surge is also improved and no longer displays the small high-frequency content previously observed. However subsequent processor reflections are poorer due to the shorter averaging range. This value of N_s corresponds to a frequency of 76.9 kHz which is significantly higher than f_0.

It is also noticeable that the envelope of positive and negative peaks of the uncompensated waveform appears to decrease and then increase when it might be expected that the envelope would gradually attenuate in a similar fashion to that of the compensated response.

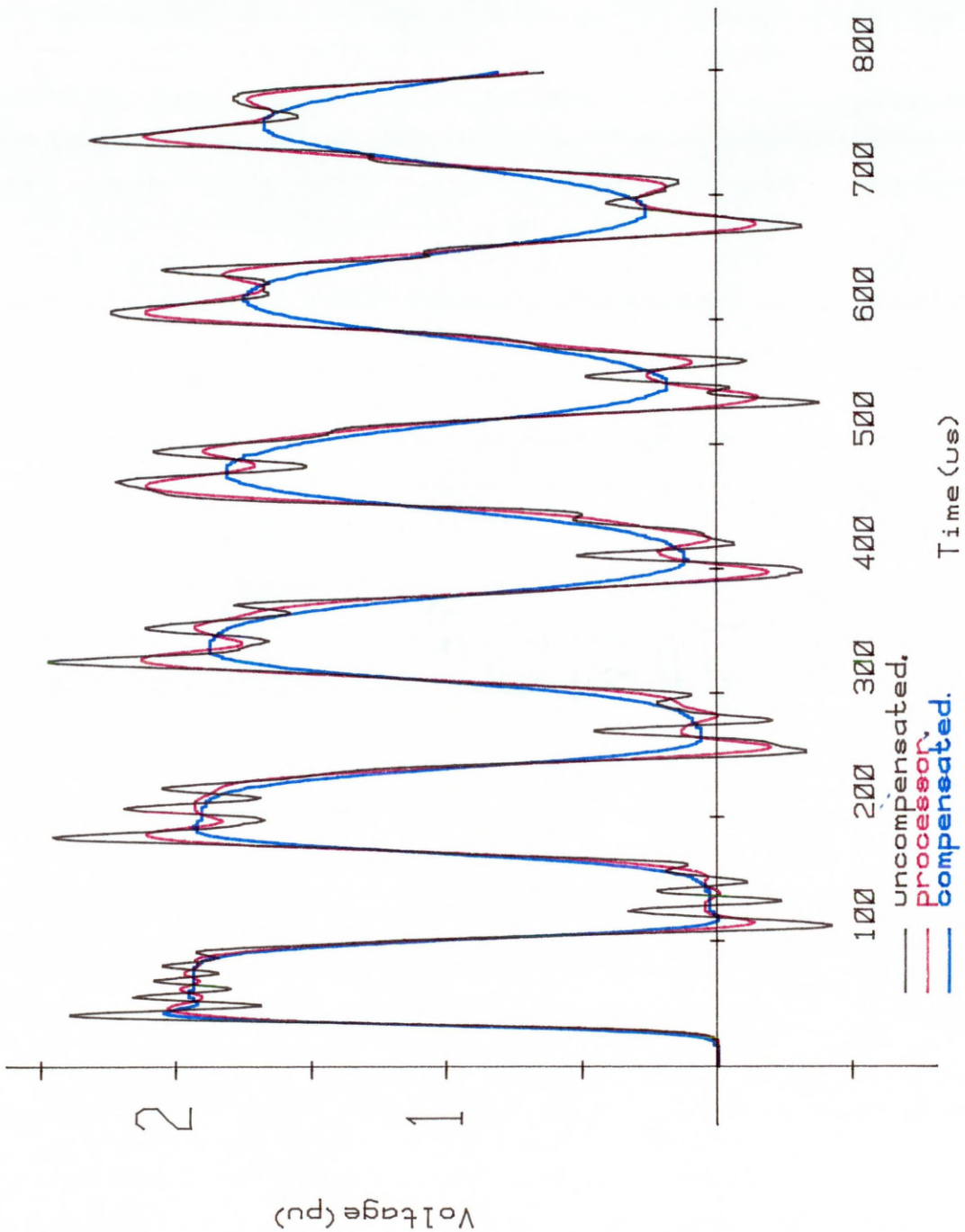

Figure 4.9(a) Responses of 10 pi-section lines with zero earth impedance (0 - 800 μs). Processor response calculated by S_{se} with N_s = 17 μs shows S_{se} to be ineffective.

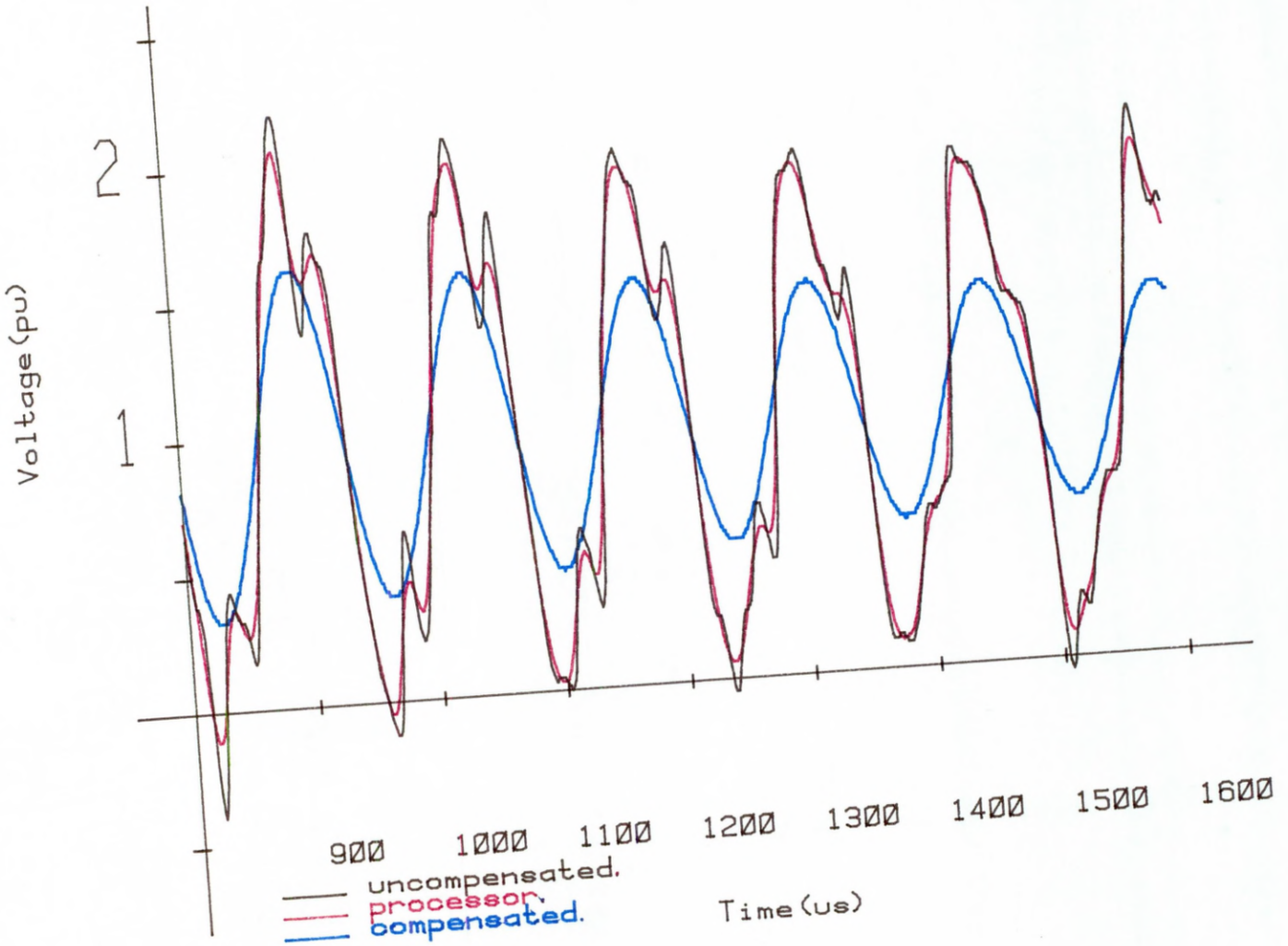

Figure 4.9 (cont'd) (b) 800 - 1600 μs.

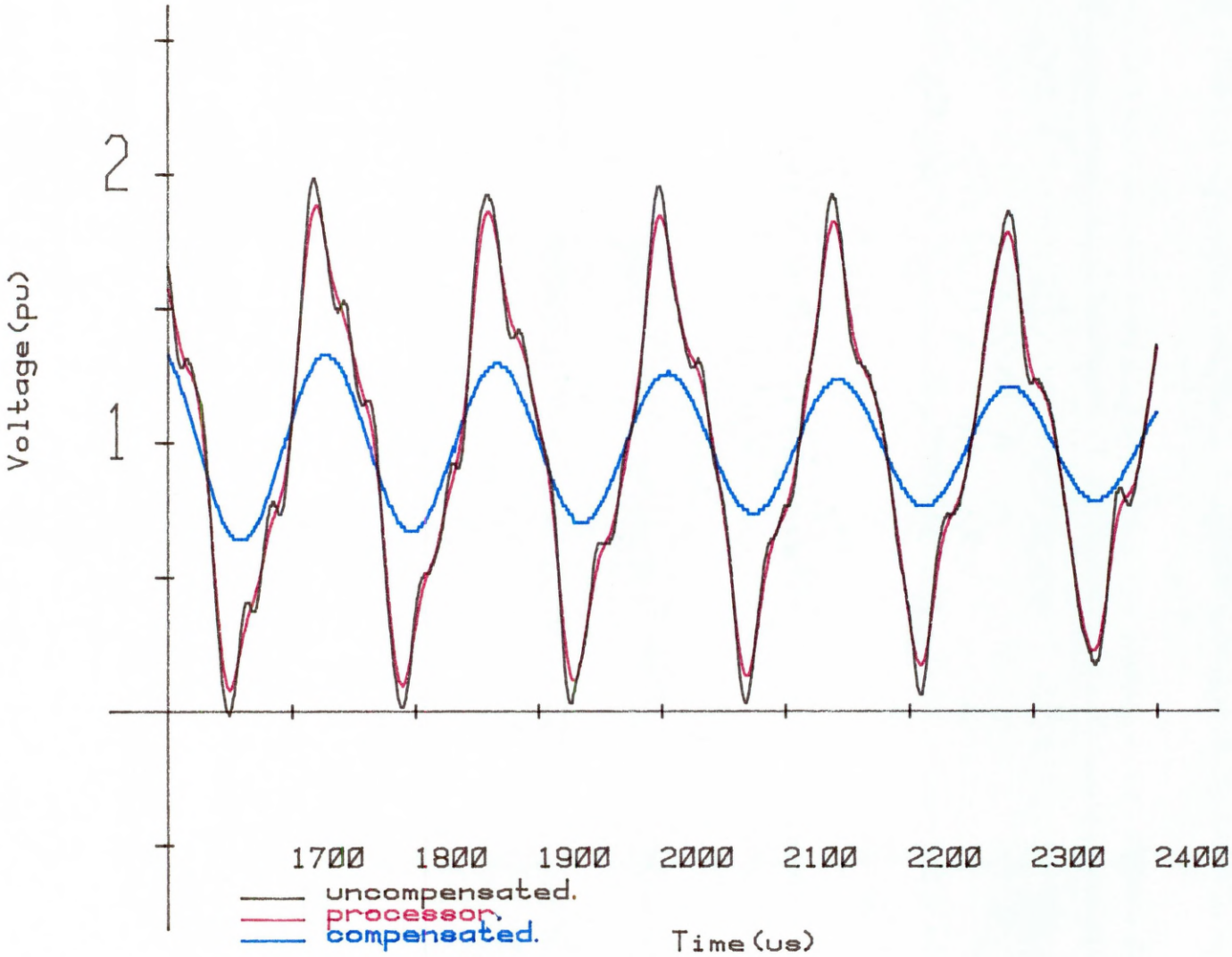

Figure 4.9 (cont'd) (c) 1600 - 2400 µs.

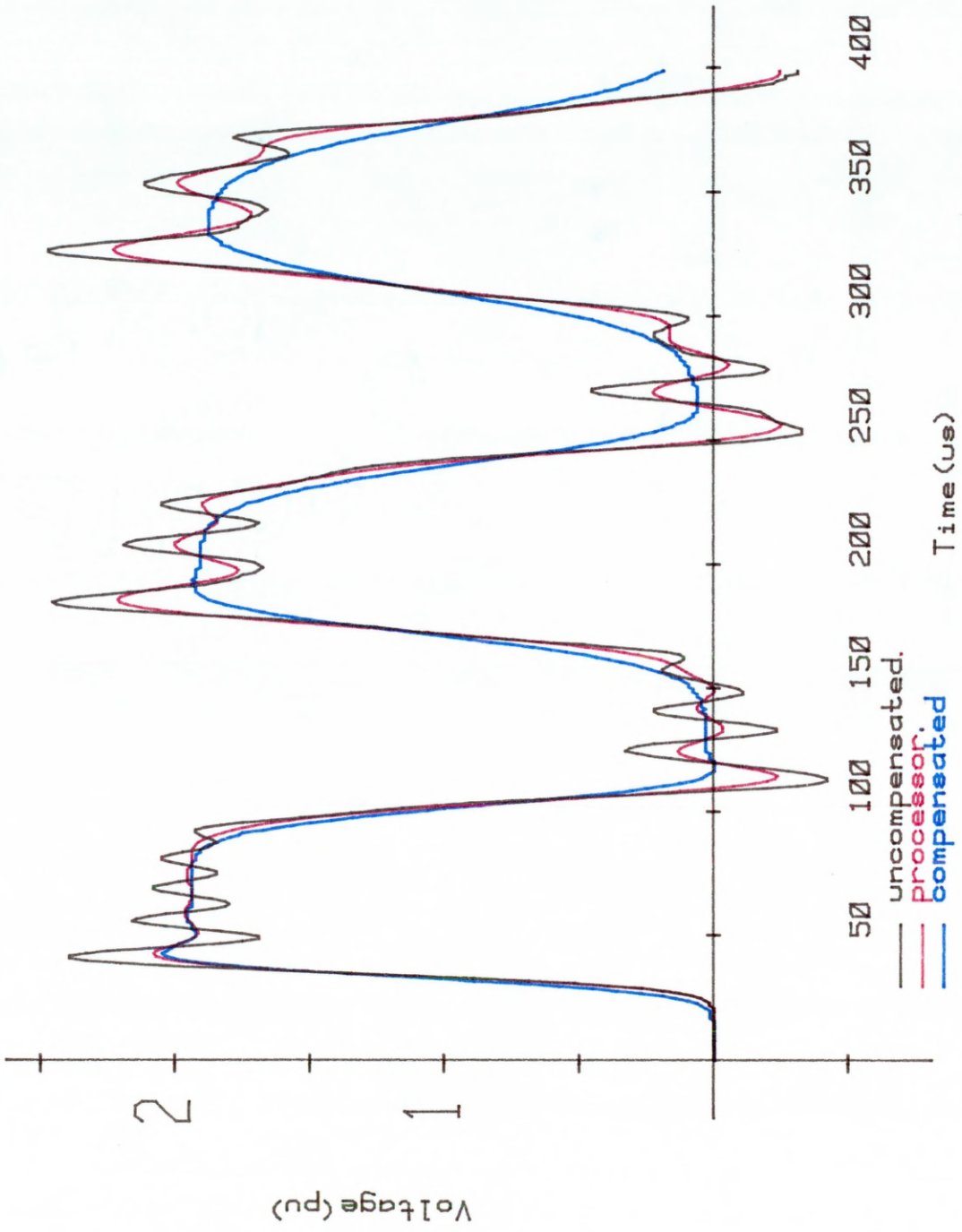

Figure 4.10 10 pi-section zero earth impedance line responses.
Processor response calculated by S_{se} with N_s = 13 μs.

The transient fundamental frequency was measured as 7.25 kHz.

4.4.1.3. 100 Mile, 20 Π-Section Line

The 20 π-section responses of Figures 4.11(a) - (e) emphasised the previous findings, the processor response being calculated with an averaging range of 21 μs. This averaging range again becomes quickly ineffective (after only 350 μs) while varying N_s, as before, to 17 μs improved the initial processor surge and initial rate of rise (Figure 4.12). The latter value of N_s corresponds to a frequency of 66.7 kHz. Therefore the oscillations predominant in the first surge of the uncompensated waveform are again close, in frequency, to the natural π-section frequency f_0.

However the uncompensated response clearly shows that frequencies of this order are attenuated after only one transient fundamental cycle. As the frequency of the Gibbs content decreases, each subsequent lower frequency is apparent in the response for an increasing period of time. The global response in this case remains square-wave in character, as opposed to the 5 and 10 π-section lines cases, and after 3500 μs (see Figure 4.11(e)) closely resembles a waveform containing only fundamental and 3rd harmonic components.

The transient fundamental frequency of the 20 π-section line was determined as 3.61 kHz.

4.4.2 Lines with Earth-Path Impedance

The model line used in section 4.4.1.1 was then modified to include the frequency-dependent R-L earth-path network of the 3-phase line. Since the mutual coupling components C_m and L_m were also situated in the model earth-return path (Figure 1.2) these components were included in the circuit modification. The receiving-end responses to DC energisation for 5, 10 and 20 π-sections were then recorded.

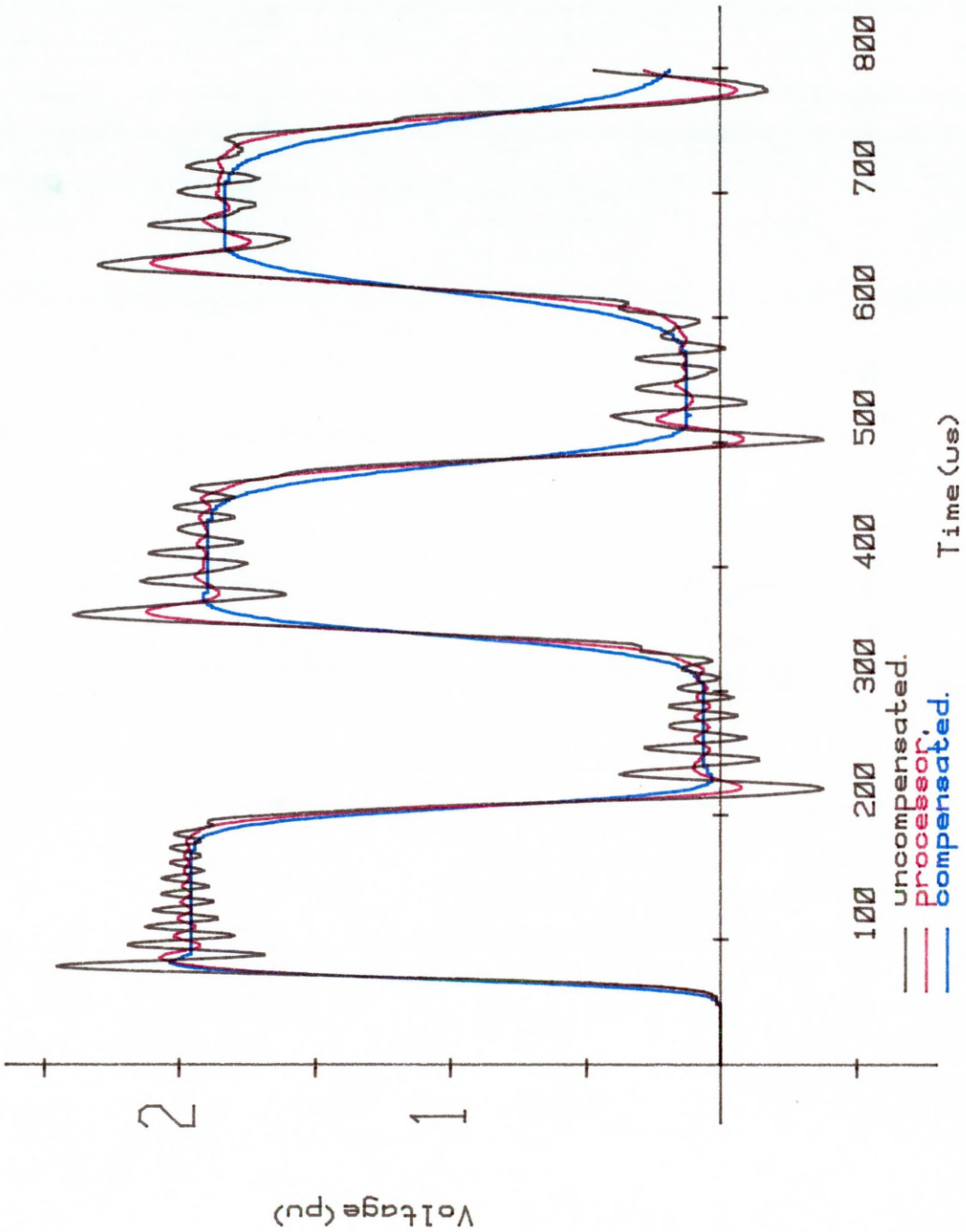

Figure 4.11(a) Responses of 20 pi-section lines with zero earth impedance (0 - 800 μs). Processor response calculated by S_{se} with N_s = 21 μs.

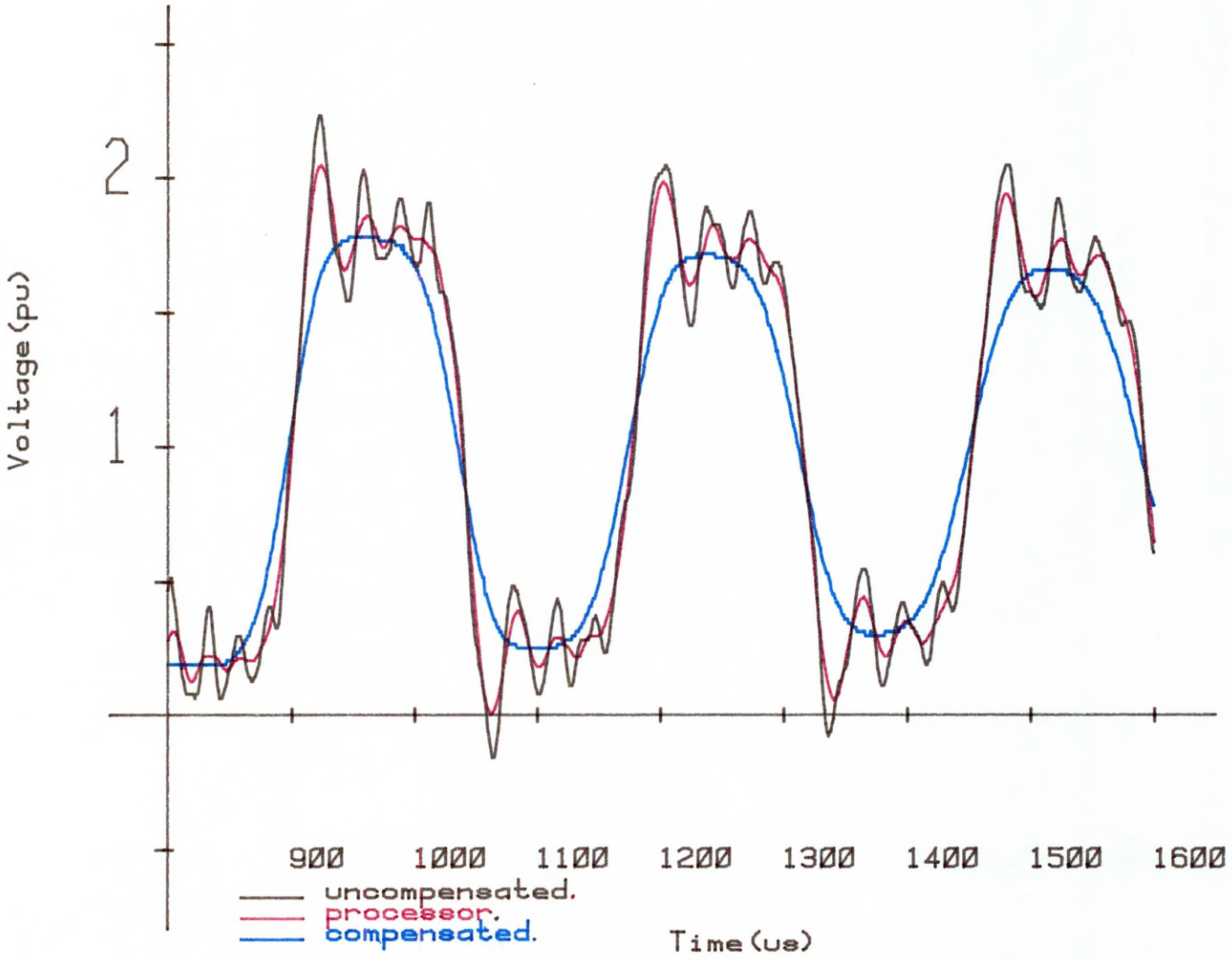

Figure 4.11 (cont'd) (b) 800 - 1600 μs.

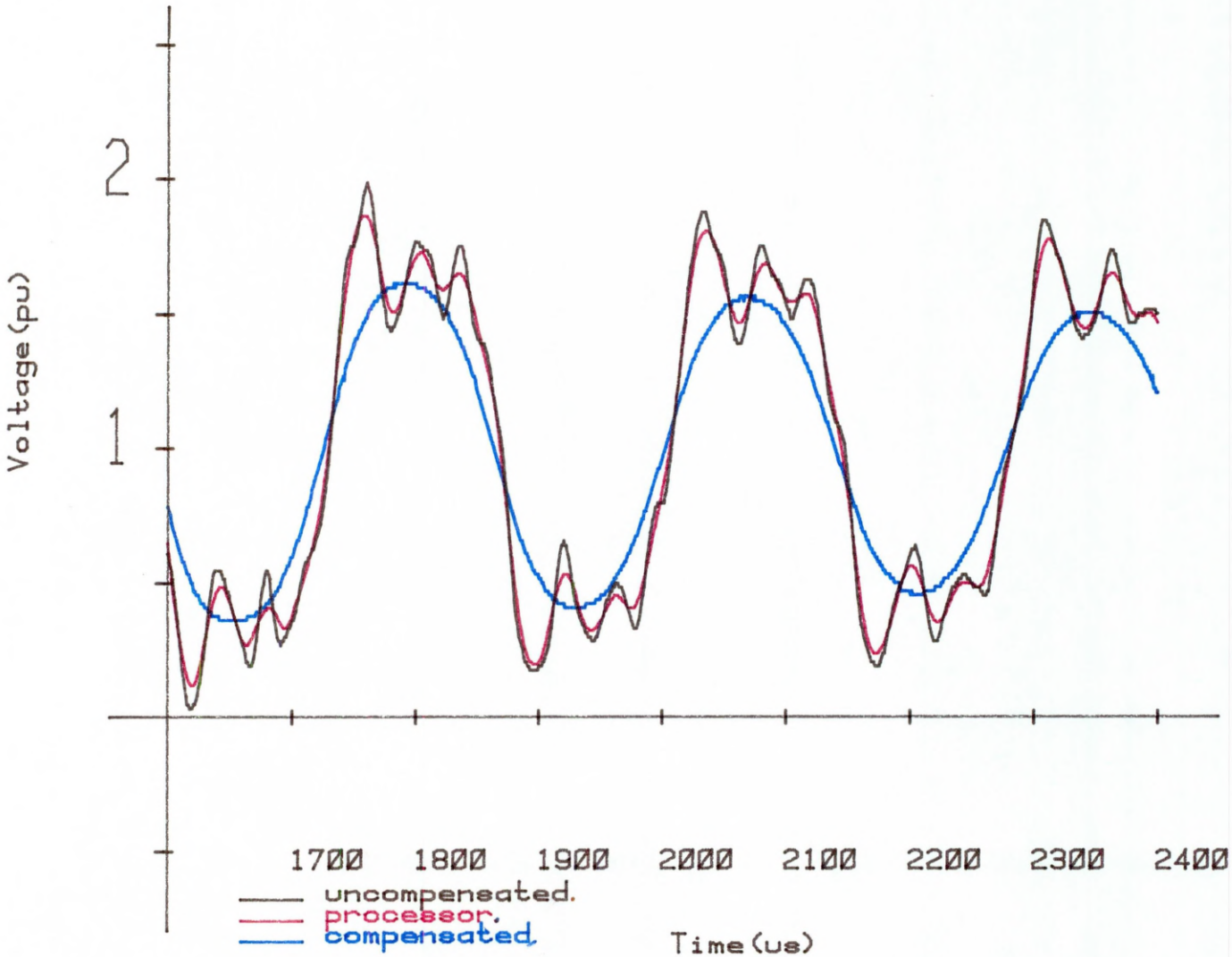

Figure 4.11 (cont'd) (c) 1600 - 2400 us.

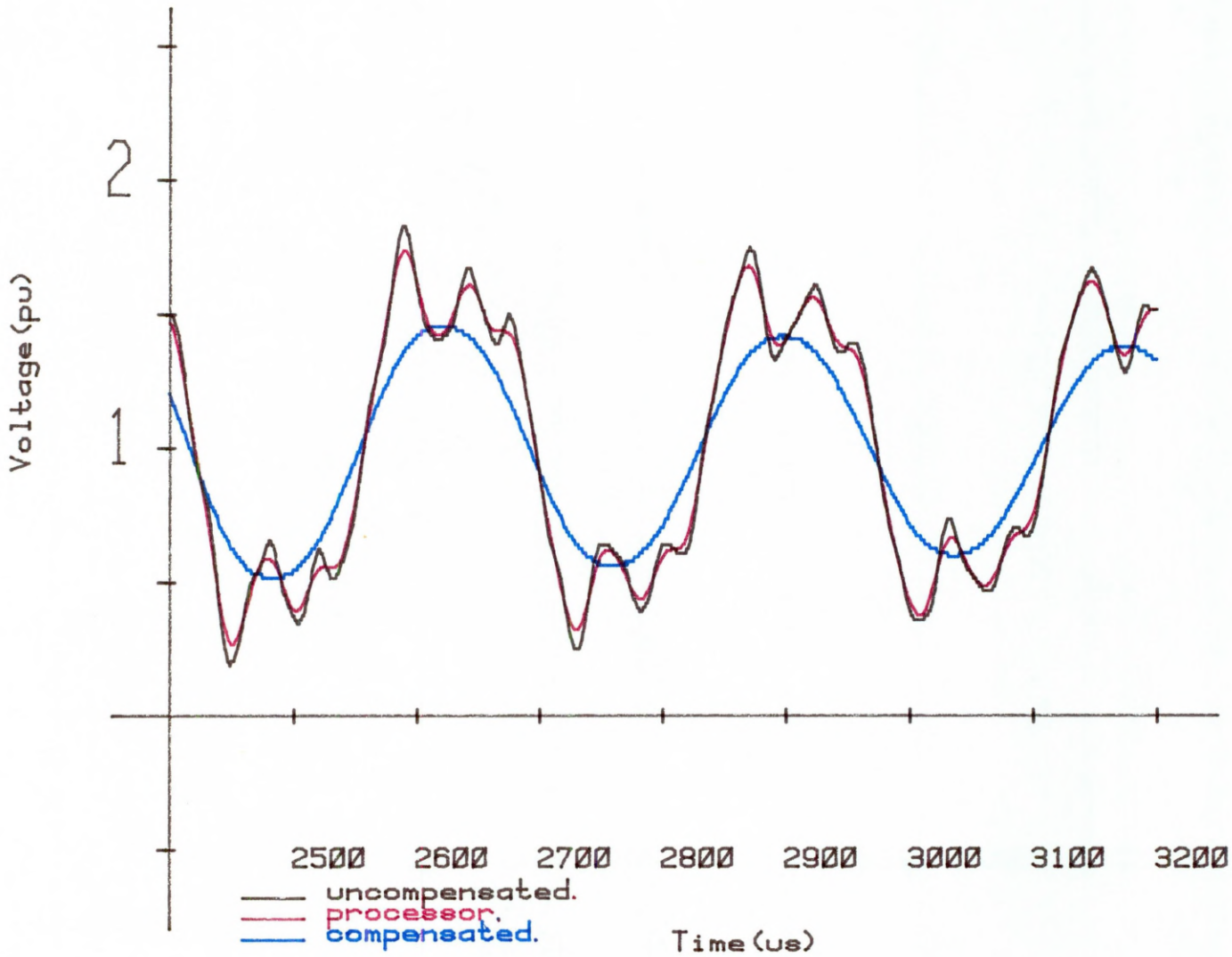

Figure 4.11 (cont'd) (d) 2400 - 3200 μs.

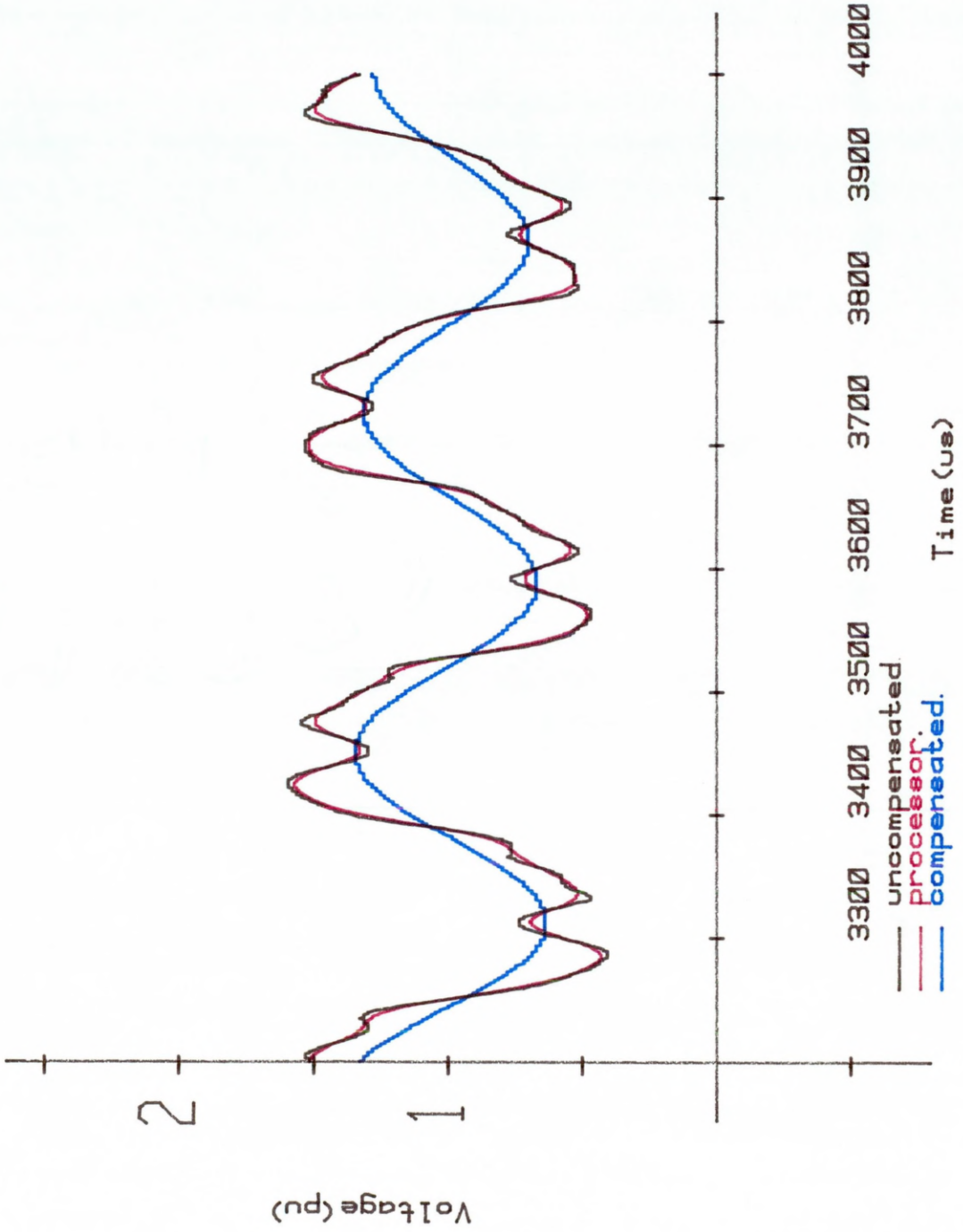

Figure 4.11 (cont'd) (e) 3200 - 4000 μs.

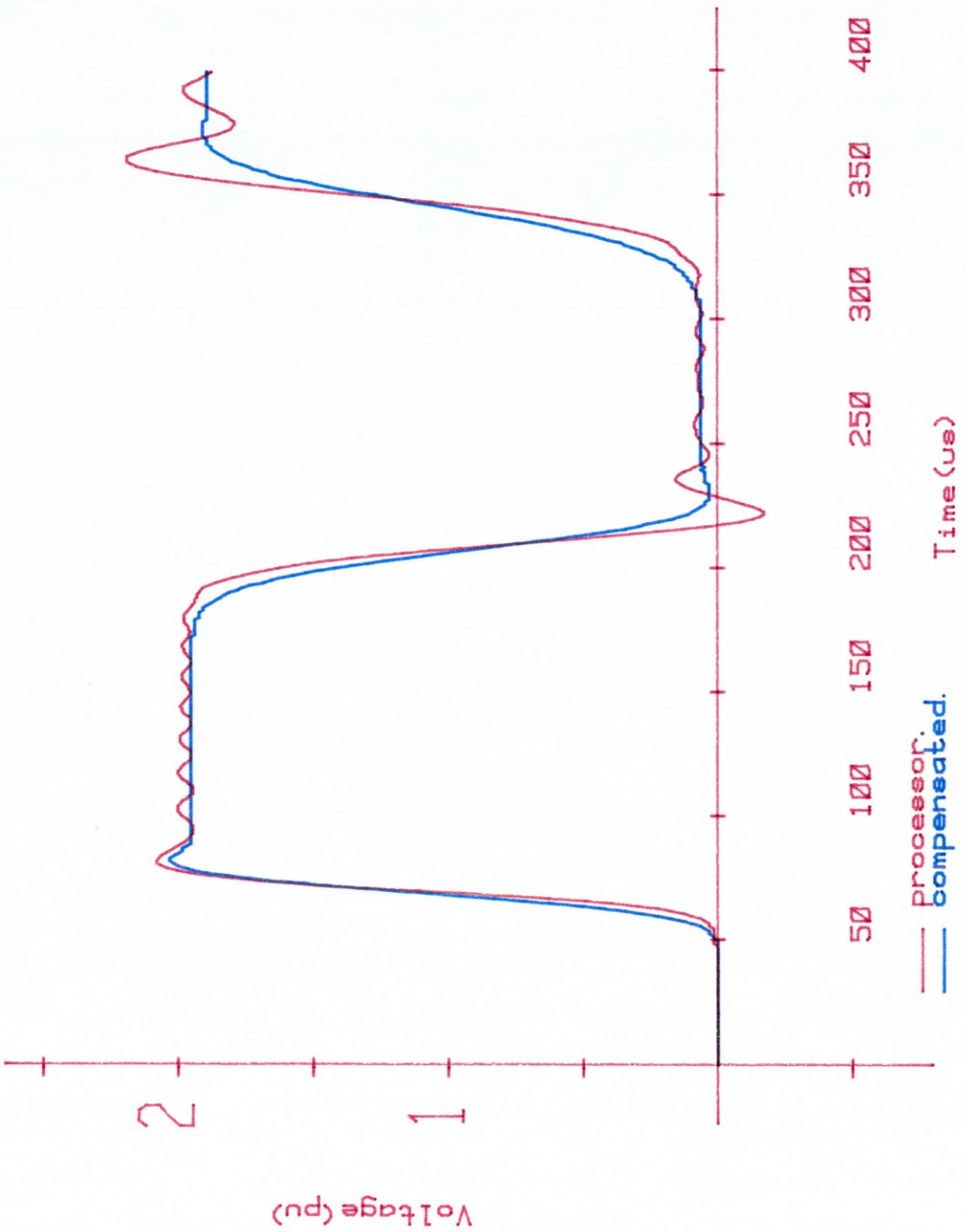

Figure 4.12 20 pi-section zero earth impedance processor and compensated waveforms. Processor response calculated by S_{se} with N_s = 17 μs.

4.4.2.1. 25 Mile, 5 Π-Section Line

The 5 π-section line receiving-end waveforms of Figures 4.13(a) - (b) show that the uncompensated response is initially similar to that obtained in the zero earth impedance line case but that the high-frequency Gibbs content is attenuated from the response after only 200 μs. This is due to the effect of the stratified-earth R-L ladder circuit where the minimum impedance 'seen' by the high-frequencies in this network will be the 69Ω resistor. The earth-path model also subjects the transient fundamental to increased attenuation which is apparent from the reduced rates of rise of the uncompensated waveform discontinuities and the global response.

The processor response calculated with N_s=15 μs was the most effective averaging range for reducing the high-frequency content and the processor waveform is an overall improvement on the resistor-damped response with the exception of the initial rate of rise.

4.4.2.2. 50 Mile, 10 Π-Section Line

The effect of the earth-path network can again be seen in the 10 π-section line responses of Figures 4.14(a) - (b). The changing high-frequency content which was apparent in the uncompensated response from the equivalent zero earth impedance line is not observed and the uncompensated waveform exhibits no Gibbs phenomena after 300 μs. The processor response, again calculated with N_s=15 μs, although displaying a small oscillatory content in the initial surge is an improvement over the damped response. The exception to this is again the initial rate of rise but for this line length it is closer to the damped response discontinuity than was observed in the 5 π-section case.

4.4.2.3. 100 Mile, 20 Π-Section Line

Figures 4.15(a) - (b) show the three responses from the 20 π-section line with the processor response calculated with N_s equal to 19 μs. The Gibbs phenomena are no longer observed in the uncompensated

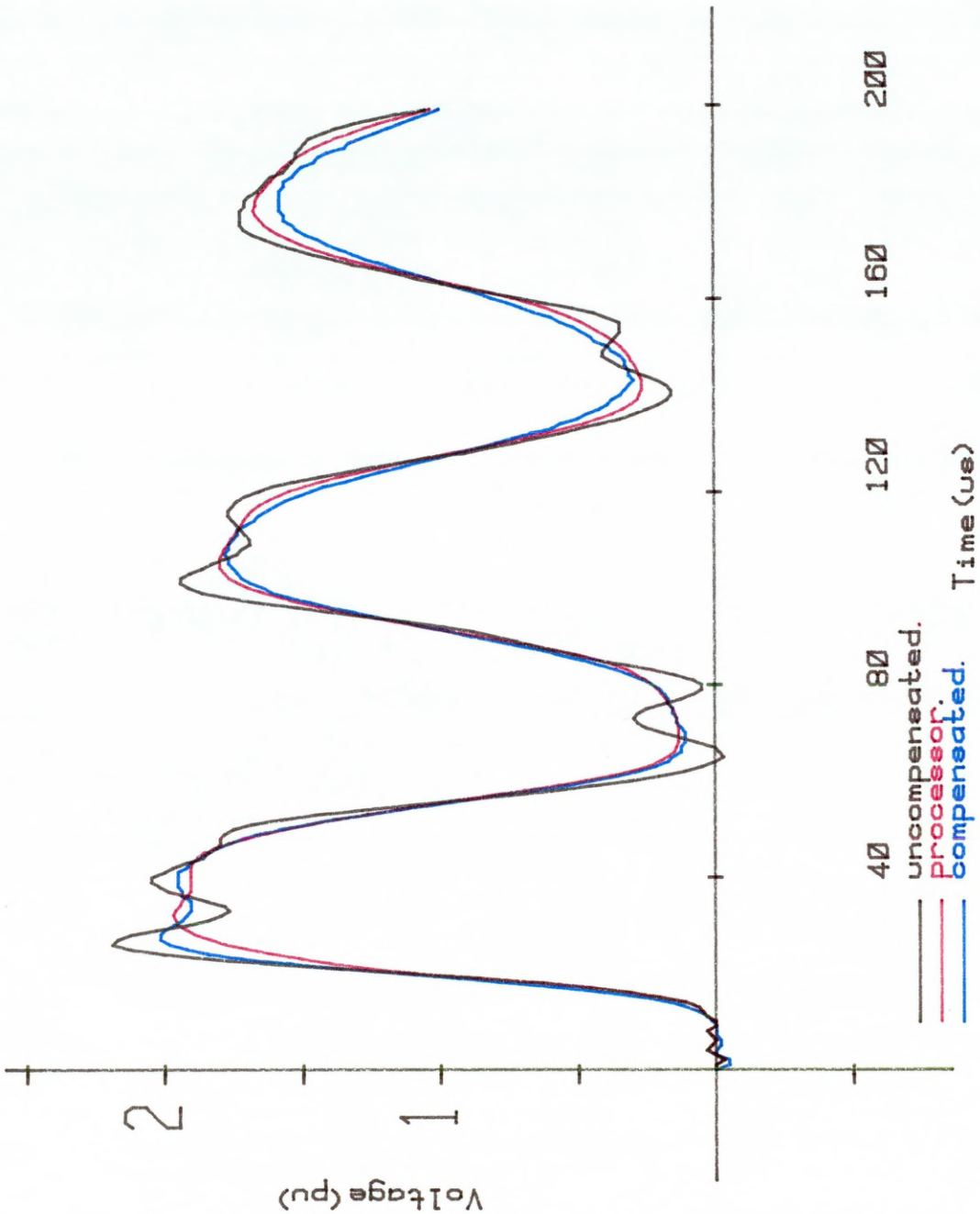

Figure 4.13(a) Responses of 5 pi-section lines with earth-path impedance (0 - 200 μs). Processor response calculated by S_{se} with N_s = 15 μs.

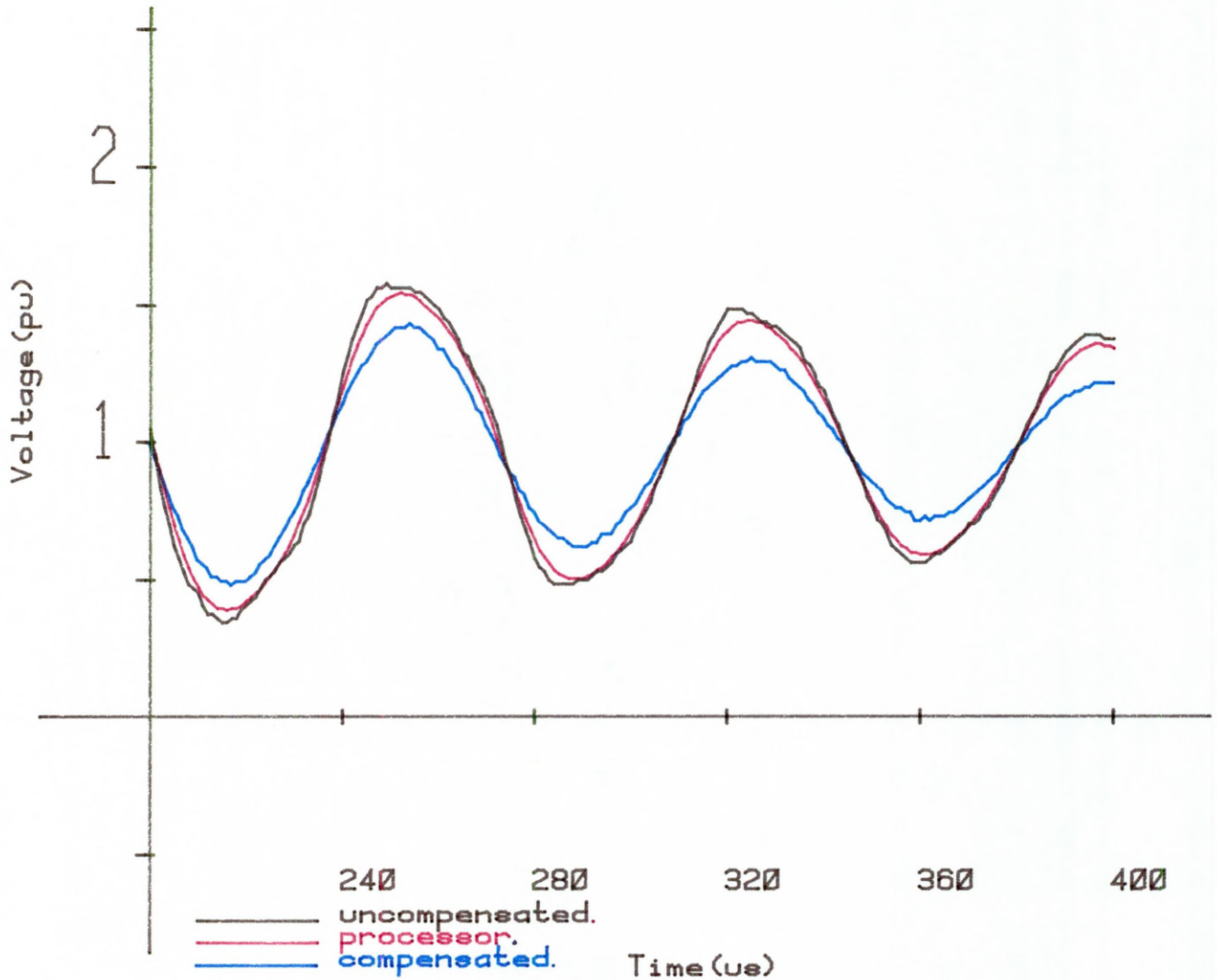

Figure 4.13 (cont'd) (b) 200 - 400 us.

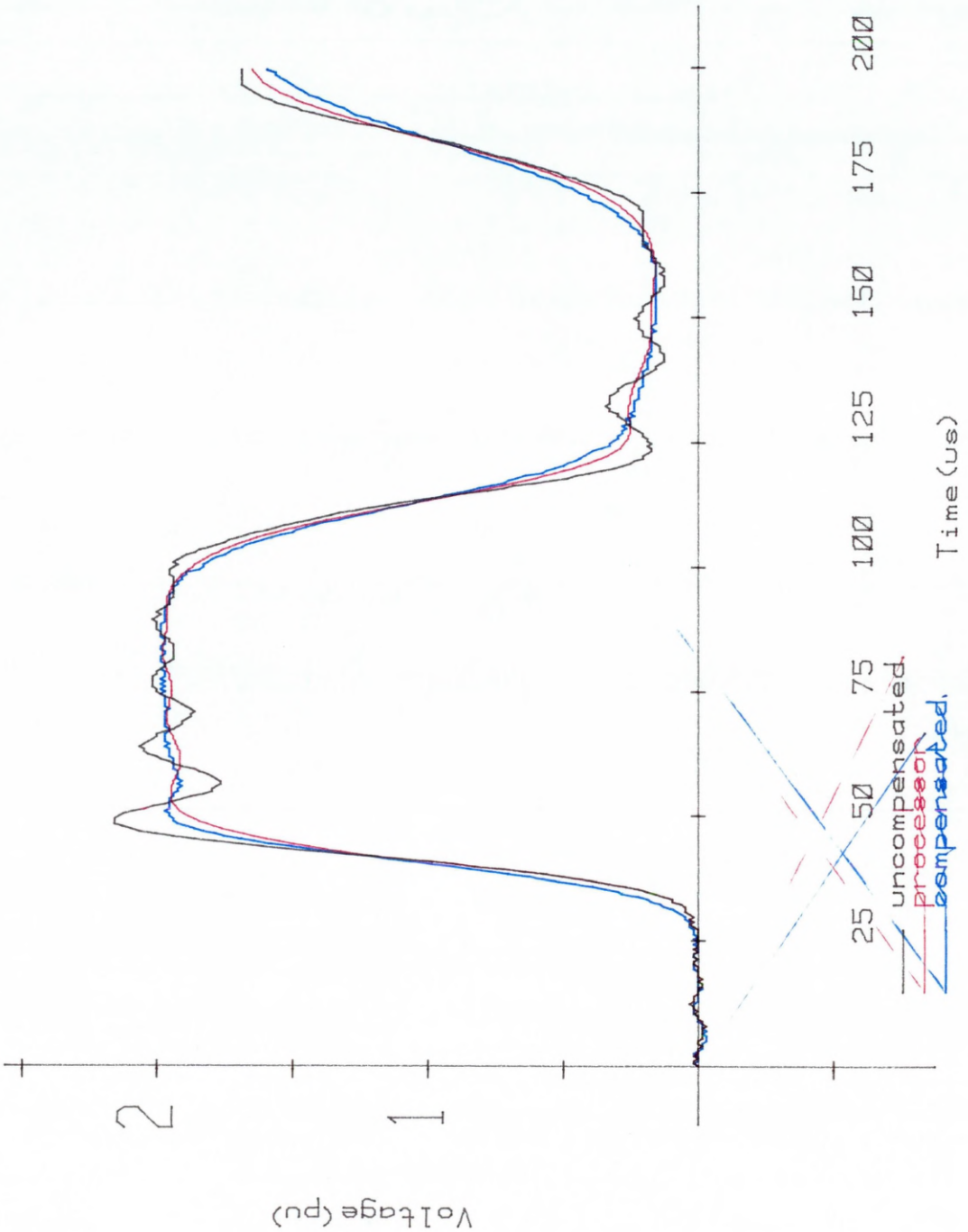

Figure 4.14(a) Responses of 10 pi-section lines with earth-path impedance (0 - 200 μs). Processor response calculated by S_{se} with N_s = 15 μs.

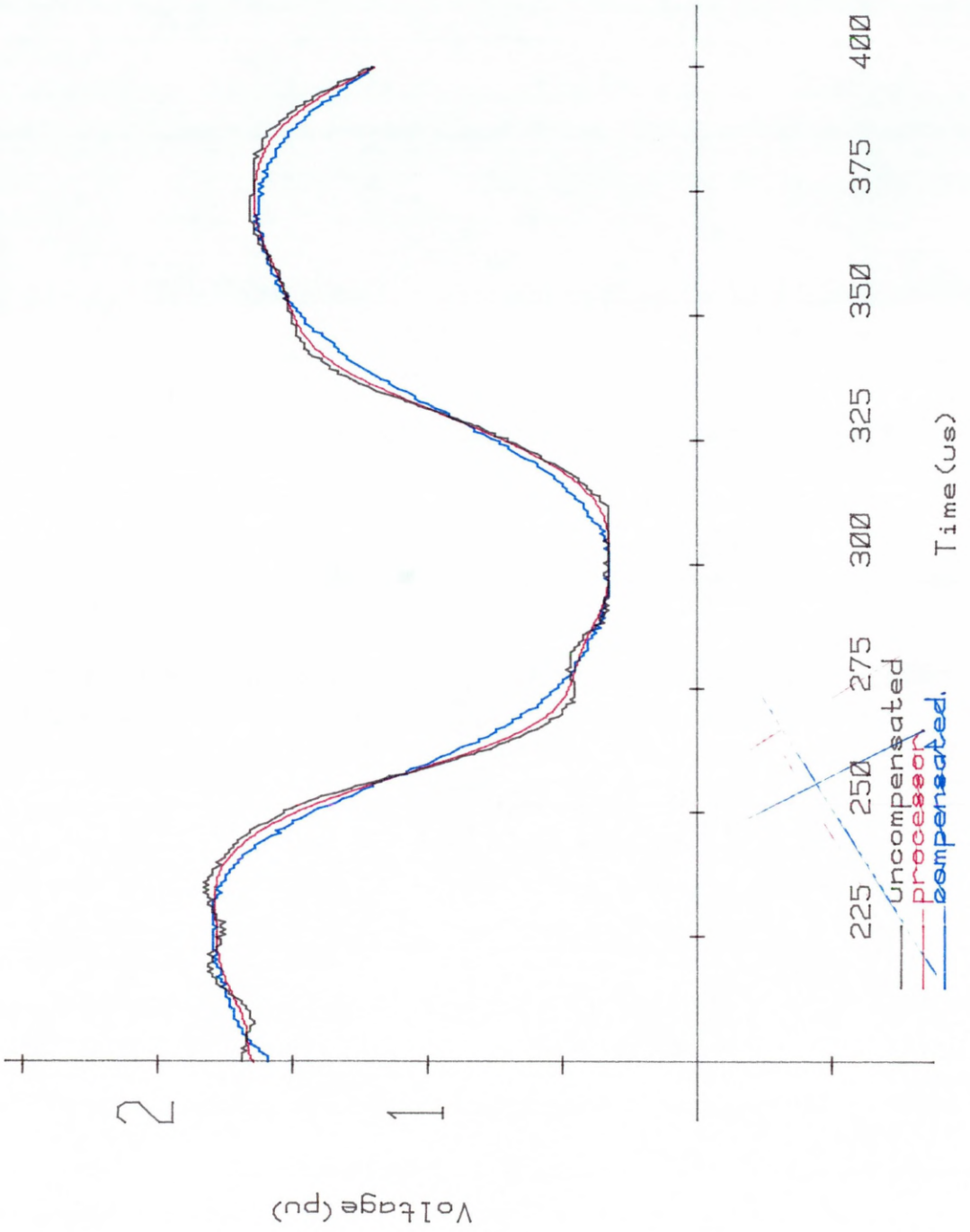

Figure 4.14 (cont'd) (b) 200 - 400 μs.

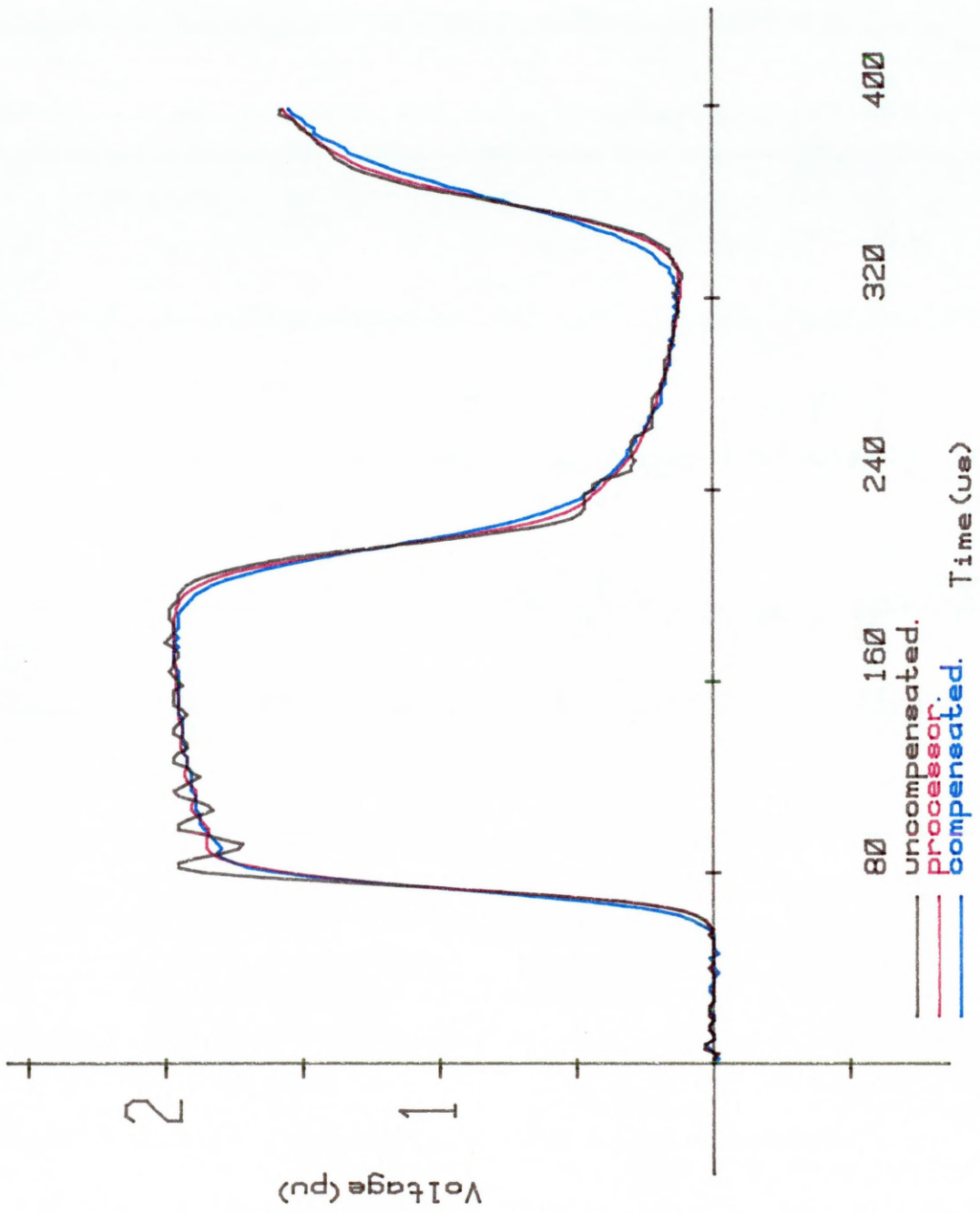

Figure 4.15(a) Responses of 20 pi-section lines with earth-path impedance (0 - 400 μs). Processor response calculated by S_{se} with N_s = 19 μs.

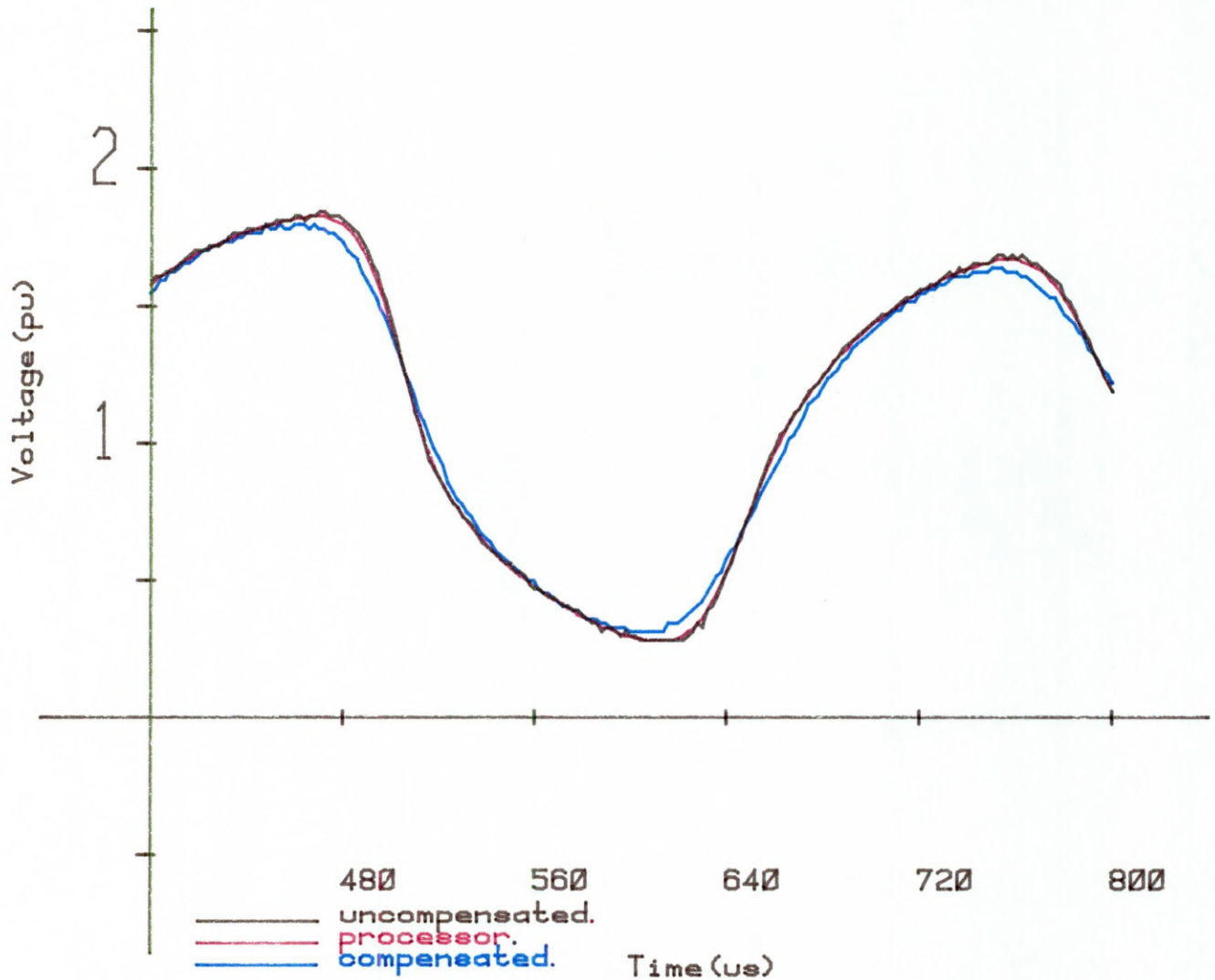

Figure 4.15 (cont'd) (b) 400 - 800 μs.

waveform after 280 μs and the processor waveform after this time is almost identical to this response.

The initial surge of the processor waveform again displays a slight oscillatory content but the first rate of rise is almost comparable with that of the damped waveform. However the best processor response was determined with N_s equal to 15 μs (Figure 4.16) and in this case the initial rate of rise is greater than in the compensated case.

4.4.3 Analysis of Experimental Standard Sigma Factor

From the waveforms shown general observations on the ability of S_{se} to reduce the Gibbs phenomena from the uncompensated model line responses are now discussed.

4.4.3.1. S_{se} for the Zero Earth Impedance Lines

The Experimental Standard Sigma Factor S_{se}, whose averaging range is automatically determined from the uncompensated waveform, is found to only effectively reduce the Gibbs phenomena in the 5 π-section line case. The 10 and 20 π-section processor responses have demonstrated the limitation of S_{se}, using the single averaging range, because of the changing high-frequency content of their uncompensated waveforms. For these line lengths S_{se} is only effective for the modification of the initial surges which still however display a slight oscillatory content in the processor response.

With the software capability of varying N_s the initial surges of the 10 and 20 π-section lines were improved which demonstrates that calculating N_s from the initial Gibbs oscillation is neither effective in modifying the subsequent receiving-end surges nor ideal for reducing the oscillations in the initial uncompensated waveform surge. The automatically determined values of N_s for the 5, 10 and 20 π-section lines were respectively 15, 17 and 21 μs. Reducing these values to 13, 13 and 17 μs respectively improved the processor initial surge in each case when compared to the corresponding compensated response.

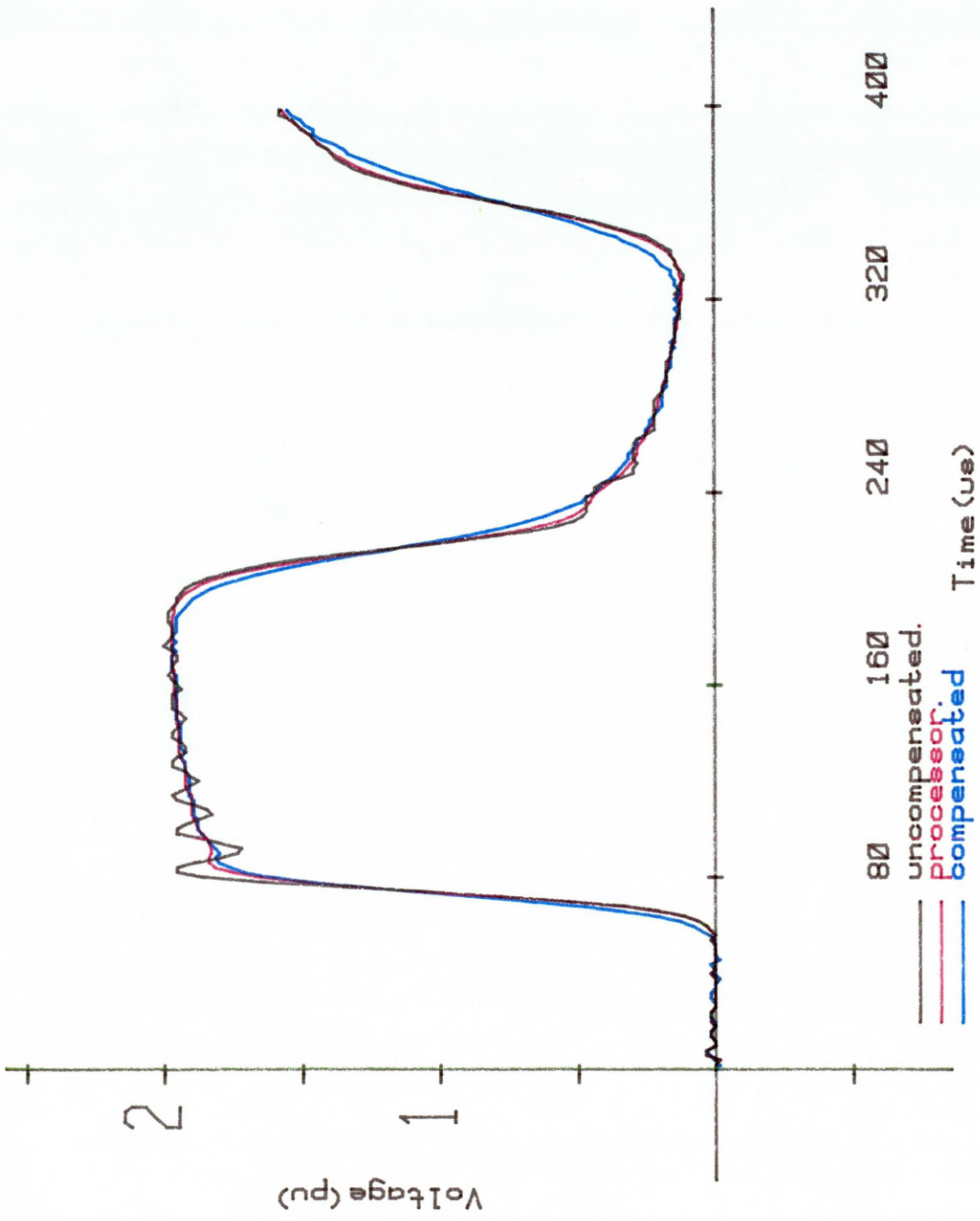

Figure 4.16 Responses of 20 pi-section lines with earth-path impedance. Improved processor response calculated by S_{se} with N_s = 15 μs.

When considering the initial rates of rise of the automatically calculated processor responses it can be stated that they improve and become comparable with their equivalent compensated line rates of rise as the length of line increases. The initial rates of rise, as stated previously, are copied from the uncompensated line response up to the point where S_{se} is implemented so that processor response continuity is retained. It is from this point that the rates of rise were considered. When varying N_s (see above) steeper initial rates of rise for the two longest lines, when compared to the corresponding compensated discontinuity, were obtained. The reduction of N_s increases waveform rates of rise while increasing N_s has the opposite effect.

Subsequent discontinuities are steeper in all processor responses when compared to the corresponding compensated case. However this can only be stated confidently for the 5 π-section line since the processor response displays no Gibbs content. Sections of this waveform do however lie outside the 0 - 2 pu range. For all lines it can be seen that the 'foot' effect[9] is more pronounced in the compensated line response.

4.4.3.2. Frequency Variation of the Gibbs Phenomena

The values of N_s which gave the best processor initial surge waveform for the 5, 10 and 20 π-section lines were determined as 13, 13 and 17 μs respectively. This indicates that the predominant frequency of this surge in all three uncompensated line cases is close to the natural π-section frequency f_0 of 65.18 kHz. Subsequent reflections of the 10 and 20 π-section uncompensated waveforms show that frequencies of this order are attenuated from the response over one transient cycle. The 20 π-section waveform clearly displays a changing Gibbs content with the frequency of subsequent Gibbs Oscillations decreasing but being apparent in the response for an increasingly longer time. The natural π-section frequency, f_0, is the highest Gibbs frequency observed in the uncompensated line responses and only occurs in the initial transient surge.

This may be explained from the attenuation-frequency characteristic of Figure 1.5 which shows that higher frequencies are subject to increased attenuation in the uncompensated line. Consequently the high-frequency content will be reduced much more rapidly than the lower frequency components of a response. This is apparent in the 20 π-section line global response which approximates to a waveform containing fundamental and 3rd harmonic components only (Figure 4.11(e)).

The global response of the compensated line transient also improves as line length increases which is also explained by the attenuation characteristic in Figure 1.5. For the 5 and 20 π-section lines the transient fundamental frequencies are 14.3 and 3.61 kHz respectively. The global response of the 20 π-section compensated line remains closer in magnitude to the uncompensated waveform for a greater number of transient fundamental cycles than in the 5 π-section line case. Since the transient fundamental frequency of this line is approximately one quarter of that determined in the 5 π-section case, the sinusoidal component which contributes to the square-wave response is subject to less attenuation. The high-frequency content of each compensated line response is attenuated which globally gives a damped waveform, basically sinusoidal in shape.

4.4.3.3. S_{se} for Earth Impedance Lines

For all three line lengths with earth-path impedance the reduction of the Gibbs Oscillations using the automatically calculated S_{se} was successful although a slight oscillatory content was observed in the initial surge of the 10 and 20 π-section processor responses. The 20 π-section response was improved by reducing N_s from 19 to 15 μs and this indicated that a 'fixed' value of N_s could be applied to process all uncompensated responses successfully since the best processor waveforms for the 5 and 10 π-section lines also used this averaging range.

As in the case of the zero earth impedance lines, the initial rates

of rise of these waveforms improved as the line length increased. Using the 'fixed' value of 15 μs for averaging gave a steeper initial rate of rise for the longest line than was observed from the damped response. Subsequent processor discontinuities are an improvement on that of the damped line responses which again show the effects of increased attenuation on the high-frequency components of the transient.

After the elimination of the Gibbs Oscillations, due to the stratified-earth circuit model, it could be stated that averaging of the uncompensated waveform is not required. However this was not undertaken since the differences between the uncompensated and processor waveforms are very small.

4.5 The Adaptive Experimental Sigma Factor S_{ae}

The processor responses for the 10 and 20 π-section zero earth impedance lines of section 4.4.1.1 demonstrated the inability of S_{se} to sufficiently reduce the magnitude of the Gibbs Oscillations present in subsequent uncompensated waveform surges. However S_{se} was effective in significantly reducing the Gibbs content of the initial surge from which N_s was calculated. This suggested that if an averaging range could be determined for each subsequent surge then an improved processor response might be obtained.

The 20 π-section uncompensated waveform shown in Figures 4.11(a) - (e) indicates that an adaptable averaging range could be calculated from the first oscillation of each receiving-end surge thereby modifying S_{se} to suit the frequency content of that particular surge. The software flexibility of the microprocessor would allow this to be investigated if a method of determining each new averaging range could be devised.

4.5.1 20 Π-Section, Zero Earth Impedance Response

Figure 4.11 shows that regions of Gibbs Oscillations initially occur

in the uncompensated waveform at pu values of approximately 0 and 2 pu. Subsequent oscillatory regions then occur above and below the 1 pu DC source value at magnitudes of < 2 and > 0 pu as line losses attenuate the transient waveform. Therefore the 1 pu DC source voltage could be used as a reference for the calculation of N_s for subsequent surges.

As described previously the first oscillation (at approximately 2 pu) is used to calculate the value of N_s. S_{se} can then be applied to modify the uncompensated response until an uncompensated waveform sample whose voltage value is less than 1 pu is detected. When a sample satisfying this criterion is encountered the microprocessor software can proceed to determine the adapted averaging range N_a from the first oscillation (at approximately 0 pu) of the next surge. The new technique defined as the Adaptive Experimental Sigma Factor S_{ae} is then implemented until the uncompensated waveform pu value becomes greater than 1 whereby a new value of N_a will be determined from the first oscillation of the next surge at 2 pu. The procedure is then repeated for the remainder of the waveform.

Implementing S_{ae} gave the processor response of Figures 4.17(a) - (e) and shows that the Gibbs phenomena of the subsequent surges are considerably reduced when compared to those calculated using S_{se} alone (see Figures 4.11(a) - (e)). A reduced oscillatory content is still observed in the processor waveform which endorses the previous finding that the first oscillation of a surge does not give the ideal averaging range to completely reduce the Gibbs content. However the overvoltage profile of the response is now much more accurate and although the waveshape calculated is not ideally square it does indicate that S_{ae} may be employed to determine overvoltage magnitudes.

4.5.2 5 and 10 Π-Section, Zero Earth Impedance Responses

The waveshape of the uncompensated 20 π-section response remained similar to that of the initial surge for the entire record length of

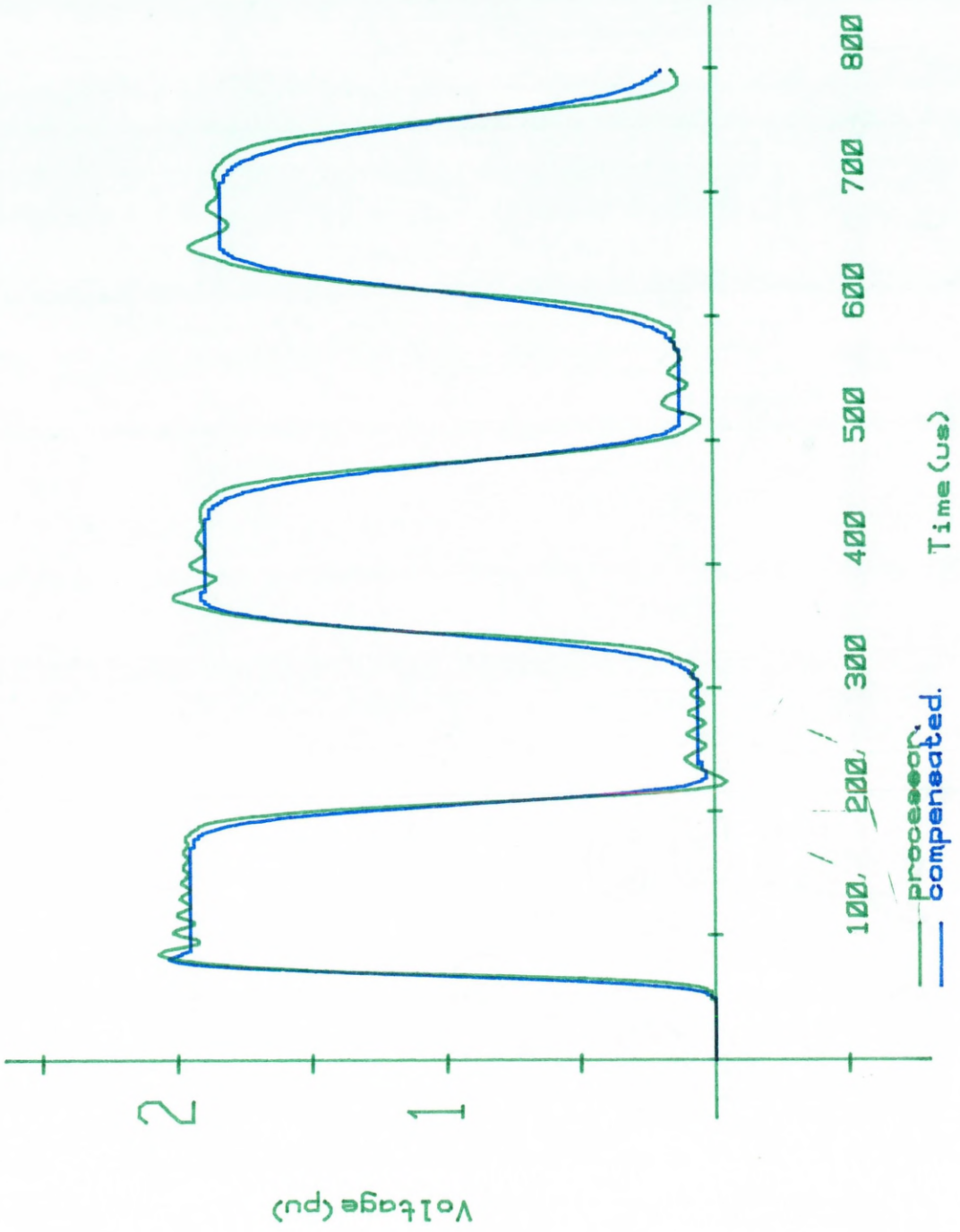

Figure 4.17(a) Processor and compensated responses of 20 pi-section lines with zero earth impedance (0 - 800 μs). Improved processor response calculated by S_{ae}.

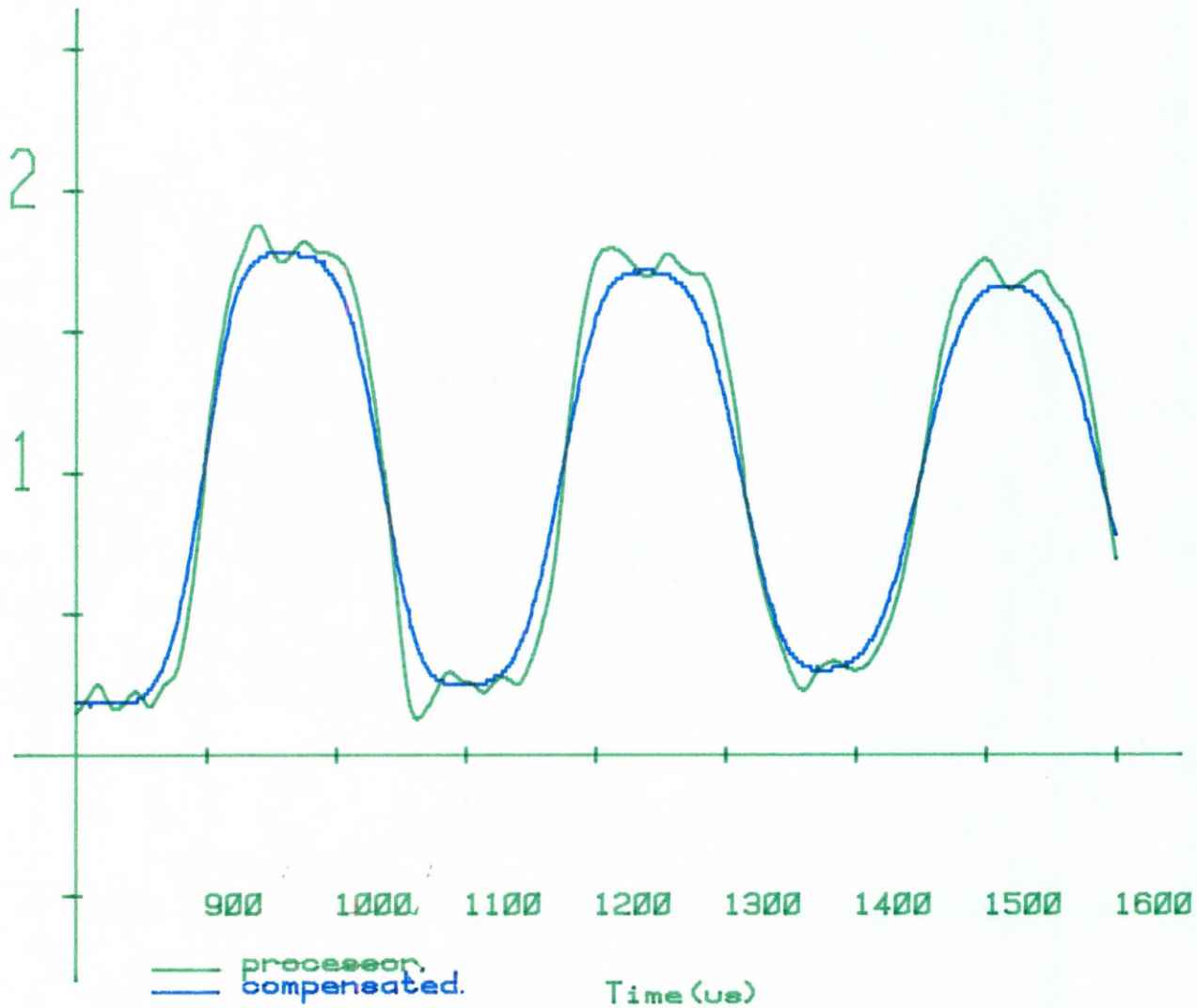

Figure 4.17 (cont'd) (b) 800 - 1600 μs.

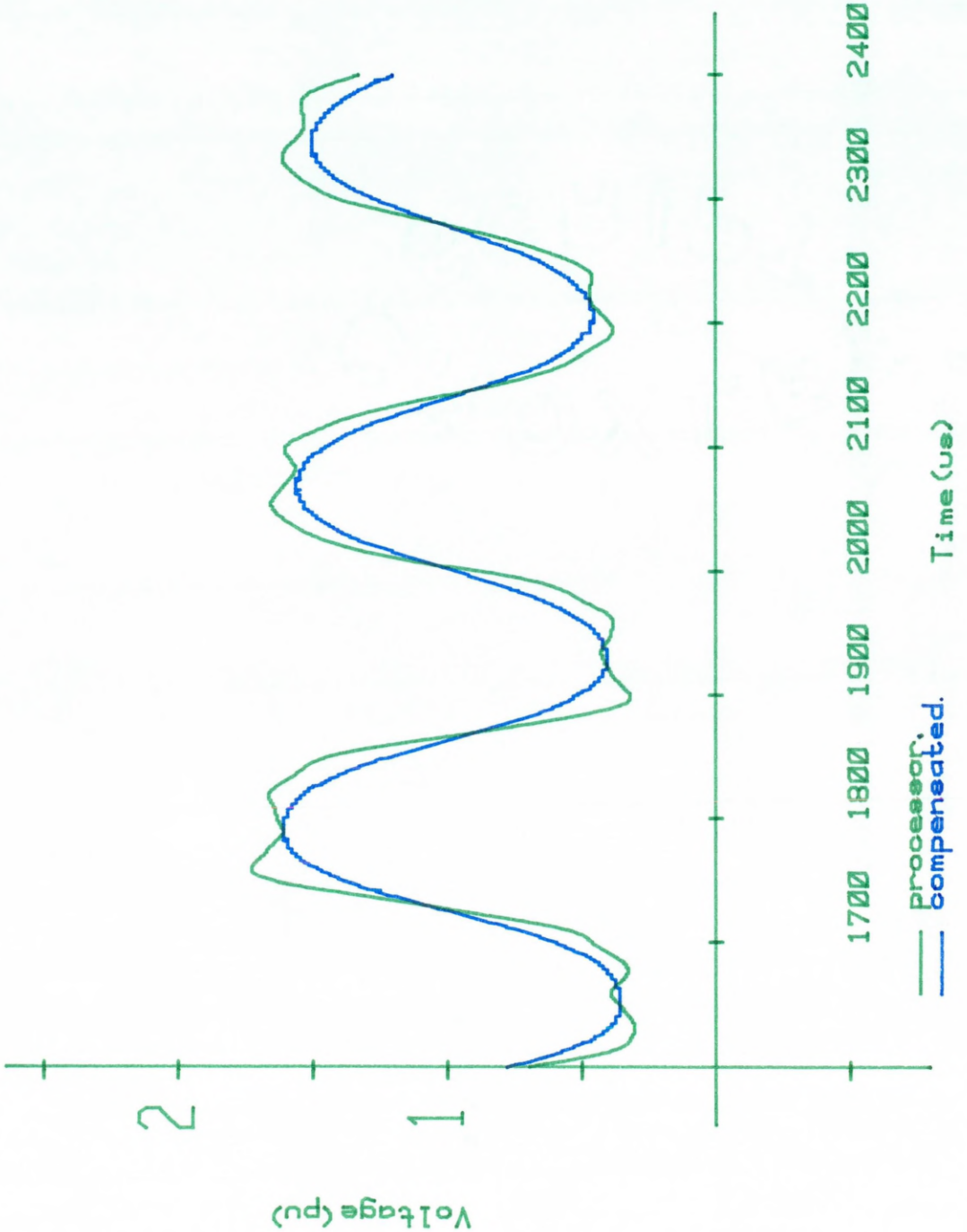

Figure 4.17 (cont'd) (c) 1600 - 2400 μs.

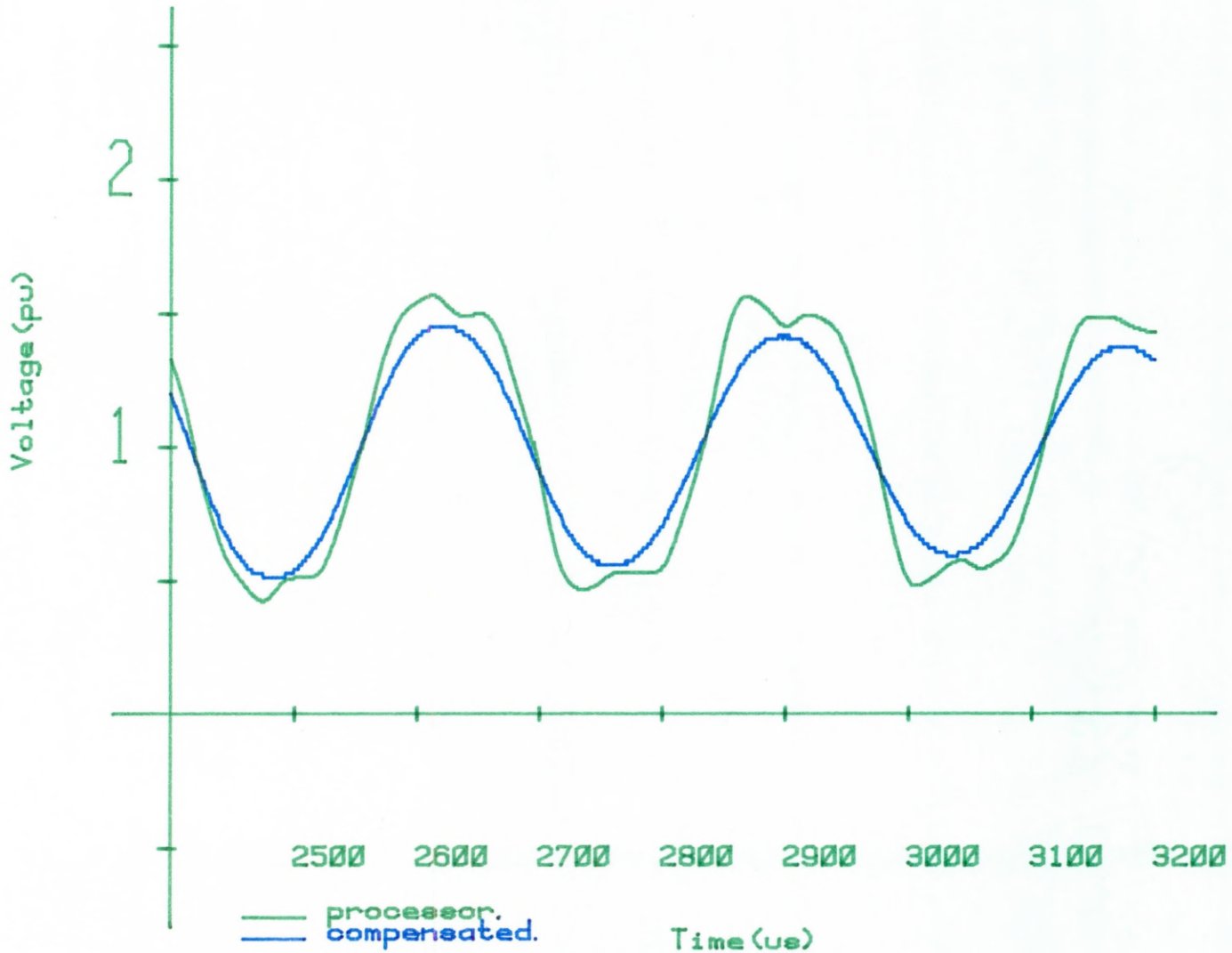

Figure 4.17 (cont'd) (d) 2400 - 3200 μs.

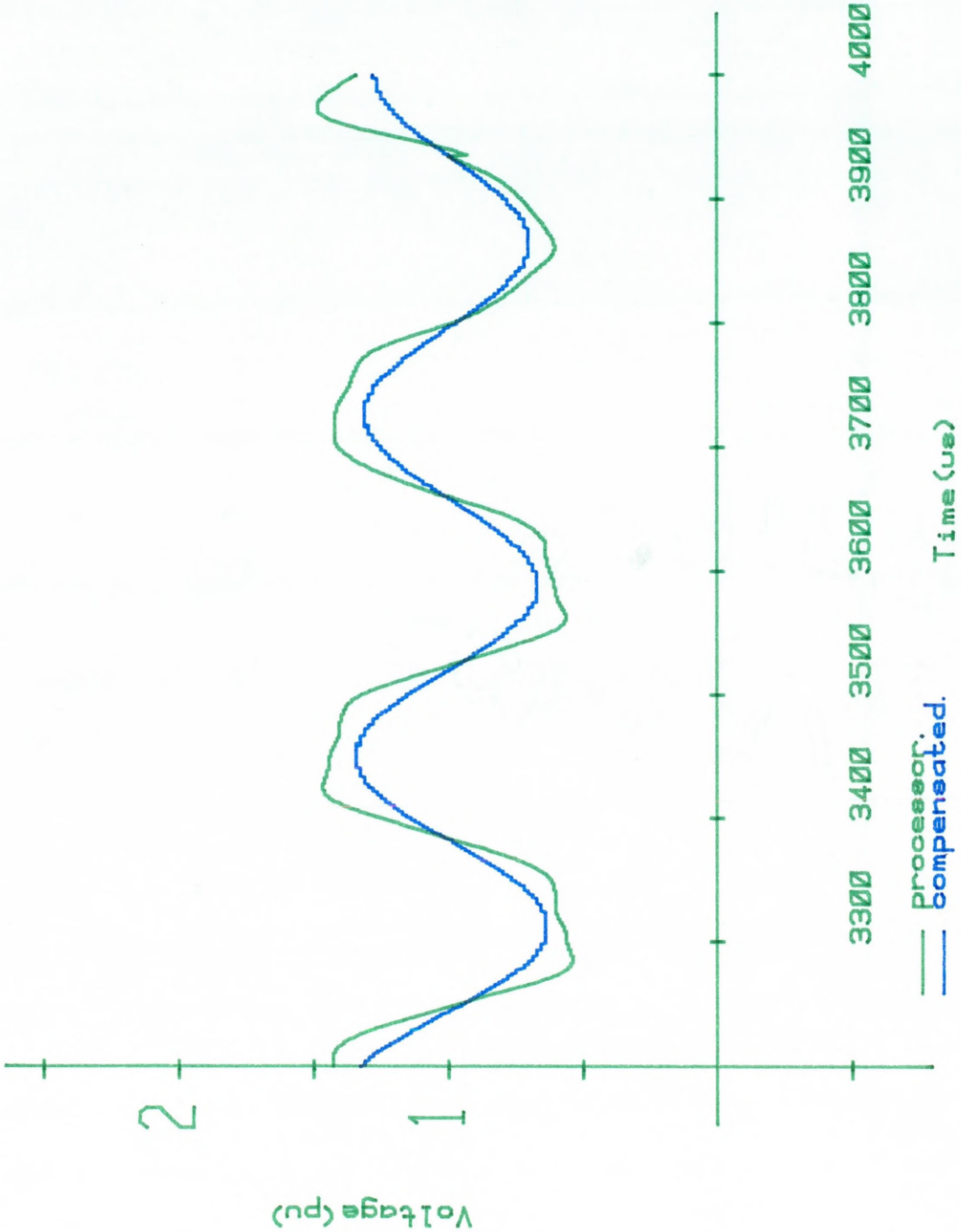

Figure 4.17 (cont'd) (e) 3200 - 4000 μs.

4000 μs i.e. the first oscillation of each surge allowed a new value of N_a to be determined. However from Figures 4.6(a) - (d) and 4.9(a) - (c) subsequent surges in the 5 and 10 π-section uncompensated responses are only characteristic of the initial surge until 150 and 1000 μs respectively whereafter the uncompensated waveforms become basically sinusoidal with a reduced high-frequency content. Therefore the use of S_{ae} is limited to the aforementioned times.

It was previously observed in the 10 π-section processor response calculated by S_{se} (section 4.4.1.2) that N_s became relatively effective in reducing the Gibbs phenomena, after 1600 μs in the global response, when the uncompensated waveform was no longer square in waveshape. From this it was suggested that a single higher averaging value would have been sufficient to satisfactorily reduce the remaining Gibbs content of the waveform after 1600 μs.

Since the software developed for S_{se} allowed the value of N_s to be user-defined, the processor responses of the 5 and 10 π-section lines after 150 and 1000 μs were investigated by applying various values of N_s to the uncompensated waveforms. It was found that oscillatory-free processor responses were obtained for averaging ranges of 19 and 35 μs for the 5 and 10 π-section lines respectively after the aforementioned times. The transient fundamental frequencies of these lines, determined in section 4.4.3.1, are 14.3 and 7.25 kHz which correspond to transient periods (denoted by T) of 70 and 138 μs respectively. It was therefore noted that the effective averaging ranges determined were approximately T/4 μs which equates to the line travel time. This assumption was verified by estimating an averaging value for the 20 π-section line which was determined at 69 μs i.e. 3.61 kHz gives the transient period T for this line as 277 μs and T/4=69 μs. When this averaging range was implemented the global processor response of this line was found to be free of any Gibbs content.

Therefore the value of N_s for the effective averaging of uncompensated waveforms whose subsequent transient surges are not square-wave in character would as a first estimate be T/4 μs.

The processor waveform of the 5 π-section line (Figures 4.18(a) - (b)) was therefore calculated by applying S_{ae} until 150 μs and then averaging using N_s=19 μs for the remainder of the uncompensated response. An improved response has been obtained using this adaptive technique. The overvoltages have been reduced and the response is now only outwith the 0 - 2 pu range from 130 - 350 μs (previously 90 - 500 μs).

The 10 π-section response (Figures 4.19(a) - (c)) is also an improvement to that determined by S_{se}. However in applying this technique to the uncompensated waveform two interesting problems were encountered.

Firstly a modified approach to S_{ae} was necessary since a small averaging range (N_a=5 μs) was calculated from the uncompensated response at 732 μs (see Figure 4.9(a)). This slight oscillation occurs on a discontinuity and prevents the averaging range being determined from the major oscillation which immediately follows. When the small averaging range calculated was initially implemented the Gibbs content of the following surge was reduced by an unacceptably small amount. This suggested that a lower limit of N_a would have to be defined.

Since the lowest averaging range calculated from the initial surges of the 1-phase lines investigated was 13 μs and on the previous assumption that these surges contained the highest Gibbs frequencies (section 4.4.3.2), the lower limit of N_a was defined as 11 μs. On the basis of this assumption the processor response in Figure 4.19 was obtained.

The second point leads to an anomaly in the averaging technique and is apparent from the processor waveform shown. The first oscillation of the 0 pu surge occurring at 536 μs gave a 'legitimate' averaging range i.e.

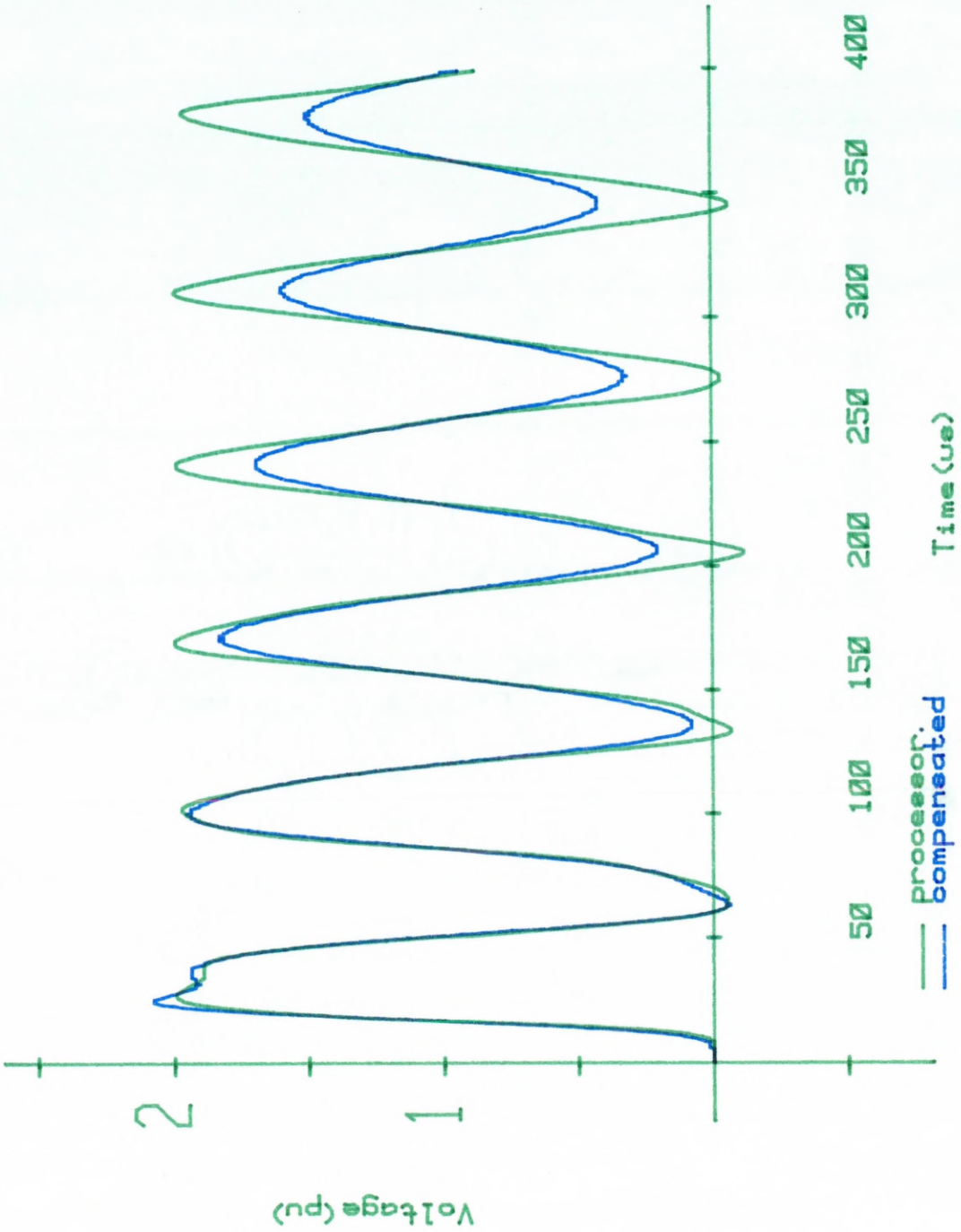

Figure 4.18(a) Processor and compensated responses of 5 pi-section lines with zero earth impedance (0 - 400 μs). Processor response calculated using S_{ae} up to 150 μs whereafter the T/4 estimation is implemented.

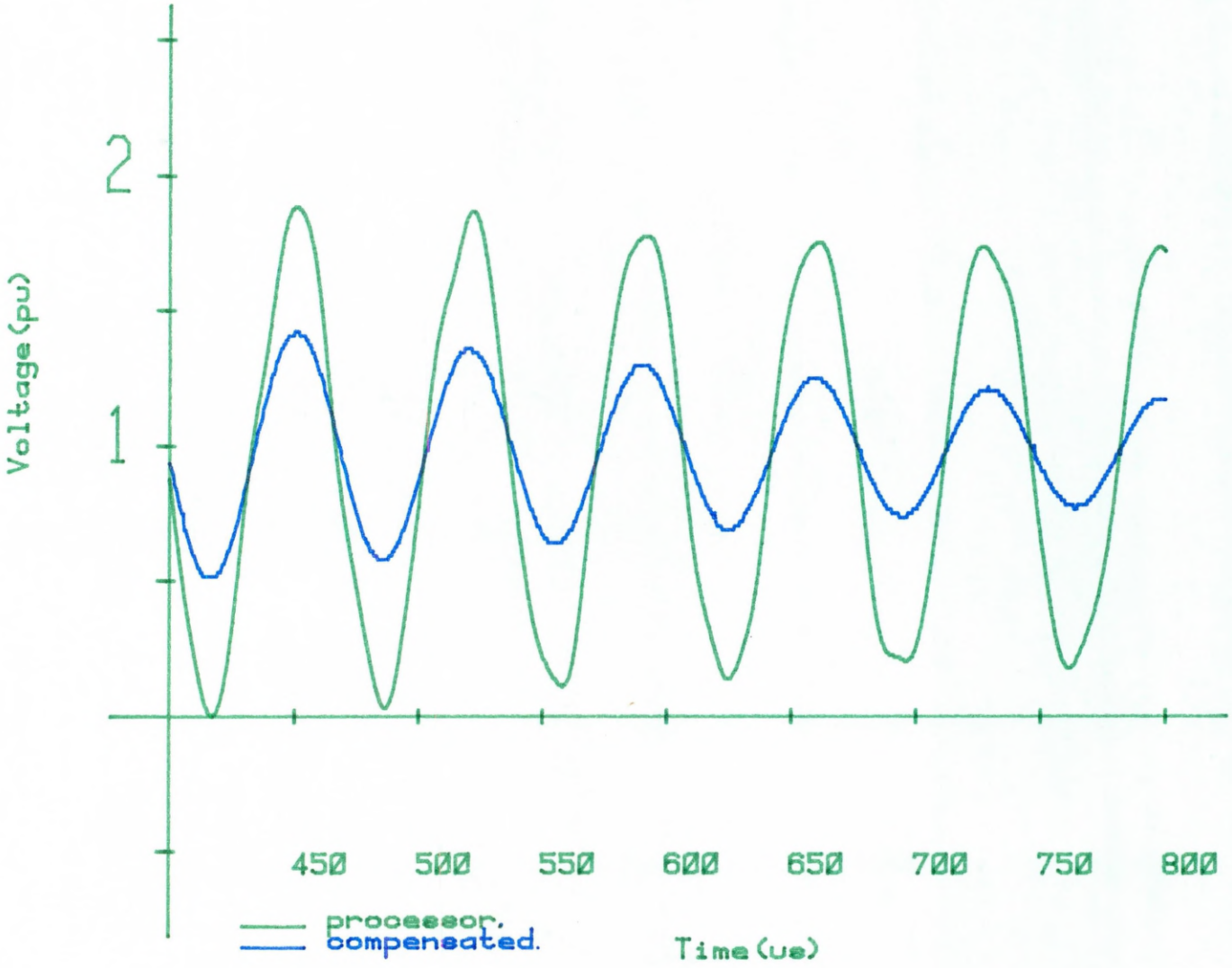

Figure 4.18 (cont'd) (b) 400 - 800 us.

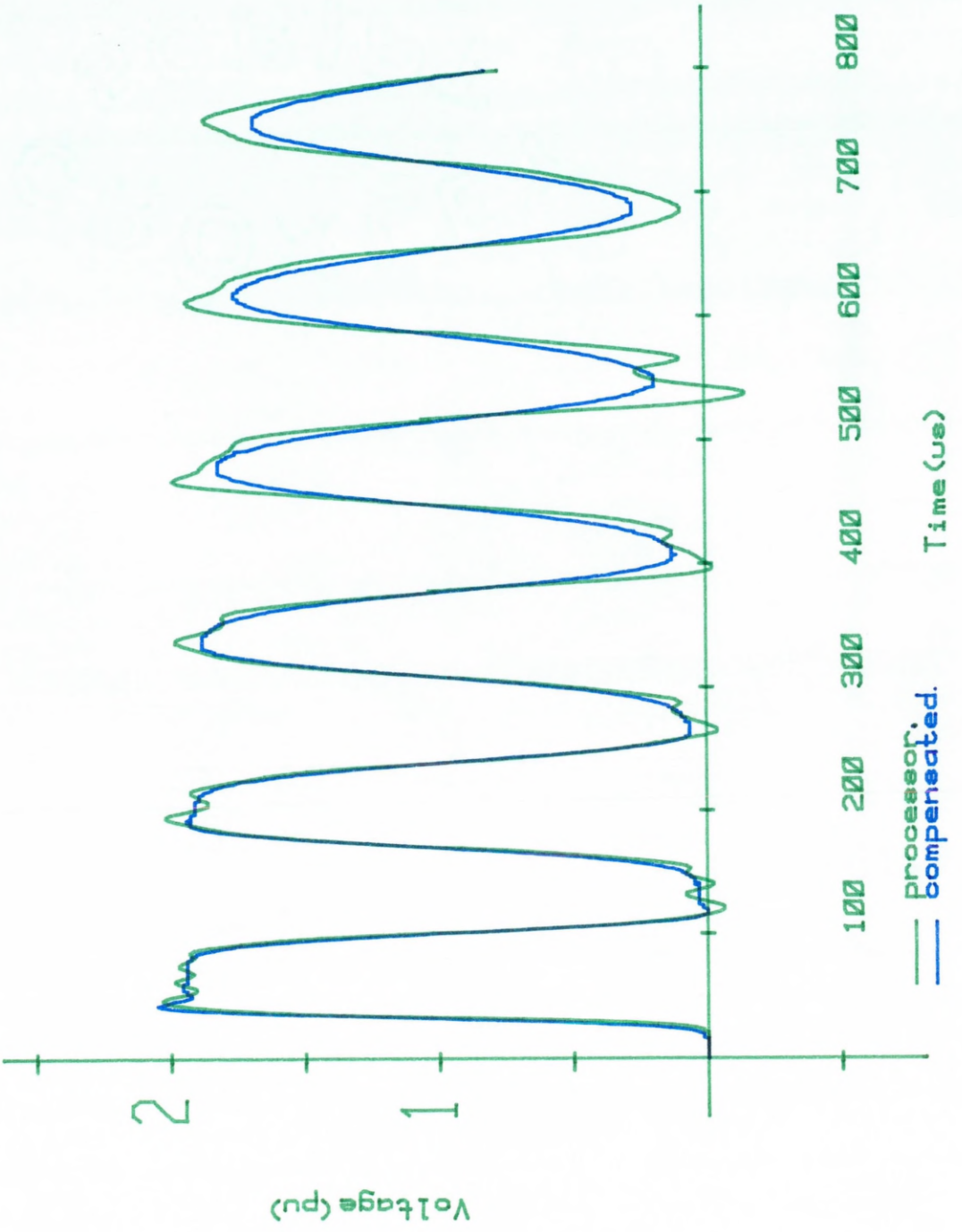

Figure 4.19(a) Processor and compensated waveforms of 10 pi-section lines with zero earth impedance (0 - 800 μs). Processor response calculated using S_{ae} up to 1000 μs whereafter the T/4 estimation is implemented.

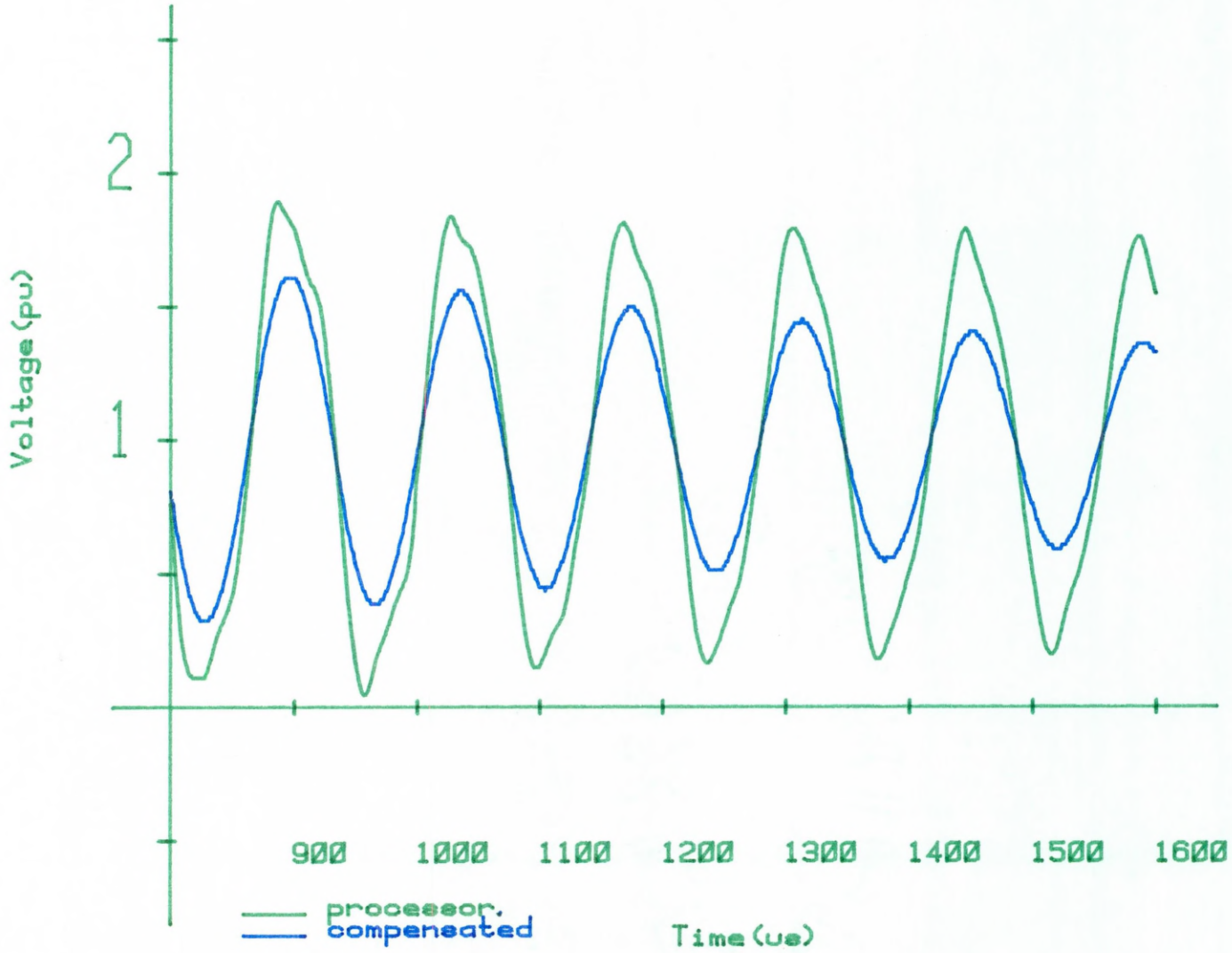

Figure 4.19 (cont'd) (b) 800 - 1600 μs.

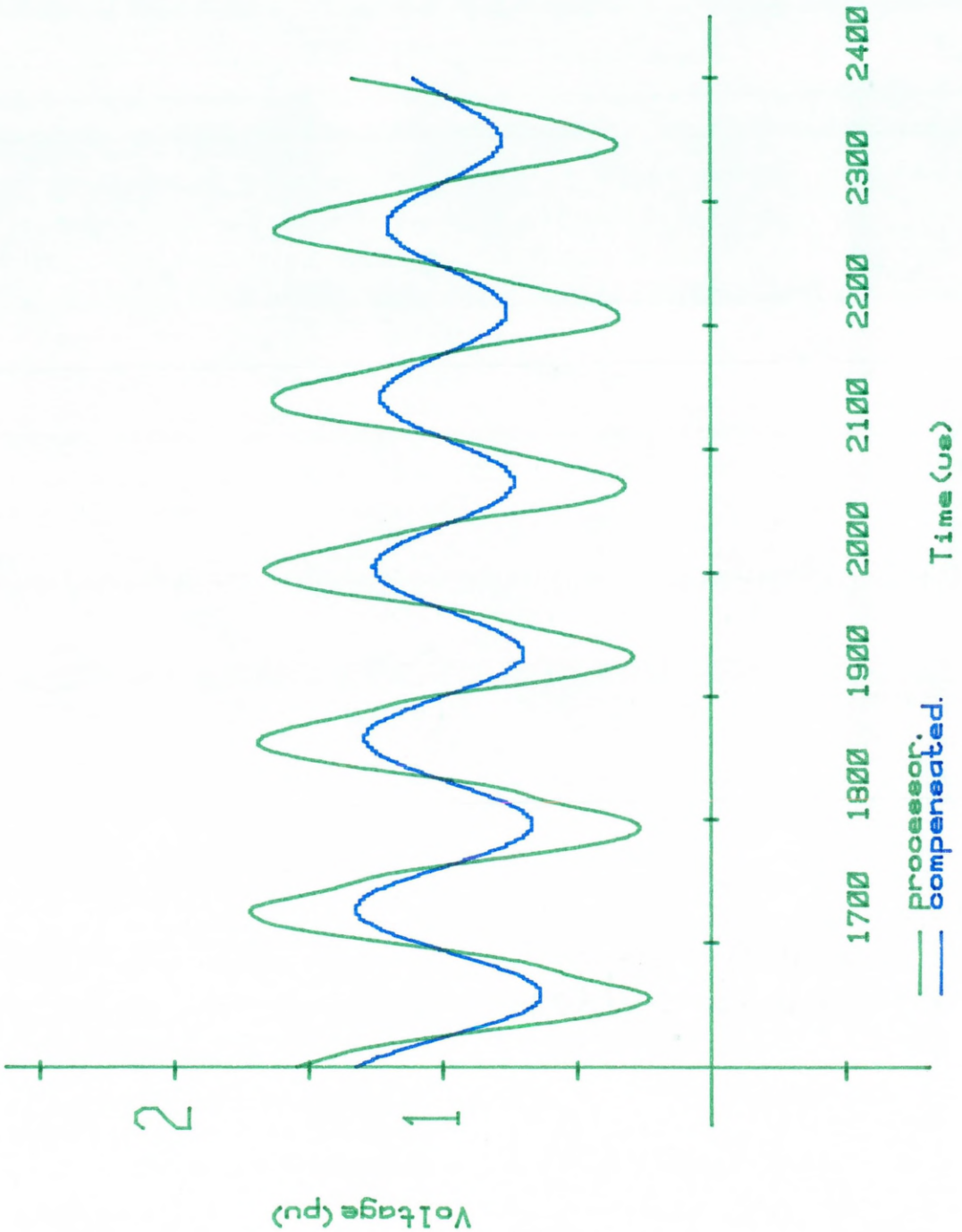

Figure 4.19 (cont'd) (c) 1600 - 2400 μs.

$>$ 11 μs, of 17 μs but as the processor response shows this is relatively ineffective. However the 'incorrect' calculation of N_a is due to the secondary oscillation in the uncompensated waveform itself and not to the method of determining N_a. This demonstrated for the first time that the accuracy of the technique was dependent on the uncompensated waveform generated. This could be overcome by limiting the calculation of new values of N_a to approximately 520 μs and then averaging using the T/4 μs estimation but it does indicate that the accuracy of the local averaging technique is restricted by the uncompensated response waveshape.

4.5.3 Analysis of the Adaptive Sigma Factor

The use of S_{ae} for the modification of the zero earth impedance uncompensated line waveforms has improved the accuracy of the processor responses calculated. The techniques involved in determining N_a and hence S_{ae} are more complicated than that developed for S_{se} and also required a greater knowledge of the uncompensated waveshapes which were to be processed.

S_{ae} is however more dependent on waveshape. This is shown by the 5 and 10 π-section uncompensated waveforms which after 150 and 1000 μs no longer resemble the initial transient surge upon whose characteristic the technique is based. This was overcome however by the empirical T/4 μs estimation. The use of N_a, whose value is equivalent to the travel time of the line, will significantly reduce the Gibbs phenomena present in an uncompensated response which is not basically square in waveshape.

The determination of ineffective values of N_a was discussed in relation to the 10 π-section line response. For small averaging ranges of the order of a few microseconds, this is solved by defining a lower limit for N_a. This is based on the assumption that the highest frequency, and therefore the lowest averaging range, occurs in the initial surge. However the problem encountered with the value of N_a which was greater than the lower limit

defined, but still ineffective, points to a limitation of the technique.

It is now apparent that accurate transient waveform representation will not be achieved by the local averaging of sampled waveforms as a reduced high-frequency content has been apparent in all the processor responses calculated but since the magnitude of the Gibbs Oscillations have been significantly reduced accurate overvoltage analysis may still be carried out.

4.6 Sinusoidal Energisation

The receiving-end waveforms so far investigated have been the result of line energisation from a +1 pu ideal DC source. However since most actual power systems operate at a frequency of 50 Hz the effects of sinusoidal energisation on the generation of Gibbs phenomena in the transient response and on the transient fundamental itself were investigated. Therefore 1-phase 5, 10 and 20 π-section lines with and without earth path impedance were energised from the TNA ideal AC source using the scaled model line frequency of 398 Hz (see section 1.3.1).

4.6.1 90 and 270° Closure

The response of these lines for point-on-wave closures of 90 and 270° were investigated initially as these closures represented instantaneous positive and negative 1 pu steps being applied to the model line.

The 20 π-section (zero earth) uncompensated receiving-end responses for these closures are shown in Figures 4.20 and 4.21 respectively. The uncompensated waveforms shown have exactly the same high-frequency content as the response obtained from DC energisation (Figure 4.11(a)) but the transient fundamental now varies with the sinusoidal source. The response for 270° closure is a mirror image in the time axis of that obtained for 90° and responses recorded for similar excitation from the other zero earth impedance line lengths verified these observations. This implied that the

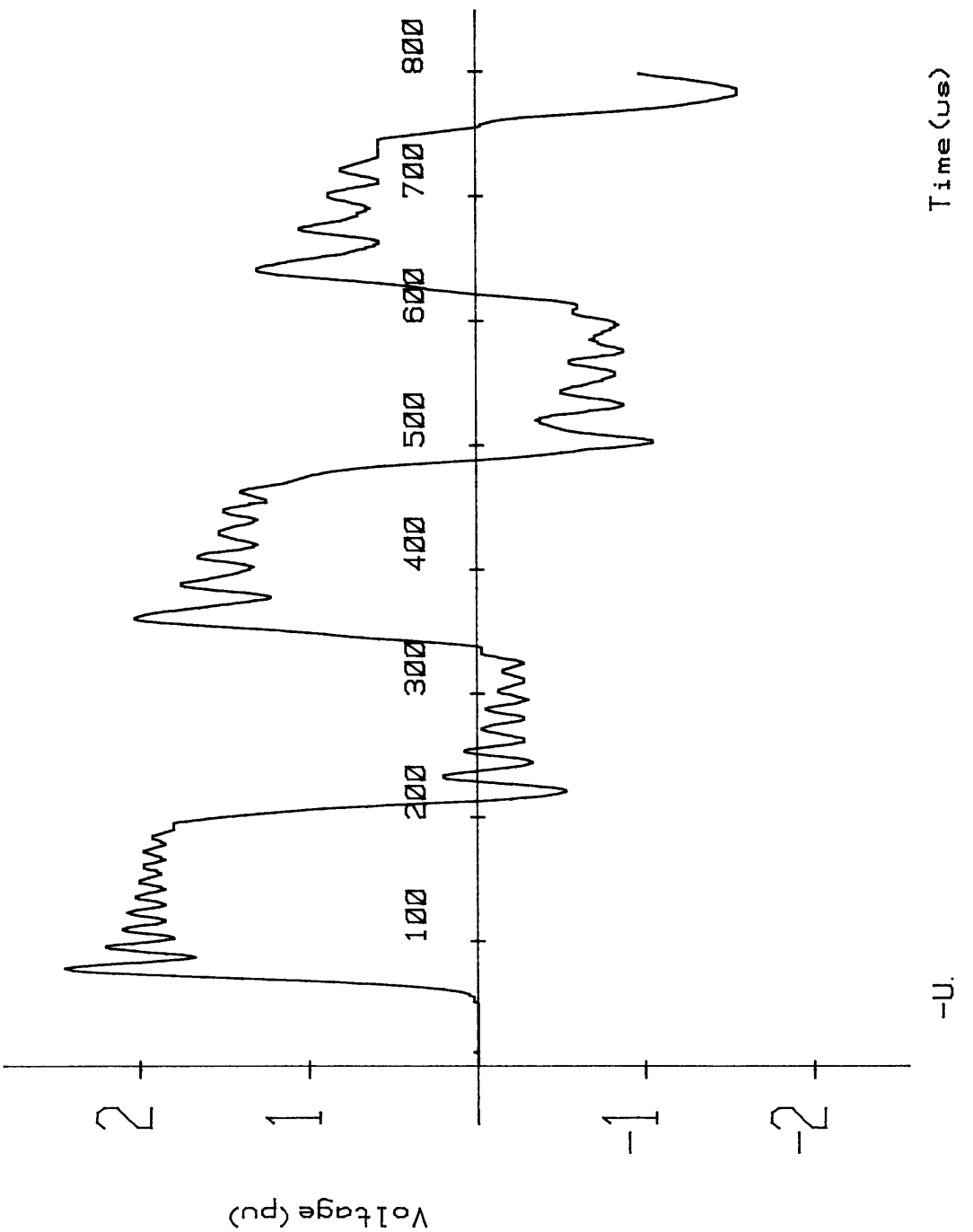

Figure 4.20 Response of 20 pi-section uncompensated line with zero earth impedance to sinusoidal energisation (90° closure).

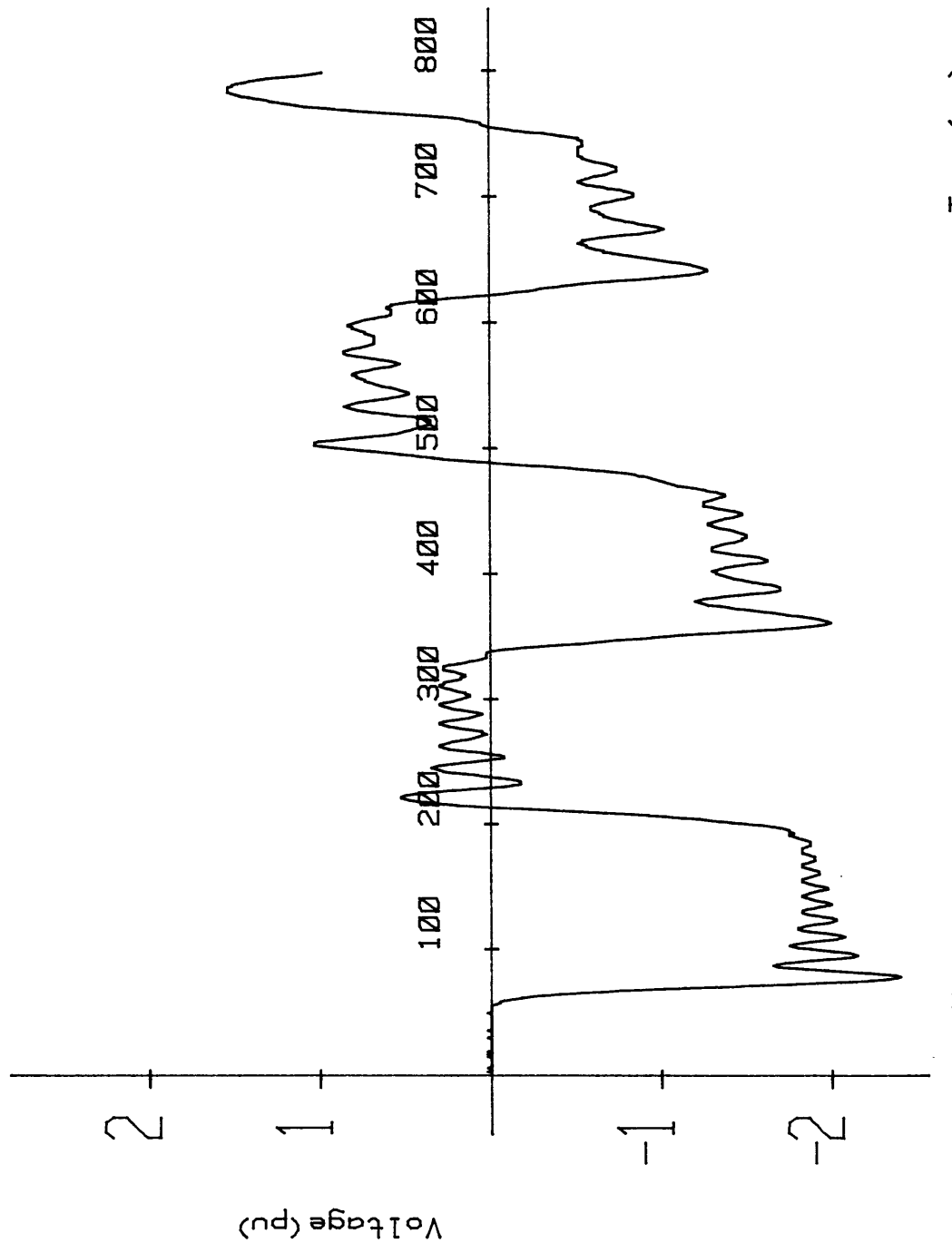

Figure 4.21 Response of 20 pi-section uncompensated line with zero earth impedance to sinusoidal energisation (270° closure).

methods which had been previously applied to the uncompensated responses for DC excitation could be used to reduce the Gibbs content of the AC source line energisation transients.

Figure 4.22 show the 20 π-section processor and resistor-damped responses using S_{ae} (section 4.5) with N_a now being calculated using the source voltage variation as the reference. The processor waveform still contains an apparent high-frequency content as was noted in the DC case but the reduction of the Gibbs phenomena, as before, remains significant. Both waveforms result from a point-on-wave closure of 90° and show that the techniques previously developed to reduce the transient Gibbs content remain effective for energisation at the peak of the voltage supply.

4.6.2 Variation of Point-on-wave Closure

The source point-on-wave closure was now varied from 0 - 90° to determine its effect on the receiving-end responses of the 20 π-section line with zero earth path. Figure 4.23 shows the uncompensated and Figure 4.24 the processor and resistor-damped responses for a closure of 60°. The magnitude of the Gibbs content in the uncompensated waveform appears to be constant in relation to the magnitude of the transient fundamental. The processor response again effectively reduces the Gibbs content indicating that the averaging ranges determined by the technique employed by S_{ae} are very similar to those calculated for 90° closure.

Similar observations can be made for the 30° closure case, the uncompensated waveforms recorded being shown in Figures 4.25(a) - (b). Although the processor response displayed in Figures 4.26(a) - (b) shows that S_{ae} still significantly reduces the Gibbs content in this case a large oscillation is noticeable at 2050 μs. When investigated further, by checking the averaging ranges calculated, it was found that an ineffective value of N_a had been determined for this surge.

Though not apparent from the processor response for 10° closure

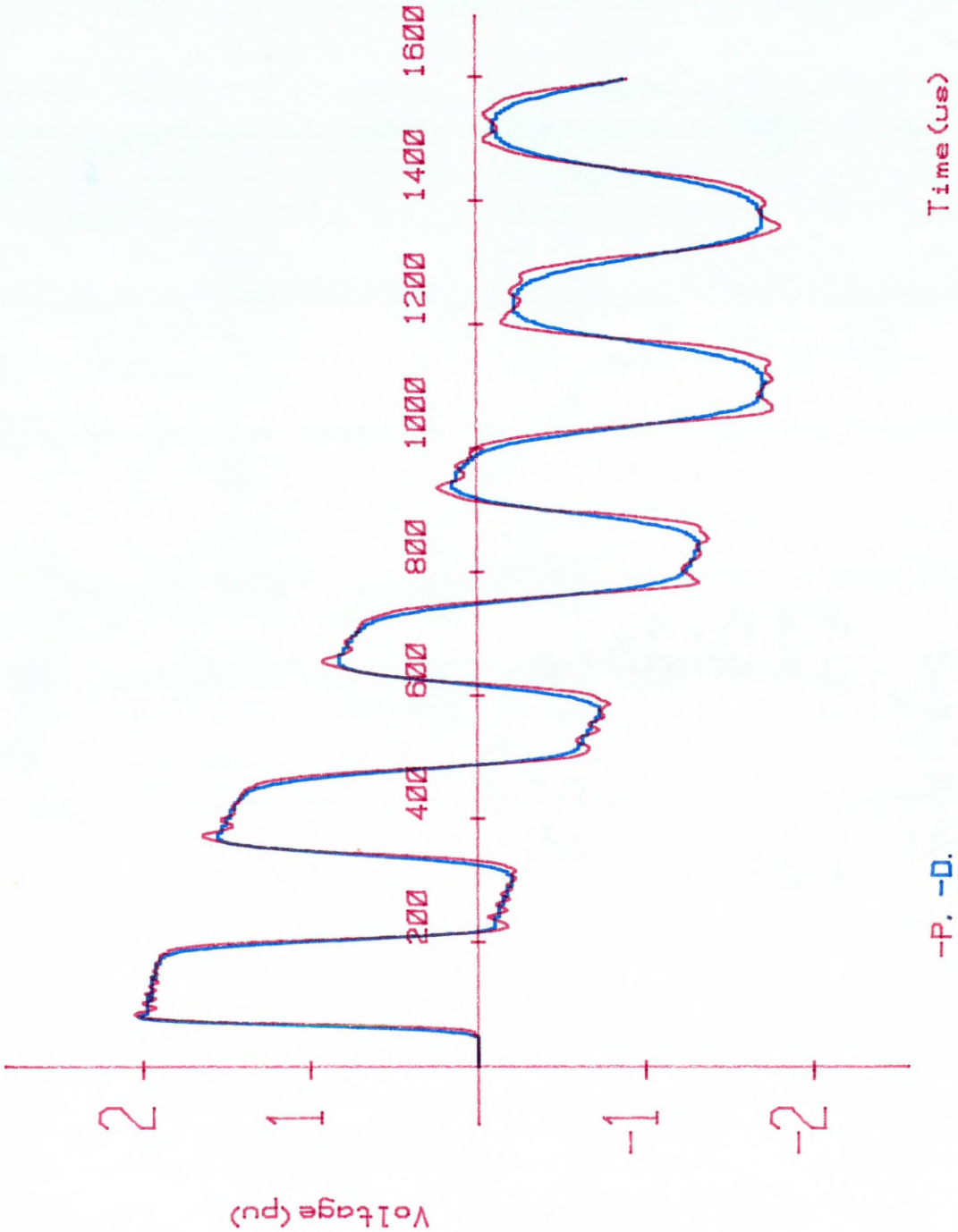

Figure 4.22 Processor (S_{ae}) and compensated waveforms of 20 pi-section lines with zero earth impedance for 90° closure.

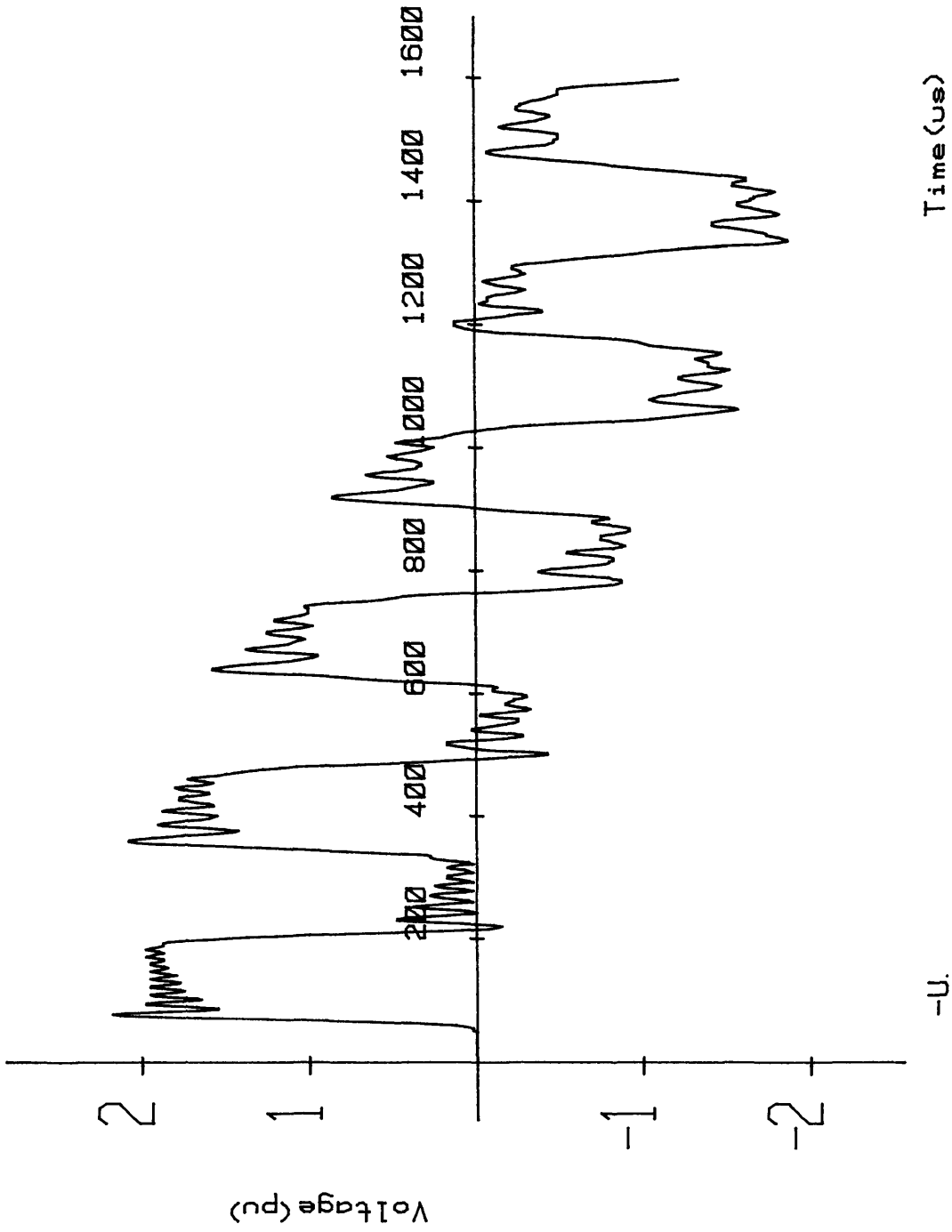

Figure 4.23 20 pi-section uncompensated line response for 60° closure.

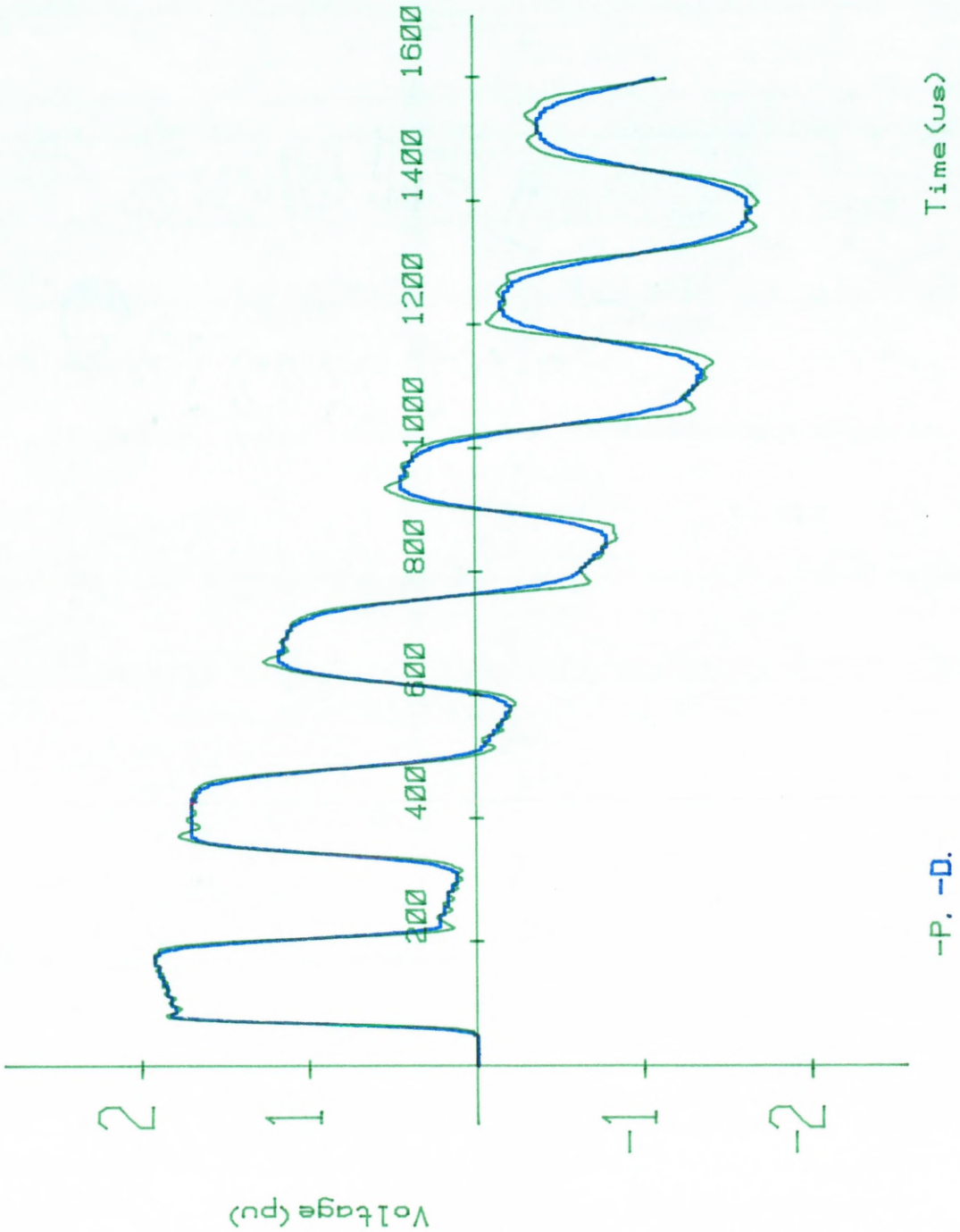

Figure 4.24 Processor (S_{ae}) and compensated waveforms of 20 pi-section lines with zero earth impedance for 60° closure.

Figure 4.25 (a) 20 pi-section uncompensated line response for 30° closure (0 - 1600 μs).

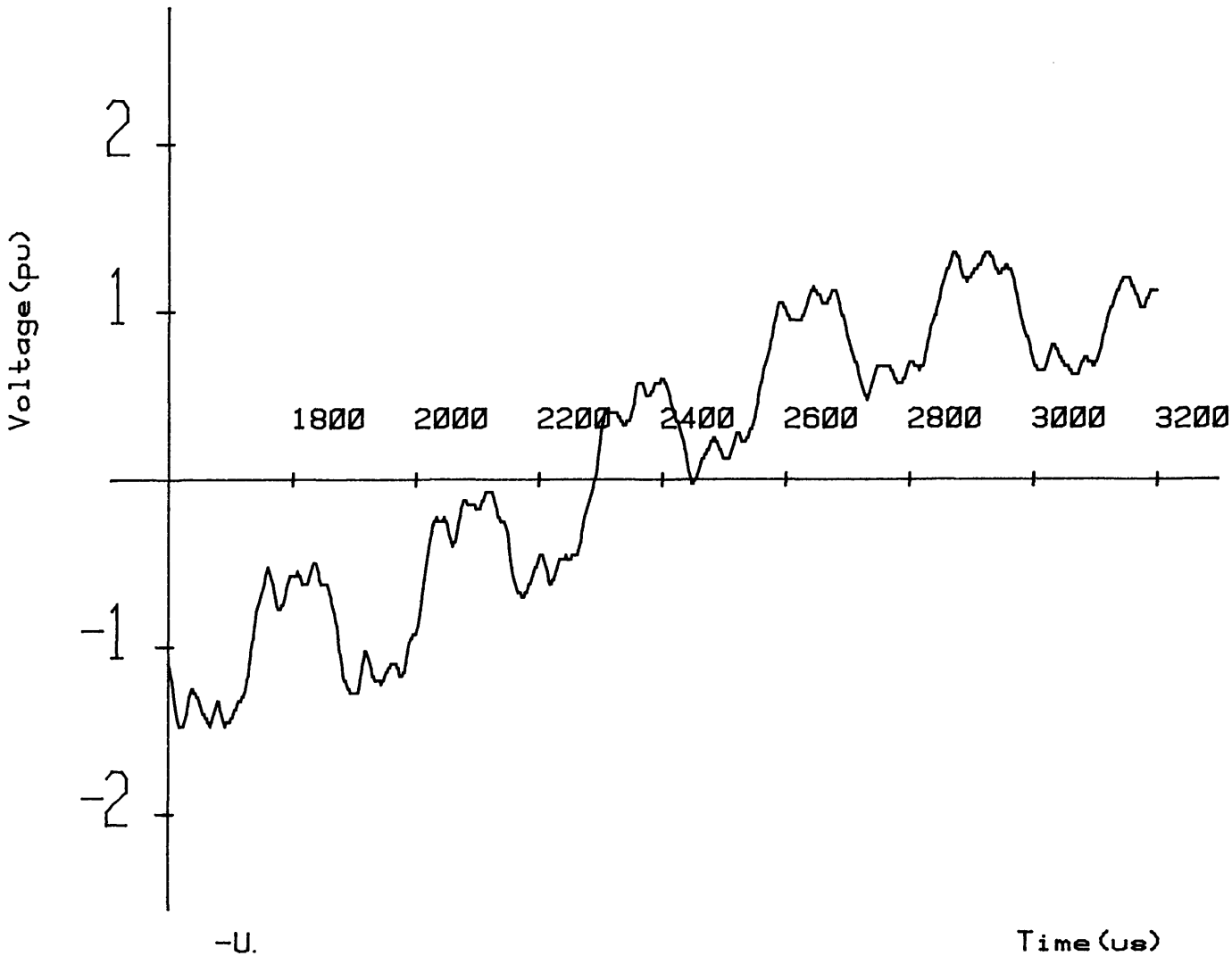

Figure 4.25(cont'd) (b) 1600 - 3200 μs.

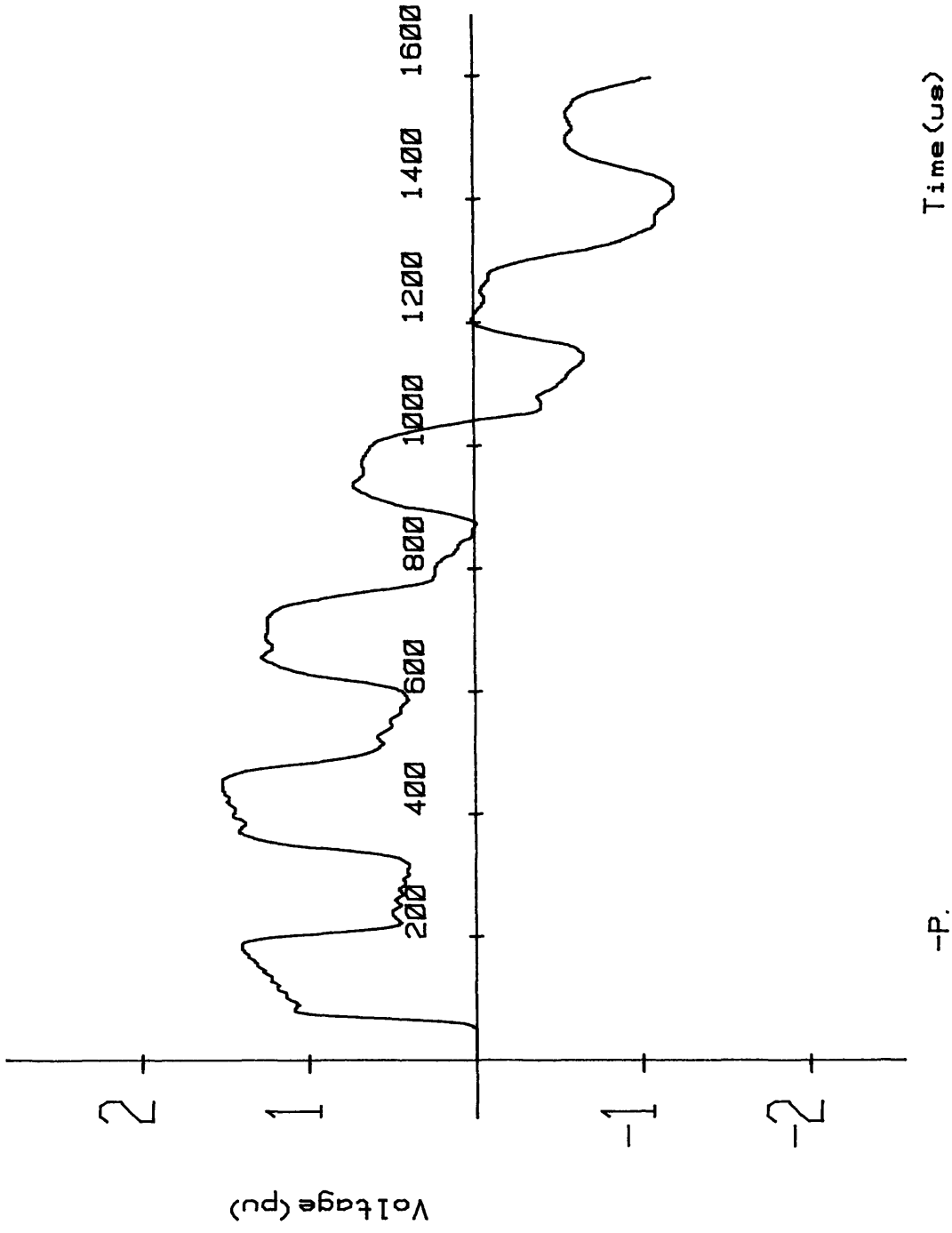

Figure 4.26 (a) 20 pi-section processor response (S_{ae}) for 30° closure (0 - 1600 μs).

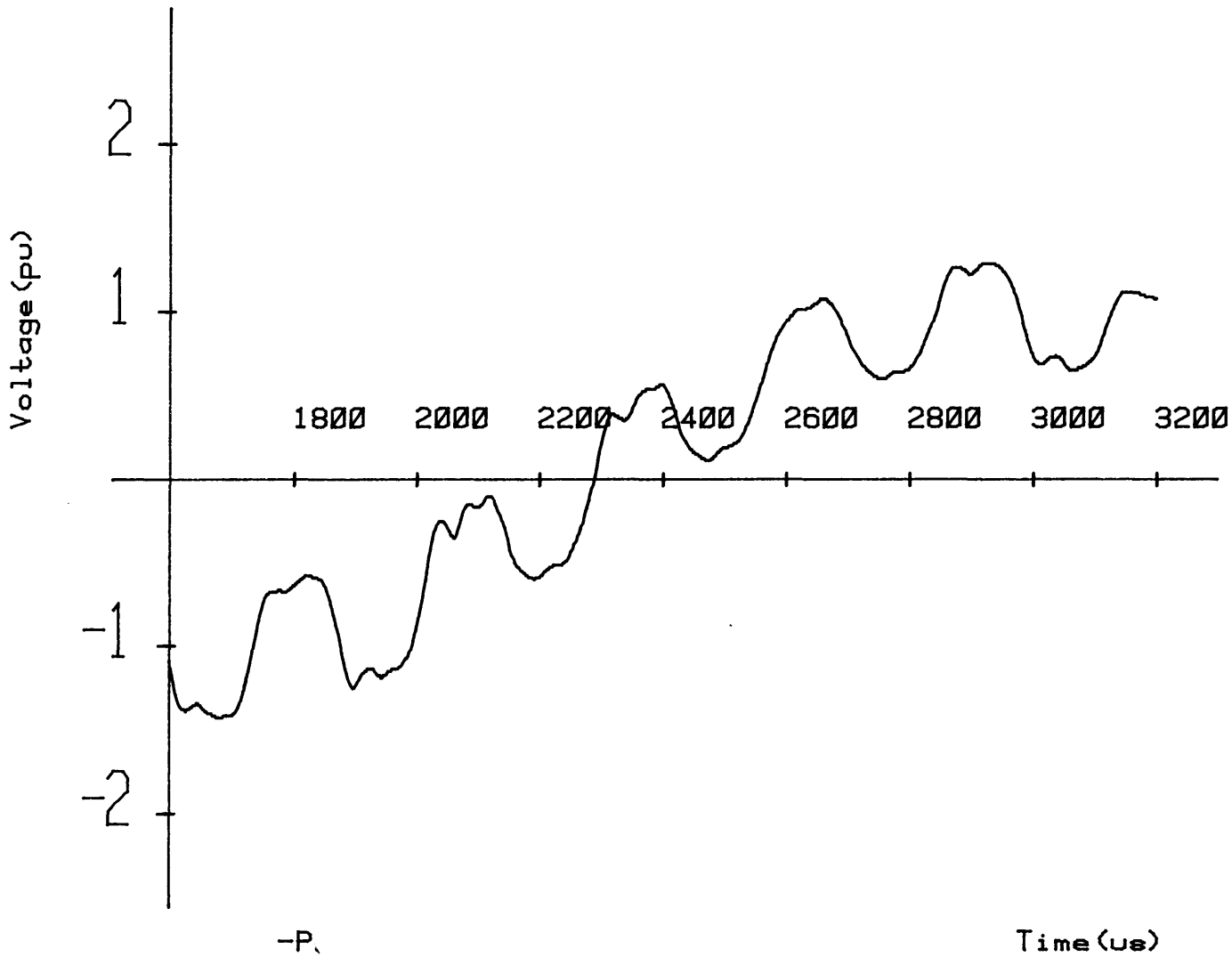

Figure 4.26 (cont'd) (b) 1600 - 3200 μs.

many ineffective averaging ranges were calculated from the uncompensated waveform of Figures 4.27(a) - (b) (the processor response is shown in Figures 4.28(a) - (b)). Inspection of this waveform shows that the Gibbs phenomena are less clearly defined due to the resolution i.e. volts/bit, of the TR used. Because the voltage range over which the oscillations vary is low, sampling errors will occur which lead to incorrect calculations for the values of N_a. This could be overcome by changing the resolution (Volts Full Scale) of the TR but this alteration would require a time-consuming software modification which is unnecessary since the resolution used is adequate for the most severe closure conditions.

However it is observed from the uncompensated waveforms for the more severe closures investigated that the Gibbs phenomena frequencies do not appear to change with variation in the angle of closure and therefore the values of N_a determined for say 90° closure could be applied over the relevant time ranges to process the uncompensated waveforms recorded for lower point-on-wave closures. This would effectively reduce the Gibbs content for any switching condition encountered thereby eliminating the need to change the TR resolution.

4.6.2.1. Zero Degrees Closure

The uncompensated response, of the 20 π-section line, for 0° closure shown in Figure 4.29 displays no Gibbs phenomena. Since there is no step disturbance and hence no high-frequency input to the model line at the sending-end the Gibbs phenomena will not be observed. Theoretically the receiving-end voltage should follow the source variation exactly but with a delay equal to the travel time of the line. However the slight oscillation detected occurs with a frequency which is related to the line travel time and arises due to the lumped-parameter nature of the line[9]. The resistor-damped response also displayed this effect. Averaging of the uncompensated waveform is therefore unnecessary for this closure condition.

Figure 4.27 (a) 20 pi-section uncompensated line response for 10° closure (0 - 1600 μs).

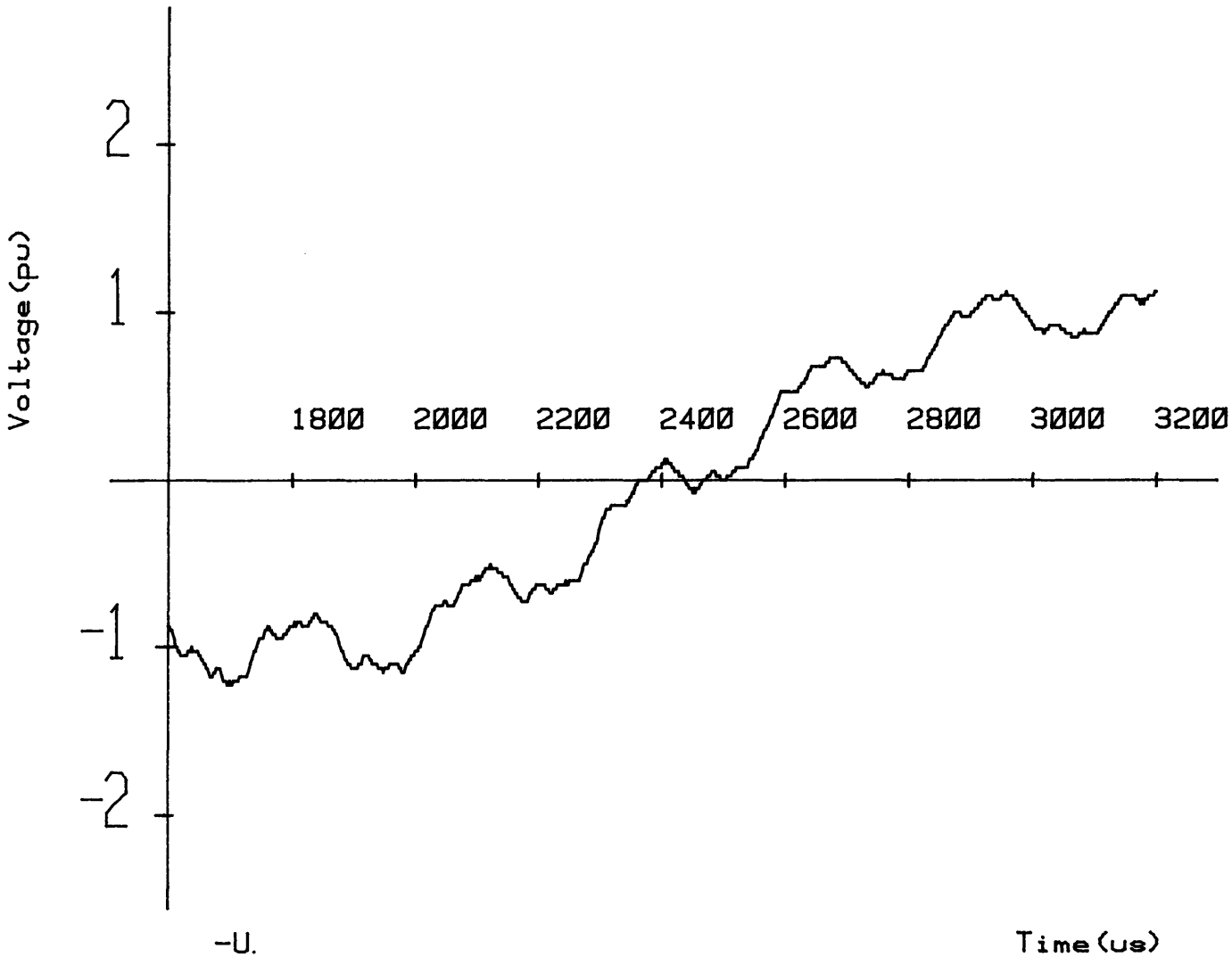

Figure 4.27 (cont'd) (b) 1600 - 3200 μs.

Figure 4.28 (a) 20 pi-section processor response (S_{ae}) for 10° closure (0 - 1600 μs).

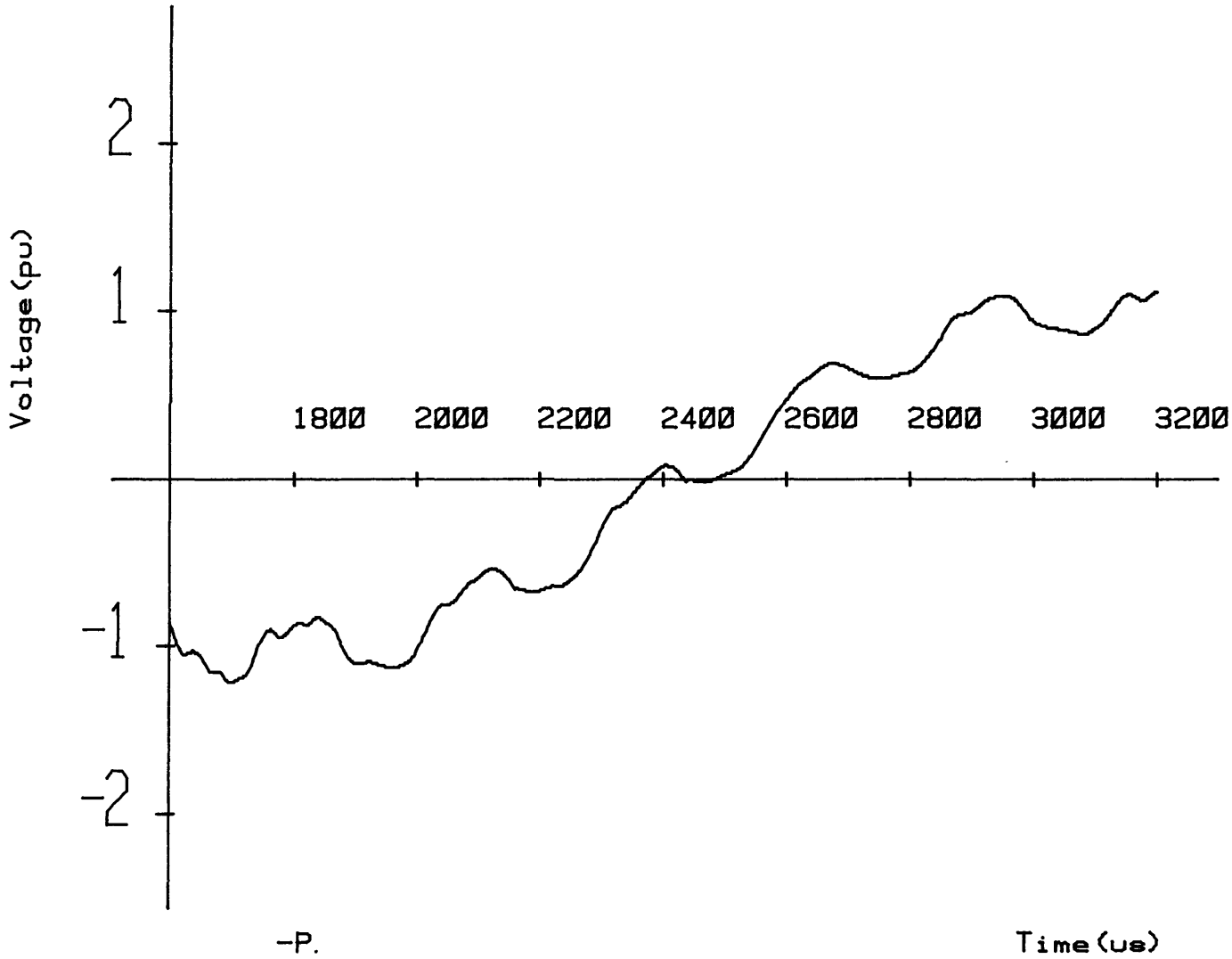

Figure 4.28 (cont'd) (b) 1600 - 3200 μs.

Figure 4.29 20 pi-section uncompensated line response for 0° closure.

4.6.3 Analysis of Sinusoidal Energisation

The results obtained for the lines with zero earth impedance demonstrated that the calculation of N_a was limited by the resolution of the TR as the point-on-wave closure approached 0°. N_a could therefore be calculated from the worst case closure, i.e. 90 or 270°, and applied to all uncompensated waveforms generated from less severe closure conditions. This may be implemented since the angle of closure does not alter the frequencies of the transient Gibbs content.

The previously determined 'fixed' averaging range of 15 μs for the 1-phase lines with earth-path impedance remained effective for sinusoidal energisation. This value of N_s can therefore be applied to all uncompensated waveforms resulting from any condition of closure and is applicable for all line lengths of this model configuration.

The exception to these recommendations is the case of 0° switching whose responses contain no Gibbs Oscillations and therefore do not require processing.

4.7 The Experimental Modified Sigma Factor S_{me}

The processor results obtained using S_{se} and S_{ae} have shown that the magnitude of the Gibbs phenomena have been significantly though not completely reduced. The rates of rise of the processor discontinuities are also an improvement on the resistor-damped responses with the exception of the initial rates of rise of the 5 and 10 π-section lines.

The Modified Sigma Factor σ_m in the Transform analysis was devised to improve the rates of rise of the response calculated by the inversion integral which incorporated σ_s. Figure 4.30(a) shows the effect of σ_m where the arbitrary averaging range chosen was half of that used for σ_s i.e. compare with Figure 4.1(b). A reduced Gibbs content is still observed in the response calculated. As stated previously, the claim that the use of both factors at the appropriate parts of the Fourier response would improve the

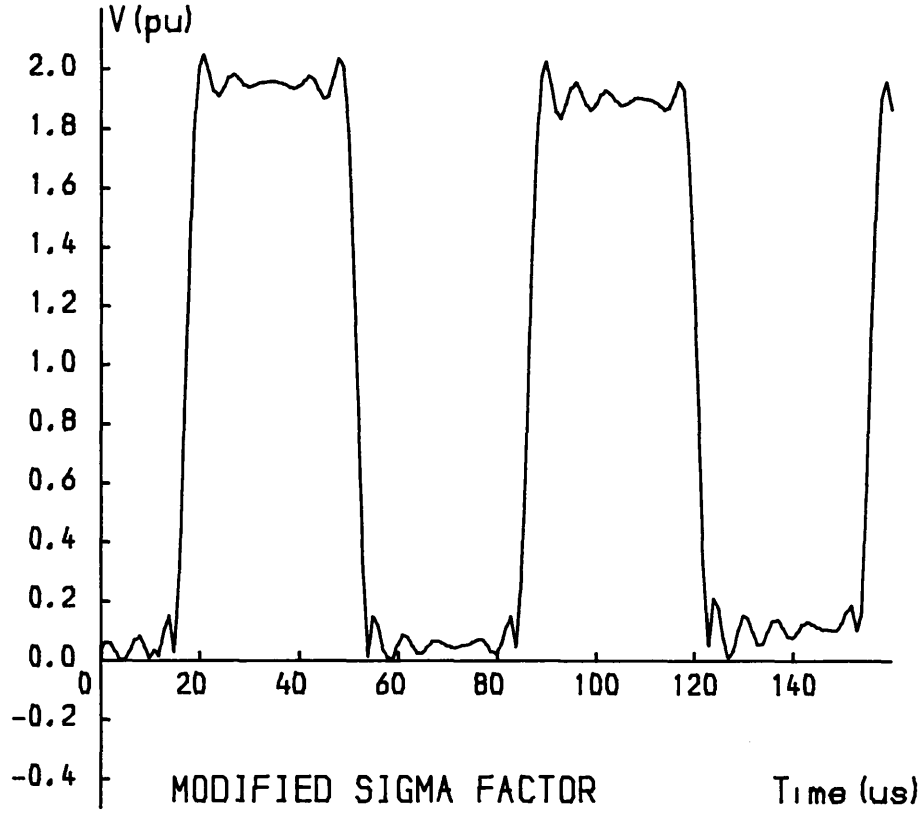

(a)

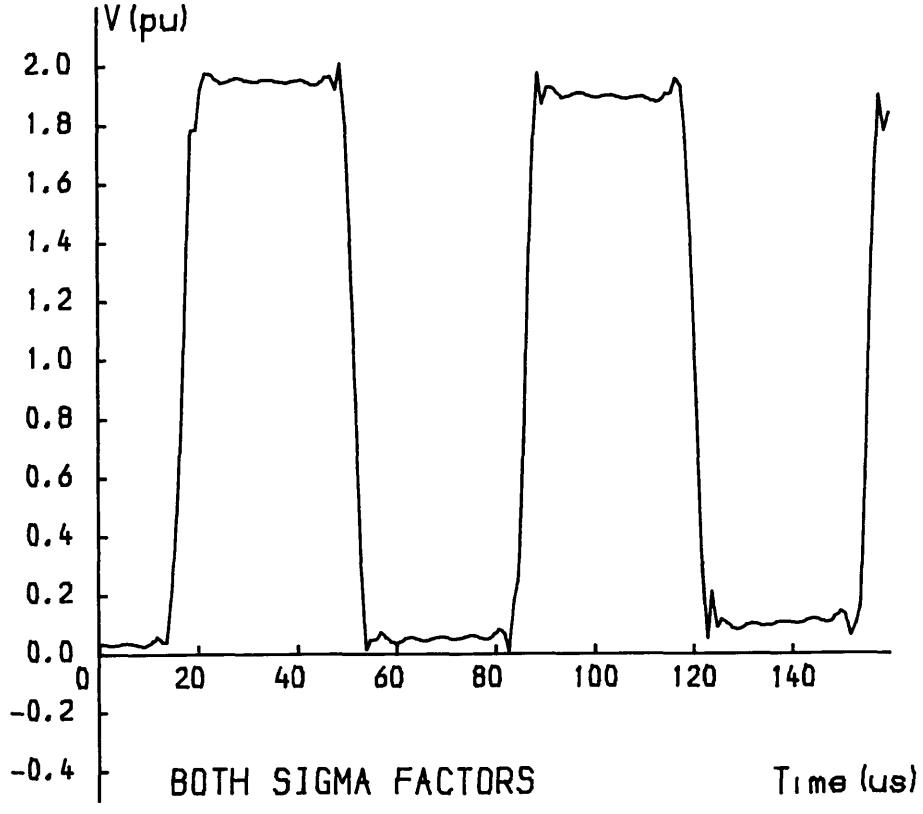

(b)

Figure 4.30 The use of σ_m and σ_s in modifying a 25 mile actual line response calculated by the Modified Fourier Transform (a) σ_m (b) σ_m and σ_s.

overall waveshape[3] was fairly accurate though calculations showed that the response continuity was disturbed where the averaging range was changed (Figure 4.30(b)). However the use of σ_s and σ_m for response modification suggested that S_{se} could be used in conjunction with an Experimental Modified Sigma Factor S_{me} to further improve the processor discontinuities and in particular the initial rates of rise.

The Fourier Transform solution of equation (4.1) i.e. excluding Sigma Factors, shown in Figure 4.1(a) gave the highest rates of rise for the response discontinuities. A Transform Analysis-Model Line analogy can be made in this respect as the waveforms from the uncompensated model line also display this characteristic i.e. the uncompensated response rates of rise are greater than those of the processor and resistor-damped responses. More practical rates of rise of voltage might be obtained from the uncompensated waveform as the model cut-off frequency f_c excludes a range of higher frequencies that will be present in an actual transmission line response. Therefore the uncompensated waveform discontinuities, which gives the worst case rates of rise from the model, could be included directly in a processor response to further improve accuracy.

To simplify the incorporation of uncompensated waveform discontinuities directly in a processor response the waveforms from the 1-phase uncompensated lines with earth path impedance of section 4.4.2 were chosen for the following reasons:-

1. By waveform inspection it was noted that their uncompensated waveform discontinuities were free of Gibbs phenomena. Therefore the use of S_{se} would not be required for these regions of the waveform. This would allow them to be incorporated directly in a processor response.

2. The reduction of the Gibbs phenomena required only the single value of N_s i.e. 15 μs, since no changing high-frequency Gibbs

content was apparent.

This would simplify the task of programming the use of S_{se} and S_{me} together in software. Therefore the initial idea to improve the processor response rates of rise consisted of retaining the uncompensated waveform discontinuities and 'fitting' them to regions of the processor response where S_{se} had been used to reduce the uncompensated waveform Gibbs content (Figure 4.31).

4.7.1 Implementation of S_{me}

For an open-circuited line the uncompensated model receiving-end waveforms show that the Gibbs phenomena occur where a lossless distributed-parameter line response would have a flat surge peak whose gradient would be zero. Therefore after the processor response is calculated using S_{se} it could be analysed to determine regions where the gradient between processor samples satisfies the above criterion (solid line of processor waveform in Figure 4.31). These regions can be noted in software and will indicate the surge peaks of the waveform. Having achieved this it would then be required to 'fit' these processed regions to the uncompensated waveform discontinuities.

Since the high-frequency components of an actual line square-wave response would be attenuated by line losses this suggested that a curve could be drawn between these processor and uncompensated waveforms (dotted line of Figure 4.31). If, for example, the initial rate of rise of the uncompensated waveform was to be made continuous with the first processor region then it would be possible to determine an uncompensated discontinuity sample value which was less in voltage magnitude than the first sample of the processed region. The difference in voltage and time between samples could also be determined by software which would give the information required to calculate a curve.

However problems existed in defining a suitable curve function and

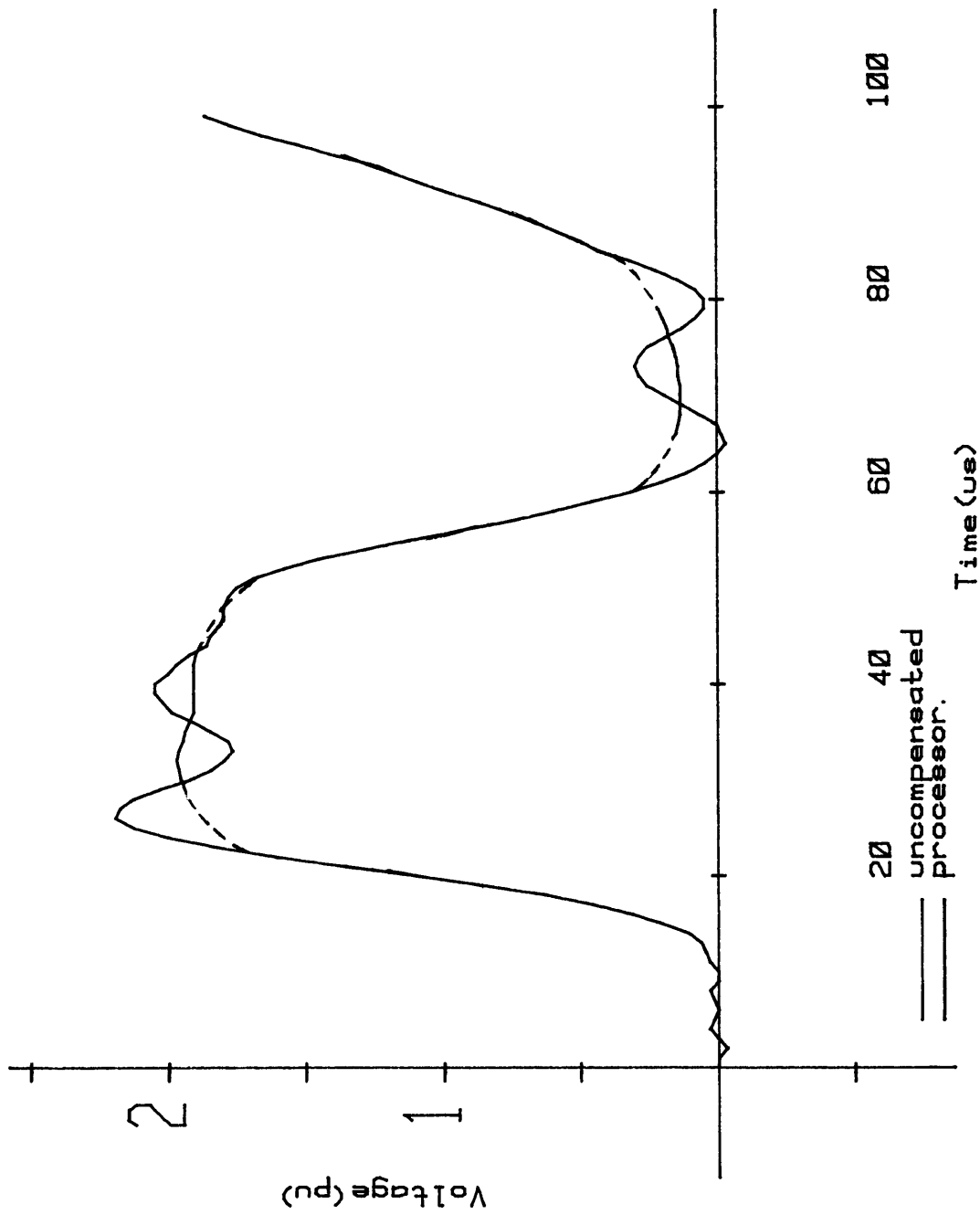

Figure 4.31 Incorporating the uncompensated waveform discontinuities in a processor response to improve processor rates of rise.

in determining the uncompensated waveform sample which would give the best result. More importantly it was realised that the method of connecting the two regions by a curve was independent of the data representing the uncompensated and processor waveforms.

It was decided that a technique for improving the processor discontinuities should be based on data correlated from the uncompensated response itself in the same manner by which S_{se} and S_{ae} had been determined.

4.7.2 The Modified Sigma Factor Averaging Range N_m

When varying N_s in order to improve processor waveform initial surges in section 4.4.1.1 it had been noted that a reduction in N_s gave improved rates of rise for the processor discontinuities. When investigated further it was found that by averaging with N_s=1 μs, i.e. H=0, that the processor response was an exact copy of the uncompensated waveform. With H=0 the sample v_n in equation (4.4) is the only sample incorporated in the voltage summation and dividing by $N_s(=1)$ therefore gives $v_{np} = v_n$. The reduction of the averaging range for sampled waveforms is thereby a direct analogy with σ_m in the Transform Analysis. Hence the variation of H and therefore N_s could be used in some manner to retain the uncompensated waveform discontinuities.

For the earth path impedance lines it has been noted that the single value of N_s=15 μs successfully reduced the Gibbs phenomena in the uncompensated responses. This defines the upper limit for averaging while the lower limit was defined as 1 μs. With an averaging range of 15 μs the Gibbs phenomena in a response would be significantly reduced while the implementation of a 1 μs range would in effect copy the uncompensated waveform discontinuities. The averaging ranges between these limits i.e. 3,5 ... 11,13 μs could also be used in an attempt to achieve the 'curve fitting' discussed previously. In order to do this the variation in the

Experimental Modified Sigma Factor Averaging Range N_m would have to be determined from the uncompensated waveform data. N_m in this case would have values of 1,3 ... 13,15 μs.

4.7.2.1. The Use of N_s to Determine N_m

Since the value of N_s, and hence H, is constant it was used to determine which value of N_m should be implemented for modifying the uncompensated waveform. In this respect the magnitude of the rate of change of voltage or voltage gradient was calculated for each uncompensated waveform sample in the following manner (refer to Figure 4.32).

For the n^{th} voltage sample, v_n, the value of the voltage sample 'H' samples previous, v_{n-H}, can be subtracted from the value of the voltage sample 'H' samples after it, v_{n+H}, to give a gradient magnitude |G| for that sample. It was reasoned that if v_n was in a region of Gibbs Oscillations then $|G_n|$ would be close or equal to zero i.e. sample 29 while if v_n was positioned midway in a discontinuity then $|G_n|$ would have a high gradient value i.e. sample 12. If v_n was positioned in the initial waveform discontinuity $|G_n|$ would give the highest gradient value that could be calculated since this discontinuity has the steepest rate of rise in a 1-phase uncompensated line transient response. |G| was assigned the unit of pu voltage per 15 μs.

A range of gradients can therefore be determined with one value pertaining to each sample of the uncompensated response. If $|G_n|$ is high then v_n comprises part of a discontinuity and N_m should be low i.e. 1 or 3 μs, while if $|G_n|$ is close or equal to zero then N_m=13 or 15 μs should be applied for waveform modification since v_n lies in a region of Gibbs phenomena. As a region of Gibbs Oscillations is approached N_m will be increased until such time that the upper limit of 15 μs is used as the region is encountered. In order to determine the values of N_m that should be implemented as $|G_n|$ decreased and approached zero, empirical calculations were carried out using the initial surges of the 5 and 20 π-section

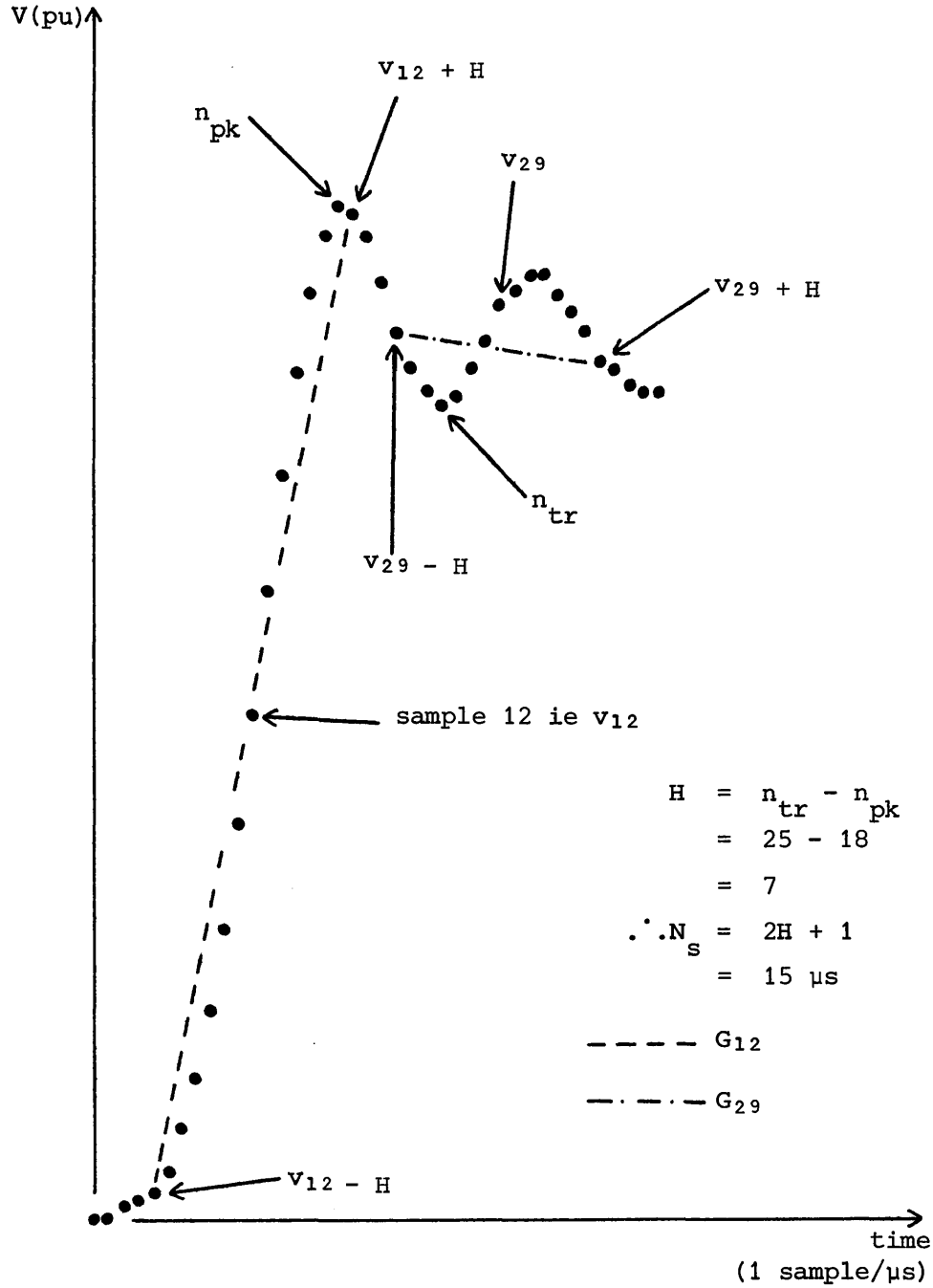

Figure 4.32 Calculation of $|G_n|$ by using N_s.

uncompensated earth-path impedance line responses.

The waveform samples of each response were plotted on graph paper and |G| for each sample calculated by Z-2D software. Those regions of the waveform for which |G| < 0.313 i.e. a low rate of change indicating a region of Gibbs Oscillations, were to be modified with N_m=15 μs. The value for |G| was arrived at empirically. The uncompensated samples to which this criterion applied were replaced by the processor values calculated using N_m=15 μs (similar to the solid-line processor response shown in Figure 4.31). Possible processor values were then plotted i.e. the dotted line in Figure 4.31, in order to give the best square-wave response which could be intuitively estimated. The value of N_m which gave the closest processor sample voltage to the estimated voltage value was then determined by calculating all possible processor values for that sample using the allowed values of N_m.

From the averaging ranges and gradients determined tables for the two lines were devised so that a particular value of N_m would be implemented for averaging for a defined range of |G| (Figure 4.33). Using these tables processor responses were obtained for both lines (Figures 4.34 and 4.36) and these can be compared with the responses calculated by S_{se} alone (Figures 4.35 and 4.37). Initial and subsequent rates of rise of the 5 and 20 π-section lines are improved by S_{me}. However, in each case, by varying N_m the processor continuity is not retained as was observed in the Transform Analysis.

From these results the initial rates of rise of the three model line waveforms were calculated for both line lengths (1 pu voltage = 275 kV) and these are shown in Figure 4.38.

4.7.2.2. Analysis of N_m

The values from the processor responses indicate that S_{me} gives higher rates of rise than by the use of S_{se} alone and that S_{me} calculates

N_m applied	$\|G\|$ (δpu/15 μs) 5π	20π
	2.141	1.656
1		
	1.875	1.484
3		
	1.641	1.328
5		
	1.406	1.172
7		
	1.172	1.016
9		
	0.938	0.781
11		
	0.547	0.547
13		
	0.313	0.313
15		
	0.0	0.0

Figure 4.33 Ranges of gradient values $|G_n|$ for which specific averaging ranges were applied for uncompensated waveform modification.

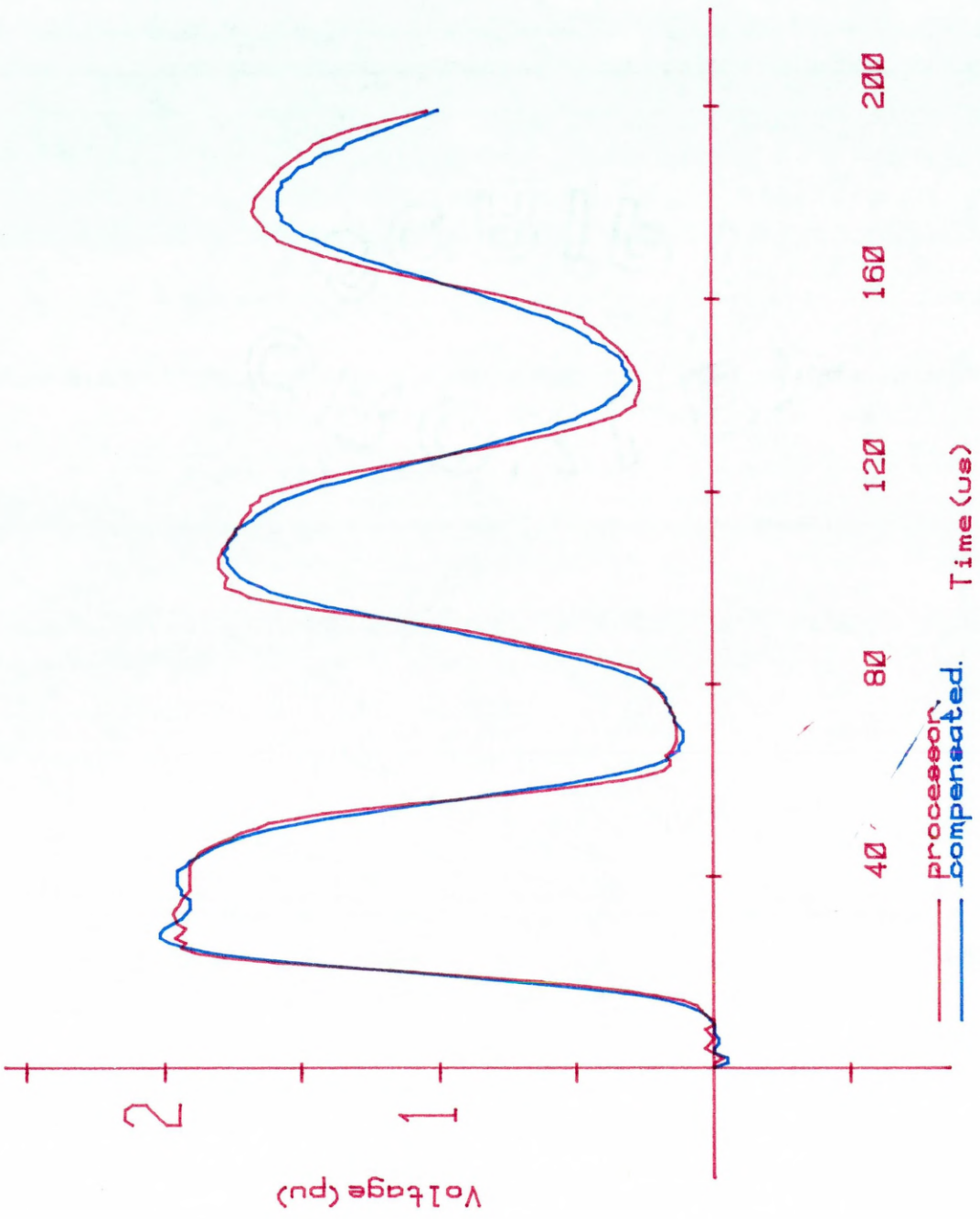

Figure 4.34 5 pi-section processor response calculated by S_{me}.

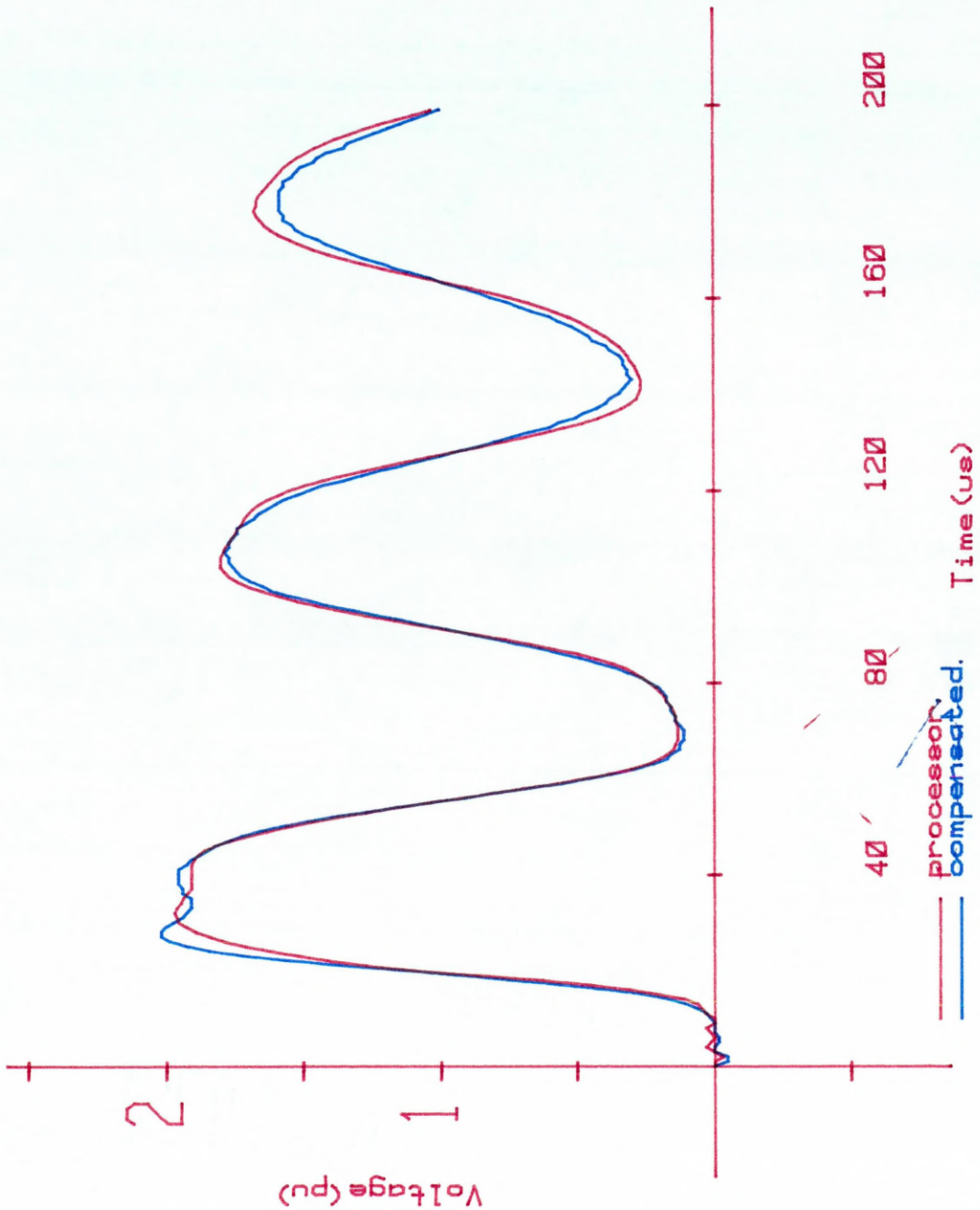

Figure 4.35 5 pi-section processor response calculated by S_{se}.

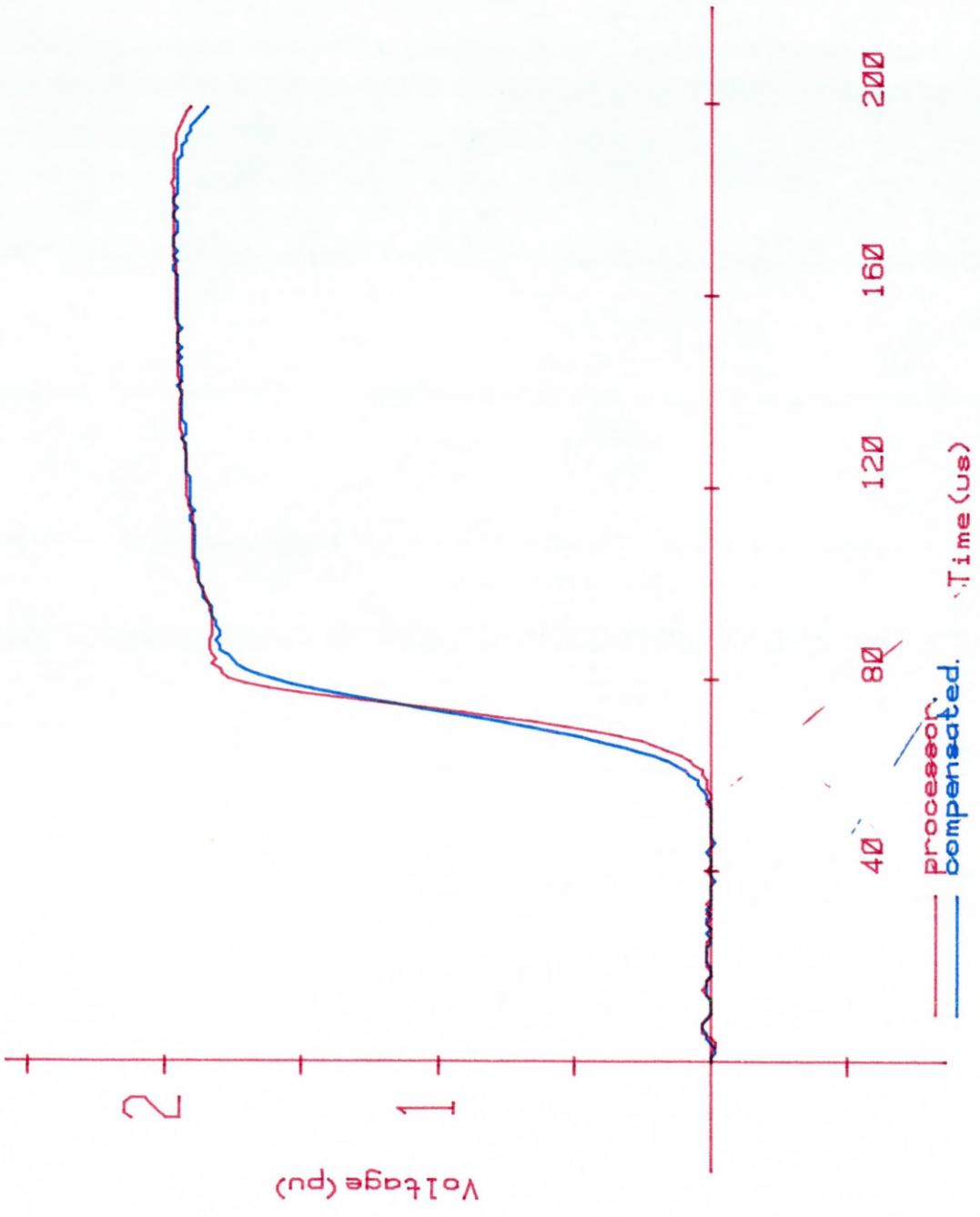

Figure 4.36 20 pi-section processor response calculated by S_{me}.

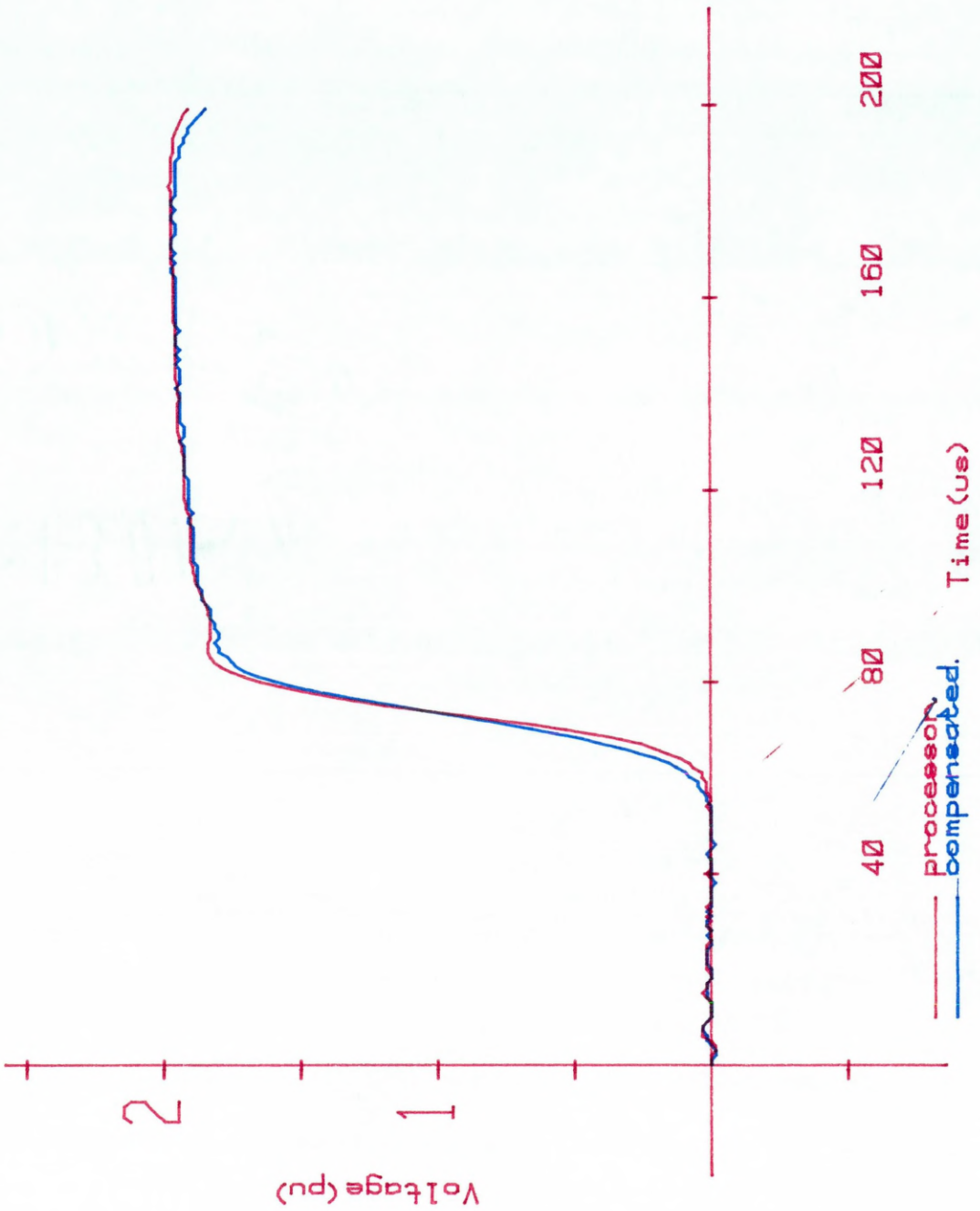

Figure 4.37 20 pi-section processor response calculated by S_{se}.

Line Configuration	RRRV (kV/μs)	
	5π	20π
Resistor-compensated	46.1	24.4
Processor response S_{se}	31.9	26.9
Processor response S_{me}	51.9	39.5
Uncompensated	54.0	39.5

Figure 4.38 RRRV of initial discontinuity of 5 and 20 pi-section line responses.

values that are close or equal to that determined from the uncompensated waveform. Although S_{me} gives improved initial and subsequent rates of rise the processor responses do display a loss of continuity. These changes are very small in magnitude and an improved representation is obtained. The technique however does have a number of disadvantages:-

1. In order to evaluate the tables of Figure 4.33 many calculations were required and some intuitive judgement used when assuming the processor response desired.

2. The tables are also only truly effective for the initial surges from which they were derived and since subsequent rates of rise are not as severe the full range of N_m would not be implemented for the remainder of the uncompensated waveform.

3. By calculating tables for two lengths of line it was found that the values of N_m were applied over differing ranges of $|G|$ since the two uncompensated responses differed in the rates of rise of waveform discontinuities. A 'general case' table of values therefore could not be applied to different lengths of a model configuration.

Therefore it was decided that a simpler method of varying N_m would have to be determined which did not require the same level of operator involvement.

4.7.2.3. Automatic Variation of N_m

In order to eliminate the pre-processing calculations which the tabular method required a simple assumption was made in order to achieve an 'automatic' version of S_{me}. The assumption was based on the change in $|G|$ for successive samples to determine the value of N_m which should be used when implementing S_{me}.

The magnitude of the rate of change of voltage, $|G|$, varied from a finite value to zero. If an increase in $|G|$ between successive uncompensated samples was calculated it was assumed that a discontinuity was being

approached and consequently N_m would be reduced. Similarly a decrease in |G| for successive samples would imply a forthcoming surge peak with its Gibbs Oscillatory content indicating that N_m should be increased. As before the limits of N_m were defined as 1 and 15 μs and the criterion that when |G| < 0.313 (section 4.7.2) that N_m(=15 μs) was used when applying S_{me} was also defined. As stated previously N_m=15 μs was determined as the most effective averaging range for this range of gradient values and an uncompensated waveform sample whose gradient satisfied this condition would be modified immediately with this value of N_m.

The processor results using this simplified technique are shown in Figures 4.39 and 4.40. The initial rates of rise for the processed responses of the 5 and 20 π-section lines were found to be 46.1 and 35.4 kV/μs respectively which although not as severe as those calculated using S_{me} (Figure 4.38) are still greater than those calculated by S_{se}. Again the waveforms display a loss of continuity due to the variation of N_m and the 5 π-section processor response (Figure 4.39) in particular shows this effect at the upper end of the initial rate of rise.

4.7.3 Discussion of the Use of S_{me}

The application of S_{me} in the processing of the uncompensated line responses gave improved square-wave representation and increased rates of rise for initial and subsequent waveform discontinuities. However, as in the Fourier analysis, loss of processor waveform continuity was evident where N_m was varied.

The techniques devised for S_{me} are dependent on the upper limit of averaging being constant. Consequently the implementation of S_{me} for the lines with zero earth impedance would be more complex due to the problems previously encountered with the decreasing frequency of the Gibbs phenomena of the uncompensated waveforms. Also considering that the processor responses obtained from these lines using S_{ae} contained a reduced Gibbs

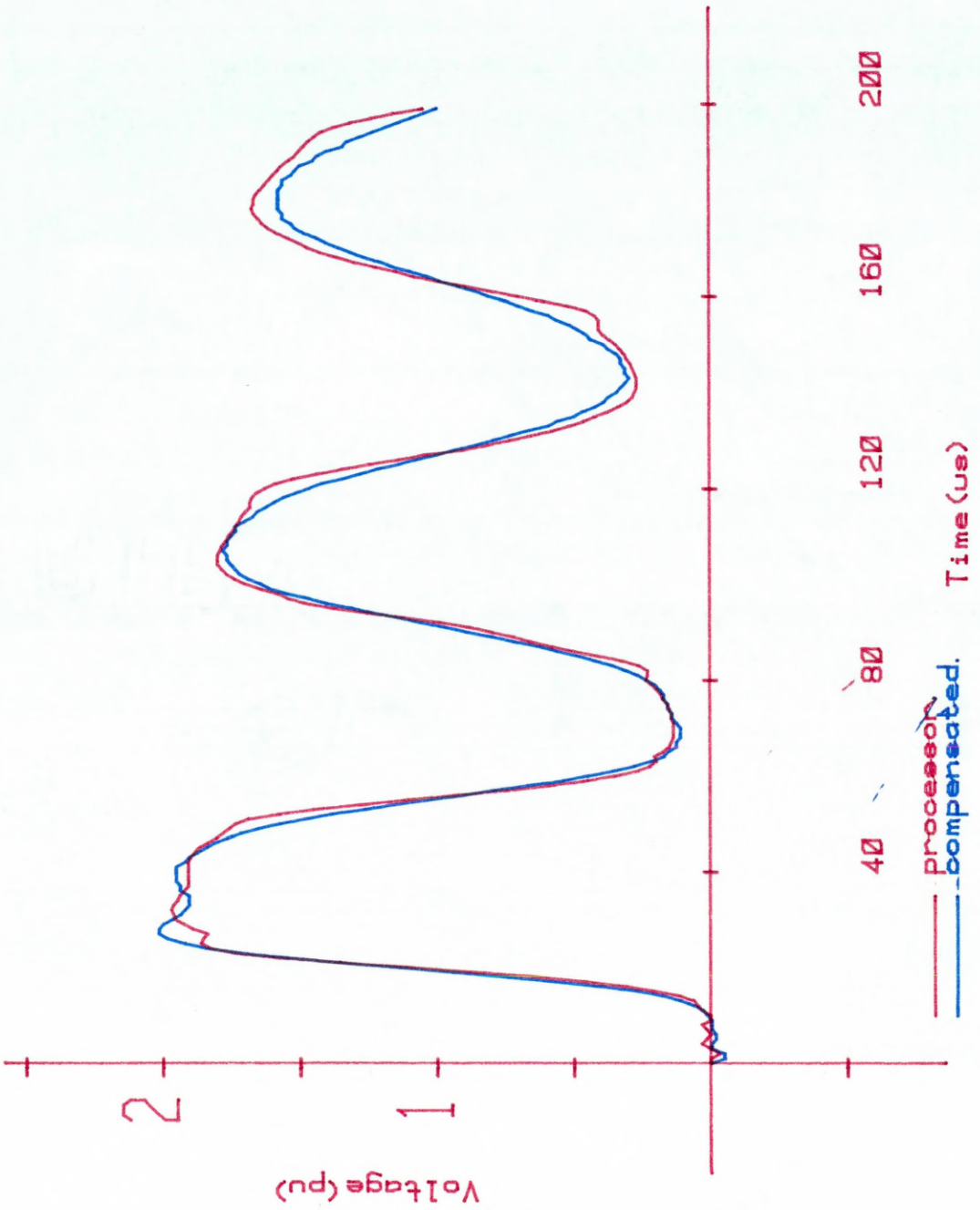

Figure 4.39 5 pi-section processor response calculated using the automatic S_{me}.

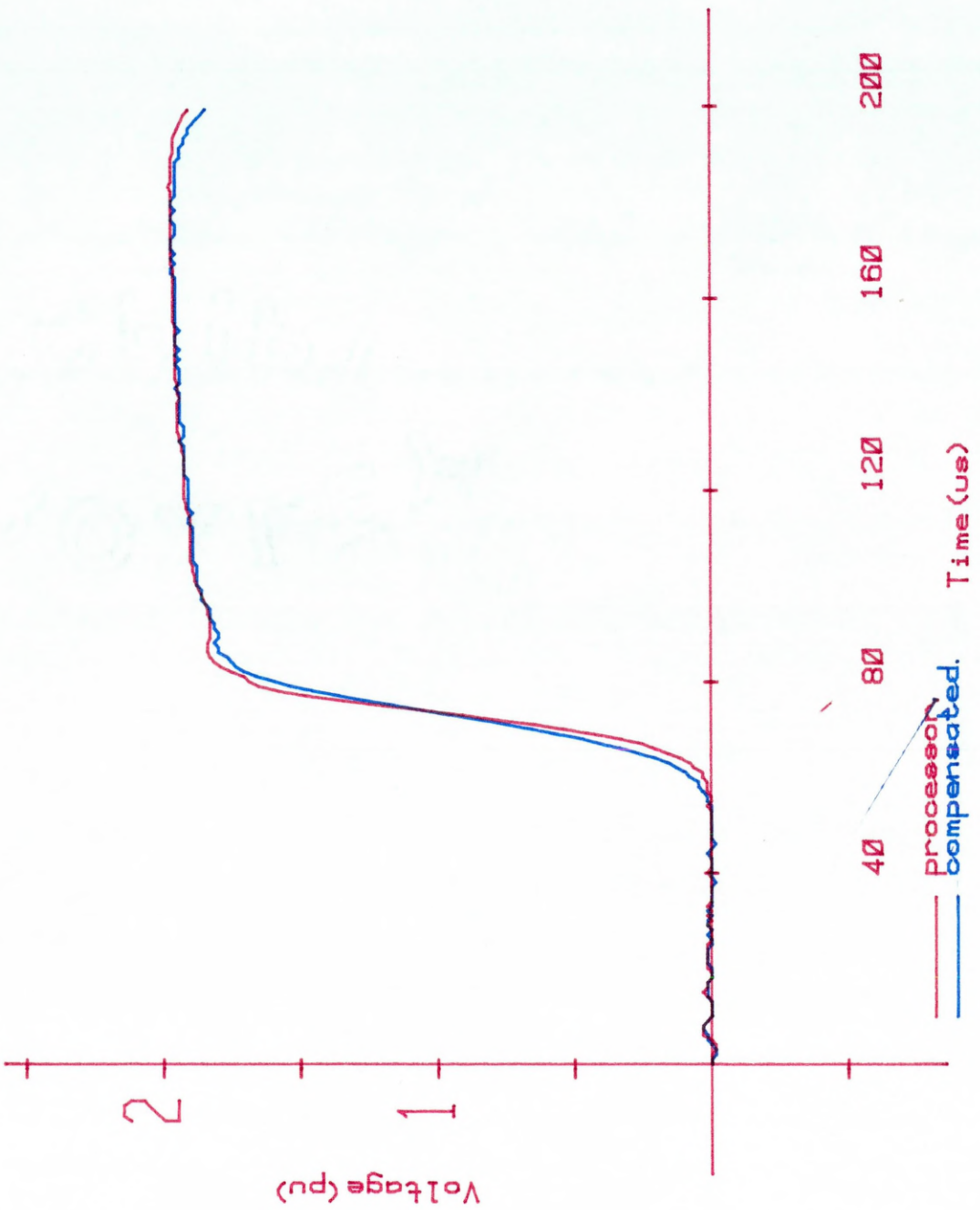

Figure 4.40 20 pi-section processor response calculated using the automatic S_{me}.

content the application of S_{me} and the subsequent loss of waveform continuity would most probably lead to an increased apparent oscillatory content being observed.

Improvements in waveshape, relating to the processor waveform rates of rise, appear to be restricted especially for the zero earth impedance line responses. However if the magnitudes of worst case rates of rise are desired they could be taken directly from the uncompensated waveforms and coupled with the overvoltage analysis using S_{ae} may still lead to greater accuracy, when determining these parameters, than that given by the resistor-damped model.

CHAPTER 5

The Effect of Source Inductance on Gibbs Phenomena

5.1 Introduction

The model transient waveforms investigated in Chapter 4 were generated by line energisation from an equivalent infinite i.e. zero impedance AC or DC source. The high-frequency components of the step input from this source type are attenuated due to the filter effect of the line giving rise to the Gibbs phenomena observed in the receiving-end responses shown. However the types of source busbar which occur in actual power systems are assumed to exist between the two extreme cases of a purely inductive and a purely resistive source, the nature of the source being dependent on the equipment connected to that busbar[20]. A busbar fed solely by generators or transformers can be represented by a voltage source behind an inductance while that fed from transmission lines alone can initially be considered as a voltage source behind a resistance.

In this case the inductive source was considered for uncompensated line energisation tests as the inductance modifies the sending-end voltage applied to the model line. The frequency content of the line input is therefore different from the infinite source case and the effect on the generation of Gibbs phenomena in the uncompensated line responses was investigated. Previous line energisation transient analysis has shown that source inductance has a marked effect not only on the transient waveshapes generated but also on the overvoltages produced at the transmission line receiving-end[4, 20, 21, 6]. In this respect similar overvoltage analysis was carried out on the single and 3-phase model lines, with and without resistor-damping, to determine if significant differences in peak overvoltage profile could be obtained when comparing resistor-damped and processor-modified responses.

5.2 Energisation from an Inductive Source

As shown in section 4.6 the energisation of an uncompensated model transmission line from an infinite AC source generates Gibbs phenomena in the receiving-end response for all point-on-wave closures with the exception of 0°. However the initial step input which occurs for these closures is now modified with the introduction of inductance into the model source representation.

The equivalent circuit for a transmission line fed from a purely inductive source is shown in Figure 5.1(a) which represents the DC voltage supply E behind the source inductance L_s which is determined from the 3-phase fault level at the source. Z_0 (assumed to be purely resistive) represents the surge impedance of the transmission line. From transient theory, when the switch is closed, the voltage appearing across Z_0 i.e. the line sending-end voltage V_s is given by

$$V_s = E(1 - e^{-At}) \tag{5.1}$$

where

$$A = Z_0/L_s \tag{5.2}$$

For the DC source V_s will be of the form of Figure 5.1(b) when the switch is closed at t=0. Therefore V_s rises to the voltage supply E with a time constant which is dependent on L_s and Z_0. The frequency content of the input to the line is therefore altered such that the very high-frequency components of the step input are no longer present for inductive source energisation. For a certain value of L_s it could therefore be assumed that the highest frequency component of the line input would be below that of f_c, the model cut-off frequency, thereby giving an uncompensated response which would be free of Gibbs Oscillations.

Tests were carried out on a single and 3-phase basis, using the inductance unit of the new TNA (section 2.6.5) to model L_s, to determine if

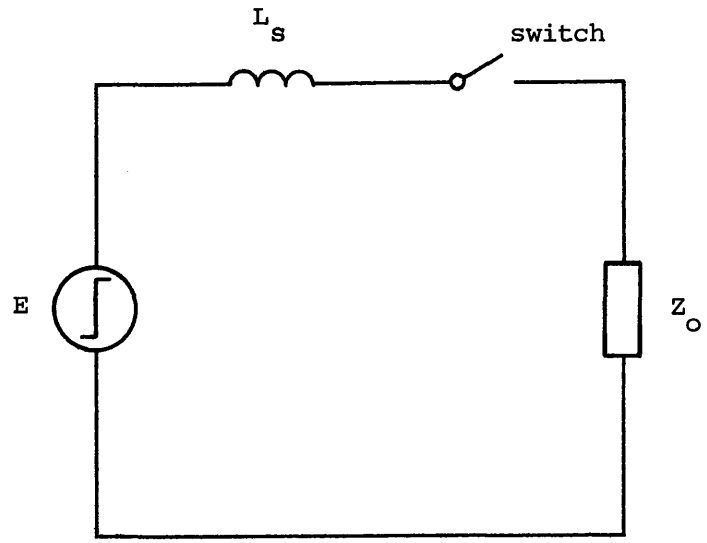

Figure 5.1(a) Equivalent circuit for a purely inductive source energising a transmission line.

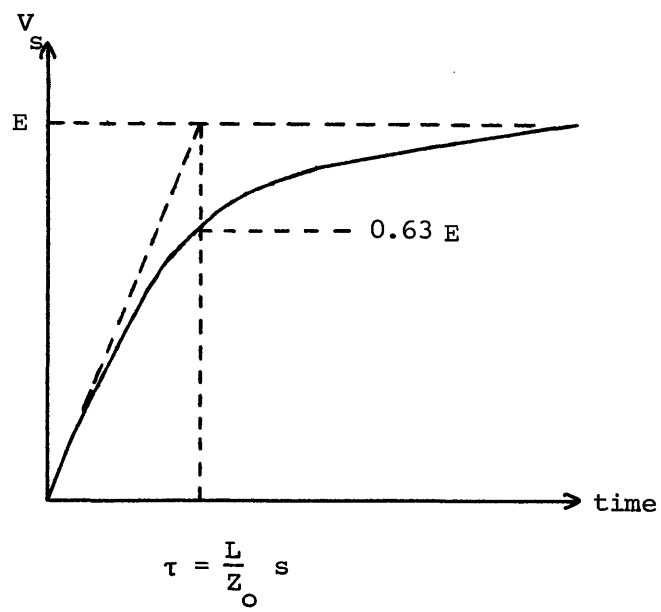

Figure 5.1(b) Line sending-end voltage for inductive source energisation.

this would be the case. All inductance values stated are for the actual line case i.e. 50 Hz. The values used in the model experiments were scaled down by 1/3 of the 50 Hz value since the model source frequency was 398 Hz (section 1.3.1).

5.3 The Oscillatory-free Response due to L_s

Figure 5.2 shows the receiving-end response of a 1-phase 20 π-section uncompensated zero earth impedance line with L_s=0.0801H and for a point-on-wave closure of 90°. The uncompensated waveform appears to be free of the high-frequency Gibbs components while other effects due to the source impedance can be observed.

The 'hump' or peak characteristic which can be seen at 230 μs is due to the initial exponential rise at the sending-end travelling to the receiving-end, being reflected back and impinging on the source inductance. This in turn travels back to the receiving-end giving the waveshape observed. This effect is then observed throughout the waveform at intervals of twice the propagation time of the line with exponential changes taking place between these peaks. This occurs since the source reflection coefficient, no longer having a negative value as in the infinite source case, changes exponentially between $\pm$1. The transient response then varies according to the 398 Hz source. Similar waveshapes have previously been observed[4].

Although no natural π-section Gibbs frequency can be detected in the waveform, results obtained previously for infinite source energisation of this line length indicated that Gibbs phenomena of a lower frequency may be present in the receiving-end response (section 4.4.1.1). It was thought that this could be the case when the response in Figure 5.2 at 1200 μs was analysed. Therefore a method of distinguishing between source inductive effects and possible Gibbs phenomena would have to be realised. The programs developed using the Runge-Kutta technique in section 7.4 were of little or no use in this respect since it was realised that the

Figure 5.2 20 Pi-section Uncompensated Line Response with a Source Inductance of 0.08H.

frequency-dependent resistance of the line series impedance and source inductance could not be taken into account. The Runge-Kutta uncompensated line responses therefore displayed a far higher Gibbs frequency content than was observed in the model line waveforms (see Figure 7.13(a), the Runge-Kutta equivalent response of Figure 5.2).

However the line responses given by Bickford[4] were calculated using travelling wave techniques in the s-domain and this method was used to calculate the distributed-parameter line response and therefore eliminate any confusion in differentiating between the Gibbs phenomena and inductive source effects.

5.3.1 Line Responses by the Lattice Technique

As described in section 1.8.2 the Lattice Method makes use of the reflection and transmission coefficients K_r and K_t at line junctions and terminations to calculate voltages and currents arising from a system disturbance. For a 1-phase transmission line knowledge of K_r for the sending and receiving-end conditions of the line is necessary together with the line travel time T[30]. K_r is given by

$$K_r = \frac{R_e - Z_o}{R_e + Z_o} \tag{5.3}$$

where Z_0 is the surge impedance of the line and R_e is the surge impedance of the termination.

For the open-circuited receiving-end $R_e = \infty$, $K_r = 1$

For the inductive source $R_e = sL$, $K_r = \frac{sL - Z_o}{sL + Z_o}$

For a step input the sending-end voltage V_s is given by

$$V_s(s) = \frac{E}{s} \cdot \frac{Z_o}{sL + Z_o} \tag{5.4}$$

Substituting equation (5.2) into (5.4) gives

$$V_s(s) = \frac{E}{s} \cdot \frac{A}{s + A} \tag{5.5}$$

The inverse Laplace transform of this gives equation (5.1).

This voltage is time dependent and taking the line delay into account the line receiving-end voltage V_r is given by

$$V_r(s) = V_s(s)[\ 2e^{-sT} + 2K_r e^{-3sT} + \ldots\ ] \qquad (5.6)$$

where e^{-sT}, e^{-3sT} etc represents the line delay using the 2^{nd} Heaviside Shifting Property and the factor of 2 in each term represents voltage doubling at the receiving end.

Expanding equation (5.6) and taking the inverse Laplace transform of the first three terms gives

$$\begin{aligned} V_r = {} & 2U(t-T)E(+1 - e^{-A(t-T)}) + \\ & 2U(t-3T)E(-1 + e^{-A(t-3T)}(\ 1 + 2A(t-3T)\ )\ ) + \\ & 2U(t-5T)E(+1 - e^{-A(t-5T)}(\ 1 + 2[A(t-5T)]^2\ )\ ) + \ldots \end{aligned}$$

The first eight terms of equation (5.6) were obtained from which a pattern for subsequent terms was established. The expression for V_r was programmed on the College mainframe and sinusoidal energisation was also included.

When incorporating the parameters used by Bickford in the program identical responses to those shown in the reference[4] were obtained. The model line parameters were then applied and gave the response shown in Figure 5.3. Comparing this to the model line response of Figure 5.2 it can be seen that the two waveforms are initially very similar but digress with time since the travelling wave technique assumes lossless propagation. Figure 5.3 therefore does not display the attenuation and distortion present in the model. However it does demonstrate that oscillations, which are not related to Gibbs phenomena, are generated by multiple reflections in a line energised from an inductive source. The slight oscillatory content observed at 1200 μs in the model response is therefore due to the introduction of L_s into the source.

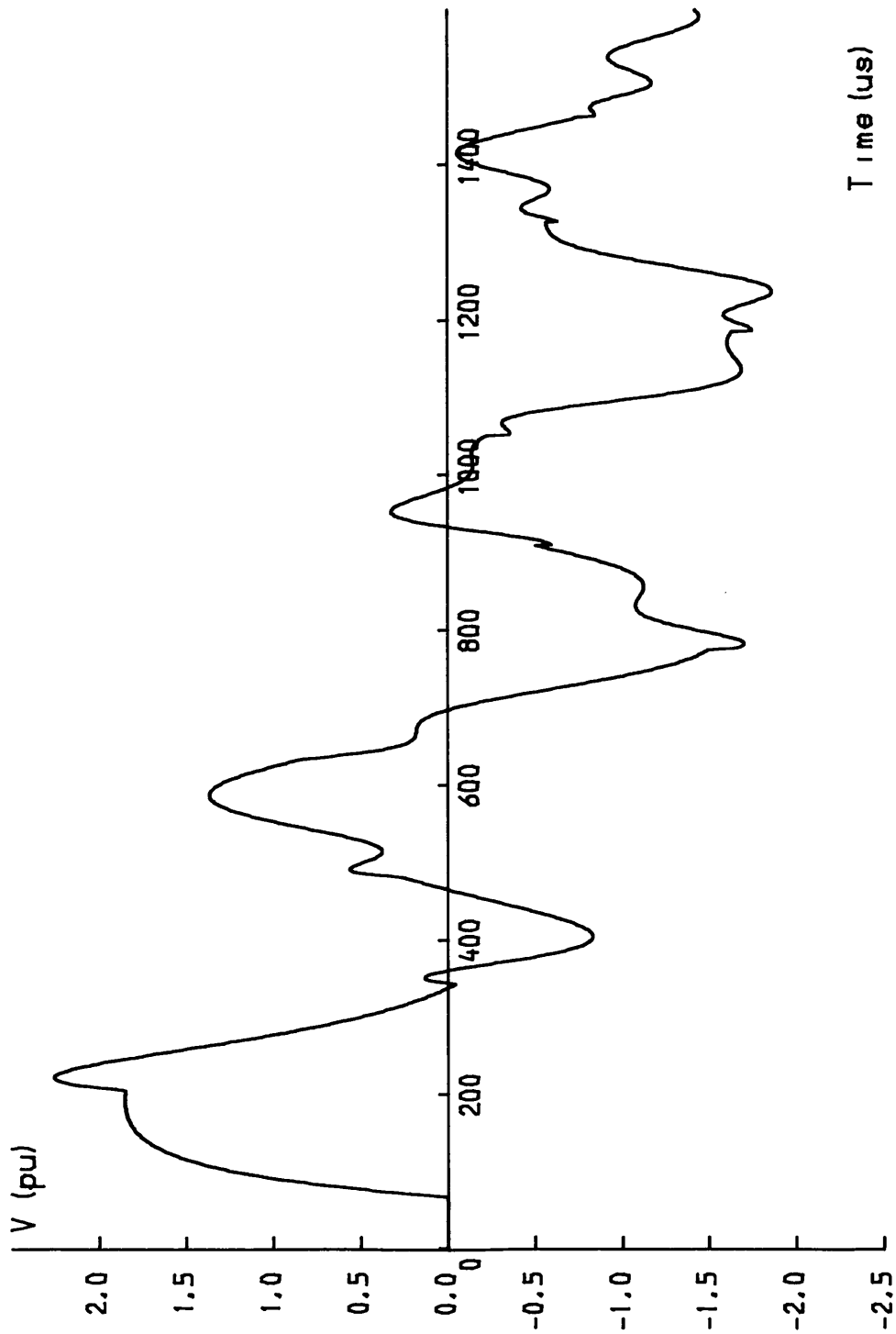

Figure 5.3 Actual Line Response calculated by Travelling-Wave Techniques. L_s = 0.08H.

Figure 5.4 displays the resistor-damped model response and shows that the increased attenuation of this line reduces the source effects significantly.

5.4 Determination of L_G

The uncompensated line waveform of Figure 5.2, verified using the travelling wave technique, demonstrated that a value of L_s equal to 0.0801H gave a transient response which was free of Gibbs Oscillations. For the 20 π-section line the lowest value of source inductance, L_G, for which no Gibbs phenomena would be observed must therefore lie between 0 (i.e. the infinite source case) and 0.0801H. In order to determine the value of L_G for this line length uncompensated waveforms were recorded for 90° closure using preferred values of L_s in this range of inductance values. Specific values of L_s were chosen in order to limit the number of waveforms to be analysed to a practical amount. These values, listed in Appendix IV.2, form part of the full range of L_s values used in the overvoltage profile studies of section 5.6.2.

At each stage in the analysis the presence of Gibbs phenomena in the model line responses was determined by comparison with the equivalent responses calculated by the travelling-wave program.

5.4.1 Lines with Zero Earth Impedance

5.4.1.1. 20 Π-Section Line

Analysis of the 20 π-section line responses as L_s was increased showed that the first significant change in waveform shape from that for the infinite source case took place with L_s=0.015H. The receiving-end response for this condition (Figure 5.5) shows that the initial oscillation of each surge is reduced such that it is no longer the predominant feature of the surge in terms of magnitude. As was previously observed the frequency of the Gibbs phenomena decreases with subsequent reflections.

Increasing L_s to 0.0201H the 'hump' effect now becomes significant

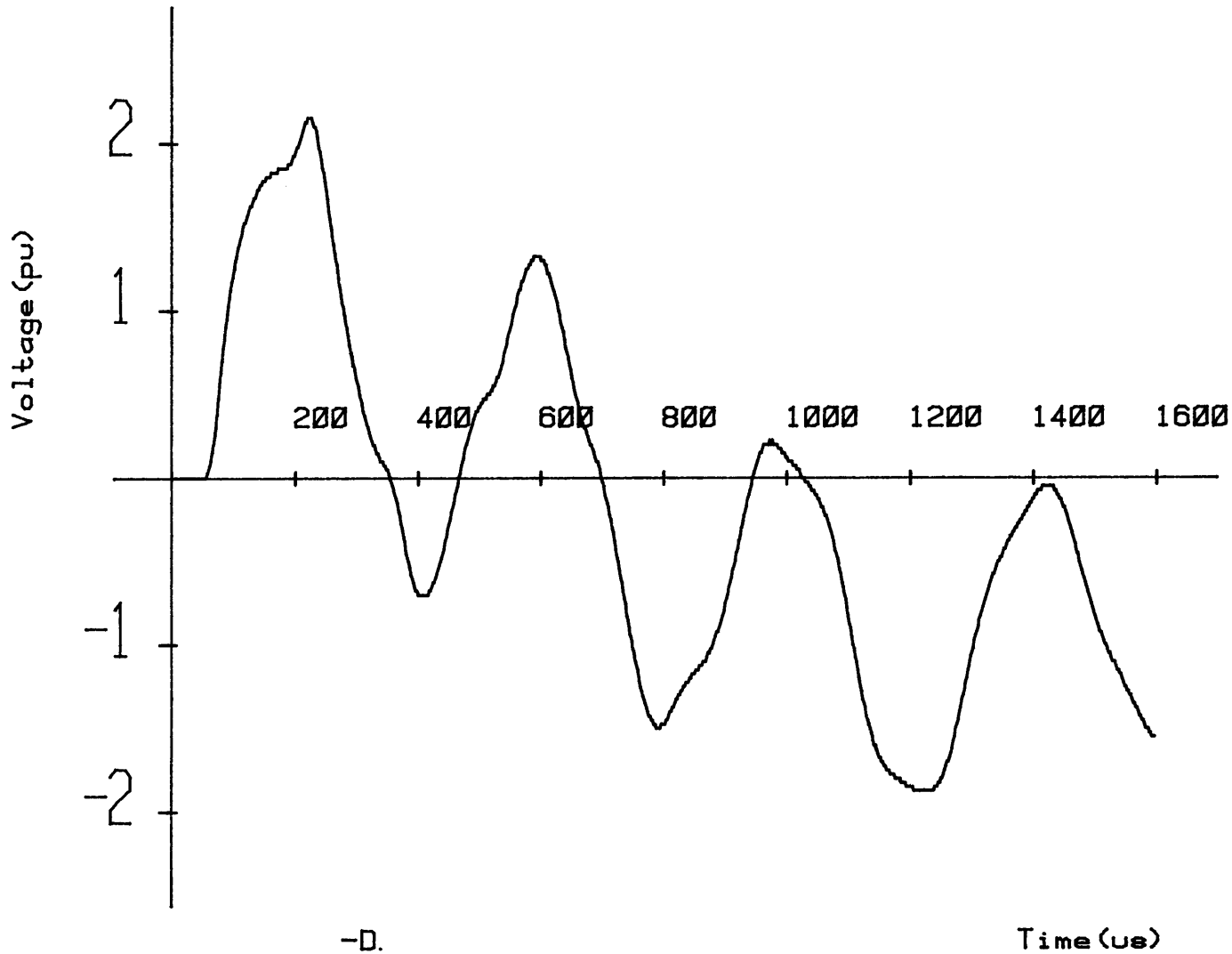

Figure 5.4 20 Pi-section Compensated Line Response with L_s = 0.08H.

Figure 5.5 20 Pi-section Uncompensated Line Response with L_s = 0.015H.

in the uncompensated line response of Figure 5.6. The magnitude of the Gibbs Oscillations are further reduced with the changing frequency nature of the Gibbs content now only apparent until 1400 μs. Figure 5.7 further demonstrates this progressive change for L_s=0.0249H and Figure 5.8 finally displays a receiving-end response which is free of Gibbs Oscillations with L_s=0.03H. Therefore for this length of line the uncompensated receiving-end responses obtained by energisation from a source with values $\geq$ 0.03H should not require modification by the Experimental Sigma Factors. For the 20 π-section line L_G is therefore defined as 0.03H.

To determine if L_G was dependent on line length similar tests were carried out on the 5 and 10 π-section lines.

5.4.1.2. 10 Π-Section Line

The receiving-end responses for the 10 π-section line for source values of 0.015, 0.0201 and 0.0249H are shown in Figures 5.9.1 - 3 respectively and similar changes in waveshape and high-frequency content to that observed for the 20 π-section line can be seen in these figures as L_s is increased. However the Gibbs phenomena are attenuated much more quickly and the source effects are more pronounced in each response than for those of the longer line with equivalent source values e.g. compare Figures 5.5 and 5.9.1. L_G for the 10 π-section line was defined as 0.0249H (Figure 5.9.3).

5.4.1.3. 5 Π-Section Line

Figures 5.10.1 - 3 display the waveforms obtained from the 5 π-section line for source values of 0.0099, 0.015 and 0.0201H respectively and further demonstrate that the inductive effects become even more significant as the line length is decreased. Figure 5.10.1 shows that source effects are solely present in the waveform after 320 μs and the response of Figure 5.10.3 displays no Gibbs content which defines L_G as 0.0201H for the 5 π-section line.

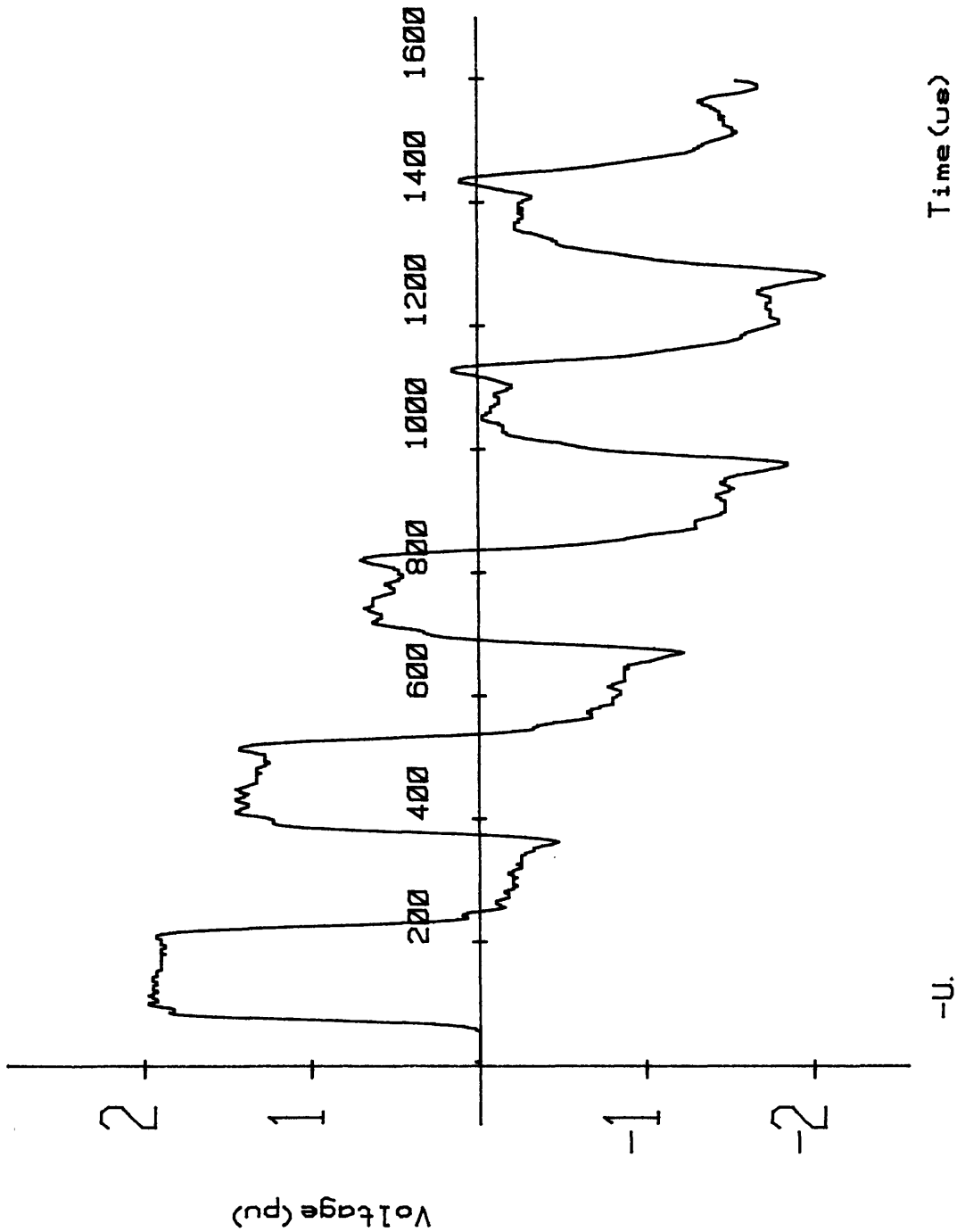

Figure 5.6 20 Pi-section Uncompensated Line Response with L_s = 0.0201H.

Figure 5.7 20 Pi-section Uncompensated Line Response with L_s = 0.0249H.

Figure 5.8 20 Pi-section Uncompensated Line Response with L_s = 0.03H.

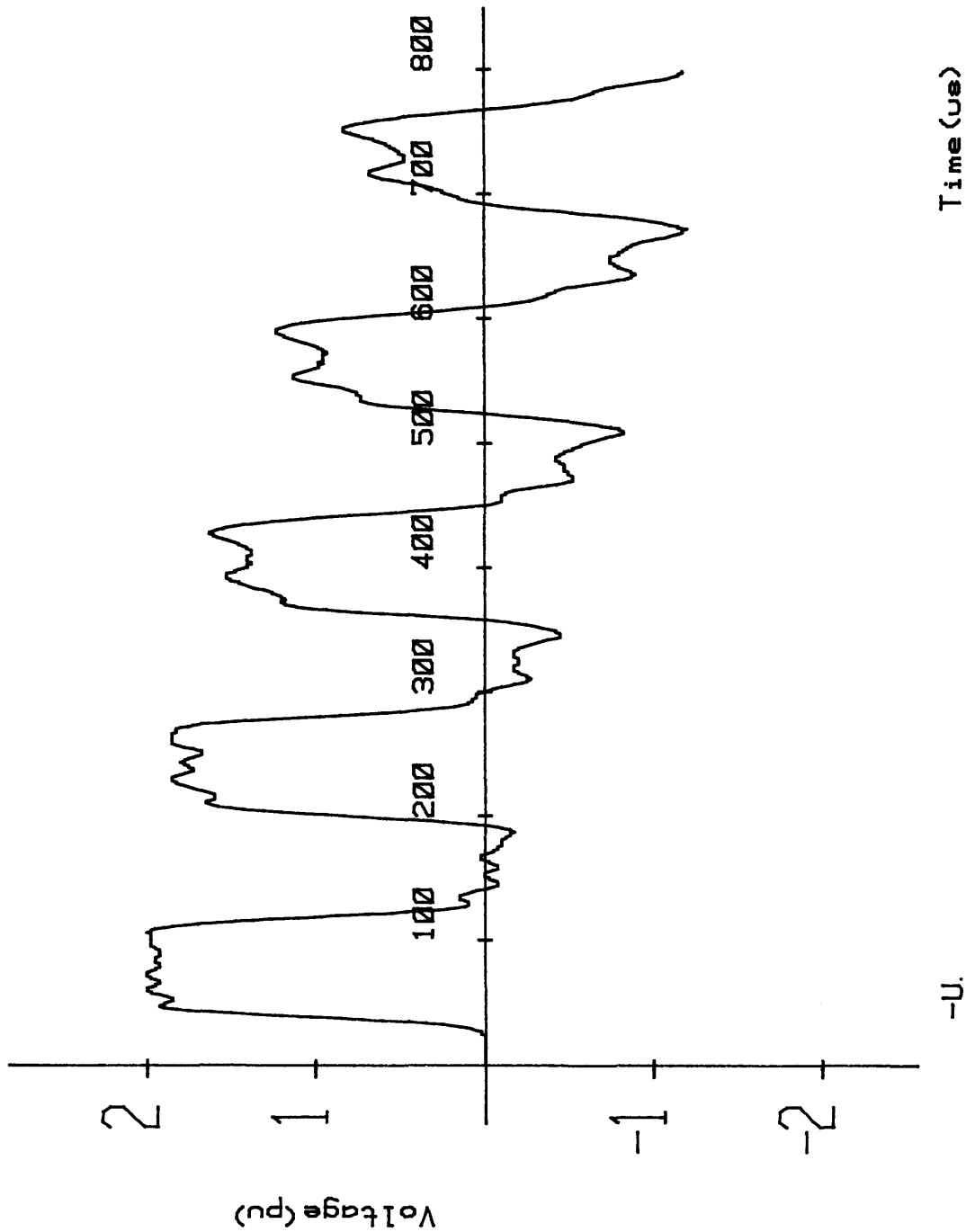

Figure 5.9.1 10 Pi-section Uncompensated Line Response with L_s = 0.015H.

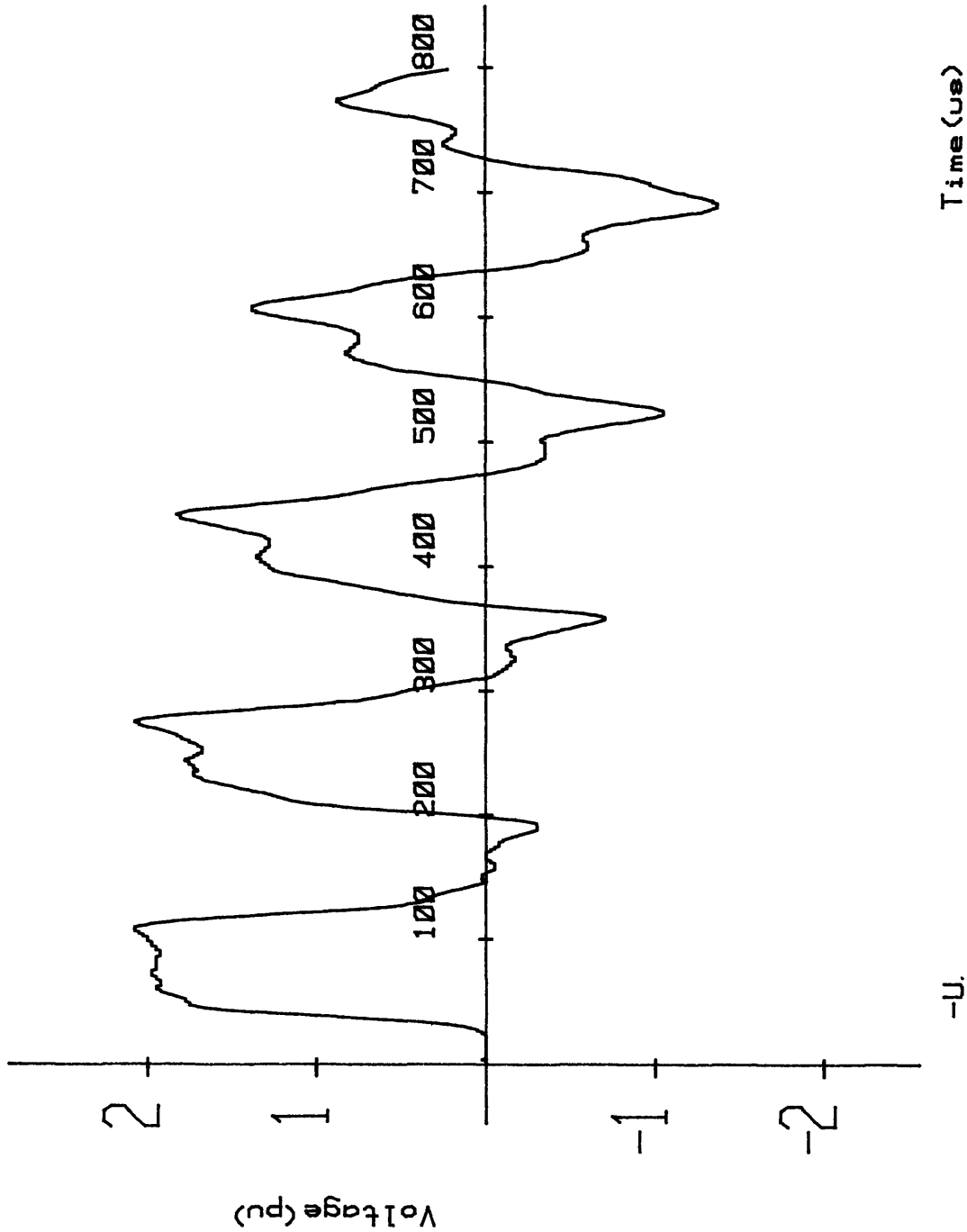

Figure 5.9.2 10 Pi-section Uncompensated Line Response with L_s = 0.0201H.

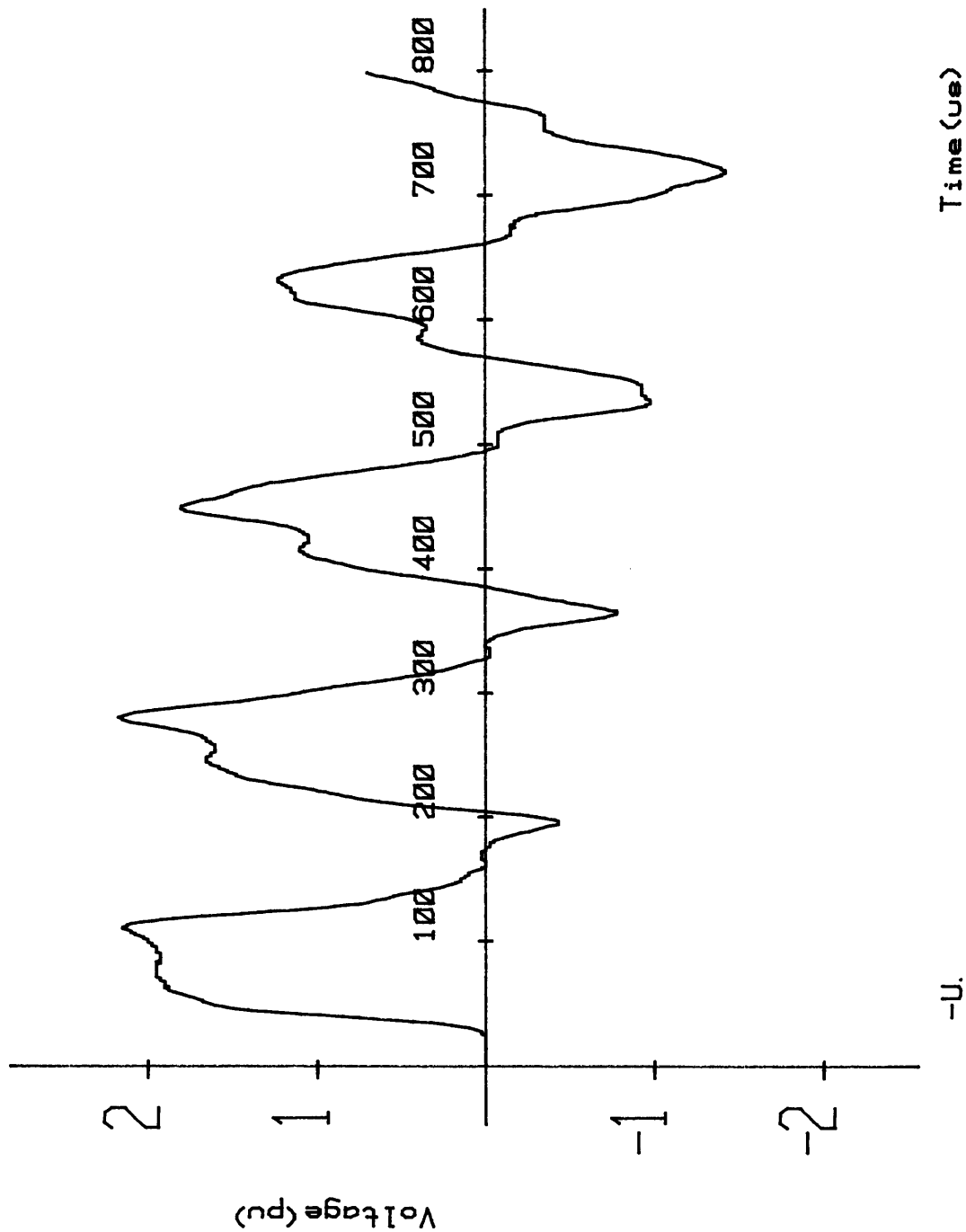

Figure 5.9.3 10 Pi-section Uncompensated Line Response with L_s = 0.0249H.

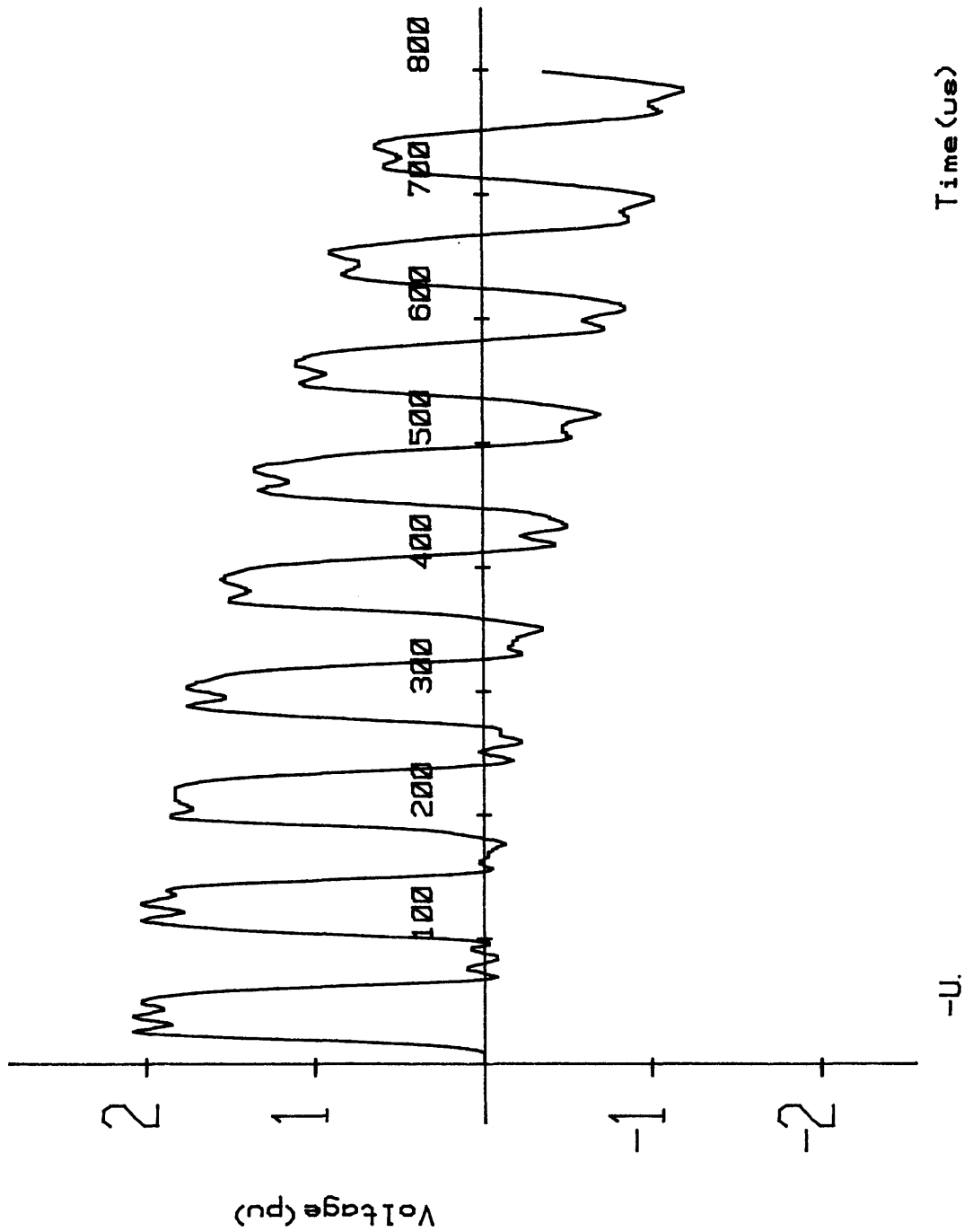

Figure 5.10.1 5 Pi-section Uncompensated Line Response with L_s = 0.0099H.

Figure 5.10.2 5 Pi-section Uncompensated Line Response with L_s = 0.015H.

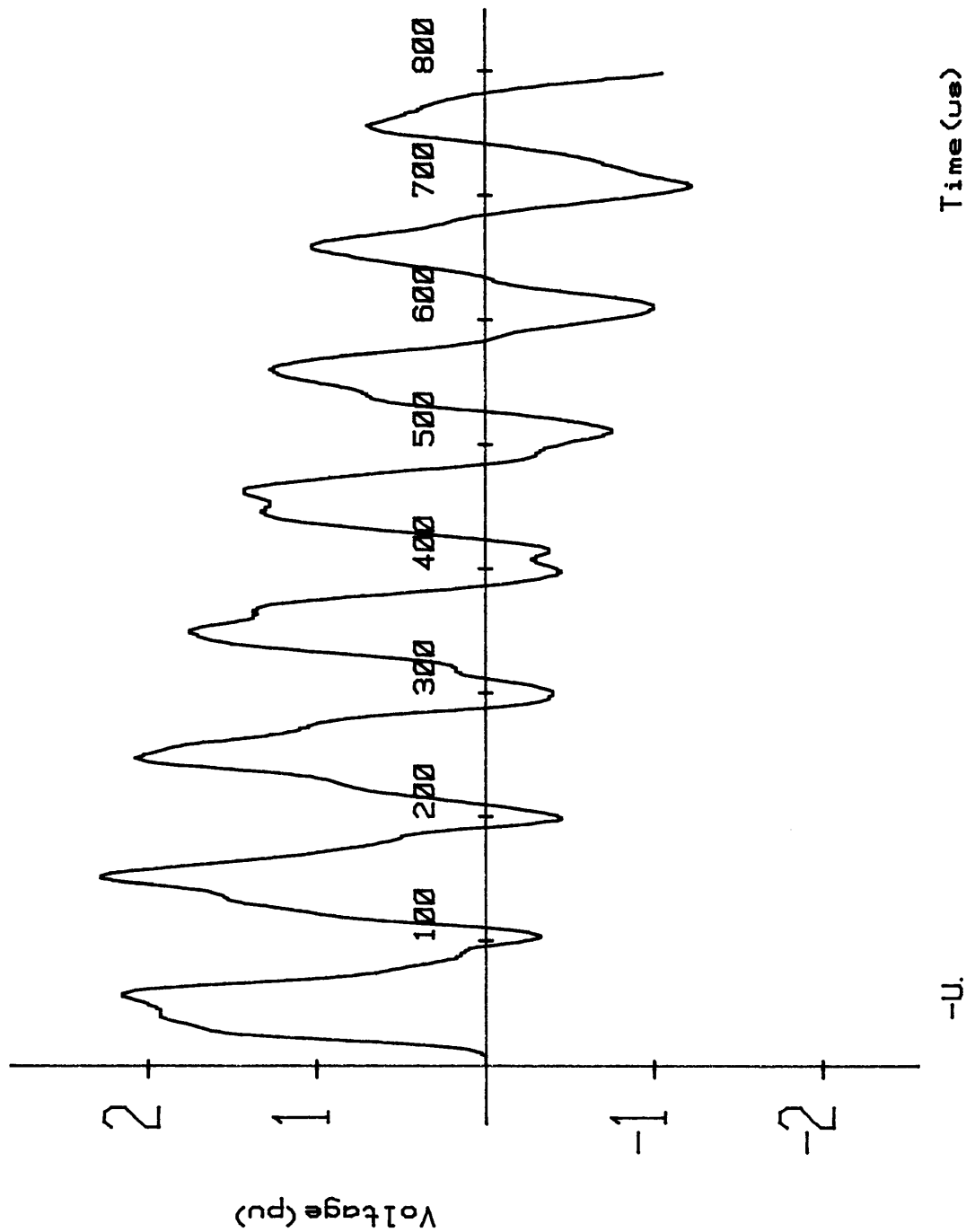

Figure 5.10.3 5 Pi-section Uncompensated Line Response with L_s = 0.0201H.

5.4.2 Lines with Earth Path Impedance

Extending the analysis to the 1-phase lines including the frequency-dependent earth path showed that the effects of increasing L_s were similar to that previously shown in the zero earth impedance line responses. Since the inclusion of the earth path had attenuated the Gibbs phenomena in the transient responses for infinite source energisation after a short time (section 4.4.2) it was expected that the value of L_G would be reduced for each line length. However for all three line lengths L_G had the same value (0.0249H).

This indicates that L_G for the 20 π-section line decreased as expected while that for the 10 π-section line remained the same. The uncompensated responses of these lines with L_s=L_G are shown in Figures 5.11.1 - 2. However L_G for the 5 π-section line has increased and this result is verified by the waveforms shown in Figures 5.11.3 - 4 where L_s has values of 0.0201 and 0.0249H respectively.

5.4.3 Simultaneous Closure of 3-Phase Lines

Simultaneous closure of the uncompensated 3-phase lines demonstrated that the waveshapes obtained were almost identical in waveshape and Gibbs content to those recorded from the 1-phase zero earth impedance model. For R-Y-B closures of 90°, 330° and 210° it was found that the red-phase waveforms were identical to the 1-phase line responses in every respect with the exception that the Gibbs components were slightly reduced in magnitude. An example of this is shown in Figure 5.12 for a source value of 0.0201H. The red-phase waveform can be compared with 1-phase response of Figure 5.6 for the same source value and closure angle. The Gibbs phenomena are eliminated after approximately 1100 μs in the 3-phase response while this occurred after 1400 μs for the 1-phase case. The slight difference in Gibbs content is attributed to the change in the surge impedance value of the 3-phase line (section 1.3.1).

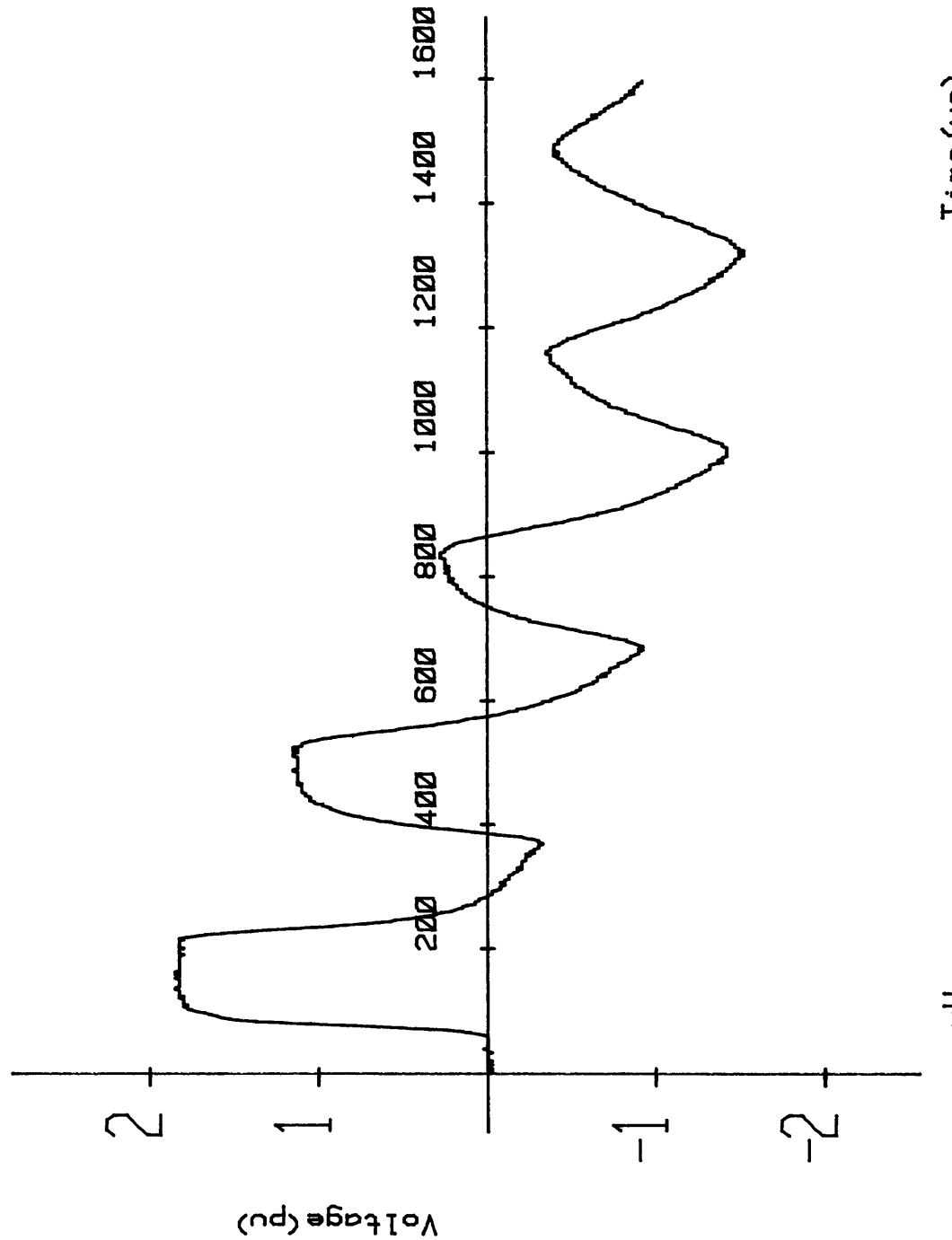

Figure 5.11.1 Response of 20 Pi-section Uncompensated Line with Earth Path with L_s = 0.0249H.

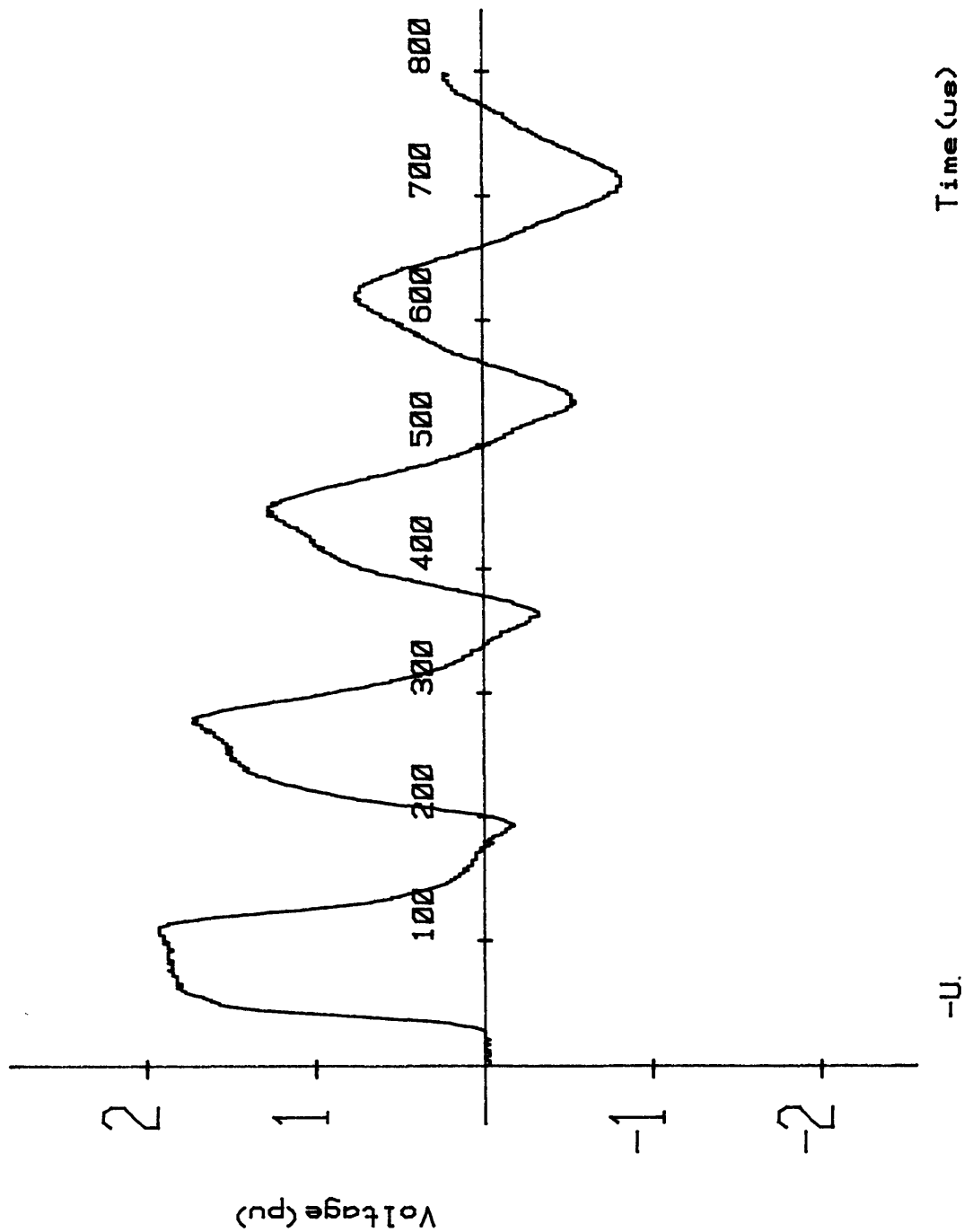

Figure 5.11.2 Response of 10 Pi-section Uncompensated Line with Earth Path with L_s = 0.0249H.

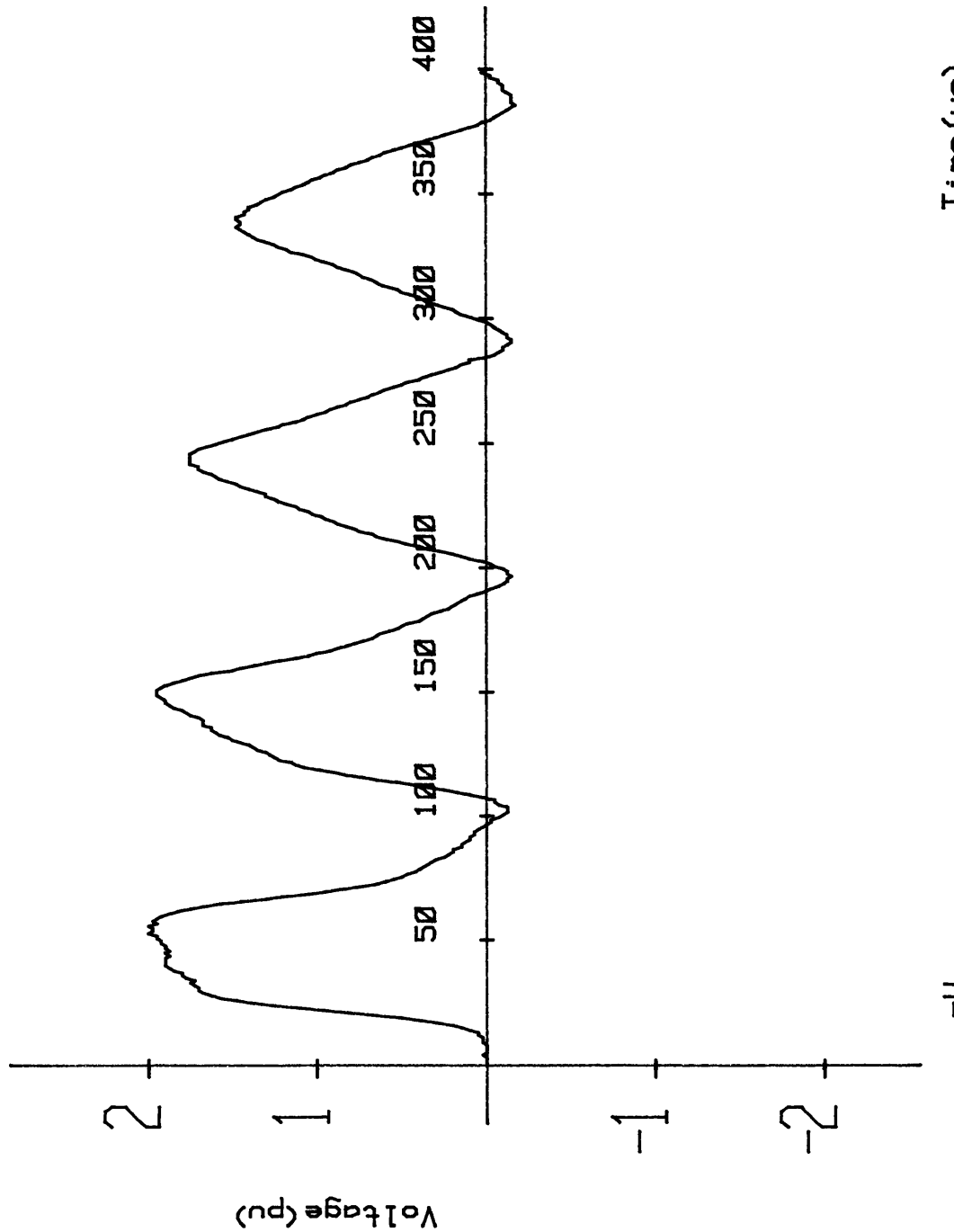

Figure 5.11.3 Response of 5 Pi-section Uncompensated Line with Earth Path with L_s = 0.0201H.

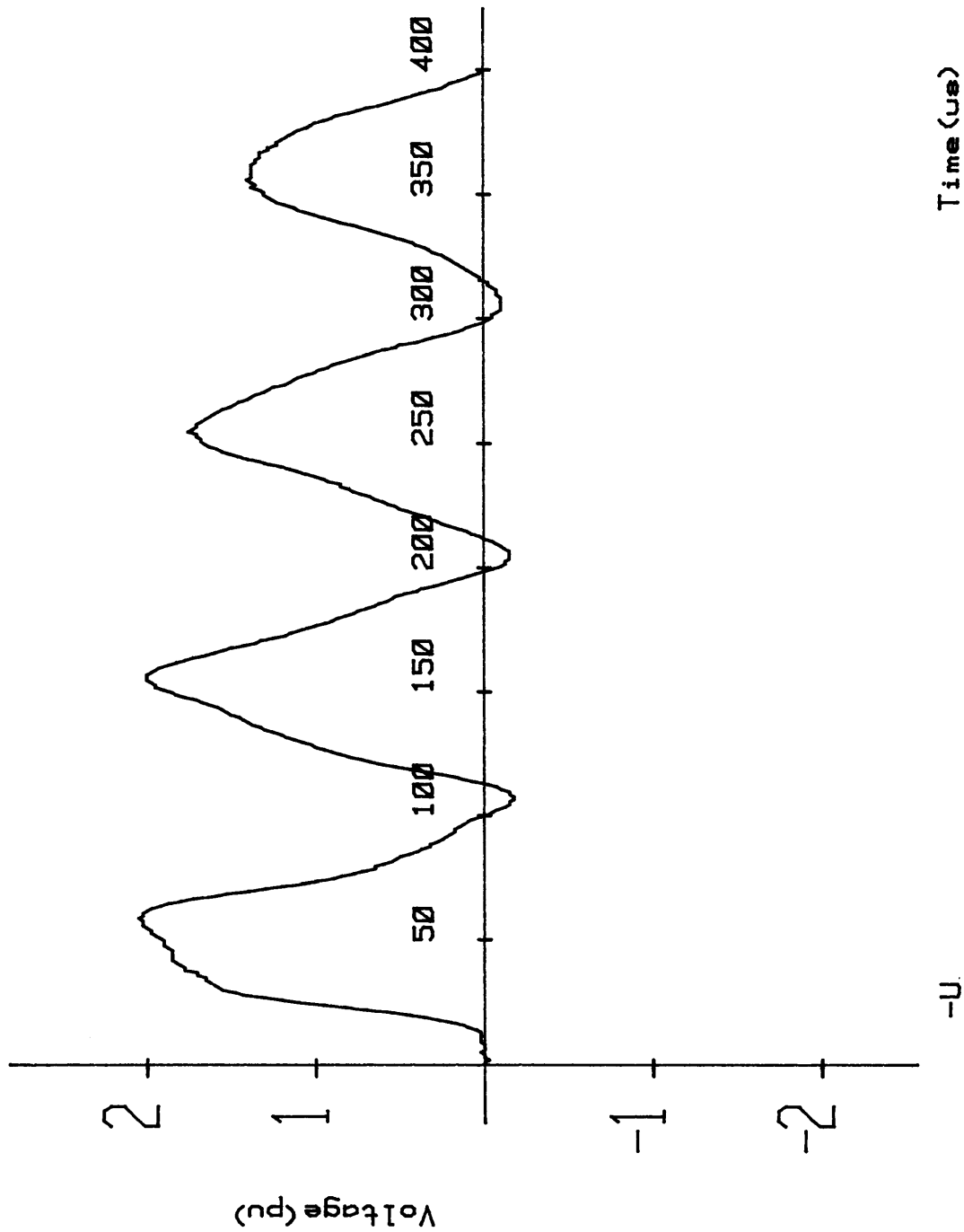

Figure 5.11.4 Response of 5 Pi-section Uncompensated Line with Earth Path with L_s = 0.0249H.

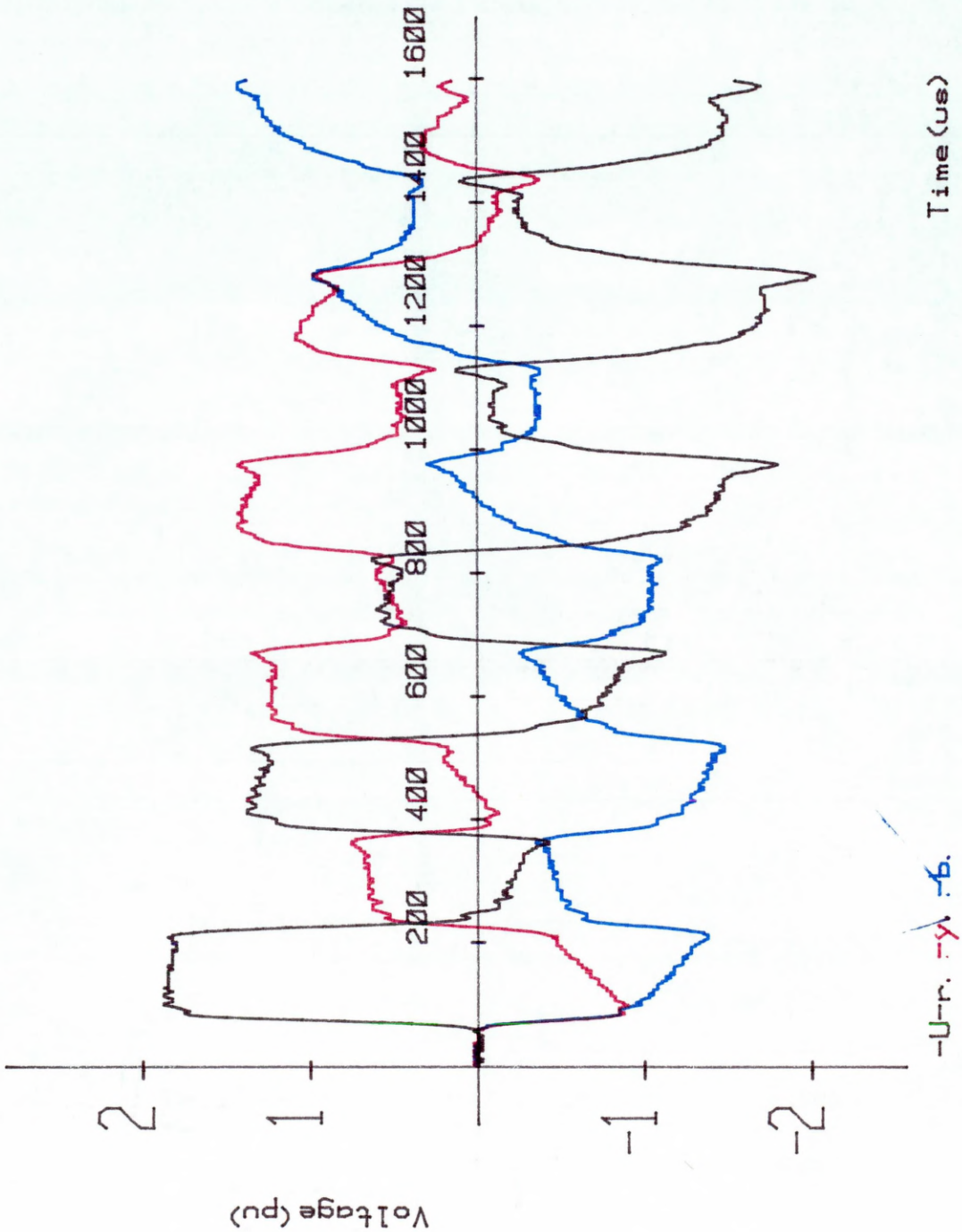

Figure 5.12 3-phase, 20 Pi-section Uncompensated Line Response with L_s = 0.0201H.

The slight reduction in Gibbs content however had no effect on the values of L_G determined for the 3-phase uncompensated lines. For each line length L_G had the same value as was determined in the corresponding 1-phase zero earth impedance case.

5.4.4 Discussion of L_G

5.4.4.1. Zero Earth Impedance Lines

From the observations for this line configuration it can be seen that L_G varies with line length. This is unexpected since the surge impedance of the model line and therefore frequency content of the modified step input do not vary with line length. Although Figure 1.4 shows that the uncompensated line surge impedance increases with frequency Z_0 does not vary significantly over the 0 - 100 pu range of frequencies i.e. 0 - 40 kHz. Since the transient fundamental frequency of the three line lengths investigated lie within this range, the highest obtained from the 5 π-section line at 14.3 kHz, Z_0 is assumed to remain constant. Therefore the variation of L_G is not dependent on surge impedance.

However for infinite source energisation it was previously observed that a larger Gibbs content was apparent, for a longer time, in the uncompensated response as line length increased. This is also the case for inductive source energisation when L_s is kept constant and can be seen from Figures 5.10.2, 5.9.1 and 5.5 where L_s=0.015H for the 5, 10 and 20 π-sections lines respectively. Hence L_G increases with line length and the magnitude of the Gibbs content in a response must be dependent on the transient fundamental frequency.

For infinite source energisation it was found that the first oscillation of a surge was predominant in magnitude for the first few reflections. The source inductance value for which this was no longer the case was the same for all three line lengths this value being 0.015H. As L_s increased the length of time for which Gibbs Oscillations could be observed

in a response decreased with the source effects becoming increasingly more predominant. Since the two averaging techniques developed were based on calculating an averaging range (N_s or N_a) from the initial oscillation of a surge this might contribute to the decision of which technique to apply to the uncompensated waveforms recorded where Gibbs phenomena were still apparent. The decrease in Gibbs frequency magnitude would therefore give rise to the problems of sample resolution experienced when varying the point-on-wave closure for AC source excitation in section 4.6.

The red-phase waveshapes obtained from simultaneous closure of the 3-phase lines were almost identical to the 1-phase zero earth impedance cases. The reduction in Gibbs content of the 3-phase line waveforms is very slight but suggests that the value of L_G for each line may be slightly less than for the 1-phase case. This is not evident however because of the preferred values of L_s chosen. The reduction in high-frequency content may be related to the increase in the phase self surge impedance (from 297Ω for the 1-phase line to 372Ω for each phase of the 3-phase line).

5.4.4.2. Earth Impedance Lines

The waveforms obtained from this line configuration demonstrated a similar progression as L_s increased to that observed for the zero earth impedance lines. The Gibbs phenomena were quickly attenuated from the responses due to the earth path but the magnitude of the source effects were also significantly reduced when compared with those observed in the zero earth line responses. The value of L_G was the same for all line lengths which had been the expected result of the tests for the zero earth impedance lines.

5.5 Averaging of Uncompensated Waveforms when $L_s < L_G$

The responses of the uncompensated model lines energised from an inductive source have shown that L_s has a significant effect on the transient waveform shape and Gibbs frequency content. L_G for each line has been ascertained and for all values greater than or equal to this inductance no

averaging of the uncompensated line responses is necessary. This defines a range of source values 0 - L_GH where the Experimental Sigma Factors are required to reduce the Gibbs phenomena.

5.5.1 Averaging of Earth Path Impedance Line Responses

Section 4.4.2 showed that a single value of N_s=15 μs was sufficient to reduce the Gibbs phenomena successfully for all line lengths of this configuration when energised from an infinite source. This was also found to be the case for all source values < L_G and is again due to the predominant damping effect of the earth path preventing a changing frequency Gibbs content in the receiving-end waveforms.

5.5.2 Averaging of Zero Earth Impedance Line Responses

For this line configuration the methods of averaging the uncompensated responses were determined chiefly by the response characteristics. In an analogous situation to the averaging of the earth-path impedance line responses it was found that the transient responses whose Gibbs content was attenuated quickly i.e. when L_s was slightly below L_G, could be modified by the application of a single value of N_s. This can be seen when applied to the 20 π-section uncompensated response of Figure 5.7 where L_s=0.0249H and L_G for this line is 0.03H. Using S_{se} with N_s=15 μs gives the processor response shown in Figure 5.13 which is free of any Gibbs associated frequency content. The compensated line waveform is plotted for comparison and the figure shows that S_{se} does not reduce the source effects as significantly as the resistor-damping.

However if S_{se} is applied to the uncompensated waveform of Figure 5.6 where L_s=0.0201H the processor response of Figure 5.14 shows that S_{se} is not as effective due to the changing frequency Gibbs content. Therefore S_{ae} was applied to the uncompensated waveform giving the processor response of Figure 5.15. This response is a slight improvement over that shown in Figure 5.14 and although the Gibbs content is not completely

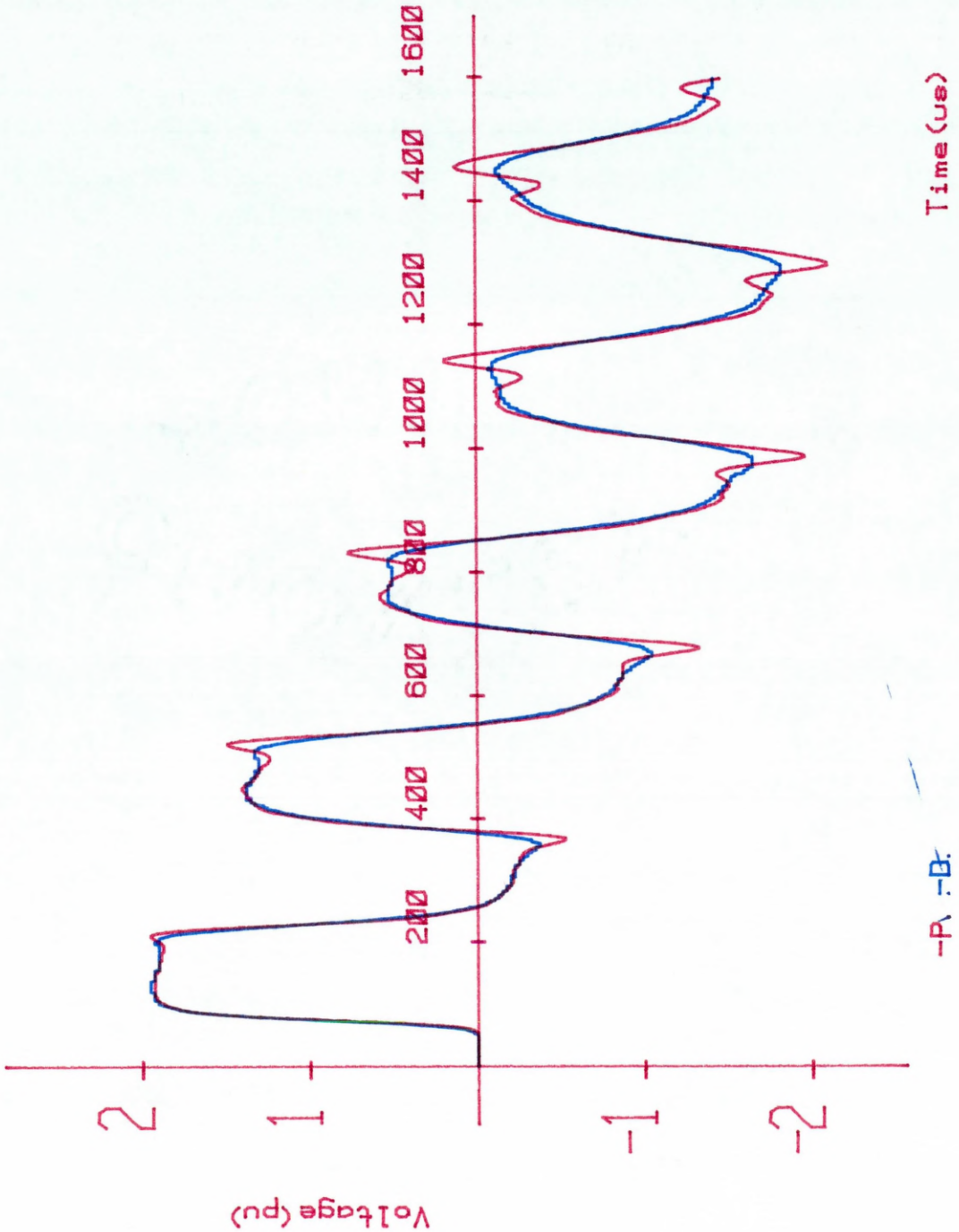

Figure 5.13 20 Pi-section Line Processor and Compensated Waveforms for L_s = 0.0249H. S_{se} effectively reduces the Gibbs phenomena.

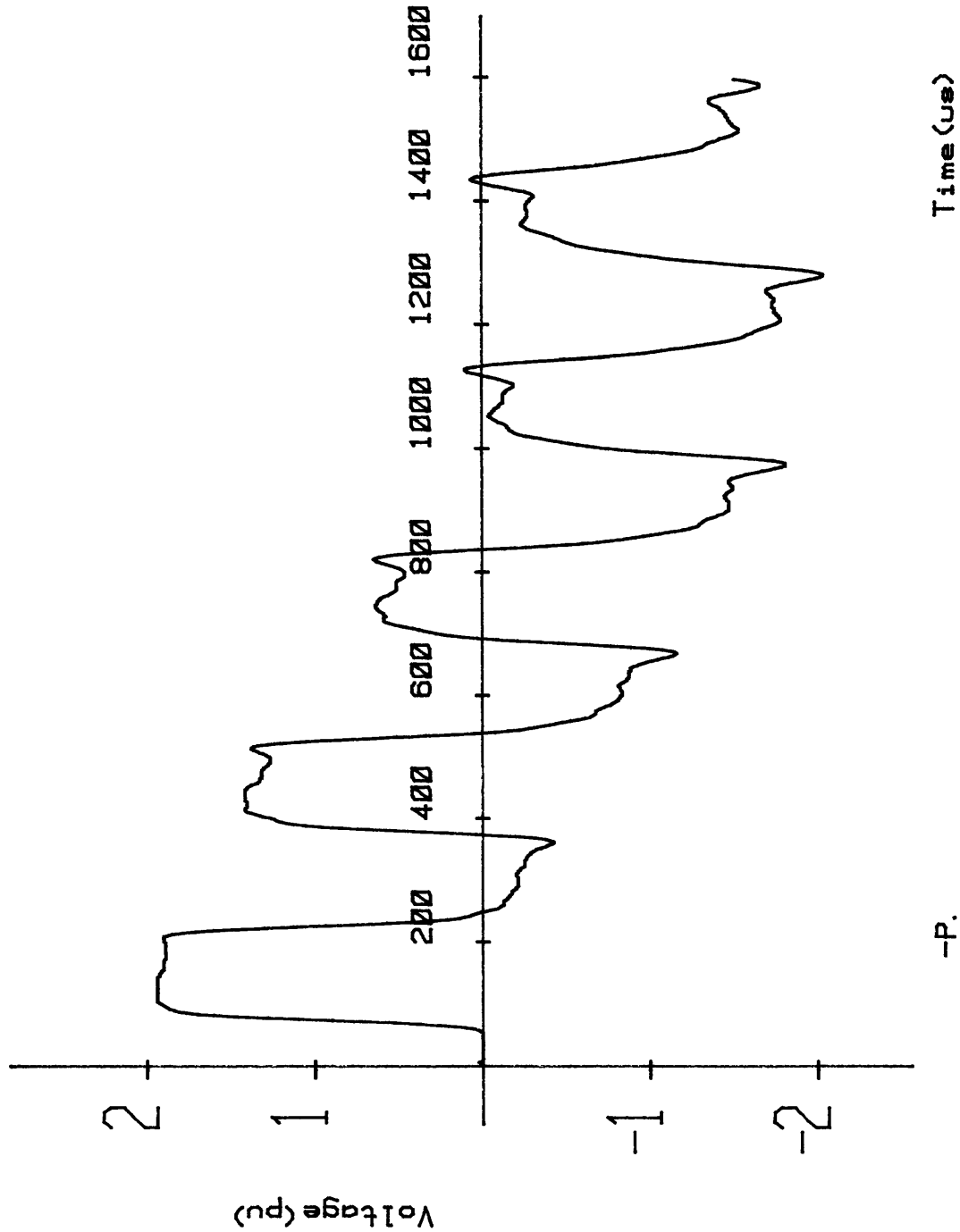

Figure 5.14 20 Pi-section Line Processor Response showing S_{se} to be ineffective when L_s = 0.0201H.

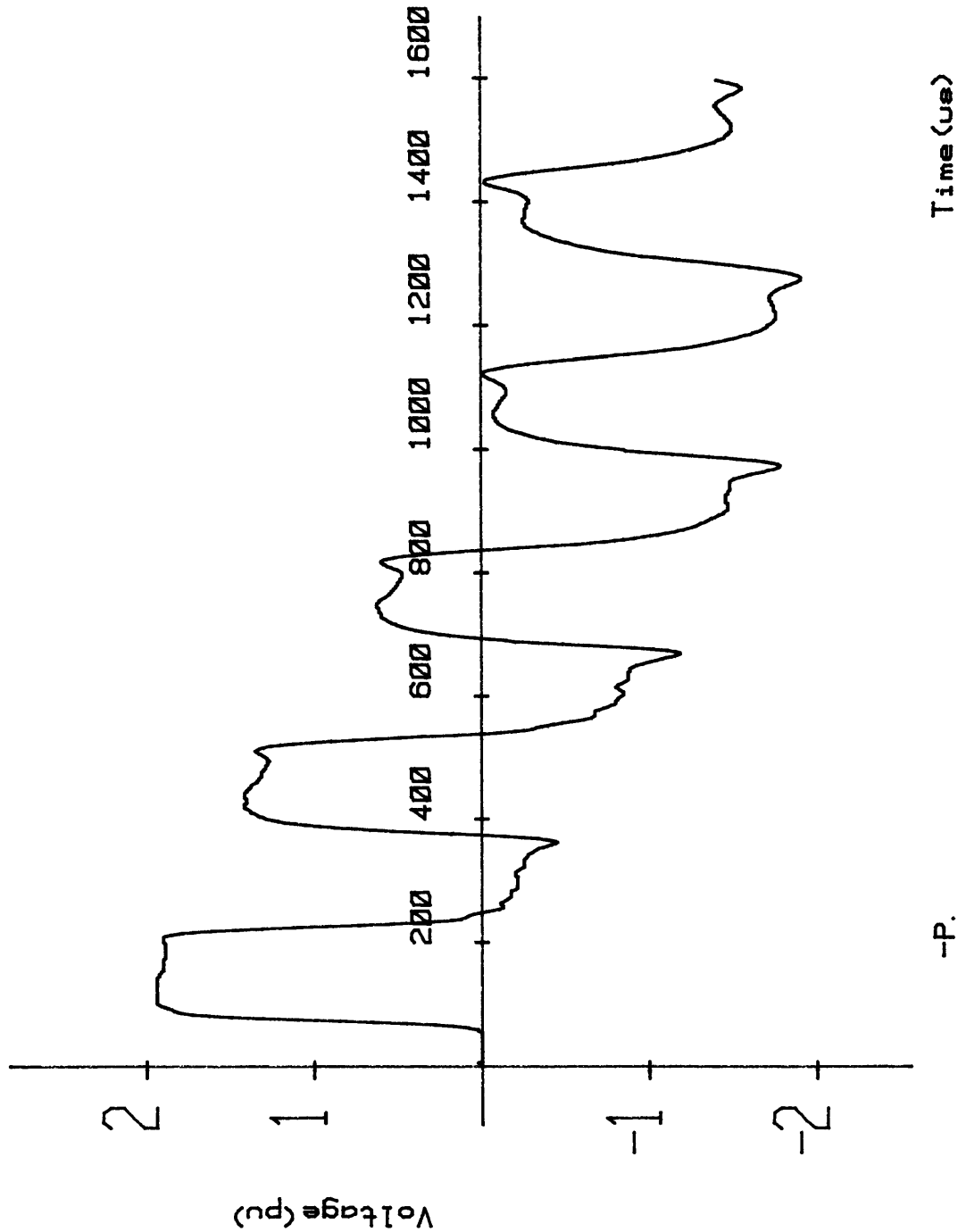

Figure 5.15 20 Pi-section Line Processor Response obtained by S_{ae} when L_s = 0.0201H.

reduced the inductive source effects are more significant in magnitude.

Due to the characteristics of the other uncompensated waveforms recorded in the range 0 - L_GH the use of S_{ae} was found to be the most effective in reducing the Gibbs phenomena. A further example of this is shown in Figure 5.16 which displays the processor response of the uncompensated waveform of Figure 5.5 with L_s=0.015H. S_{ae} again reduces the magnitude of the oscillations significantly although not completely. This can be compared with the resistor-compensated waveform of Figure 5.17.

A similar treatment was implemented for the shorter line lengths where S_{ae} was used to process the uncompensated waveforms as L_s was increased from 0H and as L_s approached L_G, S_{se} was then implemented.

5.6 The Effect of Source Inductance on Peak Overvoltages

The uncompensated waveforms obtained from inductive source energisation have so far shown that resistor-damping or the application of Experimental Sigma Factors is not required when $L_s \geq L_G$. Actual system source values however exceed L_G with most generator impedances in the limits 0 - 0.5H[9]. Peak overvoltage and source impedance analysis of an identical model system incorporating damping resistors has also been undertaken for a 0 - 1H range of L_s[20]. It was therefore decided to carry out a similar experimental procedure using the latter range of source inductance values to determine if major differences in the overvoltage profiles of the compensated and uncompensated lines would arise in the region where the Experimental Sigma Factors, S_{se} and S_{ae}, were not required i.e. L_G - 1H. These energisation studies were carried out on a 1-phase basis for 90° point-on-wave closure and for 3-phase simultaneous closure (R-phase at 90°) using the compensated and uncompensated lines. Earth-path impedance was also included in the 1-phase analysis.

It was assumed that the peak overvoltage values obtained from the uncompensated line would fall into two categories.

Figure 5.16 20 Pi-section Processor Response obtained using S_{ae} with L_s = 0.015H.

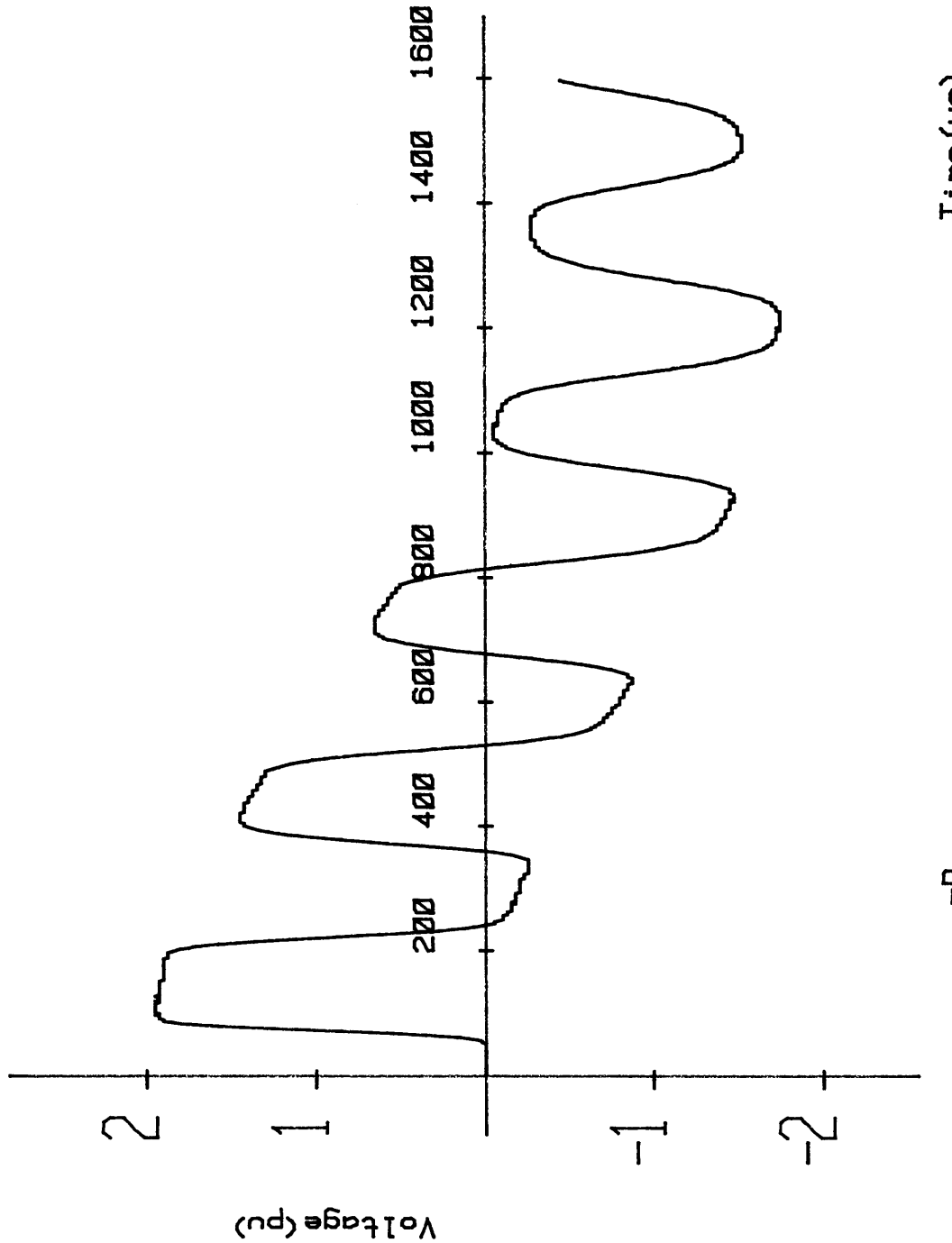

Figure 5.17 20 Pi-section Compensated Response with L_s = 0.015H.

1. Processor values, from S_{se} and S_{ae}, when $L_s < L_G$

2. Uncompensated values when $L_s \geq L_G$

However when the studies were carried out it was found, as L_s was increased beyond L_G, that high-frequency components reappeared in the uncompensated line responses.

5.6.1 High-Frequency Components due to the TNA Model Source

The reappearance of this high-frequency content is shown in the 20 π-section, zero earth impedance, uncompensated line response of Figure 5.18. L_s in this case is 0.18H and the oscillatory content can be observed until approximately 500 μs. These phenomena were initially observed in the receiving-end waveform on the initial rate of rise for a source value of 0.1H but only significantly affected the first surge peak voltage value at 0.12H. The increased effect of this phenomena, as L_s is further increased, is therefore apparent in Figure 5.18. S_{se} was applied to the uncompensated waveform shown and an averaging range of N_s=15 μs completely reduced the oscillations (see Figure 5.19). The phenomena were not observed in the resistor-compensated line response of Figure 5.20.

For the same line with L_s=0.5H the oscillations are observed in Figure 5.21 as being much closer to the lower end of the first rate of rise with a large perturbation occurring immediately after the effect of source switching reaches the receiving-end at 69 μs. For this source value the oscillations are apparent until approximately 800 μs and indicates that as L_s is increased the magnitude of the high-frequency oscillations also increases. Again the application of S_{se} with N_s=15 μs successfully reduced the phenomena (Figure 5.22) which were not observed in the compensated line response (Figure 5.23).

From the responses for all three lengths of 1-phase uncompensated lines it was observed that the oscillations first appeared at approximately the same value of L_s and affected the initial surge peak at 0.1H for the 5

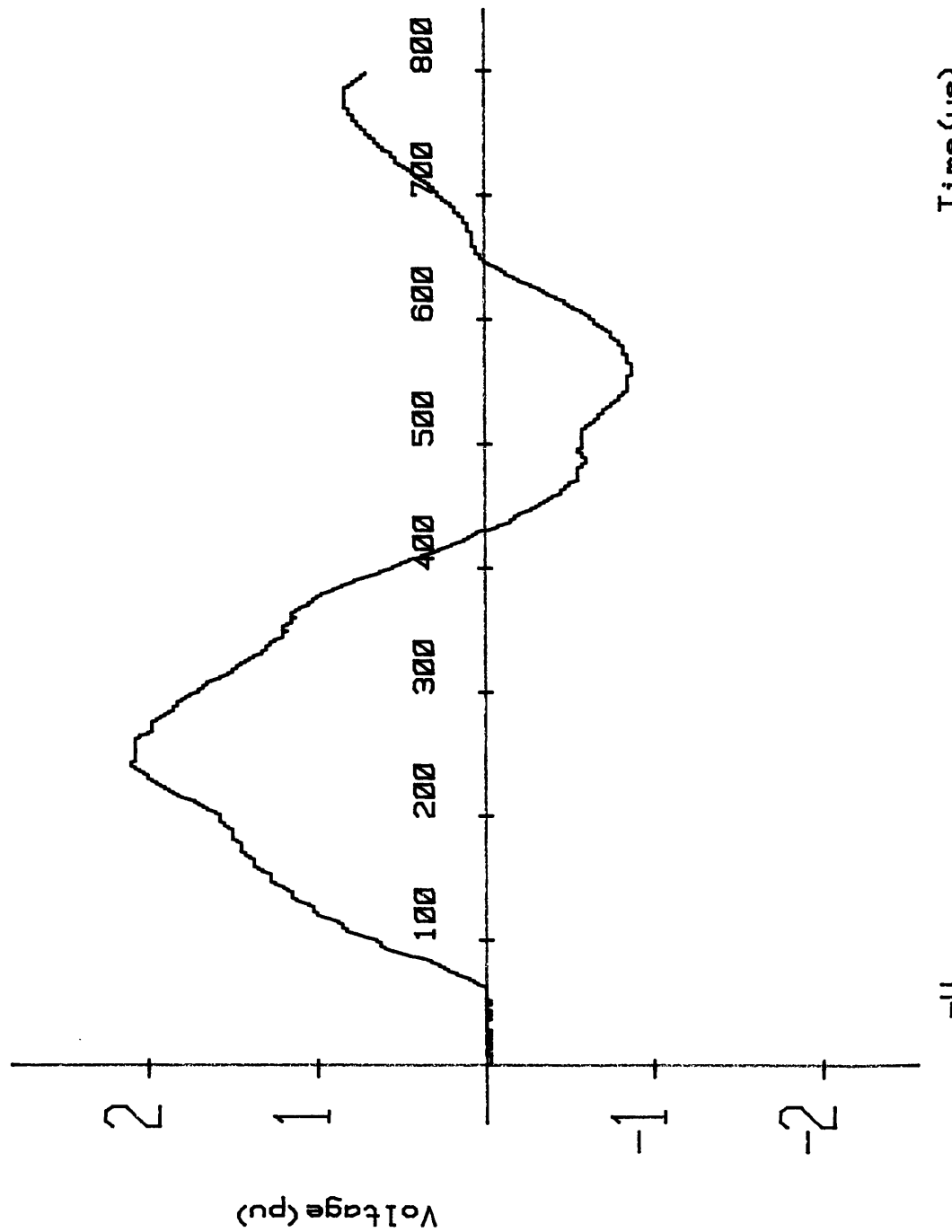

Figure 5.18 High-frequency Oscillations in the 20 Pi-section Uncompensated Line Response with L_s = 0.18H.

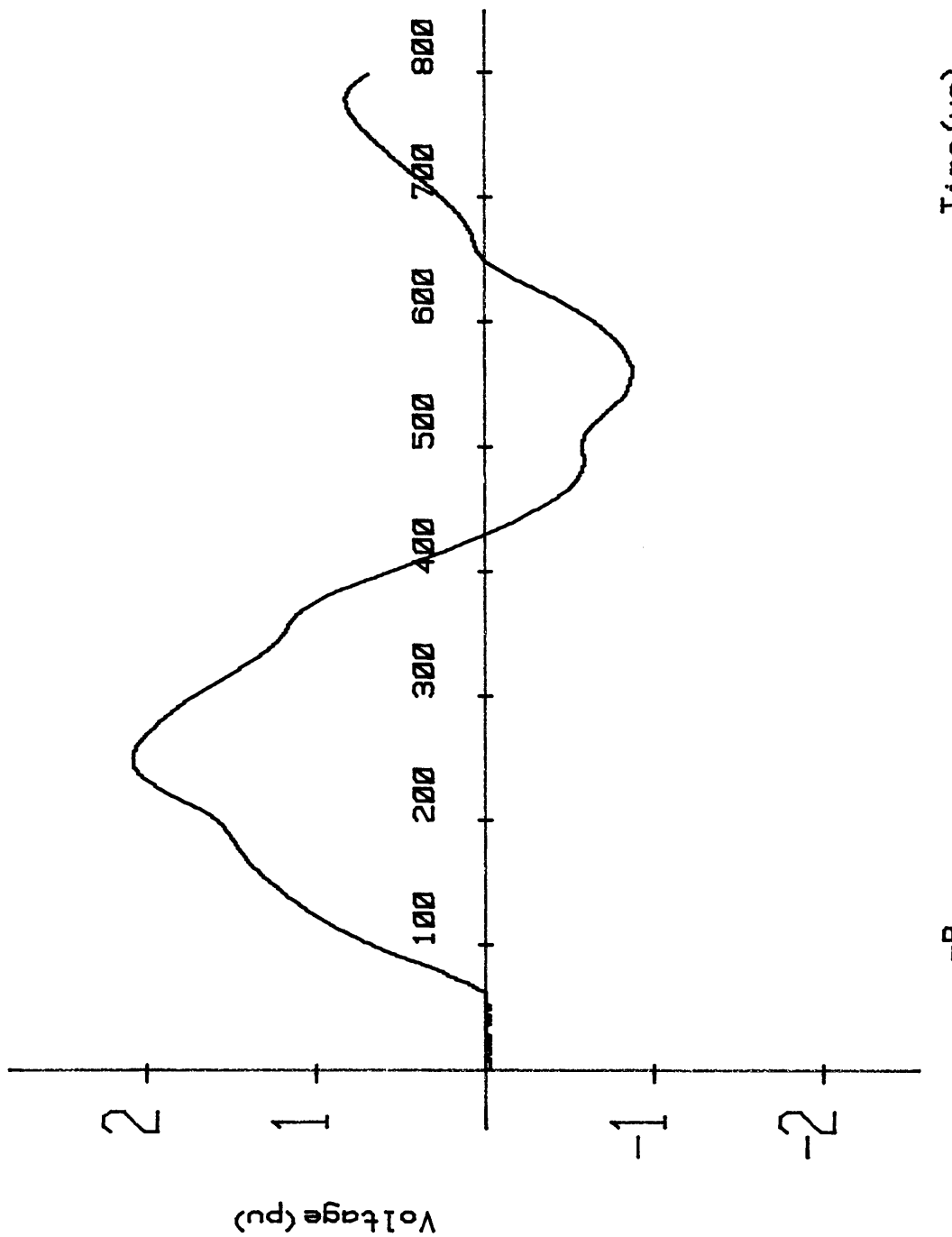

Figure 5.19 Reduction of the High-frequency content by S_{se} with N_s = 15μs.

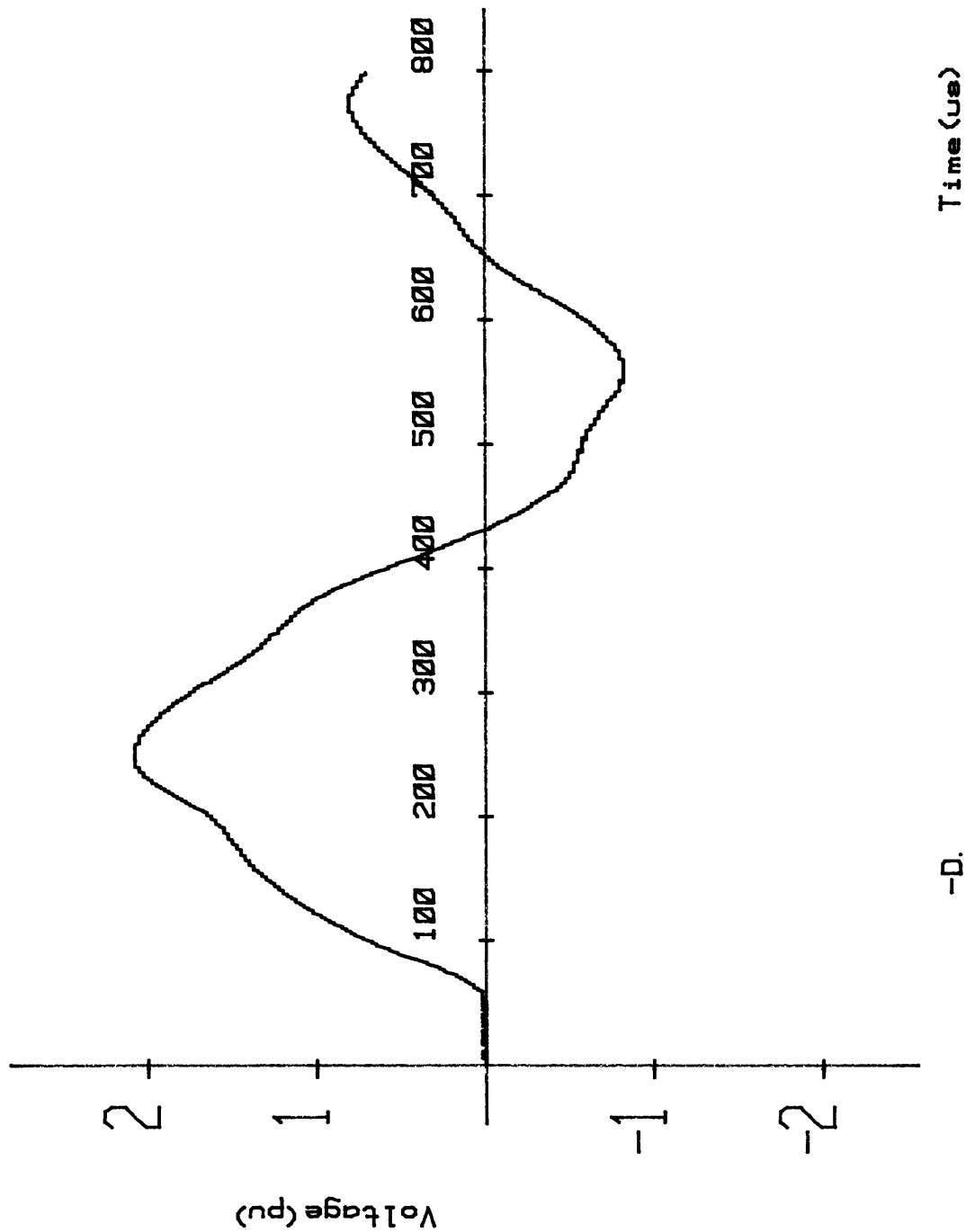

Figure 5.20 20 Pi-section Resistor-compensated Line response with L_s = 0.18H.

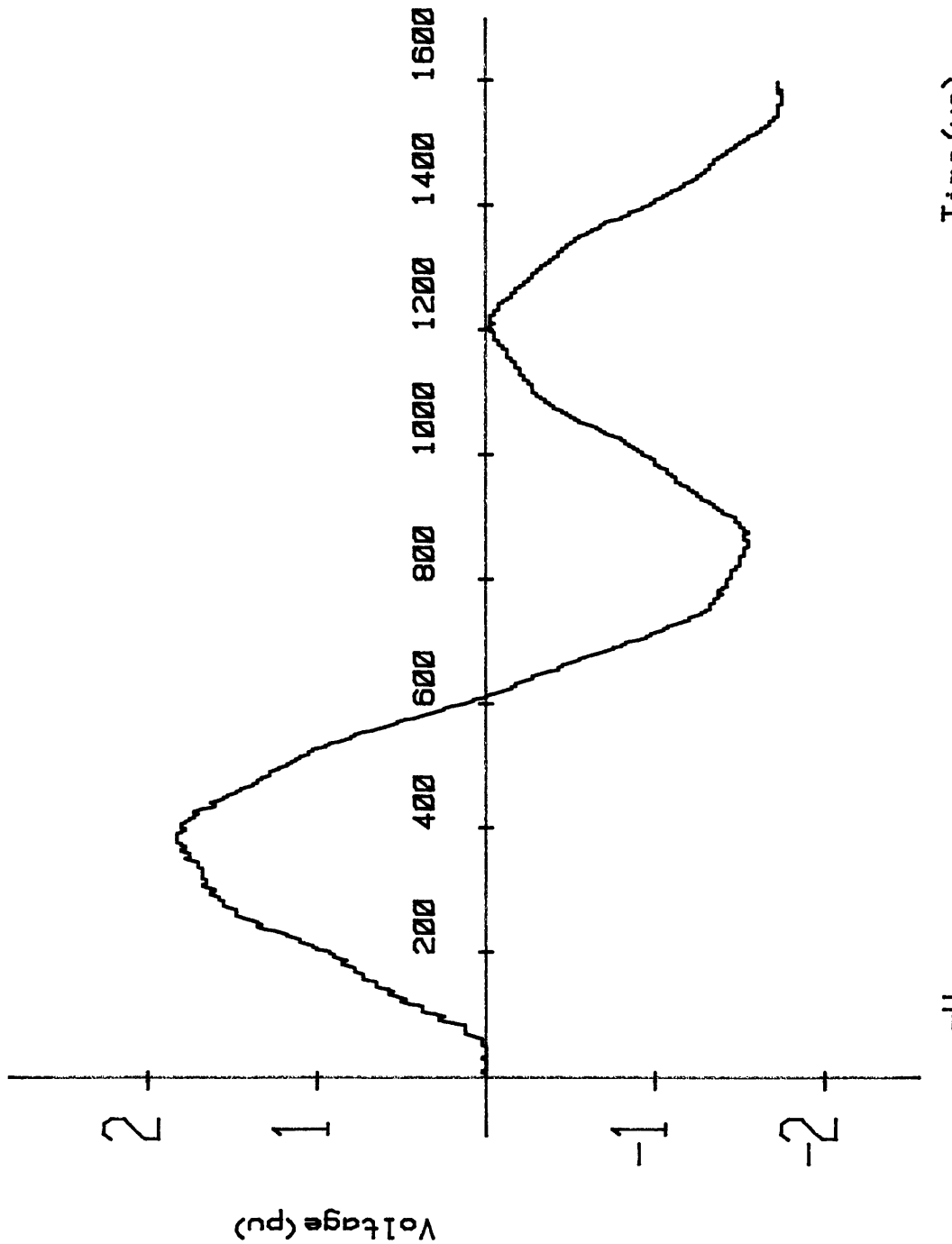

Figure 5.21 20 Pi-section Uncompensated Response with L_s = 0.5H. The High-frequency content has increased.

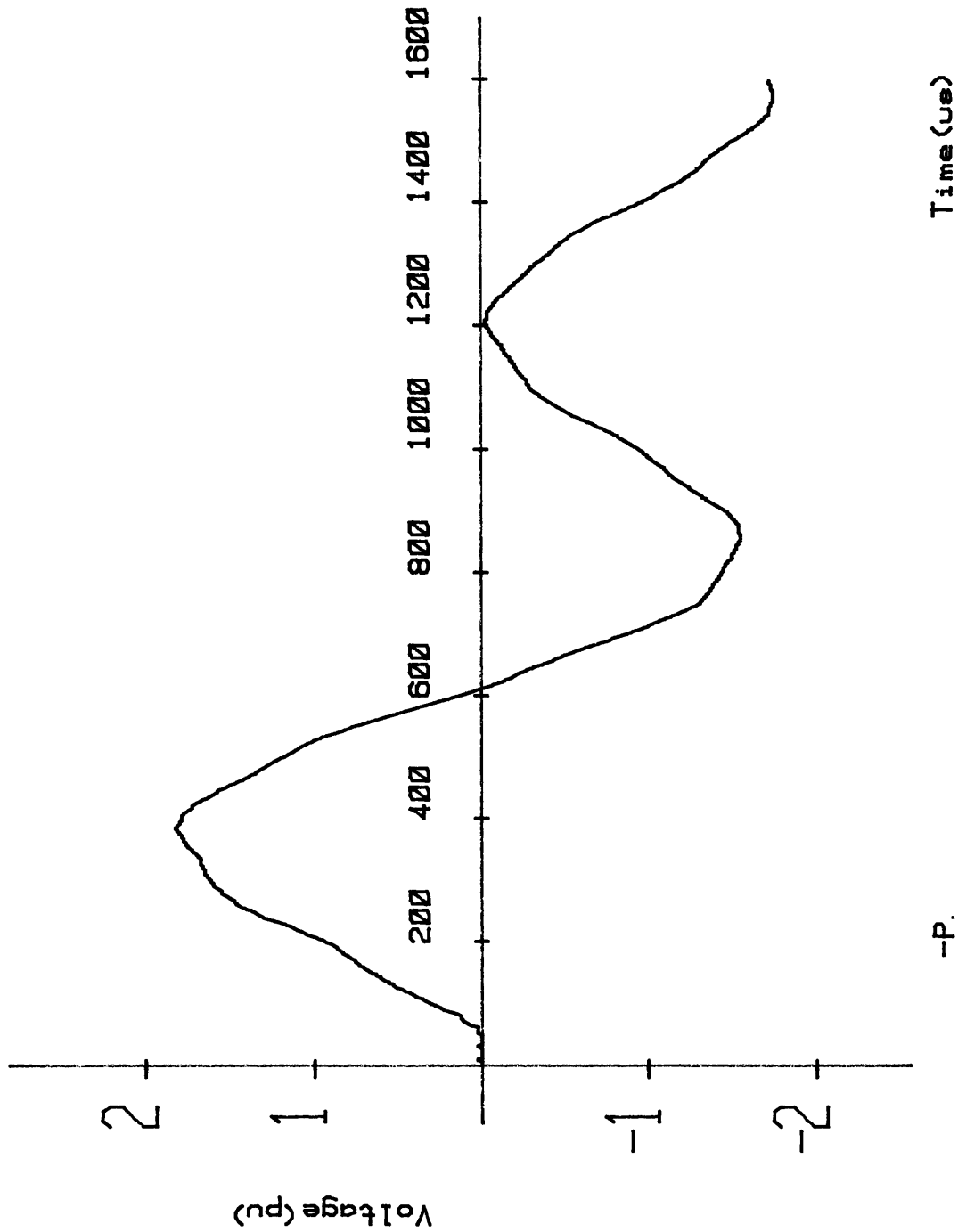

Figure 5.22 Reduction of the High-frequency content by S_{se} with N_s = 15μs.

Figure 5.23 20 Pi-section Resistor-Compensated Line Response with L_s = 0.5H.

π-section line and 0.12H for both longer lines. In order to reduce these oscillations S_{se} was applied to the uncompensated responses and for all line lengths the value of N_s which successfully reduced the high-frequency content was determined at 15 μs.

With the frequency-dependent earth path included in the uncompensated model line configuration these high-frequency effects were only apparent at the lower end of the initial rate of rise due to the damping of the high-frequencies by the earth path. Therefore S_{se} was not applied to these 1-phase uncompensated waveforms as the oscillations were eliminated before they could affect the initial surge peak voltage value.

5.6.1.1. Discussion

The values of L_s for which these oscillations initially began to appear and at which they affected the initial surge peak in the uncompensated responses of the zero earth impedance lines were approximately the same for each line length. It was therefore assumed that the oscillations must be related to the introduction of the TNA source inductance and not to a condition of resonance occurring since the effects became apparent at the same source value for different line lengths.

For all values of L_s from 0.12 - 1H the averaging range which successfully reduced the oscillations was found to be constant at N_s=15 μs and suggests that they are related to the natural π-section frequency of 65.18 kHz. However the range of L_s over which these oscillations are apparent is large. This suggests that the supply frequency resonance condition occurring between the source inductance and line capacitance is not responsible while the frequency of the source inductance and sending-end shunt capacitance is decreasing as L_s increases. The only explanation which can be given is that the oscillations are related to the physical construction of the model inductors used for source representation. As L_s is increased the number of turns used by the TNA inductors increases and for example a

parameter such as the capacitance between turns may be responsible for the high-frequency phenomena observed.

The processor responses shown indicate that the Experimental Standard Sigma Factor S_{se} must be used for values of $L_s \geq 0.12H$ to obtain oscillatory-free responses for the lines with zero earth impedance thereby drastically reducing the range of source values where no averaging techniques are required to L_G - 0.12H for this line configuration. The high-frequency phenomena were also observed in the 3-phase simultaneous closure experiments and appeared for the source values that were determined in the zero earth impedance line analysis.

Since the earth impedance line responses were not greatly affected by this phenomena no averaging was applied and the peak values recorded were taken directly from the uncompensated waveforms when $L_s \geq L_G$.

5.6.2 Overvoltage Profiles

The peak overvoltage values were then recorded with the necessary averaging applied to uncompensated waveforms subject to the high-frequency phenomena discussed previously and are tabulated in Appendices IV.2 to IV.10. Uncompensated/processor and resistor-damped peak voltage values were then plotted to a base of L_s to give overvoltage profiles similar to those given by Bickford et al[20, 6].

The profiles for the 5, 10 and 20 π-section compensated and uncompensated models are given for:-

1. the 1-phase lines with zero earth impedance in Figures 5.24 - 5.26.
2. the 1-phase lines with earth-path impedance in Figures 5.27 - 5.29.
3. the 3-phase lines with mutual coupling and earth-path impedance due to simultaneous closure in Figures 5.30 - 5.32

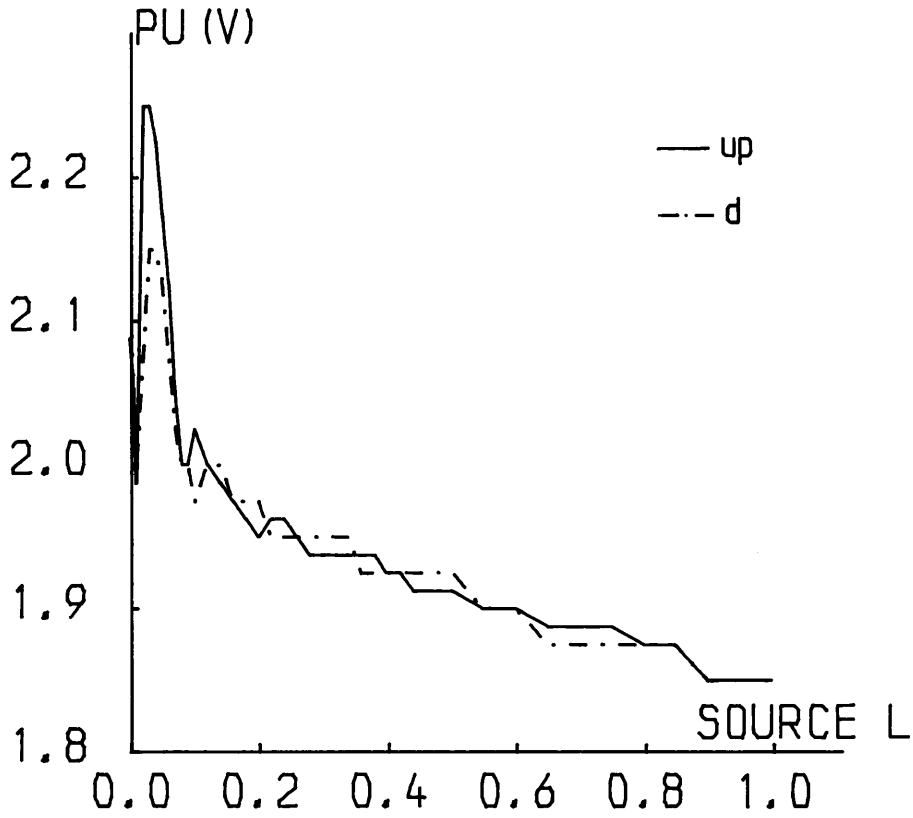

Figure 5.24 Variation of maximum receiving-end voltage with L_s for the 1-phase, zero earth return, 5 pi-section lines.

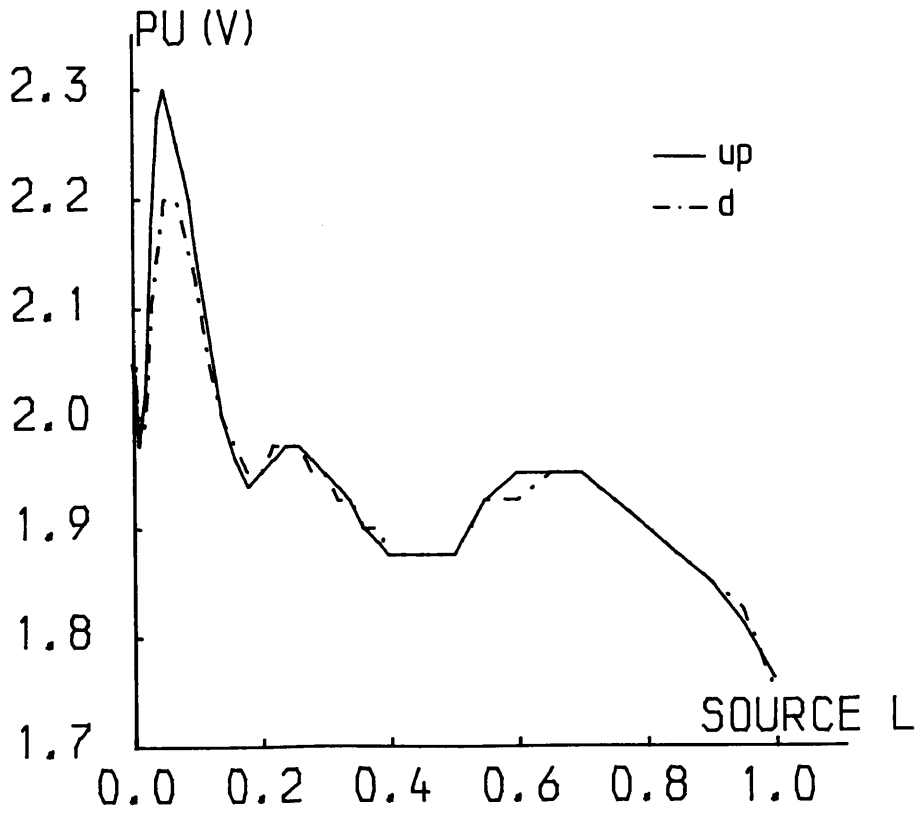

Figure 5.25 Variation of maximum receiving-end voltage with L_s for the 1-phase, zero earth return, 10 pi-section lines.

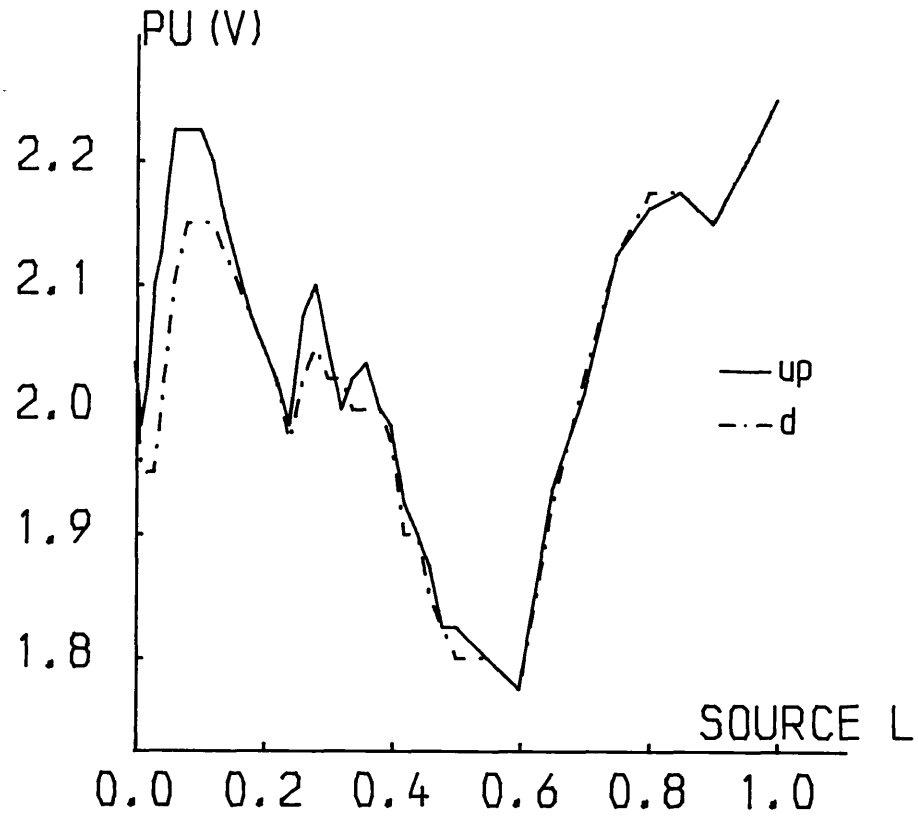

Figure 5.26 Variation of maximum receiving-end voltage with L_s for the 1-phase, zero earth return, 20 pi-section lines.

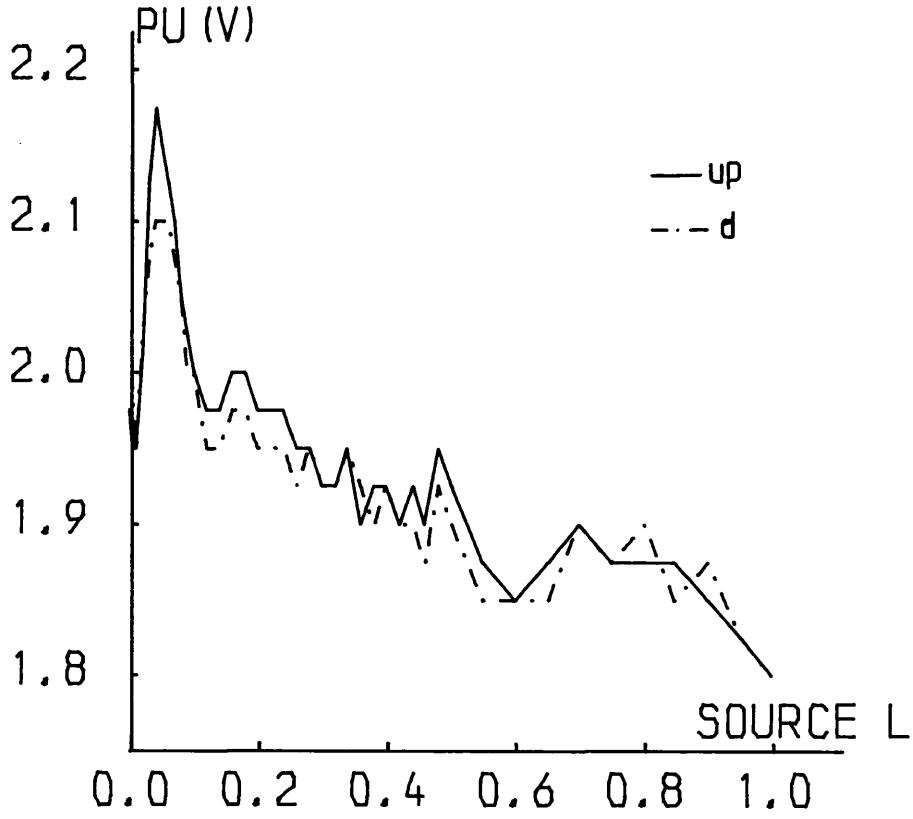

Figure 5.27 Variation of maximum receiving-end voltage with L_s for the 1-phase, earth-path impedance, 5 pi-section lines.

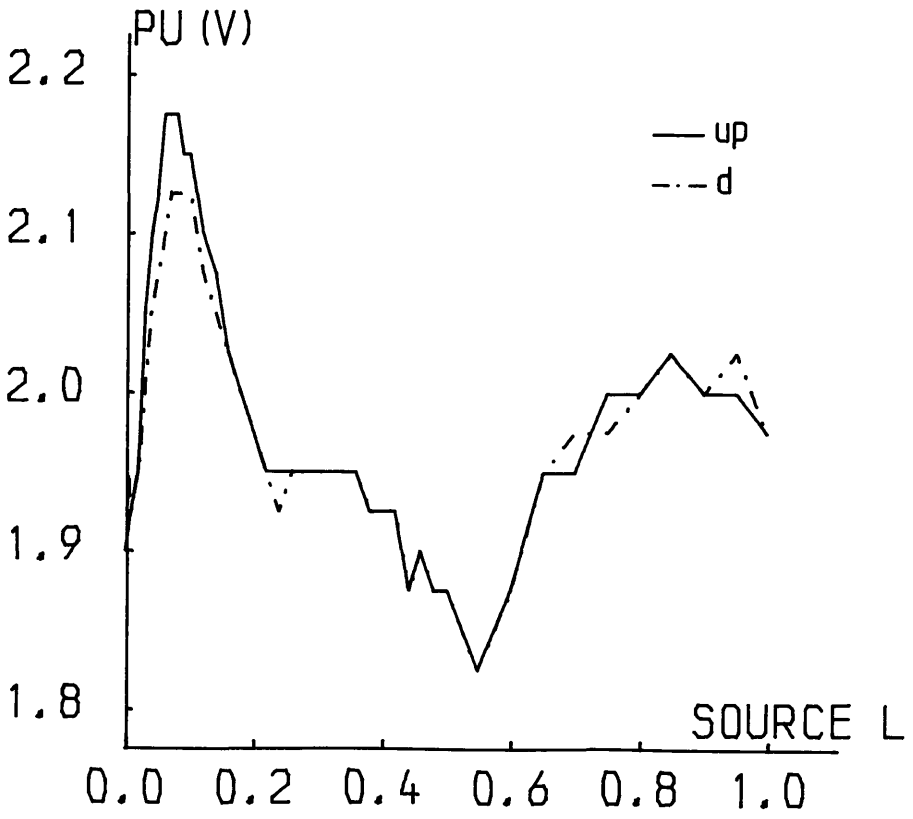

Figure 5.28 Variation of maximum receiving-end voltage with L_s for the 1-phase, earth-path impedance, 10 pi-section lines.

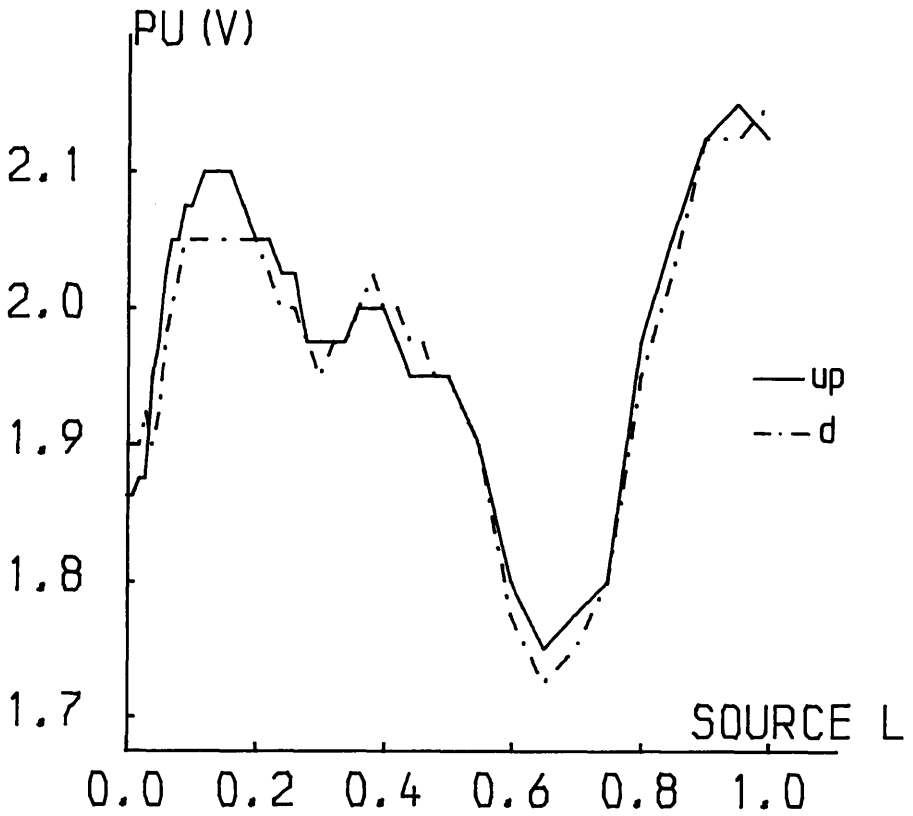

Figure 5.29 Variation of maximum receiving-end voltage with L_s for the 1-phase, earth-path impedance, 20 pi-section lines.

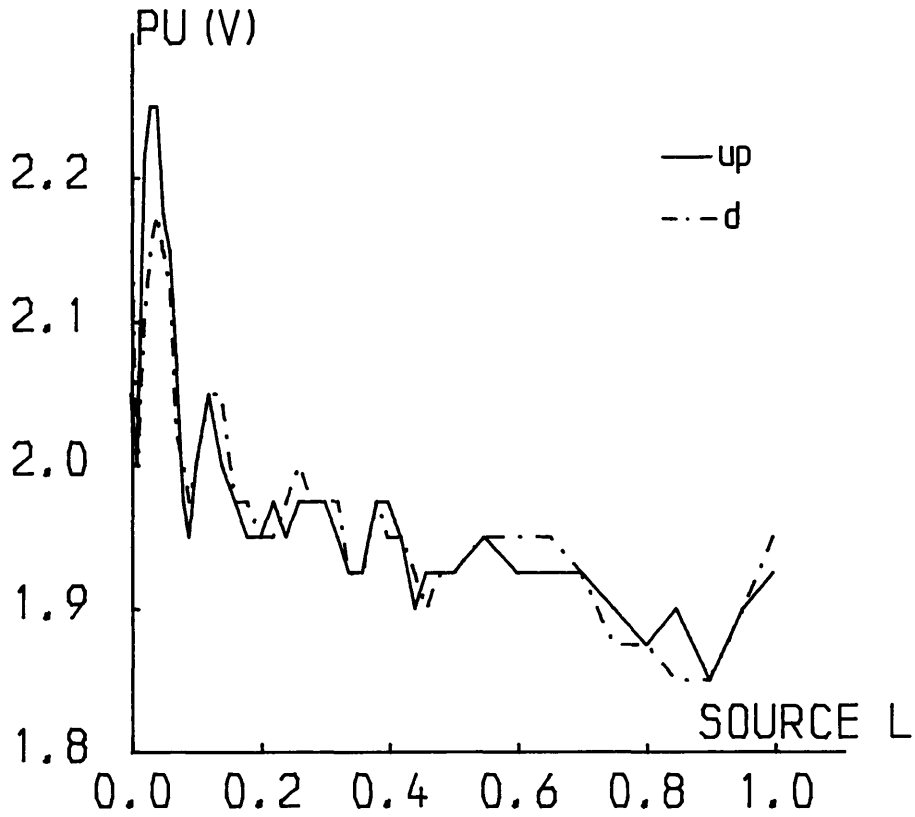

Figure 5.30 Variation of maximum receiving-end voltage with L_s for the 3-phase 5 pi-section lines due to simultaneous closure.

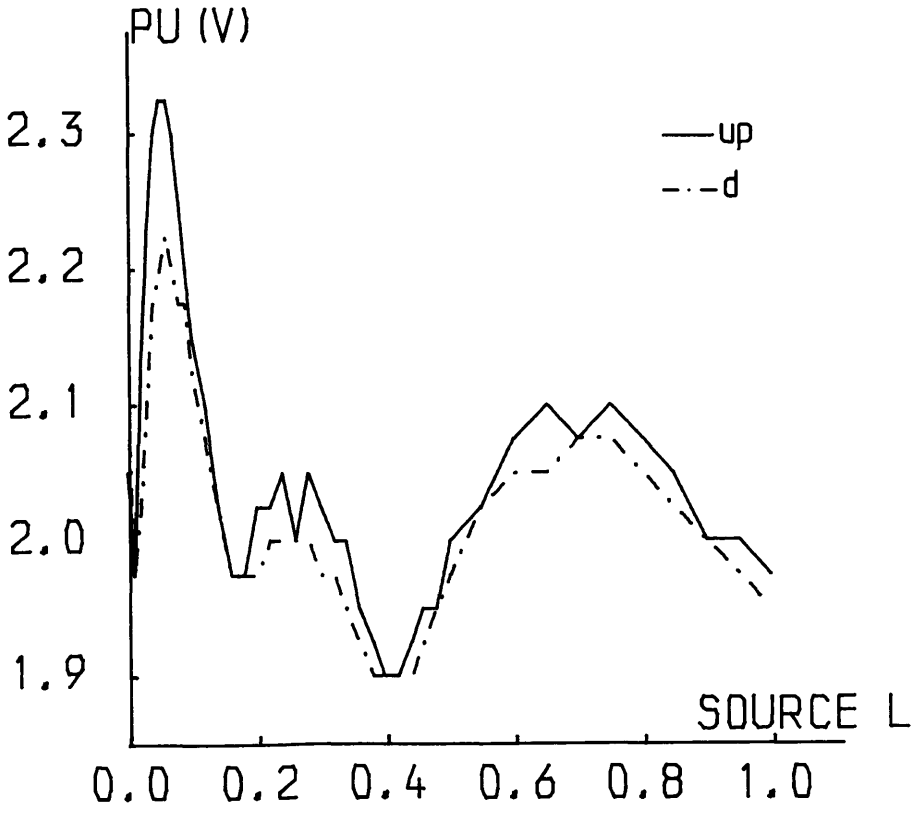

Figure 5.31 Variation of maximum receiving-end voltage with L_s for the 3-phase 10 pi-section lines due to simultaneous closure.

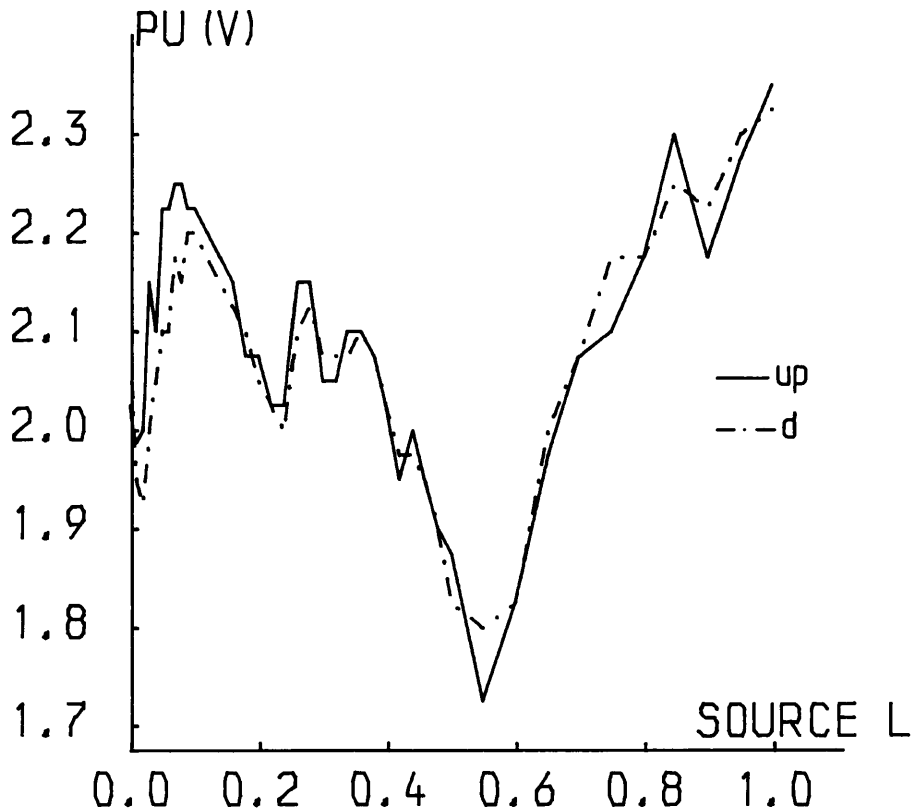

Figure 5.32 Variation of maximum receiving-end voltage with L_s for the 3-phase 20 pi-section lines due to simultaneous closure.

Each profile consists of two sets of overvoltages where 'up' indicates the uncompensated/processor value and 'd' represents the compensated or damped line value.

5.6.2.1. Analysis of Overvoltages Profiles

From these figures it can be seen that the three model line configurations give overvoltage profiles each of which display an initial peak characteristic for both the compensated and uncompensated lines. The value of L_s at which the maximum pu voltage of this characteristic occurs and the range of L_s over which it can be observed both increase with line length. The maximum pu value of the characteristic increases when the line length is doubled from 5 to 10 π-sections but then decreases for the 20 π-section lines in all cases. The peak pu value of the characterisic is the maximum value recorded in the 0 - 1H range with the exception of the 20 π-section line lengths. The overvoltage curves for this line length increase dramatically for source values greater than 0.6H in each case due to the source inductance and line capacitance giving rise to a condition approaching power frequency resonance[20].

The characteristic is observed in all profiles in the range 0 - 0.2H and it is in this region that a consistent and significant difference in the peak overvoltages of the compensated and uncompensated lines occur. For the remainder of the inductance range i.e. 0.2 - 1H, the pu difference between the profiles is close or equal to zero. The characteristic peak occurs because the source inductive effects become increasingly more significant in the uncompensated line receiving-end responses, as L_s is increased from zero, than in those of the compensated line whose attenuation significantly reduces these effects. The difference in magnitude of these source effects for the compensated and uncompensated/processor waveforms was previously noted in Figures 5.2 and 5.4 and Figure 5.13 for source values of 0.0801H and 0.0249H respectively. However from Figures 5.18 - 5.23 it is observed that significant waveform differences are now no longer apparent as L_s is further increased

and that the processor and compensated waveforms are now almost identical in waveshape and amplitude.

The presence of L_s in the source means that the frequency of the transient response is no longer dependent on the line travel time but on the natural frequency of the source inductance and line capacitance which decreases as L_s increases. From Figure 1.5 it was observed that the attenuation of the compensated and uncompensated π-sections become approximately equal at lower frequencies. This may explain why the profiles become increasingly similar since the transient fundamental frequency decreases as L_s is increased.

Since the only significant difference in pu overvoltage is realised in the 0 - 0.2H region this range of L_s was analysed to give values for the average and maximum pu difference between the compensated and uncompensated overvoltage curves occurring for each model configuration and line length. These results are given in Figure 5.33 and show that the characteristic is observed over an increasing range of L_s as line length increases. For line lengths greater than the longest considered experimentally i.e. 20 π-sections or 100 miles, it could therefore be assumed that the range of source inductance values where the uncompensated line overvoltages will be significantly higher than those of the compensated line will increase.

No relation between average or maximum pu difference and line length can be observed from the experimental results although it can be stated that these parameters have values which are consistently lower in the 1-phase earth impedance case. However the average pu difference for all cases ranges from 0.025 - 0.085 pu with the maximum value varying from 0.05 - 0.175 pu. 0.175 pu corresponds to 39.3 kV for an actual 275 kV system.

Configuration/ Line length		Range of characteristic (H)	Average pu difference	Maximum pu difference
Z	5	0.07	0.0775	0.175
E	5	0.09	0.025	0.075
3	5	0.08	0.05	0.1
Z	10	0.165	0.064	0.125
E	10	0.22	0.032	0.075
3	10	0.145	0.085	0.125
Z	20	0.225	0.08	0.175
E	20	0.265	0.034	0.05
3	20	0.22	0.062	0.125

where Z = 1-phase, zero earth impedance line

E = 1-phase, earth-path impedance line

3 = 3-phase line, simultaneous closure

5 represents 5 pi-section line length

Figure 5.33 Average and maximum pu differences between uncompensated and compensated line profiles.

5.7 Discussion of Source Inductance

The inclusion of inductance in the source representation and the subsequent reduction of the high-frequency content of the line sending-end voltage leads to uncompensated line receiving-end responses which are free of Gibbs Oscillations. The overvoltage profiles also show that significant differences in maximum receiving-end voltage also occur which will lead to greater accuracy in the prediction of overvoltages from the uncompensated model line. Since the maximum length of line considered was only 100 miles long, further analysis of longer lines may lead to the range of source values, over which the compensated and uncompensated line overvoltages differ significantly, being extended.

The analysis has also shown that waveform verification by the Runge-Kutta method is limited due to the inability of the numerical technique to include the frequency-dependent variation of resistance of the inductive components of the system. The Runge-Kutta technique was however used to verify overvoltage profiles using the resistor-damped line configuration (see section 7.4). The use of the Lattice Method in the Laplace s-domain was used to check the accuracy of the values of L_G determined for the 1-phase lines with zero earth impedance and indicates that further development of the Lattice technique will be useful in the investigation of other systems where, for example, load inductance or line compensation are included.

CHAPTER 6

Spectral Analysis of Model Line Waveforms

6.1 Introduction

The averaging of discrete waveform samples in the time-domain using the Experimental Sigma Factors has shown that a significant reduction of the Gibbs content of uncompensated line transients, as a result of infinite or inductive source energisation, can be achieved. However the waveforms obtained from energisation of the 10 and 20 π-section 1-phase zero earth impedance lines, discussed in section 4.4.1.2, demonstrated the changing nature of the Gibbs phenomena with frequencies other than the natural π-section frequency becoming apparent in the transient global response. This necessitated the development of the Adaptive Experimental Sigma Factor S_{ae} the application of which reduced the phenomena significantly but not completely. In order to understand this effect more clearly, the frequency content of the model line transients was investigated using Fourier Transform analysis techniques. A greater knowledge of the frequency components of which these waveforms consist may lead to the development of improved averaging techniques for processor modification.

A continuous-time or analogue signal described by the function f(t) can be analysed in this way by taking the Fourier Transform of the function using equation (1.13) i.e.

$$F(\omega) = \int_{-\infty}^{\infty} f(t)\ e^{-j\omega t}\ dt$$

$F(\omega)$ then displays the frequency components of the function and is referred to as the spectrum of f(t). A similar transformation exists for discrete-time signals which gives a discrete frequency spectrum equivalent to the continuous case. This is the Discrete Fourier Transform or DFT[41].

Spectral analysis is now increasingly used in preparation for the

Digital Filtering of the discrete-time signals analysed, these filters reducing unwanted noise or interference from the signals. Since the Gibbs phenomena can be viewed as 'unwanted interference' in the digitised line transient response it was initially assumed that if the Gibbs frequency components could be identified, by spectral analysis using the DFT, they could then be filtered from the uncompensated response by implementation of a software Digital Filter.

6.2 The Discrete Fourier Transform

The Discrete Fourier Transform is given by

$$X(\tfrac{K}{N\Delta T}) = \sum_{n=0}^{N-1} x(n)\ e^{-j2\pi Kn/N} \qquad (6.1)$$

where

$x(n)$ = series of waveform sample values or sample record

ΔT = sampling period or time between samples

N = number of samples in record

K = the frequency components 0,1,..,N-1

$X(\tfrac{K}{N\Delta T})$ = $X(K)$ = Complex amplitudes of frequency components

The resolution Δf of components in the frequency domain is given by

$$\Delta f = \frac{1}{N\Delta T} \qquad (6.2)$$

where $N\Delta T$ the sample record length must represent a complete cycle or number of cycles of the time-domain waveform since equation (6.1) assumes periodicity of the sampled waveform. This is not the case for a transient response but by taking one cycle of the transient fundamental periodicity is implied. A complete cycle must be taken to prevent a reduction in the calculated frequency component accuracy[41].

In order to satisfy the Nyquist sampling theorem and prevent signal aliasing[42] the frequency of sampling must be greater than twice the highest frequency present in the waveform i.e. ΔT must be sufficiently small

to allow correct identification of that frequency component.

Equation (6.1) can be simplified by the substitution

$$e^{-j2\pi Kn/N} = \cos(\frac{2\pi Kn}{N}) - j \sin(\frac{2\pi Kn}{N}) \quad (6.3)$$

which allows a straightforward definition of the DFT in software.

6.2.1 The DFT of a Square Wave

The receiving-end waveform of a transmission line has previously been calculated by the inverse Modified Fourier Transform of equation (4.1) with the inclusion of Lanczos Sigma Factor σ_s giving an improved square-wave response. The Fourier Transform of an ideal square wave gives a sin(X)/X distribution in the frequency domain[26] which suggested that the DFT be applied to this function to determine the accuracy of the DFT routine written (Appendix V) and also to display the frequency spectra of the 'ideal' line response.

Implementing (4.1), with model line L, C and R values to omit scaling, the response of a 25 mile line to step excitation was calculated with the limit of integration Ω = 3 MHz and $d\omega$ = 1 kHz. The resultant receiving-end waveform is shown Figure 6.1(a). If the DFT of this waveform was determined the predominant feature in the frequency domain would be the DC component of 1 pu. This would reduce the relevant magnitudes of the high-frequency components which in the uncompensated model line waveforms to be investigated would be of most interest. To allow more detailed inspection of these frequencies the voltage values of the line response were modified by subtracting the step 1 pu value from each sample reducing the DC content to effectively zero (Figure 6.1(b)).

Since the highest frequency in the Fourier Transform calculation was defined as 3 MHz the receiving-end voltage values were calculated every ΔT=0.1 μs to satisfy the Nyquist sampling criterion. By taking one complete cycle from 17 - 87 μs, which comprised 700 samples of the receiving-end

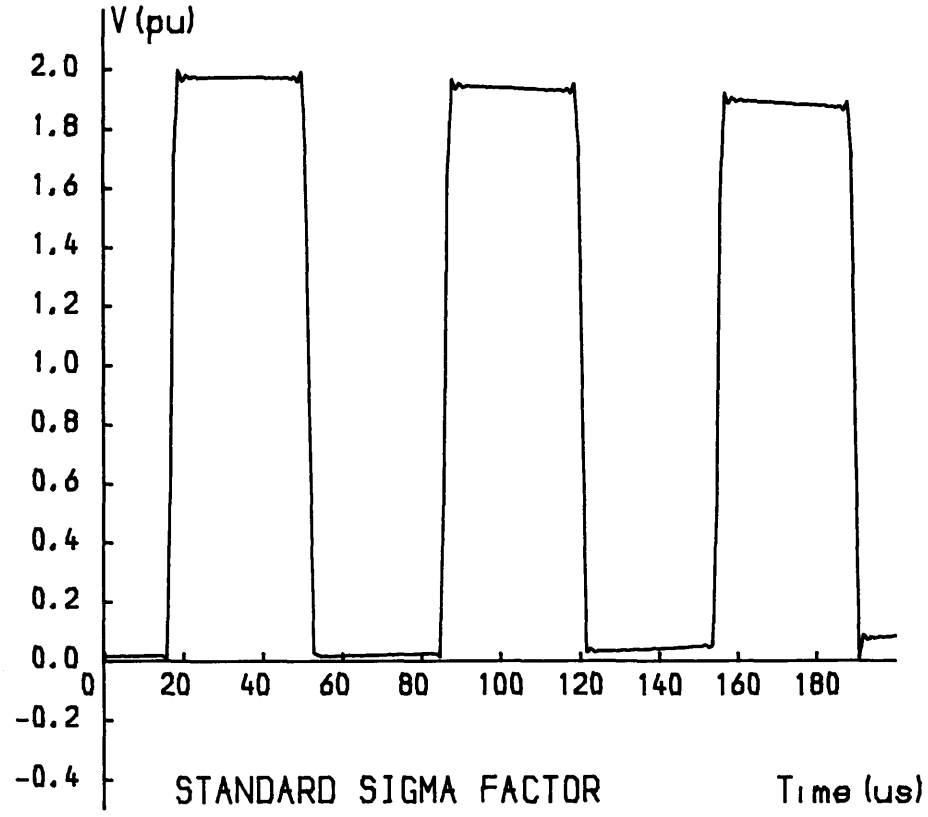

Figure 6.1(a) 25 mile line response to step excitation calculated by the Modified Fourier Transform.

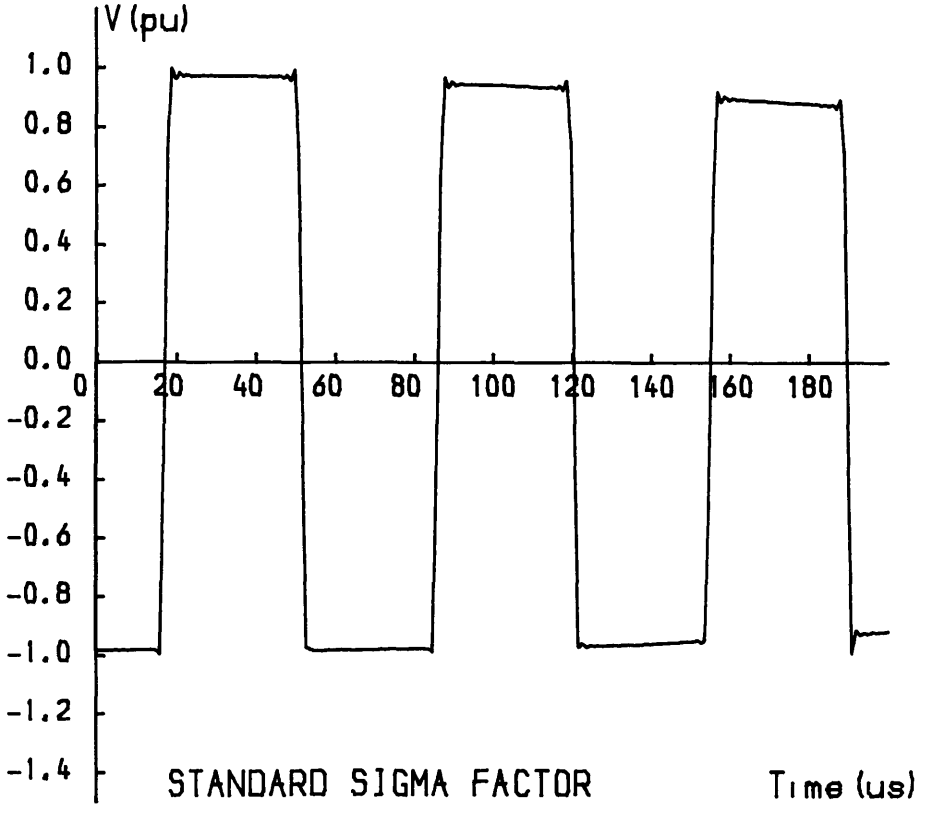

Figure 6.1(b) The response with the DC content removed.

waveform, the DFT was calculated and the resulting frequency spectrum is shown in Figure 6.2(a). The components are spaced at intervals of 14.29 kHz i.e. $\frac{1}{N\Delta T}$ and give an acceptable indication of the waveform frequency content. Note the asterisk displays the magnitude of the DC content which has been effectively reduced by subtracting the 1 pu step value.

Schwartz[42] and Bozic[43] demonstrate that the frequency resolution Δf can be reduced by 'zero padding' i.e. the addition of zero values to the original sample sequence x(n). Both the original and zero augmented sequences have the same Discrete Fourier Transform but the frequency component spacing is now reduced due to the increased record length $N\Delta T$. This allows the user to define any frequency component resolution. Defining Δf as 2 kHz the number of samples required for the DFT of the square-wave response is calculated from equation (6.2) as 5000. x(0) - x(699) contain the original waveform data while x(700) - x(4999) contain the added zero values. The improved frequency spectrum due to zero padding is shown in Figure 6.2(b) which now clearly displays the expected sin(X)/X result.

6.2.1.1. Analysis of the Square-Wave Frequency Content

The square wave consists of a fundamental and odd harmonic components whose magnitudes decrease with increase in frequency. The transient fundamental frequency for this line length is 14.29 kHz and from the analytical sin(X)/X solution the expected harmonic components were calculated. These are listed in Figure 6.3(a) and compared with the values obtained from the DFT of Figure 6.2(b). The theoretical magnitude of the components at these frequencies can also be determined and are normalised with respect to the fundamental e.g.

$$X_n(K) = \frac{|X(K)|}{|X(0)|} \qquad (6.4)$$

These are also compared to those calculated from the DFT (Figure 6.3(b)).

The results in Figure 6.3 show that high accuracy is obtained

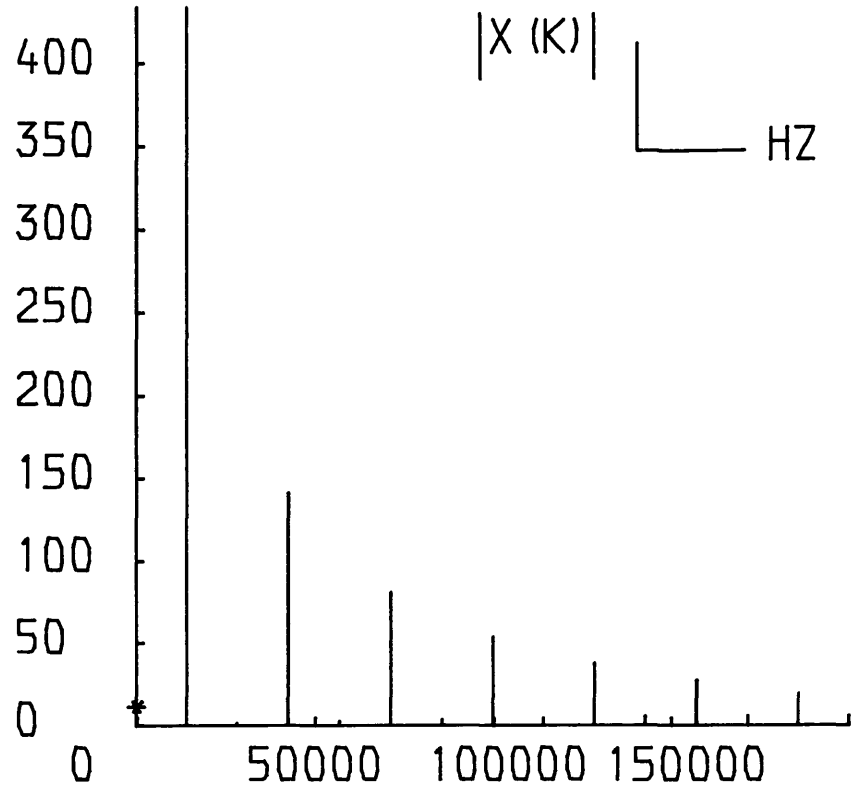

Figure 6.2(a) DFT of the 25 mile line response.
Δf = 14.29 kHz.

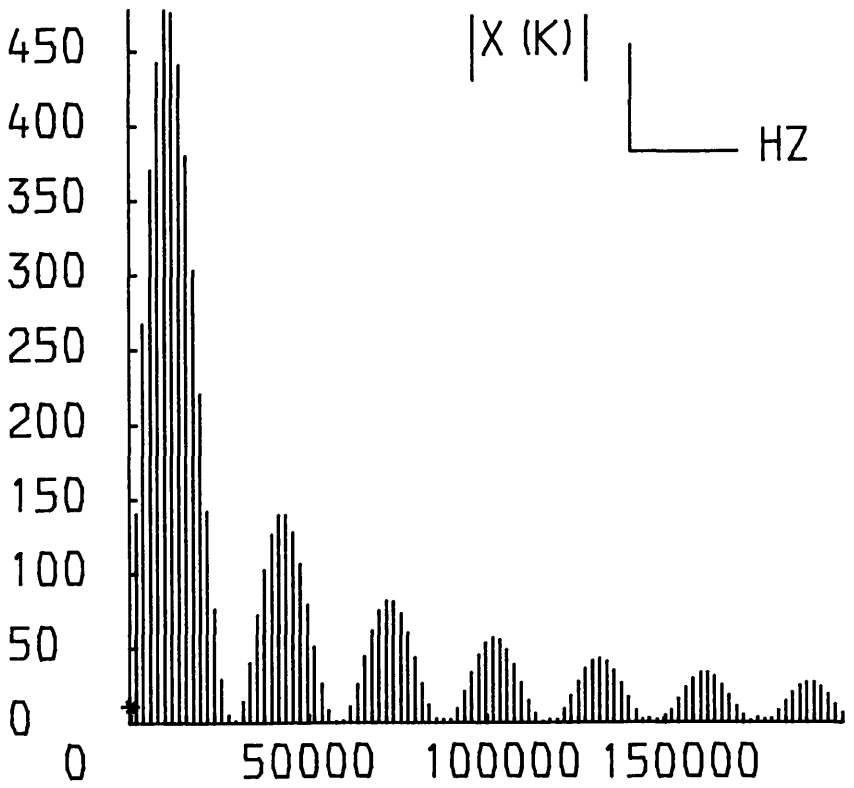

Figure 6.2(b) DFT of the 25 mile line response.
Δf = 2 kHz.

Harmonic	f(kHz) Analytic	f(kHz) DFT
3rd	42.9	42.0
5th	71.4	72.0
7th	100.0	102.0
9th	128.6	132.0

Figure 6.3(a) Frequencies of the odd harmonic components of the square wave.

Harmonic	Xn(K) Analytic	Xn(K) DFT
3rd	0.33	0.29
5th	0.20	0.17
7th	0.14	0.12
9th	0.11	0.09

Figure 6.3(b) Normalised magnitudes of the square wave odd harmonic components.

using the DFT in spectral analysis and it is emphasised that the theoretical values are for an ideal square wave which is not band-limited i.e. $f \rightarrow \infty$ and which is free from the effects of attenuation.

6.3 The DFT of Model Line Waveforms

The frequency component distribution calculated from the Modified Fourier Transform square wave response allows some assumptions to be made regarding the possible frequency content of the model line responses. Since the receiving-end waveforms of the open-circuited model line are square in nature for ideal source energisation the frequency components which should be predominant are the transient fundamental and the odd harmonic components whose frequencies lie below the model line cut-off frequency f_c of 92.2 kHz (see Appendix I.6). A component at the natural π-section frequency of 65 kHz would also be expected for the uncompensated line waveforms.

The 5 π-section model line waveforms of Figure 4.6 which have a transient frequency of 14.29 kHz should therefore only display the 3^{rd} and 5^{th} harmonic components in the amplitude spectra in addition to the fundamental. In the 20 π-section line cases i.e. the responses of Figure 4.11, the transient fundamental is 3.61 kHz which implies that a greater number of odd harmonic components will be observed in the frequency spectrum of this line i.e. up to and including the 25^{th} harmonic component of 90.25 kHz. The 65 kHz component is also anticipated in the uncompensated line spectra.

The amplitude spectra of these two line lengths for both uncompensated and compensated lines were calculated by transferring eight sets of sample sequences from the Z-2D to the DEC-20 for analysis, the eight sequences consisting of the first two cycles of each transient response. As before x(n) was modified in each case to minimise the DC content before the DFT of equation (6.1) was applied.

6.3.1 5 Π-Section Line Frequency Spectra

6.3.1.1. First Cycle of Transient Waveform

The frequency spectra of the first transient cycle for the uncompensated and resistor-damped 5 π-section lines are shown in Figures 6.4 and 6.5 respectively. Each figure comprises the magnitude (a) and phase (b) of the complex components calculated by (6.1) and a 0 - 100 kHz range with a frequency resolution of 1 kHz displayed.

Although both frequency spectra are similar up to 30 kHz the magnitude of the fundamental component is greater in the uncompensated line case. For frequencies greater than 30 kHz however significant differences in the two spectra can be observed. The uncompensated line spectrum displays three distinctive peaks which are centred at 44, 63 and 82 kHz. Their normalised magnitudes are 0.29, 0.19 and 0.12 respectively. It was previously assumed that predominant features would appear at the harmonic frequencies of 42 and 71 kHz and at the natural π-section frequency of 65 kHz. The high-frequency components at 44 and 63 kHz partly confirm this. However no significant 5^{th} harmonic component can be observed and the component at 82 kHz is unexpected.

The amplitude spectrum of the compensated line waveform above 30 kHz displays 5 distinctive peaks at 33, 45, 63, 77 and 93 kHz. The 3^{rd} harmonic component i.e. 45 kHz has a magnitude of only 0.15 which is a significant reduction when compared to the uncompensated line value of 0.29. Again no 5^{th} harmonic can be observed and a reduced content at 63 kHz is present.

6.3.1.2. Second Cycle of Transient Waveform

The amplitude spectra for the second transient cycle of the uncompensated and resistor-damped waveforms are shown in Figures 6.6(a) and (b) respectively. The shape of the frequency spectra in both cases are similar to those determined for the first transient period with a noted

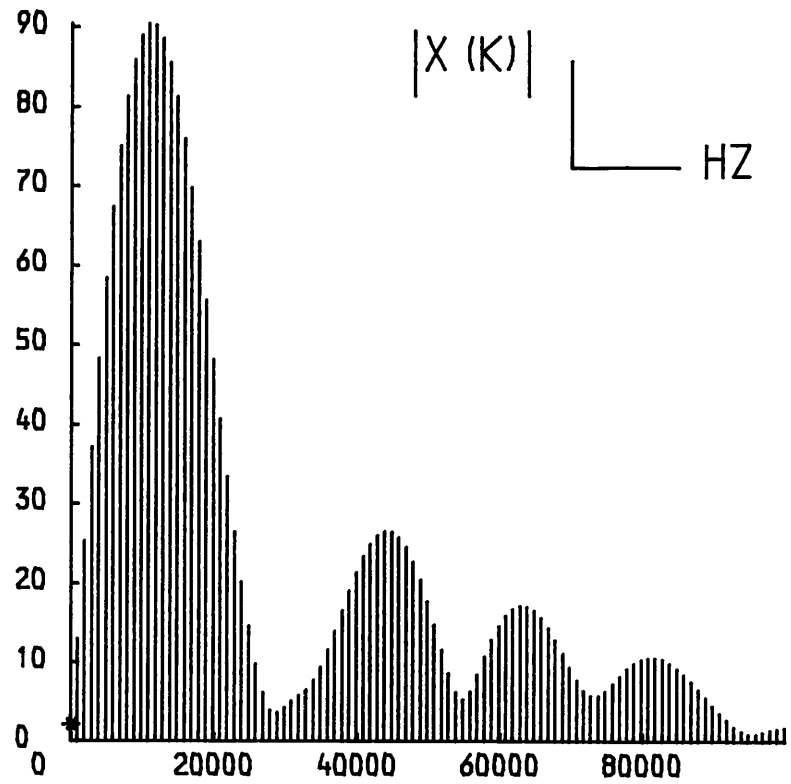

(a)

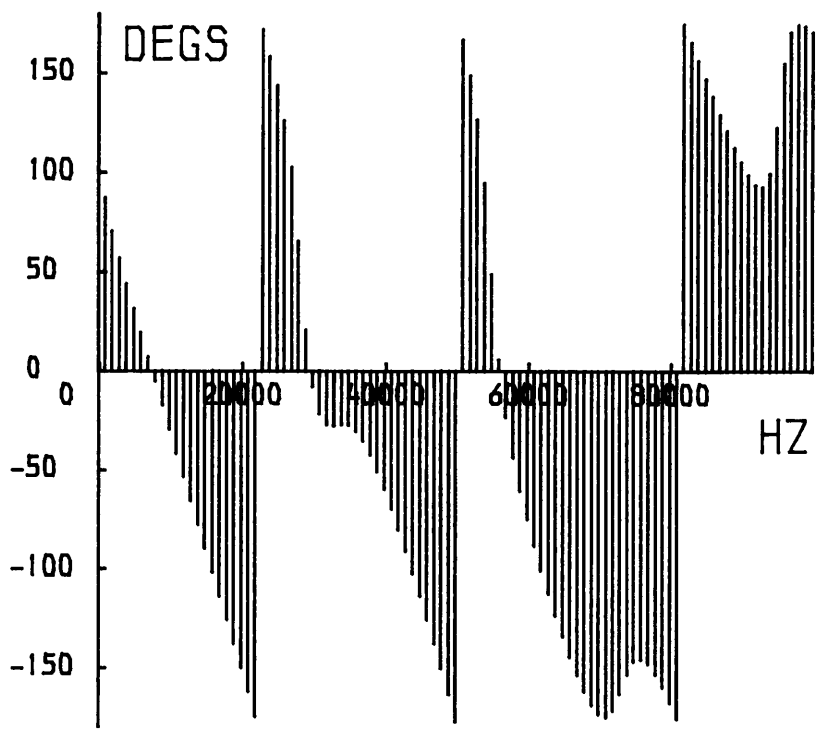

(b)

Figure 6.4 Frequency spectrum of 5 pi-section uncompensated line response, 1st transient cycle
(a) Magnitude; (b) Phase.

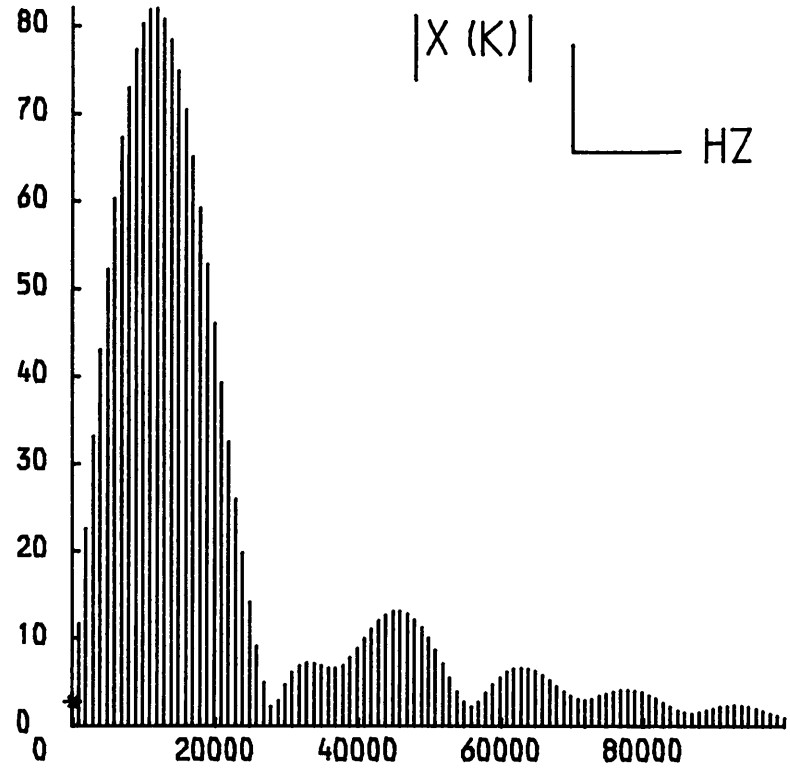

(a)

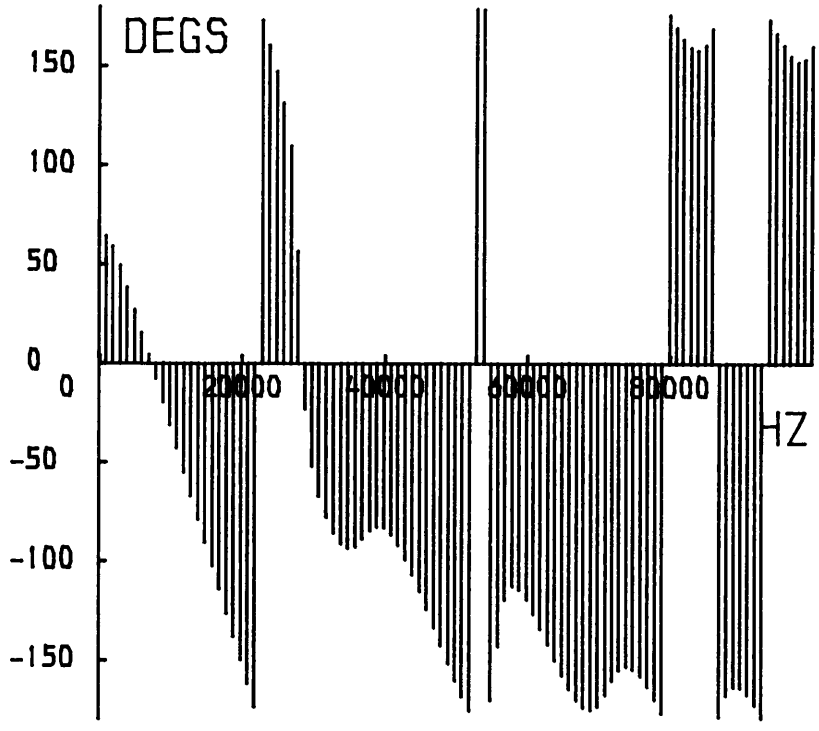

(b)

Figure 6.5 Frequency spectrum of 5 pi-section compensated response, 1st transient cycle.
(a) Magnitude; (b) Phase

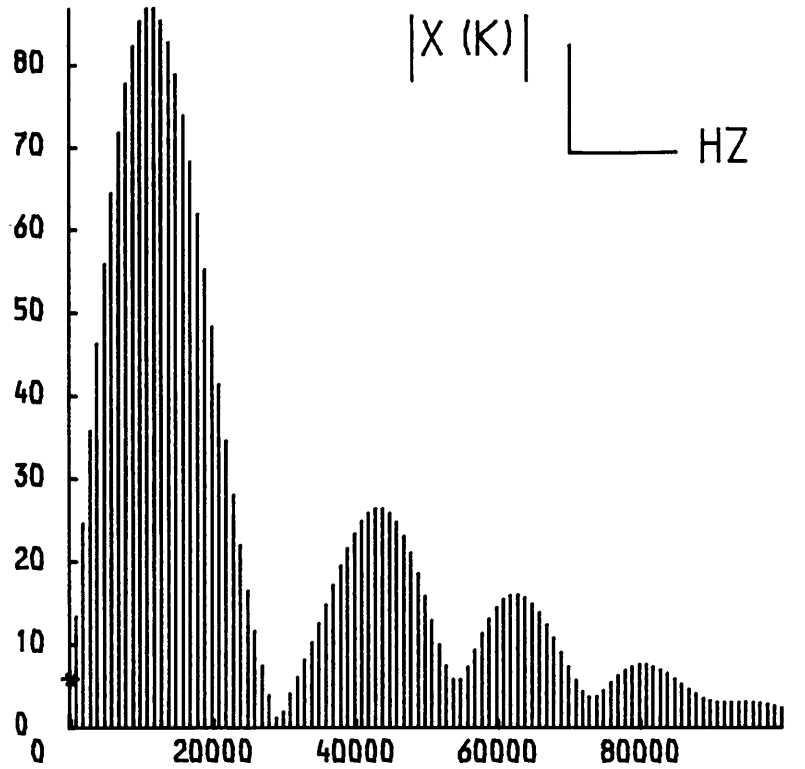

(a)

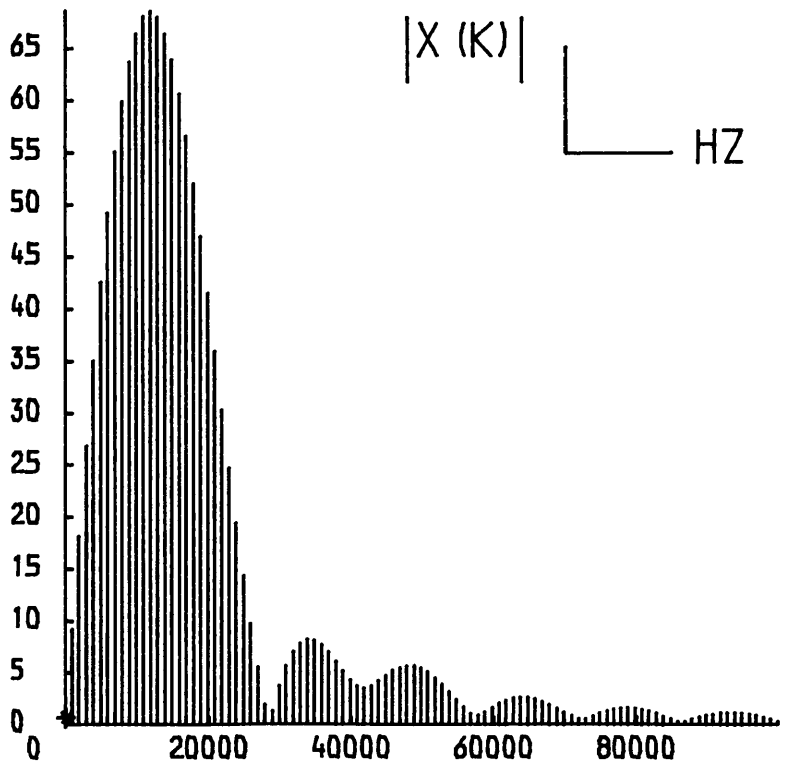

(b)

Figure 6.6 Amplitude spectra of 5 pi-section lines, 2nd transient cycle.
(a) Uncompensated; (b) Compensated.

reduction however in all component magnitudes. Although the fundamental frequency component in both cases is reduced, notably in the damped case, the change in magnitude of the higher frequency components is of greater interest. Their normalised magnitudes were calculated with respect to the new fundamental peak values to indicate the relative change in frequency content between the transient cycles.

The three peaks in the uncompensated case were determined in magnitude as 0.29, 0.19 and 0.09 for the 44, 63 and 82 kHz components respectively. When compared to their values for the first cycle only the 82 kHz component is reduced in relation to the fundamental. The change in frequency content observed from the compensated line spectra shows that the component at 33 kHz is now greater in magnitude than the 45 kHz component with frequencies above this also significantly reduced.

The differences between the frequency spectrum for subsequent compensated line transient cycles emphasises the effect of increased attenuation, even at frequencies as low as the 3^{rd} harmonic, due to the inclusion of the compensating resistors in the model. Attenuation is also present in the uncompensated line but as the spectra for subsequent transient cycles show only very high frequencies i.e. 82 kHz are significantly reduced.

6.3.1.3. Discussion

The uncompensated line spectra show that even though the natural π-section frequency f_0 appears to be initially predominant in the time-domain waveform other high-frequency components can be observed in the amplitude spectra at approximately 44 and 82 kHz. For both transient cycles the 3^{rd} harmonic component has the largest magnitude. The anticipated 5^{th} harmonic was not a significant feature while the 82 kHz component was unexpected. Comparing the spectra for both transient cycles shows that the 82 kHz component is the only high-frequency component significantly reduced which is explained by the attenuation of the model

π-section increasing with frequency (see Figure 1.5).

The compensated line amplitude spectra did not display a sin(X)/X frequency distribution and the only significant component which was anticipated was observed at the 3rd harmonic frequency. The 33 kHz component was not anticipated and a significant feature was observed at 63 kHz i.e. approximately f_0, although it was significantly reduced in magnitude with respect to the uncompensated line component at this frequency. The attenuation due to the inclusion of the damping resistors is seen by comparing the magnitudes of the high-frequency components for subsequent transient cycles.

The phase responses for the first transient cycle display approximate linearity until 60 kHz in both cases and the amplitude spectra show that the uncompensated line waveform components are greater than each corresponding value of the compensated case.

6.3.2 Components above the Model Cut-Off Frequency

All spectra show that there are frequencies above the previously stated π-section cut-off frequency of 92.2 kHz. This is caused by digitisation of the analogue waveform and in the incorrect assumption that the model line has an ideal low-pass filter characteristic.

6.3.2.1. Errors due to Waveform Discretisation

1. The model line waveforms are sampled by the TR so that an analogue voltage from the line may lie exactly halfway between two successive digital voltage levels one of which has to record the analogue value. This results in quantisation noise which has a maximum error of ±0.5 Volts/bit.

2. The complete cycle for each sample sequence was defined as those sample values which occurred closest to 0 pu (after removal of the DC component) and which also satisfied the required

number of samples to give the transient fundamental frequency i.e. NΔT. The first and last values in a sequence may contribute to a small discontinuity effect in x(n) which will give rise to an apparent high-frequency content[41].

6.3.2.2. The Model Line as a Practical Low-Pass Filter

Based on the assumption that the theoretical cut-off frequency of the model π-section is accurate no frequency components above the 92.2 kHz cut-off should be observed in the amplitude spectrum. However the stated value of f_c is approximate since it is calculated using the L and C values of a lossless π-section. The suggestion of an ideal low-pass filter characteristic is incorrect since practical characteristics vary considerably from the theoretical case. The two filter responses are shown in Figure 6.7.

6.3.3 20 Π-Section Line Frequency Spectra

6.3.3.1. First Cycle of Transient Waveform

A similar procedure was undertaken for the 20 π-section line compensated and uncompensated transient cycles. The amplitude spectra for the first and second transient cycles of the uncompensated line response are shown in Figures 6.8(a) and 6.9(a) respectively with the corresponding resistor-damped line response spectra in part (b) of each figure.

It was previously assumed that the number of odd harmonic components observed in the frequency domain would increase, with a decrease in the transient fundamental frequency, and this is verified by the uncompensated line spectra shown. The transient frequency of this line length is 3.61 kHz and the harmonic frequencies anticipated from the theoretical sin(X)/X solution are listed in Figure 6.10. The frequency of the peaks which occur in the uncompensated model line spectrum of Figure 6.8(a) are given for comparison.

The results demonstrate that the DFT clearly identifies most of the harmonic components in the frequency range up to 50 kHz. However the

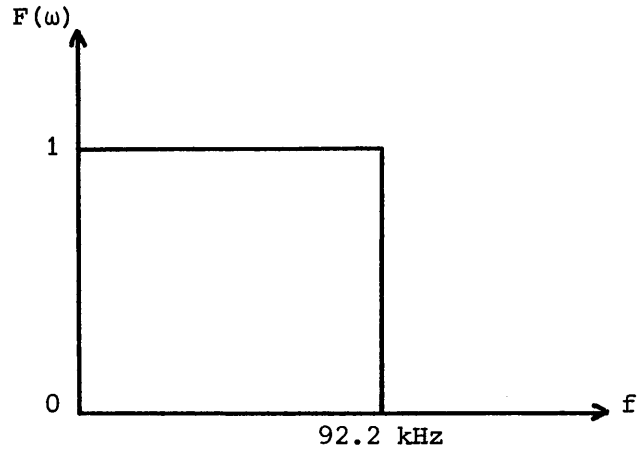

(a)

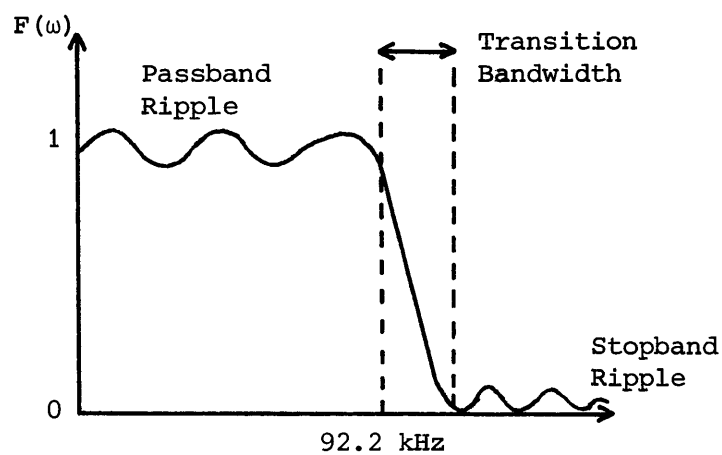

(b)

Figure 6.7 Low-pass Filter Characteristics
(a) Ideal; (b) Practical

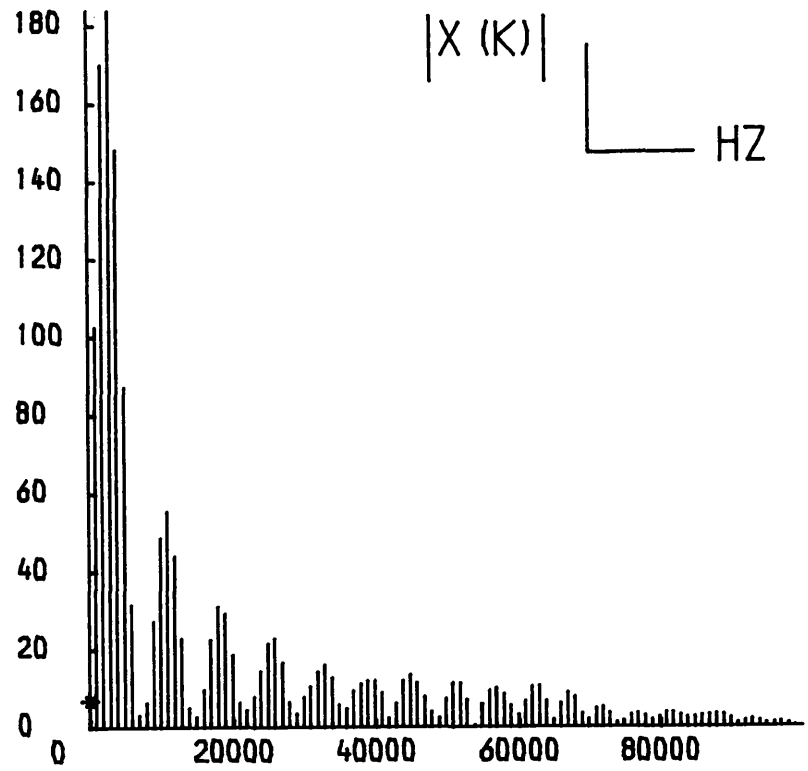

(a)

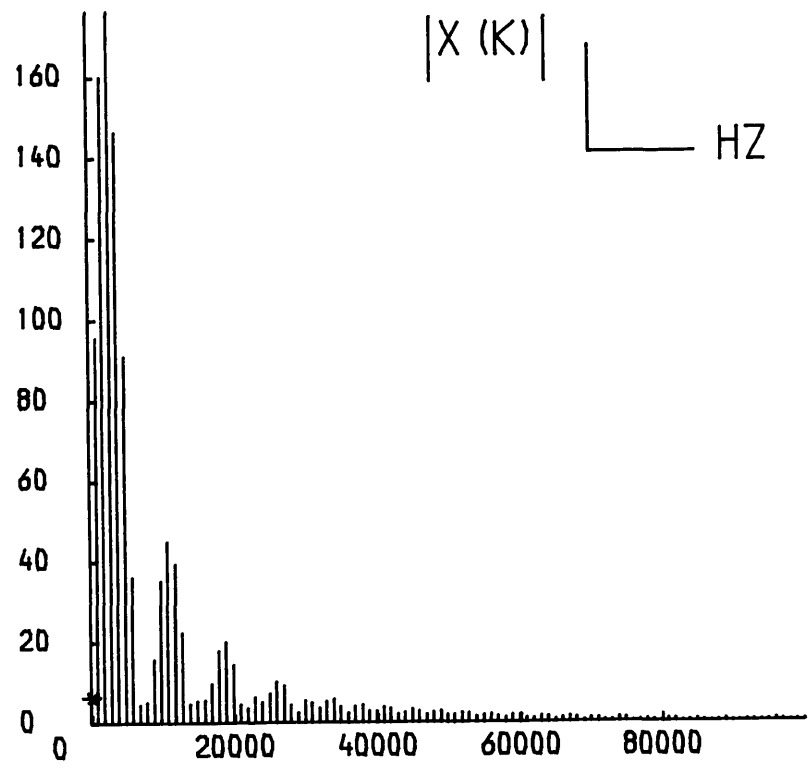

(b)

Figure 6.8 Amplitude spectra of 20 pi-section lines, 1st transient cycle.
(a) Uncompensated; (b) Compensated

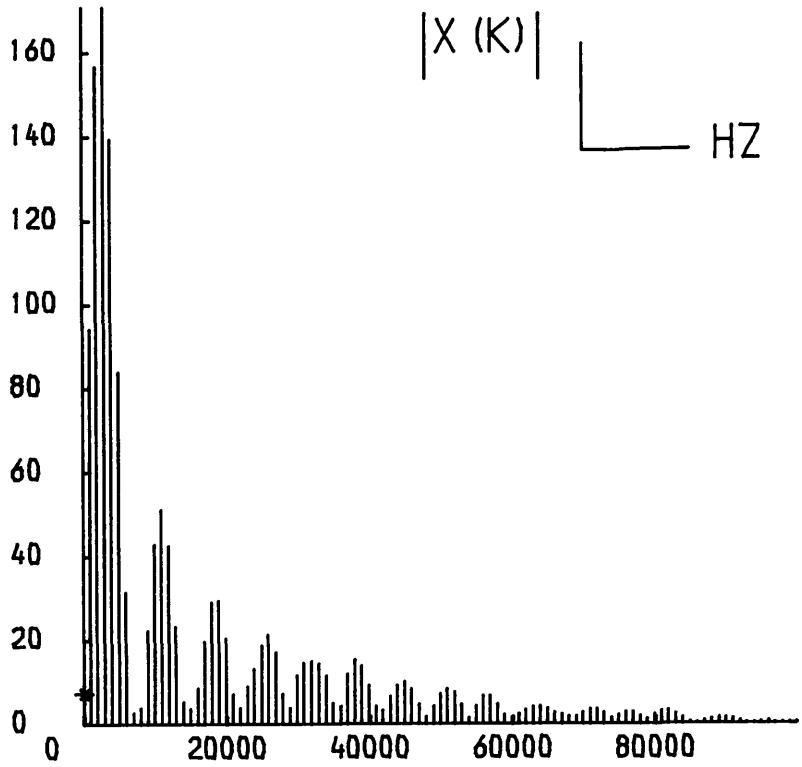

(a)

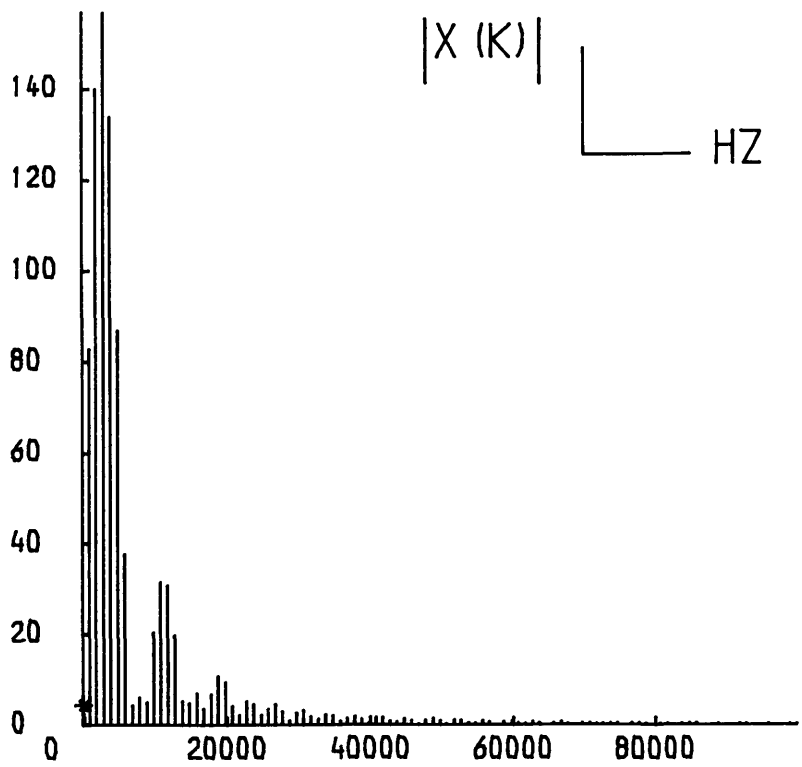

(b)

Figure 6.9 Amplitude spectra of 20 pi-section lines, 2nd transient cycle.
(a) Uncompensated; (b) Compensated

Harmonic	f(kHz) Analytic	f(kHz) DFT
3rd	10.8	11
5th	18.1	18
7th	25.3	26
9th	32.5	33
11th	39.7	40
13th	46.9	45
	-	51
15th	54.2	-
	-	57
17th	61.4	63
19th	68.6	67
	-	72
21st	75.8	77
23rd	83.0	82
25th	90.3	88

Figure 6.10 Frequencies of odd harmonic components for the 20 pi-section uncompensated line.

uncompensated line response contains frequencies at 51 and 57 kHz where the theoretical 15th harmonic of 54.2 kHz was expected and a component at 72 kHz is observed to be approximately midway between the theoretical 19th and 21st harmonics.

The damped line response spectrum of Figure 6.8(b) only clearly displays a sin(X)/X distribution until 26 kHz i.e. the 7^{th} harmonic, but the magnitude of component frequencies above this do decrease steadily as f -> 100 kHz.

6.3.3.2. Second Cycle of Transient Waveform

The second transient cycle spectra of Figure 6.9 again demonstrate the reduction of the high-frequency content, most notably in the resistor-damped case. The 5 π-section uncompensated line spectra displayed a significant reduction of the 82 kHz component only between the first and second transient cycles but the 20 π-section line spectra of Figures 6.8(a) and 6.9(a) show that components at frequencies of 60 kHz and above are now significantly attenuated.

If this trend of high-frequency attenuation is considered for further subsequent transient cycles then only the fundamental and 3^{rd} harmonic frequencies will be observed in the global response. The progressive elimination of the high-frequencies is evident from the 20 π-section uncompensated waveform shown in Figure 4.11 whose global response displays an approximate fundamental and 3^{rd} harmonic content.

6.4 The Limitation of Frequency-Domain Filtering

The determination of frequencies which should be filtered from an uncompensated line response is not a simple task especially in the case of the longer line whose amplitude spectra displays much more information concerning frequency content. The following discussion therefore only considers the simple case of the 5 π-section line.

The first consideration in attempting to obtain a response free from Gibbs phenomena would be to filter out the 63 kHz component in the 5 π-section uncompensated line spectrum of Figure 6.4(a) i.e. the component close to f_0. The appearance of the 82 kHz component is not understood but on the basis that it is not related to the transient fundamental frequency could also be assumed to be erroneous. These frequencies could therefore be filtered from the model line waveform by a multiple bandstop filter.

The remaining contributary frequencies would therefore be the transient fundamental, the 3^{rd} harmonic and the remaining components in the ranges 67 - 80 kHz and 84 - f_c kHz. However no significant 5^{th} harmonic is present and higher-order harmonic components necessary for square-wave representation are also absent due to the low-pass filter effect of the line. Therefore it can be deduced that the components remaining will not give a square-wave response and indeed the response would still display Gibbs Oscillations.

Therefore filtering in the frequency domain will not give an oscillatory-free response since the frequencies required for square-wave representation are not present due to model line design. The uncompensated square-wave obtained will improve as the line is lengthened, thereby lowering the transient fundamental frequency, and allowing an increased number of odd harmonic components to contribute to the response. However, as the 20 π-section line frequency spectra have shown, analysis would become increasingly complex if not impossible.

6.5 Use of a Low-Pass Digital Filter

A low-pass digital filter program was readily available and was used to verify that the DFT of the 5 π-section uncompensated line in Figure 6.4(a) was accurate. Since the filter software was not developed by the author only a basic description of the filter equation used in the program is given. A detailed analysis of Digital Filter Theory can be found in a variety

of publications[43, 44].

The program is based on a Finite Impulse Response Filter design and is given by the convolution summation

$$y(n) = \sum_{k=0}^{N-1} h(k)\ x(n-k) \qquad (6.5)$$

where

y(n) = the filtered output samples

x(n) = the input samples of waveform

h(n) = the impulse response coefficients of the filter.

h(n), the impulse response of the filter, is determined from the ideal frequency response $H(e^{j2\pi f})$ (see Figure 6.7(a)).

The program required three input variables for execution. These were:-

1. The Passband Frequency f_p (in kHz)
2. The Transition Bandwidth (2 kHz chosen) i.e. see Figure 6.7(b)
3. The number of impulse coefficients, N, required. The upper limit of this variable is dictated by the transition bandwidth chosen (N = 1000)

A sequence of input samples x(n) was also required and was generated by Runge-Kutta software. The filtered responses of the 5 π-section line for passbands of 40 - 90 kHz were calculated and are shown in Figures 6.11(a) - (f).

Figure 6.11(a) displays the transient fundamental (broken line) and is compared with the uncompensated input waveform to the filter. Increasing f_p to 50 kHz should allow the 3rd harmonic content to be observed but as Figure 6.11(b) shows a pure 3rd harmonic effect is not obtained from the filter output.

The filtered response with f_p=60 kHz in Figure 6.11(c)

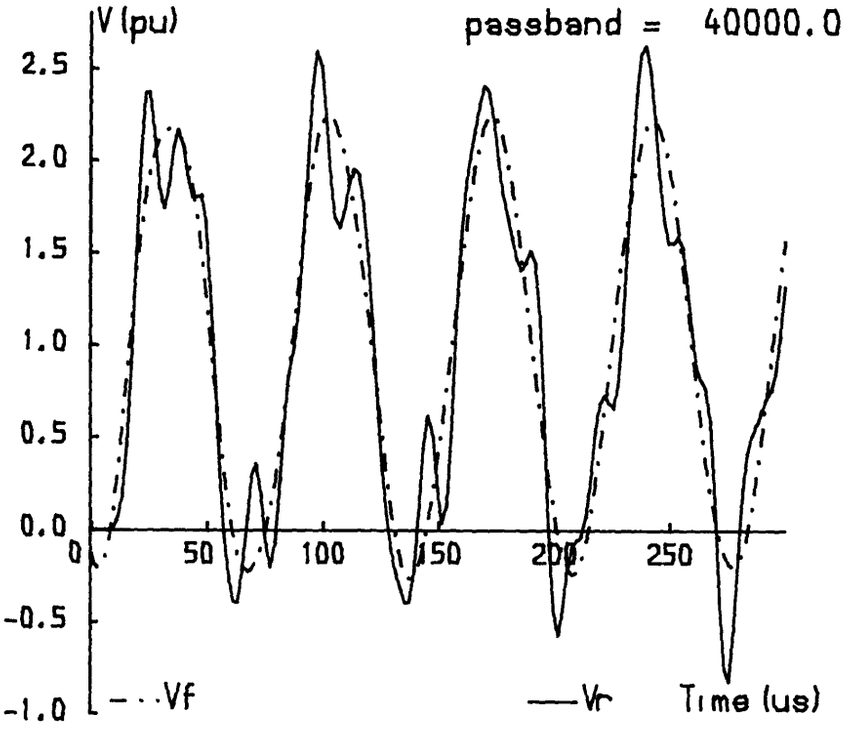

(a)

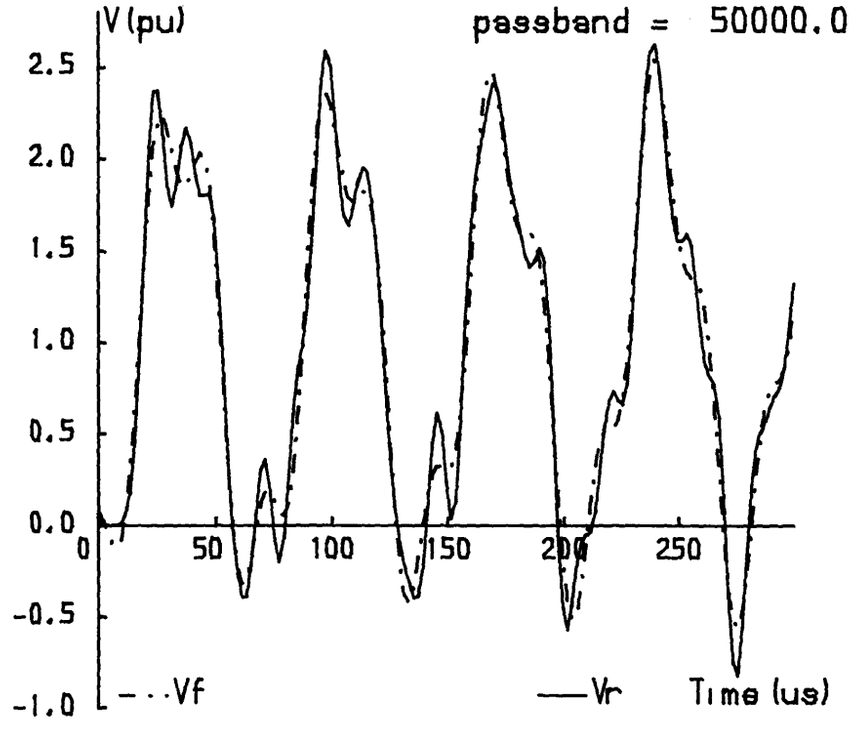

(b)

Figure 6.11 Low-pass filtering of 5 pi-section uncompensated line response.
(a) f_p = 40 kHz; (b) f_p = 50 kHz

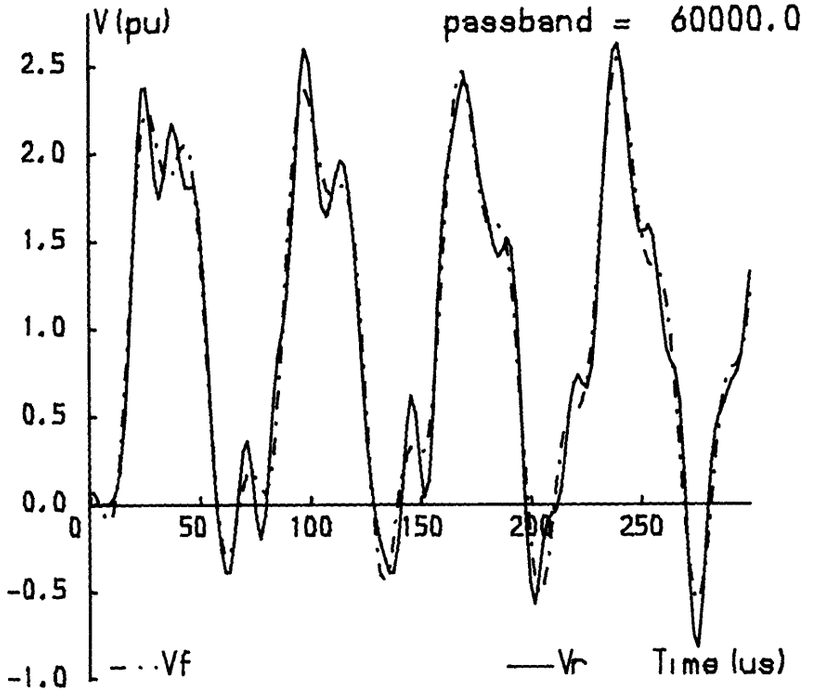

(c)

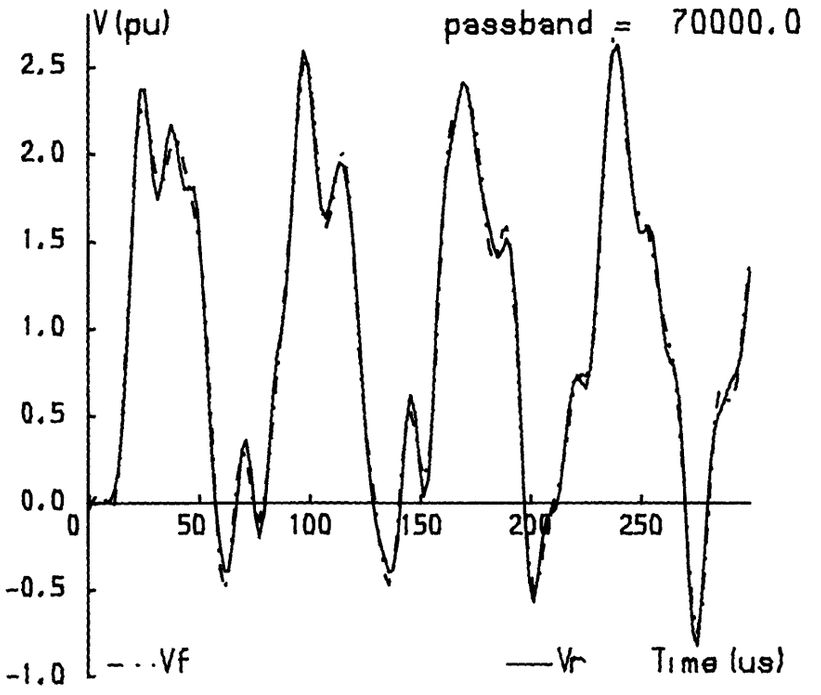

(d)

Figure 6.11 (cont'd) Low-pass filtering of 5 pi-section uncompensated line response.
(c) f_p = 60 kHz; (d) f_p = 70 kHz

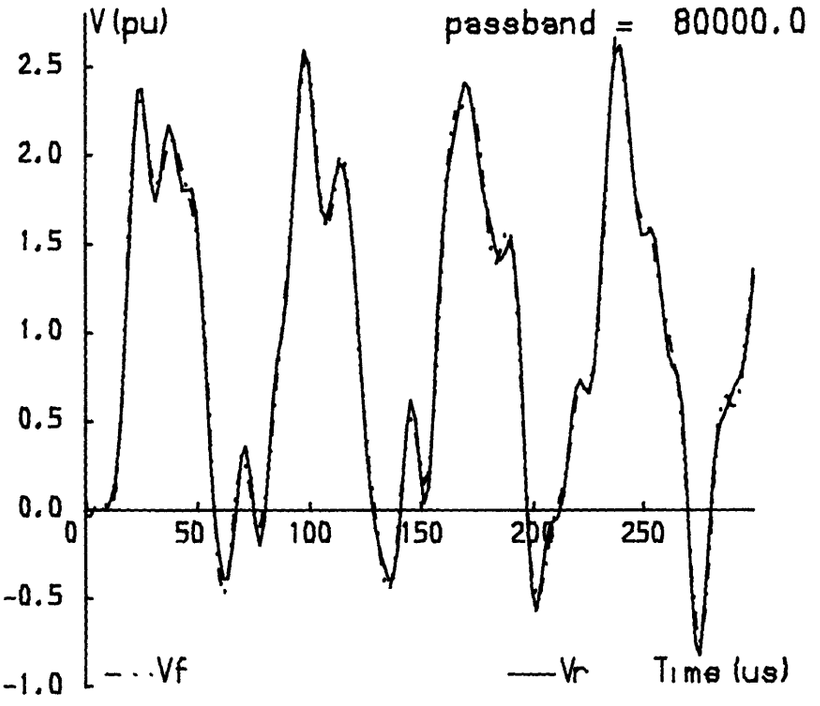

(e)

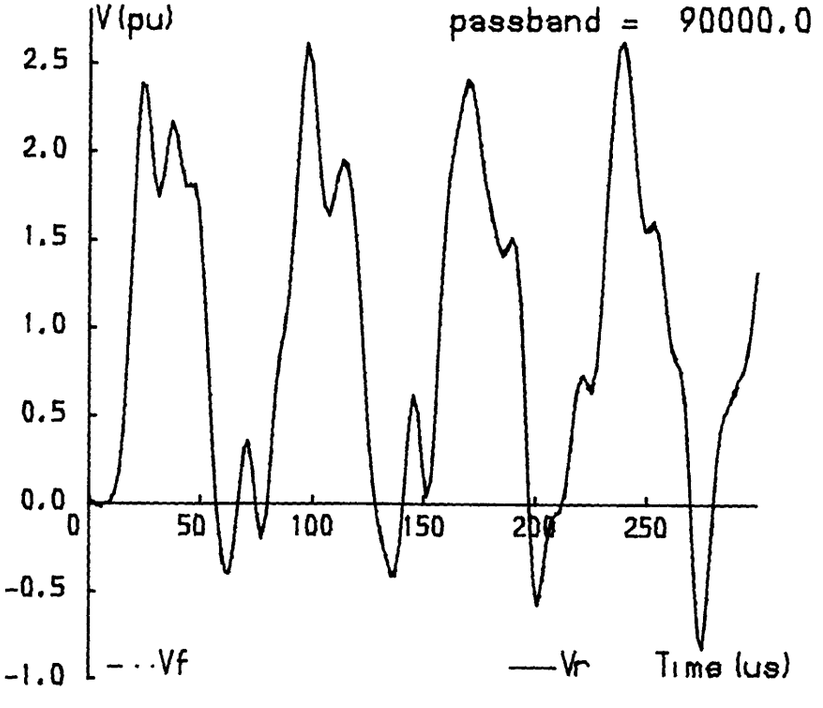

(f)

Figure 6.11 (cont'd) Low-pass filtering of 5 pi-section uncompensated line response.
(e) f_p = 80 kHz; (f) f_p = 90 kHz

demonstrates very little change to that obtained for 50 kHz cut-off which implies that any frequency content in the region 50 - 60 kHz is small. This can be observed from the DFT in Figure 6.4(a) for this frequency range. Incorporating the natural π-section frequency however alters the filtered response in Figure 6.11(d) when f_p is increased to 70 kHz.

Further increases in f_p show that there is no significant 5^{th} harmonic effect when comparing the almost similar filtered waveforms of Figures 6.11(d) and 6.11(e) which again shows the DFT to be accurate. Finally with f_p at 90 kHz the input waveform is almost reconstituted (Figure 6.11(f)) which suggests that the cut-off frequency of the line is close to the calculated value of 92.2 kHz.

6.6 Summary of Spectral Analysis

The work described in the preceding text is regarded as being exploratory in nature and although no solution for the reduction of the Gibbs phenomena was obtained the understanding of the model line was greatly enhanced.

The effects of line attenuation and how it alters the transient high-frequency content of the response of the uncompensated 20 π-section line with zero earth impedance have been clarified. As the line length increases the number of odd harmonics present will increase which improves the square-wave nature of the response but higher-order harmonic content however is reduced quickly due to the model line attenuation. This explains why the 20 π-section uncompensated waveform remains square in waveshape while the responses of the shorter lines quickly become sinusoidal.

The 5 π-section line analysis discussed the absence of an anticipated frequency, the 5^{th} harmonic whose frequency was less than the model cut-off value, and the appearance of an unexpected component at 82 kHz. The absence of one component and the presence of another may be related in this instance although the reason for this is not apparent. The

Low-pass Digital Filter waveforms verified that the DFT of the 5 π-section line was accurate by observing the change in the filtered response for an increasing passband frequency value. However the analysis of the frequency spectrum is not complete if the filtered response of Figure 6.11(b) is considered. In this case an ideal fundamental and 3^{rd} harmonic waveform was not observed even for the initial cycle of the filter output.

From the analysis carried out, filtering in the frequency domain would not lead to any improvement in the processed responses from that obtained by the application of the Experimental Sigma Factors S_{se} and S_{ae} to the uncompensated waveforms. However further analysis would be beneficial particularly in determining why expected frequencies are not observed while unexpected frequency components are calculated. This may further enhance the understanding of the model line design.

CHAPTER 7

Verification of Model Line Transients by the Runge-Kutta Method

7.1 Introduction

In order to verify the experimental transient response of the model line for the various circuit configurations investigated, a fourth-order Runge-Kutta numerical integration software routine[45, 46] was developed to solve the differential equations associated with the uncompensated and compensated model lines. Verification was necessary since the transient responses were obtained in some cases by the physical modification of the model line i.e. the removal and addition of the damping resistors (section 2.5.1). The technique has been used previously to calculate switching transients[22, 4] and this chapter follows the development of the method from a simple 1-phase line with zero earth impedance to the more complex 3-phase line with mutual coupling and frequency-dependent earth path.

In all sixteen computer files were written which include the effects of source inductance and non-simultaneous closure. Other examples such as load resistance and energisation of a line from a line source are discussed briefly and illustrate the ease with which the technique can be adapted to cater for a particular circuit configuration. Each circuit configuration required two files to represent the model with and without damping resistors.

The programs were written on the DEC-20 mainframe due to the arithmetic power of the machine. Familiarity with the system, the associated graphics package (FGHOST) and plotter prior to the research period allowed the research to commence (October 1981) until the Z-2D microprocessor system was purchased (March 1982). Hard-copy results could therefore be obtained from the mainframe for direct comparison with model line waveforms.

7.2 1-phase Uncompensated Line with Zero Earth Impedance

The model line is represented by π-sections of lumped inductance, capacitance and resistance and from this representation a first-order differential equation for each reactive component in the line can be established and solved by the Runge-Kutta method employed (see Appendix VI.1).

Step energisation of a 2 π-section circuit, with inductive and capacitive elements only, was initially investigated in order to gain experience in the method and to determine the step length 'h' which would be required for accurate calculation of the resultant receiving-end response. Initially the receiving-end voltage appeared to be attenuated but since the circuit was lossless this was attributed to the use of too long a step length. It was eventually determined that a step length of the order of microseconds was required and after a few more program runs the expected result was obtained with h=1 μs. The expected response had been previously calculated by Laplace techniques.

A 5 π-section line program was then written, with resistance included, using values taken from the 5 π-section model line. The corresponding circuit and differential equations are shown in Figures 7.1 and 7.2. It was observed from Figure 7.2 that a pattern emerged for the rates of change of current for π-sections 2 - 5 and for the rates of change of voltage for π-sections 1 - 4. This allowed a general program to be developed to determine the receiving-end voltage of an 'n' π-section model line the differential equations for which are shown below written in the FORTRAN language used for all Runge-Kutta programs.

```
      F(1)=((E*SM-Y(NI+1)-Y(1)*R1)/L1)
      DO 310 I=2,NI
310   F(I)=((Y(NI-1+I)-Y(NI+I)-Y(I)*R1)/L1)
      DO 320 I=NI+1,NVAR-1
320   F(I)=((Y(I-NI)-Y(I-NI+1))/C1)
      F(NVAR)=(Y(NI)/C2)
```

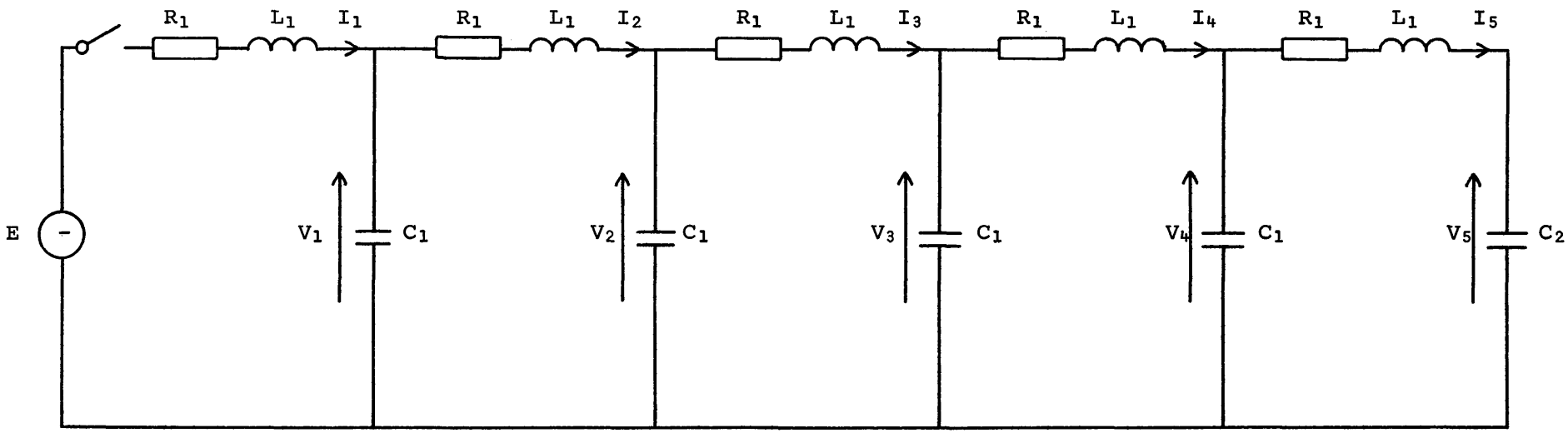

Figure 7.1 5 pi-section uncompensated line with zero earth impedance showing variables used in Runge-Kutta program.

$$\frac{dI_1}{dt} = \frac{E - V_1 - I_1R_1}{L_1} \qquad \frac{dV_1}{dt} = \frac{I_1 - I_2}{C_1}$$

$$\frac{dI_2}{dt} = \frac{V_1 - V_2 - I_2R_1}{L_1} \qquad \frac{dV_2}{dt} = \frac{I_2 - I_3}{C_1}$$

$$\frac{dI_3}{dt} = \frac{V_2 - V_3 - I_3R_1}{L_1} \qquad \frac{dV_3}{dt} = \frac{I_3 - I_4}{C_1}$$

$$\frac{dI_4}{dt} = \frac{V_3 - V_4 - I_4R_1}{L_1} \qquad \frac{dV_4}{dt} = \frac{I_4 - I_5}{C_1}$$

$$\frac{dI_5}{dt} = \frac{V_4 - V_5 - I_5R_1}{L_1} \qquad \frac{dV_5}{dt} = \frac{I_5}{C_2}$$

Figure 7.2 Differential equations for the 5 pi-section uncompensated line with zero earth impedance.

The accuracy of this program was verified by using the model line parameter values given by Bickford[6] and successfully matching the receiving-end voltage calculated by the program with that given in the reference.

Results were then taken using the 5 π-section model line values and the response to step excitation is shown in Figure 7.3. This can be compared with the model line response of Figure 7.4 and shows that good waveform correlation is achieved. However the high-frequency content of the Runge-Kutta waveform is greater than that observed in the model response. This is because the numerical method does take into account the frequency-dependent resistance of the line series impedance i.e. skin effect. The resistance value used in the software was constant at 0.83Ω. This was determined experimentally by Toland[11] at the model line power supply frequency of 398 Hz.

To demonstrate the flexibility of the software approach the effect of increasing the number of π-sections for the 25 mile line representation was investigated thereby approaching the response that would be obtained from a 25 mile distributed-parameter line. This was achieved by halving the inductance, capacitance and resistance per π-section each time the number of π-sections used for representation was doubled. As a consequence the step length had to be reduced for response accuracy. As expected, the increasing number of π-sections used to model this line length, gave Gibbs Oscillations of a higher frequency with a corresponding reduction in their amplitude[9]. The rate of rise of voltage at the discontinuities also increases with the increase in number of π-sections as is seen in Figures 7.5(a) and (b) for 10 and 20 π-sections representations respectively.

The program N3SND.FOR (Appendix VI.2) shows the standard format for all files written. The programs are interactive in that the user can choose the number of π-sections and in the 1-phase case whether an AC (point-on-wave for closure user-defined) or DC source (+1 pu step) is desired.

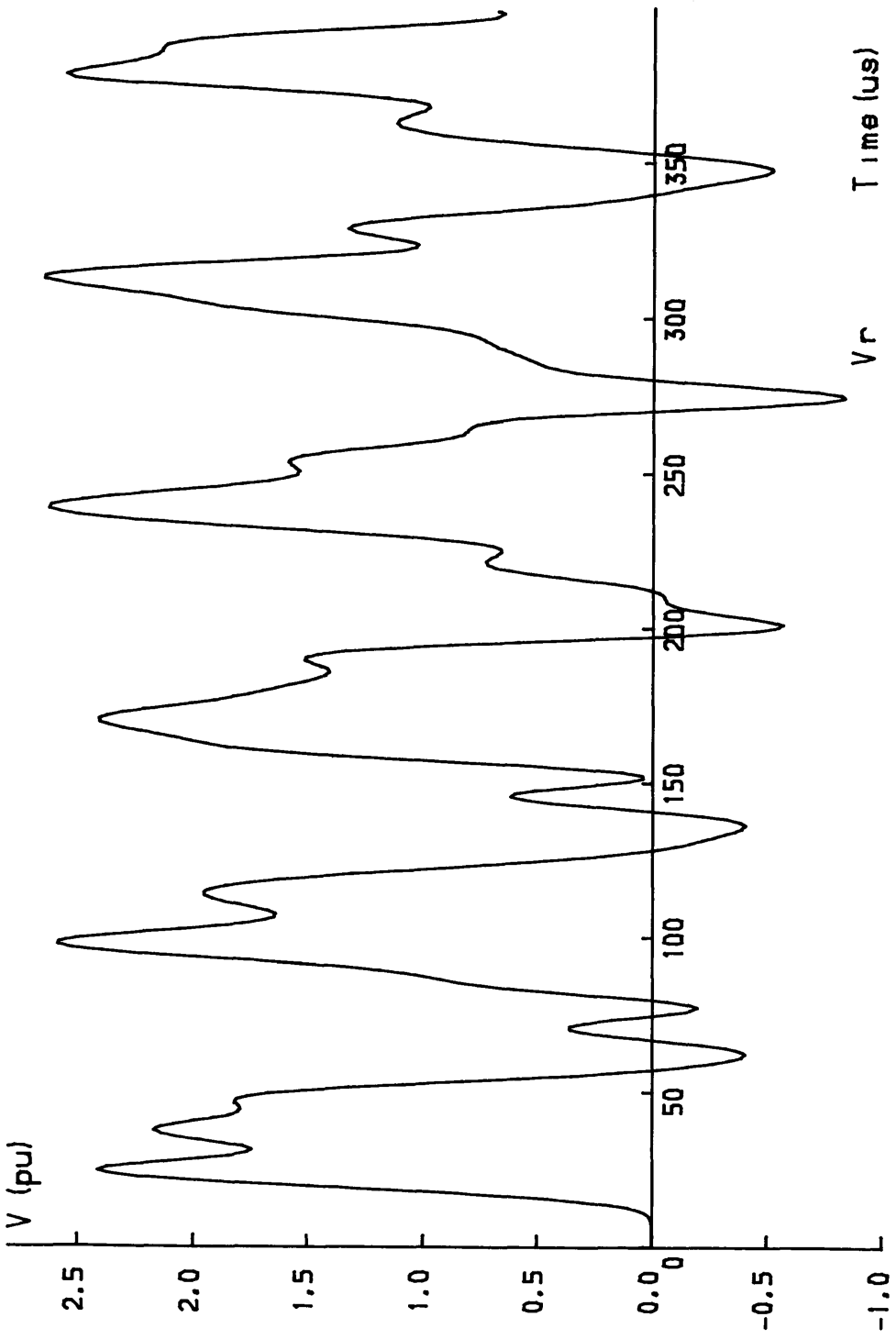

Figure 7.3 Receiving-end response for step excitation of the 5 pi-section uncompensated line calculated by the Runge-Kutta technique.

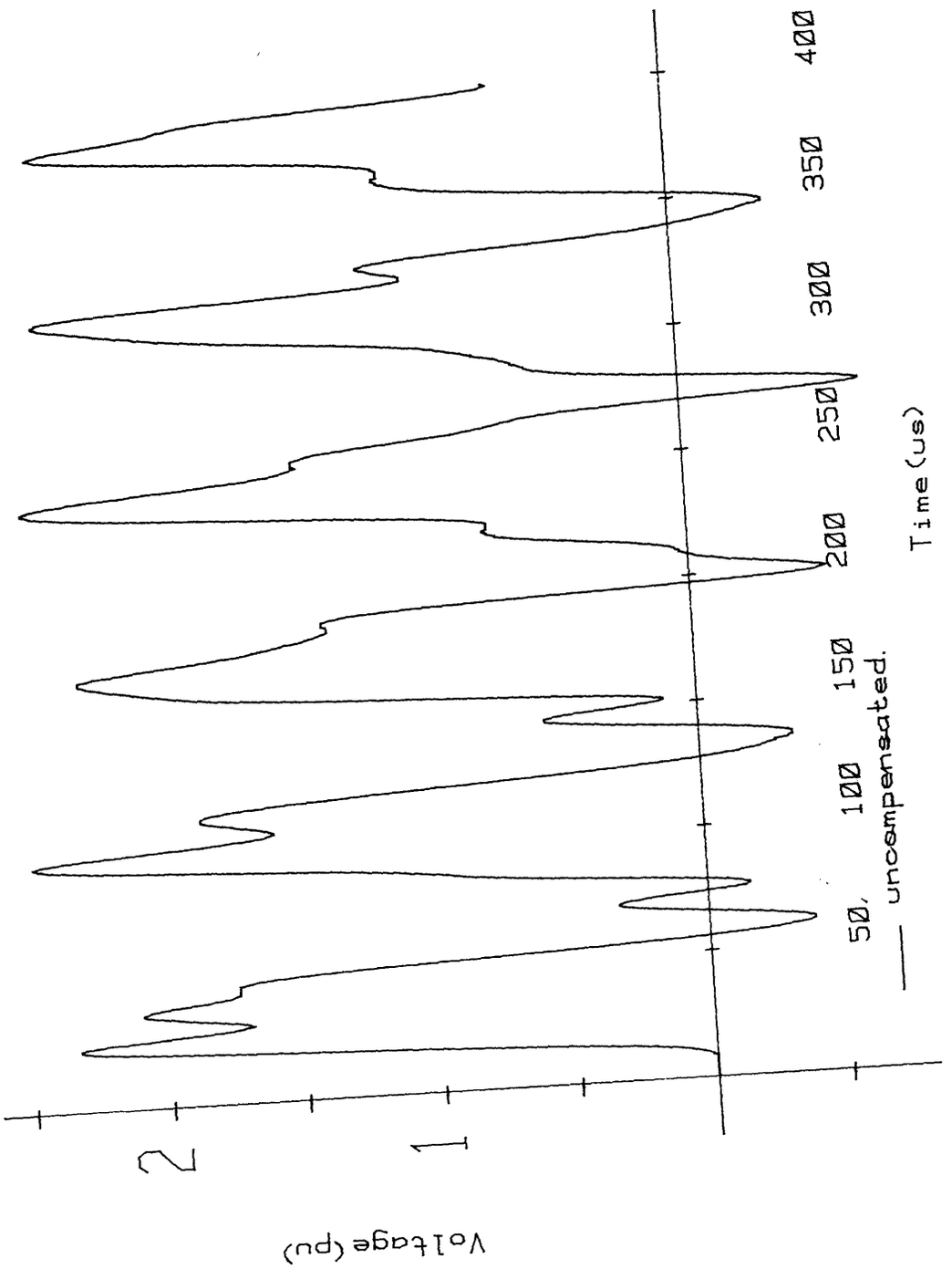

Figure 7.4 Receiving-end response to step excitation of the 5 pi-section uncompensated model line.

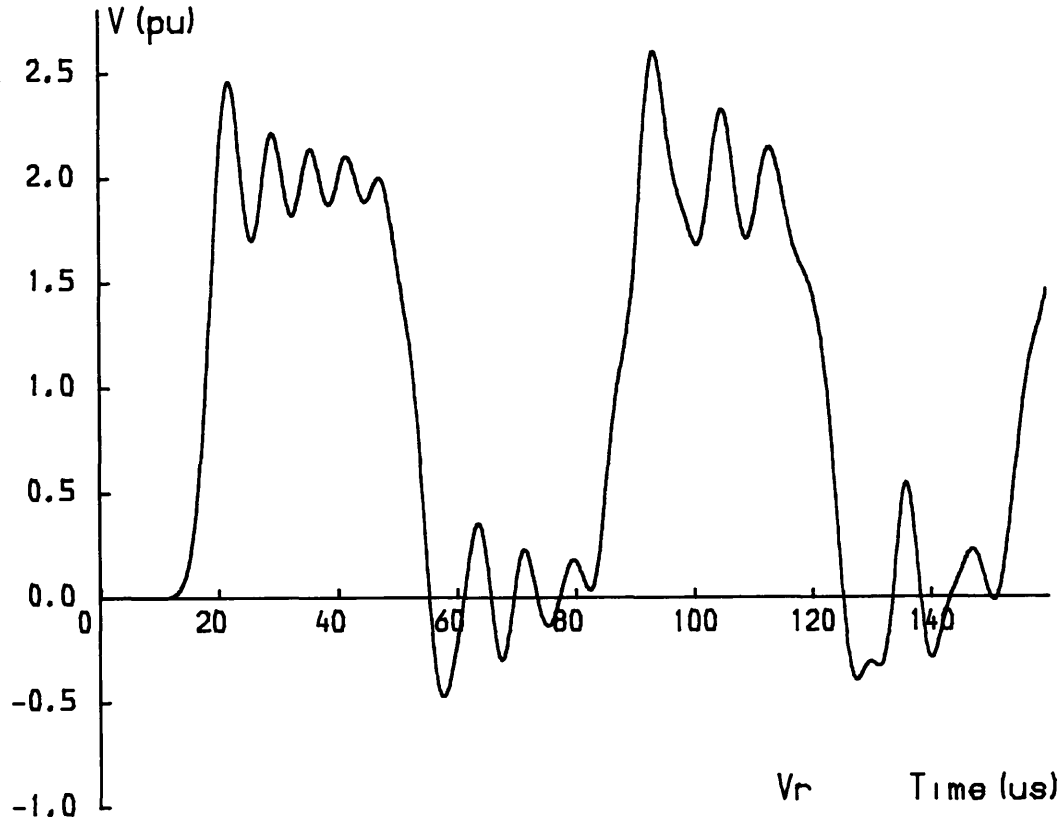

(a)

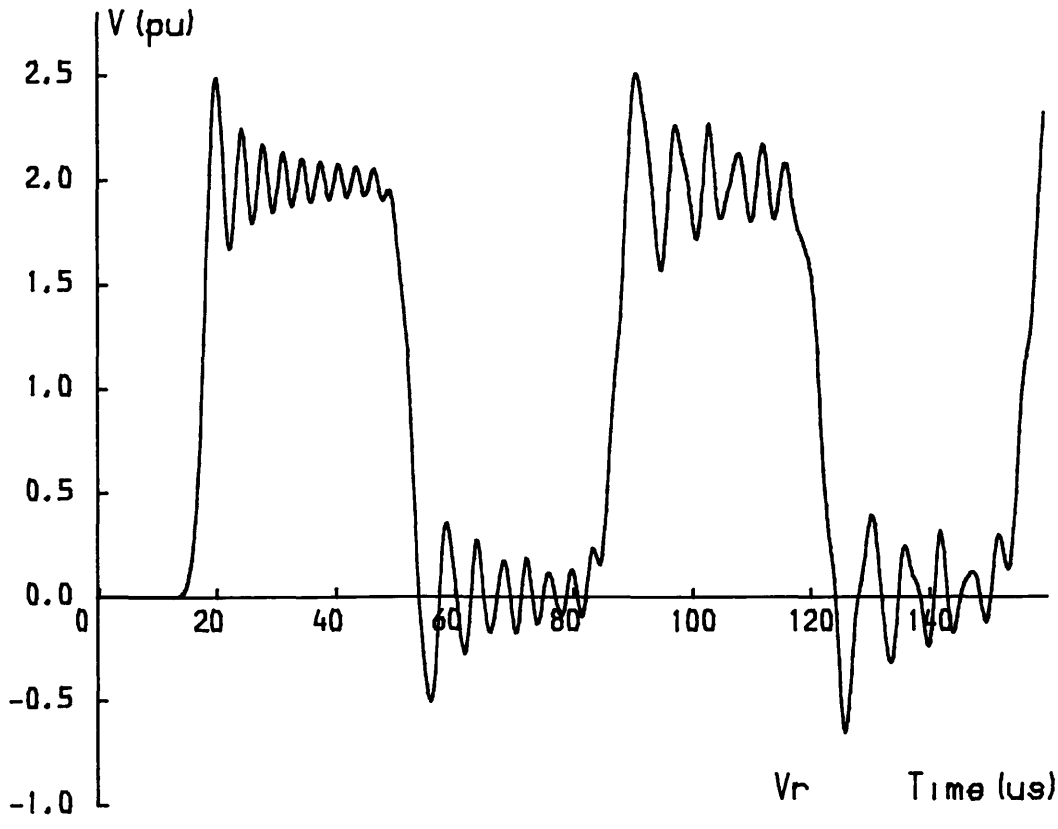

(b)

Figure 7.5 Response of a 25 mile model line represented by (a) 10 pi-sections; (b) 20 pi-sections.

The program also allows the user to plot the receiving-end waveform over a maximum spread of 4000 μs, chosen to limit the size of graphics file generated and the peak receiving-end voltages can be recorded along with the time at which they occur.

7.2.1 1-phase Resistor-compensated Line with Zero Earth Impedance

The definition of a differential equation for each variable in the uncompensated line case was achieved but the configuration of the resistor-damped circuit introduced some difficulty in this respect as it was not possible to define a rate of change of current for the damping resistor R_4 (Figures 7.6(a) and (b)). An equation for $\frac{dI_1}{dt}$ was obtained however and by using Kirchhoffs Laws I_2 and I_3 could be defined (Figure 7.6(c)). By KVL from Figure 7.6(a):-

$$I_2R_4 = I_1R_1 + L_1 \frac{dI_1}{dt}$$

$$I_2 = I_1 \frac{R_1}{R_4} + \frac{L_1}{R_4} \frac{dI_1}{dt} \qquad (7.1)$$

and by KCL

$$I_3 = I_1 + I_2$$

This was repeated for I_5, I_6 etc and since the calculation of these currents were performed 'outwith' the Runge-Kutta algorithm, the rate of change of current in equation (7.1) was defined as the current change per second. Therefore the values for $\frac{dI_1}{dt}$, $\frac{dI_4}{dt}$ etc. were multiplied by the factor h^{-1} to give the correct magnitudes for I_2 and I_3:-

$$I_2 = I_1 \frac{R_1}{R_4} + \frac{L_1}{R_4} \frac{dI_1}{dt} * \frac{1}{h} \qquad (7.2)$$

where the value of $\frac{dI_1}{dt}$ used is the average of the derivatives for I_1 over the time step (see RHS of equation (8.12)) i.e. the value used to predict I_1 at x+h. This definition gave the computed response shown in Figure 7.7 and can be compared with the compensated model line response in Figure 7.8. Again waveform correlation is good although the model line response again

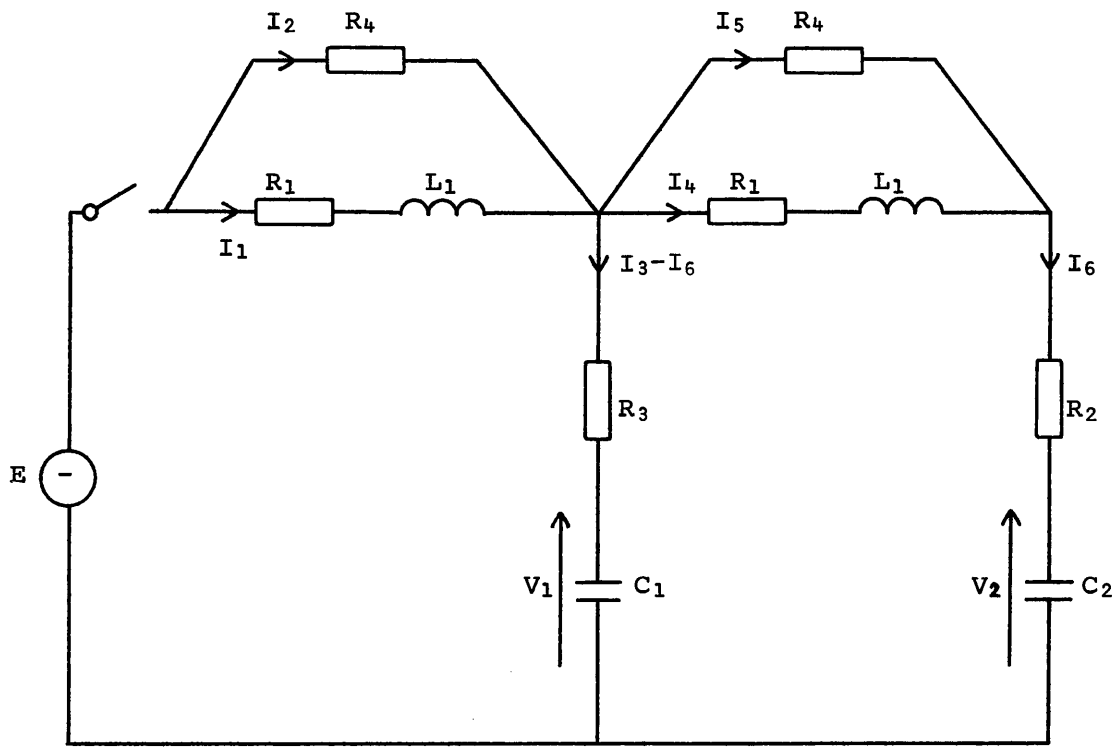

(a)

$$\frac{dI_1}{dt} = \frac{E - I_1R_1 - (I_3 - I_6)R_3 - V_1}{L_1} \qquad \frac{dV_1}{dt} = \frac{I_3 - I_6}{C_1}$$

$$\frac{dI_4}{dt} = \frac{(I_3 - I_6)R_3 + V_1 - I_4R_1 - I_6R_2 - V_2}{L_1} \qquad \frac{dV_2}{dt} = \frac{I_6}{C_2}$$

(b)

$$I_2 = I_1 \frac{R_1}{R_4} + \frac{L_1}{R_4} \frac{dI_1}{dt} \qquad I_5 = I_4 \frac{R_1}{R_4} + \frac{L_1}{R_4} \frac{dI_4}{dt}$$

$$I_3 = I_1 + I_2 \qquad I_6 = I_4 + I_5$$

(c)

Figure 7.6(a) Variables defined for a 2 pi-section compensated line

(b) The corresponding differential equations.

(c) Variables outwith the Runge-Kutta technique.

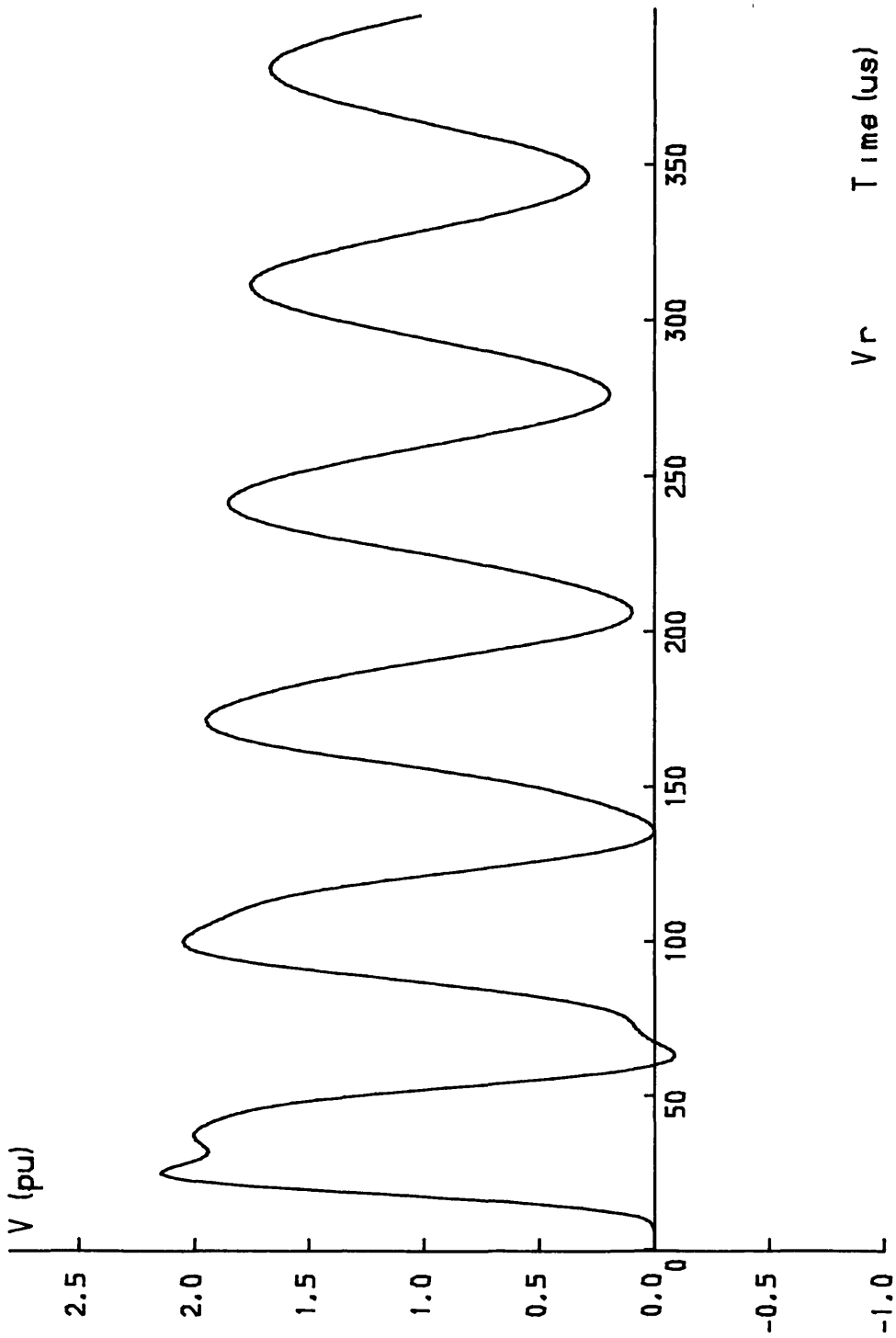

Figure 7.7 Response of a 5 pi-section compensated line with zero earth impedance calculated by Runge-Kutta.

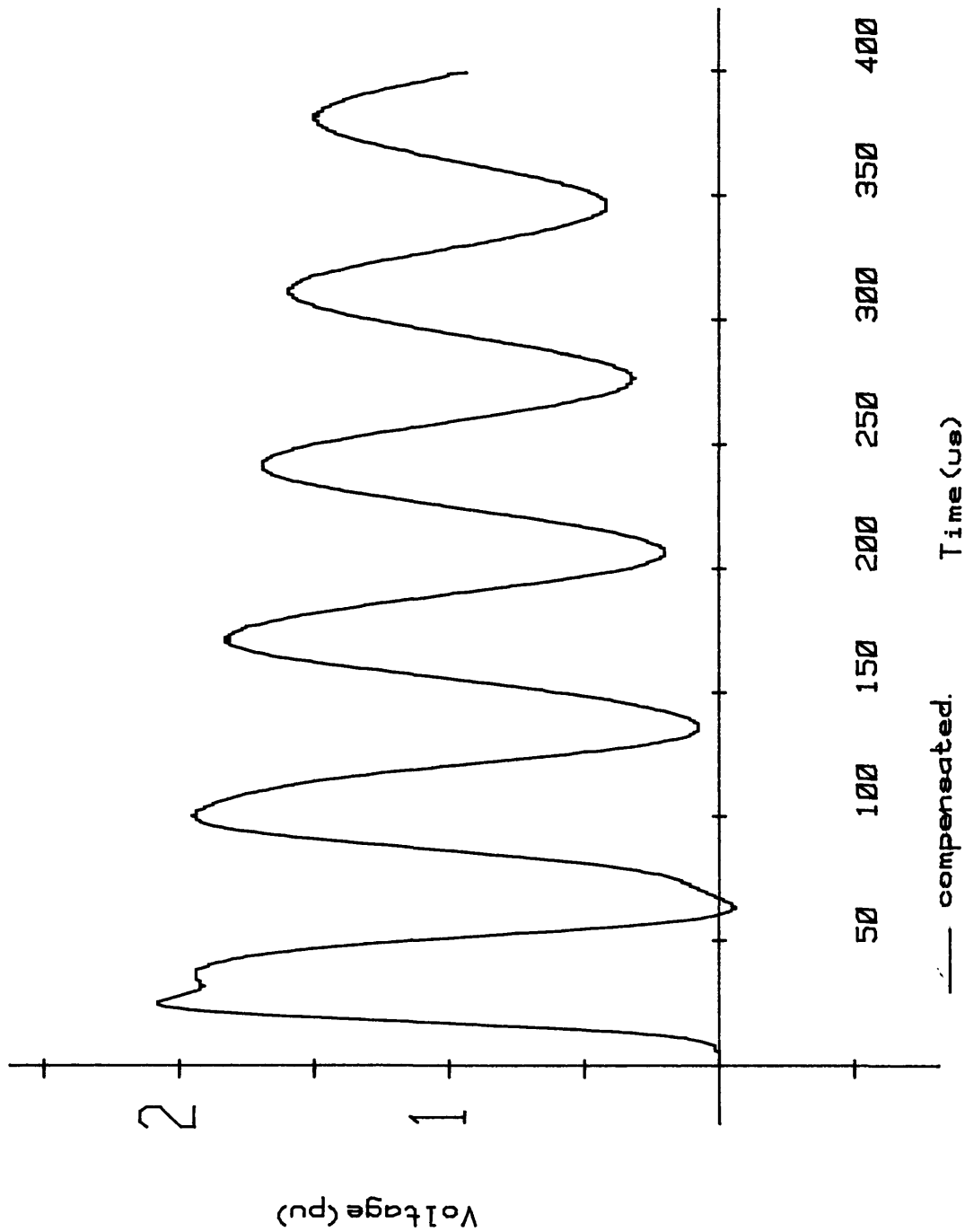

Figure 7.8 Response of the 5 pi-section compensated model line.

displays greater attenuation.

It was found that the inclusion of the damping resistors and specifically the parallel connection of R_4 across the line series impedance required that the step length be reduced to 0.25 μs in order to give an accurate response. The resistor R_4 must therefore allow a greater rate of change of current than that which previously occurred due to the series reactance L_1 alone in the circuit of Figure 7.1. The calculation of a compensated response therefore required more computation time due to the reduced step length but calculations of the order of a few hundred microseconds were not prohibitive when using the mainframe computer. Some additional software was written to plot the receiving-end responses at 1 μs intervals instead of 0.25 μs intervals thus reducing the size of the graphics files generated.

7.3 1-phase Uncompensated Line with Earth-path Impedance

This circuit incorporates the mutual coupling of the 3-phase line and also the R-L frequency-dependent earth path derived from Carsons equations[10]. This more complex configuration was chosen so that the effect of the earth path could be observed in the experimental transient responses investigated in section 4.4.2. It also allowed the differential equations of this network to be derived and verified in the Runge-Kutta software which would be useful when defining the 3-phase circuit equations for the simultaneous closure overvoltage studies of section 5.6.2.

A single π-section representation is shown in Figure 7.9(a) and the corresponding differential equations in Figure 7.9(b). Although the inclusion of the earth path increased the number of variables per π-section from 2 (see section 7.2) to 6, a programming pattern was again established and an 'n' π-section program devised.

This program emphasised the need for transient waveform verification when model line responses from this configuration could not be

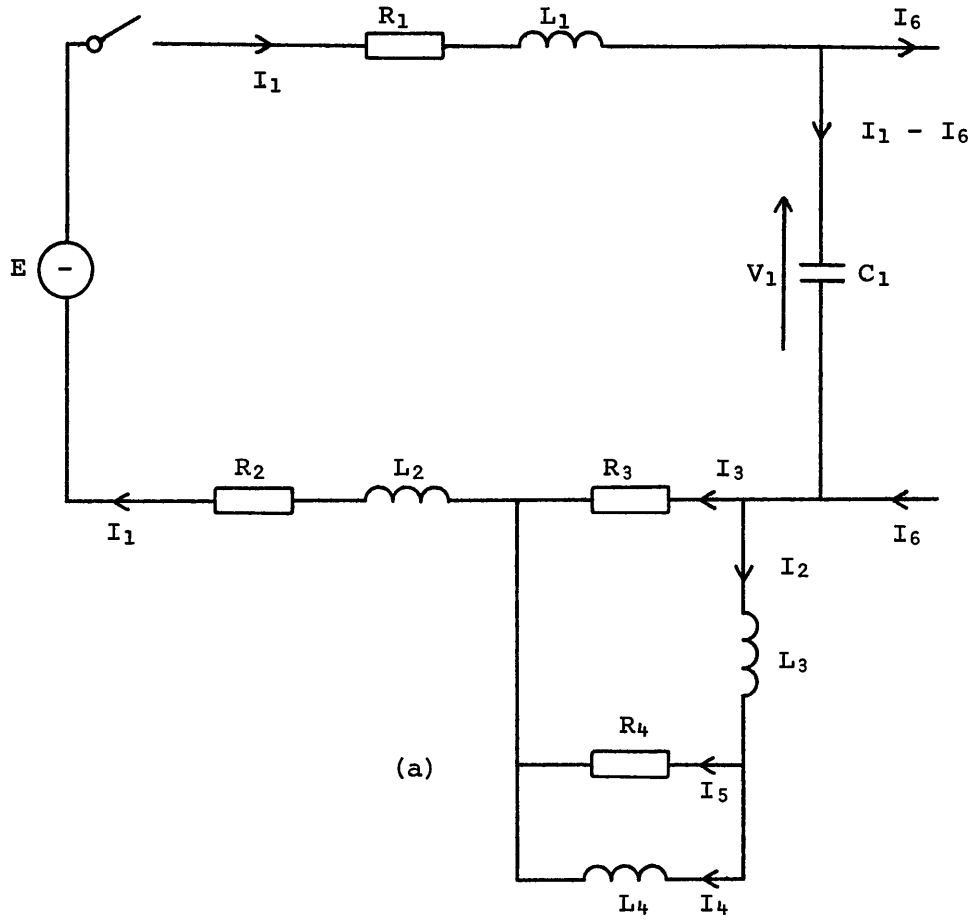

$$\frac{dI_1}{dt} = \frac{E - V_1 - I_3R_3 - I_1(R_1 + R_2)}{L_1 + L_2} \qquad \frac{dV_1}{dt} = \frac{I_1 - I_6}{C_1}$$

$$\frac{dI_2}{dt} = \frac{I_3R_3 - I_5R_4}{L_3}$$

$$\frac{dI_3}{dt} = \frac{dI_1}{dt} - \frac{dI_2}{dt}$$

$$\frac{dI_4}{dt} = \frac{I_5R_4}{L_4}$$

$$\frac{dI_5}{dt} = \frac{dI_2}{dt} - \frac{dI_4}{dt}$$

(b)

Figure 7.9(a) Single pi-section including mutual coupling and frequency-dependent earth path.

(b) Differential equations.

matched initially with those calculated by the Runge-Kutta method. It was found that an additional earth path had been introduced by the TR signal input circuitry which previously had been shorted out when investigating the lines with zero earth impedance. However the use of the DL019 Line Disturbance Monitor (section 2.8) isolated the correct model line response which was then successfully matched with the Runge-Kutta result.

7.3.1 1-phase Resistor-compensated Line with Earth-path Impedance

In section 7.2.1 rates of change of current for I_2 and I_3 could not be defined thus leading to their evaluation outwith the integration algorithm. However the mutual coupling inductor L_2 present in the earth path allowed differential equations to be defined for I_2 and I_3. From Figure 7.10:

$$L_1 \frac{dI_1}{dt} + L_2 \frac{dI_3}{dt} = E - I_1R_1 - (I_3 - I_{10})R_6 - V_1 - I_4R_3 - I_3R_2 \quad (7.3)$$

therefore

$$\frac{dI_1}{dt} = \frac{E - I_1R_1 - (I_3 - I_{10})R_6 - V_1 - I_4R_3 - I_3R_2 - L_2\frac{dI_3}{dt}}{L_1} \quad (7.4)$$

The differential equation of I_3 was defined using L_2 alone by selecting the mesh which includes compensating resistor R_2, and $\frac{dI_2}{dt}$ determined by KCL. Therefore no calculations outwith the routine were necessary and 8 variables per π-section are defined. The receiving-end responses for the 20 π-section uncompensated and compensated lines due to step excitation are shown in Figure 7.11 and these compare favourably with the corresponding model line waveforms recorded in Figure 4.15(a).

7.4 1-phase Lines with Source Inductance

The introduction of inductance into the model source for the investigation of the effect of L_s on the Gibbs phenomena in Chapter 5 necessitated that slight modifications be made to the differential equations already defined for the 1-phase lines discussed. The sending-end shunt capacitance (Figure 7.12(a)) cannot now be omitted as was the case for infinite source energisation. Figure 7.12(a) shows the modified sending-end

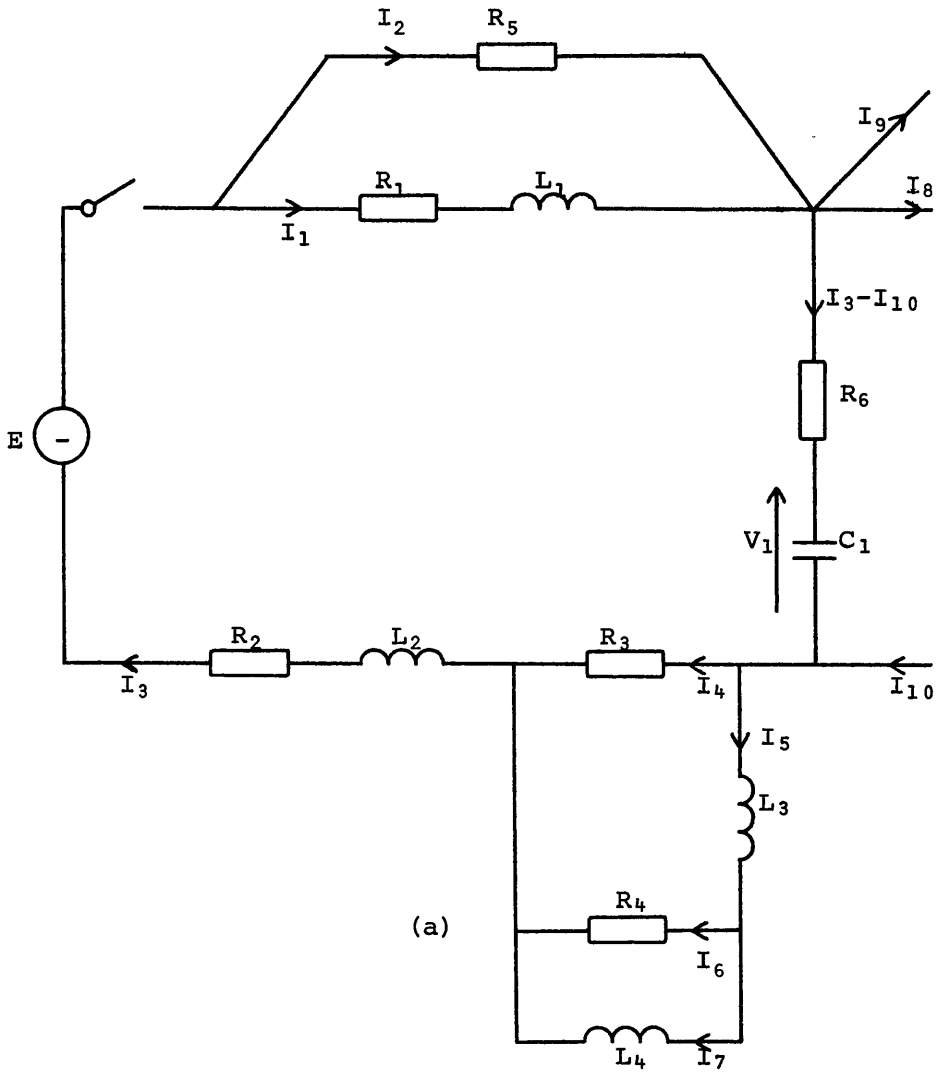

$$\frac{dI_1}{dt} = \frac{E - I_1R_1 - (I_3 - I_{10})R_6 - V_1 - I_4R_3 - I_3R_2 - L_2\frac{dI_3}{dt}}{L_1}$$

$$\frac{dI_3}{dt} = \frac{E - I_2R_5 - (I_3 - I_{10})R_6 - V_1 - I_4R_3 - I_3R_2}{L_2}$$

$$\frac{dI_2}{dt} = \frac{dI_3}{dt} - \frac{dI_1}{dt}$$

$$\frac{dI_5}{dt} = \frac{I_4R_3 - I_6R_4}{L_3}$$

$$\frac{dI_4}{dt} = \frac{dI_3}{dt} - \frac{dI_5}{dt}$$

$$\frac{dI_7}{dt} = \frac{I_6R_4}{L_4}$$

$$\frac{dI_6}{dt} = \frac{dI_5}{dt} - \frac{dI_7}{dt}$$

$$\frac{dV_1}{dt} = \frac{I_3 - I_{10}}{C_1}$$

(b)

Figure 7.10(a) Single compensated pi-section including mutual coupling and frequency dependent earth path.

(b) Differential equations.

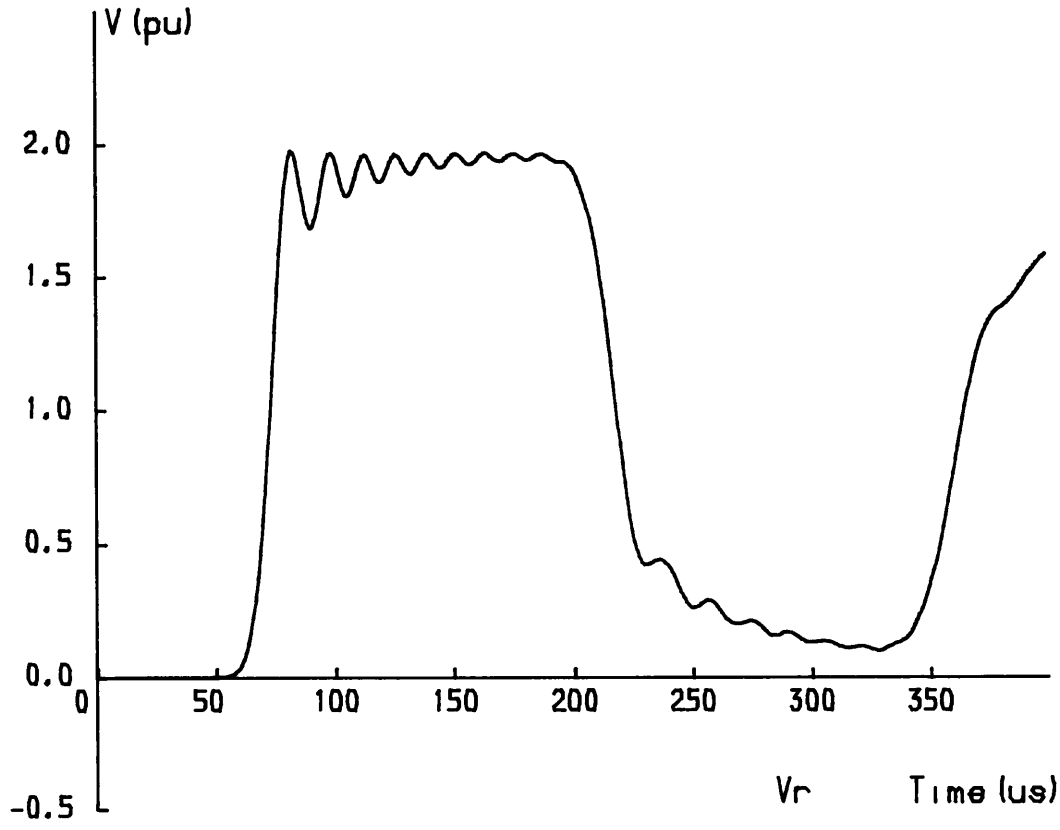

(a)

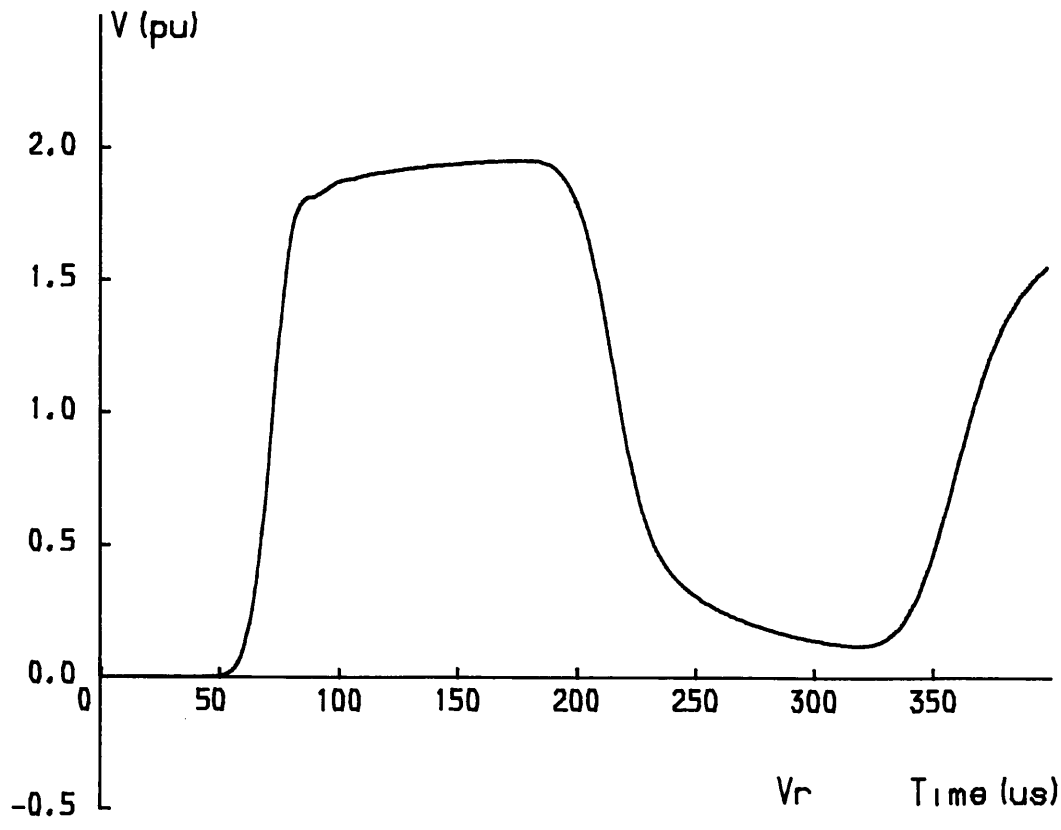

(b)

Figure 7.11 Responses of the 20 pi-section line including frequency-dependent earth parth (a) uncompensated; (b) compensated.

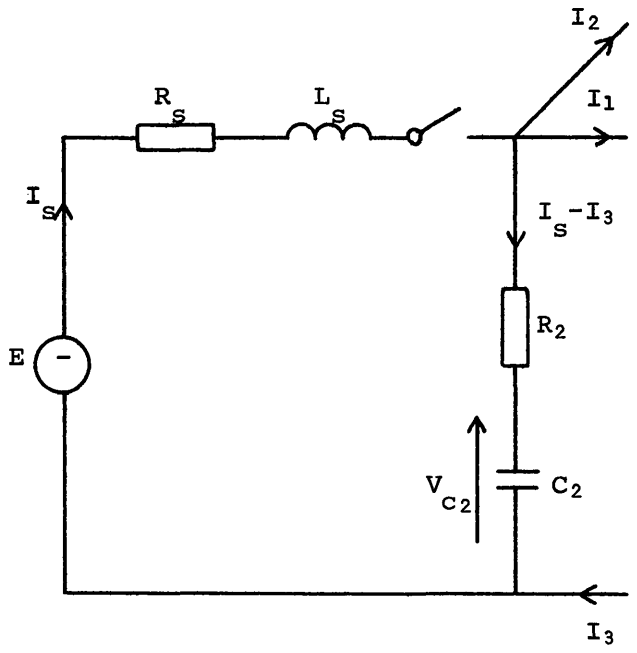

(a)

$$\frac{dI_s}{dt} = \frac{E - I_s R_s - (I_s - I_3)R_2 - V_{c_2}}{L_s}$$

$$\frac{dV_{c_2}}{dt} = \frac{I_s - I_3}{C_2}$$

(b)

Figure 7.12(a) Sending-end circuit modification for source inductance.
(b) Differential equations.

circuit configuration for the resistor-damped line of section 7.2.1.

Differential equations for the shunt capacitance voltage and the source current must be defined and furthermore V_{C2} and the voltage across R_2 now replace the supply voltage E in the ideal source case (see Figure 7.6). Figures 7.13(a) and (b) display the Runge-Kutta responses for the 20 π-section uncompensated line with zero earth impedance for source values of 0.0801H and 0.03H respectively and these correspond to the model line waveforms shown in Figures 5.2 and 5.8. Comparison of the corresponding figures show that Gibbs Oscillations are still apparent in the calculated responses because skin effect was not programmed into the numerical technique. This restriction was discussed in section 7.2 and is highlighted further by the inclusion of source inductance. The DC resistance of L_s i.e. R_s in Figure 7.12(a) was incorporated to increase the accuracy of the calculated response but when determining L_G i.e. the value of L_s which gave an oscillatory-free transient response, the numerical method consistently gave values which were larger than those obtained experimentally (section 5.4). Figure 7.13(b) shows the Runge-Kutta response with L_s=L_G (experimental value) for the 20 π-section zero earth impedance line and a high-frequency Gibbs content is still apparent. In the equivalent model line response of Figure 5.8 no Gibbs phenomena were observed.

However the compensated line Runge-Kutta programs were used to give peak overvoltage/source inductance profiles for comparison with those obtained experimentally in section 5.6.2. The experimental overvoltage profile for the 20 π-section compensated line with earth-path impedance is compared with that determined by the corresponding Runge-Kutta program of section 7.3.1 in Figure 7.14. The figure shows that the Runge-Kutta overvoltages are consistently higher in magnitude than the experimental values but that the profile shapes are almost identical. The numerical method may therefore be used to verify the overvoltage profile shapes that would be obtained from the

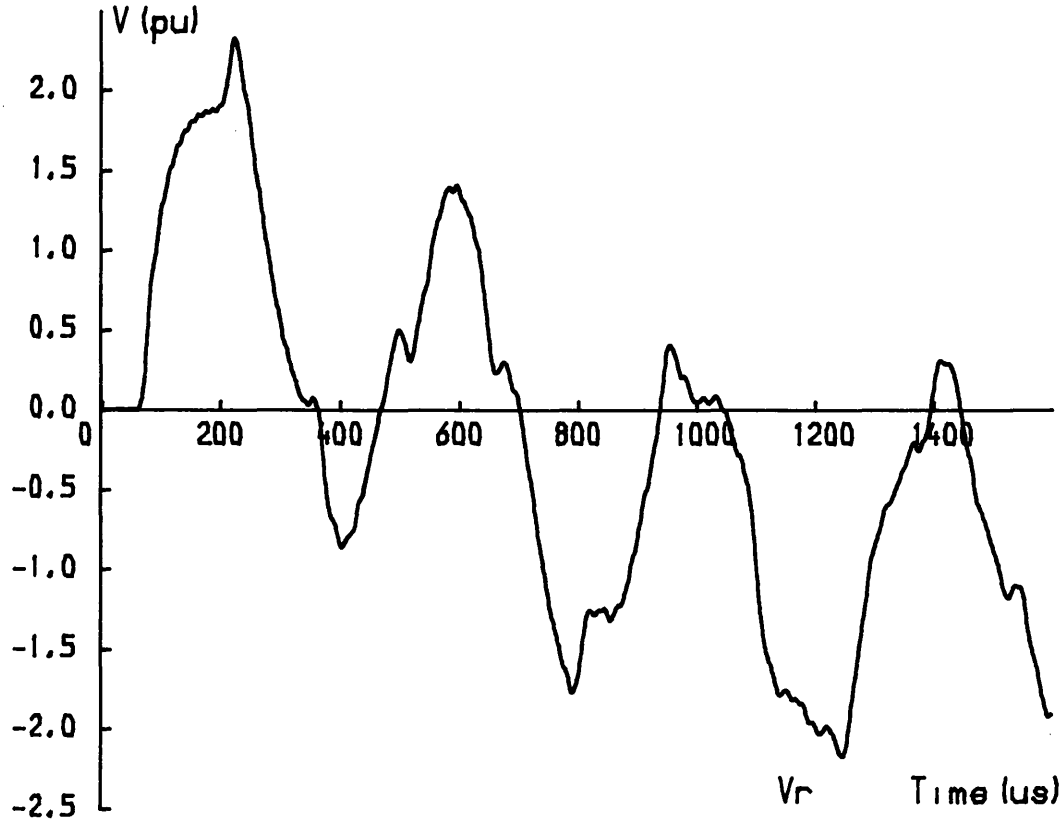

(a)

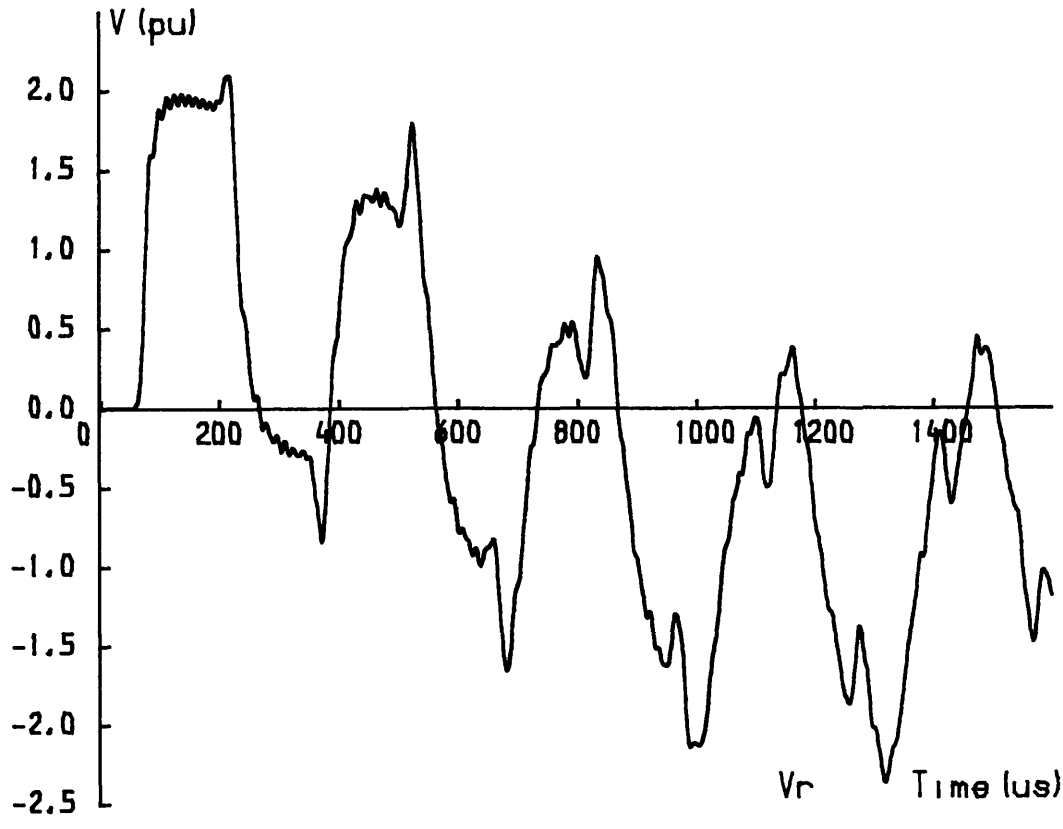

(b)

Figure 7.13 Runge-Kutta responses of a 20 pi-section uncompensated line with zero earth impedance energised from an inductive source of (a) 0.08H and (b) 0.03H.

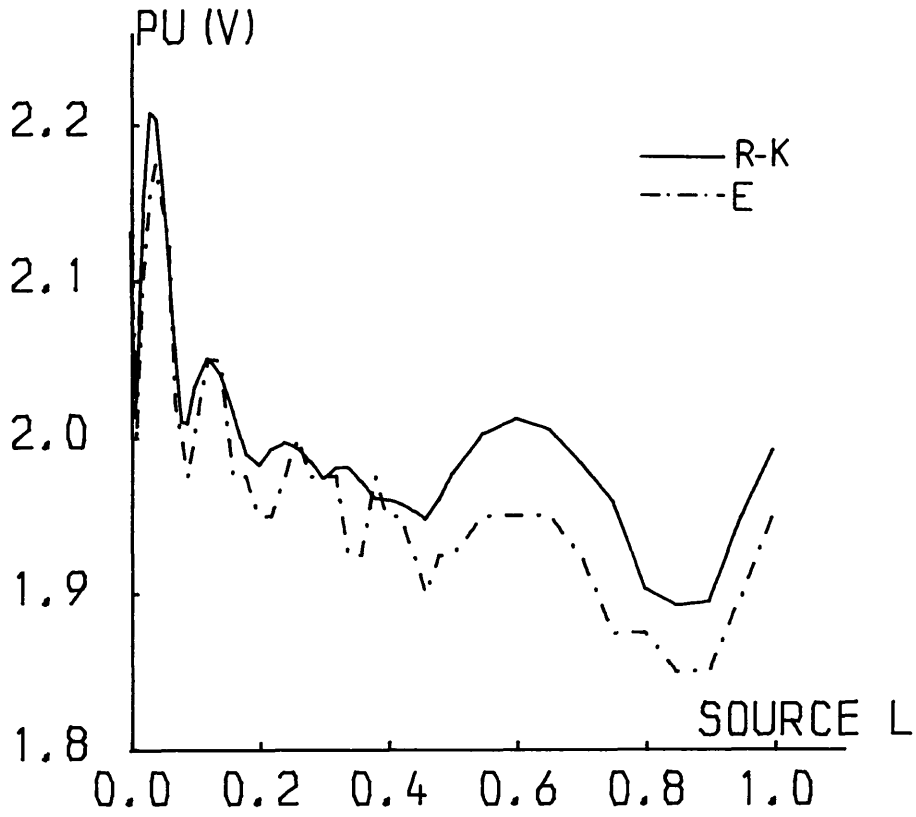

Figure 7.14 Overvoltage profiles of the 20 pi-section compensated line with earth-path impedance. The Runge-Kutta (R-K) overvoltages are consistently greater in magnitude than the experimental (E) results.

switching of a compensated model line from an inductive source.

7.5 3-phase Uncompensated Line

The 3-phase uncompensated line program was written to ensure that the overvoltage/source inductance 3-phase analysis in Chapter 5 was accurate. A single 3-phase π-section is shown in Figure 7.15 for a non-simultaneous closure condition with the red phase energised first.

The corresponding differential equations are defined in Figure 7.16 with the extra variables required for this condition being the voltages across the phase sending-end shunt capacitances C_2 and mutual coupling capacitor C_4. The voltages $V_{c2y} + V_{c4}$ and $V_{c2b} + V_{c4}$ in the differential equations of dI_2/dt and dI_3/dt are replaced by E_Y and E_B respectively as each phase closes thereby giving the simultaneous closure equation definition. The red phase is assumed to close at t=0 μs while the user can specify the closure of Y and B at any time and in any sequence. Figure 7.17 shows the three receiving-end phase-neutral voltages of a 5 π-section line calculated for the closure conditions of the R-phase at 90°, the Y-phase 200 μs later at 0° and the B-phase 400 μs later at 270°. Although this program was written primarily for simultaneous closure the option of sequential closure was included.

7.5.1 3-phase Resistor Compensated Line

A single 3-phase π-section of the compensated line for simultaneous closure is shown in Figure 7.18 with the corresponding differential equations given in Figure 7.19. As in the uncompensated case non-simultaneous closure was included as it required little modification to the equations already defined. However Figure 7.19 indicates that 18 variables per π-section are required and shows the increased complexity involved in the Runge-Kutta method. Figure 7.20 shows the receiving-end responses for simultaneous closure (R-phase at 90°) of a 5 π-section compensated line which verified the responses obtained from the model line.

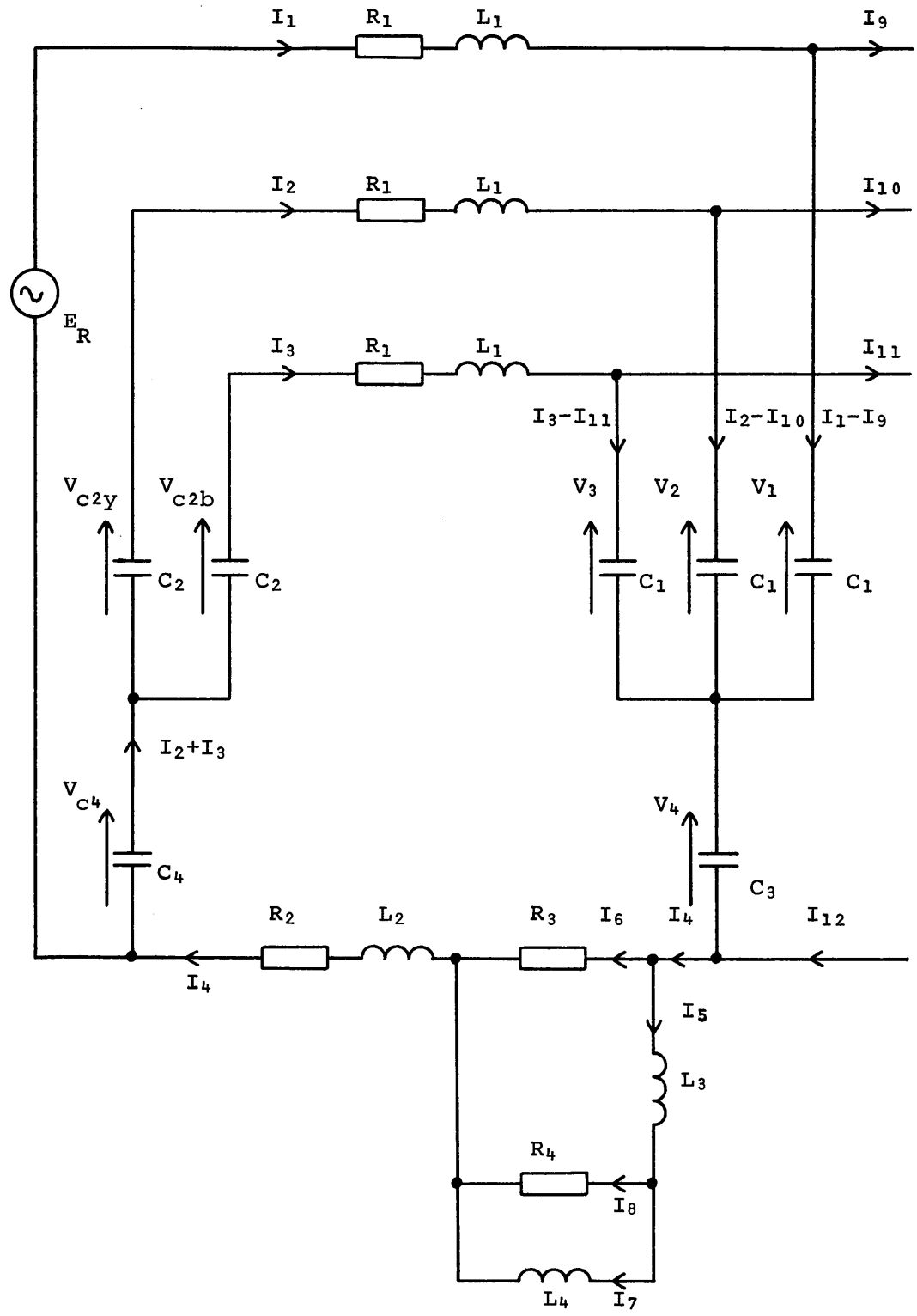

Figure 7.15 Non-simultaneous closure of the uncompensated 3-phase line (R-phase closed).

Let $V_T = V_4 + I_6R_3 + I_4R_2 + L_2\frac{dI_4}{dt}$

$$\frac{dI_1}{dt} = \frac{E_R - I_1R_1 - V_1 - V_T}{L_1} \qquad \frac{dV_1}{dt} = \frac{I_1 - I_9}{C_1}$$

$$\frac{dI_2}{dt} = \frac{V_{C_4} + V_{C_2Y} - I_2R_1 - V_2 - V_T}{L_1} \qquad \frac{dV_2}{dt} = \frac{I_2 - I_{10}}{C_1}$$

$$\frac{dI_3}{dt} = \frac{V_{C_4} + V_{C_2B} - I_3R_1 - V_3 - V_T}{L_1} \qquad \frac{dV_3}{dt} = \frac{I_3 - I_{11}}{C_1}$$

$$\frac{dI_4}{dt} = \frac{dI_1}{dt} + \frac{dI_2}{dt} + \frac{dI_3}{dt} \qquad \frac{dV_4}{dt} = \frac{I_4 - I_{12}}{C_3}$$

$$\frac{dI_5}{dt} = \frac{I_6R_3 - I_8R_4}{L_3}$$

$$\frac{dI_6}{dt} = \frac{dI_4}{dt} - \frac{dI_5}{dt} \qquad \frac{dV_{C_4}}{dt} = -\frac{(I_2 + I_3)}{C_4}$$

$$\frac{dI_7}{dt} = \frac{I_8R_4}{L_4} \qquad \frac{dV_{C_2Y}}{dt} = -\frac{I_2}{C_2}$$

$$\frac{dI_8}{dt} = \frac{dI_5}{dt} - \frac{dI_7}{dt} \qquad \frac{dV_{C_2B}}{dt} = -\frac{I_3}{C_2}$$

Figure 7.16 Differential equations for uncompensated 3-phase line with R-phase closed.

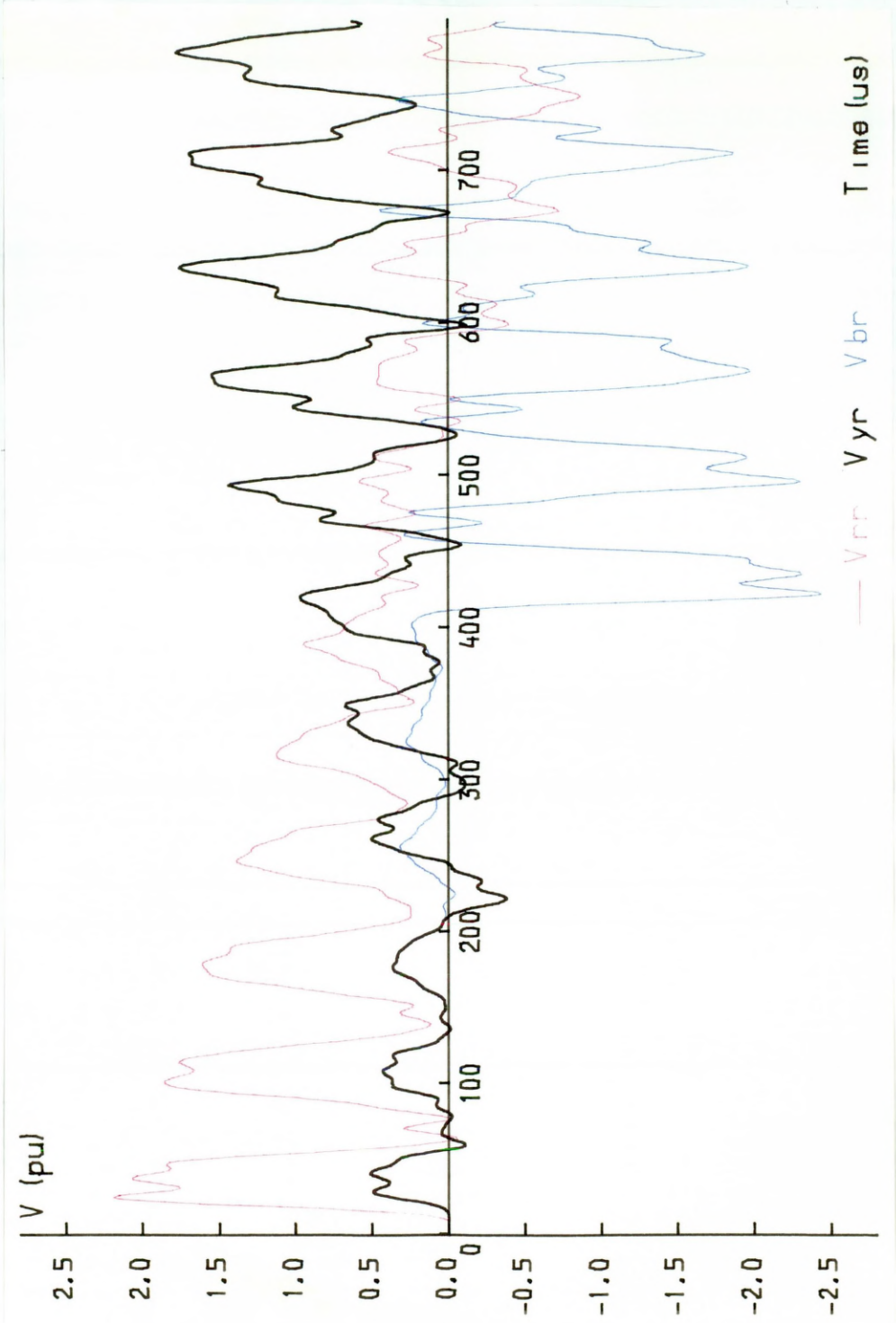

Figure 7.17 Response to non-simultaneous closure of an uncompensated 5 pi-section line.
Y-B closure sequence: 30, 60° after R-phase energised at 90°.

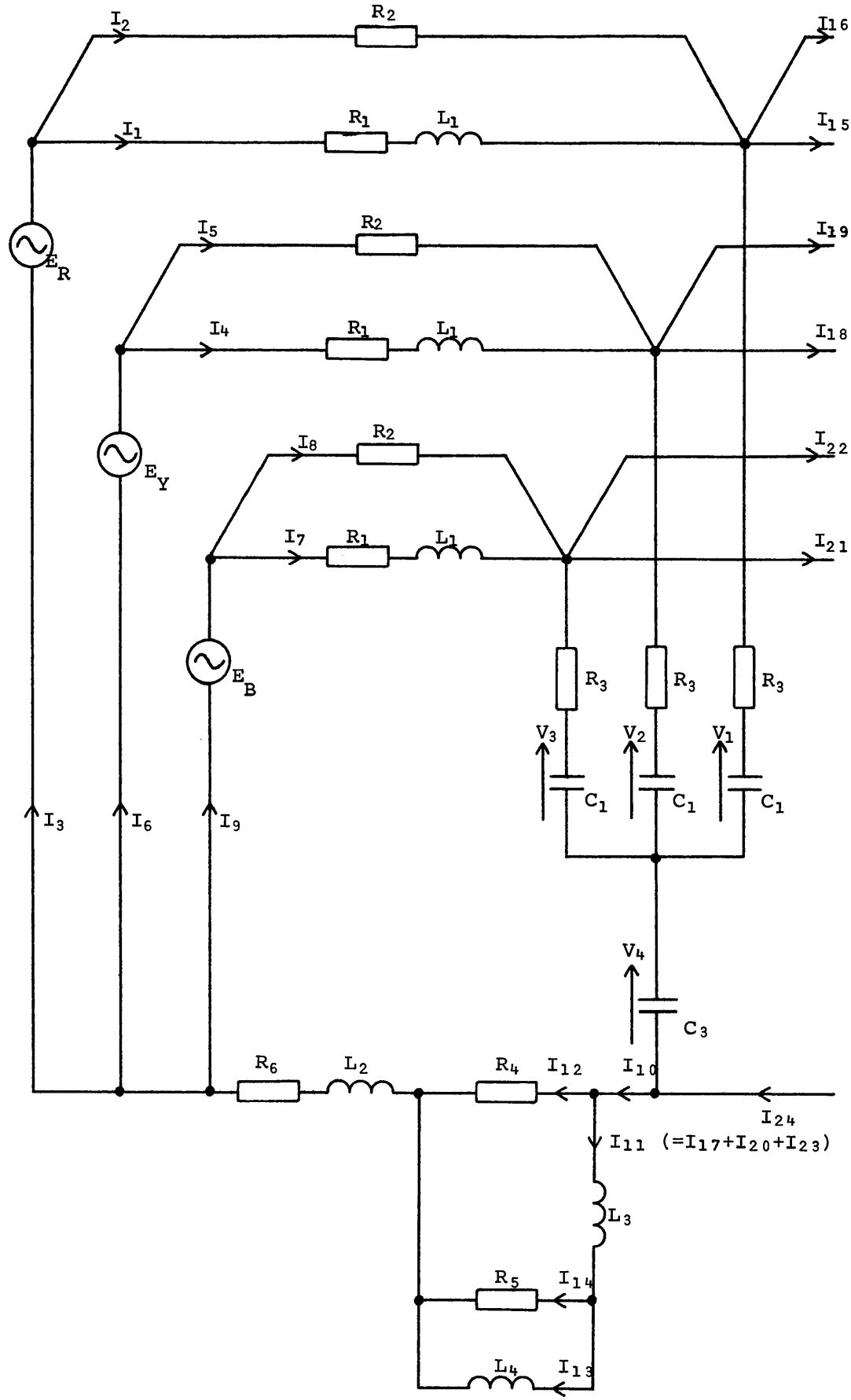

Figure 7.18 Simultaneous closure of the compensated 3-phase line.

Let $V_T = V_4 + I_{12}R_4 + I_{10}R_6$

$$\frac{dI_1}{dt} = \frac{E_R - I_1R_1 - I_3R_3 - V_1 - V_T - L_2\frac{dI_{10}}{dt}}{L_1} \qquad \frac{dV_1}{dt} = \frac{I_3 - I_{17}}{C_1}$$

$$\frac{dI_3}{dt} = \frac{E_R - I_2R_2 - I_3R_3 - V_1 - V_T}{L_2} \qquad \frac{dV_2}{dt} = \frac{I_6 - I_{20}}{C_1}$$

$$\frac{dI_2}{dt} = \frac{dI_3}{dt} - \frac{dI_1}{dt} \qquad \frac{dV_3}{dt} = \frac{I_9 - I_{23}}{C_1}$$

$$\frac{dI_4}{dt} = \frac{E_Y - I_4R_1 - I_6R_3 - V_2 - V_T - L_2\frac{dI_{10}}{dt}}{L_1} \qquad \frac{dV_4}{dt} = \frac{I_{10} - I_{24}}{C_3}$$

$$\frac{dI_6}{dt} = \frac{E_Y - I_5R_2 - I_6R_3 - V_2 - V_T}{L_2}$$

$$\frac{dI_5}{dt} = \frac{dI_6}{dt} - \frac{dI_4}{dt}$$

$$\frac{dI_7}{dt} = \frac{E_B - I_7R_1 - I_9R_3 - V_3 - V_T - L_2\frac{dI_{10}}{dt}}{L_1}$$

$$\frac{dI_9}{dt} = \frac{E_B - I_8R_2 - I_9R_3 - V_3 - V_T}{L_2}$$

$$\frac{dI_8}{dt} = \frac{dI_9}{dt} - \frac{dI_7}{dt}$$

$$\frac{dI_{10}}{dt} = \frac{dI_3}{dt} + \frac{dI_6}{dt} + \frac{dI_9}{dt}$$

$$\frac{dI_{11}}{dt} = \frac{I_{12}R_4 - I_{14}R_5}{L_3}$$

$$\frac{dI_{12}}{dt} = \frac{dI_{10}}{dt} - \frac{dI_{11}}{dt}$$

$$\frac{dI_{13}}{dt} = \frac{I_{14}R_5}{L_4}$$

$$\frac{dI_{14}}{dt} = \frac{dI_{11}}{dt} - \frac{dI_{13}}{dt}$$

Figure 7.19 Differential equations for simultaneous closure of the compensated 3-phase line.

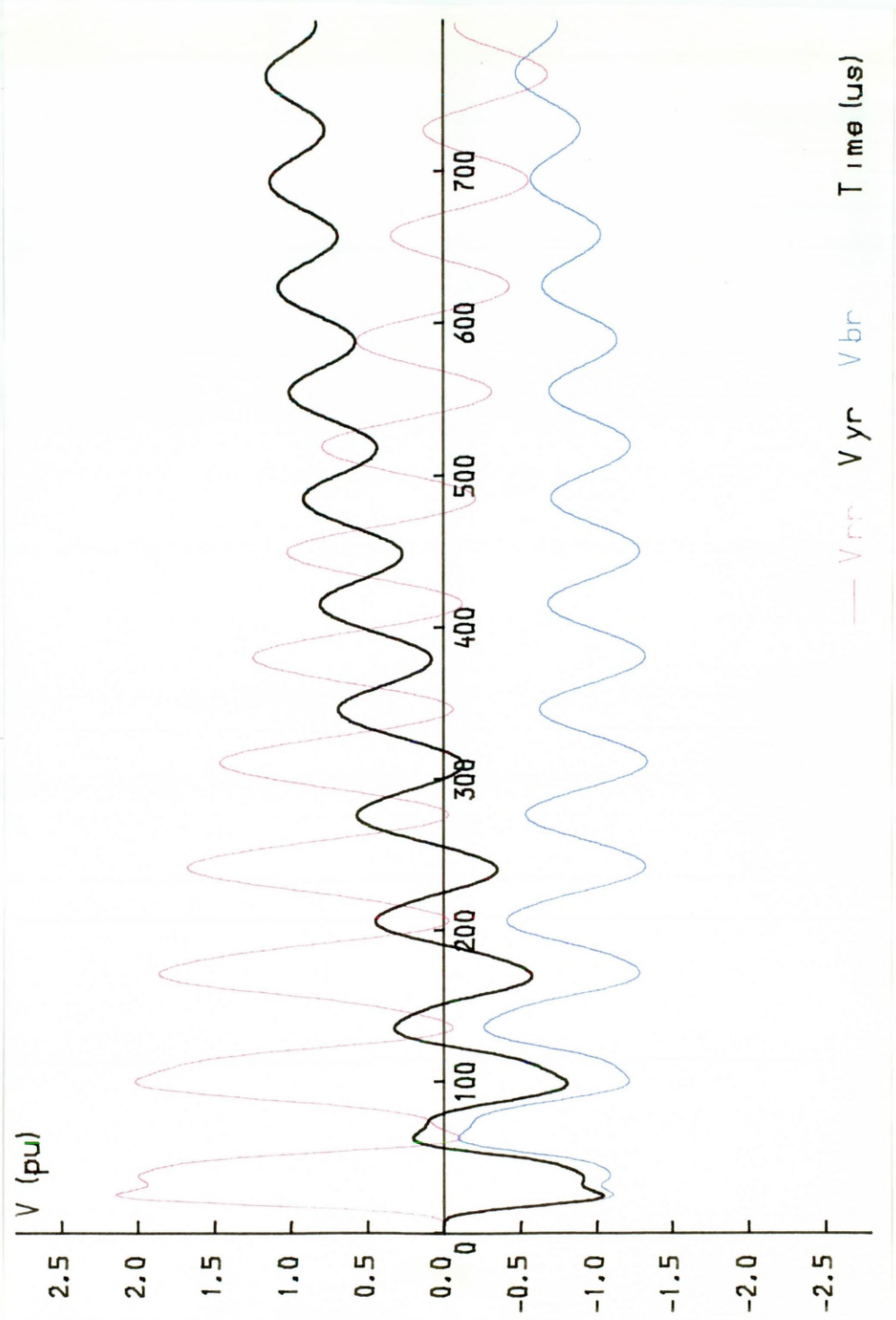

Figure 7.20 Response to simultaneous closure (R-phase at 90°) of a 5 pi-section compensated line.

7.6 Loading Effect of the TR Input Circuitry

The examples of source inductance and non-sequential closure show that the Runge-Kutta method gives some flexibility in that a circuit can be changed at the sending-end and the existing software requires little modification to accommodate that change. This was also found to be true for the remote end of the line when studying the loading effect of the TR on the model. The expertise gained also allowed the development of a program to investigate the energisation of a line from a transmission line source (discussed in Chapter 8).

The loading effect of the TR signal input, the parameters of which are 1MΩ and 48 ρF, on the uncompensated model line were investigated by modification of the existing 1-phase, zero earth impedance, Runge-Kutta software. The receiving-end circuit modification is shown in Figure 7.21(a). Although the TR was shown to have a negligible effect on the line response recorded, an interesting point concerning the step length arose. The Runge-Kutta programs written for the compensated lines discussed previously required a step length of 0.25 μs in order to give an accurate and stable response whereas a 1 μs step was sufficient in the uncompensated line cases. However the definition of the receiving-end shunt resistance in the software required that the step length be reduced to that used in the compensated line case for accurate response calculation. Therefore the connection of the load resistance is analogous to the parallel connection of the compensating resistor across the line series impedance shown in section 7.2.1.

7.6.1 Energisation of a Line from a Line Source

To investigate the effect on the Gibbs phenomena for this particular condition (Chapter 8) again involved little modification to the existing 1-phase software. Figure 7.22 shows that the model representation and therefore the differential equations of each line are the same. The only additional software written to predict the response of this system was to

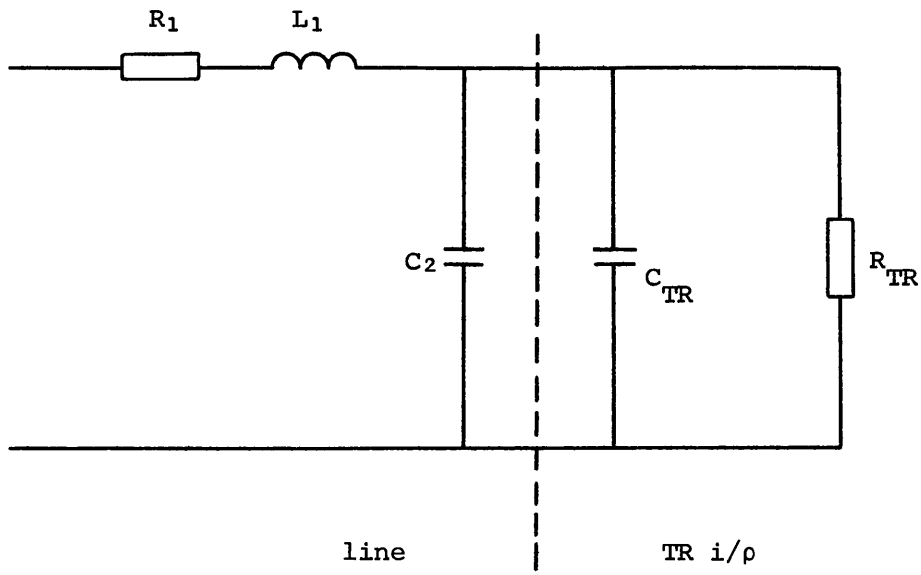

where C_{TR} = 48 ρF R_{TR} = 1 MΩ

Figure 7.21 Connection of TR input circuit at the uncompensated line receiving end.

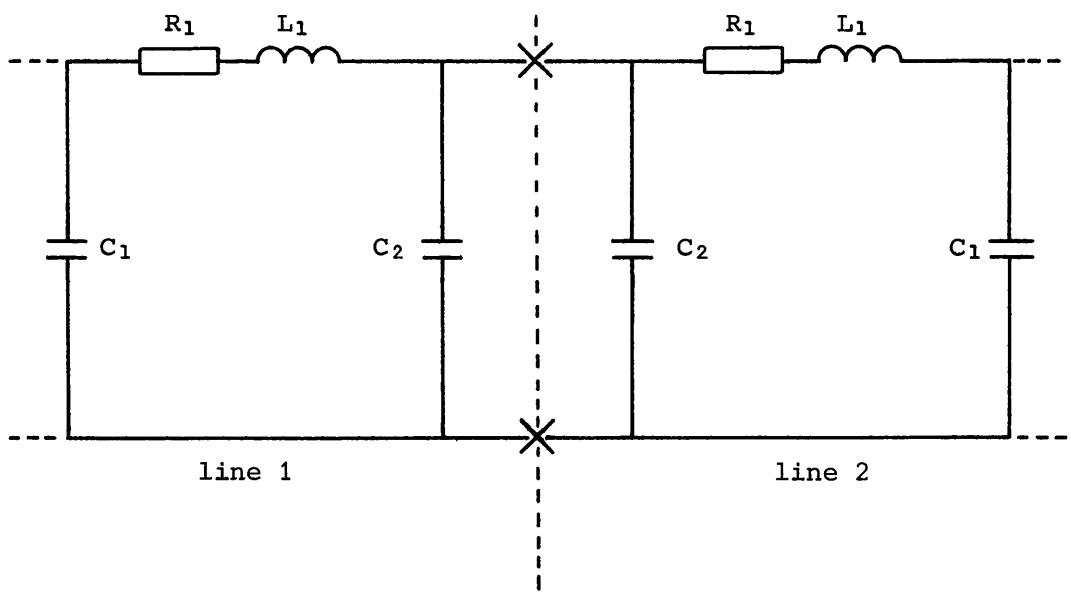

Figure 7.22 Energising a transmission line from a transmission line source.

rearrange the voltage and current variables (stored in the Y array) in the Runge-Kutta programs after the 2^{nd} line had been energised. The uncompensated and compensated receiving-end responses of line 2 (10 π-sections) energised from a 5 π-section line (line 1) are shown in Figure 7.23.

7.7 Runge-Kutta Software Overview

The Runge-Kutta routine is an accurate method for the solution of a system of differential equations. It has been extremely useful in verifying solutions to the model line at every stage since the comparison of experimental results in some cases required the modification of the line by the physical addition or removal of the compensating resistors.

The method for deriving the programs, shown in section 7.2, involved defining a five π-section circuit of the line to be simulated and establishing the repetitive nature of the differential equations to obtain the expressions that could be programmed in software. This allowed flexibility when investigating longer lengths of line and also saved time. This format allows a certain flexibility and requires little change if the user wishes to modify the circuit at the source or remote ends as previously shown. However it does require a detailed knowledge of the circuits and their differential equations to be able to do this.

Initially it was thought that the software written should allow an inexperienced user to input the circuit into the program by the nodal definition of components but in the final analysis this would, however, have created more software than was necessary for what are essentially specific model line configurations. A software package (GECAP) was available which used the nodal data input technique but it was found that it was limited in the maximum number of nodes which could be defined (25) and was inadequate even for the definition of a 20 π-section 1-phase line with zero earth impedance.

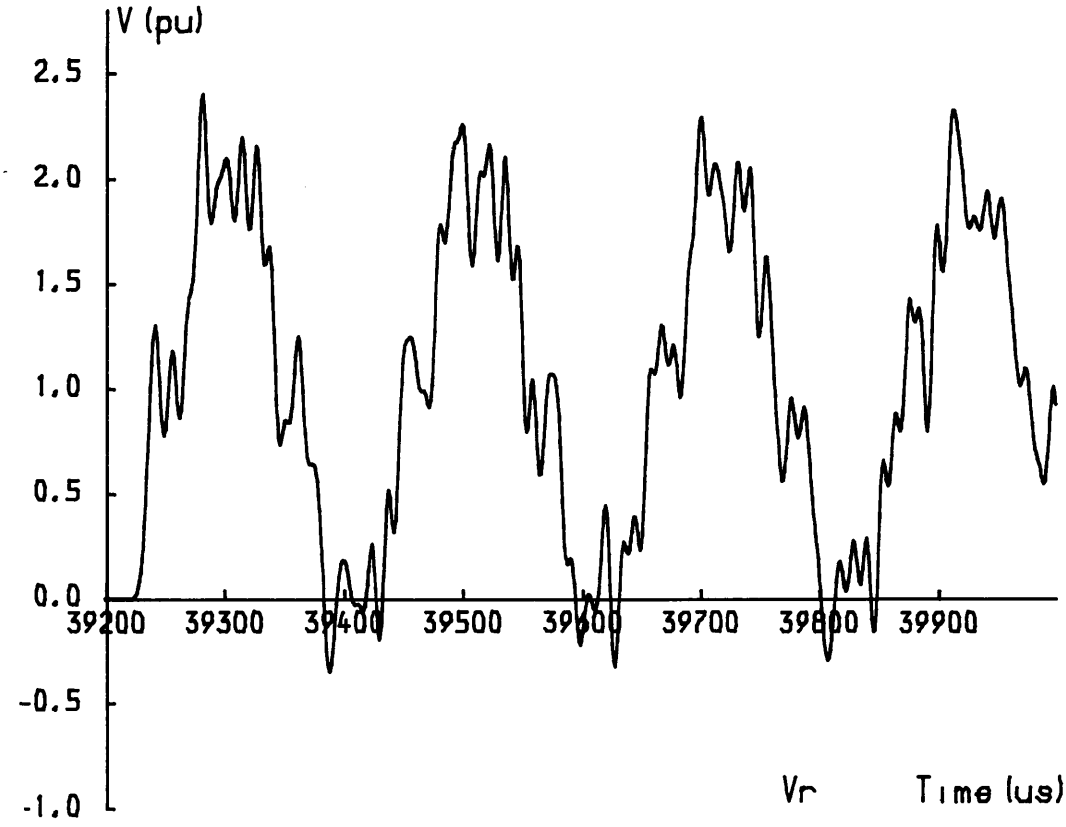

(a)

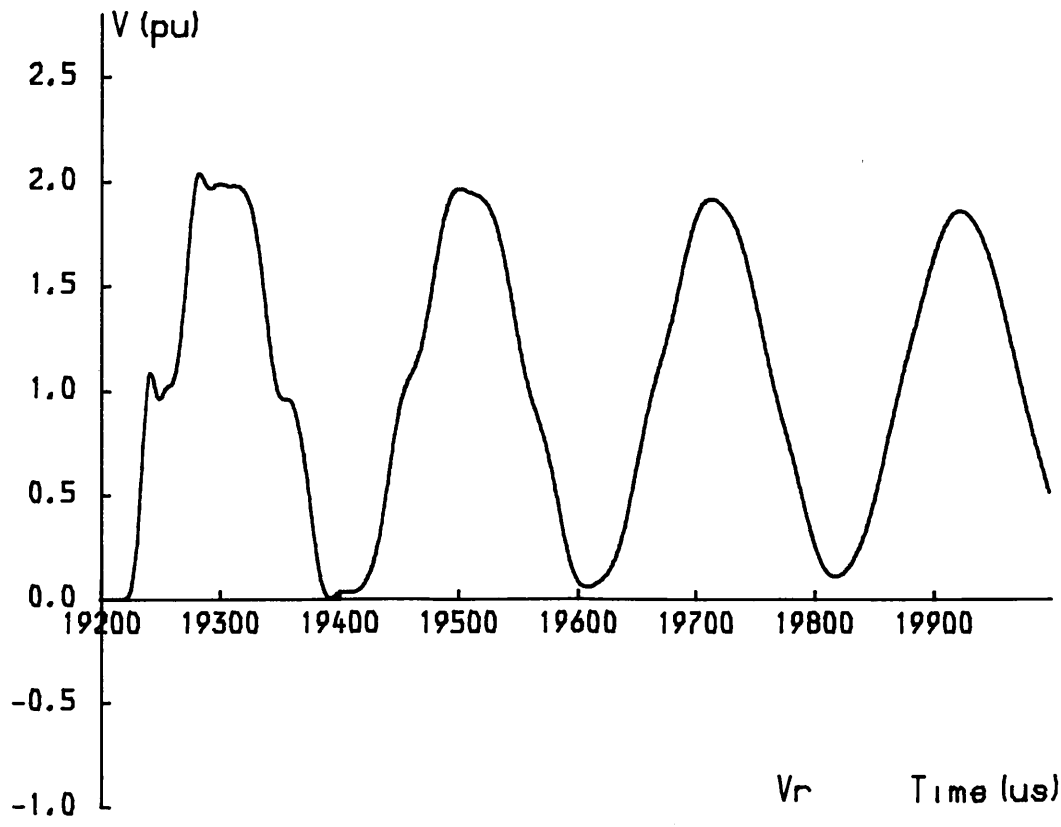

(b)

Figure 7.23 Receiving-end responses of a 10 pi-section line energised from a 5 pi-section line.
(a) Uncompensated. (b) Compensated.

The 1-phase program described in section 7.2 was transferred from the DEC-20 mainframe to the Z-2D system with the intention of making the project independent of any other system to avoid time-sharing but after test runs it became apparent that the 8-bit processor of the Z-2D took too long to calculate a response. For 40 variables i.e. a 1-phase 20 π-section uncompensated line, and 1600 time steps, the 36-bit mainframe took approximately 2.5 seconds of CPU time, the corresponding time on the Z-2D being 540 seconds. Consequently the problem would be accentuated with the verification of damped responses and the more complex circuits used. Consequently the Z-2D was not employed for waveform verification by the Runge-Kutta technique.

The use of the Runge-Kutta technique has been developed from the straightforward 1-phase line case to the more complex 3-phase line with frequency-dependent earth path. It has been invaluable in ensuring that the connections of the model line were correct and useful in investigating the effects that the recording equipment (TR) may have had (see sections 7.3 and 7.6). It has verified at each stage that the experimental responses obtained were correct and ensured the accuracy of the results obtained in this investigation.

It is doubtful, however, that the technique should be advanced further when the differential equations shown in section 7.2 for the 1-phase uncompensated line and those defined for the compensated 3-phase line (Appendix VI.2) are compared. The increase in complexity is apparent and will restrict the use of the method in aiding investigation into more complex systems due to the time and effort that would be necessary to ensure accurate differential equation definition. However the technique could still be used to verify the response of 3-phase lines due to non-simultaneous closure and would be very useful in the investigation of more complex 1-phase systems.

In spite of this the software approach does allow total automation in the sense that repetitive computer runs on systems with varying parameters can be carried out using the mainframe BATCH facilities. It was used in this instance to gather overvoltage information for the compensated lines for a range of source inductance values (section 7.4).

CHAPTER 8

Summary of Discussion

8.1 Introduction

The microprocessor modification of uncompensated model line transient waveforms, resulting from line energisation, has been investigated in an extensive study. The equipment required for the generation, recording, modification, display and plotting of the model line responses has been described and the software associated with this system discussed. The software was developed as an integral part of the study comprising of a number of Z-2D files for the application of the Experimental Sigma Factors, Runge-Kutta programs for model line waveform verification and Modified Fourier Transform and Lattice Technique programs for waveform comparison. Spectral analysis was also achieved by the Discrete Fourier Transform software.

Three Experimental Sigma Factors S_{se}, S_{ae} and S_{me} have been derived for the modification of the sampled uncompensated waveforms, these techniques being analogous to the use of the mathematical Sigma Factors used in Fourier Transform analysis. The effect of these experimental factors as a means of reducing the uncompensated waveform Gibbs phenomena has been analysed for the cases of open-circuited single and 3-phase lines energised from ideal and inductive sources. Extensive use of the display and plotting facilities has allowed the effectiveness of the averaging techniques to be ascertained by comparison of the resulting processor waveforms with resistor-compensated line responses.

The frequency content of the uncompensated and compensated transient waveforms has been calculated by the Discrete Fourier Transform to determine if improved averaging techniques could be devised by gaining a greater knowledge of the frequency components predominant in the model line responses. The Digital Filtering of uncompensated waveforms has also

been investigated.

8.2 The Experimental Standard Sigma Factor S_{se}

The Experimental Standard Sigma Factor S_{se} was the first local averaging technique employed where the associated averaging range, N_s, was determined automatically from the initial Gibbs Oscillation of the uncompensated receiving-end response. The ability of S_{se}, with this single value of N_s, to reduce the Gibbs phenomena has been shown to be significant only in the case of the 1-phase lines with earth path impedance. The processor responses of the 1-phase lines with zero earth impedance show that S_{se} is ineffective due to the changing frequency of the Gibbs content in the uncompensated waveforms.

In all 1-phase uncompensated responses resulting from infinite source energisation the predominant frequency of the Gibbs phenomena in the transient initial surge was found to be close or equal to the natural π-section frequency f_0. This frequency corresponds to a period of approximately 15 μs and consequently the value of N_s determined from the initial oscillation was close or equal to this value. Using this averaging range, processor modification has been successful in reducing the Gibbs content of the uncompensated responses obtained from the 1-phase lines with frequency-dependent earth path. The processor waveforms, in comparison with the compensated responses, display improved global response and steeper rates of rise for the three line lengths energised. The exception to this is the rate of rise of the initial discontinuity for the 5 and 10 π-section responses. However the initial rate of rise of the processor response improves as line length increases and for the longest line i.e. 20 π-sections, is steeper than that observed in the corresponding compensated case.

The averaging range calculated automatically from the 20 π-section line was 19 μs but an operator-defined value of 15 μs gave an improved processor response. Therefore for this 1-phase line configuration a 'fixed' value

of N_s could be applied to successfully reduce the high-frequency content of the uncompensated waveforms obtained from longer lengths of line. For lines lengths of more than 20 π-sections, the processor response should display a steeper initial rate of rise than will be observed in the compensated line response.

The processor waveforms calculated from the uncompensated responses of the 1-phase lines with zero earth impedance have demonstrated that S_{se} is ineffective after the initial transient surge due to the decreasing frequency of the Gibbs content present in subsequent surges. S_{se} was only relatively effective in the case of the 5 π-section line however, the surge peak voltages of the processor response lying outside the expected 0 - 2 pu range. Again the value of N_s calculated automatically from the initial oscillation did not give the best averaging range for modification of the initial surge. Therefore an adaptive averaging technique was developed to significantly reduce the changing Gibbs content of these responses.

8.3 The Adaptive Sigma Factor S_{ae}

By adapting the technique used for the determination of the Experimental Standard Sigma Factor S_{se}, the Experimental Adaptive Sigma Factor S_{ae} was derived. This uses the initial oscillation of each surge of a zero earth impedance response to calculate an averaging range, N_a, which is applied specifically to that surge. Therefore the averaging technique effectively adapted to the changing frequency of the Gibbs Oscillations that were encountered.

The calculation of a new averaging range for a subsequent surge was determined by using the excitation voltage as a reference. The Gibbs Oscillations for the responses of the open-circuited model line were evident at approximately 0 and 2 pu around the 1 pu (DC source) excitation voltage. The source voltage was therefore used as a reference to decide when a new averaging range N_a was to be calculated.

Implementing S_{ae} significantly reduced the Gibbs phenomena in the 20 π-section, zero earth impedance, uncompensated waveform but a reduced Gibbs content in each processor surge was however still apparent. This implies that the initial oscillation does not give an accurate indication of the frequency content of the surge. However the reduction of the magnitude of the Gibbs content was significant and was assumed to be sufficient so that the application of S_{ae} would give acceptable accuracy in the determination of the transient peak overvoltage.

When applying S_{ae} to the uncompensated responses of the shorter lines, in particular the 10 π-section line, it was found that increased operator involvement was required to obtain a processor response with a significantly reduced Gibbs content. This was brought about due to the waveshape encountered.

The first observation made was that after 1000 μs this uncompensated waveform no longer had a square-wave characteristic indicating that the above method would no longer apply. The result of this was the development of the empirical T/4 μs estimation which would be used to modify uncompensated waveforms which were not square-wave in character. This approximation proved to be accurate when averaging the 5, 10 and 20 π-section line responses. The second observation made was that by implementing S_{ae} a small inaccurate averaging range was determined by the technique due to a high-frequency oscillation present on the waveform discontinuity (see Figure 4.9(a) at 732 μs). The technique assumed this to be the initial oscillation of the next transient surge. This problem was overcome by defining a lower limit for averaging on the assumption that the Gibbs Oscillations with the highest frequency, and therefore lowest averaging range, occurred in the initial uncompensated waveform surge.

However the third observation demonstrated that the method used for waveform modification would not be entirely satisfactory. The calculation

of a value of N_a from the uncompensated waveform at 536 μs (see Figure 4.9(a)) was a 'legitimate' averaging value in that it was above the lower limit (11 μs) set previously. However as the processor response calculated by S_{ae} (Figure 4.19(a)) showed this value for averaging was ineffective in reducing the Gibbs content of that surge. This demonstrated for the first time that the averaging range determined from the initial oscillation of a surge could be inaccurate and that the criterion for local averaging might have to be re-defined.

The use of the T/4 μs estimation and the definition of a lower limit of averaging demonstrate that increased operator involvement is required in order to obtain a processor response which is accurate with respect to overvoltage magnitude. The technique developed for the implementation of S_{ae}, although only applicable to the specific waveshape in question, initiated the development of these two rules which limit the averaging ranges required for the modification of uncompensated waveforms.

8.4 Energisation from an Infinite AC Source

The preceding analysis relates to the responses obtained from DC step energisation. The effect of AC source energisation was similar to that for the DC case in that the initial step input generated Gibbs phenomena of exactly the same frequency and content in the uncompensated receiving-end responses. The transient fundamental though now follows the AC voltage supply wave. S_{se} and S_{ae} could therefore be applied to these responses for significant reduction of the Gibbs content. The problem of voltage sample resolution does arise for point-on-wave closures that approach 0 or 180° but if effective averaging ranges can be determined for the worst case closure then these can be applied over the same time ranges to reduce the Gibbs Oscillations thus overcoming this limitation.

8.5 The Experimental Modified Sigma Factor S_{me}

The processing of uncompensated line responses by the application of S_{se} and S_{ae} gave processor waveform discontinuities which were steeper than those of the corresponding compensated waveforms with the exception of the initial rates of rise in the 5 and 10 π-section lines with and without earth-path impedance. To improve this characteristic, and also subsequent discontinuities, the Experimental Modified Sigma Factor S_{me} was developed. An initial attempt to 'fit' uncompensated waveform discontinuities to processor waveform surge peaks i.e. where the Gibbs content had been reduced by S_{se}, by curve-fitting between these two regions was investigated but subsequently discarded since the technique was not directly related to the data representing the uncompensated waveform.

In the Fourier Transform analysis σ_m, using a shorter averaging range than σ_s, improved the rates of rise of the response calculated by the inversion integral. It was also found that the use of a shorter averaging range in modifying the sampled uncompensated responses gave improved processor waveform rates of rise when applied to the response discontinuities. Therefore N_m, the Variable Experimental Modified Sigma Factor Averaging Range, was designated a low value e.g. 1 μs, at waveform discontinuities while having a high averaging value e.g. 15 μs, when processing regions of Gibbs phenomena in the uncompensated waveform.

The value of the variable averaging range, N_m, to be applied for waveform modification was determined by using the Standard Averaging Range N_s to calculate a voltage gradient magnitude $|G|$ for each uncompensated waveform sample. If $|G|$ for a sample was high it was assumed that the sample was part of a waveform discontinuity while a low value for $|G|$ indicated that the sample was situated in a region of Gibbs phenomena. Using this criterion two techniques were devised to determine the value of N_m which should be implemented for the particular section of the

waveform considered.

The first technique consisted of defining a specific value of N_m (variable from 1 to 15 μs) to a specific range of |G|. Although this tabular method gave improved processor waveshapes the technique was highly operator dependent in that a vast amount of pre-processing calculation was necessary to determine the best value of N_m to achieve this improvement.

The preparatory work involved made this technique impractical however and consequently N_m was then varied automatically, the variation based on the change in |G| for successive samples. This variation of N_m gave processor responses where the waveform remained continuous but with small discontinuities occurring when N_m was changed. This was also observed in the Fourier analysis and gave the impression of a high-frequency content in the processor response.

Since the investigation of S_{me} was carried out on the uncompensated waveforms from the 1-phase lines with earth-path impedance, the upper limit of N_m was constant i.e. 15 μs. Consequently the application of S_{me} for the 1-phase lines with zero earth impedance would be increasingly more complex due to the changing averaging ranges implemented by S_{ae}. In addition a reduced high-frequency content was still apparent in the processor responses calculated by S_{ae} for these lines. Consequently by including the automatic technique devised for S_{me} an increase in the high-frequency content, due to the variation of N_m, would be apparent which would further degrade the processor response calculated.

Therefore by improving the rates of rise of the processor response, a small apparent high-frequency content is observed. However if values for the rates of rise of voltage are desired this parameter may be taken from the uncompensated waveform directly since the worst case rate of rise occurs in this response. This may be assumed since the filter effect of the model line excludes a range of higher frequencies that might be present in an actual line

response. It also may be argued that since the attenuation of the high-frequency range is greater in the uncompensated model than in the actual line case (see Figure 1.5) that it is feasible to determine this parameter as described. Greater accuracy may therefore be obtained in this manner as these rates of rise are significantly higher than in the compensated case (see Figures 4.13(a) and 4.15(a)).

8.6 Energisation from an Inductive Source

The inclusion of inductance in the source representation modified the line sending-end input voltage such that the high-frequency content of the input was reduced. As the source inductance L_s was increased a condition was reached where the highest frequency component of the line sending-end voltage was less than the model line cut-off frequency f_c. For this condition Gibbs phenomena were not apparent in the uncompensated line receiving-end response and this source value was defined as L_G, the minimum value of L_s for which this occurred. Consequently local averaging was not required.

Comparison of the uncompensated and compensated line responses, for source inductance values where $L_s \geq L_G$, showed that resistor compensation significantly damped the transient waveform source effects i.e. the 'hump' or 'peak' characteristics. The two averaging techniques S_{se} and S_{ae}, implemented when $L_s < L_G$, while reducing the uncompensated waveform Gibbs content did not significantly affect these source effects. Consequently a significant and consistent difference in peak overvoltage was demonstrated for the two line configurations in the overvoltage profiles obtained. The major difference in these profiles was observed in the inductance range 0 - 0.2H. The range of source values for which this difference in peak overvoltage was observed increases with line length and therefore for lines greater than the maximum of 20 π-sections investigated an extension of this range should become evident. The overvoltage difference

varies from 0.05 - 0.175 pu and since actual generator inductances lie in the range 0 - 0.5H the uncompensated line with processing facilities should give greater accuracy in determining overvoltages in this range.

The value of L_G was found to increase with line length for the zero earth impedance lines while remaining constant for the model lines including earth-path impedance. L_G also varied with line length for simultaneous closure experiments on the 3-phase model line, the values determined for L_G being the same as those of the 1-phase zero earth impedance cases. The waveshapes obtained from the 3-phase model line were the same as those observed in the 1-phase lines with zero earth impedance but the magnitude of the Gibbs content was slightly reduced. This is due to the change in surge impedance parameters of the line configurations.

A high-frequency component, related to the natural π-section frequency f_0, reappeared in the uncompensated responses of the 3-phase lines and the 1-phase lines with zero earth impedance. This phenomena was observed for a source value of 0.12H and the magnitude of these oscillations increased as L_s was further increased. However the oscillations were successfully reduced by applying an averaging range of 15 μs in each case. These high-frequency components are thought to be caused by the TNA inductors used to represent the source inductance.

8.7 Spectral Analysis of Model Line Waveforms

In order to obtain a greater knowledge of the frequency components in the model line transient waveforms, spectral analysis of the responses, using the Discrete Fourier Transform, was carried out. It was hoped that by obtaining more information concerning the Gibbs phenomena that improved averaging techniques might be devised. This however was not achieved but the analysis increased the understanding of the model line characteristics.

The analysis demonstrated the effects of increased attenuation of

the compensated line and showed that the frequency content of the model line responses were more complex than anticipated. In calculating an actual line response by the Modified Fourier Transform and determining the frequency spectrum of the receiving-end square-wave response, assumptions were made regarding the expected frequency spectra of the model line waveforms. Discussing the 5 π-section uncompensated line spectra it was found that some of the major frequency components predicted could be observed in the frequency spectrum calculated i.e. the 3^{rd} harmonic and natural π-section frequency components, while the expected 5^{th} harmonic was not observed. A significant high-frequency component at 82 kHz was also calculated. An explanation for this cannot readily be given but suggests that further examination would be of benefit in understanding the uncompensated model line. Although Digital Filtering of the Gibbs phenomena was found to be inadequate a Low-pass Digital Filter program was used to verify the frequency spectra obtained.

8.8 Conclusions on the Experimental Sigma Factors

The reduction of Gibbs phenomena, present in the uncompensated line receiving-end responses, by the application of the Experimental Sigma Factors has been reasonably successful. By applying S_{se}, using the 'fixed' value of N_s, to the responses from the 1-phase uncompensated lines with earth-path impedance improvements in processor waveform global response and discontinuities have been achieved when compared to the transient responses of the compensated line. Although the processor initial rate of rise of the 5 and 10 π-section lines is reduced, this improves as line length increases and is greater in the 20 π-section case. For the shorter lines the uncompensated waveform initial rate of rise may be taken for the worst case value.

Processor waveshapes completely free of the Gibbs phenomena cannot be obtained using the techniques devised when considering the

processor responses calculated for the zero earth impedance lines. Although S_{ae} has been successful in significantly, though not completely, reducing the magnitude of the Gibbs content accurate determination of transient overvoltages can still be achieved with processor waveform initial rates of rise again improving with line length. However the responses from these lines have revealed much about the averaging techniques and methods used to implement them due to the changing frequency of the Gibbs content. This has necessitated increased operator-dependency and complexity of programming for significant reduction of the Gibbs phenomena but benefits can still be gained despite this with particular reference being made to the overvoltage profiles obtained from inductive source energisation.

The increased complexity used in applying the averaging techniques has shown that the success of the averaging method derived is dependent on waveshape. This was verified by the number of problems encountered as the investigation developed:-

1. When applying S_{ae}, therefore calculating a new averaging range for each subsequent surge, a reduced high-frequency content is still observed in the processor response. Therefore the averaging range calculated from the initial oscillation is not the most effective for Gibbs reduction. The method of calculating each new averaging range, N_a, is dependent on waveshape i.e. regions of Gibbs Oscillations occurring alternatively above and below the source voltage with the initial oscillation predominant in magnitude in each surge. Implementing S_{ae} was straightforward in the case of the 20 π-section uncompensated waveform since it retained the square-wave characteristic for the complete record length of 4000 μs. The processor response calculated (Figure 4.17) shows that S_{ae} is effective.

2. The 10 π-section line response however (Figure 4.9(b)) is no longer square-wave in nature after 1000 μs and this necessitated

the development of the empirical T/4 μs estimation. This approximation defines an upper limit for the averaging range. The dependency on waveshape of the technique was further demonstrated when averaging this waveform using S_{ae} until 1000 μs. A small oscillation on the waveform discontinuity, which prevented the technique in calculating the new value of N_a from the initial oscillation of the next surge meant that a lower limit of averaging had to be defined. This was based on the assumption that the highest frequency of the Gibbs Oscillations occurred in the initial surge and had a frequency of 65.18 kHz i.e the natural π-section frequency f_0. This set a lower limit for local averaging.

3. However the most important factor concerns the 'legitimate' averaging range that was calculated at 536 μs (see Figure 4.9(a)) which did not effectively reduce the Gibbs phenomena. The averaging range calculated lay between the previously defined lower and upper limits but was still ineffective (Figure 4.19(a)). This indicated that the method for determining the averaging range, from the waveform samples, could be inaccurate and was dependent on the waveshape generated.

4. The final factor is not dependent on waveshape but on the sample resolution of the recording instrument, the Transient Recorder. With an AC source for point-on-wave closures that approached 0° the determination of effective averaging ranges became increasingly less accurate which was not immediately apparent from the processor responses since the magnitude of the transients were reduced accordingly. This was also demonstrated in inductive source energisation when L_s approached L_G where the Gibbs phenomena were reduced in magnitude. The Gibbs content was not completely reduced in this instance either since

the sample resolution did not allow accurate determination of the required averaging range value. This was ignored since the source effects were much more predominant in overvoltage magnitude.

Waveshape dependency can be further illustrated by inspection of the response in Figure 8.1. This shows the receiving-end waveform of a 10 π-section uncompensated line (line 2) energised from a 5 π-section uncompensated line (line 1, both lines having zero earth impedance) fed from a DC source. The equivalent compensated response is shown in Figure 8.2. The waveform initially displays the voltage doubling of the 0.5 pu voltage surge which propagates to the remote end of line 2 after energisation. However the receiving-end voltage surges and their Gibbs content do not occur alternatively above and below this 'new' source voltage since the negative surge which travels to the source of line 1 is reflected back and on arrival at the remote end of line 2 doubles and adds to the surge already observed. This alters the waveform shape from that previously seen for the case of line energisation from an ideal or inductive source and therefore S_{ae} cannot be implemented correctly using the 0.5 pu source voltage as a reference in this case. Hence the software would have to be altered which emphasises that the averaging techniques would have to be modified accordingly with each new system configuration investigated.

8.8.1 Future Work

The problems discussed have occurred for the lines whose responses display a decreasing Gibbs frequency content. The dependency on waveshape for the determination of averaging ranges may be overcome however by adapting the approach to the problem and incorporating some of the observations made from the preceding analysis.

The previously defined lower and upper limits of averaging may be used in this instance for waveform modification. By applying the lower limit to the initial uncompensated waveform surge and subsequently increasing the

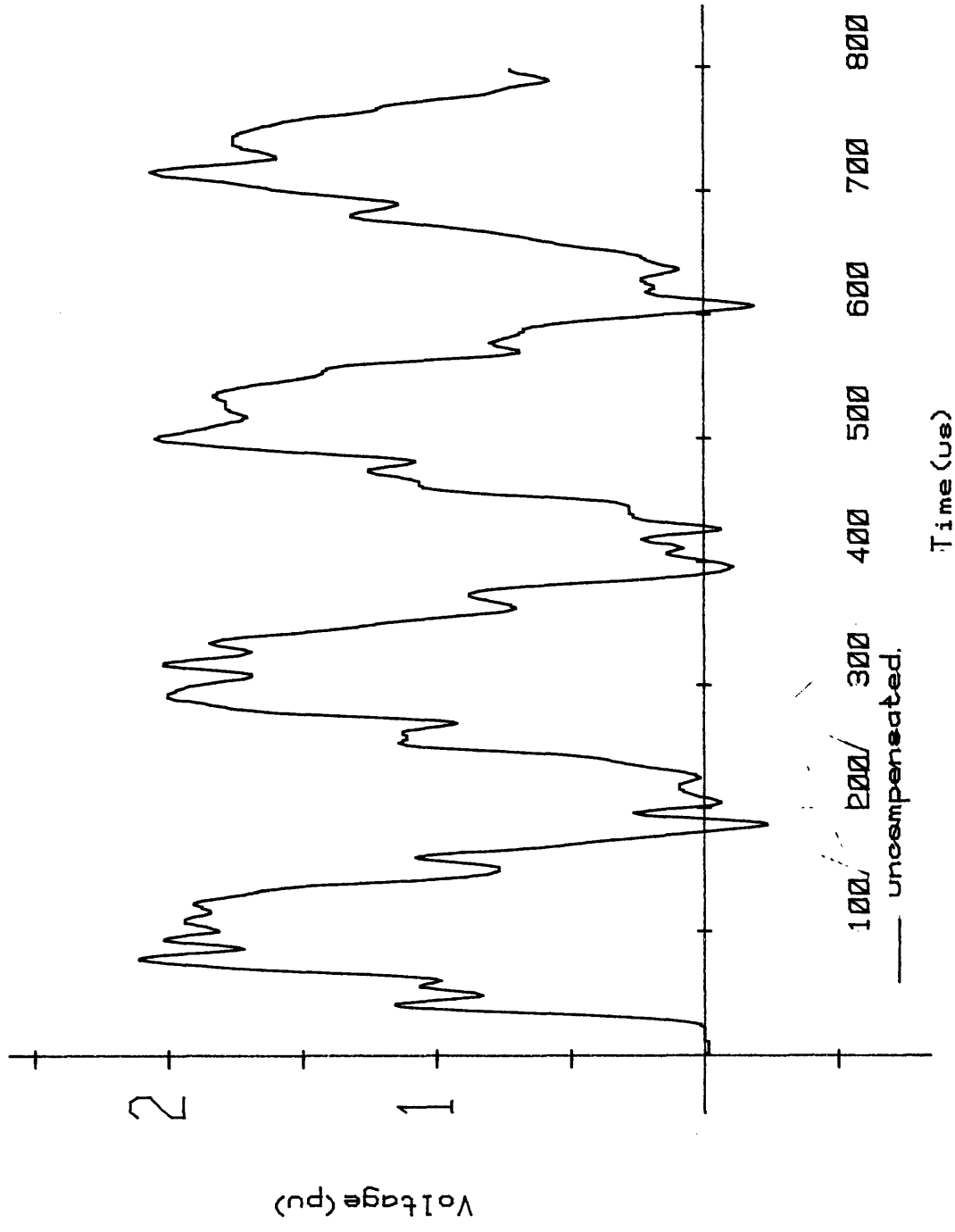

Figure 8.1 Receiving-end response of a 10 pi-section line (line 2) energised from a 5 pi-section line (line 1). Lines uncompensated with zero earth impedance, DC source in line 1.

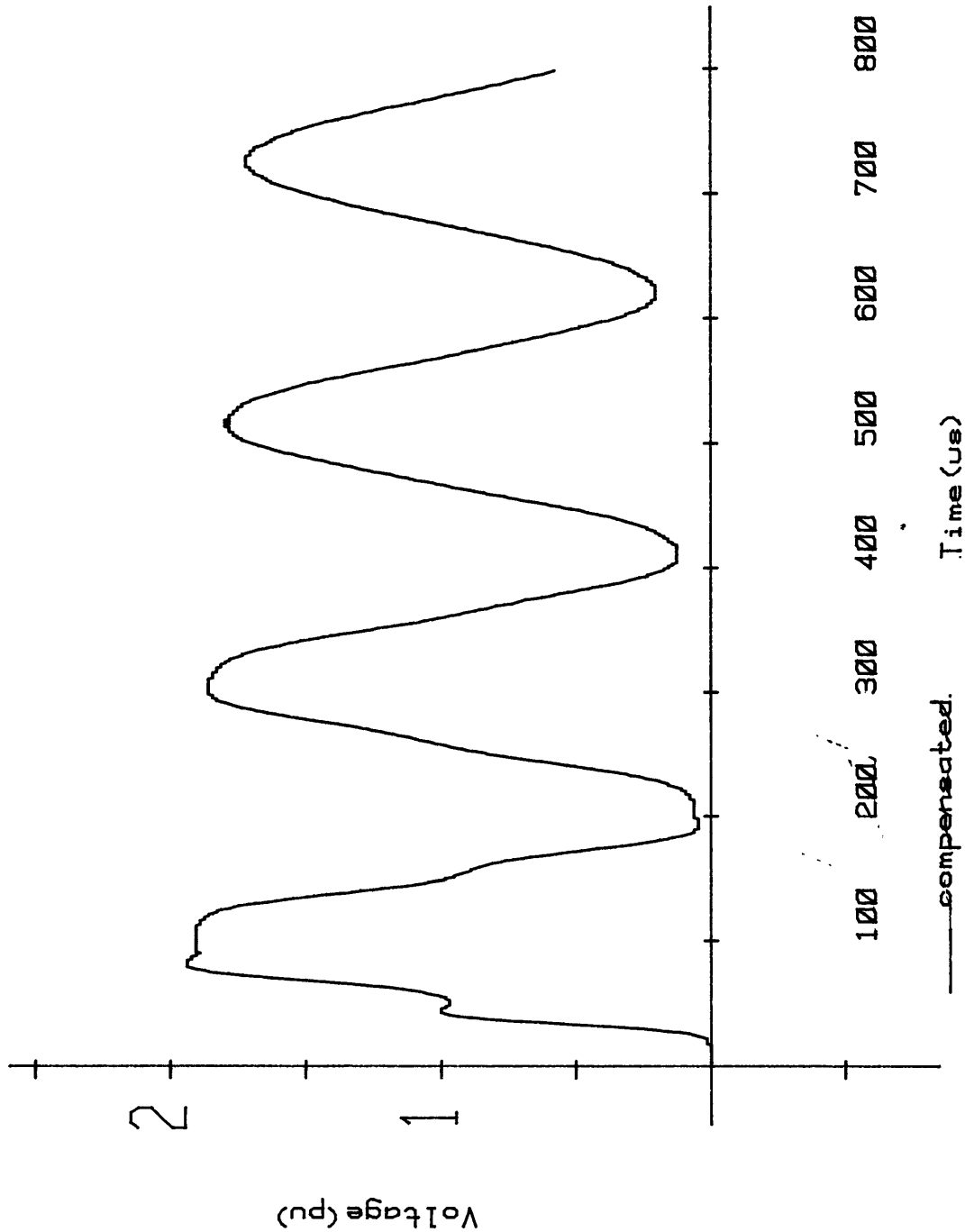

Figure 8.2 Receiving-end response of a 10 pi-section line (2) energised from a 5 pi-section line (1). Lines compensated with zero earth impedance, DC source in line 1.

averaging range with time until the T/4 μs approximation is implemented now gives values of N_a which are a function of time instead of waveshape. Inspection of the uncompensated 20 π-section zero earth impedance response in Figure 4.11 shows that the frequency of the Gibbs Oscillations decreases with time. Therefore the averaging ranges that would be required for effective modification would increase correspondingly with time, in this case from the lower limit of 15 μs to the upper limit i.e. the T/4 μs estimation, of 69 μs.

This technique could then be applied to the 5 and 10 π-section line responses where the lower limit would be approximately the same and as a first approximation the T/4 μs upper limit would again be implemented. Without modifying the technique this could also be applied to the line-to-line energisation transient of Figure 8.1, in this case the T/4 μs estimation being defined for a 15 π-section line.

This method therefore avoids the difficulties associated with determining the averaging ranges directly from the waveform samples but would require the most effective averaging range for each surge to be determined. However this would not involve lengthy analysis since the software written allows the averaging range to be changed and the result quickly calculated. Line energisation from an inductive source would involve greater analysis since the Gibbs content varies with L_s but the analysis would be justified since the increase in peak overvoltage obtained from the processor waveforms is significant and for longer line lengths the range of inductance over which this difference is observed should also increase. This technique could not be applied to the 1-phase line responses including earth path impedance although this is not a disadvantage since a single averaging range is effective for modification in this case.

The use of both S_{se} and S_{ae} (where N_a would be time-dependent) may be useful when considering the 3-phase line response due to

non-simultaneous pole closure. Figure 8.3 shows the phase-to-neutral receiving-end voltage of the red phase of a 5 π-section uncompensated 3-phase line when the red phase is energised at t=0 and the Y and B phases respectively 200 and 400 μs later. This may be compared with the Runge-Kutta calculated response in Figure 7.17. This response shows that the Gibbs phenomena are attenuated from the response after only 170 μs which is analogous to the response of the 1-phase line with earth-path impedance. Consequently S_{se} could be applied until 200 μs when the Y-phase is energised. However the response displays no significant effect for this closure since the Y-phase is energised for a point-on-wave value of 0°. Upon closure of the B-phase (at 270°) however at 400 μs the Gibbs phenomena become significant and the resulting waveshape is initially irregular due to mutual coupling effects. Therefore from this time the time-dependent S_{ae} may be implemented for the successful reduction of the Gibbs content. Figure 8.4 shows the processor response calculated by S_{se} and shows that it is only effective until approximately 400 μs. Therefore the averaging ranges for reducing Gibbs phenomena generated by subsequent pole closures would be required.

The use of S_{se} and the time-dependent S_{ae} may lead to even greater accuracy in the processor responses which already have demonstrated the advantages of the local averaging technique.

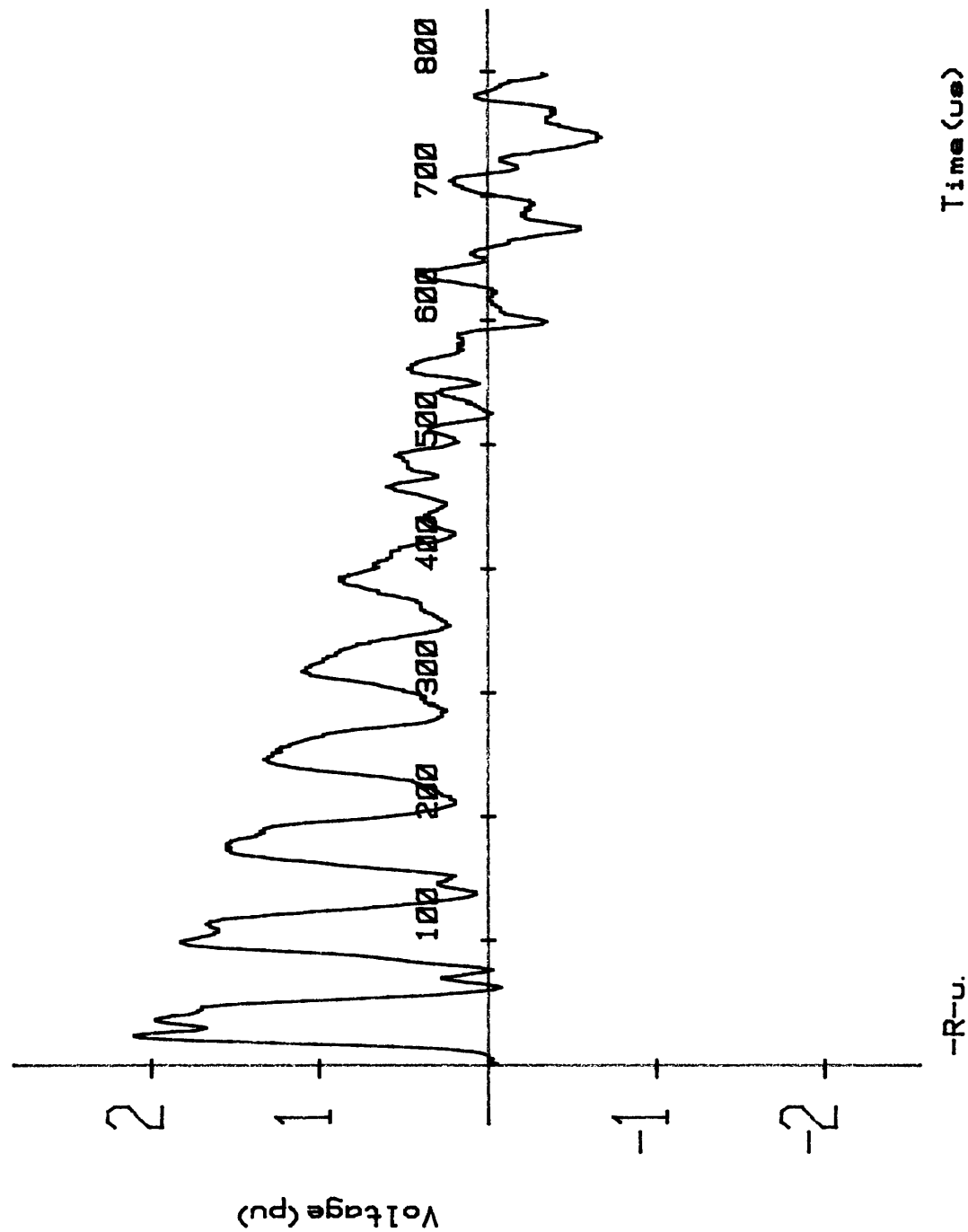

Figure 8.3 Receiving-end response (R-phase only) of a 5 pi-section, 3-phase uncompensated line. Y-B closure sequence: 30, 60° after R-phase is energised at 90°.

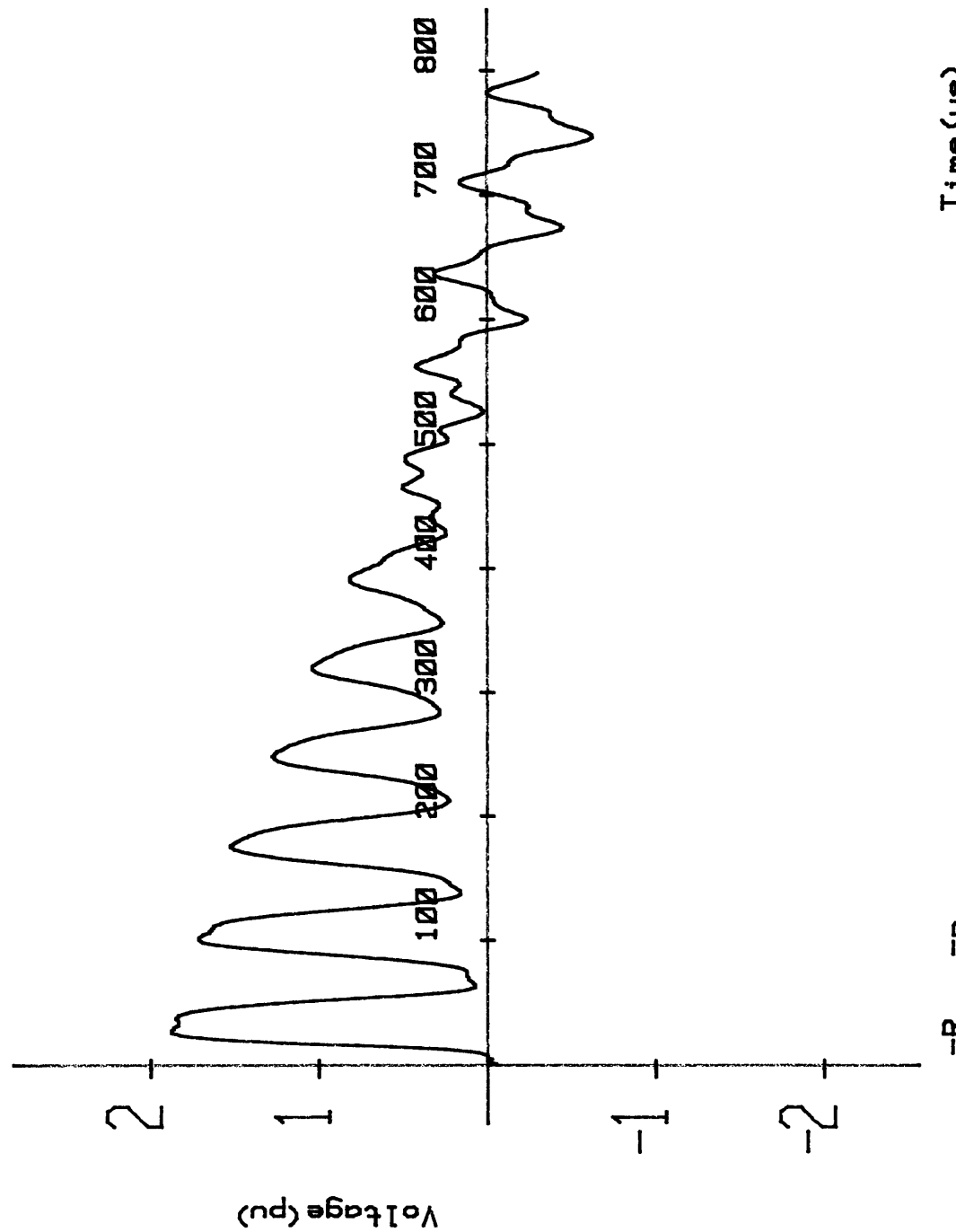

Figure 8.4 Processor response (R-phase only) by using S_{se}.

APPENDIX I

Actual and Model Line Parameters

I.1. Actual Line Parameters

Consider the incremental length δx of a transmission line shown in Figure A1.1 where R, L and C are the resistance, inductance and capacitance of the line per unit length. The voltage and current at the input of the line element are V and I respectively while the voltage and current at the element output are $(V + \delta V)$ and $(I + \delta I)$. Hence

$$- \frac{\delta V}{\delta x} = IR + L \frac{\delta I}{\delta t} \tag{8.1}$$

and

$$- \frac{\delta I}{\delta x} = C \frac{\delta V}{\delta t} \tag{8.2}$$

If V and I are sinusoidal quantities then

$$\frac{\delta V}{\delta t} = j\omega V \quad \text{and} \quad \frac{\delta I}{\delta t} = j\omega I$$

Substituting in (8.1) and (8.2) yields

$$- \frac{\delta V}{\delta x} = (R + j\omega L)I$$

$$- \frac{\delta I}{\delta x} = (j\omega C)V$$

and on further differentiation

$$\frac{\delta^2 V}{\delta x^2} = (R + j\omega L)(j\omega C)V$$

$$\frac{\delta^2 I}{\delta x^2} = (R + j\omega L)(j\omega C)I$$

or

$$\frac{\delta^2 V}{\delta x^2} = \gamma^2 V \tag{8.3}$$

$$\frac{\delta^2 I}{\delta x^2} = \gamma^2 I \tag{8.4}$$

where

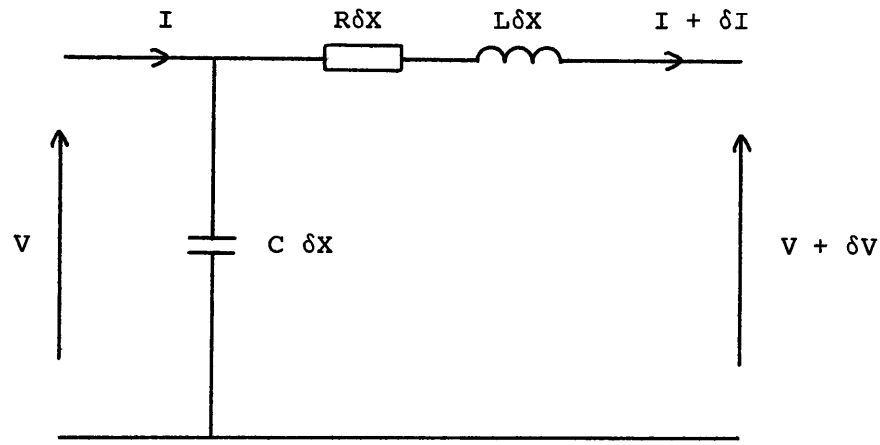

Figure A1.1 Incremental section (of length δX) of a uniformly distributed line.

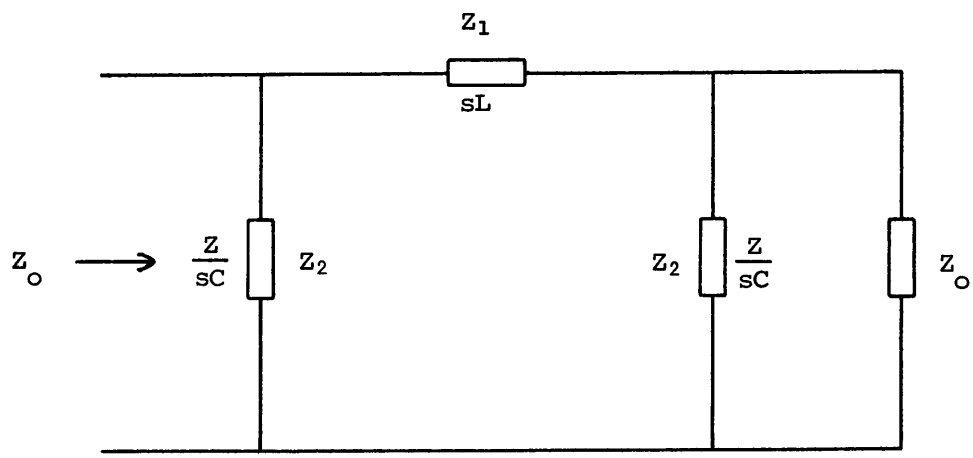

Figure A1.2 Determination of surge impedance of a lossless pi-section.

$$\gamma = \sqrt{(R + j\omega L)(j\omega C)} \tag{8.5}$$

γ is complex and is called the propagation coefficient. It may be written

$$\gamma = \alpha + j\beta \tag{8.6}$$

where α is the attenuation coefficient and β is the phase-change coefficient.

Equations (8.3) and (8.4) are second-order differential equations and by differentiation and substitution the solutions are readily shown[47] to be

$$V = Ae^{-\gamma x} + Be^{\gamma x} \tag{8.7}$$

and

$$I = \frac{\gamma}{R+j\omega L} (Ae^{-\gamma x} - Be^{\gamma x}) \tag{8.8}$$

For an infinitely long line the voltage and current both tend to zero as x tends to infinity which implies that B = 0 giving

$$V = Ae^{-\gamma x}$$

and

$$I = \frac{\gamma}{R+j\omega L} Ae^{-\gamma x}$$

The ratio of voltage to current

$$\frac{V}{I} = \frac{R+j\omega L}{\gamma} = \sqrt{\frac{R+j\omega L}{j\omega C}}$$

is termed the surge impedance of the line and is denoted by Z_0. Rewriting γ from equation (8.5)

$$\gamma = j\omega \sqrt{LC} \left(1 - j\frac{R}{\omega L}\right)^{1/2}$$

and using the Binomial Theorem

$$\gamma = \frac{R}{2} \sqrt{\frac{C}{L}} \left[1 - \frac{R^2}{8\omega^2 L^2}\right] + j\omega \sqrt{LC} \left[1 + \frac{R^2}{8\omega^2 L^2}\right] \tag{8.9}$$

The real part of (8.9) corresponds to α the attenuation coefficient

in equation (8.6) with units in nepers/mile while the imaginary part of (8.9) is the phase-change coefficient β in (8.6) in radians/mile.

I.2. Variation of Actual Line Parameters with Frequency

The parameters were calculated for 5 miles of line to correspond to the 5 miles/π-section representation of the model line.

Frequency (kHz)	Surge impedance (ohms)	Attenuation (Np)	Phase-Change (degrees)
0.05	296.3	0.00053	0.5
0.5	295.2	0.00086	4.9
1.0	295.1	0.00118	9.9
2.0	295.1	0.00160	19.8
3.0	295.1	0.00197	29.6
4.0	295.1	0.00230	39.5
5.0	295.1	0.00259	49.4
6.0	295.1	0.00285	59.3
7.0	295.1	0.00309	69.2
8.0	295.1	0.00330	79.0
9.0	295.1	0.00345	88.9
10.0	295.1	0.00357	98.8

I.3. Uncompensated Model Line Parameters

The uncompensated π-section is shown in Figure A1.2 terminated in its characteristic impedance Z_0. The input impedance i.e. Z_0 is given by

$$Z_0 = \frac{Z_2(Z_1 + Z_t)}{Z_2 + Z_1 + Z_t}$$

where

$$Z_t = \frac{Z_2 Z_0}{Z_2 + Z_0}$$

This can be rearranged to give

$$Z_0 = \sqrt{\frac{Z_1 Z_2{}^2}{Z_1 + 2Z_2}} \tag{8.10}$$

If the impedances are substituted into (8.10) where

$$Z_1 = R + j\omega L$$

and

$$Z_2 = \frac{2}{j\omega C}$$

then the expression

$$Z_0 = \sqrt{\frac{\frac{L}{C} - j\frac{R}{\omega C}}{1 - \frac{\omega^2 LC}{4} + j\frac{\omega CR}{4}}} \tag{8.11}$$

gives the surge impedance of the uncompensated π-section.

I.4. Frequency Variation of Uncompensated Model Parameters

Frequency (kHz)	Surge Impedance (ohms)	Attenuation (Np)	Phase Change (degrees)
0.4	787.7	0.00053	0.5
4.0	785.6	0.00064	5.0
8.0	787.8	0.00077	10.0
16.0	796.9	0.00104	20.0
24.0	812.8	0.00139	30.2
32.0	836.8	0.00190	40.6
40.0	871.1	0.00255	51.4
48.0	919.3	0.00343	62.8
56.0	988.0	0.00449	74.8
64.0	1090.5	0.00584	87.9
72.0	1256.8	0.00796	102.7
80.0	1579.5	0.01154	120.4

I.5. Frequency Variation of Compensated Model Parameters

The values for surge impedance, attenuation and phase change were taken from the experimental analysis carried out by Ovenstone[18]. The power loss component was so high that measurements could only be taken up to 60 kHz.

Frequency (kHz)	Surge Impedance (ohms)	Attenuation (Np)	Phase Change (degrees)
0.4	788	0.00177	0.49
4.0	795	0.0021	5.4
8.0	798	0.0028	10.5
12.0	800	0.0038	15.8
16.0	808	0.0065	20.6
20.0	812	0.0113	25.5
24.0	818	0.021	30.4
28.0	824	0.0335	35.5
32.0	830	0.0441	40.3
36.0	836	0.0565	45.5
40.0	848	0.068	50.2
44.0	860	0.083	55.7
48.0	870	0.1011	61.1
52.0	878	0.119	67.6
56.0	898	0.1395	72.3
60.0	916	0.1638	78.1
66.0	946	-----	87.2
70.0	980	-----	93.5
75.0	1032	-----	101.1
80.0	1116	-----	110.1

I.6. Model Line Cut-Off Frequency f_c

The uncompensated model line cut-off frequency, f_c, can be evaluated from equation (8.10). Assuming a lossless π-section i.e. R = 0 then

$$Z_1 = sL$$

and

$$Z_2 = \frac{2}{sC}$$

Substituting into (8.10) gives

$$Z_0 = \sqrt{\frac{4/C^2}{s^2 + \frac{4}{LC}}}$$

This has a nominal cut-off at a value of

$$s^2 = \frac{-4}{LC}$$

Therefore the nominal cut-off frequency is

$$\omega = \sqrt{\frac{4}{LC}}$$

where L and C are the total π-section values. For the particular values of L_p and C_p given in section 2.4 f_c = 92.2 kHz.

APPENDIX II

Cromemco Z-2D Programs

II.1. Program SIN3P.FOR

```
C       Assembler routines called
C
        EXTERNAL DATAI,BLINE,CONV,INPLT,PLOT,LBPLOT
        EXTERNAL TIK,REAXE,WPDISP,WPKEY
C
        BYTE    Q1,Q2,Q3,Q4,Q5,Q7,Q8,Q9,Q10,Q11,QL1,QL2
        BYTE    KYLT,BU,BP,BD,WP,PLDS
        DIMENSION INDPL(9)
C
C       Common data areas,between FORTRAN and assembler
C       modules,FORTRAN main and FORTRAN subroutines
C
        COMMON  /IDATA/IDATA(4096)/LAVSTA/LAVSTA/PLDS/PLDS
        COMMON  /NTIME/NTIME/NETM/NETM/IFLAG/IFLAG/IUP/IUP
        COMMON  /IXAX/IXAX/IVP/IVP/LTIME/LTIME/LABEL/LABEL
        COMMON  /IMXRTE/IMXRTE/ANGLER/ANGLER/SAMPTM/SAMPTM
        COMMON  /INC/INC/NBLOCK/NBLOCK/IBUFF/IBUFF(64)
        COMMON  /ISUB/ISUB/NOPOS/NOPOS/ICOL/ICOL
        COMMON  /ITIM1/ITIM1/ITIM2/ITIM2/ISTEP/ISTEP
        COMMON  /MDATA/MDATA/IRANGE/IRANGE/LAVEND/LAVEND
        COMMON  /FSIN/FSIN(3)/KYCO/KYCO/KYLT/KYLT
        COMMON  /PV/PV(9)/PT/PT(9)/NOPHSE/NOPHSE
        COMMON  /IHALF/IHALF/LIMIT/LIMIT/INCREM/INCREM
        COMMON  /SPOW/SPOW/PHSEMX/PHSEMX
C
1010    CALL    GRAFIX
        CALL    INIT
        CALL    XAREA(1,1,378,241,0)
C
C       SCALING: 0 -> 450 signifies -2.8 pu -> +2.8 pu
C       If pu scaling changes modify '450'
C
        CALL    SCALE(-20,1000,0,450)
C
C       Label Monitor Axes
C
        CALL    XTEXT(720,0,15,'time (us)^')
        CALL    XTEXT(35,418,15,'v^')
        CALL    XTEXT(35,396,15,'o^')
        CALL    XTEXT(36,370,15,'l^')
        CALL    XTEXT(35,346,15,'t^')
        CALL    XTEXT(35,325,15,'a^')
        CALL    XTEXT(35,304,15,'g^')
        CALL    XTEXT(35,279,15,'e^')
        CALL    XTEXT(28,250,15,'(^')
        CALL    XTEXT(40,250,15,'p^')
        CALL    XTEXT(53,250,15,'.^')
        CALL    XTEXT(64,250,15,'u^')
        CALL    XTEXT(80,250,15,'.^')
        CALL    XTEXT(88,250,15,')^')
        QL2=X'59'
```

```
C
C       Input data (if necessary)
C
        WRITE(3,10)
10      FORMAT(' Data transfer from TR ? ')
        READ(3,20)Q1
20      FORMAT(A1)
        IF(Q1.NE.X'59')GOTO 200
        WRITE(3,30)
30      FORMAT(' TR Sweep,TNA R-ph closure,Source Z ? ')
        READ(3,40)ISWEEP,IANGLE,QL1
40      FORMAT(I6,I6,A1)
        SWEEP=FLOAT(ISWEEP)
        ANGLER=FLOAT(IANGLE)
        CALL    OPEN(6,'SWITCH3 DAT',0)
        WRITE(6,50)SWEEP,ANGLER,QL1
50      FORMAT(F10.3,F10.3,1X,A1)
        ENDFILE 6
        CALL    PHASEM
        IF(FSIN(1).EQ.PHSEMX)WRITE(3,51)
        IF(FSIN(2).EQ.PHSEMX)WRITE(3,52)
        IF(FSIN(3).EQ.PHSEMX)WRITE(3,53)
51      FORMAT(' Enter R-ph 1st')
52      FORMAT(' Enter Y-ph 1st')
53      FORMAT(' Enter B-ph 1st')
60      WRITE(3,70)
70      FORMAT(' Waveform to transfer :-'/
     1' 1-R U(nmodified)'/
     2' 2-Y U'/
     3' 3-B U'/
     4' 4-R R(esistor)'/
     5' 5-Y R'/
     6' 6-B R'/
     7' 7-End of Transfer'/
     8' ')
        READ(3,80)NOPHSE
80      FORMAT(I1)
        IF(NOPHSE.EQ.7)GOTO 200
90      CALL    DATAI
        WRITE(3,100)
100     FORMAT(' Data Transferred ? ')
        READ(3,110)Q3
110     FORMAT(A1)
        IF(Q3.NE.X'59')GOTO 90
        IF(PHSEMX.EQ.0.0)GOTO 115
        PHSEMX=0.0
        SPOW=FSIN(1)
        IF(NOPHSE.EQ.2.OR.NOPHSE.EQ.5)SPOW=FSIN(2)
        IF(NOPHSE.EQ.3.OR.NOPHSE.EQ.6)SPOW=FSIN(3)
        CALL    PUSECH
C
C       Routine to determine 0V level of response
C       and place this on time axis(225) on monitor
C
115     LEVELF=IDATA(1)
        N=1
120     LV1=0
        LV2=0
        IMXRTE=25
```

```
        DO 130 I=N,IMXRTE
130     IF(IDATA(I).EQ.LEVELF)LV1=LV1+1
140     DO 150 I=N,IMXRTE
        IF(IDATA(I).EQ.LEVELF)GOTO 150
        LEVEL2=IDATA(I)
        N=I
        GOTO 160
150     CONTINUE
160     DO 170 I=N,IMXRTE
170     IF(IDATA(I).EQ.LEVEL2)LV2=LV2+1
        IF(LV1.LT.LV2)LEVELF=LEVEL2
        IF(LV1.LT.LV2)GOTO 120
        IF(N.EQ.IMXRTE)GOTO 180
        N=N+1
        LV2=0
        GOTO 140
180     IDATA(1)=LEVELF
C
C       SCALING: 225 = 450/2
C
        LEVELD=225-LEVELF
C
        DO 190 I=1,4096
190     IDATA(I)=IDATA(I)+LEVELD
        SAMPTM=SWEEP/4000
C
C       Calculate peak voltage of transferred response
C       while in the working memory area
C
        CALL    PEAKV
C
C       Store waveform on disc
C
        IF(NOPHSE.EQ.1)CALL OPEN(6,'UUURRRR DAT',0)
        IF(NOPHSE.EQ.2)CALL OPEN(6,'UUUYYYY DAT',0)
        IF(NOPHSE.EQ.3)CALL OPEN(6,'UUUBBBB DAT',0)
        IF(NOPHSE.EQ.4)CALL OPEN(6,'DDDRRRR DAT',0)
        IF(NOPHSE.EQ.5)CALL OPEN(6,'DDDYYYY DAT',0)
        IF(NOPHSE.EQ.6)CALL OPEN(6,'DDDBBBB DAT',0)
        INC=1
        NBLOCK=1
        DO 195 I=1,4096
        MDATA=IDATA(I)
        CALL    STOBUF
195     CONTINUE
        ENDFILE 6
        GOTO 60
C
C       Start here if previous data(on disc) to be analysed
C
200     CALL    OPEN(6,'SWITCH3 DAT',0)
        READ(6,210)SWEEP,ANGLER,QL1
210     FORMAT(F10.3,F10.3,A1)
        ENDFILE 6
        CALL    PHASEM
        IF(FSIN(1).EQ.PHSEMX)CALL OPEN(6,'UUURRRR DAT',0)
        IF(FSIN(2).EQ.PHSEMX)CALL OPEN(6,'UUUYYYY DAT',0)
        IF(FSIN(3).EQ.PHSEMX)CALL OPEN(6,'UUUBBBB DAT',0)
        LIMIT=4096
```

```
        CALL    GETVAL
        ENDFILE 6
        SPOW=FSIN(1)
        IF(FSIN(2).EQ.PHSEMX)SPOW=FSIN(2)
        IF(FSIN(3).EQ.PHSEMX)SPOW=FSIN(3)
        CALL    PUSECH
        SAMPTM=SWEEP/4000
        ISWEEP=SWEEP
C
C       Draw axes and number pu axis on monitor
C
220     CALL    BLINE
        CALL    TIK
C
C       Determination of averaging range from receiving-end
C       waveform whose sending-end switches closest
C       to 90 or 270
C
        IPLUS1=IMXRTE+1
        ISIGN1=1
        IF(IDATA(IPLUS1)-IDATA(IMXRTE).LT.0)ISIGN1=-1
        DO 270 I=IMXRTE,4096
        IF(ISIGN1.EQ.1)GOTO 250
        IF(IDATA(I+1)-IDATA(I))270,270,260
250     IF(IDATA(I+1)-IDATA(I))260,270,270
260     IPEAK=I
        ISIGN1=-ISIGN1
        GOTO 280
270     CONTINUE
280     DO 310 I=IPEAK,4096
        IF(ISIGN1.EQ.1)GOTO 290
        IF(IDATA(I+1)-IDATA(I))310,310,300
290     IF(IDATA(I+1)-IDATA(I))300,310,310
300     ITROFF=I
        GOTO 320
310     CONTINUE
320     IHALF=ITROFF-IPEAK
        WRITE(3,330)IHALF,IPEAK,ITROFF
330     FORMAT(3I6)
        IF(IHALF.GT.20)IHALF=1
340     IRANGE=2*IHALF+1
C
C       Determine the starting point on the waveform for
C       averaging,modify(if necessary) and store on disc
C
345     DO 410 NPHSE=1,3
        IF(NPHSE.EQ.1)CALL OPEN(6,'UUURRRR DAT',0)
        IF(NPHSE.EQ.2)CALL OPEN(6,'UUUYYYY DAT',0)
        IF(NPHSE.EQ.3)CALL OPEN(6,'UUUBBBB DAT',0)
        LIMIT=4096
        CALL    GETVAL
        ENDFILE 6
        INC=1
        NBLOCK=1
        IF(NPHSE.EQ.1)CALL OPEN(6,'PPPRRRR DAT',0)
        IF(NPHSE.EQ.2)CALL OPEN(6,'PPPYYYY DAT',0)
        IF(NPHSE.EQ.3)CALL OPEN(6,'PPPBBBB DAT',0)
C
C       If the source closes at 0 degrees it is
```

```
C       assumed that no averaging is required
C
        IF(FSIN(NPHSE).LT.0.017.OR.QL2.EQ.X'4E')LIM3=1
        IF(FSIN(NPHSE).LT.0.017.OR.QL2.EQ.X'4E')GOTO 390
C
C       Determine first averaged value which is less in
C       magnitude than uncompensated response. This is defined
C       as the starting point for averaging
C
        LIM1=IPEAK-IHALF
350     LAVSTA=LIM1
        LAVEND=LAVSTA
        CALL    AVERGE
C
C       SCALING: 225 from 450/2
C
        MSHIFT=MDATA-225
        ISHIFT=IDATA(LIM1)-225
C
        IF(IABS(MSHIFT).LT.IABS(ISHIFT))LIM1=LIM1-1
        IF(LIM1.LT.LAVSTA)GOTO 350
        IF(MSHIFT.EQ.ISHIFT)GOTO 370
360     LIM1=LIM1+1
        LAVSTA=LIM1
        LAVEND=LAVSTA
        CALL    AVERGE
C
C       SCALING: 225 from 450/2
C
        MSHIFT=MDATA-225
        ISHIFT=IDATA(LIM1)-225
C
        IF(IABS(MSHIFT).LE.IABS(ISHIFT))GOTO 370
        GOTO 360
370     LAVEND=4096-IHALF
        LIM3=LAVEND+1
        NDCOPY=LIM1-1
C
C       Copy uncompensated response until start of averaging
C       for processor-modified waveform
C
        DO 380 ICOPY=1,NDCOPY
        MDATA=IDATA(ICOPY)
380     CALL    STOBUF
C
C       Calculate the rest of the uP response
C
        CALL    AVERGE
390     DO 400 ICOPY=LIM3,4096
        MDATA=IDATA(ICOPY)
400     CALL    STOBUF
        ENDFILE 6
410     CONTINUE
C
C       Operator Interaction
C
        CALL    OPEN(6,'UUURRRR DAT',0)
        LIMIT=4096
        CALL    GETVAL
```

```
        ENDFILE 6
        IDSRGE=ISWEEP/5
415     DO 416 I=1,9
416     INDPL(I)=0
        WRITE(3,420)
420     FORMAT(' Operator Interaction ? ')
        READ(3,421)Q10
421     FORMAT(A1)
        IF(Q10.NE.X'59')GOTO 429
        WRITE(3,830)
830     FORMAT(' Peak values: (C)alculate,(P)rint,(N)o ')
        READ(3,840)Q11
840     FORMAT(A1)
        IF(Q11.EQ.X'4E')GOTO 850
        IF(Q11.EQ.X'50')GOTO 875
        NOPEAK=1
        IF(Q1.EQ.X'59')NOPEAK=7
        DO 860 NOPHSE=NOPEAK,10
        IF(NOPHSE.EQ.1)CALL OPEN(6,'UUURRRR DAT',0)
        IF(NOPHSE.EQ.10)CALL OPEN(6,'UUURRRR DAT',0)
        IF(NOPHSE.EQ.2)CALL OPEN(6,'UUUYYYY DAT',0)
        IF(NOPHSE.EQ.3)CALL OPEN(6,'UUUBBBB DAT',0)
        IF(NOPHSE.EQ.7)CALL OPEN(6,'PPPRRRR DAT',0)
        IF(NOPHSE.EQ.8)CALL OPEN(6,'PPPYYYY DAT',0)
        IF(NOPHSE.EQ.9)CALL OPEN(6,'PPPBBBB DAT',0)
        IF(NOPHSE.EQ.4)CALL OPEN(6,'DDDRRRR DAT',0)
        IF(NOPHSE.EQ.5)CALL OPEN(6,'DDDYYYY DAT',0)
        IF(NOPHSE.EQ.6)CALL OPEN(6,'DDDBBBB DAT',0)
        LIMIT=4096
        CALL    GETVAL
        ENDFILE 6
        IF(NOPHSE.EQ.10)GOTO 860
        CALL    PEAKV
860     CONTINUE
875     WRITE(3,880)(PV(I),PT(I),I=1,9)
880     FORMAT(' Ur 'F10.7,' pu at 'F9.2,' us'/
     1' Uy 'F10.7,' pu at 'F9.2,' us'/
     1' Ub 'F10.7,' pu at 'F9.2,' us'/
     1' Dr 'F10.7,' pu at 'F9.2,' us'/
     1' Dy 'F10.7,' pu at 'F9.2,' us'/
     1' Db 'F10.7,' pu at 'F9.2,' us'/
     1' Pr 'F10.7,' pu at 'F9.2,' us'/
     1' Py 'F10.7,' pu at 'F9.2,' us'/
     1' Pb 'F10.7,' pu at 'F9.2,' us'/
     1' ')
850     IF(QL1.NE.X'59')GOTO 424
        WRITE(3,422)
422     FORMAT(' Averaging required for source Z used ? ')
        READ(3,423)QL2
423     FORMAT(A1)
        QL1=X'4E'
        IF(QL2.EQ.X'59')GOTO 424
        GOTO 345
424     WRITE(3,425)IHALF
425     FORMAT(' Half range value is 'I4'. New value ? ')
        READ(3,426)Q9
426     FORMAT(A1)
        IF(Q9.NE.X'59')GOTO 429
        WRITE(3,427)
```

```
427     FORMAT(' Enter new half range value ')
        READ(3,428)NEWRGE
428     FORMAT(I6)
        IHALF=NEWRGE
        GOTO 340
C
C       Waveform Display(s)
C
429     WRITE(3,430)
430     FORMAT(' Single (S)/Three (T) -phase display ? ')
        READ(3,440)Q7
440     FORMAT(A1)
        BU=X'75'
        BP=X'70'
        BD=X'64'
        IF(Q7.EQ.X'53')GOTO 450
        BU=X'72'
        BP=X'79'
        BD=X'62'
450     WRITE(3,460)
460     FORMAT(' For 1-ph display,choose phase R,Y or B,'/
     1' for 3-ph display,choose waveform U,P or D ')
        READ(3,470)WP
470     FORMAT(A1)
        WRITE(3,480)BU,BP,BD,BU,BP,BU,BD,BP,BD,BU,BP,BD
480     FORMAT(' Waveforms/phases to display :-'/
     1' 1- 'A1,/
     2' 2- 'A1,/
     3' 3- 'A1,/
     4' 4- 'A1,' . 'A1,/
     5' 5- 'A1,' . 'A1,/
     6' 6- 'A1,' . 'A1,/
     7' 7- 'A1,' . 'A1,' . 'A1/
     8' ')
        READ(3,490)NWP
490     FORMAT(I1)
        WRITE(3,500)IDSRGE
500     FORMAT(' Normal display range is'I6'us'/
     1' '/
     2' Normal (N),Half (H) or Twice (T) range ? ')
        READ(3,510)Q8
510     FORMAT(A1)
        INCREM=1
        MULRGE=100
        ISTEP=1
        IF(Q8.EQ.X'4E')GOTO 520
        INCREM=2
        MULRGE=50
        IF(Q8.EQ.X'48')GOTO 520
        INCREM=1
        MULRGE=200
        ISTEP=2
520     WRITE(3,530)
530     FORMAT(' Limits for waveform display (in us) ')
        READ(3,540)ISTART,IEND
540     FORMAT(I6,I6)
        ITIM1=1
        IF(ISTART.NE.0)ITIM1=(ISTART/SAMPTM)
        ITIM2=(IEND/SAMPTM)
```

```
        IFLAG=2
550     KYLT=WP
        ICOL=15
        IF(IFLAG.EQ.1)ICOL=0
        KYCO=120
        CALL    WPDISP
C
C       Indicate to WAVDOP that display is required
C
        PLDS=X'44'
C
        IF(WP.NE.X'52'.AND.WP.NE.X'55')GOTO 622
        IF(NWP.EQ.2.OR.NWP.EQ.3)GOTO 622
        IF(NWP.EQ.6)GOTO 622
        JXTIM=110
        ICOL=11
        IF(IFLAG.EQ.1)ICOL=0
        KYLT=BU
        KYCO=150
        DO 620 I=ITIM1,ITIM2,ISTEP
        CALL    XDOT(JXTIM,IDATA(I),ICOL)
620     JXTIM=JXTIM+INCREM
        CALL    WPKEY
        INDPL(1)=1
622     IF(WP.NE.X'59'.AND.WP.NE.X'55')GOTO 624
        IF(NWP.EQ.3)GOTO 624
        IF(Q7.EQ.X'53'.AND.NWP.EQ.2)GOTO 628
        IF(Q7.EQ.X'53'.AND.NWP.EQ.6)GOTO 628
        IF(Q7.EQ.X'54'.AND.NWP.EQ.1)GOTO 640
        IF(Q7.EQ.X'54'.AND.NWP.EQ.5)GOTO 624
        ICOL=11
        KYLT=BU
        KYCO=150
        IF(Q7.EQ.X'53')GOTO 623
        ICOL=8
        KYLT=BP
        KYCO=200
623     IF(IFLAG.EQ.1)ICOL=0
        CALL    OPEN(6,'UUUYYYY DAT',0)
        CALL    WAVDOP
        ENDFILE 6
        CALL    WPKEY
        INDPL(2)=1
624     IF(WP.NE.X'42'.AND.WP.NE.X'55')GOTO 626
        IF(NWP.EQ.2)GOTO 626
        IF(Q7.EQ.X'53'.AND.NWP.EQ.3)GOTO 636
        IF(Q7.EQ.X'53'.AND.NWP.EQ.6)GOTO 630
        IF(Q7.EQ.X'54'.AND.NWP.EQ.4)GOTO 640
        ICOL=11
        KYLT=BU
        KYCO=150
        IF(Q7.EQ.X'53')GOTO 625
        ICOL=4
        KYLT=BD
        KYCO=250
625     IF(IFLAG.EQ.1)ICOL=0
        CALL    OPEN(6,'UUUBBBB DAT',0)
        CALL    WAVDOP
        ENDFILE 6
```

```
        CALL    WPKEY
        INDPL(3)=1
626     IF(WP.NE.X'52'.AND.WP.NE.X'50')GOTO 628
        IF(NWP.EQ.3)GOTO 628
        IF(Q7.EQ.X'53'.AND.NWP.EQ.1)GOTO 640
        IF(Q7.EQ.X'53'.AND.NWP.EQ.5)GOTO 632
        IF(Q7.EQ.X'54'.AND.NWP.EQ.2)GOTO 628
        IF(Q7.EQ.X'54'.AND.NWP.EQ.6)GOTO 628
        ICOL=8
        KYLT=BP
        KYCO=200
        IF(Q7.EQ.X'53')GOTO 627
        ICOL=11
        KYLT=BU
        KYCO=150
627     IF(IFLAG.EQ.1)ICOL=0
        CALL    OPEN(6,'PPPRRRR DAT',0)
        CALL    WAVDOP
        ENDFILE 6
        CALL    WPKEY
        INDPL(4)=1
628     IF(WP.NE.X'50'.AND.WP.NE.X'59')GOTO 630
        IF(NWP.EQ.1.OR.NWP.EQ.3)GOTO 630
        IF(NWP.EQ.5)GOTO 630
        ICOL=8
        IF(IFLAG.EQ.1)ICOL=0
        KYLT=BP
        KYCO=200
        CALL    OPEN(6,'PPPYYYY DAT',0)
        CALL    WAVDOP
        ENDFILE 6
        CALL    WPKEY
        INDPL(5)=1
630     IF(WP.NE.X'42'.AND.WP.NE.X'50')GOTO 632
        IF(NWP.EQ.1)GOTO 632
        IF(Q7.EQ.X'53'.AND.NWP.EQ.5)GOTO 636
        IF(Q7.EQ.X'54'.AND.NWP.EQ.2)GOTO 640
        IF(Q7.EQ.X'54'.AND.NWP.EQ.4)GOTO 640
        ICOL=8
        KYLT=BP
        KYCO=200
        IF(Q7.EQ.X'53')GOTO 631
        ICOL=4
        KYLT=BD
        KYCO=250
631     IF(IFLAG.EQ.1)ICOL=0
        CALL    OPEN(6,'PPPBBBB DAT',0)
        CALL    WAVDOP
        ENDFILE 6
        CALL    WPKEY
        INDPL(6)=1
632     IF(WP.NE.X'52'.AND.WP.NE.X'44')GOTO 634
        IF(NWP.EQ.2)GOTO 634
        IF(Q7.EQ.X'53'.AND.NWP.EQ.4)GOTO 640
        IF(Q7.EQ.X'54'.AND.NWP.EQ.3)GOTO 636
        IF(Q7.EQ.X'54'.AND.NWP.EQ.6)GOTO 634
        ICOL=4
        KYLT=BD
        KYCO=250
```

```
        IF(Q7.EQ.X'53')GOTO 633
        ICOL=11
        KYLT=BU
        KYCO=150
633     IF(IFLAG.EQ.1)ICOL=0
        CALL    OPEN(6,'DDDRRRR DAT',0)
        CALL    WAVDOP
        ENDFILE 6
        CALL    WPKEY
        INDPL(7)=1
634     IF(WP.NE.X'59'.AND.WP.NE.X'44')GOTO 636
        IF(NWP.EQ.1)GOTO 636
        IF(Q7.EQ.X'53'.AND.NWP.EQ.2)GOTO 640
        IF(Q7.EQ.X'53'.AND.NWP.EQ.4)GOTO 640
        IF(Q7.EQ.X'54'.AND.NWP.EQ.5)GOTO 636
        ICOL=4
        KYLT=BD
        KYCO=250
        IF(Q7.EQ.X'53')GOTO 635
        ICOL=8
        KYLT=BP
        KYCO=200
635     IF(IFLAG.EQ.1)ICOL=0
        CALL    OPEN(6,'DDDYYYY DAT',0)
        CALL    WAVDOP
        ENDFILE 6
        CALL    WPKEY
        INDPL(8)=1
636     IF(WP.NE.X'42'.AND.WP.NE.X'44')GOTO 640
        IF(NWP.EQ.1.OR.NWP.EQ.2)GOTO 640
        IF(NWP.EQ.4)GOTO 640
        ICOL=4
        IF(IFLAG.EQ.1)ICOL=0
        KYLT=BD
        KYCO=250
        CALL    OPEN(6,'DDDBBBB DAT',0)
        CALL    WAVDOP
        ENDFILE 6
        CALL    WPKEY
        INDPL(9)=1
C
C       Having displayed waveform(s),time axis is now
C       labelled using CV3.Z80 module
C
640     CONTINUE
650     IFLAG=IFLAG-1
        IF(IFLAG.EQ.0)CALL REAXE
        ITMSC1=IDATA(1)-1
        K=211
        LTIME=MULRGE*SAMPTM
        NTIME=ISTART+LTIME
        LABEL=NTIME
        IUP=0
C
C       8 time axis values to be displayed
C
        DO 660 I=1,8
        NETM=K-50
        CALL    XDOT(K,ITMSC1,15)
```

```
        CALL    XDOT(K,ITMSC1-2,15)
        CALL    XDOT(K,ITMSC1-3,15)
        CALL    CONV
        NTIME=NTIME+LTIME
        K=K+100
660     CONTINUE
C
C       Plot or new display
C
        IF(IFLAG.EQ.0)GOTO 415
        WRITE(3,670)
670     FORMAT(' Plot display ? ')
        READ(3,680)Q5
680     FORMAT(A1)
        IF(Q5.EQ.X'59')GOTO 720
690     WRITE(3,700)
700     FORMAT( ' New display ? ')
        READ(3,710)Q4
710     FORMAT(A1)
        IF(Q4.NE.X'59')GOTO 1010
        IF(IFLAG.EQ.1)GOTO 550
C
C       Waveform plot(s)
C
720     CALL    INPLT
C
C       Indicates to WAVDOP that plot is required
C
        PLDS=X'50'
        KYLT=WP
        KYCO=120
        CALL LBPLOT
        IF(INDPL(1).EQ.0)GOTO 740
        JXTIM=110
        DO 730 I=ITIM1,ITIM2,ISTEP
        IXAX=JXTIM
        IVP=IDATA(I)
        CALL    PLOT
730     JXTIM=JXTIM+INCREM
        KYLT=BU
        KYCO=150
        CALL    LBPLOT
        CALL    CHGPEN
740     IF(INDPL(2).EQ.0)GOTO 750
        CALL    OPEN(6,'UUUYYYY DAT',0)
        CALL    WAVDOP
        ENDFILE 6
        KYLT=BU
        KYCO=150
        IF(Q7.EQ.X'53')GOTO 745
        KYLT=BP
        KYCO=200
745     CALL    LBPLOT
        CALL    CHGPEN
750     IF(INDPL(3).EQ.0)GOTO 760
        CALL    OPEN(6,'UUUBBBB DAT',0)
        CALL    WAVDOP
        ENDFILE 6
        KYLT=BU
```

```
        KYCO=150
        IF(Q7.EQ.X'53')GOTO 755
        KYLT=BD
        KYCO=250
755     CALL    LBPLOT
        CALL    CHGPEN
760     IF(INDPL(4).EQ.0)GOTO 770
        CALL    OPEN(6,'PPPRRRR DAT',0)
        CALL    WAVDOP
        ENDFILE 6
        KYLT=BP
        KYCO=200
        IF(Q7.EQ.X'53')GOTO 765
        KYLT=BU
        KYCO=150
765     CALL    LBPLOT
        CALL    CHGPEN
770     IF(INDPL(5).EQ.0)GOTO 780
        CALL    OPEN(6,'PPPYYYY DAT',0)
        CALL    WAVDOP
        ENDFILE 6
        KYLT=BP
        KYCO=200
        CALL    LBPLOT
        CALL    CHGPEN
780     IF(INDPL(6).EQ.0)GOTO 790
        CALL    OPEN(6,'PPPBBBB DAT',0)
        CALL    WAVDOP
        ENDFILE 6
        KYLT=BP
        KYCO=200
        IF(Q7.EQ.X'53')GOTO 785
        KYLT=BD
        KYCO=250
785     CALL    LBPLOT
        CALL    CHGPEN
790     IF(INDPL(7).EQ.0)GOTO 800
        CALL    OPEN(6,'DDDRRRR DAT',0)
        CALL    WAVDOP
        ENDFILE 6
        KYLT=BD
        KYCO=250
        IF(Q7.EQ.X'53')GOTO 795
        KYLT=BU
        KYCO=150
795     CALL    LBPLOT
        CALL    CHGPEN
800     IF(INDPL(8).EQ.0)GOTO 810
        CALL    OPEN(6,'DDDYYYY DAT',0)
        CALL    WAVDOP
        ENDFILE 6
        KYLT=BD
        KYCO=250
        IF(Q7.EQ.X'53')GOTO 805
        KYLT=BP
        KYCO=200
805     CALL    LBPLOT
        CALL    CHGPEN
810     IF(INDPL(9).EQ.0)GOTO 690
```

```
        CALL    OPEN(6,'DDDBBBB DAT',0)
        CALL    WAVDOP
        ENDFILE 6
        KYLT=BD
        KYCO=250
        CALL    LBPLOT
        GOTO 690
820     END
C
C       Load IBUFF(128 Bytes) with data
C       When full store on disc
C
        SUBROUTINE STOBUF
        COMMON  /IBUFF/IBUFF(64)/INC/INC/MDATA/MDATA
        COMMON  /NBLOCK/NBLOCK
        IBUFF(INC)=MDATA
        IF(INC.NE.64)GOTO 10
        WRITE(6,REC=NBLOCK)IBUFF
        NBLOCK=NBLOCK+1
        INC=1
        GOTO 20
10      INC=INC+1
20      RETURN
        END
C
C       Retrieve data from disc into IBUFF for
C       calculation,display or plot
C
        SUBROUTINE GETBUF
        COMMON  /IBUFF/IBUFF(64)/ISUB/ISUB/NOPOS/NOPOS
        NI=ISUB
        BLOCK=NI/64.00
        NBLOCK=BLOCK
        IF((NBLOCK-BLOCK).NE.0)NBLOCK=NBLOCK+1
        READ(6,REC=NBLOCK)IBUFF
10      NOPOS=NI-64
        IF(NOPOS.LE.0)GOTO 20
        NI=NI-64
        GOTO 10
20      NOPOS=NI
        RETURN
        END
C
C       Display or plot waveforms stored on disc
C
        SUBROUTINE WAVDOP
        BYTE    PLDS
        COMMON  /IBUFF/IBUFF(64)/ISUB/ISUB/ICOL/ICOL
        COMMON  /NOPOS/NOPOS/ITIM1/ITIM1/ITIM2/ITIM2
        COMMON  /INCREM/INCREM/IXAX/IXAX/IVP/IVP/PLDS/PLDS
        COMMON  /ISTEP/ISTEP
        JXTIM=110
        NOPOS=65
        DO 10 ISUB=ITIM1,ITIM2,ISTEP
        IF(NOPOS.LE.64)GOTO 20
        CALL    GETBUF
20      IF(PLDS.EQ.X'44')CALL XDOT(JXTIM,IBUFF(NOPOS),ICOL)
        IF(PLDS.EQ.X'44')GOTO 30
        IXAX=JXTIM
```

```
        IVP=IBUFF(NOPOS)
        CALL    PLOT
30      NOPOS=NOPOS+ISTEP
10      JXTIM=JXTIM+INCREM
        RETURN
        END
C
C       Message to change pen after each waveform plot
C       if > 1 waveform to be plotted
C
        SUBROUTINE CHGPEN
        BYTE    Q6
10      WRITE(3,20)
20      FORMAT(' Changed Pen ? ')
        READ(3,30)Q6
30      FORMAT(A1)
        IF(Q6.NE.X'59')GOTO 10
        RETURN
        END
C
C       Loads IDATA(4096) with waveform disc file
C
        SUBROUTINE GETVAL
        COMMON  /IDATA/IDATA(4096)/IBUFF/IBUFF(64)
        COMMON  /NOPOS/NOPOS/LIMIT/LIMIT/ISUB/ISUB
        NOPOS=65
        DO 10 ISUB=1,LIMIT
        IF(NOPOS.NE.65)GOTO 20
        CALL    GETBUF
20      IDATA(ISUB)=IBUFF(NOPOS)
10      NOPOS=NOPOS+1
        RETURN
        END
C
C       Searches for 1 pu on waveform for determining
C       OV level and starting point for calculation
C       of averaging range
C
        SUBROUTINE PUSECH
        COMMON  /IDATA/IDATA(4096)/IMXRTE/IMXRTE/SPOW/SPOW
C
C       SCALING:80 bits/pu
C
        PU=80.0*SPOW
C
        IPU=IFIX(PU)
        DO 10 I=2,4096
        IF(IABS(IDATA(1)-IDATA(I)).LT.IPU)GOTO 10
        IMXRTE=I
        GOTO 20
10      CONTINUE
20      RETURN
        END
C
C       Process uncompensated response by local averaging
C
        SUBROUTINE AVERGE
        COMMON  /IDATA/IDATA(4096)/MDATA/MDATA
        COMMON  /LAVSTA/LAVSTA/LAVEND/LAVEND/IHALF/IHALF
```

```
      COMMON  /IRANGE/IRANGE
      DO 10 I=LAVSTA,LAVEND
      MDATA=IDATA(I)
      DO 20 J=1,IHALF
      K=I+J
      L=I-J
20    MDATA=MDATA+IDATA(K)+IDATA(L)
      MDATA=MDATA/IRANGE
      IF(LAVEND.EQ.LAVSTA)GOTO 10
      CALL    STOBUF
10    CONTINUE
      RETURN
      END
C
C     Determine which phase switches closest to 90 or 270
C     for IMXRTE and averaging range
C
      SUBROUTINE PHASEM
      COMMON  /FSIN/FSIN(3)/PHSEMX/PHSEMX/ANGLER/ANGLER
      PI=3.14159274101257320
      FSIN(1)=ANGLER
      FSIN(2)=ANGLER+240.0
      FSIN(3)=ANGLER+120.0
      DO 10 I=1,3
      RAD=(FSIN(I)*2.0*PI)/360.0
10    FSIN(I)=ABS(SIN(RAD))
      PHSEMX=AMAX1(FSIN(1),FSIN(2),FSIN(3))
      RETURN
      END
C
C     Determine peak voltage values and times at which
C     they occur on the digitised waveforms
C
      SUBROUTINE PEAKV
      COMMON  /IDATA/IDATA(4096)/NOPHSE/NOPHSE
      COMMON  /SAMPTM/SAMPTM/PV/PV(9)/PT/PT(9)
      IPKVAL=0
      DO 10 KPEAK=1,4096
C
C     SCALING:225 from 450/2
C
      IF(IABS(IDATA(KPEAK)-225).LE.IABS(IPKVAL))GOTO 10
      IPKVAL=IDATA(KPEAK)-225
C
      IPKTIM=KPEAK
10    CONTINUE
C
C     SCALING:80 bits/pu
C
      PV(NOPHSE)=IPKVAL/80.00
      PT(NOPHSE)=IPKTIM*SAMPTM
      RETURN
      END
```

II.2. Program DI3.Z80

```
;       Transfer of waveform data from TR through
;       the Z-2D 8PIO board into IDATA(4096)

;       Port 0:Control flags to T.R.
;       Port 1:Control flags to Cromemco
;       Port 2:Data from T.R. to Cromemco


        ENTRY   DATAI           ;Entry from SIN3P.FOR


        COM     IDATA           ;Store waveform from T.R.
ADD1:   DS      8192            ;8k of storage
        REL

BASE    EQU     60H             ;Base address of 8PIO board

;       Initialise 8PIO

DATAI   LD      A,0F9H          ;Ports 1,2 to i/p,0 to o/p
        OUT     BASE+6,A        ;Polling 'OUT' to port 6
        LD      B,00H           ;Load A and B with zero
        LD      A,00H
        OUT     BASE+0,A        ;Clear TR control lines
        LD      IX,ADD1         ;storage address to I-reg

;       Begin handshake procedure

        LD      A,10H           ;O/P Enable
        OUT     BASE+0,A
        LD      A,30H           ;O/P Request
        OUT     BASE+0,A
WAIT:   IN      A,BASE+1        ;O/P Flag set ?
        BIT     1,A
        JR      Z,WAIT          ;No,wait

;       Transfer data

DARDY:  IN      A,BASE+1        ;Yes,Data Ready Flag set ?
        BIT     0,A
        JR      Z,DARDY         ;No,wait
        IN      A,BASE+2        ;Yes,input data
        LD      (IX+0),A        ;Store data as
        LD      (IX+1),B        ;    two-byte integer
        INC     IX              ;Increment index reg. twice
        INC     IX              ;    for next data
        IN      A,BASE+1        ;End of data transfer ?
        BIT     1,A
        JR      Z,DOUB          ;If finished,double
        LD      A,70H           ;Handshaking with T.R. for
        OUT     BASE+0,A        ;    next data byte
        LD      A,30H           ;Word request to logic '0'
        OUT     BASE+0,A
        JR      DARDY           ;Get next byte

;       Routine to double integer values
```

```
DOUB:   LD      HL,20FFH        ;Count for data doubling
        LD      C,01H           ;C reg gives value of MSB
        LD      IX,ADD1         ;Point to 1st 2-byte value
        SCF                     ;Set carry flag
CLCAR:  CCF                     ;Clear carry flag
        LD      A,(IX+0)        ;Load value into A reg.
        RLA                     ;Double by L shift thru CF
        LD      (IX+0),A        ;Return value to storage
        JR      C,CLOAD         ;If value > 255,carry set
        JR      UPIX            ;If not,(IX+1) remains zero
CLOAD:  LD      (IX+1),C        ;CF set (IX+1) has overflow
        CCF                     ;Clear carry for next value
UPIX:   INC     IX              ;Point to next value
        INC     IX
        DEC     HL              ;Countdown
        DEC     HL
        LD      A,00H
        SUB     H               ;If H zero doubling ended
        JR      NZ,CLCAR
DONE:   RET                     ;Return to FORTRAN SIN3P

        END
```

II.3. Program BL3.Z80

```
;       Using IDATA(1) time and voltage axes
;       are drawn. Voltage axis is labelled

;       Graphic routines external to BL3.Z80

        EXT     XLINE,XDOT,XTEXT

;       Routines called by SIN3P.FOR

        ENTRY   BLINE,TIK,REAXE,WPDISP,WPKEY

        COM     IDATA
ADD1:   DS      8192            ;8k working area
        REL

        COM     TICK
ST08:   DS      8
        REL

        COM     ST011
ST011:  DS      8
        REL

;       Commons for 3-ph key display

        COM     KYLT
LTKY:   DS      1
        REL

        COM     ICOL
COLI:   DS      2
        REL

        COM     KYCO
COKY:   DS      2
        REL

;       Load Time axis data for routine

BLINE   LD      HL,225          ;SCALING:Y-coord of time
        LD      (ADD1),HL       ;axis ie 450/2 in IDATA(1)

        LD      HL,63           ;1st X-coord of Time axis
        LD      (ST01),HL       ;    ,also line colour
        LD      HL,15           ;Colour of axes
        LD      (ST013),HL
        LD      HL,ST013
        LD      (ST015),HL
        LD      HL,960          ;2nd X-coord of Time axis
        LD      (ST02),HL       ;Save
        LD      HL,ST02         ;Load ST02 address in ST03
        LD      (ST03),HL
        LD      HL,ADD1         ;Get Y-coord of Time axis
        LD      (ST04),HL       ;    from 1st value of data
        LD      HL,ST013        ;Load ST01 address in ST05
```

```
        LD      (ST05),HL       ;    for line colour(white)
;
;       Load P.U. axis data for routine
;
        LD      HL,110          ;X-coord of PU axis
        LD      (ST016),HL
        LD      HL,20           ;1st Y-coord of PU axis
        LD      (ST017),HL

        LD      HL,450          ;SCALING:2nd Y-coord
        LD      (ST018),HL

        LD      HL,ST016        ;Store X-coord address
        LD      (ST019),HL      ;    in ST019
        LD      HL,ST018        ;Store 2nd Y-coord address
        LD      (ST019+2),HL    ;    in ST019+2
        LD      HL,ST013        ;Store white colour address
        LD      (ST019+4),HL    ;    in ST019+4

;       Draw p.u. and time axes
;       Called again for new display after
;       axis corruption

REAXE   LD      HL,ST01
        LD      DE,ADD1         ;Set up register-pairs with
        LD      BC,ST03         ;   pointers for subroutine
        CALL    XLINE           ;   call to draw Time axis
        LD      BC,ST019        ;Set pointers in reg-pairs
        LD      DE,ST017        ;    for graphic subroutine
        LD      HL,ST016        ;    to display PU axis
        CALL    XLINE
        RET

;       Scale PU axis by plotting ticks(white)
;       which consist of two dots each

TIK     LD      HL,107          ;X-coord of dot 1
        LD      (ST06),HL
        LD      HL,109          ;X-coord of dot 2
        LD      (ST06+2),HL     ;Save for XDOT sub.

;       SCALING parameter since 80 bits/pu
;       Change if pu excitation or TR Volts
;       Full Scale is altered

        LD      BC,80

        LD      A,04H           ;4 ticks to plot ie
        LD      (ST07),A        ;  1,2,-1,-2 pu
        LD      A,02H           ;2 dots per tick
        LD      (ST07+1),A
        OR      A               ;Clear CF
        LD      HL,(ADD1)       ;Get time axis Y-coord
        ADD     HL,BC           ;Add 80 for 1 pu
        LD      (ST08),HL
        ADD     HL,BC           ;Add 80 for 2 pu
        LD      (ST08+2),HL
        LD      HL,(ADD1)       ;Get zero value
        OR      A               ;Clear CF
```

```
        SBC     HL,BC           ;Value for -1 pu
        LD      (ST08+4),HL
        SBC     HL,BC           ;Value for -2 pu
        LD      (ST08+6),HL
        LD      HL,ST06         ;X-coord pointer
TWICE:  LD      DE,ST08         ;Y-coord pointer
        LD      BC,ST013        ;Dot colour(white)
        PUSH    HL              ;Save HL,DE,BC since
        PUSH    DE              ;  XDOT corrupts
        PUSH    BC
VSCAL:  CALL    XDOT            ;Plot dot
        POP     BC              ;Recover pointers
        POP     DE
        POP     HL
        INC     DE              ;Point to next Y
        INC     DE
        PUSH    HL              ;Save pointers
        PUSH    DE
        PUSH    BC
        LD      A,(ST07)        ;Tick count-1
        DEC     A
        LD      (ST07),A
        JR      NZ,VSCAL
        POP     BC              ;Recover pointers
        POP     DE
        POP     HL
        INC     HL              ;Point to X-coord of
        INC     HL              ;    second dot
        LD      A,(ST07+1)      ;No. of dots/tick -1
        DEC     A
        LD      (ST07+1),A
        JR      Z,FIN           ;Finished ?
        LD      A,04H           ;4 dots for 2nd X-coord
        LD      (ST07),A
        JR      TWICE           ;Plot 2nd dots

;       Label pu axis ie 1,2,-1,-2 pu

FIN:    LD      DE,5            ;For number position

;       SCALING parameter:same as previous

        LD      BC,80

        LD      HL,(ADD1)       ;Get zero pu
        ADD     HL,BC
        ADD     HL,BC           ;Y-coord for 2 pu
        SBC     HL,DE           ;Reposition number
        LD      (ST011),HL
        SBC     HL,BC           ;Y-coord for 1 pu
        LD      (ST011+2),HL
        SBC     HL,BC           ;Zero
        SBC     HL,BC           ;Y-coord for -1 pu
        LD      (ST011+4),HL
        SBC     HL,BC           ;Y-coord for -2 pu
        LD      (ST011+6),HL
        LD      HL,75           ;X-coord of pu nos.
        LD      (ST010),HL
        LD      A,'2'           ;2 for XTEXT
```

```
        LD      (STO14),A
        LD      A,'^'           ;Delimiter for XTEXT
        LD      (STO14+1),A
        LD      HL,STO14
        LD      (STO15+2),HL
        LD      HL,STO10        ;Set pointers
        LD      DE,STO11
        LD      BC,STO15
        CALL    XTEXT           ;Write 2 for +2 pu
        LD      HL,STO10        ;Set pointers
        LD      DE,STO11+6
        LD      BC,STO15
        CALL    XTEXT           ;Write 2 for -2 pu
        LD      A,'1'           ;Prepare to write
        LD      (STO14),A       ;    1 pu
        LD      HL,STO10
        LD      DE,STO11+2
        LD      BC,STO15
        CALL    XTEXT           ;Write 1 for +1 pu
        LD      HL,STO10
        LD      DE,STO11+4
        LD      BC,STO15
        CALL    XTEXT           ;Write 1 for -1 pu
        LD      A,'-'           ;-ve sign for - pu
        LD      (STO14),A
        LD      HL,50           ;X-coord of -ve sign
        LD      (STO10),HL
        LD      HL,STO10
        LD      DE,STO11+4
        LD      BC,STO15
        CALL    XTEXT           ;-ve sign for -1 pu
        LD      HL,STO10
        LD      DE,STO11+6
        LD      BC,STO15
        CALL    XTEXT           ;-ve sign for -2 pu
        RET

;       Routine for 3-ph key display

WPDISP  LD      HL,STOTXT+1
        JR      WPD
WPKEY   LD      HL,STOTXT       ;Include -ve sign
WPD     LD      (BCST+2),HL
        LD      A,(LTKY)        ;Letter to be displayed
        LD      (STOTXT+1),A
        LD      HL,COLI         ;Address of letter colour
        LD      (BCST),HL
        LD      HL,COKY         ;Address of letter coord
        LD      DE,C0000        ;0 coord
        LD      BC,BCST         ;Address of colour and text
        CALL    XTEXT
        RET

;       Storage for axes and labelling displays

STO1:   DS      2
STO2:   DS      2
STO3:   DS      2
STO4:   DS      2
```

```
ST05:   DS      2
ST06:   DS      4
ST07:   DS      2
ST09:   DS      2
ST010:  DS      2
ST013:  DS      2
ST014:  DS      2
ST015:  DS      4
ST016:  DS      2
ST017:  DS      2
ST018:  DS      2
ST019:  DS      6

;       Storage for 3-ph key display

STOTXT: DB      '-'
        DS      1
        DB      '^'
BCST:   DS      4
C0000:  DEFW    5

        END
```

II.4. Program CV3.Z80

```
;       The time axis is labelled by taking
;       values from SIN3P.FOR

;       Graphic routine called by CV3.Z80

        EXT     XTEXT

;       Routines called by SIN3P and Z80 modules

        ENTRY   CONV,ASCON

        COM     NTIME           ;Timebase value
ADD3:   DS      2
        REL

        COM     NETM            ;X-coord for timebase
ADD4:   DS      2               ;    value display
        REL

        COM     IFLAG           ;Flag to indicate
ADD5:   DS      2               ;whether to display or
        REL                     ;remove value

        COM     IUP             ;Flag to change Y-coord
ADD6:   DS      2               ; of value > 3 digits
        REL

        COM     ASC             ;Data area for integers
ASCII:  DS      6               ; converted to ASCII
        REL

CONV    LD      A,'^'           ;Text delimiter at end
        LD      (ASCII+5),A     ;    of ASCII message
        LD      HL,(ADD3)       ;Integer data for ASCII
        CALL    ASCON           ; conversion for XTEXT sub.
        LD      (STO20+2),IX    ;Store pointer to 1st
                                ;   non-zero ASCII no.
        LD      A,B             ;Is no. 4 or more digits ?
        CP      2
        JR      NC,REMOVE       ;If yes use other Y-coord
        LD      A,(ADD6+1)      ;Check flag for last
        CP      0               ;   Y-coord used when
        CPL                     ;   value > 3 digits
        LD      (ADD6+1),A
        JR      NZ,REMOVE
        LD      DE,YHITE2       ;Load alternative Y-coord
        JR      REM1
REMOVE: LD      DE,YHITE
REM1:   LD      A,(ADD5)        ;Remove timebase scaling ?
        CP      1
        JR      Z,ORDPLO
        LD      HL,DCOLOR       ;Display in background
        LD      (STO20),HL      ; colour ie remove
        JR      TIMBAS          ; timebase value
ORDPLO: LD      HL,COLOR        ;Display in white
```

```
        LD      (ST020),HL
TIMBAS: LD      BC,ST020
        LD      HL,ADD4
        CALL    XTEXT           ;Write value to monitor
        RET

;       ASCII conversion routine

ASCON:  LD      IY,P10TAB       ;Power of Ten Table
        LD      IX,ASCII        ;Address ASCII code store
LOOPO:  XOR     A               ;Clear accumulator
        LD      D,(IY+1)
        LD      E,(IY+0)        ;Load power of ten to DE
LOOP1:  OR      A               ;Clear carry
        SBC     HL,DE           ;HL minus power of 10
        JR      C,JUMP1         ;Go if negative
        INC     A               ;Increment count
        JR      LOOP1
JUMP1:  ADD     HL,DE           ;Restore integer
        ADD     A,30H           ;Convert no. to ASCII
        LD      (IX+0),A        ;Store ASCII code
        INC     IX              ;Increment for next ASCII
        INC     IY
        INC     IY              ;Next power of 10
        LD      A,E             ;Conversion complete ?
        CP      1
        JR      NZ,LOOPO
        LD      IX,ASCII        ;Eliminate ASCII zeroes
        LD      B,00H           ;B-reg holds zero count
        JR      FECHO
COWNT:  INC     B
        INC     IX              ;Point to next character
FECHO:  LD      A,(IX+0)        ;Get next ASCII character
        CP      30H             ;ASCII 0 ?
        JR      Z,COWNT         ;If yes inc B count and IX
        RET

;       Power of ten table and store

P10TAB: DEFW    10000
        DEFW    1000
        DEFW    100
        DEFW    10
        DEFW    1
YHITE:  DEFW    28
YHITE2: DEFW    50
COLOR:  DEFW    15
DCOLOR: DEFW    0
ST020:  DS      4

        END
```

II.5. Program IP3.Z80

```
;       Digital plotter is initialised. X and Y
;       axes are plotted and labelled
;       Routines called by IP3.Z80 module

        EXT     ASCON,CHECKO

;       Routines called by SIN3P and Z80 modules

        ENTRY   INPLT,VARSTO,TRANS

;       Data passed from SIN3P and Z80 modules

        COM     ASC
ASCII:  DS      6
        REL

        COM     TICK
ST08:   DS      8
        REL

        COM     ST011
ST011:  DS      8
        REL

        COM     LTIME
ADD9:   DS      2
        REL

        COM     LABEL
ADD10:  DS      2
        REL

TBASE   EQU     0A0H            ;Device B Base Address
BAUD    EQU     90H             ;Baud Rate 2400,1 stop bit
NORMAD  EQU     00H             ;Bit 7,// O/P norm address

INPLT   LD      A,00H           ;Initialise byte
        LD      (DSAVE),A       ;     transfer count
        LD      A,BAUD          ;Set baud rate and stop bit
        OUT     TBASE+0,A
        LD      A,NORMAD        ;Set normal addressing
        OUT     TBASE+4,A
        LD      IY,SEOM         ;Set output mode and
        CALL    TRANS           ;    handshake protocol
        LD      IY,SCALE        ;Scale plotter and
        CALL    TRANS           ;    draw Y-axis
        LD      IY,PLXAX        ;Draw X axis and label
        CALL    TRANS           ;    both axes

        LD      IX,ST08         ;Address for Tick data
        LD      C,4             ;No. Y-axis ticks plotted
TICAG:  LD      H,(IX+1)        ;Prepare to convert data
        LD      L,(IX+0)
        PUSH    IX              ;Save tick data address
        CALL    ASCON           ;Convert to ASCII string
        CALL    CHECKO          ;Three byte no. ?
```

```
        LD      IY,VAST3        ;Store data at address
        CALL    VARSTO          ;    during plot routine
        LD      IY,TICKY        ;Start address of tick plot
        CALL    TRANS           ;Data from uP to plotter
        POP     IX              ;Retrieve address of data
        INC     IX              ;Point to next value
        INC     IX
        DEC     C               ;All ticks plotted ?
        JR      NZ,TICAG        ;No,plot next one

        LD      IX,STO11        ;Address for Y axis
                                ;    labelling data
        LD      C,4             ;4 labels 1,2,-1,-2 pu
PRTNO2: LD      A,'2'           ;ASCII 2 to plot
        LD      (VAST5),A       ;    data block
PRTNO:  PUSH    IX              ;Save pointer
        LD      H,(IX+1)        ;Get Y-coord of label
        LD      L,(IX+0)
        CALL    ASCON           ;Convert
        CALL    CHECKO          ;Three byte no. ?
        LD      IY,VAST4        ;Store converted integer
        CALL    VARSTO          ;    in plot data block
        LD      IY,NUMBER       ;Plot figure
        CALL    TRANS
        DEC     C               ;Label count -1
        JR      Z,NEGSN         ;Figures plotted,plot -'s
        POP     IX              ;Retrieve pointer
        INC     IX              ;Point to next Y-coord
        INC     IX
        LD      A,'1'           ;ASCII 1 to block
        LD      (VAST5),A
        LD      A,C
        CP      1
        JR      NZ,PRTNO
        JR      Z,PRTNO2        ;1's plotted,plot 2nd '2'

NEGSN:  LD      A,'-'           ;ASCII -ve to plot block
        LD      (VAST14),A
        LD      C,2             ;2 -ve signs to plot
        LD      IX,STO11+4      ;Point to Y-coord of -1 pu
NEGTW:  PUSH    IX              ;Save pointer
        LD      H,(IX+1)        ;Get Y-coord
        LD      L,(IX+0)
        CALL    ASCON           ;Convert to ASCII
        CALL    CHECKO          ;Three byte no. ?
        LD      IY,VAST13       ;Store converted value
        CALL    VARSTO          ;    in plot data block
        LD      IY,NEGSIN       ;Plot -ve sign
        CALL    TRANS
        POP     IX              ;Point to Y-coord for
        INC     IX              ;    -2 pu
        INC     IX
        DEC     C               ;-ve sign count -1
        JR      NZ,NEGTW
        LD      C,8             ;No. of timebase values
        LD      A,32H           ;1st X digit for timebase
        LD      (VAST6),A       ;Store in plot data block
        LD      (VAST8),A
        LD      HL,(ADD10)      ;Fetch 1st timebase figure
```

```
AGAIN:  PUSH    HL              ;Save timebase value
        CALL    ASCON           ;Convert value for plotter
        POP     HL              ;Retrieve timebase value
        LD      D,B             ;Store no. of ASCII 0's
        LD      A,00H           ;Load acc. with ASCII NOP
        LD      IX,VAST9        ;Add. plot timebase store
LDNOP:  LD      (IX+0),A        ;NOP instead of ASCII 0
        INC     IX
        DEC     B               ;Finished loading NOP's ?
        JR      NZ,LDNOP
        LD      IY,ASCII        ;Point to 1st non-zero
FSTNO:  INC     IY              ;    ASCII number
        DEC     D
        JR      NZ,FSTNO
STPLNO: LD      A,(IY+0)        ;Non-zero ASCII nos.
        CP      '^'             ;    loaded into plot
        JR      Z,HAND          ;    data block
        LD      (IX+0),A
        INC     IX
        INC     IY
        JR      STPLNO
HAND:   LD      IY,TICKX        ;Plot tick and
        CALL    TRANS           ;     timebase values
        LD      A,(VAST6)       ;Increment 100's digit ie
        INC     A               ;    1st digit of X-coord
        LD      (VAST6),A       ;    of tick and label
        LD      (VAST8),A       ;Store
        LD      DE,(ADD9)       ;Next timebase X position
        ADD     HL,DE
        DEC     C
        JR      NZ,AGAIN
        RET

;       Transfer Control Instructions and Plotting Data

TRANS:  LD      A,(DSAVE)       ;DSAVE stored in D-reg for
        LD      D,A             ;    byte transfer count
CHTBE:  IN      A,TBASE+0       ;Check status reg for TBE
        BIT     7,A             ;T B empty ?
        JR      Z,CHTBE         ;No,check again
        LD      A,(IY+0)        ;Start sequence
        CP      0FFH            ;End of command string ?
        JR      Z,EOS           ;Yes,return
        OUT     TBASE+1,A       ;No,byte to plotter
        INC     D               ;Byte transfer count +1
        LD      A,D             ;100 bytes to plotter ?
        CP      100
        JR      NZ,OPBYTE       ;No,continue with transfer
HANDSH: IN      A,TBASE+0       ;T B empty ?
        BIT     7,A
        JR      Z,HANDSH        ;No,check again
        LD      A,11H           ;Yes,transfer handshake
        OUT     TBASE+1,A       ;    byte for buffer space
WORD1:  IN      A,TBASE+0       ;Reply received ?
        BIT     6,A
        JR      Z,WORD1         ;No,check again
        IN      A,TBASE+1       ;Yes
        CP      12H             ;Buffer accept 100 bytes ?
        JR      NZ,WORD1        ;No,wait until it can
```

```
        LD      D,00H           ;Yes,reset bytes sent count
OPBYTE: INC     IY              ;Next byte of string
        JP      CHTBE
EOS:    LD      A,D             ;Byte transfer count
        LD      (DSAVE),A       ;    saved in DSAVE
        RET

;       Subroutine to store ASCII-coded integer
;       to memory defined by IY index reg.

VARST0: LD      B,03H           ;3 Byte no.,so 3 for count
STASH:  LD      A,(IX+0)        ;Load 1st non-zero-ASCII
        LD      (IY+0),A        ;Store
        DEC     B               ;Count -1
        INC     IY              ;Next address
        INC     IX              ;Next byte
        JR      NZ,STASH
        RET

;       Data block to set plotter output mode
;       and handshake protocol

SEOM:   DW      2E1BH,':M'
        DW      2E1BH,';@',':0',2E1BH
        DW      '1I','00','1;',';7','81'
        DW      0FF3AH

;       Data block to scale plotter and plot Y axis

SCALE:  DW      2E1BH,'S(','-C','02','1,'
        DW      '00',',0',',0','54',';0','AP'
        DW      '11',',0','54',';0','DP','P;'
        DW      '1A','01','2,',';0','UP'
        DW      0FF3BH

;       Data block to draw X axis and label both axes

PLXAX:  DW      'AP','36','2,','52'
        DB      ';'
        DW      'DP','P;','9A','06','2,','52'
        DW      'P;',';U','AP','5-','2,','05'
        DB      ';'
        DW      'ID',',0',';1','BL','oV'
        DW      'tl','ga','(e','.p','.u'
        DB      ')'
        DB      03H
        DW      'P;','8A','00','0,','D;','1I'
        DW      '0,','L;','TB','mi','(e','Su'
        DB      ')'
        DB      03H
        DB      ';'
        DB      0FFH

;       Data block to tick Y axis

TICKY:  DW      'AP','01',',7'
VAST3:  DS      3
        DW      'P;',';D','TY','P;',';U'
        DB      0FFH
```

```
;       Data block to scale Y axis ie 1,2 pu etc

NUMBER: DW      'IS','.0',',3','.0',';8','AP','06'
        DB      ','
VAST4:  DS      3
        DW      'D;','1I','0,','L;'
        DB      'B'
VAST5:  DS      1
        DB      03H
        DW      'S;',';I'
        DB      0FFH

;       Data block to tick and label X axis

TICKX:  DW      'AP'
VAST6:  DS      1
        DW      '11','2,','52','P;'
        DW      ';D','TX','P;',';U','AP'
VAST8:  DS      1
        DW      '11','2,','05','S;',';I','BL'
VAST9:  DS      5
        DB      03H
        DB      ';'
        DB      0FFH

;       Data block to plot negative signs for pu axis

DSAVE:  DS      1
NEGSIN: DW      'IS','.0',',3','.0',';8','AP','04'
        DB      ','
VAST13: DS      3
        DW      'D;','1I','0,','L;'
        DB      'B'
VAST14: DS      1
        DB      03H
        DW      'S;',';I'
        DB      0FFH
        END
```

II.6. Program PL3.Z80

```
;       Waveform data is passed from SIN3P and plotted

;       Z80 routines called

        EXT     ASCON,VARSTO,TRANS

;       Routines called by SIN3P and Z80 files

        ENTRY   PLOT,CHECKO,LBPLOT

;       Data passed from SIN3P.FOR

        COM     IXAX            ;Store for X-coord of plot
ADD7:   DS      2
        REL

        COM     IVP             ;Store for Y-coord of plot
ADD8:   DS      2
        REL

;       Commons for LBPLOT

        COM     KYLT
LTKY:   DS      1
        REL

        COM     KYCO
COKY:   DS      2
        REL

PLOT    LD      HL,(ADD7)       ;Load X-coord into HL
        CALL    ASCON           ;Convert X-coord to ASCII

;       No check needed as it is a 3-digit number

        LD      IY,XCOORD       ;Load index reg with data
        CALL    VARSTO          ;    destination,store
        LD      HL,(ADD8)       ;Load Y-coord. into HL
        CALL    ASCON           ;Convert Y-coord to ASCII
        CALL    CHECKO          ;Check no. of ASCII 0's
        LD      IY,YCOORD       ;    so IX points to 1st
        CALL    VARSTO          ;    of 3 digits,store in
        LD      IY,PUPD         ;    plotter data block
        CALL    TRANS           ;Send plotter data block
        RET

LBPLOT  LD      A,'-'
        LD      (SPCNEG),A      ;Sign if X is not 110
        LD      BC,110          ;Test for 110 value of X
        SCF                     ;Set carry flag
        CCF                     ;Clear carry flag
        LD      HL,(COKY)       ;Fetch coord
        SBC     HL,BC           ;Is it 110 ?
        JR      NZ,GETLET       ;No
        LD      A,00H           ;Yes, NOP instead of
```

```
        LD      (SPCNEG),A      ;    -ve sign
GETLET: LD      A,(LTKY)        ;Letter for key label
        LD      (LETTER),A
        LD      HL,(COKY)       ;Fetch no. for ASCII
        CALL    ASCON           ;    conversion

;       No check needed as KYCO is a 3-digit number

        LD      IY,XKEY
        CALL    VARSTO          ;Store in data block
        LD      IY,KEYPLT       ;Send data block
        CALL    TRANS
        RET


CHECKO: LD      A,B
        CP      3               ;ASCII no. have 3 O's ?
        JR      NZ,BFOUR        ;No,try 4 otherwise
        DEC     IX              ;IX ->1st of 3 digits
        LD      A,OOH           ;Fill with NOP
        LD      (IX+O),A
        JR      CHSTOP          ;Finished
BFOUR:  LD      A,B             ;4 ?
        CP      4
        JR      NZ,BFIVE        ;No,try 5
        DEC     IX              ;Yes
        LD      A,OOH
        LD      (IX+O),A
        DEC     IX
        LD      (IX+O),A        ;Fill with NOP's
        JR      CHSTOP          ;Finished
BFIVE:  LD      A,B             ;5 ?
        CP      5
        JR      NZ,CHSTOP       ;No
        DEC     IX              ;Leave ASCII O(last digit)
        DEC     IX              ;    and fill 3,4 with NOP
        LD      A,OOH
        LD      (IX+O),A
        DEC     IX
        LD      (IX+O),A
CHSTOP: RET

;       Block containing plotter commands and plot data

PUPD:   DW      'AP'
XCOORD: DS      3
        DB      ','
YCOORD: DS      3
        DB      ';'
        DW      'DP'
        DB      ';'
        DB      OFFH

;       Block containing key labelling data

KEYPLT: DW      'UP','P;'
        DB      'A'
XKEY:   DS      3
        DW      'O,','S;',';I','BL'
```

```
SPCNEG: DS      1
LETTER: DS      1
        DB      03H
        DB      ';'
        DB      0FFH

        END
```

APPENDIX III

Modified Fourier Transform

III.1. Program to Calculate Modified Fourier Transform Responses

```
C       This program calculates the voltage at the
C       receiving-end of a distributed-parameter line
C       (using the Modified Fourier Transform) due to
C       step excitation
C
C
        DIMENSION TIME(2500),AMPL(2500),MSTIME(20)
        COMPLEX AW,CCOSH,X
        COMPLEX CTL,CBL,CPS1,CPS2
        CCOSH(X)=(CEXP(X)+CEXP(-X))/(2.0,0.0)
C
C       Values of inductance/mile,capacitance/mile,
C       resistance/mile and the length of line
C
        C=880E-12
        FL=5.42E-4
        R=0.166
        D=25.0
        PI=4.0*ATAN(1.0)
        NALLOW=0
C
C       Input of data
C
        WRITE(5,10)
10      FORMAT(' Frequency Limits(Omega) ? ',$)
        READ(5,20)IOMEGA
20      FORMAT(I)
        WRITE(5,30)
30      FORMAT(' Value of "a" (Pole Shift Factor) ? ',$)
        READ(5,40)IA
40      FORMAT(I)
        A=FLOAT(IA)
        WRITE(5,50)
50      FORMAT(' Frequency Step Length ? ',$)
        READ(5,60)ISTEP
60      FORMAT(I)
        WRITE(5,70)
70      FORMAT(' Time Range(Microseconds), ')
        WRITE(5,80)
80      FORMAT(' and Time Step Length ? ',$)
        READ(5,90)ILEN,ITIME
90      FORMAT(I,I)
        WRITE(5,100)
100     FORMAT(' For no Sigma Factor,enter "0", '/
        1 ' Standard Sigma Factor,enter "1", '/
        2 ' Modified Sigma Factor,enter "-1" '/
        3 ' For Both Sigma Factors,enter "2" ')
        READ(5,110)NSIG
110     FORMAT(I)
        IF(NSIG.NE.2)GOTO 170
```

```
      WRITE(5,120)
120   FORMAT(' No. of averaging changes ? ')
      READ(5,130)NCHANG
130   FORMAT(I)
      DO 160 I=1,NCHANG
      WRITE(5,140)
140   FORMAT(' Time of averaging change(us) ? ')
      READ(5,150)MSTIME(I)
150   FORMAT(I)
160   CONTINUE
      NSIG=1
      INDIC=1
      NALLOW=2
C
C     Calculation of Vr
C
170   ISUB=0
      DO 230 I=0,ILEN,ITIME
      IF(NALLOW.NE.2)GOTO 180
      IF(I.NE.MSTIME(INDIC))GOTO 180
      NSIG=-NSIG
      INDIC=INDIC+1
180   ISUB=ISUB+1
      CPS1=(0.0,0.0)
      DO 220 W=-IOMEGA,IOMEGA,ISTEP
      IF(W.EQ.0.0)GOTO 220
      AW=CMPLX(A,W)
      CTL=(CEXP((AW)*I*1E-6))*ISTEP
      CBL=(AW)*CCOSH(D*CSQRT((R+(AW)*FL)*(AW)*C))
      CPS2=CTL/CBL
      IF(NSIG)190,210,200
190   CPS2=CPS2*(SIN(W*PI/(2*IOMEGA)))/(W*PI/(2*IOMEGA))
      IF(NSIG.EQ.-1)GOTO 210
200   CPS2=CPS2*(SIN(W*PI/IOMEGA))/(W*PI/IOMEGA)
210   CPS1=CPS1+CPS2
220   CONTINUE
      TIME(ISUB)=I
      AMPL(ISUB)=CABS(CPS1)*1/(PI*2)
230   CONTINUE
C
C     Graphical output
C
      FLEN=FLOAT(ILEN)
      CALL PAPER(1)
      CALL PSPACE(0.4,0.9,0.4,0.9)
      CALL MAP(0.0,FLEN,-0.5,2.2)
      CALL AXES
      CALL POSITN(0.0,0.0)
      DO 240 I=1,ISUB
      CALL JOIN(TIME(I),AMPL(I))
240   CONTINUE
      CALL MAP(0.0,100.0,-2.8,2.8)
      CALL CTRMAG(15)
      CALL PLOTCS(2.0,2.7,'V',1)
      CALL CTRSET(2)
      CALL PLOTCS(4.0,2.7,'(PU)',4)
      CALL CTRSET(1)
      CALL PLOTCS(86.0,-2.7,'T',1)
      CALL CTRSET(2)
```

```
CALL PLOTCS(88.0,-2.7,'IME(US)',7)
CALL CTRSET(1)
IF(NSIG.EQ.0)
1 CALL PLOTCS(10.0,-2.7,'NO SIGMA FACTORS',16)
IF(NSIG.EQ.1)
1 CALL PLOTCS(10.0,-2.7,'STANDARD SIGMA FACTOR',21)
IF(NSIG.EQ.-1)
1 CALL PLOTCS(10.0,-2.7,'MODIFIED SIGMA FACTOR',21)
IF(NSIG.EQ.2)
1 CALL PLOTCS(10.0,-2.7,'BOTH SIGMA FACTORS',18)
CALL GREND
STOP
END
```

APPENDIX IV

Source Inductance/Peak Overvoltage Results

IV.1. Source Inductance/Peak Overvoltage Tables

The following tables give the peak overvoltage values, shown graphically in Figures 5.24 - 5.32, obtained from the model line energisation experiments described in section 5.6.2. The three columns consist of the 50 Hz value of source inductance L_s, the peak voltage values obtained from the uncompensated line, with or without the application of averaging techniques, UP(Uncompensated or Processor) and the peak voltage values recorded from the compensated or damped line in column D.

With reference to the UP column the following key can be referred to which indicates whether an uncompensated or processor value is chosen and the averaging technique used when averaging of the uncompensated waveform was necessary.

1. * indicates that the uncompensated value was used i.e. no averaging techniques were necessary since the uncompensated waveform displayed no Gibbs phenomena.
2. m indicates that the peak value was obtained by averaging of the uncompensated waveform using S_{ae}.
3. A UP peak value with no symbol indicates that averaging of the uncompensated waveform was achieved by using S_{se} with N_s=15 μs.

All 1-phase results were taken for the worst case point-on-wave closure of 90° while 3-phase simultaneous closure was carried out with a closure of 90° on the red phase.

IV.2. 5 Π-Section Line Zero Earth Impedance

L_s(H)	UP(pu)	D(pu)	L_s(H)	UP(pu)	D(pu)
0.0	2.0875	2.1	0.24	1.9625	1.95
0.0024	2.075	2.1	0.2601	1.95	1.95
0.0051	2.0625	2.05	0.2799	1.9375	1.95
0.0075	2.05	2.0	0.3	1.9375	1.95
0.0099	1.9875	2.0	0.321	1.9375	1.95
0.015	2.1	2.025	0.339	1.9375	1.95
0.0201	2.25 *	2.075	0.36	1.9375	1.925
0.0249	2.2 *	2.125	0.381	1.9375	1.925
0.03	2.25 *	2.15	0.399	1.925	1.925
0.0351	2.225 *	2.15	0.42	1.925	1.925
0.0399	2.225 *	2.15	0.441	1.9125	1.925
0.045	2.2 *	2.125	0.459	1.9125	1.925
0.0501	2.175 *	2.125	0.48	1.9125	1.925
0.06	2.125 *	2.075	0.501	1.9125	1.925
0.0699	2.05 *	2.025	0.549	1.9	1.9
0.0801	2.0 *	2.0	0.6	1.9	1.9
0.09	2.0 *	2.0	0.651	1.8875	1.875
0.0999	2.025	1.975	0.699	1.8875	1.875
0.12	2.0	2.0	0.75	1.8875	1.875
0.1401	1.9875	2.0	0.801	1.875	1.875
0.1599	1.975	1.975	0.849	1.875	1.875
0.18	1.9625	1.975	0.9	1.85	1.85
0.2001	1.95	1.975	0.951	1.85	1.85
0.2199	1.9625	1.95	0.999	1.85	1.85

IV.3. 10 Il-Section Line Zero Earth Impedance

L_s(H)	UP(pu)	D(pu)	L_s(H)	UP(pu)	D(pu)
0.0	2.05 m	2.025	0.24	1.975	1.975
0.0024	2.0375m	2.05	0.2601	1.975	1.975
0.0051	2.0375m	2.05	0.2799	1.9625	1.95
0.0075	2.0125m	2.0	0.3	1.95	1.95
0.0099	1.975 m	1.975	0.321	1.9375	1.925
0.015	1.9625	1.975	0.339	1.925	1.925
0.0201	2.025	2.0	0.36	1.9	1.9
0.0249	2.15 *	2.025	0.381	1.8875	1.9
0.03	2.175 *	2.1	0.399	1.875	1.875
0.0351	2.25 *	2.125	0.42	1.875	1.875
0.0399	2.275 *	2.15	0.441	1.875	1.875
0.045	2.3 *	2.175	0.459	1.875	1.875
0.0501	2.3 *	2.2	0.48	1.875	1.875
0.06	2.275 *	2.2	0.501	1.875	1.875
0.0699	2.25 *	2.2	0.549	1.925	1.925
0.0801	2.225 *	2.175	0.6	1.95	1.925
0.09	2.2 *	2.15	0.651	1.95	1.95
0.0999	2.15 *	2.125	0.699	1.95	1.95
0.12	2.075	2.05	0.75	1.925	1.925
0.1401	2.0	2.0	0.801	1.9	1.9
0.1599	1.9625	1.975	0.849	1.875	1.875
0.18	1.9375	1.95	0.9	1.85	1.85
0.2001	1.95	1.95	0.951	1.8125	1.825
0.2199	1.9625	1.975	0.999	1.7625	1.75

IV.4. 20 Π-Section Line Zero Earth Impedance

L_s(H)	UP(pu)	D(pu)	L_s(H)	UP(pu)	D(pu)
0.0	2.0375m	2.025	0.24	1.9875	1.975
0.0024	2.0625m	2.025	0.2601	2.075	2.025
0.0051	2.0125m	2.0	0.2799	2.1	2.05
0.0075	2.025 m	2.0	0.3	2.05	2.025
0.0099	1.9875m	1.95	0.321	2.0	2.025
0.015	1.9625m	1.95	0.339	2.025	2.0
0.0201	2.025	1.95	0.36	2.0375	2.0
0.0249	2.125	1.95	0.381	2.0	2.0
0.03	2.1 *	1.95	0.399	1.9875	1.975
0.0351	2.1 *	1.975	0.42	1.925	1.9
0.0399	2.125 *	2.0	0.441	1.9	1.9
0.045	2.175 *	2.025	0.459	1.875	1.85
0.0501	2.175 *	2.05	0.48	1.825	1.825
0.06	2.225 *	2.1	0.501	1.825	1.8
0.0699	2.225 *	2.125	0.549	1.8	1.8
0.0801	2.225 *	2.15	0.6	1.775	1.775
0.09	2.225 *	2.15	0.651	1.9375	1.925
0.0999	2.225 *	2.15	0.699	2.0125	2.025
0.12	2.2	2.15	0.75	2.125	2.125
0.1401	2.15	2.125	0.801	2.1625	2.175
0.1599	2.1125	2.1	0.849	2.175	2.175
0.18	2.075	2.075	0.9	2.15	2.15
0.2001	2.05	2.05	0.951	2.2	2.2
0.2199	2.025	2.025	0.999	2.25	2.25

IV.5. 5 Π-Section Line Earth Path Impedance

L_s(H)	UP(pu)	D(pu)	L_s(H)	UP(pu)	D(pu)
0.0	1.975	2.0	0.24	1.975 *	1.95
0.0024	1.975	1.975	0.2601	1.95 *	1.925
0.0051	1.95	1.975	0.2799	1.95 *	1.95
0.0075	1.95	1.95	0.3	1.925 *	1.925
0.0099	1.95	1.95	0.321	1.925 *	1.925
0.015	1.9625	1.975	0.339	1.95 *	1.95
0.0201	2.0125	2.025	0.36	1.9 *	1.925
0.0249	2.075 *	2.05	0.381	1.925 *	1.9
0.03	2.125 *	2.075	0.399	1.925 *	1.925
0.0351	2.125 *	2.1	0.42	1.9 *	1.9
0.0399	2.175 *	2.1	0.441	1.925 *	1.9
0.045	2.15 *	2.125	0.459	1.9 *	1.875
0.0501	2.15 *	2.1	0.48	1.95 *	1.925
0.06	2.125 *	2.1	0.501	1.925 *	1.9
0.0699	2.1 *	2.075	0.549	1.875 *	1.85
0.0801	2.05 *	2.05	0.6	1.85 *	1.85
0.09	2.025 *	2.0	0.651	1.875 *	1.85
0.0999	2.0 *	2.0	0.699	1.9 *	1.9
0.12	1.975 *	1.95	0.75	1.875 *	1.875
0.1401	1.975 *	1.95	0.801	1.875 *	1.9
0.1599	2.0 *	1.975	0.849	1.875 *	1.85
0.18	2.0 *	1.975	0.9	1.85 *	1.875
0.2001	1.975 *	1.95	0.951	1.825 *	1.825
0.2199	1.975 *	1.95	0.999	1.8 *	1.8

IV.6. 10 Π-Section Line Earth Path Impedance

L_s(H)	UP(pu)	D(pu)	L_s(H)	UP(pu)	D(pu)
0.0	1.9	1.925	0.24	1.95 *	1.925
0.0024	1.9125	1.925	0.2601	1.95 *	1.95
0.0051	1.9125	1.95	0.2799	1.95 *	1.95
0.0075	1.9125	1.95	0.3	1.95 *	1.95
0.0099	1.925	1.925	0.321	1.95 *	1.95
0.015	1.925	1.95	0.339	1.95 *	1.95
0.0201	1.95	1.95	0.36	1.95 *	1.95
0.0249	2.0 *	1.975	0.381	1.925 *	1.925
0.03	2.05 *	2.0	0.399	1.925 *	1.925
0.0351	2.075 *	2.025	0.42	1.925 *	1.925
0.0399	2.1 *	2.05	0.441	1.875 *	1.875
0.045	2.125 *	2.075	0.459	1.9 *	1.9
0.0501	2.125 *	2.075	0.48	1.875 *	1.875
0.06	2.175 *	2.1	0.501	1.875 *	1.875
0.0699	2.175 *	2.125	0.549	1.825 *	1.825
0.0801	2.175 *	2.125	0.6	1.875 *	1.875
0.09	2.15 *	2.125	0.651	1.95 *	1.95
0.0999	2.15 *	2.125	0.699	1.95 *	1.975
0.12	2.1 *	2.075	0.75	2.0 *	1.975
0.1401	2.075 *	2.05	0.801	2.0 *	2.0
0.1599	2.025 *	2.025	0.849	2.025 *	2.025
0.18	2.0 *	2.0	0.9	2.0 *	2.0
0.2001	1.975 *	1.975	0.951	2.0 *	2.025
0.2199	1.95 *	1.95	0.999	1.975 *	1.975

IV.7. 20 Π-Section Line Earth Path Impedance

L_s(H)	UP(pu)	D(pu)	L_s(H)	UP(pu)	D(pu)
0.0	1.8625	1.9	0.24	2.025 *	2.0
0.0024	1.8875	1.9	0.2601	2.025 *	2.0
0.0051	1.8625	1.9	0.2799	1.975 *	1.975
0.0075	1.8625	1.9	0.3	1.975 *	1.95
0.0099	1.8625	1.9	0.321	1.975 *	1.975
0.015	1.8625	1.9	0.339	1.975 *	1.975
0.0201	1.875	1.9	0.36	2.0 *	2.0
0.0249	1.875 *	1.9	0.381	2.0 *	2.025
0.03	1.875 *	1.925	0.399	2.0 *	2.0
0.0351	1.925 *	1.9	0.42	1.975 *	2.0
0.0399	1.95 *	1.9	0.441	1.95 *	1.975
0.045	1.975 *	1.925	0.459	1.95 *	1.975
0.0501	1.975 *	1.925	0.48	1.95 *	1.95
0.06	2.025 *	1.975	0.501	1.95 *	1.95
0.0699	2.05 *	2.0	0.549	1.9 *	1.9
0.0801	2.05 *	2.025	0.6	1.8 *	1.775
0.09	2.075 *	2.05	0.651	1.75 *	1.725
0.0999	2.075 *	2.05	0.699	1.775 *	1.75
0.12	2.1 *	2.05	0.75	1.8 *	1.8
0.1401	2.1 *	2.05	0.801	1.975 *	1.95
0.1599	2.1 *	2.05	0.849	2.05 *	2.025
0.18	2.075 *	2.05	0.9	2.125 *	2.125
0.2001	2.05 *	2.05	0.951	2.15 *	2.125
0.2199	2.05 *	2.025	0.999	2.125 *	2.15

IV.8. 5 Π-Section 3-Phase Line Simultaneous Closure

L_s(H)	UP(pu)	D(pu)	L_s(H)	UP(pu)	D(pu)
0.0	2.05	2.15	0.24	1.95	1.975
0.0024	2.05	2.1	0.2601	1.975	2.0
0.0051	2.025	2.075	0.2799	1.975	1.975
0.0075	2.025	2.05	0.3	1.975	1.975
0.0099	2.0125	2.0	0.321	1.95	1.975
0.015	2.125	2.075	0.339	1.925	1.925
0.0201	2.2 *	2.1	0.36	1.925	1.925
0.0249	2.225 *	2.15	0.381	1.975	1.975
0.03	2.25 *	2.15	0.399	1.975	1.95
0.0351	2.25 *	2.15	0.42	1.95	1.95
0.0399	2.25 *	2.175	0.441	1.9	1.925
0.045	2.25 *	2.175	0.459	1.925	1.9
0.0501	2.175 *	2.15	0.48	1.925	1.925
0.06	2.15 *	2.125	0.501	1.925	1.925
0.0699	2.075 *	2.025	0.549	1.95	1.95
0.0801	1.975 *	2.0	0.6	1.925	1.95
0.09	1.95 *	1.975	0.651	1.925	1.95
0.0999	2.0	2.0	0.699	1.925	1.925
0.12	2.05	2.05	0.75	1.9	1.875
0.1401	2.0	2.05	0.801	1.875	1.875
0.1599	1.975	1.975	0.849	1.9	1.85
0.18	1.95	1.975	0.9	1.85	1.85
0.2001	1.95	1.95	0.951	1.9	1.9
0.2199	1.975	1.95	0.999	1.925	1.95

IV.9. 10 Π-Section 3-Phase Line Simultaneous Closure

L_s(H)	UP(pu)	D(pu)	L_s(H)	UP(pu)	D(pu)
0.0	2.05 m	2.075	0.24	2.05	2.0
0.0024	2.05 m	2.075	0.2601	2.0	2.0
0.0051	2.025 m	2.05	0.2799	2.05	2.0
0.0075	2.0 m	2.025	0.3	2.025	1.975
0.0099	1.975 m	1.975	0.321	2.0	1.975
0.015	1.9875	1.975	0.339	2.0	1.95
0.0201	2.125	2.025	0.36	1.95	1.925
0.0249	2.2 *	2.075	0.381	1.925	1.9
0.03	2.225 *	2.1	0.399	1.9	1.9
0.0351	2.25 *	2.125	0.42	1.9	1.9
0.0399	2.3 *	2.175	0.441	1.925	1.9
0.045	2.325 *	2.2	0.459	1.95	1.925
0.0501	2.325 *	2.2	0.48	1.95	1.95
0.06	2.325 *	2.225	0.501	2.0	1.975
0.0699	2.3 *	2.2	0.549	2.025	2.025
0.0801	2.25 *	2.175	0.6	2.075	2.05
0.09	2.2 *	2.175	0.651	2.1	2.05
0.0999	2.15 *	2.125	0.699	2.075	2.075
0.12	2.1	2.075	0.75	2.1	2.075
0.1401	2.025	2.025	0.801	2.075	2.05
0.1599	1.975	1.975	0.849	2.05	2.025
0.18	1.975	1.975	0.9	2.0	2.0
0.2001	2.025	1.975	0.951	2.0	1.975
0.2199	2.025	2.0	0.999	1.975	1.95

IV.10. 20 Π-Section 3-Phase Line Simultaneous Closure

L_s(H)	UP(pu)	D(pu)	L_s(H)	UP(pu)	D(pu)
0.0	2.025 m	2.05	0.24	2.025	2.0
0.0024	2.025 m	2.05	0.2601	2.15	2.1
0.0051	2.0 m	2.025	0.2799	2.15	2.125
0.0075	2.0 m	2.025	0.3	2.05	2.075
0.0099	1.9875m	1.95	0.321	2.05	2.075
0.015	1.975 m	1.975	0.339	2.1	2.075
0.0201	2.0	1.925	0.36	2.1	2.1
0.0249	2.05	1.95	0.381	2.075	2.075
0.03	2.15 *	2.0	0.399	2.025	2.025
0.0351	2.125 *	2.025	0.42	1.95	1.975
0.0399	2.1 *	2.05	0.441	2.0	1.975
0.045	2.15 *	2.05	0.459	1.95	1.95
0.0501	2.225 *	2.1	0.48	1.9	1.9
0.06	2.225 *	2.1	0.501	1.875	1.825
0.0699	2.25 *	2.175	0.549	1.725	1.8
0.0801	2.25 *	2.15	0.6	1.825	1.825
0.09	2.225 *	2.2	0.651	1.975	2.0
0.0999	2.225 *	2.2	0.699	2.075	2.075
0.12	2.2	2.175	0.75	2.1	2.175
0.1401	2.175	2.15	0.801	2.175	2.175
0.1599	2.15	2.125	0.849	2.3	2.25
0.18	2.075	2.1	0.9	2.175	2.225
0.2001	2.075	2.05	0.951	2.275	2.3
0.2199	2.025	2.025	0.999	2.35	2.325

APPENDIX V

Program for Transient Frequency Analysis by the DFT

```
C       Plot Dft Of Model Line Waveforms
        DIMENSION XS(0:4096),RMAG(0:4096)
        DIMENSION PMAG(0:4096),RPART(0:4096),RIMAG(0:4096)
        PI=4.0*ATAN(1.0)
C       Data File
        WRITE(5,14)
14      FORMAT(' Data File Name (0-5 characters) ? ',$)
        READ(5,15)NAME
15      FORMAT(A5)
400     OPEN(UNIT=20,FILE=NAME,ACCESS='SEQIN')
        READ(20,*)ISMPN,DT,OFFSET
        READ(20,*)(XS(I),I=0,ISMPN-1)
        DO 1000 I=0,ISMPN-1
1000    XS(I)=(XS(I)-OFFSET)/128.0
410     DO 294 I=ISMPN,4096
294     XS(I)=0.0
C
        WRITE(5,301)
301     FORMAT(' Enter desired freq. resolution ',$)
        READ(5,302)IDF
302     FORMAT(I)
        ISMPN=1/(IDF*DT)+1
        WRITE(5,303)DT,ISMPN
303     FORMAT(' Sample interval is ',F9.7,'  sample no. is ',I6)
        WRITE(5,304)
304     FORMAT(' Enter lower and upper freqs. for plot ',$)
        READ(5,305)IFRLW,IFRUP
305     FORMAT(I,I)
        FRLW=FLOAT(IFRLW)
        FRUP=FLOAT(IFRUP)
        IFRST=IFRLW/IDF
        IFRSP=IFRUP/IDF
        ISMP1=ISMPN-1
        T=ISMPN*DT
        DW=(2.0*PI)/ISMPN
C
C       Discrete Fourier Transform
C
        DO 300 K=IFRST,IFRSP
        CSU=0.0
        SSU=0.0
        DO 310 N=0,ISMP1
        ANGLE=DW*K*N
        CSU=CSU+XS(N)*COS(ANGLE)
310     SSU=SSU+XS(N)*SIN(ANGLE)
        RMAG(K)=SQRT(CSU*CSU+SSU*SSU)
        RPART(K)=CSU
        RIMAG(K)=-SSU
        IF(CSU.EQ.0.0)CSU=0.0001
        PMAG(K)=ATAN(-SSU/CSU)*57.29578
        IF(CSU.GT.0.0)GOTO 300
        IF(SSU.GT.0.0)GOTO 309
        PMAG(K)=PMAG(K)+180.0
```

```
        GOTO 300
309     PMAG(K)=PMAG(K)-180.0
300     CONTINUE
C
        WRITE(5,403)
403     FORMAT(' Phase (P) or Magnitude (M) plot ? ',$)
        READ(5,404)QUES2
404     FORMAT(A1)
        YLOW=-180.0
        YHI=180.0
        IF(QUES2.EQ.'P')GOTO 415
        YLOW=0.0
        RMAX=RMAG(IFRST)
        DO 330 I=IFRST+1,IFRSP
330     IF(RMAG(I).GT.RMAX)RMAX=RMAG(I)
        YHI=RMAX
C
C       Graphical output
C
415     CALL PAPER(1)
        CALL MAP(FRLW,FRUP,YLOW,YHI)
        CALL AXES
        IF(QUES2.EQ.'P')GOTO 420
        DO 350 I=IFRST,IFRSP
        RI=FLOAT(I)/T
        CALL POSITN(RI,0.0)
        CALL JOIN(RI,RMAG(I))
        IF(RI.EQ.0.0)CALL PLOTCS(RI,RMAG(I),'*',1)
350     CONTINUE
        CALL MAP(0.0,1.0,0.0,1.0)
        CALL PLOTCS(0.9,0.8,'HZ',2)
        CALL POSITN(0.85,0.8)
        CALL JOIN(0.7,0.8)
        CALL JOIN(0.7,0.95)
        CALL POSITN(0.64,0.99)
        CALL JOIN(0.64,0.9)
        CALL POSITN(0.48,0.99)
        CALL JOIN(0.48,0.9)
        CALL PLOTCS(0.51,0.95,'X(K)',4)
        GOTO 500
420     DO 360 I=IFRST,IFRSP
        RI=FLOAT(I)/T
        CALL POSITN(RI,0.0)
360     CALL JOIN(RI,PMAG(I))
        CALL MAP(0.0,1.0,0.0,1.0)
        CALL PLOTCS(0.94,0.4,'HZ',2)
        CALL PLOTCS(0.05,0.95,'DEGS',4)
500     CALL GREND
        STOP
        END
```

APPENDIX VI

The Runge-Kutta Technique

VI.1. Fourth-Order Runge-Kutta Method

Given a first-order differential equation

$$f(x,y) = \frac{dy}{dx}$$

an initial value y(x) and a step length 'h', y(x+h) can be evaluated using a fourth-order Runge-Kutta numerical integration technique where,

$$y(x+h) = y(x) + \frac{h}{6} * (G_0+2G_1+2G_2+G_3) \quad (8.12)$$

where $G_0 = f(x,y)$ (8.13)

$$G_1 = f(x+0.5h,y+0.5hG_0) \quad (8.14)$$

$$G_2 = f(x+0.5h,y+0.5hG_1) \quad (8.15)$$

$$G_3 = f(x+h,y+hG_2) \quad (8.16)$$

are the four derivatives required.

VI.2. Program N3SND.FOR

```
C       LINE: 3-ph,mutual earth-return with
C             damping resistors
C       EXCITATION: 1 pu peak,3-ph sinusoidal,
C                   infinite source
C                   20 pi-sections maximum
C       Maximum Plot Spread: 4000 us
C       COMMENTS: Simultaneous/non-simultaneous closure
C                 R-ph closes at t=0
C                 Step length 0.2 us
C                 Points plotted at 1us intervals
C
C
        DIMENSION H(565),G0(565),G1(565),G2(565),G3(565)
        DIMENSION Y(565),F(565)
        DIMENSION V1(4001),V2(4001),V3(4001),BASE(4001)
        REAL L1,L2,L3,L4
C
C       Values of lumped inductance,capacitance
C       and resistance
C
        L1=2.71E-3
        L2=0.68E-3
        L3=0.376E-3
        L4=0.324E-3
        C1=4400E-12
        C2=2200E-12
        C3=17200E-12
        C4=8600E-12
        R1=0.83
        R2=6800.0
        R3=16.5
        R4=69.0
        R5=9.25
        R6=0.79
        R7=33.0
C
C       Source values(1 pu)
C
        E1=1.0
        E2=1.0
        E3=1.0
C
C       Initialise(398 Hz used on model line)
C
        PI=4.0*ATAN(1.0)
        W=2.0*PI*398.0
        SL=1.0E-6
        R=1.0E6
C
C       Input Data
C
        WRITE(5,20)
20      FORMAT(' '/
        1 ' No. of Pi-sections ?                    ',$)
        READ(5,30)NPI
```

```
30      FORMAT(I)
        NI=NPI*14
        NV=NPI*14
        NVAR=NI+NV
        NEWVAR=NVAR
C
        NDPOSC=1
        NDY=1
        NDB=1
        YPHASE=0.0
        BPHASE=0.0
        WRITE(5,40)
40      FORMAT(' '/
        1 ' Pole Scatter required ?                    ',$)
        READ(5,50)QUES1
50      FORMAT(A2)
        IF(QUES1.EQ.'N')GOTO 80
        WRITE(5,60)
60      FORMAT(' '/
        1 ' Enter pole scatter of Y and B in us '/
        2 ' reminder: 10 degrees = 69.8 us             ',$)
        READ(5,70)YPHASE,BPHASE
70      FORMAT(F,F)
        YPHASE=YPHASE*SL
        BPHASE=BPHASE*SL
        NDY=0
        NDB=0
        NDPOSC=0
        NEWVAR=NVAR+5
C
80      WRITE(5,90)
90      FORMAT(' '/
        1 ' Point-on-wave closure for R-ph ? '/
        2 ' 10 degrees , enter 10                      ',$)
        READ(5,100)NPOINT
100     FORMAT(I)
        PHI1=(NPOINT*2*PI)/360.0
        PHI2=PHI1+(240.0*2*PI)/360.0
        PHI3=PHI1+(120.0*2*PI)/360.0
C
        WRITE(5,110)
110     FORMAT(' '/
        1 ' Step Length ?                              ',$)
        READ(5,120)H1
120     FORMAT(F)
        PLOT=1.0/H1
        NPLOT=INT(PLOT)
        NOPLOT=NPLOT-1
        H1=H1*SL
C
        WRITE(5,130)
130     FORMAT(' '/
        1 ' How Long for Waveform Calculation ?        ',$)
        READ(5,140)T
140     FORMAT(F)
        T=T*SL
C
        WRITE(5,150)
150     FORMAT(' '/
```

```
        1 ' Lower and Upper Limits for Graph Plot     ',$)
        READ(5,160)IX1,IX2
160     FORMAT(I,I)
        X1=IX1*SL
        X2=IX2*SL
C
        WRITE(5,170)
170     FORMAT(' '/
        1 ' Print of receiving-end peak values ?      ',$)
        READ(5,180)QUES2
180     FORMAT(A2)
C
C       Runge-Kutta algorithm
C
        INC=0
        X=0.0
190     I301=0
        DO 200 I=1,NEWVAR
200     H(I)=Y(I)
        GOTO 380
210     DO 220 I=1,NEWVAR
220     GO(I)=F(I)
        Z=H1/2.0
        X=X+Z
230     DO 240 I=1,NEWVAR
240     Y(I)=H(I)+Z*F(I)
        GOTO 380
250     DO 260 I=1,NEWVAR
260     G1(I)=2.0*F(I)
        GOTO 230
270     DO 280 I=1,NEWVAR
280     G2(I)=2.0*F(I)
        X=X+Z
        Z=H1
        GOTO 230
290     DO 300 I=1,NEWVAR
300     G3(I)=F(I)
        DO 310 I=1,NEWVAR
310     Y(I)=H(I)+(H1/6.0)*(GO(I)+G1(I)+G2(I)+G3(I))
C
C       Peak values(if desired)
C
        IF(QUES2.EQ.'N')GOTO 350
        IF(ABS(Y(NVAR-4)+Y(NVAR-12)+Y(NVAR-11)).LE.ABS
     1  (PKV1))GOTO 320
        PKV1=Y(NVAR-4)+Y(NVAR-12)+Y(NVAR-11)
        PKT1=X*R
320     IF(ABS(Y(NVAR-4)+Y(NVAR-9)+Y(NVAR-8)).LE.ABS(PKV2))
     1  GOTO 330
        PKV2=Y(NVAR-4)+Y(NVAR-9)+Y(NVAR-8)
        PKT2=X*R
330     IF(ABS(Y(NVAR-4)+Y(NVAR-6)+Y(NVAR-5)).LE.ABS(PKV3))
     1  GOTO 340
        PKV3=Y(NVAR-4)+Y(NVAR-6)+Y(NVAR-5)
        PKT3=X*R
340     IF(NDPOSC.EQ.1)GOTO 350
        IF(X.GE.YPHASE)NDY=1
        IF(X.GE.BPHASE)NDB=1
        IF(NDY.EQ.1.AND.NDB.EQ.1)NDPOSC=1
```

```
C
C       Storage of receiving-end voltages
C
350     IF(X.LT.X1)GOTO 370
        IF(X.GT.X2)GOTO 370
        NOPLOT=NOPLOT+1
        IF(NOPLOT.NE.NPLOT)GOTO 370
        INC=INC+1
        V1(INC)=Y(NVAR-4)+Y(NVAR-12)+Y(NVAR-11)
        V2(INC)=Y(NVAR-4)+Y(NVAR-9)+Y(NVAR-8)
        V3(INC)=Y(NVAR-4)+Y(NVAR-6)+Y(NVAR-5)
        BASE(INC)=X*R
        NOPLOT=0
370     IF(X-T)190,430,430
C
C       Differential Equations
C
380     S1=E1*SIN(W*X+PHI1)
        S2=E2*SIN(W*X+PHI2)
        S3=E3*SIN(W*X+PHI3)
        IF(NDPOSC.EQ.1)GOTO 390
        IF(NDY.EQ.0)S2=Y(NVAR+1)+Y(NVAR+2)+Y(NVAR+3)
        IF(NDB.EQ.0)S3=Y(NVAR+1)+Y(NVAR+4)+Y(NVAR+5)
390     TOT1=Y(NI+10)+Y(NI+12)+(Y(10)*R6)
        F(1)=((S1-Y(NI+2)-Y(NI+3)-Y(1)*R1-TOT1-L2*F(10))/L1)
        F(3)=((S1-Y(NI+1)-Y(NI+2)-Y(NI+3)-TOT1)/L2)
        F(2)=F(3)-F(1)
        F(4)=((S2-Y(NI+5)-Y(NI+6)-Y(4)*R1-TOT1-L2*F(10))/L1)
        F(6)=((S2-Y(NI+4)-Y(NI+5)-Y(NI+6)-TOT1)/L2)
        F(5)=F(6)-F(4)
        F(7)=((S3-Y(NI+8)-Y(NI+9)-Y(7)*R1-TOT1-L2*F(10))/L1)
        F(9)=((S3-Y(NI+7)-Y(NI+8)-Y(NI+9)-TOT1)/L2)
        F(8)=F(9)-F(7)
        F(10)=F(3)+F(6)+F(9)
        F(11)=(Y(NI+11)/L3)
        F(12)=F(10)-F(11)
        F(13)=(Y(NI+13)/L4)
        F(14)=F(11)-F(13)
        DO 400 I=15,NI-13,14
        K=NI+I
        SC1=Y(K-13)+Y(K-12)+Y(K-5)
        SC2=Y(K-10)+Y(K-9)+Y(K-5)
        SC3=Y(K-7)+Y(K-6)+Y(K-5)
        TOT2=Y(K+9)+Y(K+11)+(Y(I+9)*R6)
        F(I)=((SC1-Y(K+1)-Y(K+2)-Y(I)*R1-TOT2-L2*F(I+9))/L1)
        F(I+2)=((SC1-Y(K)-Y(K+1)-Y(K+2)-TOT2)/L2)
        F(I+1)=F(I+2)-F(I)
        F(I+3)=((SC2-Y(K+4)-Y(K+5)-Y(I+3)*R1-TOT2-L2*F(I+9))/L1)
        F(I+5)=((SC2-Y(K+3)-Y(K+4)-Y(K+5)-TOT2)/L2)
        F(I+4)=F(I+5)-F(I+3)
        F(I+6)=((SC3-Y(K+7)-Y(K+8)-Y(I+6)*R1-TOT2-L2*F(I+9))/L1)
        F(I+8)=((SC3-Y(K+6)-Y(K+7)-Y(K+8)-TOT2)/L2)
        F(I+7)=F(I+8)-F(I+6)
        F(I+9)=F(I+2)+F(I+5)+F(I+8)
        F(I+10)=(Y(K+10)/L3)
        F(I+11)=F(I+9)-F(I+10)
        F(I+12)=(Y(K+12)/L4)
400     F(I+13)=F(I+10)-F(I+12)
        IF(NDPOSC.EQ.1)GOTO 410
```

```
      CURENT=Y(6)+Y(9)
      IF(NDY.EQ.1.AND.NDB.EQ.0)CURENT=Y(9)
      IF(NDY.EQ.0.AND.NDB.EQ.1)CURENT=Y(6)
      F(NVAR+1)=(-CURENT/C4)
      F(NVAR+2)=(-Y(6)/C2)
      F(NVAR+3)=-F(6)*R7
      F(NVAR+4)=(-Y(9)/C2)
      F(NVAR+5)=-F(9)*R7
410   DO 420 I=NI+1,NVAR-27,14
      L=I-NI
      F(I)=F(L+1)*R2
      F(I+1)=(F(L+2)-F(L+16))*R3
      F(I+2)=((Y(L+2)-Y(L+16))/C1)
      F(I+3)=F(L+4)*R2
      F(I+4)=(F(L+5)-F(L+19))*R3
      F(I+5)=((Y(L+5)-Y(L+19))/C1)
      F(I+6)=F(L+7)*R2
      F(I+7)=(F(L+8)-F(L+22))*R3
      F(I+8)=((Y(L+8)-Y(L+22))/C1)
      F(I+9)=((Y(L+9)-Y(L+23))/C3)
      F(I+11)=F(L+11)*R4
      F(I+13)=F(L+13)*R5
      F(I+10)=F(I+11)-F(I+13)
420   F(I+12)=F(I+13)
      F(NVAR-13)=F(NI-12)*R2
      F(NVAR-12)=F(NI-11)*R7
      F(NVAR-11)=(Y(NI-11)/C2)
      F(NVAR-10)=F(NI-9)*R2
      F(NVAR-9)=F(NI-8)*R7
      F(NVAR-8)=(Y(NI-8)/C2)
      F(NVAR-7)=F(NI-6)*R2
      F(NVAR-6)=F(NI-5)*R7
      F(NVAR-5)=(Y(NI-5)/C2)
      F(NVAR-4)=(Y(NI-4)/C4)
      F(NVAR-2)=F(NI-2)*R4
      F(NVAR)=F(NI)*R5
      F(NVAR-3)=F(NVAR-2)-F(NVAR)
      F(NVAR-1)=F(NVAR)
      I301=I301+1
      IF(I301.EQ.1)GOTO 210
      IF(I301.EQ.2)GOTO 250
      IF(I301.EQ.3)GOTO 270
      GOTO 290
C
C     Output
C
430   IF(QUES2.EQ.'N')GOTO 450
      WRITE(5,440)PKV1,PKT1,PKV2,PKT2,PKV3,PKT3
440   FORMAT(' '/
     1 ' R-ph peak of ',F ' pu at ',F ' us '/
     2 ' Y-ph peak of ',F ' pu at ',F ' us '/
     3 ' B-ph peak of ',F ' pu at ',F ' us '/
     4 ' ')
450   IC=IX2-IX1
      X1=FLOAT(IX1)
      X2=FLOAT(IX2)
      ICC=IC
      IF(IX1.EQ.0)ICC=ICC-1
      CALL PAPER(1)
```

```
      CALL MAP(X1,X2,-2.8,2.8)
      CALL AXES
      CALL REDPEN
      CALL POSITN(X1,V1(1))
      DO 460 I=1,ICC
460   CALL JOIN(BASE(I),V1(I))
      CALL BLKPEN
      CALL POSITN(X1,V2(1))
      DO 480 I=1,ICC
480   CALL JOIN(BASE(I),V2(I))
      CALL BLUPEN
      CALL POSITN(X1,V3(1))
      DO 500 I=1,ICC
500   CALL JOIN(BASE(I),V3(I))
      CALL BLKPEN
      CALL MAP(0.0,100.0,-2.8,2.8)
      CALL PLOTCS(2.0,2.7,'V',1)
      CALL PLOTCS(4.0,2.7,'(PU)',4)
      CALL PLOTCS(86.0,-2.7,'T',1)
      CALL PLOTCS(88.0,-2.7,'IME(US)',7)
      CALL REDPEN
      CALL POSITN(50.0,-2.7)
      CALL JOIN(54.0,-2.7)
      CALL PLOTCS(56.0,-2.7,'V',1)
      CALL PLOTCS(58.0,-2.7,'RR',2)
      CALL BLKPEN
      CALL PLOTCS(64.0,-2.7,'V',1)
      CALL PLOTCS(66.0,-2.7,'YR',2)
      CALL BLUPEN
      CALL PLOTCS(72.0,-2.7,'V',1)
      CALL PLOTCS(74.0,-2.7,'BR',2)
      CALL GREND
      STOP
      END
```

References

1. Guile A E and Paterson, *Electrical Power Systems,Volume 2,* Permagon Press, 1972.
2. Battisson M J et al, "British Investigations on the Switching of Long E.H.V. Transmission Lines," , CIGRE, 1970, pp. 1-16, Paris,Report 13-02.
3. Day S J,Mullineux N and Reed J R, "Developments in Obtaining Transient Response using Fourier Transforms,Part I," *IJEEE,* Vol. 3, 1965, pp. 501-510.
4. Bickford J P and Doepel P S, "Calculation of Switching Transients with Particular Reference to Line Energisation," *Proc. IEE,* Vol. 114, No. 4, 1967, pp. 465-470.
5. Pender J T, "A Combined Steady-state and Transient a.c. Network Analyser," *IJEEE,* Vol. 6, 1968, pp. 353-361.
6. Bickford J P,Mullineux N and Reed J R, *Computation of Power Systems Transients,* IEE Monograph Series (Peregrinus Ltd.), 1976.
7. Ritchie W M and Barker A, "Insulation Co-ordination of GIS Installations," , Universities Power Eng. Conference, 1986, pp. 102-105.
8. Lanczos C, *Applied Analysis,* Pitman, 1957.
9. Greenwood A, *Electrical Transients in Power Systems,* Wiley-Interscience, 1971.
10. Carson J R, "Wave Propagation in Overhead Wires with Ground Return," *Bell System Tech.,* Vol. 5, No. , 1926, pp. 539.
11. Toland H, *Transient Recovery Voltages in 275kV Transmission Systems,* PhD dissertation, Strathclyde University, 1972.
12. Mullineux N and Reed J R, "Effects of a Lumped Parameter Representation of a Continuous System," *IJEEE,* Vol. 5, 1967, pp. 395-401.
13. Ritchie W M, "Power System Transient Analysis using Analogue Techniques," , Universities Power Eng. Conference, 1974, pp. 1-12.
14. Bishop H W,Crompton E and Chow T W S, "Developments in the Transient Analysis of Electrical Power Systems," , Universities Power Eng. Conference, 1985, pp. 1-4.
15. Morsztyn K, "Computer Controlled Transient Network Analyser Hybrid TNA," , UMIST, 1974, pp. 1-36, Proceedings Symposium on Power System Overvoltages.
16. Ritchie W M and Pender J T, "The Modern TNA and it's Role in Analysis and Design of Electrical Systems," *Proc. IEE,* Vol. 125, No. 2, 1978, pp. 129-134.
17. Crowe L C, "Model Line Transient Modification," DCT Elec. Eng. Dept., Private Communication 1978.
18. Ovenstone W J, "The Development of a Model Transmission Line," DCT Elect. Eng. Dept. Publication, Honours Project 1976.
19. Clark J F C, "Line Energisation," DCT Elect. Eng. Dept. Publication, Honours Project 1977.
20. Bickford J P and El-Dewieny R M K, "Energisation of Transmission Lines from Inductive Sources," *Proc. IEE,* Vol. 120, No. 8, 1973, pp. 883-890.
21. Bickford J P and El-Dewieny R M K, "Energisation of Transmission Lines from Mixed Sources," *Proc. IEE,* Vol. 121, No. 5, 1974, pp. 355-360.
22. Bickford J P, "The Calculation of Restriking Voltages using a Digital Computer," *AEI Engineering Computation Supplement,* 1963, pp. 24-28.
23. Bewley L V, *Travelling Waves in Transmission Systems,* Wiley, 1933.
24. Barthold L O and Carter G K, "Digital Travelling-Wave Solutions," *Trans. AIEE,* Vol. 80, No. 3, 1961, pp. 812-820.
25. Wedepohl L M, "Application of Matrix Methods to the Solution of Travelling-Wave Phenomena in Polyphase Systems," *Proc. IEE,* Vol. 110, No. 12, 1963, pp. 2200-2212.

26. Hsu H P, *Outline of Fourier Analysis,* Simon and Schuster Inc., 1967.
27. Galloway R H,Shorrocks W B and Wedepohl L M, "Calculation of Electrical Parameters for Short and Long Polyphase Transmission Lines," *Proc. IEE,* Vol. 111, No. 12, 1964, pp. 2051-2059.
28. Battisson M J, Day S J, Mullineux N, Parton K C and Reed J R, "Some Effects of the Frequency Dependence of Transmission-Line Parameters," *Proc. IEE,* Vol. 116, No. 7, 1969, pp. 1209-1216.
29. Day S J,Mullineux N and Reed J R, "Developments in Obtaining Transient Response using Fourier Transforms,Part II," *IJEEE,* Vol. 4, 1966, pp. 31-36.
30. Battisson M J,Day S J,Mullineux N,Parton K C and Reed J R, "Calculation of Switching Phenomena in Power Systems," *Proc. IEE,* Vol. 114, No. 4, 1967, pp. 478-486.
31. Battisson M J, Day S J, Mullineux N and Reed J R, "Calculation of Transients on Transmission Lines with Sequential Switching," *Proc. IEE,* Vol. 117, No. 3, 1970, pp. 587-590.
32. Uram R and Miller R W, "Mathematical Analysis and Solution of Transmission-Line Transients, Part I, Theory," *Trans. IEEE,* Vol. 83, 1964, pp. 1116-1123.
33. Uram R and Ferro W E, "Mathematical Analysis and Solution of Transmission-Line Transients, Part 2, Applications," *Trans. IEEE,* Vol. 83, 1964, pp. 1123-1134.
34. Pasahow E J, *Microcomputer Interfacing,* McGraw-Hill, 1981.
35. ESONE Committee, "CAMAC: A Modular Instrumentation System for Data Handling," Tech. report, EURATOM, 1969, Report EUR 4100e.
36. Barden W, *The Z-80 Microprocessor Handbook,* Sams and Co. Incorporated, 1978.
37. Wadsworth N, *Z80 Software Cookbook,* Scelbi Publications, 1979.
38. Cromemco, "SDI Graphics," Cromemco Inc., Computer Reference Manual.
39. Cromemco, "Z-80 Macro Assembler," Cromemco Inc., Computer Reference Manual.
40. Cromemco, "Fortran IV," Cromemco Inc., Computer Reference Manual.
41. Brigham E O, *The Fast Fourier Transform,* Prentice-Hall,Inc., 1974.
42. Schwartz M and Shaw L, *Signal Processing,* McGraw-Hill, 1975.
43. Bozic S M, *Digital and Kalman Filtering,* Edward Arnold, 1979.
44. Cappellini V,Constantinides A G and Emiliani P, *Digital Filters and their Applications,* Academic Press, 1978.
45. Lowry H V et al, *Advanced Mathematics for Technical Students,* Longman, 1971.
46. Dodes I A, *Numerical Analysis for Computer Science,* North-Holland, 1978.
47. Connor F R, *Wave Transmission,* Edward Arnold Ltd., 1972.